# Hydrology of the Elmley Marshes

**Helen Gavin**

Department of Geography
University College London

Thesis submitted for the degree of Doctor of Philosophy

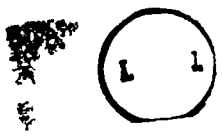

## Abstract

Despite the importance of the hydrological regime for the functioning of wetland environments, the understanding of hydrological processes, particularly evaporative dynamics and clay soil moisture fluxes, is limited and the original research outlined in this thesis constitutes a real contribution to further the scientific understanding of wetland systems. Two lines of investigation are followed based upon field experiments and monitoring of groundwater and ditch water levels together with soil moisture over time and space.

The first investigation assesses the effectiveness of the Environmentally Sensitive Area (ESA) scheme of the North Kent Marshes to achieve its objective of soft moist ground conditions through the manipulation of ditch water levels. Results demonstrate that due to the clay soil texture and low hydraulic conductivity of the marsh substrate, little relationship exists between the position of ditch water levels and groundwater. Flooding the marsh surface with brackish ditch water does promote high surface soil moistures and optimal habitat for waterfowl. However the deleterious effects upon soil structure and floristic diversity by flooding large areas need to be taken in consideration for the sustainable management of the wetland.

Results from this investigation prove that precipitation and evaporation are the dominant fluxes of water, and so the second investigation focused upon the loss of water from the wet grassland by evaporation. There are two foci of research. Firstly the relationship between surface resistance and soil moisture content is examined, so that 'correct' surface resistance values could be input to the Penman Monteith method to compute actual evaporation according to the wetness of the marsh soil. Research results show a complex relationship with decreasing rates of actual evaporation below potential rates with soil moisture loss, and a functional relationship has been quantified. Secondly the actual evaporative water loss of the wetland was determined taking into account the small-scale heterogeneity of surface wetness conditions. The Weighted Penman Monteith (WPM) approach was followed referencing results against data by the Bowen Ratio Energy Balance method. Research results show that the WPM method could be used to compute the actual evaporation loss, however the adoption of the Priestly-Taylor approach with suitable values of $\alpha$ is a simpler method and of equal accuracy.

# Contents

# List of Figures

# List of Tables

## Acknowledgements

Special thanks are offered to my supervisor Professor Clive Agnew (Department of Geography, University of Manchester) for the immense support and guidance he has provided throughout my PhD. I have also benefited from the advice and assistance of Dr. Julian Thompson (Department of Geography, UCL), Dr. Mike Acreman (CEH Wallingford), and Mr. Rob Cameron (English Nature). Many thanks are due to Janet Hope and Tula Cloke (Department of Geography, UCL) for their help in the laboratory; Nick Hamm, Sophie Evitt, and Andrew McGovern for fieldwork assistance, and Elanor McBay (Geography Department Drawing Office, UCL) who produced Figures 1.1d, 2.3 and 2.4.

Instrumentation was supplied by CEH Wallingford and the Department of Geography, UCL. I am indebted to Mike Stroud and David Cooper (CEH Wallingford) for their wise words regarding equipment.

This research would not have been possible without the very generous support, interest and assistance of the staff of the Elmley Conservation Trust, Philip Merricks and Tod Reid, who allowed access to the marshes enabling *in situ* measurements to be collected.

Finally I also thank Alastair Graham for his love and support which has contributed to the completion of this thesis.

This project was part funded by a Teaching Assistantship from the Department of Geography, UCL. The remaining funding came from the EU project 'System for HYdrology using Land Observation for model Calibration' (SHYLOC). Additional small grants were obtained from the Graduate School, UCL.

# Chapter 1 Research Objectives and Study Site

The objective of this research is to increase scientific understanding both for the study site and wet grasslands generally. This chapter introduces the research undertaken at Elmley Marshes, a wet grassland in the North Kent Marshes, and the structure of the thesis. The strategy employed to investigate the relationships between ditch water levels, the water table and soil moisture, and the nature and quantity of the loss of water from the wet grassland from evaporation are outlined. The logical framework and conceptual model of the research are presented.

## 1.1 Introduction

Wetland environments are becoming increasingly valued as their functions and benefits both to humankind and to the wider environment are appreciated and documented (RSPB *et al.* 1997). The range of habitats that can be classified as wetlands are extremely diverse including marshes, fens, peatland, and open water areas, and which support assemblages of unique flora and fauna (Mitsch and Gosselink (2000). In addition to ecological benefits, there are also additional 'goods' provided by wetland environments in terms of hydrological, sediment and chemical processes.

This research is based on the premise that hydrology can be considered as the most important determinant of wetland processes; a change in hydrology can invoke changes in the ecological and physical functioning. The salient issue is the lack of hydrological monitoring to aid management in most wetlands (Clymo *et al.* 1995). Successful management of wetland environments requires sound hydrological science and there is a need for hydrological research in wetland environments to increase understanding of wetland functioning. In this way management can be more effective to maximise the protection and wise use of these environments.

### 1.1.1 Study site

The study site Elmley Marshes are located on the Isle of Sheppey, within the North Kent Marshes wetland complex in Southeast England (Figure 1.1). The North Kent

Marshes comprise an area of brackish and freshwater grazing marsh, saltmarsh and mudflats. The ecological quality of the North Kent Marshes is reflected in the number of regional, national and international policy designations. These apply mainly on the basis on its conservation value for breeding and overwintering waterfowl, and also due to the presence of locally and nationally scarce plant and invertebrate species assemblages. The North Kent Marshes has been classed as an area of Area of High Conservation Value, which includes two National Nature Reserves, and five sites of Special Scientific Interest. In addition the North Kent Marshes comprise part of the Swale, a site of international importance by the Ramsar Convention on Wetlands and a Special Protection Area under the European Union Directive 79/409/EEC on the conservation of wild birds (Briscoe, 1988).

The Elmley Marshes are wet grassland of some 930 ha on the southern part of the Isle of Sheppey (Figure 1.1d). They are composed of a series of fields intersected by ditches used for pasture but managed in such a way to achieve conservation objectives. Elmley National Nature Reserve was designated in May 1998 and is home to more than 300,000 wildfowl and waders.

## 1.2 Research Objectives

Despite the importance of the hydrological regime for the functioning of the marshes, the dearth of hydrological research relating to the study site has been noted (Hollis *et al.* 1993, Bascombe *et al.* 1995). There are two points of focus:

1. Assess the relationship between ditch water levels and the water table and soil moisture.
2. Investigate the nature and quantity of the loss of water from the wet grassland by evaporation.

As the understanding of hydrological processes in wetland environments, such as wet grasslands, particularly evaporative dynamics and clay soil moisture fluxes, is greatly limited, this research provides a case study for an internationally important wetland site focusing upon these neglected variables. Both research topics need to be studied for effective management of this wetland environment.

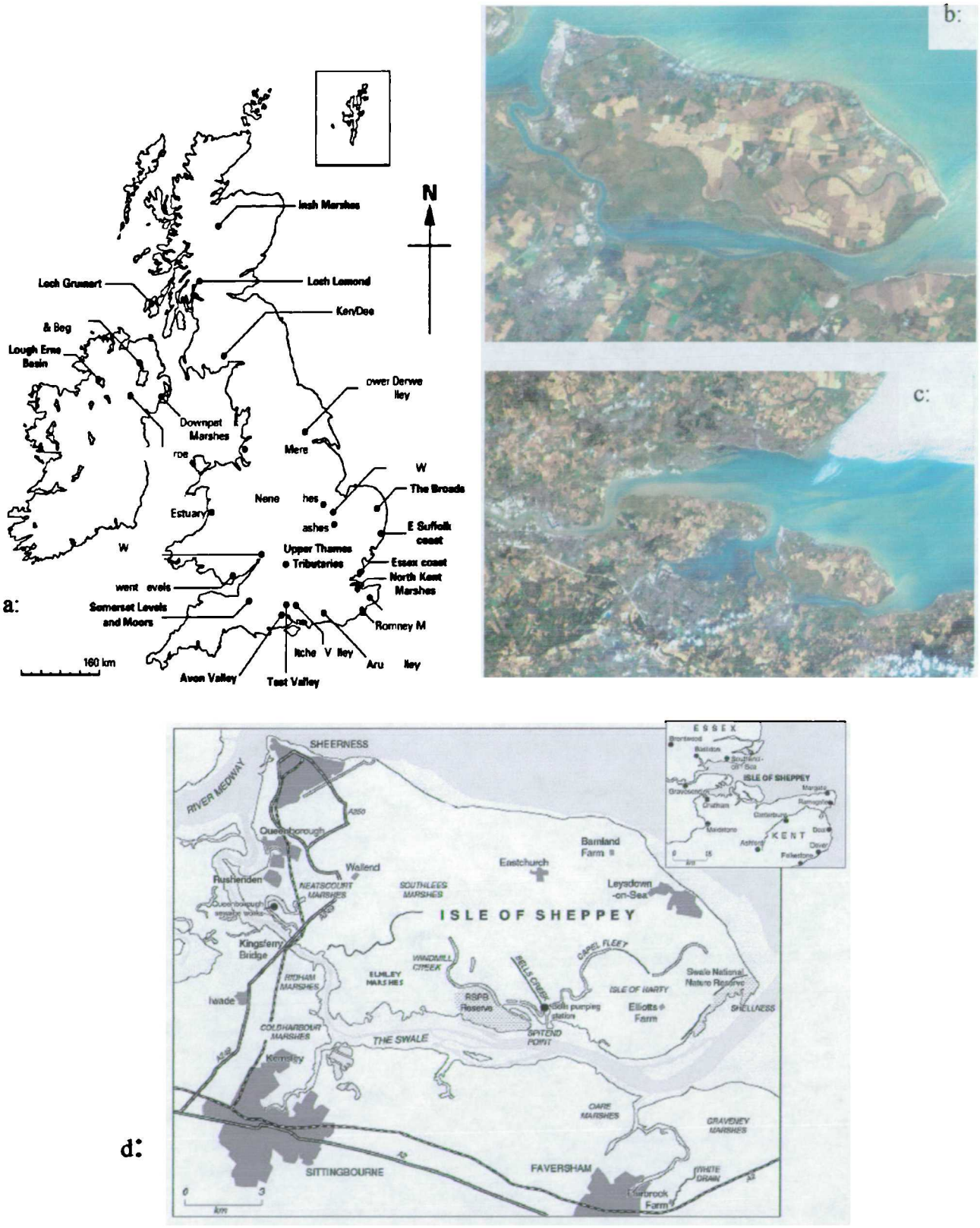


Figure 1.1. Major wet grassland areas in the UK and the North Kent Marshes. Figure a shows wet grassland areas in the UK with sites in bold include areas designated as Environmentally Sensitive Areas (ESA). Source: RSPB *et al.* (1997). Figures b and c are derived from a Landsat TM image of the North Kent and Essex coast with b: focusing upon the study site Elmley Marshes upon the Isle of Sheppey. Figure c: displays the wider area as also shown in d. Source of Landsat TM image: BNSC WOUK2000 CD-ROM.

The logical framework diagram, Table 1.1, shows the line of reasoning and steps necessary in answering each of the lines of investigation discussed below, in addition to listing the data and equipment required.

A conceptual model of the research undertaken is presented in Figure 1.2, partitioned in such a way to allow comparison with the logical framework diagram in Table 1.1. It can be seen from the conceptual model that in order to perform a full hydrological investigation of the wetland, the soil characteristics, water movement and availability, heterogeneity of the surface and the effects of these factors upon the evaporative loss of water need to be investigated.
That is, in order to examine the relationship between the ditch water level, water table and soil moisture requires information upon the soil hydrological characteristics of texture, salinity and hydraulic conductivity. The position of the water table and soil saturation need to be monitored spatially with distance from ditches. Research is needed into the effect of soil moisture levels upon evaporation in order to predict the rate of water loss. Grazing of the marsh vegetation and temporal change in surface wetness heterogeneity with time (from large open water patches in winter to predominantly dry grass areas intersected with ditches in summer) also impact upon the evaporation rate. Figure 1.3 illustrates the study area in detail marking the position of instruments and equipment used in this investigation.

### 1.2.1 Effectiveness of the management of the wet grassland

The Marshes are covered by an Environmental Sensitive Area (ESA) scheme operated by MAFF (Ministry of Agriculture Fisheries and Food) which is detailed in section 3.1. Farmers participating in the scheme receive compensatory payments to follow ecologically sensitive land management in accordance to the criteria of the scheme. There are a number of specified environmental objectives and performance criteria for each ESA; those of the North Kent Marshes ESA involve four objectives structured into a three-tier system. Of particular interest to this project is Objective 2:

> "To maintain and enhance the wildlife conservation value of grazing marsh without detriment to the landscape by maintaining high water levels in ditches" (MAFF 1994).

Table 1.1. The Logical Framework Diagram of the research investigation. The Research Questions are stated and each investigation detailed in terms of approach, data collected and equipment used and data analysis. The three investigations link together as shown in Figure 1.2. All research were performed at Elmley Marshes (Figures 1.1 and 1.3)

| **Research Question 1:** ***What is the relationship between ditch water level and the water table and soil moisture in the adjacent field?*** | |
|---|---|
| Justification | Basis of the ESA prescription implying seepage from ditches maintains high water tables and soft moist ground conditions. Research findings will promote a better understanding of the hydrological processes aiding more effective management. |
| Approach | Characterise the soil hydraulic parameters including the electrical conductivity of the marsh soil and ditch water. Relate the change in ditch water level to changes in the water table and soil moisture of the study field, and determine rates of water movement in the saturated and unsaturated zones to assess the spatial extent of the seepage from ditches. |
| Data | A Ditch water levels and water table over time and space<br>B Soil moisture over space, depth and time<br>C Precipitation and evaporation<br>D Soil characteristics; texture, structure, organic fraction, bulk density, porosity, salinity, hydraulic conductivity, soil moisture characteristic |
| Equipment | A Stageboards and piezometers<br>B Neutron scattering for depth measurements and Surface Capacitance Insertion Probe (SCIP) for spatial investigation, electrical resistance blocks (ERB) and gravimetric sampling for long-term measurements<br>C Automatic Weather Station<br>C Lab facilities, field electrical conductivity probe |
| Analysis | The DITCH model allows the prediction the movement of water between ditches and surrounding fields to examine the consequence of various ditch management regimes.<br>The BUDGET model can simulate the change in soil moisture through the data input and of precipitation and evaporation respectively only. |

| **Research Question 2:** ***What is the effect of soil moisture upon the evaporation rate?*** | |
|---|---|
| Justification | Research of this type for grass surfaces in the UK is limited. Original research. Research findings will promote a better understanding of the hydrological processes aiding more effective management. |
| Approach | Derive the parameters of the Penman Monteith formula to simulate the Elmley Marshes environment in terms of wetness levels. Determine the effect of soil moisture levels by computing values of actual evaporation by the water balance referencing against potential evaporation. Establish whether a relationship can be made between soil moisture and surface resistance so that actual evaporation can be computed using the Penman Monteith formula. |
| Data | A Soil moisture data in with depth in space and time<br>B Actual and potential evaporation |
| Equipment | A Electrical resistance blocks, neutron probe soil sampling equipment<br>B Automatic Weather Station |
| Analysis | Quantification of a relationship will enable computation of actual evaporation from the Penman Monteith model over a range of soil moisture levels. |

| **Research Question 3:** ***What is the actual evaporation loss from the heterogeneous wetland surface?*** | |
|---|---|
| Justification | Research of this type for wetland environments is limited. Original research. |
| Approach | Establish whether the Weighted Penman Monteith approach can be used obtain a spatially distributed value of evaporation over the marsh. Determine the change in surface types of the wetland over time and assign surface resistance values depending upon moisture levels. Reference against AET from the BREB method. Assess the relationship to the equilibrium evaporation and effects of local heat advection. |
| Data | A Actual and potential evaporation<br>B Spatial and temporal change in extent of the surface area of grass, open water and bare soil |
| Equipment | A Bowen Ratio Energy Balance and Automatic Weather Station |
| Analysis | The results link together the relationship between actual and potential evaporation and the inundation of the marsh. Employs the results of the second investigation to assign surface resistance values to the grass areas. The results indicate if the Weighted Penman Monteith approach can be used to simulate the actual evaporation from the wetland taking account of its spatial heterogeneity. |

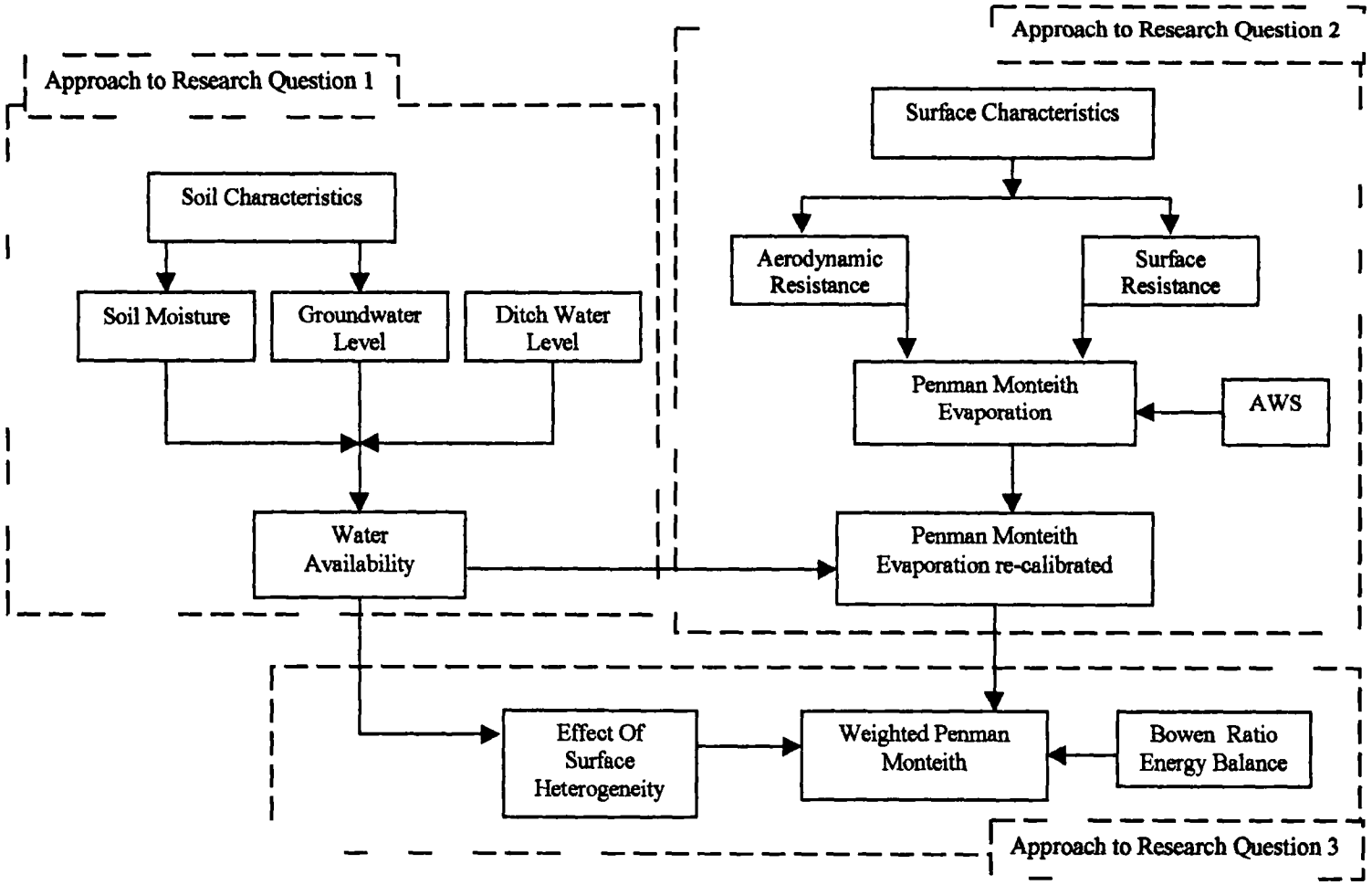


Figure 1.2. Conceptual model of the research investigation. The diagram is partitioned to show the order of research as related to the research questions expressed in Table 1.1. The soil hydrological characteristics are determined, and the relationship between the ditch water levels, groundwater and soil moisture investigated using the models BUDGET and DITCH. With an understanding of the water availability to the grass vegetation, the constraints upon the loss of water through evaporation are then examined. This is achieved by determining a relationship between soil moisture and the surface resistance term of the Penman Monteith formula. The effects of spatial heterogeneity upon evaporation from the marsh are also examined, with an attempt to compute values of evaporation from the heterogeneous wetland surface accounting of the change in areal extent of the different surface types over time.

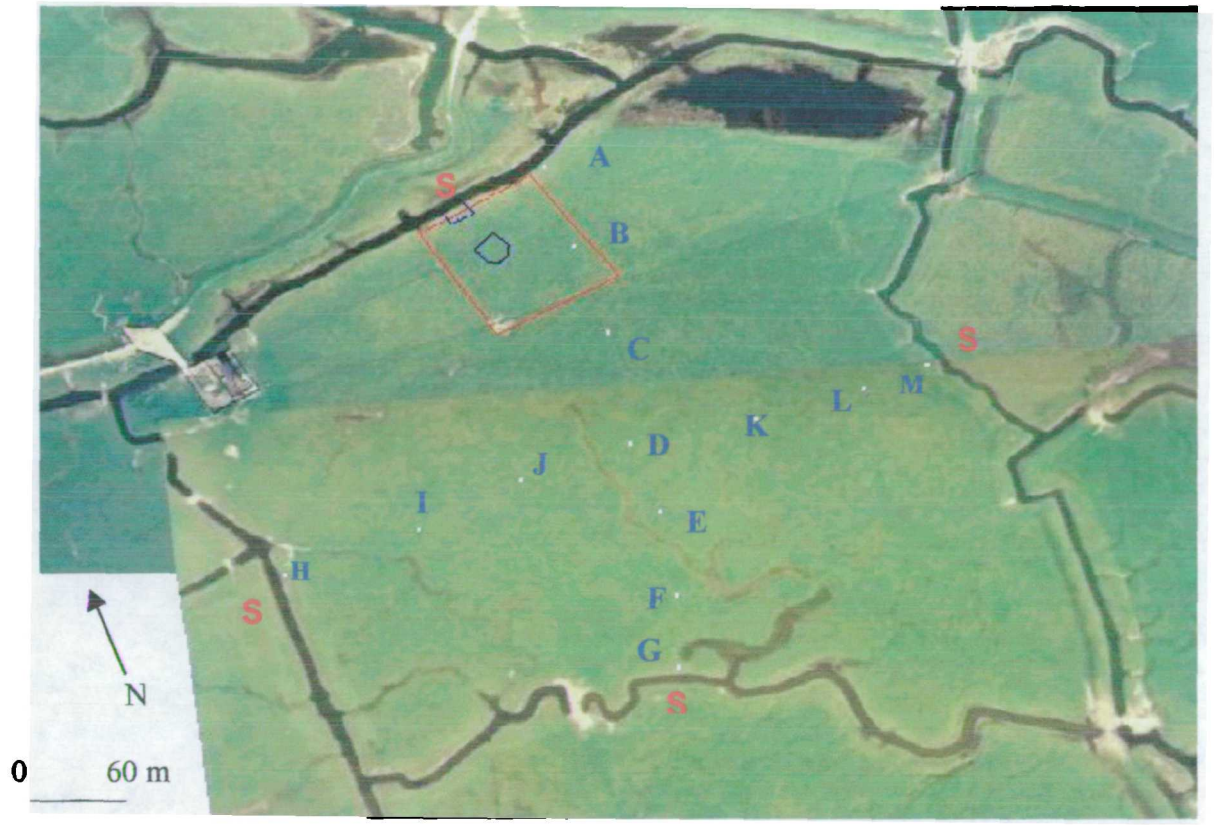


Figure 1.3. The study area in detail.
An aerial view (above: overlay of two photographs) and diagram (right) of the layout of the main enclosure (blue shield shape above) and smaller enclosure (blue open-ended square above) adjacent to the north ditch of the study field (also known as Elmley Fleet).
Marked upon the aerial photograph are the transect piezometers (small white squares) aligned north-south (A-G) and west-east (H-M). Also marked are the location of the stageboards (marked with S), positioned at the end of the piezometer transects and are referred to in the text as the east, south and west ditches.
The red square outlines the grid in which the surface soil moisture was monitored with the SCIP.
On the diagram the shaded squares are the piezometers 1, 2, 3 in which a pressure transducer is located. These piezometers were subject to pump tests performed to determine the saturated hydraulic conductivity.
The main enclosure houses most of the instruments used in this research. The ThetaProbe, Equitensiometer and pressure transducers are wired into the logger in the main enclosure. In the small enclosure the position of the stageboard (S), pressure transducer (P) in the north ditch, and the neutron access tube are labelled.

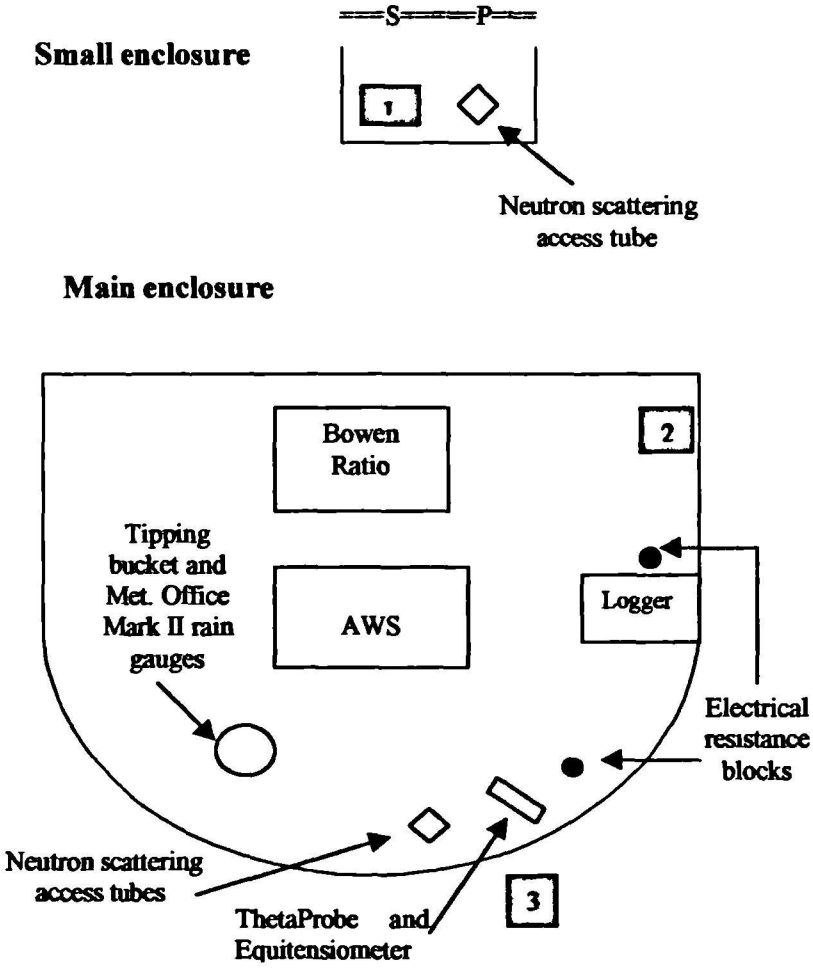

Tier 1a, the Wet Grassland Tier, focuses on the traditional use of ditches as wet fences and provide drinking water for stock, and specifies the required ditch water levels to achieve the above objective. The objective is to use the ditches as irrigation channels rather than for drainage i.e. to recharge the water table in the middle of the surrounding parcels of land by high ditch water levels to maximise wildlife conditions. "The underlying aim is to manipulate the water environment in such a way as to create moist, soft ground conditions together with areas of standing water, at these times of year critical to feeding and breeding success particularly of waders. Tier 1a was included into the ESA scheme specifically to promote this objective" (FRCA 1997 p12).

Studies of the manipulation of the marsh water table through ditch water level control have been undertaken in other wet grassland areas covered by similar ESA prescriptions (Armstrong 1993, Armstrong and Rose 1998, Youngs *et al.* 1991 Youngs *et al.* 1989, Towner and Youngs 1986, Youngs 1990) and other wetland sites (Boelter 1972, Gilman 1994). These studies show that the magnitude of water table control is predominantly affected by the hydraulic conductivity of the soil, and that even at sites with high hydraulic conductivity there is a maximum spatial influence of the ditches. In the case of North Kent, elementary research by Hollis *et al.* (1993) indicated that the manipulation of ditch water levels had little effect upon the in-field water table due to the low hydraulic conductivity of the clay marsh soil. In the absence of any hydrological monitoring undertaken by MAFF to ascertain whether the effects of ditch water level management have met the desired objective of soft moist ground conditions, this research was initiated to examine fully the relationship between the drainage ditches and the adjacent parcels of land.

It can be argued that there is a need for preliminary hydrological research in areas to be designated an ESA before the scheme is implemented. Such research would further the understanding of the system and determine the best mechanisms for meeting desired objectives through hydrological ends so that the compensatory payments are not being misspent. That the management restrictions of ESA prescriptions are imposed without prior research in order to achieve political rather than environmental objectives is a gross misjudgement and needs to be addressed.

1.2.1.1 Research Question 1: *What is the relationship between ditch water levels and the water table and soil moisture in the adjacent field?*

This research is undertaken to assess the success of the ESA hydrological management prescription. The logical framework of this investigation can be found in Table 1.1. Groundwater and ditch water level data have been monitored in addition to observations of the soil moisture of the marsh at the ditch edge and at distance. The soil characteristics of the study site including hydraulic conductivity have been determined. In this way the spatial and temporal influence of the ditch water levels upon the water table and soil moisture of the marsh can be determined. Three models are employed: Dupuit-Forchheimer analysis (section 4.2), Drain Interaction with Channel Hydrology (DITCH) (Armstrong 1993, Armstrong and Rose 1998) and BUDGET (Raes 1996). Dupuit-Forchheimer analysis and DITCH have been employed to quantify the magnitude of the recharge and discharge fluxes from the ditch system across the marsh. In addition the model BUDGET has been used to ascertain whether the change in soil moisture monitored over the marsh can be modelled using only, and therefore assumed to be directly a function of, the rainfall and evaporative fluxes over the area.

The steps taken are thus:

- Characterise the soil hydraulic parameters, bulk and particle density, texture, porosity, organic matter content, and soil moisture characteristics in addition to the electrical conductivity of the marsh soil and ditch water.
- Determine the hydraulic conductivity of the marsh soil with depth in both the unsaturated and saturated zones.
- Relate the change in ditch water level to the spatial and temporal changes in the water table and soil moisture of the study field, to assess the spatial extent of the seepage from ditches. Use the models Dupuit-Forchheimer analysis, BUDGET and DITCH to simulate hydrological processes operating over the marshes.

### 1.2.2 The loss of water by evaporation.

The research described above, and that undertaken by Hollis *et al.* (1993) suggest that the dominant hydrological fluxes of the marshes are precipitation and evaporation. The hydrological cycle is characterised by inundation during winter months and depletion of standing water and soil moisture during summer. Over the study period the seasonal range of soil moisture levels monitored in the surface soil have ranged from over 60% to below 10%. The research undertaken to assess the loss of water from the marsh investigates the influence of soil moisture, and of surface wetness heterogeneity.

Measurement of the quantity and nature of water loss through evaporation in wet grasslands, and of wetland environments as a whole, is rare. Consequently there is a dearth of information relating to the controls of soil moisture upon evaporative loss for grassland systems in the UK (Cain 1998) which the research presented here addresses. Calculations of evaporation using Penman Monteith for water balance and irrigation studies have largely been concerned with agricultural crops and commercial tree plantations due to economic considerations (Kelliher *et al.* 1993). While it is true to say that the evaporation of grass has been investigated, it is mostly under 'reference conditions' of an actively growing uniform stand, adequate water supply with a grass height between 0.08-0.15 cm completely shading the ground, with a fixed surface resistance of 70 $sm^{-1}$ (Smith *et al.* 1992, Doorenbos and Pruitt 1977, Jensen *et al.* 1990). As such it can be stated that '*there is little or no testing of the model in naturally vegetated areas*' (Wessel and Rouse 1994, p111). There exists a need to assess the evapotranspiration from natural grassland areas, which do not have an adequate water supply in the summer. In order to do this, the effect of decreasing soil moisture upon the evaporation rate needs to be investigated.

#### 1.2.2.1 Research Question 2: *What is the effect of soil moisture upon the evaporation rate?*

The research undertaken attempts to link the change in soil moisture of the marsh with the surface resistance term in the Penman Monteith equation. The logical framework of this investigation can be seen in Table 1.1. Values of surface resistance are

determined using the approach of Russell (1980) by rearranging the Penman Monteith equation. This necessitates *a priori* values of actual evaporation and potential evaporation loss that are computed from a soil moisture balance approach and the Penman Monteith model (with the variable surface resistance set to zero) respectively. In this way values of surface resistance are derived over a period of soil moisture decline which, when used in the Penman Monteith equation, would enable the computation of actual evaporation loss.

The steps taken are thus:

- Determine the effect of decreasing soil moisture by computing values of actual evaporation by the water balance approach.
- Establish a relationship between soil moisture and surface resistance so that actual evaporation can be computed using the correct resistances in Penman Monteith formula.

1.2.2.2 Research Question 3: *What is the actual evaporation loss from the heterogeneous wetland surface?*

The soil moisture of the marsh is not spatially homogenous. Wet grassland environments usually comprise a variety of surface types or patches; for example open water, wet inundated grass and drier areas that change in extent temporally and spatially, and the Elmley Marshes are no exception to this. The possible effects upon the evaporation over the marsh by small-scale heterogeneity in wetness levels form Research Question 3: *What is the actual evaporation loss from the heterogeneous wetland surface?* The logical framework of this investigation can be found in Table 1.1. The approach taken to monitor actual evaporation from the wetland follows the Weighted Penman Monteith (WPM) method of Wessel and Rouse (1994). The approach requires appropriate resistances for each 'surface type' present over the wetland which are weighted according to their spatial coverage. Results from this approach are compared against the Bowen Ratio Energy Balance station.

The steps taken are thus:

- Determine the dominant contributing source area and fetch requirements.
- Determine temporal and spatial coverage of the 'surface types' of grass, open water and bare soil and correct surface resistances.
- Determine the evaporation rate of the wetland following the WPM approach and assess accuracy against data from the Bowen Ratio Energy Balance station.
- Compute the WPM approach for these selective time periods to determine the representative evaporation from the marsh according to the representative source area.

## 1.3 Structure of the Thesis

The thesis is structured similarly to the logical framework diagram; that is each research question is considered in turn in sequential chapters. Due to broad nature of the research, relevant discussions of the concepts and fundamental process are placed in salient chapters and appendices. An examination of data acquisition and quality including instrument calibration is found in Appendix A. A summary of each chapter can be defined as such:

Chapter 1: Research Objectives and Study Site

This chapter introduces the study site, research rationale and objectives, and outlines the logical framework diagram and conceptual model.

Chapter 2: Wetlands

This chapter places the study site, Elmley Marshes, in a wider research context of wetland environments focusing upon wet grassland environments.

Chapter 3: Ditch water: soil water relationships. Part 1 Soil characteristics.

This chapter discusses the objective and methodology of Research Question 1: *What is the relationship between ditch water levels and the water table and soil moisture in the adjacent field?* The research approach and data collection are presented. The concepts and fundamental processes of water flow in the saturated and unsaturated zones are discussed together with methods to determine the hydraulic conductivity and soil moisture characteristic curve salient to the research of this chapter.

Original research from the investigation include:

- Soil characteristics (sections 3.3.1.1 – 3.3.1.1.5) including particle size, bulk and particle density, organic content and porosity.
- Soil and ditch water electrical conductivity and effects of difference in density (sections 3.3.1.6 – 3.3.1.9).
- Measurement of the hydraulic conductivity and infiltration with the Bouwer and Rice approach (section 3.3.2.1) and the Guelph permeameter (section 3.3.2.2).
- Derivation of the soil moisture characteristic employing the Gupta and Larson (1979) approach (section 3.3.3.1), pressure plate apparatus (section 3.3.3.2), data coupling of a tensiometer and neutron scattering (section 3.3.3.3), and the ThetaProbe and Equitensiometer in the surface soil (section 3.3.3.4).

Chapter 4: Ditch water: soil water relationships. Part 2 Soil hydraulics

This Chapter continues from Chapter 3 to report the results of monitoring the water table and ditch stage, and modelling performed to quantify and predict the relationship between ditch water levels, position of the water table, and recharge fluxes. The water table is modelled using the Dupuit-Forchheimer approach and also using the Drain Interaction with Channel Hydrology (DITCH) model.

Original research from the investigation include:

- Relationship between the water table and potentiometric head (section 4.1) and the relationship between ditch levels and saturation in the soil, using the piezometer transects over the west to east and north to south of the study field.
- Dupuit-Forchheimer modelling (section 4.2).
- Discussion of the DITCH model, simulation of the water table of the study area, and computation of the ditch recharge and discharge functions (section 4.3).

Chapter 5: Ditch water: soil water relationships. Part 3 Soil moisture

This chapter continues from Chapter 4 to present final research results and analysis for Research Question 1. This chapter contains the results of soil moisture profile monitoring with the neutron probe and soil sampling over 1998 and 1999. The soil moisture profile was modelled with BUDGET to ascertain the dominant water fluxes. Results are also presented of the investigation into marsh inundation and spatial and temporal change in moisture content of the surface soil layer adjacent to a ditch.

These results are interpreted in view of the Tier 1b prescription of the ESA, which stipulates inundation of the marsh surface.

Original research and data collection from the investigation include:

- Results of monitoring moisture content of the soil profile over time and space identifying the trend of soil moisture with depth and location over time (section 5.1).
- Modelling the soil profile with the BUDGET model; its performance to simulate observed soil moisture change for moisture contents at the ditch edge and at distance (section 5.2).
- Inundation mapping of the study area and the change in extent of the surface 'types' i.e. land cover of the marsh. Monitoring of surface soil moisture change over time and space. A novel approach has been used employing geostatistics to determine the optimum sampling strategy to identify spatial change for the surface soil (section 5.3).

Chapter 6: Discussion of Research Question 1

This chapter synthesises the results of the investigation of Research Question 1: *What is the relationship between ditch water levels and the water table and soil moisture in the adjacent field?* and discusses the effectiveness of the ESA management prescriptions.

Chapter 7: Wetland evaporation. Part 1 Soil moisture: surface resistance relationship

This chapter discusses the rationale and methodology of Research Question 2*: What is the effect of soil moisture upon the evaporation rate?* A review of published work examining the effect of soil moisture upon the evaporation rate is presented. The research results and analysis for this investigation are discussed and a functional relationship derived. This relationship is compared against published models.

Original research from the investigation include:

- Actual evaporation calculated by the water balance approach and potential evaporation using the Penmen Monteith model for the wet grassland study site.
- Quantification of the relationship between surface resistance and soil moisture.
- Derivation of a functional relationship to predict surface resistance from the soil moisture content.

- Comparison of the derived relationship to published models.

Chapter 8: Wetland evaporation, Part 2 Actual evaporation loss

This chapter follows from Chapter 7 and presents the rationale and methodology used to address Research Question 3: *What is the actual evaporation loss from the heterogeneous wetland surface?* The Weighted Penman Monteith (WPM) approach and necessary data is described. The principles of the Bowen Ratio Energy Balance (BREB) approach are outlined. The WPM values of actual evaporation are compared against that of the BREB.

Original research from the investigation include:

- Mapping the change of surface areas over time and designation of surface resistance values according to soil moisture content.
- Actual evaporation calculated by the WPM and BREB for the wet grassland study site.
- The relationship between WPM and BREB.
- Relationship of AET from WPM and BREB to the equilibrium evaporation rate.

Chapter 9: Summary and conclusions

This chapter summarises and considers the research findings of the hydrological investigation at Elmley Marshes.

Appendix A: Data acquisition and quality

Appendix A contains details relating to the instruments employed in this research, data collection and data quality. The results of instrument calibration to the soil of the study area are presented. The appendix is organised in the following way:

- Discussion of the data quantity and quality from the sensors of the Automatic Weather Station (AWS). The steps taken to derive data at periods of sensor malfunction are described (section A.1).
- Examination of the difference in output between the net radiometer output of the AWS, Didcot Instruments, to the Bowen Ratio station, NR-Lite (section A.2).
- Design, structure and location of the stageboards and piezometers at the study site (section A.3). The pressure transducers used for pump tests are described (section A.4).

- Operation and theory of the soil moisture monitoring equipment employed at the Marshes with the results of the instrument calibration to the soil of the marshes. The instruments discussed are the neutron probe (section A.5), Surface Capacitance Insertion Probe (SCIP) (section A.6), ThetaProbe (section A.7) and electrical resistance blocks (section A.8).
- A review of soil moisture monitoring in the surface layer of soil assesses the precision of the various instruments employed (section A.9).

Appendix B: Geostatistics

Appendix B contains a discussion of the concept of geostatistical sampling, the tool used to determine optimum sampling of soil moisture of the surface soil using the Surface Capacitance Insertion Probe (section 5.3.2.1). The appendix is organised in the following way:

- An introduction to the theory of geostatistics, particularly the use of geostatistics in soil science (sections B.1-5).
- The concept of the semivariogram is discussed with reference to the optimal number of samples required and the method of nested sampling for reconnaissance studies (sections B.6-B.7).

# Chapter 2 Wetlands

This chapter places the study site, Elmley Marshes, in a wider research context of wetland environments focusing upon wet grassland environments.

## 2.1 Introduction

Traditionally perceived as wastelands, wetland environments are becoming increasingly valued as their functions and benefits both to humankind and to the wider environment are appreciated and documented. The range of habitats that can be classified as wetlands are extremely diverse as exemplified by the definition of wetlands by the Ramsar Convention on Wetlands of International importance especially as Waterfowl Habitat:

> "Areas of marsh, fen, peatland or water, whether natural or artificial, permanent or temporary, with water that is static or flowing, fresh, brackish or salt, including areas of marine water the depth of which at low tide does not exceed six metres. Wetlands may incorporate riparian and coastal zones adjacent to the wetlands, and islands or bodies of marine water deeper than six metres at low tide lying within the wetland."

The Convention, established in the city of Ramsar Iran 1971, initiated the infrastructure for the designation, conservation and wise use of wetlands in member countries (Frazier 1996). Under the definition of the Convention, diverse habitats such as mangrove swamps, tidal salt marshes, upland peat bogs, and wet grasslands can be classified as wetlands. Wetlands that fulfil certain criteria can be nominated to be included in the Ramsar list of internationally important wetland sites, which includes as the North Kent Marshes. Such criteria include (Frazier 1996):

- It is a particularly good representative example of a natural or near-natural wetland, characteristic of the appropriate biogeographical region.
- It supports an appreciable assemblage of rare, vulnerable or endangered species or subspecies of plants or animals, or an appreciable number of individuals of any one or more of these species.

- It regularly supports 20,000 waterfowl; or where data on populations are available, it regularly supports 1% of the individuals in a population of one species or subspecies of waterfowl.

The criteria above focus upon the ecological role of wetlands as habitats for populations of waterfowl, plants or animals. While the Ramsar definition and criteria of designation convey much of the essential character of wetlands they can be criticised for lacking scientific exactness. However the definition and classification of wetlands is fraught with problems due to their diversity and dynamic nature which can evolve over time, and the difficulty in defining their boundaries with precision (Finlayson and Moser 1991). Other definitions and classifications of wetlands focus upon the physical characteristics of wetland environments such as the presence of water, hydric soils and hydrophytic vegetation.

In addition to ecological benefits, there is a growing awareness of the additional 'goods' provided by wetland environments in terms of hydrological, sediment and chemical processes. For example Adamus and Stockwell (1983) list amongst others groundwater recharge and discharge, flood water storage and desynchronisation, sediment trapping, nutrient retention and removal in addition to food chain support and habitats for wildlife and fisheries.

Hydrology is probably the single most important determinant for the establishment and maintenance of specific types of wetland and wetland processes (Mitch and Gosselink 2000). A change in the hydrology of the wetland can impinge upon, and lead to changes in, the ecological and physical functioning. The salient issue is the lack of hydrological monitoring to aid management in most wetlands. There is a need for hydrological research in wetland environments to increase scientific understanding to maximise the protection and wise use of these environments. Currently data collection and monitoring programmes in wetland environments focus mainly on ecological aspects such as the presence and density of waterfowl due to the active nature of conservation organisations such as Birdlife International, the International Union for Conservation and Nature, and World Wildlife Fund in managing wetland areas. The lack of hydrological information for wetland environments is common and can act as an obstacle to research (Clymo *et al.* 1995, Gilman 1994).

This thesis aims to increase understanding of wetland hydrological processes by undertaking research in a wet grassland. The study site is the Elmley Marshes on the Isle of Sheppey, see Figures 1.1 and 1.3, which forms part of the North Kent Marshes, a conglomeration of brackish and freshwater grazing marsh, saltmarsh and mudflats. The Elmley Marshes are wet grassland of some 930 ha on the southern part of the Isle of Sheppey. It is composed of a series of fields intersected by ditches used for pasture but managed in such a way to achieve conservation objectives. Elmley National Nature Reserve was designated in May 1998 and is home to more than 300,000 wildfowl and waders. The marshes can be considered representative of the wet grassland areas of the North Kent Marshes.

## 2.2 Wet grasslands

It is necessary to describe briefly wet grassland environments, using the study site of Elmley Marshes as an example. In this way the physical, ecological and management issues of Elmley Marshes can be discussed in relation to wet grasslands as a whole.

### 2.2.1 Introduction

Wet grasslands predominate in lowland areas in the UK, see Figure 1.1a, which are periodically flooded or waterlogged by freshwater. The majority of wet grasslands are sited on lowland floodplains in England, with a few in Scotland Wales and Northern Ireland. The traditional management of these areas for grazing pasture, with a network of ditches to retain water and act as wet fences for stock control, has promoted vegetation dominated by grasses, sedges and rushes (RSPB *et al.* 1997). The term 'wet grassland' encompass semi-natural floodplain grassland, washland, water meadows, lakeside wet grasslands, and wet grasslands with intensive water level management on drained soils.

Wet grasslands depend on the maintenance of the balance between hydrology and land use (Swetnam *et al.* 1998, Treweek *et al.* 1996). Conservation of wet grasslands can be managed through hydrological manipulation, such as the maintenance of high water tables as specified in some of MAFF's Environmentally Sensitive Areas (ESA) schemes for example. This ameliorates the habitat for specific target species but can create potential conflicts. Swetnam *et al.* (1998) discuss the deterioration of the flora

of Southlake Moor covered by the Somerset Levels and Moors ESA, when water tables are raised to successfully encourage nesting birds. Often management for conservation focuses upon such visible populations rather than the combined floral and faunal attributes of the site. Indeed English Nature have identified wet grassland areas as a priority habitat for birds due to the dependence of such Red Data Book species as Golden plover and snipe (Brown and Grice 1993, Fuller 1982).

The wet grassland areas of the North Kent Marshes, including the Elmley Marshes, are examples of wet grasslands with intensive water level management, and can be further defined as coastal grazing marsh, with brackish qualities through its reclamation from saltmarsh.

Together with the Elmley Marshes other wetlands that can be classified as 'wet grasslands with intensive water level management on drained soils' include the Somerset levels and Moors, parts of the Norfolk Broads and the Halvergate Marshes (RSPB *et al.* 1997). All or part of these wetland areas have been fragmented and lost and are now managed in traditional manner that requires the manipulation of the ditch water levels. This is discussed further in sections 2.2.5 and 2.2.4 respectively.

### 2.2.2 Physical characteristics

Permanent grass is the traditional land use for the North Kent Marshes. The drainage system consists of a network of channels dividing the landscape into fields of varying sizes. Sluices drain water through the influence of gravity at low tides. The channels were originally the tidal creeks of the former saltmarsh together with man-made ditches. A popular definition of the location of the grazing marshes of North Kent was that of Green (1971) which specified the area between the sea wall and the 12.62 m contour. This area is broadly defined as the coastline of the Cliffe/Hoo peninsula and the southern part of the Isle of Sheppey together with the south bank of the Swale plus the Medway estuary (Figure 1.1d). The total area of the marshes is approximately 4300 ha (TEP 1996) which lie along the Thames and Medway estuaries and along the Swale (Gilham and Holmes 1950).

Much of the marshland is flat with complex relief on a micro scale caused by its reclamation from saltmarsh. There also exist mounds of up to 0.5 m in height formed

by a variety of causes including anthills and the deposition of silt on the bankside from ditch dredgings.

> "The land retains much of the former saltmarsh topography, with irregular twisting drainage creeks and shallower low-lying remnant creeks called rills, framed in places by the higher ground of the marsh edge and adjoining slopes. This topography not only contributes to the exposed, flat landscape character, combining a mosaic of habitats present today, it also influenced the types of agricultural practises, principally extensive stock grazing, with arable cultivation confined to higher better drained land." ADAS (1997, p47).

Within the marshland, creeks and ditches are interlinked to enclose the marshes and create fields of varying sizes. Former creek channels and saltmarsh rills are present in the fields becoming progressively smaller along their course (Hazelden *et al.* 1986) and behave as conduits for water in times of inundation. Spoil from ditch dredging operations are deposited on the banksides accentuating natural levees and forming relative depressions in the centre of the fields (Hazelden *et al.* 1986).

Gilham and Holmes (1950) provide a comprehensive history of the reclamation of the North Kent Marshes over time. They suggest that Romans initiated the transformation of the saltings into grazing marshes from evidence of Roman pottery in the marsh sediment and the presence of garrison towns at Sittingbourne and Rochester. In addition the presence of discontinuous peat horizons formed in Roman times indicates stability in the relative levels of land and sea during that period (Fordham and Green 1980). Pottery remains and historical evidence suggest that large areas were once reclaimed and repeatedly lost to sea through neglect or breaches in sea walls. A recent example of this is the major flood in 1953. The current responsibility for maintenance of the sea walls lies with the Environment Agency. The reclaimed marshland is lower than the seaward saltings at 1-3 m O.D. and 2-5 m O.D. respectively (Hazelden *et al.* 1986). This is due to a combination of subsidence and shrinkage of the marshland through the drying of sediment and the loss of matter through oxidation, and the alluvial build-up of the saltings.

The North Kent Marshes are underlain by the London Clay Formation deposited in the early Tertiary period, which reaches a maximum thickness of over 150 m in North Kent (King 1981). Boreholes near Kingsferry Bridge (Figure 1.1d) show the London

Clay to be present at a depth of between 8.63 and 12.2 m O.D. (Barham *et al.* 1991). The overlying deposits of alluvium comprise of bluish-grey marine clay with intermittent bands of peat, silt and sand. The clays, silts and silty sand sediments of the London Clay Formation (King 1981) almost wholly underlie the North Kent Marshes. The London Clay formation can be considered impermeable and acts as an aquiclude for the three aquifers below, the principal one being the extensive chalk deposit. This is overlain in places by the limited aquifers of the Tertiary Beds (Blackheath, Oldhaven, Thanet and Woolwich) and Head deposits (Terrace and Plateau gravels) which may yield limited amounts of groundwater (Hollis *et al.* 1993, IGS 1970). The alluvium and soil represents a further aquifer of limited permeability.

The North Kent Marshes have a permanent water table and deposits of thick, highly clayey marine alluvium derived from the underlying base of London Clay (Fordham and Green 1980, Green and Burnham 1973). Having been affected by salt due to its history of reclamation, the soils are unusual in this sense and constitute the largest area of such soils in Britain (Hazelden *et al.* 1986). The soils of Elmley Marshes are classified as the Wallasea series, a non-calcareous clayey alluvial gleys (Fordham and Green 1980) overlain by a highly organic surface layer.

### 2.2.3 Ecology

Although the historic view of wet grasslands considered them as areas that could be put to better use though drainage and arable conversion leading to loss and fragmentation, wet grasslands are now becoming increasingly recognised as highly valuable habitats for plants, invertebrates, mammals and waterfowl. The juxtaposition of open water in the ditch systems, wet riparian fringes and drier areas all within the wet grassland form interlinked habitats that are extremely valuable for wildlife. Characteristic species found in these habitats have been listed by English Nature (1997). Typical grassland plants include marsh orchid, marsh marigold, marsh bedstraw, raged robin and meadow sweet. Garganey (*Anas quercuedula*), redshank (*Tringa totanus*), lapwing (*Vanellus vanellus*), snipe (*Gallinago gallinago*) and yellow wagtail (*Motacilla slava*) in addition to overwintering waterfowl are commonly supported. Within the ditch systems are wild parsnip (*Pastinaca sativa*), frogbit (*Hydrochairas morsusramae*), sharp leafed pondweed (*Potamogeton*

*acutifolius*) together with ramshorn snails (*Planor barius sp.*), diving beetles (*Dytiscus sp.*) and dragonflies (*Aeshna sp., Libellula sp.,* and *Sympetrum sp.*) can be found.

The ecological quality of the North Kent Marshes is reflected in the number of regional, national and international policy designations it holds.

> "These apply largely on the basis on its conservation value for breeding and overwintering waterfowl, but also due to the presence of locally and nationally scarce plant and invertebrate species assemblages. The North Kent Marshes has been classed as an area of Area of High Conservation Value which includes two National Nature Reserves, one Local Nature Reserve, five sites of Special Scientific Interest, three Kent Trust for Nature Conservation sites, and four RSPB reserves. In addition the Swale has been identified as a site of international importance by the Ramsar Convention on Wetlands and a Special Protection Area under the European Union Directive 79/409/EEC on the conservation of wild birds" (Briscoe, 1988).

One of the main underlying reasons for the ecological importance of the North Kent Marshes, is the presence of a salinity gradient in the ditches and grazing marsh. The salinity ranges from extremely saline to brackish creating a mosaic of microhabitats, all in close proximity.

> "The grazing marshes...exhibit much variety both in the salinity of the ditches, which ranges from fresh to strongly brackish, and in the topography of the fields, where dry sea walls and counterwalls contrast with damp runnels and depressions. Both species rich and species-poor grasslands are found here, with grazing mainly by sheep and cattle. A distinctive brackish flora occurs in the ditches which intersect the grazing marshes." IUCN (1987, p387).

Harpley (1999, p11-12) gives a description of the fauna and flora present on the Elmley Marshes.

> "The reserve is of great ornithological interest particularly for its large population of wintering and passage of wildfowl and waders amongst which white-fronted goose, widgeon and grey plover reach levels of national importance. The abundant breeding birds include mallard, coot, moorhen, lapwing, redshank, meadow pipit and skylark while nesting shoveler and pochard exceed 1% of the

British population. Raptors are particularly well represented, with marsh and hen harriers, merlin, kestrel, short-eared owl, barn owl and little owl regularly recorded.

"The invertebrate fauna of Elmley Marshes is also of national importance with flies, beetle, and bugs amongst the 31 uncommon species recorded. The abundant worms, insects, crustaceans and molluscs found in the wet fields, ditches, marshes and mudflats provide valuable food sources for the many birds using the varied habitats of the reserve. There is also evidence for the area to be a stronghold for water voles.

"The majority of the marshland is grazed by sheep and cattle, giving a short to medium length sward dominated by grasses such as brown bent (*Agrostis capillaris)*, red fescue (*Festuca rubra)*, perennial ryegrass (*Lolium perenn)e*, meadow barley (*Hordeum secalinum)*, and crested dog's-tail (*Cynosurus cristatus)*. Herbs such as white clover (*Trefolium repens)*, birds foot trefoil (*Lotus corniculatus)*, mouse eared chickweed (*Cerastium fontanum*), hairy buttercup (*Ranunculus sardous)* and hawkbits (*Leontodon spp.)* are frequent, particularly in the well grazed areas. The damper parts and temporary rills support a distinctive flora with marsh foxtail (*Alopecurus geniculatus*), salt marsh grasses (*Puccinellia spp.*) saltmarsh rush (*Juncus gerardi)* and lesser sea spurrey (*Spergularia marina)* typically present. Scarce plants include the divided sedge (*Carex divisa*), slender hare's ear (*Bupleurum tenuissum*), small goosefoot (*Chenopodium botryodes*), and annual beardgrass (*Polypogon monspeliensis*). Sea barley (*Hordeum marinum*), and sea clover (*Trifolium squamosum*), grow in the drier areas and on the sea walls.

"The ditch flora varies according to the salinity with the majority of ditches supporting brackish communities dominated by sea club-rush (*Scirpus maritimus*), fennel pondweed (*Potamogen pectinatus*), and the nationally scarce brackish water crowfoot (*Ranunculus baudotii*), and soft hornwort (*Ceratophyllum submersum*). Reed bed (*Phragmites australis*), has developed in a few places, and further inland the fresher ditches support a more diverse flora, with emergent species such as branched bur-reed (*Sparganium erectum*), lesser reedmace (*Typha angustifolia*), glaucous bulrush (*Schoenoplectus tabernaemontani*), common spikerush (*Eleocharis plustris*), water plantain (*Alisma plantago-aquatica*), and fool's water cress (*Apium nodiflorum*).

Botanical monitoring of 40 stands was undertaken by ADAS (1997) to determine the vegetation community according to the National Vegetation Classification (NVC) classification. Results indicated that stands surveyed were of mesotrophic grassland communities with a poor correlation to standard NVC communities. The predominant vegetation community of the marshes can be ascribed to MG6 (Lolium perenne/Cynosurus cristatus grassland), MG7 (Lolium perenne leys) and MG11 (Festuca rubra/Agrostis stoloifera/Potentilla anserina grassland). ADAS (1997, p33) state that "the grassland found on the North Kent grazing marsh is generally species poor when compared to other unimproved grassland communities but contains several local and national rarities. This grassland type appears to have been overlooked in much of the phytosociological literature but can be regarded as a distinct community specific to south-east England, with its distribution centred on the Thames estuary. The occurrence of this grassland, together with other nationally restricted plant communities found within the grazing marsh complex creates an extremely diverse habitat of high wildlife conservation value."

### 2.2.4 Management

Green (1971) highlights the need for sympathetic management of wet grassland areas to maintain their ecological quality and prevent further fragmentation and drainage. The increased value placed upon wet grassland areas have caused an increase in the number of management schemes and grants available which promote the maintenance and restoration of traditional low intensity grazing regimes though financial incentives or compensatory payments. The schemes include the Countryside Stewardship scheme, Wildlife Enhancement Scheme and the Environmentally Sensitive Area scheme.

The essential management operations in wet grassland environments to maximise habitats for waders and wildfowl involve the manipulation of water levels with constraints upon grazing density, mechanical operations and the application of fertilisers. This is reflected in the management prescriptions of the ESA scheme for the wet grassland areas of the Essex coast, Broads, Somerset Levels and Moors together with the North Kent Marshes.

Control of grazing density and restrictions upon the use of machinery over certain periods aims to prevent trampling of nests and chicks. Control of stocking levels can also allow the production of sward lengths of preferred height to target species (Figure 2.1). Water level management aims to control the position of the water table and degree of surface flooding through pumps, sluices or other water control structures (Figure 2.2). This is to ensure that the invertebrate prey of the waders remain close to the surface. The annual water level management regime of the wet grassland areas listed above all follow a common theme favoured by the target organism of breeding wildfowl and wintering waterfowl which does not also impair areas of botanical interest:

Typical water management regime is as follows (RSPB *et al.* 1997):

- 1 December to 31 March. Maintain ditch water levels at no less than mean field height to promote shallow surface water to cover over 30-60% of the site. This could be achieved by pumps or more sustainably by creating splashback channels. The objective is to attract winter waterfowl and waders and to develop the grassland conditions favoured by widgeons, Bewick's swans and lapwings. Partial flooding of the area is encouraged so that soil invertebrates are not totally destroyed by the anoxic flooded soil so as to provide a feeding source of the birds.
- 1 April to 30 April. Allow areas of surface flood to decrease to 20% by the end of this period. Some flooding is required to concentrate aquatic invertebrates into small pools to provide feeding sources. Maintain flooding to about 10% by the end of June. Areas of high botanical interest however should not remain flooded after April 1 to prevent deleterious effects upon the soil physical conditions and vegetation.
- 1 July to 30 November maintain water level in ditches to mean field levels or ensure there is a certain depth.

Management guidelines such as these above are common to areas of wet grassland ESA schemes, despite differences in soil type and water variability which would affect the success of obtaining the objective of high water tables and surface flooding through ditch water level control. It can be argued that there is a need for preliminary hydrological research in areas prior to being covered by agri-environment schemes.

Figure 2.1. Breeding habitat preferences of wet grassland birds. Source: RSPB *et al.* 1997.

Such research would further the understanding of the system and determine the best mechanisms for meeting desired objectives through hydrological ends so that the compensatory payments are not being misspent. Currently standard hydrological prescriptions being imposed to achieve political ends without prior research. Consequently unsustainable levels of success are achieved. In the case of the North Kent and the Essex Coast ESA, the original prescription to achieve wet grass conditions targeted the maintenance of high ditch water levels only. During the review of each scheme four years after initiation (ADAS 1997 and 1998 for North Kent and Essex respectively), the prescriptions were amended to include a component of surface flooding as described above, yet again decisions were not based on any hydrological information.

Wilson (1997, p304-305) identified six reasons behind the scarcity of research upon the ecological and environmental conservation impacts of all ESA schemes:

- The recent nature of the scheme has meant that long-term ecological monitoring of most of the prescriptions in the scheme has not been possible.
- The ESA scheme have become major political issues with increasing pressure upon government agencies to promote the scheme as a success, especially as more EU member states start to implement the scheme. To this end studies have focused on the socio-economic success of the scheme perhaps to the expense of more intangible results related to ecological monitoring.
- Only a few permanent monitoring plots have been established on farms within ESAs due to limited funds. As a result even if significant changes are observed, limited datasets make it difficult to generalise over larger areas.
- The permanent plots established require regular inspection and some farmers may not be interested in divulging information either due to the fear of losing payment in the case of the failure of the scheme, or the potential application of more constrictive restrictions such as a further reduction in stocking rates.
- Utility of remote sensed information is restricted due to the patchy and small scale coverage of areas under the scheme.
- A lack of faith in to the ecological knowledge of the farmers and managers of the land in ESAs due to the widely held notion that environmental management and monitoring of ecological change should be controlled by state related agencies. As a result farmer's knowledge has been neglected.

The Elmley Marshes are managed by the Elmley Conservation Trust and used as pasture but governed along lines suggested by Green in such a way to promote conservation objectives. The Trust has managed Elmley Marshes under an agreement with English Nature (formerly the National Conservancy Council, NCC) since 1987. The management prescriptions follow those of the ESA scheme that covers the area and the ECT try to further maximise habitat conditions through enhanced sympathetic grazing with sheep and cattle, and the creation of splashback channels and scrapes, generating a mosaic of different habitat areas in close proximity. The management regime has the objectives (Harpley 1999) to protect and manage sensitively the natural character of the North Kent Marshes, by maintaining the diverse fresh and brackish ditches, rills, seasonally flooded and dry grassland, ungrazed saltmarsh, tall

emergent vegetation, rough grassland and sea wall communities, all within the single expansive wild landscape unique to Elmley. This is to be undertaken principally of the benefit of wintering birds especially waders and wildfowl, breeding birds, especially the dry grassland and wader community, migrant birds, aquatic ditch edge and rill flora including rare species reliant on the salinity variation, and for dry grassland flora and fauna.

The success of the Elmley Conservation Trust is such that the Elmley National Natural Reserve was designated in May 1998; the first such designation given to an active farming estate accrediting that Elmley Marshes are managed in a uniquely sensitive way.

The ditches at Elmley are used as wet fences segmenting the marsh into a series of fields. At some point along its length each ditch is dammed to allow passage or access to adjacent field so that in essence the ditches are linear ponds. In order to regulate water levels, water control features are placed within the dam which consist of L-shaped piping connecting the two adjacent ditches (Figure 2.2). The ditch water level is controlled by the height of the pipe end, which is normally set to mean field height to comply with the ESA prescriptions, but can be lowered or raised for other management purposes when required. Figure 2.3 illustrates the network of dams and control structures managed by the Elmley Conservation Trust. The control structures also operate to distribute water about the ditch system using a number of 'main' ditches that feed water to and from smaller ditches enabling a certain amount of 'flushing' to be achieved (Figure 2.4).

Further to this, water is pumped onto the surface at some areas of marsh and artificial scrapes and small channels or rills have been created to induce water to flow onto the fields at times of high ditch stage. This is necessary as when the ditches are cleared of silt, the dredgings are placed on the ditch edges creating a saucer effect where the field interior is lower than the ditch edge. By cutting channels or breaches through these mounds water can flow onto the marsh at stage levels lower than those necessary if mounds had no breaches. The channels are engineered so that they allow water to flow onto the marsh at stage levels equal to mean field height.

The study field chosen for this investigation has an overall saucer shape alongside three ditches but possesses relict saltmarsh channels and rills that allow the flow of

water onto the marsh when the ditch stage exceeds their elevation. Figure 5.10 shows these rills in planimetric form, with Figure 1.3 providing an aerial view. Enhanced banks feature on the west and east ditches while the south ditch has a particularly visible rill structure stretching inland.

### 2.2.5 Loss of wet grasslands

The loss of wet grasslands in the UK has been attributed to many factors including the changes in agricultural practises, improvements in land drainage and sea defence practices, water abstraction, industrial development and fragmentation and isolation of sites. The dominant forces causing the loss of wet grasslands are attributed to UK and EC agricultural policies (RSPB *et al.* 1997), which encouraged the conversion of grassland areas to arable crop production. These policies included the post-war moves to ensure self-sufficiency for food supplies, together with Britain's entry into the European Economic Union and the adoption of the Common Agricultural Policy (CAP) which favoured grain production over meat by offering considerable grants for drainage.

Fuller (1987) reports that in England and Wales, the total area of wet grassland has declined from 7.8 million hectares in 1937 to 4.8 million hectares in 1987; a loss of 39% over this period. Only 0.6 million ha of semi-natural and rough grazing grasslands remain in England and Wales, which comprise 11% of the current grassland area and only 3% of the extent in 1939.

The NCC (1984) claim that "overall the various studies suggest that the extent of grazing marsh in eastern and southern England is likely to have declined by about 50% in the last 50 years. This is comparable with the losses recorded for most other major habitats in lowland Britain during approximately the same period." The current estimate of the extent of wet grasslands remaining in England and Wales is in the order of 220,000 ha, but much is agriculturally improved and therefore of reduced ecological value; only 20,000 ha are thought to be of unimproved grassland of high conservation value (RSPB *et al.* 1997, English Nature 1997).

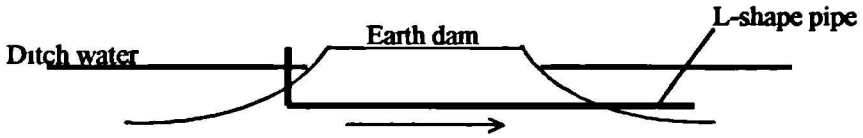


Figure 2.2. Water level control structure employed at Elmley Marsh. The photograph above shows a flexi-pipe employed to maintain water at mean field height. The plan representation illustrates how the L-shaped pipes extend through the dam with the upstream one end at mean field height, set at the upstream direction, and the other end located beneath the normal summer water level. The arrow shows the direction of flow.

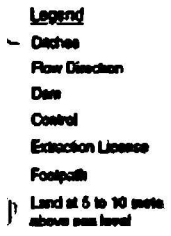


Figure 2.3. The network of ditches, dams, control structures and direction of flow over the Elmley Conservation Trust Estate. Source: Tod Reid.

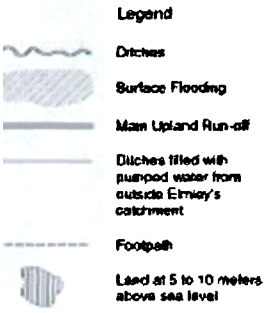


Figure 2.4. The distribution of natural surface flooding and location of main ditches of the Elmley Conservation Trust Estate. The study field is located at grid point 949681 where it can be seen that the ditch to the north regularly floods along its edge. Source: Tod Reid.

Thornton and Kite (1990) undertook an investigation into the rate of loss in the Thames estuary between 1939 and 1989. The Thames estuary forms an ecological unit with the Medway and Swale estuaries (Green 1971); this includes the Thameside marshes in addition to those in Essex and North Kent. Their results indicate an overall decline in the areal extent of grazing marsh of 70% (Table 2.1). The rates of loss experienced in the Thames estuary is reflected elsewhere, with the loss of 48% in Romney Marsh and 37% in the Norfolk and Suffolk Broads (English Nature 1997).

Table 2.1. Extent and loss of the grazing marshes in the London, Essex and Kent area. Source: Thornton and Kite (1990).

| Area | Original extent in 1939 ha | Area in 1989 ha | Marsh remaining as % of 1935 |
|---|---|---|---|
| London | 2767 | 415 | 15 |
| Essex | 5614 | 1538 | 27 |
| Kent | 4899 | 2634 | 54 |
| Total | 13280 | 4587 | 70 |

Thornton and Kite (1990) report that the once extensive tracts of marsh in the Thames estuary have become increasingly fragmented with 65 separate areas of grazing marsh remaining from a once continuous stretch. In 1989 two thirds of sites were less than 25 ha in size with only nine of 100 ha, but that these nine sites comprise 80% of the present expanse of grazing marsh.

Fragmentation of wet grasslands through drainage can threaten their survival, particularly those areas that juxtapose drained arable fields (Williams and Hall 1987, ADAS 1997). This is due to "the lowered water tables of the drained areas [which] reduces the propensity to flooding of the undrained marshes" (Oliver 1991, p42). Small sites are also less able to withstand pressure from pollution (including thistle invasion) and disturbance by public access, thus making such sites harder to conserve. Discussing the Thames estuary, Thornton and Kite (1990, p27) state that "the continued use of the marshes by birds and other species requiring large tracts of marsh depend on the maintenance of suitable habitats within and outside this system. If the decline of this habitat continues, the integrity of this ecological unit and its ability to support internationally significant population and wildfowl and waders is threatened."

ADAS (1997, p47) discuss the effects of the decline in extent of wet grassland on the hydrology of the North Kent Marshes, however the situation is true for all areas of wet grassland that have suffered fragmentation:

> "The consequences of such a shift from permanent pasture to arable and agriculture to urban have been very serious for the flora, fauna, landscape and historical interest of the North Kent Marshes. The once continuous areas of grazing marsh have been fragmented into smaller blocks, separated by either urban development or drained, levelled and improved grassland and arable land. Such fragmentation leads to a much greater edge effect...and may also result in the habitat falling below the minimum critical size to support those species occurring within it. The conversion of grazing marsh to arable involves underdrainage and in many cases levelling of the land. Such actions destroy the two key features of semi-natural grazing marsh that contributes to the mosaic of conditions typical of this habitat and the character of the landscape: the retention of surface water in winter and the relict saltmarsh topography. For underdrainage to be successful, the ditches into which the drains feed, need to be deepened to act

as efficient water carriers. Such improvements result in a loss of habitat for many aquatic plant ands invertebrate species, and the run off from agricultural chemicals compounds the problems for those species which remain."

Thornton and Kite's report shows that North Kent now holds the relative majority (54%) of remaining grazing marsh in the south-east of England. The North Kent Marshes differ from those in Essex and others in south and east England in terms of the dates of loss, which in turn indicates conversions to different land uses (Williams and Hall 1987). As discussed earlier, the financial benefits of arable conversion resulted in 70% of the original marsh extent being lost to this land use. While most of the change in the London and Essex Marshes occurred before 1968, the majority of land use transformation in North Kent happened after this date. This is probably due to the late construction of reliable flood defences that allowed North Kent to escape the post war agricultural intensification. After improvements in the sea defences the marshes were ditched to lower the groundwater levels (MAFF 1962). This gave farmers the confidence to plough closer to the sea wall, and underdrainage and field amalgamation started after 1965/6 (Hazelden *et al.* 1986) and continued into the 1980s (TEP 1996). The salt affected nature of the marsh soils however has meant that many drainage schemes have been unsuccessful (Marks and Robins 1986).
The rate of decline slowed during the 1970s but the average national estimate of loss was still in the order of 8000 ha (Carter 1982). It is reported that the area of grazing marsh in Kent has not changed substantially since the late 1980s but there remains a continuing nationwide downward trend in the extent of grazing marsh (Thornton and Kite 1990). Fortunately the reductions for arable production under CAP in 1987 together with the launch of set aside program in 1988 reduced pressure on the grazing marshes and by 1989 49% of the grazing marsh was designated SSSI status (Thornton and Kite 1990). In 1993 the North Kent Marshes was declared an Environmentally Sensitive Area (MAFF 1994).

Green (1971) stated the need for economic subsidisation to enable the continued use of the North Kent Marshes for traditional grazing regimes in the face of financial inducements to drain the land such as availability of grants and the high return of arable production. It was due to such views that the ESA scheme was developed.

> "It is the relationship between traditional grazing regimes and the high conservation value of the land that underlines the importance of continuing traditional agricultural practices over large blocks of land to maintain the wildlife interests of the area." (Green 1971, p30).

English Nature (1997, p44) corroborate Green by stating that:

> "Unless conservation measures to retain wet grassland are in place – with emphasis on the maintenance of the water levels, flooding regimes and appropriate grazing and cutting - most sites will deteriorate. The conversion to grassland to arable has put pressures on wetland wildlife, as ditches have been over-deepened and water levels lowered, and used for spray irrigation. The plants and invertebrates of ditches require a high and relatively stable water level".

### 2.2.6 Future threats

Although the rate of wet grassland loss has declined over recent years, with schemes in place to offer financial incentives for traditional management, the threat of further loss arises from the economic pressures upon pastoral farmers, the demand for land for housing and industry and sea level rise. These factors are applicable to most if not all wet grassland areas in the UK.

#### 2.2.6.1 Agricultural collapse and industrial pressure

A number of factors have combined to bring about a significant reduction in the profitability of pastoral agriculture within the UK. The main factors include the strength of sterling; the BSE crisis with the associated Over Thirty Months Scheme and beef export ban; and deregulation of the milk market.

The financial losses experienced by pastoral farmers in light of these factors have been severe (FRCA 1997). It is expected that farmers may try to minimise losses by increasing sheep numbers or possibly conversion to arable cultivation on suitable land. Alternatively, tracts of land could be used for non-agricultural purposes that may be incompatible with environmentally sensitive management. For others, adoption of land into ecologically sensitive management schemes may enable them to stay in farming.

2.2.6.2 Sea level rise

> "Britain will lose many areas of coastal associated freshwater wetland as sea levels rise...some have been partly drained for agriculture while others form nature reserves of international importance. The costs of raising embankments or installing flood barriers will not be justifiable based on the agricultural benefits likely to be attained. It is thus likely that former coastal wetlands will be converted to shallow seas having marginal or more extensive salt marsh. It is not possible to be precise about which wetland areas will be lost, because of the present imprecision in values of predicted sea level rise. A traditional grazing regime with a pleasing interlink between agriculture and conservation will be lost, but in general there will major conservation gains [through the development of saltmarsh]." Moss (1992, p52).

The long term effects of sea level rise from the coupled effects of thermal expansion and the melting of glaciers and ice sheets, could result in an increase of sea level between 15 and 95 mm by 2100 by the IPCC (1995) using 'low' and 'high' climate and ice-melt sensitivities respectively. Further to this effect, is the crustal downwarping of south-east Britain estimated at 1.9 mm $yr^{-1}$ (Shennan 1989), due to the release of glacio-isostatic pressure following the last interglacial period.

For coastal marshes such as those in North Kent and Essex, it is the presence of sea walls that will influence the outcome of a future scenario of a sea level rise of 0.5m (Boorman 1992).

> "A key factor in the impact of any rise in sea level is what lies inland of existing salt marshes. If the hinterland is low and sloping and there are no sea defences or natural barrier, a rise in sea level will result in increased erosion along the sea ward margin. This will mobilise sediments and allow further marsh development at higher levels. The rise in sea level means that the sea reaches further inland allowing the saltmarsh to extend landwards. The overall effect will be that the marsh will migrate landwards at a level corresponding the new sea level, but with its internal structure and vegetation more or less unchanged...however in Britain saltmarshes are mostly backed by low-lying areas of reclaimed marsh protected

by a sea wall. The sea wall is crucial in determining the fate of the saltmarsh when sea level rises. The sea wall, while its position remains unchanged will prevent the landward migration of the saltmarsh...Salt marshes can be regenerated by moving the sea walls landwards and allowing reclaimed land to revert to saltmarsh. " Boorman (1992, p14).

The problem for the marshes of North Kent and Essex is that the land inside the sea wall is lower lying than the saltmarsh and so would suffer from inundation, but the presence of the sea walls would enable only gradual saltmarsh development (Boorman 1992). The RSPB (1992) claim that a 0.8m rise in sea level in the Essex Marshes would lead to a 20% loss of intertidal flats; a rise of one metre would result in a 30 - 50% loss. The North Kent Marshes are considered to be under greater threat than the Essex Marshes due to the greater amount of 'low' marsh and its associated vegetation but there is a 'lack [of] detailed information about the Kent Marshes' (Boorman 1992, p19).

The National Rivers Authority (1991) declared that MAFF will only fund the strengthening of defences if it is cost effective. The Department of the Environment policy (1992) for coastal planning is such that "in low lying undeveloped coastal areas, options for coastal planning may include a policy of managed defence. In such areas, it should not be presumed that it would be economically justified to maintain existing coastal defences. Planing policies should take this into account".

In view of these statements, the North Kent Marshes may not be declared cost-effective in which case a programme of managed retreat as described by Boorman (1992) may be initiated resulting in the invasion by the sea into areas of grazing marsh. As there is limited space for the landward migration of the grazing marshes, sea level rise could result in a further loss and fragmentation of the current expanse of North Kent Marshes.

# Chapter 3 Ditch water: soil water relationships. Part 1 Soil Characteristics

This chapter discusses the objective and methodology required to address Research Question 1: *What is the relationship between ditch water levels and the water table and soil moisture in the adjacent field?* The research approach and necessary data are described. Chapters 3 - 5 present the research results and analysis for this investigation. A review is presented of the concepts and fundamental processes of water flow in the saturated and unsaturated zones, and methods to determine the hydraulic conductivity and soil moisture characteristic curve salient to the research of this chapter. Appendix A contains details pertinent to this chapter relating to the principles of operation of the neutron scattering probe (section A.5), ThetaProbe and Equitensiometer (section A.7) together with the results of calibration of the instruments to the soil of the study site.

Research results include:

- Soil characteristics (sections 3.3.1.1 – 3.3.1.1.5): particle size, bulk and particle density, organic content and porosity.
- Soil and ditch water electrical conductivity and effects of difference in density (sections 3.3.1.6 – 3.3.1.9).
- Measurement of the hydraulic conductivity and infiltration with the Bouwer and Rice approach (section 3.3.2.1) and the Guelph permeameter (section 3.3.2.2).
- Derivation of the soil moisture characteristic curve employing the Gupta and Larson approach (section 3.3.3.1), pressure plate apparatus (section 3.3.3.2), coupling of a tensiometer and neutron scattering (section 3.3.3.3), and the ThetaProbe and Equitensiometer in the surface soil (section 3.3.3.4).

Chapter 4 presents the results of monitoring the water table and ditch stage and modelling performed to quantify and predict the relationship between ditch water levels and the position of the water table, and recharge fluxes. Chapter 5 details moisture monitoring of the soil profile and the results of soil moisture modelling together with an investigation into the spatial and temporal change in surface soil moisture.

## 3.1 Introduction and justification of the research programme

The justification of this investigation is to assess the MAFF North Kent Marshes Environmental Sensitive Area (ESA) scheme that covers the study site. The common factor linking the 22 existing ESAs in England is that they are all areas of 'landscape, wildlife and historic interest of national importance and dependant upon the use of beneficial farming practises' (Agricultural Development Advisory Service (ADAS) 1997). Through compensatory payments made to farmers who uptake any part of the ESA scheme (the scheme is voluntary and lasts for ten years with an option of termination after five) it is hoped the designation will help to preserve the environmental interest of the specified areas. A research programme is established in each ESA based on a national monitoring strategy (ADAS 1997) to assess whether or not the objectives of the scheme are being met.

The North Kent Marshes ESA, an area of 13,715 ha, was designated in 1993 to safeguard the remaining marshes from the continual threat of agricultural intensification and industrial development (ADAS 1997). The monitoring programme initiated in the North Kent Marshes was developed by ADAS and MAFF and implemented by the former.

It involved (ADAS 1997):

- Land Cover. Aerial photography was used to describe the extent and distribution of the various classes of land cover in 1993 at the start of the scheme and three years later in 1996.
- Historical Features. An inventory of features within the ESA was undertaken and an assessment of how landuse change may affect them.
- Vegetation. A botanical study undertaken in 1993 to describe the grassland communities on the grazing marshes. A ditch vegetation survey undertaken in 1994 on land entered into agreement with Tier 1a (Tier structure described below).
- Ornithological interest. Counts of wintering and breeding birds in a sample section of the ESA in 1993 and a re-survey in 1996 to assess change.
- Linear and point features. A ground survey was taken within a sample of the ESA in 1993 to describe specific features and a re-survey undertaken in 1996.

There are a number of specified environmental objectives and performance criteria for each ESA; those of the North Kent Marshes ESA involve four objectives structured into a three-tier system. Of particular interest to this project is Objective 2:

> "Objective 2: To maintain and enhance the wildlife conservation value of grazing marsh without detriment to the landscape by maintaining high water levels in ditches and dykes" MAFF (1994).

Open water channels are a characteristic feature of the landscape; "an intricate network of sinuous and straight ditches traditionally formed wet fences which subdivided the flat and open land of the exposed grazing marsh and sheltered grazing marsh into grazing fields, delineated land ownership and helped to drain the land" ADAS (1997 p37). The Wet Grassland Tier of the scheme, Tier 1a, focuses on the traditional use of ditches and dykes to act as wet fences and provide drinking water for stock, prescribing high water levels to maximise wildlife conditions by creating suitable habitats. Participating farmers receive an annual payment of £165 per ha (MAFF 1994). "The underlying aim is to manipulate the water environment in such a way as to create moist, soft ground conditions together with areas of standing water, at these times of year critical to feeding and breeding success particularly of waders. Tier 1a was included into the ESA scheme specifically to promote this objective" (FRCA 1997 p12). The management prescriptions for Tier 1a (MAFF 1994) are as follows:

> During the period 1 December to 30 April maintain water levels in ditches at not less than mean field level so as to create shallow pools and do not let water out of the ditches and dykes until this has been achieved except under flood warning conditions. Provide at least 30 cm of water in the bottoms of ditches and dykes from 1 May until 30 November.

The objective of the management prescriptions is to use ditches as irrigation channels rather than for land drainage i.e. to recharge the water table in the middle of the surrounding parcels of land by high ditch water levels to maximise conditions for wildlife. This follows the reversal of classic drainage theory that while the ditches were originally dug to drain land, they can be harnessed for conservation purposes as irrigation channels to saturate the soil. The assumption in the Tier 1a prescription is that seepage from the ditches into the surrounding parcels of land maintains water tables giving rise to high soil moisture. High soil moisture levels create soft

penetrable soil conditions and therefore optimal habitat creation. In a field bordered by ditches, such as the study site at Elmley, maintaining higher water levels in the ditches than the marshland water table can create a hydraulic head. Water movement is initiated in the direction of the hydraulic gradient, and the ditch acts to irrigate the land.

The creation of soft moist ground conditions from the manipulation of the ditch water levels is to increase the penetrability of the soil for feeding waterfowl. A study of snipe by Green (1988) and Green *et al.* (1990) showed that the penetrability of the surface of grassland meadows, in which the birds feed, influenced the duration of their breeding season and that this in turn was influential upon the breeding success. The mechanism of this effect was identified as damp penetrable surface soil allowing snipe to probe the surface soil and feed upon soil invertebrates particularly earthworms that would be present but not available to the birds if the soil dried out becoming impenetrable. Penetrable soil throughout the summer permits extended breeding times through increased availability of food. The results of the investigation revealed that both invertebrate density and penetrability of the soil influenced the birds' feeding patterns, and the degree of surface flooding influenced their diet. In times of surface flooding snipe fed upon insect larvae and snails upon ditch edges compared to earthworms from meadows at periods of no surface flooding. While earthworms are the preferred diet of snipe, surface flooding leads to a reduction in earthworm density in the soil due to the anoxic conditions. Green *et al.* (1990) conclude that due to the deleterious effects upon earthworms of surface flooding, the optimal habitat conditions would be best created through the maintenance of high water tables. An enhanced habitat for snipe would be that of a network of ditches and varied surface topography providing abundant damp penetrable areas even when the water table is low. These results are also applicable to other waterfowl as illustrated in Figure 2.1.

From the description of the North Kent Marshes ESA management prescriptions above it is clear that there is an assumption of a direct relationship between field moisture conditions and ditch water levels. The marshes have a clay substrate however and considering the low permeability of such soils the basic hydrological

view must be *that there is little water movement through the soil and that the drainage and recharge function of the ditches is limited in a spatial extent.* This has implications for the effectiveness of the Wet Grassland prescriptions. Studies of the manipulation of the marsh water table through ditch water level control have been undertaken in other wet grassland areas covered by similar ESA prescriptions (Armstrong 1993, Armstrong and Rose 1998, Youngs *et al.* 1991 Youngs *et al.* 1989, Towner and Youngs 1986, Youngs 1990), and other wetland sites (Burke 1961, Boelter 1972, Nicholson *et al.* 1989, Gilman 1994). These studies show that the magnitude of water table control is predominantly affected by the hydraulic conductivity of the soil, and that even at sites with high hydraulic conductivity there is a maximum spatial influence of the ditch. The Somerset levels and Moors were investigated by Youngs *et al.* (1991) where it was found that the water levels within fields could be manipulated using this approach. This is of particular interest as management prescriptions of the ESA scheme covering the wet grassland areas of the Essex coast, Broads, Somerset Levels and Moors together with the North Kent marshes are near identical. As the Somerset Levels and Moors was one of the first ESA designations, the success of the prescriptions at this peat-based site was the basis of transferring the prescriptions to other areas. However the differences in soil type and hydrological regime at each site are likely to result in different levels of success when such a blanket approach is applied. The optimal arrangement should be that each ESA has management prescriptions particular to the physical conditions of the area, tailored specially to achieve set objectives based on prior environmental monitoring.

In the clay-based areas of North Kent Marshes and Essex Coast ESAs, the original prescription to achieve wet grass conditions targeted the maintenance of high ditch water levels only. During the review of each scheme four years after initiation (ADAS 1997 and 1998 for North Kent and Essex respectively), the prescriptions were amended to include a component of surface flooding, yet again decisions were not based on any hydrological information. The review of the North Kent Marshes ESA scheme was undertaken to assess its mid-term performance. The report by ADAS (1997, p.v) 'presents interim results of a longer-term monitoring program and gives an early evaluation of the impact of the scheme'.

At the start of the scheme 89% of the ESA was under agricultural management; 45%

of which was managed as semi-natural grazing. A further 35% was in arable production, with 8% accounting for improved grassland. Initial results have been described as 'mostly very positive' (FRCA 1997, p5), showing a maintenance of the baseline conditions of environmental factors surveyed at the start of the scheme. Results of interest to this research include:

- 67 agreements are in place representing 3400 ha of grassland. Together with land entered into the precursor of the ESA scheme, grassland management agreements with English Nature this means that over 80% of the grassland is under environmental management. 43% of the environmentally important semi natural grazing marsh is under agreement.
- 600 ha under agreement at Tier 1a. Compared to the target goal of 1200 ha this was considered to be a low take up. It was declared that there was insufficient evidence to assess whether Objective 2 had been met.

The Farming and Rural Consultative Agency, FRCA, (formerly ADAS) (1997) produced a further document with proposals for the future of the ESA for the years 1998-2003 based on results from the ADAS report (1997). Relating to Tier 1a the organisation comments that:

> "A better understanding of water relationships on the marshes is needed and the continuing drought has highlighted the need to re-appraise Tier 1a. There is a consensus that objectives must be re-set in the light of the existing and growing constraints in terms of water resources' ADAS (1997, p 6).

*However there is no monitoring programme associated with the ESA to assess the influence of Tier 1a such as the regular recording of stage and groundwater levels and the spatial extent of surface flooding.*

This is surprising as Swetnam *et al.* (1998) state the importance given by MAFF to the success of ESA schemes and ensuring that the original management guidelines were appropriate to the site, as ESA management prescriptions are not tailored to match the circumstances of specific sites. Value for money is deemed important so that a reasonable return is made of the investment of public money through the reaching of objectives (Swetnam *et al.* 1998). However, the scarcity of research upon

the ecological and environmental conservation impacts of ESA schemes has been noted by Wilson (1997) (section 2.2.4).

The FRCA proposed a change to the Tier structure to create Tier 1b specifying a certain proportion of surface flooding. This represents a 'significant evolution of the scheme' (FRCA 1997, p12) to a more targeted approach rather than the current blanket prescription. Those areas under Tier 1a agreement that have been successful in meeting the objectives of Objective 2 are identified by the FRCA as conforming to the following criteria:

- areas of spring activity
- areas under a regime of pumping or water storage reservoirs with abstraction licenses
- low lying marsh areas which are naturally susceptible to flooded conditions

In areas where these factors are absent it is thought that further achievement of the objectives of Tier 1a seem improbable. The modified approach, Tier 1b with payment of £150 per ha, is specifically aimed at encouraging breeding waders and would be subject only to those areas (FRCA 1997, p13):

- With the potential of attracting breeding waders
- With sufficient volume of water to allow ditchfull conditions and surface ponding during March to May (it is acknowledged that pumping is probably necessary)
- Where high water levels would not exclude species such as the Water Vole
- Where the agreement holder would agree a more specific grazing regime involving exclusion of stock (principally cattle) during March to Jane and more intensive grazing in autumn to condition the grass sward

Land entered into Tier 1b must follow the guidelines (FRCA 1997, p15):

- shallow (up to 0.2 m) surface water over at least 20% of the area from 1 December to 31 March
- shallow surface water over at least 15% of the site during April
- shallow surface water over 10% of the site to the end of May
- at least 300 mm depth of water in ditches during the summer and autumn months

### 3.1.1 Research approach

In this investigation an appraisal will be made of the success of the Wet Grassland prescriptions in maintaining high soil moisture levels by manipulation of the water levels in ditches. In the case of the North Kent ESA no hydrological monitoring or investigation has been undertaken by the regulatory authorities to see if the effects of ditch water level management have met the desired objective of soft moist ground conditions. It is argued that there is a need for preliminary hydrological research, and basic monitoring schemes should be set in place before the initiation of any such schemes. This is imperative to further hydrological understanding of the site, and ensures that the best mechanisms for meeting desired objectives through hydrological ends are being implemented, so compensatory payments are being used wisely.

The approach outlined in Table 1.1 (reproduced in part as Table 3.1) is that followed to address Research Question 1: *What is the relationship between ditch water levels and the water table and soil moisture in the adjacent field?* The results generated by this research programme are considerable and span three chapters. Final analysis is presented in Chapter 5.

## 3.2 Discussion of concepts and fundamental processes

It is necessary to briefly review the mechanisms of water flow in the saturated and unsaturated zone, in addition to the methods available to monitor and determine the hydrological parameters pertinent to this study.

### 3.2.1 Water flow in the saturated and unsaturated zone

Through experiments on water flow in saturated columns of sand Darcy (1856) established the law that founds the basis of water movement in a saturated medium (Youngs 1988, Ward and Robinson 1990):

$$V = -K\left(\frac{\partial h}{\partial l}\right) \qquad \text{Equation 3.1}$$

Where:
V is the macroscopic flow velocity of the groundwater (units of velocity)

K is the hydraulic conductivity (units of velocity)

$\frac{\partial h}{\partial l}$ is the hydraulic gradient, comprising the change in hydraulic head with distance along the direction of flow (units of length)

The negative sign indicates flow in the direction of decreasing head. Flow reduces to zero under the absence of a hydraulic gradient.

Darcy's law describes steady macroscopic flow in a confined isotropic medium. Soil is a complex medium comprising pore spaces of variable size, shape, direction and degree of connectivity. Water flow is constricted by these factors resulting in highly variable microscopic flow patterns. The complicated nature of the microscopic water flow in soil leads to the use of macroscopic flow terms which comprise the overall average of the microscopic flow velocities over the total volume considered such as Darcy's law (Hillel 1971, 1998).

Table 3.1. The logistical framework diagram for Research Question 1: What is the relationship between ditch water levels and the water table and soil moisture in the adjacent field?

| **Research Question 1:** ***What is the relationship between ditch water level and the water table and soil moisture in the adjacent field?*** | |
|---|---|
| Justification | Basis of the ESA prescription implying seepage from ditches maintains high water tables and soft moist ground conditions. Research findings will promote a better understanding of the hydrological processes aiding more effective management. |
| Approach | Characterise the soil hydraulic parameters including the electrical conductivity of the marsh soil and ditch water. Relate the change in ditch water level to changes in the water table and soil moisture of the study field, and determine rates of water movement in the saturated and unsaturated zones to assess the spatial extent of the seepage from ditches. |
| Data | A Ditch water levels and water table over time and space<br>B Soil moisture over space, depth and time<br>C Precipitation and evaporation<br>D Soil characteristics; texture, structure, organic fraction, bulk density, porosity, salinity, hydraulic conductivity, soil moisture characteristic |
| Equipment | A Stageboards and piezometers<br>B Neutron scattering for depth measurements and Surface Capacitance Insertion Probe (SCIP) for spatial investigation, electrical resistance blocks (ERB) and gravimetric sampling for long-term measurements<br>C Automatic Weather Station<br>C Lab facilities, field electrical conductivity probe |
| Analysis | The DITCH model allows the prediction the movement of water between ditches and surrounding fields to examine the consequence of various ditch management regimes. The BUDGET model can simulate the change in soil moisture through the data input and of precipitation and evaporation respectively only. |

Youngs (1988) reports that by the end of the nineteenth century Darcy's law had been applied to estimate groundwater movement in shallow aquifers. In shallow unconfined systems where horizontal flow dominates due to the existence of vertical equipotentials, the Dupuit-Forchheimer assumption can be used with little error to estimate flow. The assumptions of the theory state that in a system of gravity flow toward a sink, such as a drainage ditch, all flow is horizontal in direction and that the hydraulic gradient at each point is proportional to the slope of the water table but independent of depth. It is assumed that the water table is drawn down to the water level in the sink and any existence of a seepage face is ignored (Youngs 1990). Although care has to be used in the application of the Dupuit-Forchheimer theory it does allow for an approximation of the height of the water table and has been widely used. The assumptions are most valid where the flow region is of greater horizontal extent than depth. Investigations into the error of Dupuit-Forchheimer solutions have been undertaken by Youngs (1990) and Kirkham (1967) who conclude that for most soils the results of employing the assumptions generate only approximations but exact answers can be gained in soils with infinite vertical hydraulic conductivity. Youngs (1965) has examined systems that have a variation in hydraulic conductivity with depth, but uniform in a horizontal plane. The application of Dupuit Forchheimer analysis yields a good approximation in those soils that exhibit an increase in hydraulic conductivity with depth but not for the reverse situation of a decrease in hydraulic conductivity with depth. Youngs *et al.* (1991) successfully employed Dupuit Forchheimer theory to model the water table of fields intersected by ditches in the Somerset Levels.

Boussinesq (1904) introduced the concept of the specific yield as the ratio of the volume of water, soil or rock will yield by gravity drainage to the volume of soil/rock. It can also be stated as the ratio of drainage flux to rate of fall of the water table, or drainable porosity. The specific yield has a negative relationship with texture becoming smaller with decreasing grain size and hence pore size between grains. Hillel (1998) issues the caveat however that the concept of a 'drainable porosity' which releases water instantaneously when the water table falls is a gross approximation, as water drainage occurs gradually with the increasing suction that accompanies the descent of the water table. The specific yield is a useful concept

however and is successfully employed in the DITCH model (Armstrong 2000, 1993, Armstrong and Rose 1998) used in this investigation (section 4.3).

Richards (1931) extended Darcy's law through application to unsaturated flow assuming hydraulic conductivity to be dependant upon the matric suction head (in turn based on the soil moisture) incorporating the energy concept introduced by Buckingham (1907). Combination with the continuity equation for water gives the transport equation for water flow in unsaturated soil (Youngs 1988). The continuity equation (mass conservation law) states that if the water input (source) is greater than that of the output (sink) the excess must be stored in the soil. Similarly if output exceeds input, the soil moisture must decrease over time (Hillel 1998, Feddes *et al.* 1988). For one-dimensional flow in the vertical direction:

$$\frac{\partial \theta}{\partial t} = \frac{\partial}{\partial z} K\psi \left( \frac{\partial \psi}{\partial z} + 1 \right) \qquad \text{Equation 3.2}$$

Where:
$\theta$ is soil moisture
$t$ is the time interval
$\psi$ is the pressure head
$z$ is the elevation above a reference datum.

The Richards equation assumes flow to occur as in a continuum i.e. that changes in soil moisture take place smoothly. In reality water flow is characterised by jerky microscopic flow due to the influence of the soil pore structure and air movement. Despite these assumptions and the difficulty in solving Richards equation due to the non-linear dependence of K and $\theta$ on the soil water content it remains the basic flow expression underlying unsaturated flow phenomenon (Feddes *et al.* 1988). Information regarding the soil moisture characteristic curve and its relationship with hydraulic conductivity is required to solve the equation.

### 3.2.2 Hydraulic conductivity

Fundamental to both saturated and unsaturated is the hydraulic conductivity, K, the rate of water movement through the soil. The hydraulic conductivity depends upon texture and structure, degree of saturation, tortuosity of the pore system and size of

the water filled pores (Rowell 1994). The value of K also depends upon the soil water content; at saturation, K is at maximal velocity with the rate of flow decreasing rapidly with a decrease in moisture content. This is due to flow taking place only through water films; at saturation all pores have a large water surface area allowing maximum velocity. As soil moisture declines pore spaces drain of water reducing the effective cross sectional available for flow. The greater the decline in soil moisture the greater the decrease in hydraulic conductivity due to the reduction of water filled pore spaces available to conduct water. This rate of change is non-linear however and is based upon the geometry and distribution of pore spaces and retention ability of the soil.

The tortuosity of the pore system increases with soil moisture decline accompanied by a decrease in the connectivity of the pores. These factors act to lower the hydraulic conductivity. At saturation, soils with coarse textures and low retention capabilities such as sand will exhibit higher values of K than fine-grained highly retentive soils such as clay. However due to the higher K and lower retention, the sandy soil will dry out faster than the clay soil, and a crossover point will be reached with continued drying, when the clay soil has a higher hydraulic conductivity compared to the sand due to its greater proportion of water filled pores.

The hydraulic conductivity of a soil can either be measured in the laboratory or using field methods. Laboratory methods include both falling and constant head design permeameters, saturating an undisturbed core sample of the soil, or a sieved and packed soil sample and measuring the steady outflow of water. This is hardly representative of field conditions however due to the very small sample used, problem of compaction, or smearing, and the difficulty of relating small-scale results to field processes.

In addition to infiltration tests at the surface using cylindrical rings, field measurement of hydraulic conductivity can be separated into saturated and unsaturated methods. Methods in saturated soil, i.e. below the water table, include pumping tests in networks or solitary piezometers or monitoring wells. A volume of water is removed or added and the rate of change of the water level measured over time. The calculation of hydraulic conductivity from such slug tests is based on the steady state response of water rise rates; the Thies equation for steady state flow to a

well (Fetter 1994). Many such tests exist and are attractive due to the small amount of equipment and effort involved.

3.2.2.1 The Bouwer and Rice test

Bouwer and Rice (1976, 1989, Bouwer 1996) and Hvorslev (1951) both present methodologies for slug tests in unconfined aquifers using piezometers or boreholes located below the water table. Slug tests are based on an analysis of the curve y(t), where y is distance from the current position of the water level at time t in a well or piezometer to the static water level (Zlotnik 1994). The Bouwer and Rice model resembles the Hvorslev model but with a difference in the shape factor, to include the effective radius, Re, over which the hydraulic difference generated by the abstraction of water is dissipated (Mas-Pla *et al.* 1997). An investigation into the performance of the two tests by Fetter (1985) revealed comparable results by both the Bouwer and Rice and Hvorslev methods.

The Bouwer and Rice test was employed to determine the saturated hydraulic conductivity of the study site (section 3.3.2.1). The Bouwer and Rice test was applied using piezometers that contained a pressure transducer logging at regular intervals to monitor the change in head (section A.4). The Bouwer and Rice test can be summarised as:

$$K = \frac{r_c^2 \ln\left(\frac{R_e}{R}\right)}{2L_e} \frac{1}{t} \ln\left(\frac{H_0}{H_t}\right) \qquad \text{Equation 3.3}$$

Where:
$K$ is the hydraulic conductivity cm $hr^{-1}$
$r_c$ is the radius of the well casing cm
$R$ is the radius of the gravel envelope cm
$R_e$ is the effective radial distance over which head is dissipated; this is also the distance over which the average value of K is being measured cm
$L_e$ is the length of the screen of the well through which water can enter cm
$H_0$ is the drawdown at time $t=0$ cm
$H_t$ is the drawdown at time $t=t$ cm
$t$ is the time since $H=H_0$ hours

Fetter (1994) states there is no method to determine the value of $R_e$ for a given well

other than the method presented by Bouwer to determine the value of the ratio $\ln(R_e/R)$ (Bouwer and Rice 1976, 1989, Bouwer 1996). If the length of the piezometer is less than the saturated thickness of the aquifer, h, which is the case for the piezometers at the study site:

$$\ln\frac{R_e}{R} = \left[\frac{1.1}{\ln\left(\frac{L_w}{R}\right)} + \frac{A + B\ln\left[\left(\frac{h - L_w}{R}\right)\right]}{\frac{L_e}{R}}\right]^{-1} \qquad \text{Equation 3.4}$$

Where:
A and B are parameters derived from curves presented by Bouwer according to the particular ratio $L_e/R$ for the piezometer employed in the test.

The advantage of the Bouwer and Rice test over the Hvorslev method is the wider range of wells that can be employed in terms of pipe geometry. The geometry of the piezometers chosen for the pump tests (section 3.3.2.1) was a major factor influencing the choice of the Bouwer and Rice test. Brown and Narasimhan (1995) and Hyder and Butler (1995) in a review of the method confirmed the validity of the Bouwer and Rice approach by computer simulation and the observation that 'most field practitioners' employ the test. Certain simplifying assumptions are employed in the test (Hyder and Butler 1995) including:

- The change in position of the water table due to a slug test is negligible so that the water table can be considered as a constant head boundary
- Flow above the water table can be ignored
- The formation is isotropic with respect to K.

Such assumptions are common for pumped techniques (Bouwer and Jackson 1974). Hyder and Butler (1995) highlight the effects of disturbance resulting from well drilling for example, in the computed rate of K calculated by the Bouwer and Rice method. Should there exist such a 'well skin' the Bouwer and Rice method can under- or overestimate the value of K for the soil as a whole depending if the disturbance creates a skin of high or low permeability from smearing or the creation of fractures. In clay soils such as those of the study site, smearing of the soil could lead to an underestimation of the K, which is then erroneously applied as a representative value for Elmley Marshes. However this is not unique to the Bouwer

and Rice test but in all applications or tests that require the excavation of wells.

3.2.2.2 Auger hole method

Another popular technique of measuring the hydraulic conductivity in the saturated zone in addition to slug tests is the auger hole method. This method is claimed to be the most widely used, simplest and reliable method of determining the hydraulic conductivity in the presence of a water table (Dorsey *et al.* 1990, Reeve 1982). The procedure consists of auguring a hole to the desired depth below the water table. After allowing water to flood the hole and rise to equilibrium, the hole is pumped and the subsequent rate of water rise measured.

This approach was attempted at the study site but the rate of response was so slow, and the difficulty in capping the auger holes so that disturbance was minimised, meant that it was unsuitable for use.

3.2.2.3 Guelph permeameter

The Guelph permeameter described by Reynolds and Elrick 1986, Elrick *et al.* 1989) has been used extensively (Stephens *et al.* 1988, Asare *et al.* 1993, Salverda and Dane 1993, Ragab and Cooper 1993a, Lilly 1994). Much comparison has been made of the relatively new technique of the Guelph permeameter to other techniques including the auger hole method (Dorsey *et al.* 1990, Gallichand *et al.* 1990, Lee *et al.* 1985, Ragab and Cooper 1993b). The Guelph permeameter allows the measurement of 'field saturated' hydraulic conductivity in the unsaturated zone. 'Field saturated' hydraulic conductivity, $K_{fs}$, refers to a 'saturated' porous medium containing entrapped air (Reynolds and Elrick 1986). Such soils would exhibit hysteresis in their soil moisture characteristic curve (SMC) (section 3.2.4). The Guelph permeameter procedure necessitates the excavation of a cylindrical well above the water table at a desired height and measuring the steady state recharge required to maintain a constant depth of water in the well once field saturation has been achieved (Reynolds and Elrick 1986). In this way measurements of $K_{fs}$ can be made in the unsaturated zone at different depths to assess variability.

Problems with the Guelph permeameter include the time taken to achieve steady state discharge due to soil heterogeneity and linked to this, the need for careful preparation of the well to prevent the formation of a well skin by smearing especially in low

permeable soils. Comparisons between the Guelph permeameter and auger hole method identify lower values of hydraulic conductivity computed by the Guelph permeameter, $K_{fs}$, than by the auger hole method, K (Gallichand *et al.* 1990, Dorsey *et al.* 1990). However this is to be expected due to the incomplete saturation of the soil when taking a measurement with the Guelph permeameter in the unsaturated zone due to entrapped air. Reynolds and Elrick (1986, 1983) defend the use of the Guelph permeameter stating that a value of $K_{fs}$ is actually preferred, as it is more representative of natural flow velocities in the unsaturated zone. Baird (1997) issues similar views, reporting favourable usage of a similar instrument to determine $K\psi$ of an unsaturated peat wetland in the Somerset Levels.

The Guelph Permeameter technique was applied to the study site to derive values of field saturated hydraulic conductivity, $K_{fs}$ (section 3.3.2.2.1). The Guelph permeameter was also used to conduct infiltration tests at the surface, to maintain a constant head of water inside an infiltration ring inserted into the surface soil (section 3.3.2.2.2).

Swelling clay soils such as observed at the study site pose particular problems in the determination of field measured hydraulic conductivity due to seasonal variations in pore distributions and geometry. Bouma (1980) quotes the example of a Dutch clay soil of which the hydraulic conductivity varied from 50 m $day^{-1}$ when dry and cracked in summer, to 0.01 m $day^{-1}$ when saturated and swollen. This is due to the extremely permeable nature of shrinking clay soils when dried due to preferential flow along created and enlarged cracks and fissures. After saturation, swelling of the soil drastically reduces the permeability of the soil allowing flow only through the soil matrix and macropores such as root holes and channels made by soil fauna. Messing and Jarvis (1990) claim that through the action of swelling, soils suffer from entrapped air that can block flow pathways. In such circumstances, field measurement of hydraulic conductivity yielding estimates of $K_{fs}$ are more appropriate or representative of actual conditions than the higher values of K measured in the laboratory or the auger hole method under saturated conditions. This concurs with Reynolds and Elrick (1986, 1983) above. Bouma (1980) and Bouma and Dekker (1981) present a method for measuring the hydraulic conductivity of a clay soil with

macropores in both the vertical and horizontal plane. A cube of soil is taken and covered with gypsum; the soil should first be saturated allowing maximum swelling to take place. The gypsum layer is removed from opposite faces of the cube so that water can infiltrate the upper surface of the cube and be collected at the lower surface. The exposed faces of the cube are then covered with gypsum, turned over and the procedure repeated for two other faces to determine the water flow in the other direction. This method allows an appraisal of the rate of water movement through the macropores of the soil in both the horizontal and vertical direction. The size of cube tested by Bouma and Dekker (1981) was 25 $cm^3$. It was not believed that this small size would be appropriate for the study site in this investigation due to the experience of the clay soil sensitivity to compression when wet. As a result a much larger sample would be required. This would involve many logistical problems due to the difficulty in extracting a soil sample from below the surface from the marsh. Despite the attractiveness of this method it was therefore decided to focus on the use of the Guelph permeameter so that a measurement could be taken *in situ*.

Reynolds and Elrick (1986 p85) state that 'the Guelph permeameter method measures the steady state liquid recharge, Qs, necessary to maintain a constant depth of water, H, in an uncased cylindrical well of radius, r, above the water table. Field saturated $K_{fs}$ and matric flux potential, $\psi m$, is then calculated from the recharge head and well radius data using the Richards (1931), Laplace, and Gardner (1958) analysis based on steady state solutions for infiltration into unsaturated soil from a well'.
$K_{fs}$ is found by solution of Richards equation for steady state flow from a well (Reynolds *et al.* 1985, Salverda and Dane 1993):

$$Qs = \frac{2\pi H^2}{C} K_{fs} + \pi r^2 K_{fs} + \frac{2\pi H^2}{C} \psi m \qquad \text{Equation 3.5}$$

Where:
C is the shape factor describing the 'bulb' of saturated soil around the water outlet tip.

The value of C is dependent upon the head: well radius and soil texture and structure. There are also minor influences such as the proximity of the liquid surface in the well to the soil surface (Amoozegar 1989, Elrick *et al.* 1989, Reynolds and Elrick 1986, 1987, Reynolds *et al.* 1985. Values for C are given in the manual of the Guelph permeameter (Soil Moisture Equipment Corp. 1987) for different H: r ratios and soil

types.

Equation 3.5 depends upon the following assumptions (Salverda and Dane 1993, p406):

1 Steady state flow is attained. This can be a problem in clay soils with macropores such as those in the study area.

2 The soil is homogeneous, isotropic and rigid. The swelling nature of clay soil pose problems but as the increase of volume of the peds in response to increased moisture levels takes place slowly, it is thought that the volume difference over the time take to conduct a test with the Guelph permeameter is negligible.

3 A semi-infinite flow domain exists so that no disturbances of the flow pattern occur.

The solution of Equation 3.5 depends upon the simultaneous equation approach using two data pairs of Qs-H due to both $K_{fs}$ and $\psi m$ being unknown. Should the assumptions above not be maintained, negative values of $K_{fs}$ and $\psi m$ can be calculated. This has lead to the criticism of the simultaneous equation approach as being 'not well conditioned' (Philip 1985).

To avoid the use of the simultaneous equations approach, $K_{fs}$ and $\psi m$ can be calculated using a single head approach (Elrick *et al.* 1989):

$$K_{fs} = \frac{CQs}{2\pi H^2 + \pi r^2 C + \frac{2\pi H}{\alpha}} \qquad \text{Equation 3.6}$$

$$\psi m = \frac{CQs}{\left[\left(2\pi H^2 + \pi r^2 C\right)\alpha + 2\pi H\right]} \qquad \text{Equation 3.7}$$

Where:

$$\alpha = \frac{K_{fs}}{\psi m} \qquad \text{Equation 3.8}$$

The value of field saturated hydraulic conductivity when derived from the single head approach is dependent upon the value of $\alpha$ being measured independently or obtained from the literature. The parameter represents the porous properties of the soil and can be defined as an 'index of capillarity' (Reynolds 1994, Campbell and Fritton 1994 and Elrick *et al.* 1989).

### 3.2.3 Soil water potential

Water flow in unsaturated soils is subject to a gravity potential, $\psi_g$, and a water potential which depends upon the prevailing soil moisture and comprises matric and osmotic potentials. Flow is subject to the sum of these, moving in the direction of a high to low gradient. Total potential $\varphi$ (units of kPa) is thus defined as:

$$\varphi = \psi_g + \psi_m + \psi_o \qquad \text{Equation 3.9}$$

Where:
$\psi_g$ is the gravitational potential
$\psi_m$ is the matric potential
$\psi_o$ is the osmotic potential

The osmotic potential is enforced through solutes in the soil and acts to lower the total potential (i.e. make more negative) by osmotic forces. The osmotic potential can be largely ignored in most soils, being less important than matric potential (Ward and Robinson 1990), however in such brackish soil conditions as the study site (section 3.3.1.6), the effect of the osmotic potential of the soil may not be negligible. Matric potential is composed of capillary and adsorption forces that together with the osmotic potential, exert a suction pressure on the soil water. Suction is expressed as a negative in relation to atmospheric pressure.

The magnitude of the suction forces acting upon water flow is related to soil textural and structural properties; the physical attraction of the water to the surfaces of the soil particles and capillary pores. Following the gradient of decreasing potential, water will flow from films surrounding soil particles to where they are thinner until equilibrium is reached. Surface tension between air and water within soil gives rise to capillary forces, with the greater self-attraction of water molecules than to water vapour resulting in the contraction of the liquid surface under tension to a curved meniscus. The curvature of the meniscus is related to, and increases with, the suction pressure exerted by the soil matrix. Adsorption of water by electrostatic forces creates thin films of water surrounding soil particles. Attraction is greatest in clay soil which, due to the small particle size and therefore large surface area, retain high water volumes under high suctions relative to sandy soils for example.

The combined action of capillary and adsorption forces is such that at a given tension

water is held more tightly by smaller particles than larger ones resulting in the observations that the coarser the soil texture the less water held under tension, and with increasing potential pores will drain in order of size, with larger pores draining at lower suction than smaller pores.

### 3.2.4 Soil moisture characteristic curve

The relationship between the moisture content of a soil, $\theta$, at a given suction pressure, $\psi$, is termed the soil moisture characteristic curve, SMC. The SMC varies for different soils based upon the textural properties as described above, and also varies within the same soil due to hysteresis. Thus for a given value of $\theta$, $\psi$ will be different if the soil is being wetted than dried. Hillel (1971, 1998) lists four causes of hysteresis:

1. Geometric non-uniformity of pore spaces leading to the 'ink bottle effect'. Pore spaces can be conceptualised as irregular shaped voids interconnected by narrower or smaller passages. Desorption (drying) depends upon the radius of the connecting passages (higher suction) whilst sorption (re-wetting) depends upon the larger diameter (lower suction) of the pore void. Both are characterised by abrupt discontinuous spurts of water that are more pronounced in coarse textured soils.
2. The contact angle effect, which refers to the degree of curvature of water, held at capillary tension to the soil particle. Under desorption, the contact angle and degree of curvature is greater than under sorption resulting in a greater suction at given soil moisture.
3. Trapping of air in pores restricting sorption pathways and therefore reducing the soil moisture.
4. Swelling, shrinking or ageing/ripening of the soil, which can result in soil structural changes (such as the creation of macropores) depending upon desorption or sorption. It is believed that this is the most important factor at Elmley Marshes.

The SMC is derived by the simultaneous measurement of the soil moisture content of the soil over a range of matric potentials or suctions, preferably over both wetting and

drying cycles to assess the degree of hysteresis. Measurement of the SMC can be undertaken directly in the field using in-situ instruments to measure the soil moisture and pressure potential, by laboratory methods which can be difficult, laborious and costly (Rawls *et al.* 1982), or indirectly by published empirical relationships.
Traditionally tensiometers have been used to generate suction values *in situ* (Curtis and Trudgill 1975). In addition to using tensiometers (section 3.3.3.3) the attempt to measure the soil suction at the study site included the coupling of an Equitensiometer and ThetaProbe (Delta-T Devices 1998a, b) connected to a data logger to yield continuous measurements (section 3.3.3.4). The instruments are discussed further by Gaskin and Miller 1996) and Topp *et al.* (1980). Calibration details can be found in section A.7.1.

Laboratory methods of measuring the SMC include the pressure plate apparatus. Curtis and Trudgill (1975) detail the use of the pressure plate apparatus to measure the soil moisture characteristic curve. Saturated samples of soil are placed upon a porous ceramic plate and a certain suction pressure applied by a compressor. Moisture is lost from the samples until an equilibrium is reached. This equilibrium relates to the amount of moisture retained in the soil at that suction pressure. The amount of moisture retained by the soil is determined by the change in weight and oven drying the sample. The time taken to establish equilibrium depends upon the soil type and can take up to 30 hours (Curtis and Trudgill 1975). An outflow burette is attached to the pressure plate apparatus and used to determine if equilibrium has been attained when the water level in the burette remains constant. A range of pressure can be applied up to 1500kPa, the soil moisture constant at which wilting point is reached.
The pressure plate apparatus has been used to determine the SMC for the Wallasea soil series with depth. A soil core was taken to 1 m depth and subsampled. This core was subsampled to provide samples at approximately every 5 cm along the core. The use of the pressure plate however suffered from maintenance problems leading only to a few measurements of different pressures being taken. Section 3.3.3.2 details the experimental procedure, problems encountered, and results.

Published empirical formulae derive the SMC from basic soil properties such as particle size distribution, organic content and bulk density. Several formulae exist, for example Rawls *et al.* (1982), Wosten and van Genuchten (1988), Vereecken *et al.*

(1989), de Jong and Loebel (1982), Puckett *et al.* (1985), Ariya and Paris (1981), Petersen *et al.* (1968).

The predictive model presented by Gupta and Larson (1979) has the form:

$$\theta\psi = [a\,x\,sand\%] + [b\,x\,silt\%] + [c\,x\,clay\%] + [d\,x\,organic\ matter\%] + [e\,x\,bulk\ density\ g\,cm^{-3}]$$

Equation 3.10

Where:
a, b, c, d, e are regression coefficients which differ in value for different $\theta$ values.

This model was derived using sieved packed soil samples in the pressure plate apparatus to measure the $\theta\psi$ relationship on a number of soils varying in texture and structure including swelling soils. Hamm (1998) reviewed alternative predictive models and concluded that for application to the study area, the Gupta and Larson model was the most satisfactory based on logistical and practical reasons. This is discussed further in section 3.3.3.1.

## 3.3 Results of the research investigation at the study site

In order to investigate the influence of ditch water level control it is necessary to analyse the Wallasea soil series of Elmley Marshes to ascertain its hydrological properties. Changes in ditch water level, the water table, and soil moisture of the study field need to be monitored over time and space. This comprises a large amount of information that is presented as follows. The remainder of this chapter contains the results of the soil characteristics in terms of texture and structure information, the SMC and hydraulic conductivity with depth.

### 3.3.1 Soil characteristics

#### 3.3.1.1 Soil series characteristics

Fordham and Green (1980) and Hazelden *et al.* (1986) have also investigated the soil of the North Kent Marshes and their results are presented where applicable to the research undertaken in this project. The soils of the grazing marshes consist almost entirely of Downholland and Wallasea soil series: non-calcareous clayey alluvial gleys (Fordham and Green 1980). The non-calcareous nature of the soils has negative

implications for successful conversion of land to arable use. The main difference between the two soil series is the presence of the amount of organic matter in the surface 15 cm of soil that is chiefly derived from the land use (Fordham and Green 1980). Downholland humose soils are found under long established grassland while Wallasea soils are non-humose and typical of arable land with improved drainage. According to this classification, the soils at Elmley are classified into the Downholland series due to the high organic content of the surface. The physical characteristics of this series are found in Tables 3.2 and 3.3. However in the special investigation of the saline soil of North Kent by the Soil Survey (Hazelden *et al.* 1986), Wallasea soils were mapped over the Elmley marshes, and identified as the soil type for such undrained grassland areas. Due to this, the soil series of the study site is hereby stated to be the Wallasea series.

Much of the analysis of the soil hydraulic parameters was done in collaboration with Hamm (1998). Soil cores were taken to depths of at least 1 m from the study site and divided into samples so that the texture, organic content and particle density of the soil could be determined. Bulk density was determined from additional cores taken from the study site.

3.3.1.2 General description

Thirteen soil cores taken near the transect piezometer nests were obtained from the site. The profile is described in Table 3.4 and as reported by Fordham and Green (1980), overall there are three basic horizons within the profile. A dense fibrous mat of high organic content in the surface 0.2 m overlies a layer of mottled grey clay with blocky texture to approximately 0.6 m depth. Below this depth exist a blue/grey unripened clay layer.

3.3.1.3 Particle size distribution

Texture analysis was performed on samples at intervals to 1 m depth using the pipette method. Results show that the soil is dominated by the clay and silt fractions (Table 3.5). The silt has the greater proportion in the 0.10-0.45 m layer indicating leaching of silt down through the profile from the upper soil layers. Fordham and Green (1980) and Hazelden *et al.* (1986) have shown the presence of silt infilled pores at a

similar depth, which create barriers to water flow. From the results of the particle size distribution and organic content analysis the soil can be classified as clay bordering on a silty clay with a organic peaty surface.

3.3.1.4 Organic content

Values of organic content were determined by the loss on ignition method on three samples per depth increment. Results are shown in Figure 3.1 and Table 3.5 and show that the top 0.15 m of soil has an extremely high organic matter content with an average value of 36%. These results are higher than those of Fordham and Green (1980) and Hazelden *et al.* (1986) showing the possible increase in humic material since their study was undertaken, or the natural variation over the North Kent marshes, as the Elmley Marshes was not a study site chosen by the researchers.

Table 3.2. Description of the soil series that covers the Elmley Marshes. Source: adapted from Fordham and Green (1980).

| Soil Series | Wallasea |
|---|---|
| Classification | Humic-alluvial gley soil. |
| Parent material | Non-calcareous clayey marine alluvium. |
| Occurrence | Major soil series in the North Kent Marshes. |
| Description | Commonly wet with moderate or small available water capacity; drainage and water level control is essential for arable cropping. Microrelief due to relict creeks is a serious problem; levelling is expensive and using estuarine dredging has only limited success due to their saline nature. |

Table 3.3. A standard profile of a Wallasea series soil. Source: Fordham and Green (1980 p119).

| Particle size | Clay or silty clay. |
|---|---|
| Colour | Black or very dark greyish brown humose topsoil, often with rusty mottles; grey with ocherous mottles below passing to grey soils with fewer brownish or reddish mottles; distinctly mottled soil starts above 0.4 m. |
| Stones | None. |
| Structure and consistence | Topsoil can be friable with strongly developed fine blocky or granular structure under old pasture; firm coarse prismatic or blocky passing to firm weakly developed prisms; massive partly ripened clay and occur below 0.6 m, but cracking penetrates deeply in dry summers; in parts, tunnelling by ants gives marked macroporosity below the surface. |
| $CaCO_3$ | None. |
| Soil moisture regime | Commonly or usually wet due to poor drainage; water stands in relict creeks and at a high level in ditches during winter and after heavy rain at other times; small available water content. |

Table 3.4. The change in soil characteristics with depth of the soil cores taken from the study area (Wallasea soil series).

| Depth m | Description |
|---|---|
| 0 | Black, fibrous, organic layer. Densely matted with roots that makes it difficult to tear or cut. Crumbly texture; soil held by roots. |
| 0.2 | Dark brown soil with red mottling in patches. Heavily rooted. Blocky structure can be broken into fragments more easily than the surface layer of soil. Can be smeared. |
| 0.3 | Band of ripened grey/brown clay with some red mottling. Blocky texture that can be easily smeared. A number of roots present. |
| 0.6 | Blue/grey – light brown clay with red mottling. No structure. Some roots present. Very easily smeared and quite malleable. |
| 0.9 | Sticky blue/grey – light brown clay with red mottling. No structure. Very easily smeared and malleable. Few/no roots present. |
| 1.2 | Very sticky blue/grey- brown. Few patches of red mottling. No structure. Impossible to handle without smearing. Few/no roots present. |
| 1.5 | Dark grey-brown fluid clay. Few/no roots present. |

The high organic content in the top 0.15 m indicates this layer holds the majority of plant roots, which is confirmed from the examination of the soil. The plant roots extend to 0.3-0.4 m depth after which some extend to 0.5-0.6 m depth. The trend of decreasing organic content with depth seems to accord with this observation. After this depth it is thought that the increasing salinity (Figure 3.4) and unripened nature of the clay soil down the profile inhibits root formation. The increase in organic matter at 0.5-0.7 m depth is unexpected and could be due organic particles being leached down the profile.

The range of organic matter commonly found at the surface of mineral soils in temperate regions is in the order of 4-10% (Brady 1990). Soils with low organic matter i.e. less than 3% are classified as mineral soils while part/organic soils are those with more than 15% organic content (Rowell 1994). The values of organic matter at the study site are extremely high at the surface and can be classified as an organic rather than mineral soil. At depths deeper than 0.2 m, the values of organic matter are still high but the percentage reduces to 10% and less (except for the increase at 0.5-0.7 m) and the soil can be classified as mineral. The response of organic matter enables the soil to retain more moisture (Hillel 1971); this is manifested in soil moisture profiles monitored at the study site.

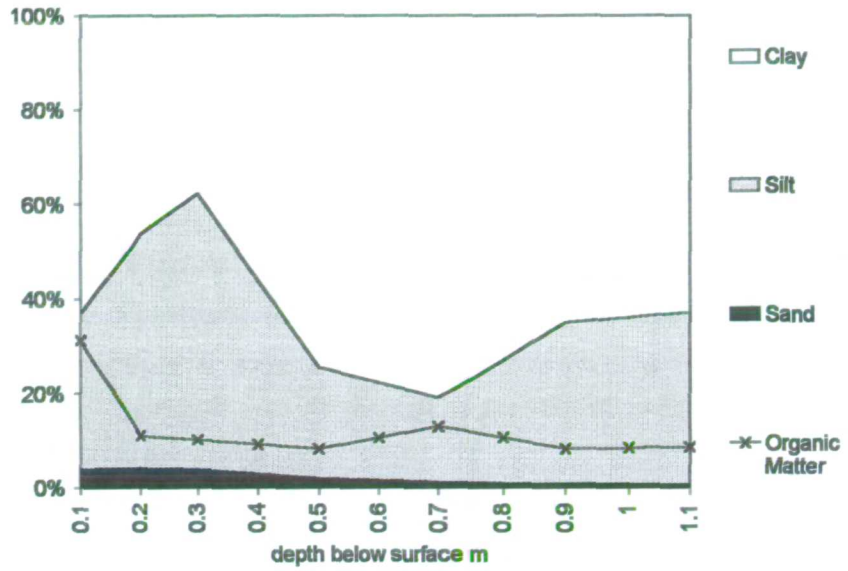


Figure 3.1. The particle size distribution and organic matter distribution with depth for the study site.

Table 3.5. The particle size distribution of Elmley Marshes, Wallasea soil series. Similar values have been reported by Fordham and Green (1980) and Hazelden *et al.* (1986) (see Table 3.6). There was error in the analysis of the sample for 0-0.05 m and so results for this layer are not shown.

| Depth of sample m | Sand % | Silt % | Clay % | Organic Matter % |
|---|---|---|---|---|
| 0.00-0.05 | | | | 65.27 |
| 0.05-0.10 | 3.87 | 33.12 | 63.01 | 31.17 |
| 0.10-0.15 | 3.37 | 51.07 | 45.56 | 11.75 |
| 0.15-0.20 | 4.25 | 49.47 | 46.28 | 10.97 |
| 0.20-0.25 | 5.18 | 48.07 | 46.74 | 10.30 |
| 0.25-0.45 | 3.90 | 58.39 | 37.72 | 10.10 |
| 0.45-0.50 | 1.99 | 23.45 | 74.55 | 8.15 |
| 0.50-0.70 | 1.13 | 17.94 | 80.93 | 12.97 |
| 0.70-0.90 | 0.78 | 34.22 | 64.99 | 8.18 |
| 1.05-1.10 | 0.64 | 36.44 | 62.92 | 8.60 |

Table 3.6. Particle size distribution and organic matter content for Wallasea and Downholland series soil from Hazelden *et al.* (1986) and Fordham and Green (1980) respectively. Fordham and Green state that the presence of clay infilled pores between 0.5 and 0.7 m depth could be the result of increased clay mobility following the leaching of salt after the flooding caused by the 1953 floods (MAFF 1962).

| Hazelden *et al.* (1986) Wallasea Series | | | | | | Fordham and Green (1980) Downholland Series | | | | |
|---|---|---|---|---|---|---|---|---|---|---|
| Depth of sample m | Sand % | Silt % | Clay % | Organic Matter % | Bulk density g $cm^{-3}$ | Depth of sample m | Sand % | Silt % | Clay % | Organic Matter % |
| 0.00-0.10 | <1 | 45 | 54 | 12 | 0.52 | 0.00-0.05 | <1 | 46 | 52 | 22 |
| 0.10-0.26 | | 42 | 55 | 0.6 | 1.31 | 0.05-0.19 | | 37 | 62 | 3.2 |
| 0.26-0.42 | | 49 | 46 | 0.8 | | 0.19-0.49 | | 34 | 65 | 2.8 |
| 0.42-0.56 | | 50 | 48 | 0.8 | 1.38 | 0.49-0.98 | | 33 | 66 | |
| 0.56-0.75 | | 40 | 59 | 0.8 | 1.3 | 0.98-1.20 | | 39 | 60 | |
| 0.75-1.00 | | 50 | 49 | 0.7 | | | | | | |

3.3.1.5 Bulk density, particle density and porosity

Bulk density can be defined as the mass of a unit volume of dry soil (i.e. both solids and pore spaces). Typical values for clay and silt rich soil can range 1.0 to 1.6 g $cm^{-3}$ (Brady 1990). The bulk density has proven difficult to determine accurately as the clay soil is very sensitive to any compression and mishandling. Great care has been applied to the samples and it is assumed any compression was negligible and values obtained are representative.

The general trend of the bulk density profile with depth, Figure 3.2 and Table 3.7, starts with low values of 0.44 g $cm^{-3}$ at the surface, due to the very high organic matter content (Adams 1973) increasing to 0.97 g $cm^{-3}$ at 0.15-0.20 m. The bulk density then climbs to a value of 1.27 g $cm^{-3}$ at 0.35-0.40 m depth. After this depth the bulk density drops and fluctuates around 1 g $cm^{-3}$, a typical value for clay soil.

As bulk density is a measure of the mass of both soil and pores in soil, so the particle density is a measure of the solids alone. Typical values of mineral soils are in the range of 2.60-2.75 g $cm^{-3}$; organic soils have a lower mass per unit volume of 0.1-1.4 g $cm^{-3}$ (Brady 1990). The specific gravity bottle method was employed to determine the density of the soil particles. Results are presented in Table 3.7.

The particle and bulk density data can be used to calculate the porosity of the soil profile (Table 3.7). The high porosity of the surface soil is due to the high proportion of organic matter creating a porous layer. The porosity values from 0.2 m depth are typical of fine-grained soils such as this. The bulk density values are comparable to those of Hazelden *et al.* (1986).

From the above data, and information about the soil moisture regime, it has been possible to construct Figure 3.3, a plot of the air capacity and water release characteristics of the surface soil at Elmley. Analysis of the plot reveals that the total amount of water in the soil remains constant with depth except at the surface. Here the higher amounts of organic matter enable the soil to hold a greater amount of water. The percentage of available water decreases down the profile. The term 'available water' normally refers to the amount of water available to plants until the wilting point is reached at 1500 kPa. In this instance however due to the problems in deriving the soil moisture characteristic curve with depth (section 3.3.3.2.1), and so

determine the soil moisture at 1500 kPa, the minimum value of available water is based upon the lowest value of soil moisture recorded over the two year monitoring period.

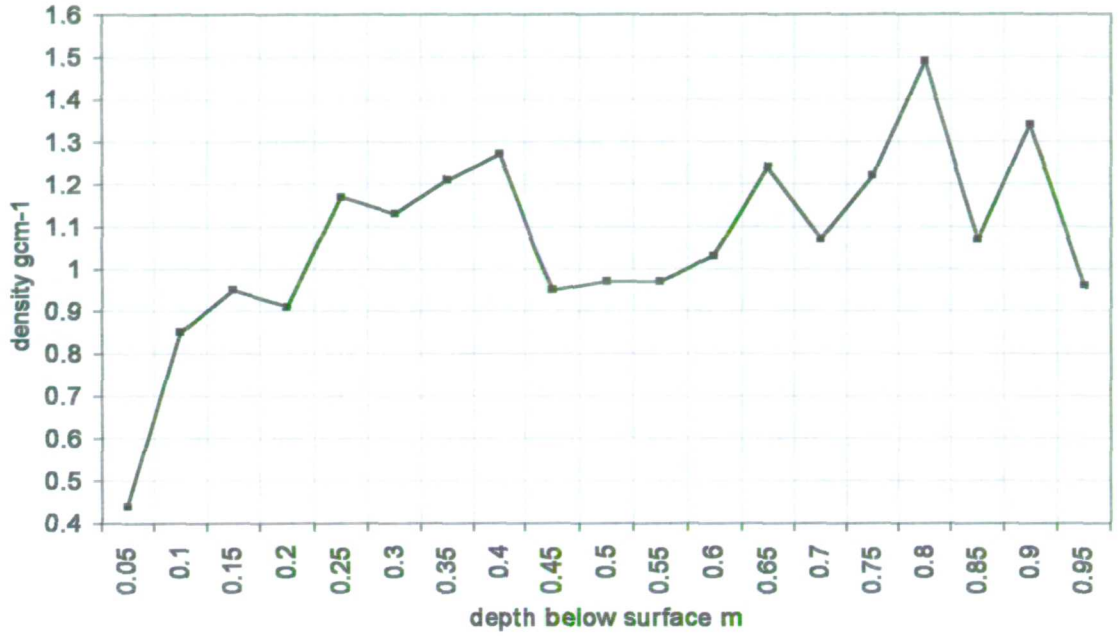


Figure 3.2. Change in bulk density with depth for the study area, Wallasea soil series.

Table 3.7. The results of the analysis of bulk density and particle density, and the derived value of porosity. The published values of bulk density by Hazelden *et al.* (1986) are also presented for comparison.

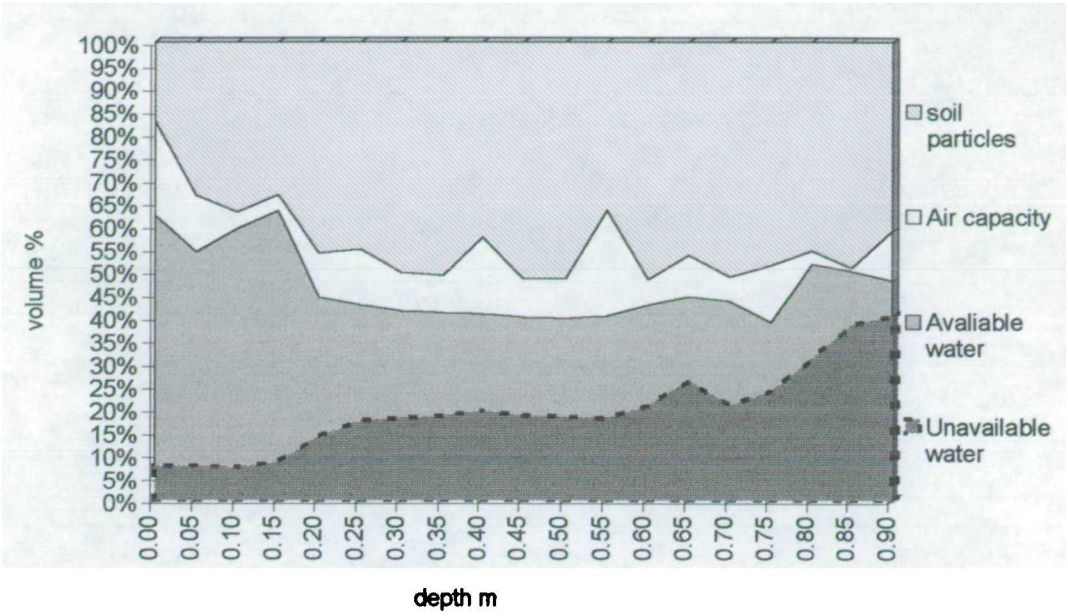


Figure 3.3. Air capacity and water release characteristics for the study site, Wallasea soil series.

It can be seen that the volume of available water, (in this case the range of high and low values exhibited by the marsh over the study period), is greater than the published values of wilting point of clay soils of approximately 20% or higher (Brady 1990, Fetter 1994, Rowell 1997). It is believed that the cracking nature of the soil of the study site enables enhanced loss of water from a larger surface area of soil resulting in low values of soil moisture retained by the soil.

3.3.1.6 Effect of soil salinity

Salt affected soils are mainly found in marine alluvium sediments at coastal locations. Such soils typically have a clay content in the range 10 - 80% and often have peaty topsoils (Loveland *et al.* 1986). Extensive areas of these soils occur in North Kent, Somerset, Essex, Romney Marsh and around the Wash in East Anglia. Salts in soil are also derived from chlorides and sulphates of calcium, magnesium, sodium and potassium sourced from irrigation water, groundwater, and the chemical weathering of soil minerals and bedrock for example. Not only are high levels of salts in soil detrimental to plant growth, but also a high level of sodium in relation to low levels of calcium and sodium can be both physically and chemically detrimental to soil

structure.

The deleterious effects of salt and sodium are to hinder healthy plant growth (Fitter and Hay 1987) by causing direct toxicity due to the high sodium, chloride and boron content in the water. Ionic imbalances in the plant are created which can reduce the availability of water by lowering the osmotic potential, known as physiological drought.

Should the soil be sodic (i.e. have a dominance of sodium salts), as in the North Kent Marshes, the exchangeable sodium percentage, ESP, of the soil will be high. High values of ESP also yield a high soil pH due to the presence of neutral salts. The ESP is the amount of exchangeable sodium expressed as a percentage of the cation exchange capacity CEC (Rowell 1994). For such soils, the treatment of salinity is not as simple as to leach away salts as this would cause structural damage through soil slaking, pore blockage and a decrease in permeability of the soil. A common classification of sodic soil is to use the value of the ESP; soils with an ESP<15 are classified as non-sodic while those with ESP $\geq$ 15 are sodic. However, research by Crescimanno *et al.* (1995) shows that soil structural damage can occur below this threshold value of an ESP of 15. Almost linear relationships were found between soil structure and hydraulic behaviour with ESP at low cationic concentrations, with aggregate stability and hydraulic conductivity shown to decrease by 25% in the range of ESP 2-5. Likewise Loveland *et al.* (1986) stated dispersal can occur in expansible alluvial clays such as the Wallasea series with an ESP as low as 10. Hazelden *et al.* (1986) report values of ESP for the Wallasea series (Table 3.8). At depths greater than 0.35 m the soil can be classified as sodic, while at the surface, the sodicity is influenced by the degree of water logging. The surface soil can be considered sodic if it suffers severe inundation. Otherwise the ESP of the soil is much lower than typically considered sodic although the results of Crescimanno *et al.* (1995) indicate that deleterious effects of sodium can still be experienced. Hazelden *et al.* (1986) report higher concentrations of sodium salts occur in soils that experience flooding from ditches. This has also been quantified from soil sampling in this investigation (section 3.3.1.7) and has implications for the proposed flooding of the marsh by ditch water to comply with Tier 1b of the ESA management scheme (section 3.1).

The results of experiments to determine the soil electrical conductivity and ESP in this investigation and by other researchers, illustrate the presence of a non-saline or

very slightly saline non-sodic surface soil overlying a saline-sodic subsoil for the North Kent Marshes. As such these soil are classed as potentially structurally unstable and unsuitable for drainage programmes. The saline sodic nature of the subsoil result in low hydraulic conductivities of the soil matrix (section 3.3.2) due to soil dispersion and pore blockage.

Table 3.8. The exchangeable sodium percentage with depth sampled on St Mary's Marshes (Wallasea soil series) at locations with differing levels of inundation. Source Hazelden *et al.* (1986, p21).

| Degree of water logging | Depth of sample m | | |
|---|---|---|---|
| | 0-0.15 | 0.35-0.50 | 0.7-0.85 |
| Very severe | 22 | 29 | 35 |
| Severe | 9 | 26 | 32 |
| Moderately severe | 6 | 19 | 23 |
| Slight or none | 5 | 15 | 22 |

3.3.1.7 Quantification of soil salinity

Soil samples have been taken to determine the electrical conductivity. Information regarding salt levels is required to assess the effects upon soil structure, water density and movement, and also to assess the possible impact upon the electrical resistance blocks used to monitor soil moisture (section 5.1.1), which are known to be sensitive to salt in the soil. The electrical conductivity has been determined following the method by Rowell (1997) and Hazelden *et al.* (1986) by taking a 1:5 soil: water extract. Hazelden *et al.* (1986) used this method for their survey of the electrical conductivity of the North Kent Marshes soil and so these results will be directly comparable. The results of the soil salinity experiments are presented in Table 3.10 and Figure 3.4. Four soil cores were taken to a depth of approximately 0.8 m for the analysis at different field visits. Equal numbers of cores were taken from both within the main enclosure and the small enclosure adjacent to the north ditch edge (Figure 1.3). The sample in the enclosure represent the salinity of the marsh at 30 m distance from the north ditch whereas the samples taken next to the ditch are representative of soil that is in direct contact with the ditch water either through seepage or regular flooding in winter. Each core was sectioned into regular intervals of 0.2 m depth and divided into a number of subsamples to use as much as the core as possible in the analysis. The conductivity of each soil water extract was determined and the average

per 0.2 m layer calculated to a confidence interval of 95%. A GLI International 914 model portable temperature, conductivity and salinity probe was employed in the investigation.

In addition to measuring the electrical conductivity of the soil, the water within the piezometers in the study field was also measured, and also in the four ditches surrounding the study field. The conductivity of water from the Met Office Mark II rain gauge was also measured when a sufficient volume had been collected.

Measurements were taken in the piezometers during nine field visits over February to September 1998 yielding a total of 578 data points. While common procedure when monitoring water quality from boreholes is to pump out the water in the well, then obtain a 'fresh' water sample when the water has risen back, it was not feasible to do this due to the slow response rates of the piezometers. Indeed having pumped out certain piezometers to perform the Bouwer and Rice pump test to compute hydraulic conductivity, the rate of recovery took several weeks (section 3.3.2.1). Thus the conductivity of the piezometer water was measured by lowering the probe into the wells without pumping out the water and so it could be argued that a 'fresh' water sample was not obtained. However the level of groundwater/phreatic surface measured in the piezometers was not static over the period of measurement indicating water flow in and out of the piezometers and therefore the water sampled by the conductivity probe was not always the same.

The number of conductivity measurements taken from the ditches (total 13) are substantially less than those for the piezometers as reflected in the higher range of values at the 95% level (Figure 3.4). It was soon recognised that the electrical conductivity measurements of the ditches would serve only as estimates due to the problems of selecting a suitable spot for repeated sampling and at a suitable reach and depth. The ditches are slow moving or static bodies of water and stratification probably occurs over the year due to the poor circulation of the water.

It was decided to take conductivity measurements next to the stageboards for reference. Overall the conductivity of the water of the four ditches bordering the study field were very slightly saline to slightly saline (Table 3.10). The values are similar for all the ditches, which is expected due to the fact they are inter connected (Figure 2.3). Conductivity values taken by English Nature (1995) in the same four

ditches surrounding the study field have been classified in the range 3.0-4.9 dS $m^{-1}$, very slightly saline to slight saline, within the ranges measured in this investigation and give confidence in the results obtained in this study.

It can be seen from Tables 3.9 and 3.10 that the conductivity ranges of the soil layers from the surface to 0.4 m depth in the enclosure can be classified as non-saline to very slightly saline according to Hazelden *et al.* (1986). However according to Miller and Gardiner (1998), some sensitive plants are affected by this level of salinity. At greater depth, the soil layers 0.4-0.6 m and 0.6-0.8 m, can be classified as being very slightly saline to slightly saline within their range of conductivity, with some to many plants affected by this level of salinity. Piezometer water measurements increase in conductivity with depth; 1 m classed as borderline to moderately saline, with 1.5 m and 2 m classed as moderately saline.

Confidence or error bars are illustrated on Figure 3.4 and are greater for the soil samples than for the piezometer results. This is due to the much smaller number of measurements of the soil samples but could also be a factor of the 'freshness' of the water in the piezometers, as previously discussed above. The confidence bars indicate a significant difference at the 95% level between the conductivity of the surface soil layers. The surface soil by the north ditch has significantly greater conductivity than in the enclosure and this is due to the inundation of the riparian zone, where the samples were taken, from the brackish ditch water. Apart from this surface layer however, the difference in conductivity is insignificant. The conductivity profile in the enclosure increases with depth indicating the action of precipitation in leaching salt from the surface. The profile next to the ditch shows a slight decrease down the profile indicating perhaps the retention of salt by the surface organic layer with only partial leaching down the profile.

This difference in conductivity with depth was also observed by the Soil Survey (Hazelden *et al.* 1986) with the soil being described as being 'non-saline topsoil and very slightly saline in the subsoil. Moderately saline soils occur on the sites of former creek channels'. Results of conductivity sampling of Hazelden *et al.* (1986) and Fordham and Green (1980) are presented in Table 3.11 with the former presenting higher values illustrating the influence of site location when taking samples for analysis. Hazelden's samples were taken on a levée close to a ditch. Fordham and

Green describe their conductivity profile as 'near a dry creek', which is not as specific in location and could have been from an area that does not experience flooding from the saline ditch water. As such, Hazelden *et al.*'s data are directly comparable to the values reported in this study from the ditch edge. Likewise the measurements from samples taken from the enclosure can also be compared to Fordham and Green's data.

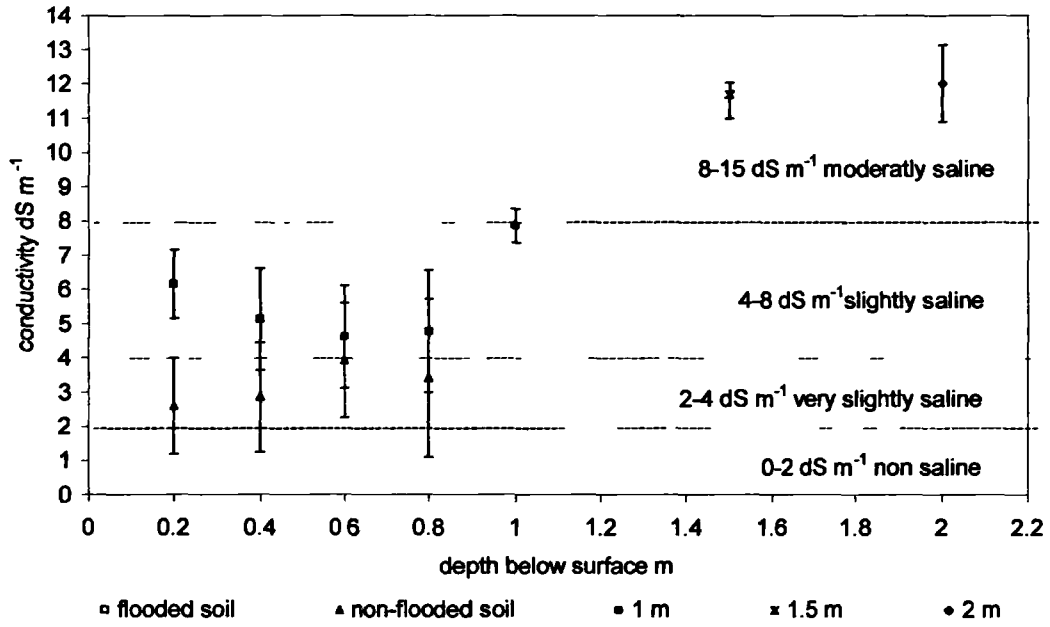


Figure 3.4. Results of soil conductivity measurements. The flooded soil is representative of ditch margin area regularly inundated with brackish water. The non-flooded soil samples were taken from within the main enclosure. The measurements at 1 m, 1.5 m, and 2 m were taken in the transect piezometers. The error bars are shown at the 95% confidence interval.

Table 3.9. Classification of soil salinity by Rowell (1997 p278), Hazelden *et al.* (1986 p23) and Miller and Gardiner (1998 p209).

| Electrical conductivity dS $m^{-1}$ | Soil classification Rowell (1997) | Soil classification Hazelden *et al.* (1986) | Plant effects Miller and Gardiner (1998) |
|---|---|---|---|
| 0-2 | Non-saline soils | Non-saline | Few plants affected |
| 2-4 | | Very slightly saline | Some sensitive plants affected |
| 4-8 | Saline soils | Slightly saline | Many plants affected |
| 8-16 | | Moderately saline | Most crop plants affected |
| 16+ | | Strongly saline | Few plants can survive |

3.3.1.8 Summary of conductivity

The trend of conductivity from the surface as measured by soil samples and the piezometer water is one of increase with depth. Such a trend is expected due to the reclamation of the area from salt marsh. The conductivity of the precipitation is low as expected at 0.1 dS $m^{-1}$ but the influence of the sea is noticed with a comparison to a value of precipitation of 0.009 dS $m^{-1}$ recorded inland over Malham, Lancashire (Rowell 1994). The salt content of the soil water and ditches has implications on plant growth, as stated in Table 3.9, through direct toxiticies or ionic imbalances. The soil at the study site will have greater osmotic potential than non-saline clay soils leading to a reduction both in the availability of water to plants and to water flow due to increased suction pressure at given soil moisture contents.

Table 3.10. The results of soil electrical conductivity measurements of the Wallasea soil series for soil samples taken within the enclosure and adjacent to the north ditch. The conductivity of the ditch water and groundwater (using the piezometers) and precipitation of the study site were also measured. The salinity classification is after Hazelden *et al.* (1986).

| Sample depth m | Electrical conductivity dS $m^{-1}$ at temperature 25°C. Range given for the 95% percentile | Range of values dS $m^{-1}$ | Salinity classification |
|---|---|---|---|
| Non-flooded soil taken from the main enclosure. Depth in m. | | | |
| 0-0.2 | 2.61 +/- 0.96 | 1.66 – 3.57 | Non-saline to very slightly saline |
| 0.2-0.4 | 2.83 +/- 1.08 | 1.75 – 3.91 | Non-saline to very slightly saline |
| 0.4-0.6 | 3.91 +/- 1.14 | 2.77 – 5.05 | Very slightly saline to slightly saline |
| 0.6-0.8 | 3.74 +/- 1.17 | 2.56 – 4.91 | Very slightly saline to slightly saline |
| Regularly flooded soil from the north ditch. Samples taken from the ditch edge. Depth in m. | | | |
| 0-0.2 | 5.51 +/- 0.48 | 5.04 – 5.99 | Slightly saline |
| 0.2-0.4 | 3.45 +/- 1.31 | 2.14 – 4.75 | Very slightly saline to slightly saline |
| 0.4-0.6 | 3.34 +/- 0.44 | 2.90 – 3.77 | Very slightly saline |
| 0.6-0.8 | 2.93 +/- 0.17 | 2.76 – 3.10 | Very slightly saline |
| Conductivity of the water in the piezometers. Averages have been calculated from all measurements taken. | | | |
| 1.0 | 7.86 +/- 0.49 | 7.36 – 8.35 | Slightly saline |
| 1.5 | 11.68 +/- 0.69 | 10.99 – 12.37 | Moderately saline |
| 2.0 | 12.02 +/- 1.12 | 10.90 – 13.14 | Moderately saline |
| Conductivity of the water in the ditches bordering the study field. Averages have been calculated from all measurements taken. | | | |
| North ditch | 3.6 +/- 0.62 | 3.41 – 3.79 | Very slightly saline |
| West ditch | 3.6 +/- 1.15 | 3.37 – 3.90 | Very slightly saline |
| East ditch | 4.2 +/- 1.11 | 3.85 – 4.55 | Very slightly saline to slightly saline |
| South ditch | 4.9 +/- 1.23 | 3.67 – 6.13 | Very slightly saline to slightly saline |
| Conductivity of the water collected in the Met. Office Mark II gauge in the enclosure. Averages have been calculated from all measurements taken. | | | |
| Precipitation | 0.1 +/- 0.01 | 0.0 9 – 0.11 | Non- saline |

Table 3.11. Values of soil conductivity by other researchers.

| Hazelden *et al.* (1986) | | Fordham and Green (1980) | |
|---|---|---|---|
| Depth of sample m | Conductivity dS $m^{-1}$ | Depth of sample cm | Conductivity dS $m^{-1}$ |
| 0.00-0.1 | 3.6 | 0.00-0.05 | 1.6 |
| 0.10-0.26 | 2.3 | 0.05-0.19 | 1.38 |
| 0.26-0.42 | 2.31 | 0.19-0.49 | 2.02 |
| 0.42-0.56 | 2.56 | 0.49-0.98 | 3.51 |
| 0.56-0.75 | 2.67 | 0.98-1.20 | 4.68 |
| 0.75-1.00 | 2.89 | | |

3.3.1.9 Effect of salt upon water density

The difference in salt content with depth and space over the study field creates a variable density system with depth and space, which has implications for the density of water and its movement within the soil system. While research on mixed convective flows, for example saltwater intrusions in coastal aquifers has been substantial, there is a dearth of investigations to determine the effects of the density driven water flow and heterogeneity in hydraulic conductivity (Schincariol and Schwartz 1990).

Water density or specific mass varies with salinity and temperature and can be computed as (Custodio 1987):

$$\rho = 1000 + 0.8054S - 0.0065(T - 4 + 0.2214S)^2 \qquad \text{Equation 3.11}$$

Where:
$\rho$ is density kg $m^{-3}$ or g $l^{-1}$
S is salinity parts per thousand (PPT) or g $l^{-1}$
T is temperature $^0C$

Fresh water has with a specific density of 1000 g $l^{-1}$, equivalent to kg $m^{-3}$ or 1 g $cm^{-3}$. As shown in Equation 3.11 this value is affected by the temperature of the water with maximum density at $4\,^0C$; at the standard temperature of $25\,^0C$, the density is 997 kg $m^{-3}$. The density of sea water at $25\,^0C$ is computed to be 1021-1023 g $l^{-1}$, using salinity data derived from total dissolved solids of 33-35 g $l^{-1}$ of oceanic waters (Custodio 1987, p11).

For saturated systems Bruggeman (1987) states that the density differences created by salinity differences in the order of 4 to 5 g $l^{-1}$ can be ignored. However research by Schincariol and Schwartz (1990) using dyed fluids of different density in a flow tank

filled with homogenous porous media has shown that density difference of only 1 g $l^{-1}$ yield unstable flow patterns. Further to this, Swartz and Schwartz (1998), using a similar experimental set-up but with a layered media of varying hydraulic conductivity, revealed that complex mixing patterns can develop from the combination of fluid density differences and heterogeneous systems.

The experiments run by Swartz and Schwartz (1998) involved a layer of low hydraulic conductivity overlying one with higher hydraulic conductivity, a pattern with potentially unstable density stratification. The soil system, as identified by soil analysis, at Elmley Marsh comprises a three layer system with a progressive decline in hydraulic conductivity and salinity concentration from the surface. This situation can be classified as stable leading to steady stratification, which is observed in the results of electrical conductivity sampling.

To determine the density of water in the soil profile in the study field it is necessary to relate the conductivity of the soil layers (Table 3.10) to a salinity measurement so that the water density can be computed. Salinity is a function of the conductivity and temperature of the water sampled. The logging conductivity probe employed in this investigation, converts measurements to salinity data to the reference temperature of $25^{0}C$. The output salinity measurement is a measure of the total dissolved solids, TDS, in the sample water and as such the quality of the water sample can be classified according to Table 3.12.

Table 3.13 contains the salinity data for each soil layers examined at Elmley Marsh including the salinity of the water in the piezometers and ditches surrounding the study field. The density of the water has been computed using Equation 3.11. The samples can all be classified as brackish according to Table 3.12 except the precipitation which, as would be expected, is classified as freshwater. As with the conductivity measurements, the salinity data presented in Table 3.13 exhibit large confidence intervals when the number of samples taken were small for example in the case of the ditch measurements. These values therefore can only provide an indication of the salinity levels of the ditch water as the seasonal fluctuation on salt content has not been investigated.

The density differences between the soil, piezometer and ditch water samples do not exceed 4 to 5 g $l^{-1}$ which, according to Bruggeman (1987), can therefore be

discounted as a possible influence on the gravity flow of water. However there are some differences in density which accord to the threshold of 1 g $l^{-1}$ of Schincariol and Schwartz (1990). Even if these differences cannot be discounted, as the overall change of salinity is one with increase with depth i.e. progressively dense water, there is a stable gradation of water density flow.

Table 3.12. Classification of water quality based upon total dissolved solids (TDS). Source Fetter (1994).

| Classification | TDS g $l^{-1}$ |
|---|---|
| Fresh | 0-1 |
| Brackish | 1-10 |
| Saline | 10-100 |
| Brine | >100 |

Table 3.13. The results of salinity measurements of the Wallasea soil series for soil samples taken within the enclosure and by the north ditch. The salinity of the ditch water and groundwater (using the piezometers) and precipitation of the study site were also measured the water density has been computed from Equation 3.11.

| Sample depth m | Salinity in units of PPT equivalent to g $l^{-1}$ at the 25 $^{0}C$. Range given for the 95% percentile | Range of values g $l^{-1}$ | Water density using average salinity values g $l^{-1}$ |
|---|---|---|---|
| Soil in the enclosure. Depth in m. | | | |
| 0.0-0.2 | 3.38 +/ - 1.13 | 2.70 – 4.96 | 999.98 |
| 0.2-0.4 | 3.33 +/ - 1.57 | 1.76 – 4.90 | 999.61 |
| 0.4-0.6 | 5.17 +/ - 1.13 | 4.04 – 6.30 | 1000.97 |
| 0.6-0.8 | 4.50 +/ - 2.7 | 1.80 – 7.20 | 1000.48 |
| Soil by the north ditch. Depth in m | | | |
| 0.0-0.2 | 7.00 +/ - 1.07 | 5.93 – 8.07 | 1002.33 |
| 0.2-0.4 | 5.50 +/ - 1.75 | 3.75 – 7.25 | 1001.22 |
| 0.4-0.6 | 6.13 +/ - 2.16 | 3.96 – 8.29 | 1001.68 |
| 0.6-0.8 | 5.13 +/ - 1.62 | 3.51 – 6.74 | 1000.94 |
| Salinity of the water in the piezometers. Averages have been calculated from all measurements taken. | | | |
| 1.0 | 4.73 +/ - 0.34 | 4.39 – 5.07 | 1000.65 |
| 1.5 | 6.96 +/ - 0.39 | 6.57 – 7.36 | 1002.30 |
| 2.0 | 7.57 +/ - 0.68 | 6.88 – 8.25 | 1002.75 |
| Salinity of the water in the ditches bordering the study field. Averages have been calculated from all measurements taken. | | | |
| North ditch | 2.55 +/ - 0.8 | 1.67 – 3.43 | 999.03 |
| West ditch | 2.18 +/ - 1.69 | 0.49 – 3.86 | 998.99 |
| East ditch | 2.50 +/ - 1.40 | 1.10 – 3.9 | 999.83 |
| South ditch | 3.03 +/ - 0.79 | 2.24 – 3.82 | 999.39 |
| Salinity of precipitation collected in the Met Office Mark II gauge in the enclosure. Averages have been calculated from all measurements taken. | | | |
| Precipitation | 0.54 +/ - 0.01 | 0.53 – 0.54 | 997.53 |

In view of these results the BUDGET model has been employed so that the salinity of the soil with depth can be included when trying to simulate the change in soil moisture. While the effect of density differences may be slight and of a stable form, the osmotic suction of the soil will increase with rising salt content inducing greater retention of water causing a reduction in water lost by evaporation. An increase in salt accumulation in the root zone and/or a reduction in soil water content increases the electrical conductivity of the soil water solution, which in turn causes a corresponding increase in the relative soil salinity, reducing the amount of water that can be extracted by the roots. This process can be simulated in the BUDGET model in the salt transport routine (section 5.2.1.4).

#### 3.3.1.10 Seasonal change in macroporosity

The Wallasea soil series has a high proportion of smectite (Hazelden *et al.* 1986) which renders it particularly susceptible to shrinkage and cracking when drying (Figure 3.5). Soil shrinkage occurs as water evaporates from pores of such small size that the clay particles move closer together as air cannot penetrate the soil (Rowell 1994). Soil can shrink vertically leading to changes in the surface elevation, and horizontally through the production of vertical cracks and fissures and once vertical cracks have formed, further drying can occur from the faces of the cracks. Adsorption of water through rewetting by precipitation and or irrigation causes the soil to swell. Should the vertical cracks not be aligned when the soil swells and regains its maximum volume, shearing and smearing of the crack faces can take place producing slickensides, planes of weakness along which the fissure will reopen with repeated cycles of wetting and drying.

Soil water movement is strongly influenced by the seasonal changes in soil structure and porosity with the soil ranging from nearly impermeable when fully wet to very permeable when cracked (Messing and Jarvis 1990). This can be observed in Figure 4.2 as a rapid change in groundwater during rain events at the end of summer (section 4.1.2) compared to the computed low hydraulic conductivity of the soil matrix.
In an extensive review of soil macroporosity by Beven and Germann (1982), macropores can be classified into four groups according to their origin:

a:

b:

c:

d:

Figure 3.5. Macroporosity of the Elmley Marshes is caused through two processes. Bioturbidation and tunnelling by animals particularly rabbits create very large pores (a) and secondly seasonal soil moisture change induces shrinkage and cracking. An example of soil cracking can be seen above. An area of ground adjacent to the triangulation pillar undergoes regular shallow inundation in winter (b), which evaporates to leave exposed wet soil. Drying produces soil polygons through horizontal cracking (c, d), which, with continued water loss cracks in the vertical direction, form discrete dry soil discs of approximately 20 mm depth. After the discs have formed some drying is observed beneath the discs but generally the dry upper layer prevents moisture loss from beneath.

- Pores formed by soil fauna. These pores can range in size depending upon the size of the burrowing animal from earthworms to rabbits for example.
- Pores formed by plant roots. These pores also have a range of sizes according to the plant that created the channels from narrow pores by grass roots to larger structures by tree roots for example.
- Cracks and fissures created by desiccation of clay soil.
- Natural soil pipes created by the erosive action of soil water flow.

The first and third groups of macropores are particularly prevalent at Elmley, due to the shrinking nature of the soil and the large population of burrowing animals which range in size from ants to foxes. Care was taken to site instruments and experiments away from animal burrows but the seasonal effects of soil shrinkage could not be avoided.

Beven and Germann (1982) discuss the implication of preferential water flow through macropores rather than through the soil matrix in that such soil water behaviour does not conform to Darcian principles. An improved flow theory for soils containing macropores would be based on a coupled domain concept in which the soil matrix domain would be described by hydraulic properties and the macropores would constitute a second domain. Such a model would also have to account for the change in macroporosity with time when applied to swelling soils. In order to construct such a model much information would be required about the nature of the macropores, for example the continuity of the pores, the hydraulic properties of flow in macropores, the spatial and temporal characteristics of the pore network and the interaction between the domains of macropores and soil matrix (Beven and Germann 1982). Beven and Germann list a number of domain models that account for the effect of macropore flow yet report that none are entirely satisfactory due to lack of data against which to calibrate the models and as such cannot be considered more than 'exploratory hypotheses'. Until the water flow and structural properties of macropores systems over time and space become more widely understood many difficulties remain in attempting to quantify and model water flow in soil macropores. Bronswijk (1988) reports the adaptation of the FLOWEX model (Wind and Van Doorne 1975, Buitendijk 1984) of transient water flow in soils, into a version

applicable to clay soils that suffer cracking, FLOCR. The FLOWEX model simulates one dimensional water flow in soils based on the combination of Darcy and continuity equations. For this approach the soil moisture characteristic curve and the change in hydraulic conductivity with soil moisture needs to be known for the study soil. The adaptation to this model so that clay soils that undergo swell and shrink cycles can be modelled, is to add a third relationship known as the shrinkage relationship. This can be defined as the relation between moisture ratio and void ratio of soil aggregates. To perform a model simulation, information is required of the change in volume due to moisture transport, with certain assumptions for the geometry of the swell/shrink cycle into cracking and subsidence. Information is also required to accurately dynamically partition precipitation falling onto the soil to infiltrate the matrix and cracks allowing the simulation of bypass flow and direct recharge of the water table.

Laboratory quantification of the shrinkage relationship can be undertaken by packing a cylinder with soil and measuring the change in diameter of the soil disk when allowed to dry gradually. In this way the volume ratio of soil: air over a range of soil moistures can be determined. However, the method does not allow the distinction to be made between the proportion of pores that are hydrologically effective from those which do not allow channelling of water. An alternative method involves the use of dyes as tracers to stain those pores that have transported the dye-water in undisturbed soil cores. The continuity and size dimensions of the pores can be determined by cutting thin sections from the core (Bouma and Dekker 1978). Yassoglou *et al.* (1994, p290) confirm that 'field data on shrinking soils are scarce' and measured the size and area of cracks in the field by tracing onto transparent sheets. However this was considered impractical for use in this study.

The importance of soil shrinkage at the study site in terms of soil water movement and evaporation rates were not fully appreciated until late into the project time scale, and experiments to determine the shrinkage properties of the Wallasea soil series of the marsh have not been undertaken. This is identified as a flaw in the research strategy as while the influence of macroporosity over the summer periods can be seen, by the change in the water table at rates faster than the computed hydraulic conductivity through the soil matrix, it cannot be quantitatively discussed. This has implications for the success of modelling the soil profile using BUDGET (section 5.2). BUDGET does not account for seasonal changes in porosity and so only the

drying cycle of the soil can be accurately modelled. Modelling the rewetting of the profile is not successful as recharge of the soil moisture through winter precipitation occurs at all depths due to the preferential flow along macropores. In BUDGET only the surface soil layer becomes wet which can lead to a large error difference between the model output and observed data.

### 3.3.2 Hydraulic Conductivity

An important parameter to determine is the soil hydraulic conductivity in the saturated and unsaturated zones. The hydraulic conductivity was measured in each of the three hydrological subsystems identified from soil analyses (section 3.3.1.2). The soil below a depth of 0.8 m was classified as permanently saturated as the position of the phreatic surface measured by the 1 m piezometers was always above this depth. The hydraulic conductivity of this saturated layer was measured using the Bouwer and Rice slug test (1976, 1989), Equation 3.3. The principles of the Bouwer and Rice test, are discussed in section 3.2.2.1. The soil above 0.8 m depth was classified as the unsaturated zone. The Guelph permeameter was used with Hamm (1998) to determine the field saturated conductivity, $K_{fs}$, at 0.4 m depth. The principles of the Guelph permeameter are discussed in section 3.2.2.3. The Guelph permeameter was also used to determine the infiltration rate through the surface soil.

#### 3.3.2.1 Saturated zone: Bouwer and Rice test (1976, 1989)

There were six occasions when the piezometers 1, 2 and 3 were pumped over 1998-1999. These piezometers were chosen as they contained pressure transducers allowing the recovery rate to be measured continually (section A.4). Table 3.14 details the period of time for each test and the derived value of hydraulic conductivity. The truncation of each monitoring period for each pump test was usually caused by water entering the piezometer nests and flooding the piezometers as it was not possible to cap the pipes due to the cables of the pressure transducers.

The procedure of the test involved pumping out the water in the piezometers and measuring the hourly change with pressure transducers. The value of Ht (position of the water level in the well after pumping) as a function of time t is plotted on semi-logarithmic paper with the former on the log axis. The values of Ho (initial level of

water immediately water pumping) and Ht are taken from the straight line section of the graph, if any, which indicates steady state drainage. Figures 3.6 and 3.7 shows the change in water level after pumping and the selection of data for inclusion in the analysis for one selected test.

The average value of the hydraulic conductivity computed by the Bouwer and Rice pump tests for Elmley Marshes at a depth of 1.5m is $2.77 \times 10^{-5}$ m $day^{-1}$, which is extremely slow within the range published for clay soils (Fetter 1994).

The soil at 1.5 m depth is unripened saline sodic fluid marine clay and therefore not surprising that the hydraulic conductivity of this soil layer is extremely slow. It is also possible that a well skin may have been produced when the piezometers were installed, yielding lower values of K than expected. One of the assumptions of the test is that change in the water table are negligible over the test so that the water table can be considered as a constant head boundary. It is believed that this assumption was been met. However the time taken for the piezometers to respond was lengthy being over a matter of months, and the data selected for inclusion in the test span over a few weeks in most cases. The position of the water table as measured by other piezometers in the vicinity did change however through the natural fluxes of precipitation and evaporation. Over the period of test three the position of the water table fell, while in tests 4-6 the water table was observed to rise. No change in the position of the water table was observed over the remaining tests. The change in water table was gradual however and it is not thought to affect the results of the pump test as the piezometer inlet tip was well below the position of the water table.

Table 3.14. Results of the six applications of the Bouwer and Rice slug method to determine hydraulic conductivity.

| Piezo meter | Period of monitoring | Data period used in analysis | No. of observations (hours) | $H_0$ m Water level at t=0 | $H_t$ (m) Water level at t=t | Value of K m $day^{-1}$ |
|---|---|---|---|---|---|---|
| 1 | 28 Jan - 7 March 1998 | 16 Feb to 7 Mar 1998 | 490 | 0.02 | 0.24 | $5.02 \times 10^{-5}$ |
| 1 | 4-9 April 1998 | 4 to 9 April 1998 | 124 | 0.44 | 0.46 | $2.25 \times 10^{-5}$ |
| 2 | 28 Jan - 6 March 1998 | 30 Jan to 6 March 1998 | 866 | 0.53 | 0.65 | $1.14 \times 10^{-5}$ |
| 1 | 6 July - 24 Nov 1998 | 7 Sept. to 18 Oct 1998 | 1000 | 0.12 | 0.27 | $4.12 \times 10^{-5}$ |
| 3 | 6 July - 24 Nov 1998 | 17 August to 18 Oct. 1998 | 1500 | 0.17 | 0.31 | $2.01 \times 10^{-5}$ |
| 1 | 24 July 1999 - 25 Feb 2000 | 28 Sept to 20 Dec 1999 | 2000 | 0.16 | 0.38 | $1.14 \times 10^{-5}$ |
| | | | | | Average value | $2.77 \times 10^{-5}$ |

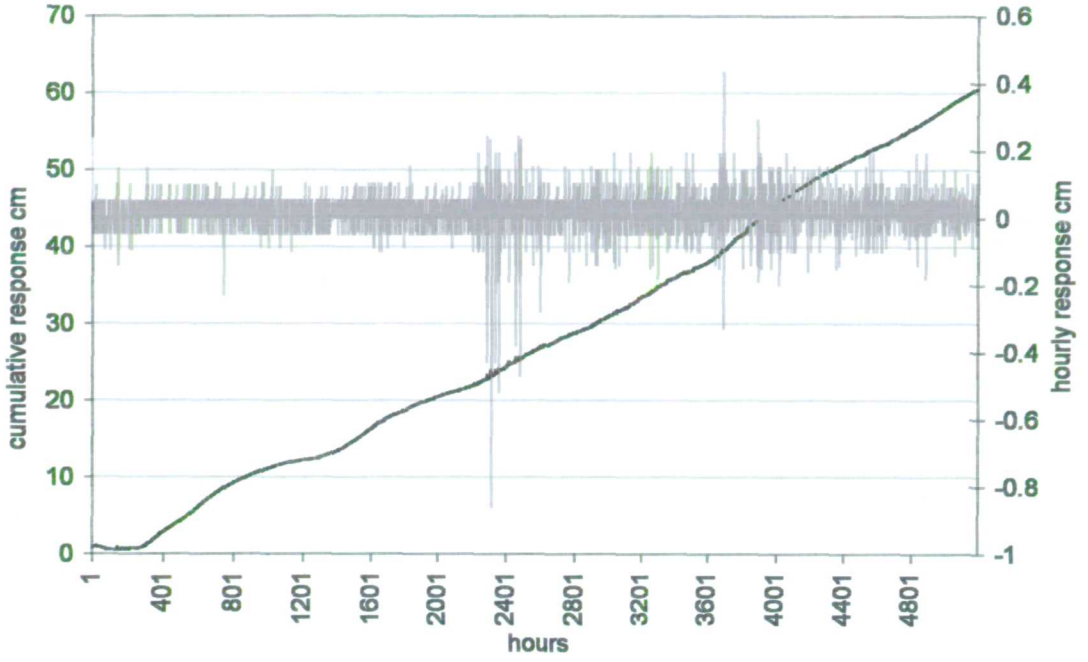


**Figure 3.6. Change in water level (hourly and cumulative) for piezometer 1 after pumping. The time period of the test is 28 January to 7 March 1998.**

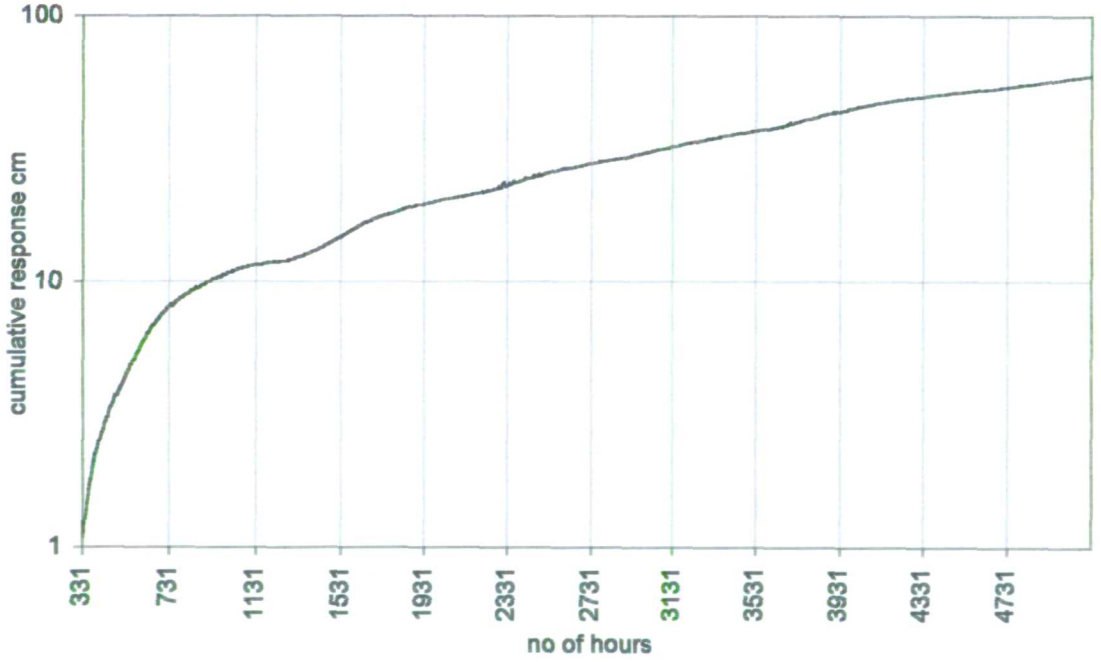


**Figure 3.7. The log transformed cumulative response of the water level in piezometer 1 after pumping (period of test 28 January to 7 March 1998). The hours between 1601 and 3601 were selected for the Bouwer and Rice analysis.**

3.3.2.2 Unsaturated zone: Guelph permeameter and infiltration tests

3.3.2.2.1 Guelph permeameter

Several attempts were made to use the permeameter but problems were experienced with the time taken to achieve steady state flow, smearing of the well surface, and presence of macro-pores such as root channels and animal holes.
One successful test was taken, at depth 0.45 m, after careful preparation of the well hole and having left the permeameter to attain steady state flow for 17 hours before measurements were taken. The assumption of field capacity was taken to enable the estimation of the soil hydraulic conductivity.

In the successful test Hamm (1998) used the single head approach to avoid the use of the simultaneous equations approach (section 3.2.2.3). The single head approach is dependent upon the value of $a$ being independently estimated. The value of $a$ depends upon the porous properties of the soil. Elrick *et al.* 1989 reports studies that show $a$ to be influences by soil structure especially if macropores are present and insensitive to soil texture. The 'Achilles heel' in the single head technique has been identified by Elrick *et al.* (1989 p186) as 'being the choice of $a$'.
Hamm (1998) selected $a$ values from the literature for clay soils of 12 $m^{-1}$ and 4 $m^{-1}$ (Campbell and Fritton 1994, Reynolds and Elrick 1990, Elrick *et al.* 1989). The choice of these $a$ produces values of $K_{fs}$ in the range $1.28 - 2.23 \times 10^{-4}$ m $day^{-1}$. The sensitivity of $K_{fs}$ to $a$ is greatest at low values as used for clay soils. Further, the low value of alpha has an influence upon the value of C. These factors introduce uncertainty into the value of $K_{fc}$ obtained. However the values obtained are in the range expected for clay soils. Table 3.15 lists the results at difference values of $a$.

Table 3.15. Value of $K_{fs}$ as measured using the Guelph permeameter at Elmley Marshes at 0.4-0.5 m depth. The value of the hydraulic conductivity ranges depending upon which value of $a$ is employed in the analysis.

| Value of $a$ $m^{-1}$ | $K_{fs}$ m $day^{-1}$ |
|---|---|
| 12 | $2.23 \times 10^{-4}$ |
| 4 | $1.28 \times 10^{-4}$ |

3.3.2.2.2 Infiltration

Both the terms infiltration 'rate' and infiltration 'capacity' are used in the literature and it is necessary to distinguish between them. The terms should not be used interchangeably as the infiltration 'rate' is a measure of the velocity of water infiltrated over time while the infiltration 'capacity' is the maximum infiltration rate (Hills 1970). Infiltration rates may be less than maximum due to the inadequate supply of water, and the infiltration capacity can change over time due to the ability of the soil to absorb water due to the length of precipitation and antecedent conditions. The infiltration rate can be determined as (Hills 1970):

$$Infiltration\ \ rate = \frac{h_1 - h_2}{t} \qquad \text{Equation 3.12}$$

Where:
$h_1$ is the initial reading
$h_2$ is the subsequent reading
$t$ = time increment

The infiltration rate was determined for the soil of the study area by using the Guelph permeameter to maintain a constant head of water (0.06 m) in an infiltration ring. An 0.11 m diameter infiltration cylinder was used and inserted into the soil to 0.05 m depth and the steady state fall in water level measured over time. Three tests were performed and the rate of change in water level monitored every minute. Soil samples were taken before and after the test to ascertain the change in moisture content.

The cumulative fall in water level over the period monitored was plotted for each of the three tests to ascertain whether steady state conditions had been attained, as indicated by a straight line plot (Figure 3.8). The second test can be considered the most reliable due to the near perfect straight line and similarly test 1 only deviates slightly from a 1:1 line. However the rate of change observed by the third test deviates such that it cannot be considered representative of steady state and has been discarded from further analysis. Results of the cumulative change over time for each test are presented in Figure 3.8, and Table 3.16 lists the values of infiltration obtained.

Table 3.16. Results of the successful infiltration tests in the surface 0.05 m.

| Test | No. of data points i.e. minutes | Average cm $min^{-1}$ | Max cm $min^{-1}$ | Min cm $min^{-1}$ | St. dev. cm $min^{-1}$ | Soil moisture before test | Soil moisture after test |
|---|---|---|---|---|---|---|---|
| 1 | 57 | 0.94 | 1.5 | 0.4 | 0.269 | 13 | 57 |
| 2 | 130 | 0.48 | 1.2 | 0.1 | 0.127 | 16 | 27 |

The infiltration rates computed are in the range of 0.5 to 0.9 cm $min^{-1}$, an equivalent infiltration capacity of 7.0 and 13.5 m $day^{-1}$ which is a considerably faster rate than hydraulic conductivity measurements calculated by the Guelph permeameter and Bouwer and Rice test. The experiments were conducted in the month of July, and the soil moisture of the area before the tests were carried out was low and had increased considerably after the test had ended (Table 3.16). The fast rate of infiltration would be a factor of the high uptake of the soil both as it is dry but also most probably cracked with macropores with a greater surface area available for water uptake (Leeds-Harrison *et al.* 1986). The presence of macropores beneath the infiltration ring would also act to conduct the infiltrating water away quickly after passing through the surface organic layer. Should the tests have continued, a decrease in the infiltration rate would have been expected, as discussed above, due to the reduced ability of the soil to transmit water.

The higher values of infiltration through the surface organic soil contrast with the lower value of hydraulic conductivity in the clay subsoil. These results help explain the occurrence of inundation of the marsh surface. The difference in the ability of the surface soil and subsoil to transmit water leads to surface ponding and inundation in winter. The marsh soil is observed to crack widely and produce fissures in summer through the loss of water by evaporation (Figure 3.5). At the onset of winter rainfall, water is infiltrated quickly through the surface and flows through the macropores and cracks to the water table. The rise of the water table and absorption of water into the soil leads to soil swelling closing the fissures, allowing water to only flow through the soil matrix and remaining macropores such as root channels. Subsequent rainfall leads to surface saturation and water ponding to the reduced transmission of the subsoil.

3.3.2.3 Conclusion for all hydraulic conductivity tests

The values derived from the Bouwer and Rice slug tests and the Guelph permeameter are extremely slow and it is possible at both depths that smearing of soil may have produced a well skin. However the saline sodic nature of the clay at depth would cause very low matrix transmissivity in any case. The values obtained are comparable to other published values for clay soils, however, and so it is thought that the tests have been successful in returning reliable and comparable values of the hydraulic conductivity. Values of $K_{fs}$ are low at 0.4-0.5 m depth but faster than the soil at 1.5 m indicating the influence of structure, salt content and presence of root channels at 0.4-0.5 m on the rate of water movement.

The infiltration results serve to highlight the different structure and texture characteristics of the surface layer compared to subsurface layers as discussed in section 3.3.1. The particular structure and high organic content and porosity values of the surface layer enables rapid flow compared to the unstructured massive clay at lower depths.

### 3.3.3 Soil moisture characteristic curve

The attempt to derive the soil moisture characteristic curve for the soil of the study site was undertaken using four different methods. Attempts to derive the relationship for soil layers to 1 m depth were undertaken using two techniques, the Gupta and Larson (1979) approach as employed by Hamm (1998) based on soil properties derived in the laboratory, and the pressure plate apparatus using sieved samples. The soil moisture characteristic curve was also derived using *in situ* methods for two soil depths. Neutron scattering was used in conjunction with a tensiometer at 0.5 m, and a ThetaProbe and Equitensiometer were buried in the soil in the surface 0.2 m layer. While values of soil moisture and matric potential from neutron scattering and the tensiometer could only be measured on field visits limiting the number of data-pairs obtained, the ThetaProbe and Equitensiometer were wired into the datalogger in the enclosure (Figure 1.3) yielding hourly measurements over the period January 1999 to March 2000. The results for each method are discussed below.

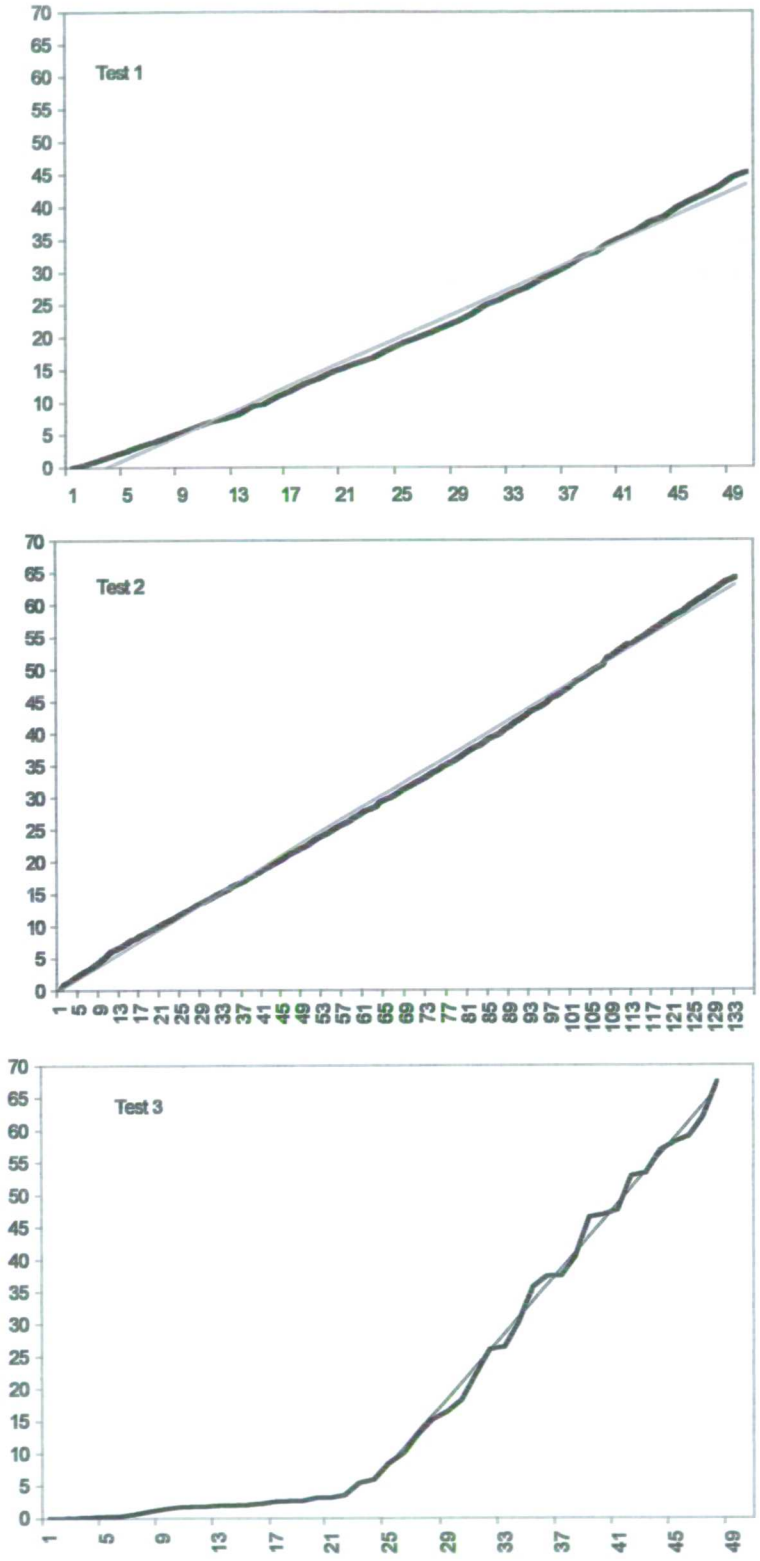


Figure 3.8. Results of the three infiltration tests conducted at the study site. Change in head (y-axis cm) over time (x-axis minute) is expressed cumulatively together with a straight line to assess the steady state response. Note the difference in duration of test 2. Tests 1 and 2 were selected for further analysis.

3.3.3.1 Gupta and Larson technique

The Gupta and Larson model (Equation 3.10) to determine the soil moisture characteristic curve was applied by Hamm (1998) to the study site as it was considered the most robust model from the literaure. The approach is discussed in section 3.2.4.

The model was used to predict the soil moisture characteristic curve to all depths for which the necessary parameters of bulk density, organic matter and particle size distribution were known. The results were compared to observations made by the ThetaProbe and Equitensiometer at depth 0.05-0.15 m below the surface, and to the measurements made at 0.5 m depth by the tensiometer and neutron scattering.
The comparison demonstrated that the Gupta and Larson technique considerably over-predicts the water content at given pressure head up to 30 – 40%. This is explained by Hamm (1998) as pertaining to the unusual soil conditions of Elmley which lie outside the environments in which the technique was constructed i.e. clay fraction greater than 65%, organic matter greater than 23% in the top 0.1 m and sand fraction contributing less than 6%.

Sensitivity analyses show that a substantial increase in the sand fraction, up to 20%, is required to replicate the measured $\theta$-$\psi$ values. However the values of the sand fraction measured in this project and published by Hazelden *et al.* (1986) and Fordham and Green (1980) (Tables 3.5 and 3.6) all report the sand fraction to be less than 5%.
Thus although the Gupta and Larson approach was deemed to be the most appropriate of the published models to be suitable for the conditions at Elmley marsh, it has been found to overestimate the water content and thus should not be employed to derive the SMC curve.

Alternative methods to derive the soil moisture characteristics have been undertaken in response to the findings above. These include the coupled use of the ThetaProbe and Equitensiometer in the surface soil, and the pressure plate apparatus using samples to a depth of 1 m below the soil surface.

3.3.3.2 Pressure plate apparatus

The pressure plate apparatus at Kings College, London was used to derive the soil moisture characteristic curve. A large soil core was taken from the marsh in the enclosure to 1 m depth. The very hard and dry nature of the marsh when the core was taken resulted in extreme difficulty when extracting the soil from the core tubes. Soil was removed from the core tube gradually so that samples were produced approximately every 5 cm. As the soil had been disturbed when removed from the core, it was sieved through a 2 mm mesh before a subsample was packed into the securing rings of the pressure plate to a depth of 1 cm. The number of samples, 22, necessitated the use of two plates; as each run was being performed using half the samples, the other half were left to gain saturation. The Upper Set contained samples from the surface to 0.4 m depth, with the Lower Set had soil from 0.4 to 1 m depth.
Standard procedure was followed, samples were completely saturated by being left to soak in water, weighed and reweighed after time in the pressure plate apparatus. The samples were saturated again, weighed, and subject to a different suction in the pressure plate. This procedure continued over a range of pressures to build up the soil moisture characteristic curve. Great care was taken to minimise loss of samples so that the change in weight after each pressure run was due to the change in moisture content alone. The samples were left for a minimum of 48 hours in the pressure plate apparatus in order to establish equilibrium. At the end of the investigation the sample were oven dried to achieve a dry soil weight so that moisture content at each pressure applied could be determined.

3.3.3.2.1 Problems using the pressure plate apparatus

Many logistical problems were encountered when using the pressure plate apparatus. The most important of these in influencing the results of the experiment are threefold and interlinked.
Firstly, it was difficult to maintain the required pressure over the 48 hour period of each experiment. The pressure initially set would decrease by the end of the experiment run, for example a pressure set at 600 kPa fell to 140 kPa (Table 3.17). On two occasions the pressure actually increased from 500 to 600 kPa, and from 200 to 400 kPa. On the occasions when the pressure was found to have fallen, the

pressure was reset to initial values for at least 20 minutes to ascertain whether the soil sample had equilibrated at the initial or fallen pressure. This was determined by the response observed in the outflow burette. It seemed that although a rush of air bubbles followed the change in pressure, it was difficult to ascertain whether water entered the burette. From this it had to be assumed that the samples reached equilibrium at the pressure shown at the end of each run.

The second logistical problem was that it is thought that the plates employed in the analysis leaked to some extent i.e. they were not completely sealed or free from cracks. Of the number of plates available for use, two were selected, which seemed in best condition with intact seals and no observable fractures. When used in the apparatus the observed rush of large air bubbles into the outflow burette did not follow manual guidelines. In addition to this, it was difficult to determine whether equilibrium had been established due to these air bubbles, the third logistical problem. One set of samples was maintained at pressure for one week, as an investigation into the length of time required to establish equilibrium. Air was still bubbling after a week, but it seemed little water entered the outflow burette after 48 hours and so it was decided this was the time period to be used thereafter. The air bubbles were believed to be caused by minute fractures in the plate itself, or its seal, allowing air to penetrate the plate. Such problems were caused by the age of the plates, approximately 20 years, though these were the plates in best condition and there were no resources available to replace them.

Despite these problems it was the intention to derive the soil moisture characteristic curve as best as could be achieved, over a range of pressures using the pressure plate apparatus, as samples to a depth of 1 m could be used in the analysis. However, the compressor of the apparatus developed a fault, which resulted in the cessation of the experimental runs due to the uncertain length of time required for the problem to be fixed. Only a small number of runs had been undertaken before the malfunction of the compressor allowing the soil moisture characteristic curve to be derived for a narrow range of pressure, 100-600 kPa. Table 3.17 lists the problems experienced using the pressure plate for each pressure run.

3.3.3.2.2 Results

The results are presented in Table 3.18 and Figure 3.9. The results are presented as averages per 0.1 m layer. The results and difficulties experienced with the apparatus cause concern over the reliability of the results of the pressure plate apparatus. The response of the soil is stratified by depth indicating the influence of changing soil properties down the profile. It can be seen that the moisture content of the samples do not uniformly decline with increasing pressure but fluctuate; moisture declines from 40 to 130 kPa but then increase to 200 kPa, decrease to 430 kPa and finally increase to 600 kPa. Further there is uncertainly over the true pressure to which the soil samples established equilibrium. It has to be concluded that the results obtained by the pressure plate apparatus are unreliable and unrepresentative of the soil moisture characteristic curve of the Wallasea soil series of the study site due to the logistical problems encountered, and will not be employed in further analysis.

3.3.3.3 Neutron scattering and tensiometer

Two tensiometers (Soil Test) were inserted in the main enclosure in early April 1998 at depths of 0.3 and 0.5 m next to the neutron scattering access tubes in the enclosure. Difficulties were experienced with the shallowest tensiometer due to a faulty 'o' ring seal which caused the tensiometer to rust and consequently no data were obtained. There were problems also with the tensiometer at 0.5 m depth but after rehabilitation suction was established. However problems were experienced again in September 1998 and the tensiometer was again removed for maintenance. Suction was re-established when reinserted into the soil. Unfortunately the condition of the tensiometer left *in situ* over the winter of 1998/1999 deteriorated with the pressure gauge filling with water and rusting. The tensiometer was rehabilitated but rusting caused further problems and was finally was removed. Data collection ceased due to the unavailability of more tensiometers.

Attention focused instead on taking samples for use in the pressure plate apparatus, which would enable an assessment of the soil moisture characteristic curve for the whole profile at regular specified pressures. However the unsuccessful use of the apparatus has necessitated the examination of the tensiometer dataset and the attempts to generate a soil moisture characteristic curve of the profile for reference purposes.

Table 3.17. The problems experienced using the pressure plate for each pressure experimental run and upper and lower sets, shown in order of pressure not procedure.

| Set pressure kPa | Problems |
|---|---|
| 100 | Pressure slipped for both sets; lower set fell to 40 kPa. A power failure occurred in the building during the run with the upper set resulting in this data being rejected. |
| 150 | Pressure slipped for both upper and lower sets to 80 kPa. |
| 200 | Lower set pressure stayed constant but the seal on the plate had perished at the end of the run and the compressor had developed a fault, ending the use of the equipment. |
| 300 | Pressure slipped for Lower set to 20 kPa. |
| 430 | Upper set pressure, originally fixed at 200 kPa, increased to 430 at the end of the run. |
| 500 | Lower set pressure originally fixed at 500 kPa increased to 600 kPa at the end of the run. |
| 600 | Pressure slipped for upper set to 140 kPa. |

Table 3.18. Results of the soil moisture characteristic curve with depth. Values were derived using the pressure plate apparatus at Kings College, London. Only a few pressure runs could be made before the malfunction of the compressor.

| Set | Depth of sample m | Soil moisture % at given pressure kPa | | | | | |
|---|---|---|---|---|---|---|---|
| | | 100 | 150 | 200 | 300 | 500 | 620 |
| Set B | 0.0-0.1 | 36 | 37 | 33 | | | 36 |
| | 0.1-0.2 | 38 | 30 | 24 | | | 35 |
| | 0.2-0.3 | 56 | 39 | 31 | | | 42 |
| | 0.3-0.4 | 66 | 44 | 34 | | | 46 |
| | 0.4-0.5 | 60 | 41 | 39 | 50 | 51 | 51 |
| Set A | 0.5-0.6 | 67 | 48 | 46 | 55 | 52 | 52 |
| | 0.6-0.7 | 75 | 51 | 55 | 63 | 58 | 58 |
| | 0.7-0.8 | 86 | 64 | 64 | 72 | 69 | 69 |
| | 0.8-0.9 | 89 | 66 | 68 | 73 | 73 | 73 |
| | 0.9-1.0 | 68 | 48 | 43 | 55 | 57 | 57 |

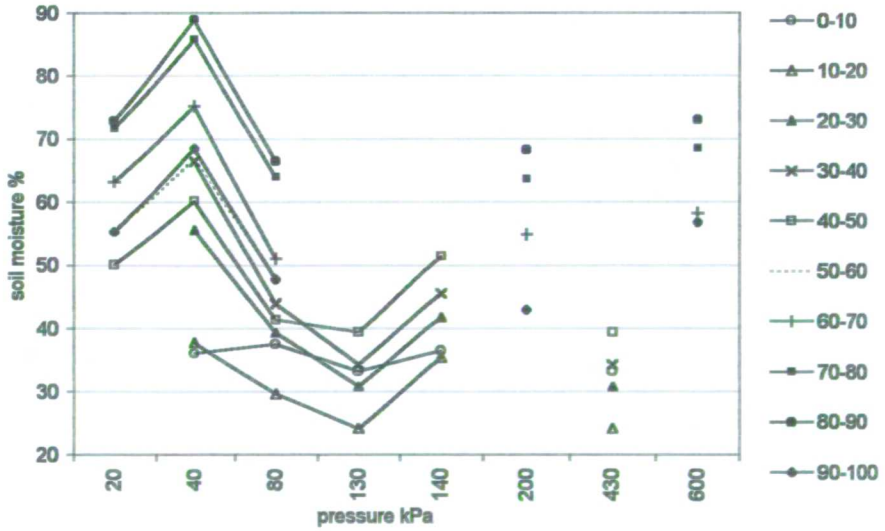


Figure 3.9. Change in soil moisture with pressure at different depths derived from pressure plate apparatus.

Matric potential observed from the tensiometer, on field visits over the period May to October 1998 when the instrument was operational, were coupled with soil moisture data measured by neutron scattering in the access tubes in the enclosure (section A.5). Figure 3.10 and Table 3.19 present the data obtained from the tensiometer against soil moisture averaged from the surface to 0.80 m depth. It can be argued that the pairing of suction data to a soil moisture measurement taken at the same depth of the soil has a more theoretical basis than using an average of the soil profile. However the average can be justified by the fact that the value of moisture content generated from neutron scattering is not a 'point' measurement but based on a 'sphere of influence' around the particular depth measured, and that this sphere increases with decreasing soil moisture. The relationship as originally derived for average soil moisture of depth 0-0.65 m as neutron scattering data indicated negligible loss after this point. However soil sampling in 1999 exhibited soil desiccation to a depth of 0.8 m. In order that a derived relationship is applicable to both years, the average soil moisture to 0.8 m depth was paired to observation of matric potential from the tensiometer.

Both Russell (1980) and Sceicz and Long (1969) derive relationships for the matric potential with water content averaged over a certain depth of the soil profile. Sciecz and Long (1969) justify this as surface resistance is mainly affected by leaf potential, which is governed in turn by the soil water potential in the top layer, as water extraction by plant roots begins at the surface progressing downwards as the soil dries (Rawlins *et al.* 1968, Gardner 1983). Russell adds that although $\psi$ varies down the profile, most of the roots are located in the surface, using the potential in the upper layers (in his case at 0.3 m depth below the surface) constitutes a 'good index'. The range of soil moisture over which matric potential varies is increased, as the lower values at the surface are incorporated into the measurement.

During May, values of matric potential fluctuate around 0 to -40 kPa from 37% to 32% volumetric soil moisture. With further soil moisture decline the matric potential increases to –450 kPa at 27% moisture content, and –680 kPa at the lowest soil moisture recorded of 25%. There is fluctuation at matric potentials greater than -600 kPa leading to uncertainty; the lack of measurements causes confusion over the value of matric potential at this moisture content. The soil had rewetted by October with a

value of –10 kPa at 29% moisture which is similar to the observation on 17 June which had experienced rewetting, indicating a possible effect of hysteresis.

Table 3.19. Matric potential data from the tensiometer inserted at 0.5 m depth. Soil moisture has been averaged over the soil profile to 0.80 m depth using data from the electrical resistance blocks as well as the two neutron access tubes data.

| 1998 | Matric potential kPa | Soil moisture % 0 - 0.80 m |
|---|---|---|
| 9 May | 0 | 37 |
| 11 May | 0 | 34 |
| 26 May | -40 | 32 |
| 17 June | 0 | 29 |
| 23 June | -130 | 29 |
| 7 July | -450 | 27 |
| 15 July | -670 | 27 |
| 21 July | -630 | 26 |
| 5 August | -680 | 25 |
| 22 October | -10 | 29 |

3.3.3.3.1 Relationship

Ten data pairs were collected over the period May to October 1998, and all taken over the drying cycle of the soil except two (17 June and 22 October 1998) which were taken as the soil was in the process of re-wetting. The hiatus in measurements between August and October was due to the removal of the tensiometer for renovation. The lack of measurements hinder further analysis; for the soil moisture characteristic curve to be derived in this way, a much larger dataset should be compiled with soil moisture monitored over a larger range of pressures over both drying and wetting cycles.

While the derivation of the soil moisture characteristic curve for the surface soil has been successful, there is a need to derive a matric potential for the soil profile as a whole due to difficulties experienced with the pressure plate apparatus. While the soil moisture characteristic curve for the profile cannot be reliably constructed from the few data-pairs available from the tensiometer and neutron probe (and electrical resistance blocks in the surface layers, section 5.1.1), it can provide reference values to indicate the relative magnitude of the matric potential at a given soil moisture. This

is of use in the second research investigation (Table 1.1 and Chapter 6).

The relationship between soil moisture and matric potential has been described in the literature by different functions, common ones being power (Gardner *et al.* 1970, Campbell 1974) or exponential functions (Brooks and Corey 1966). There is no agreed consensus in the literature over the form of the soil moisture characteristic curve due its shape and range being dependent upon soil textural factors. It was found when the $\theta\psi$ (average 0-0.8 m depth) data listed in Table 3.19 were subject to a power curve, there was considerable overestimation of the matric potential at high soil moistures and underestimation at low moisture content. Good fits were found both by the approach by Gregson *et al.* (1987), and the semi-logarithm fit by Williams *et al.* (1983), but when extrapolated outside the moisture range of the data, $\psi$ was considered too high at $\theta$=22% (the lowest value recorded of soil moisture average 0-0.80 in 1999). This decision is speculative however due to the lack of data.

A better relationship was found by the two-part function approach suggested by Hutson and Cass (1987), who adapted an exponential relationship to a parabolic form at high soil moistures. The two-part function is applicable at all water contents removing any allowance made with other models for the air entry potential. The observed data have a point of inflection at $\theta_1$ where the shape of the curve changes. This is represented in the two-part function as the switch between curves. It was found that the curve that best represented the data from the Wallasea soil series was a function that coupled a parabolic form to a rational function, thus the former function is applied at moisture contents above $\theta_1$ at 26.7%, with the switch to the latter below this threshold. The resulting curve is displayed in Figure 3.10 against the observed data with error bars of the fitted curve computed to the 95% confidence level. Details of the measurement error for the fitted function are displayed in Table A.10 in Appendix A.

For $\theta > \theta_1$ $$\psi = \frac{a\left(1-\frac{\theta}{\theta_s}\right)^{0.5}\left(\frac{\theta_1}{\theta_s}\right)^{-b}}{\left(1-\frac{\theta_1}{\theta_s}\right)^{0.5}}$$ Equation 3.13

Where:

$\psi$ is matric potential kPa (expressed as positive)
$\theta$ is volumetric soil moisture %
$\theta_s$ is the saturation moisture content at 34%
The constants a and b have the values 6 and 19 respectively

For $\theta < \theta_1 \quad \psi = \dfrac{a + b\theta}{1 + c\theta + d\theta^2}$ Equation 3.14

Where the constants a, b, c, d have the value –2457.09, 87.55, 0.046, and –0.0028 respectively

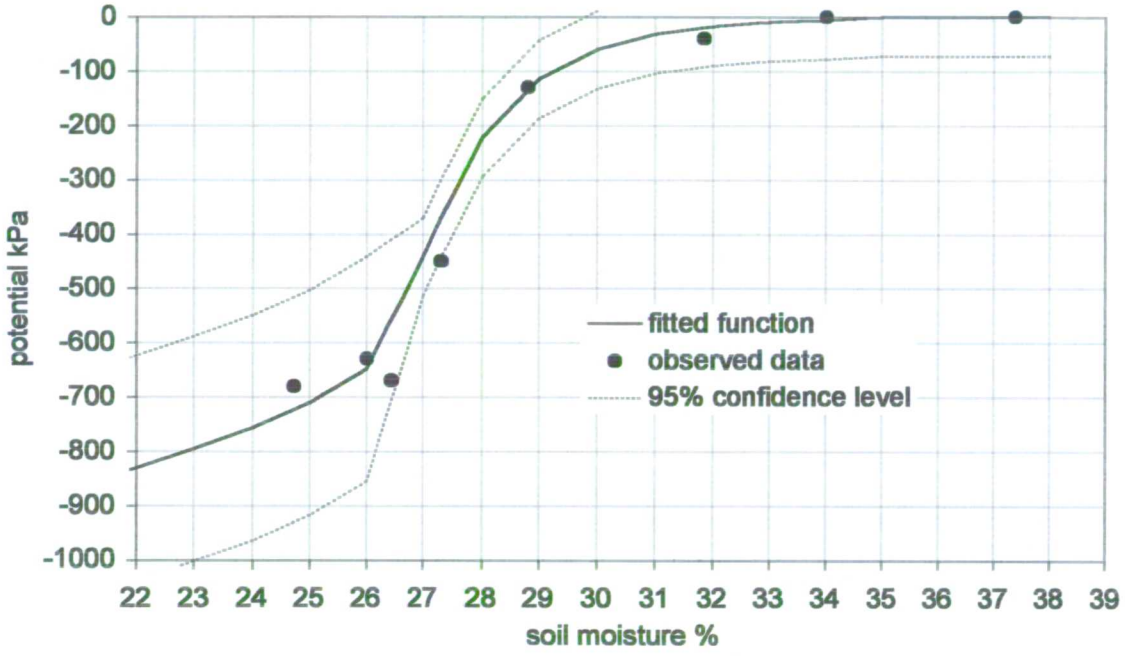


Figure 3.10. The $\theta\psi$ relationship for moisture conditions averaged over 0.80 m depth observed with the neutron probe and tensiometer. The correlation co-efficient for both functions is very strong at $r^2$=0.99. The dashed lines represent the 95% confidence interval of the two-part function, which are wide due to the small dataset upon which the regression was determined.

### 3.3.3.4 ThetaProbe and Equitensiometer

The derivation of the soil moisture characteristic curve for the surface soil layer was more successful using the ThetaProbe and Equitensiometer. These two instruments were buried in the marsh soil and connected to a datalogger in January 1999 to yield continuous hourly measurements of soil moisture and matric potential (section A.7). In this way the relationship is derived *in situ* over both the natural drying and wetting cycle of the soils allowing an assessment of the degree of hysteresis for the surface

organic layer.

Hourly paired measurements of soil moisture and matric potential over January 1999 to March 2000 were subtotalled to generate daily averages. This dataset was then processed to remove those data pairs that did not have a valid reading of matric potential. This occurred when the voltage output of the Equitensiometer exceeded its factory calibration range to convert to values of matric potential and happened frequently over the summer period of 1999 when the ThetaProbe registered values of soil moisture of 10-11%.

Figure 3.11 shows the result of deriving the soil moisture characteristic curve with the ThetaProbe and Equitensiometer. The data has been split to show the drying and wetting cycles to highlight hysteresis. This was achieved by distinguishing the periods of data when the soil was drying, March to June 1999, and when the soil was wetting, December 1999 to March 2000. The period when fluctuations were observed in the value of soil matric potential but the soil moisture remained constant at 10-11%, June to November 1999, was also identified.

The drying curve is very smooth compared to the wetting curve and a distinct difference, hysteresis, between the curves can be seen. The fluctuating values of matric potential at soil moistures of 10-11% are due to short rainfall events and are illustrated in Figure 3.12. It would be expected that a similar level of fluctuation is observed in the ThetaProbe also but this is not the case and gives rise for concern. The range of pressure over which the Equitensiometer fluctuates is considerable with pressure reducing from values outside the range of the instrument (displayed on the chart as -10000 kPa for illustrative purposes only) to -90 kPa as the soil temporarily wets after the input of water by precipitation. The lack of response of the ThetaProbe over this period has been discussed in section A.9 and the values of soil moisture compared to other those obtained by other methods in the surface soil layer (electrical resistance blocks, SCIP and soil sampling). Between June and September 1999 the values of soil moisture output from the ThetaProbe was comparable to values obtained by other methods (Figure A.14) although there is an absence of fluctuations as observed by the Equitensiometer. From September to December 1999 however the other methods all show an increase in soil moisture, which is not observed by the ThetaProbe. It is believed that the lack of change in the output of the ThetaProbe from June to December 1999 was due to a loss of contact between the pins of the ThetaProbe and the soil into which it is embedded through soil shrinkage. The

presence of air pockets, however small, around the pins causes the probe to output values of soil moisture lower than it would be in the absence of air pockets. The ThetaProbe started to respond in a 'normal' or expected manner from mid December, possibly due to winter rainfall causing the soil to wet-up and swell so that full contact was re-established with the pins. Thus the fluctuations recorded by the Equitensiometer over the summer 1999 in response to precipitation are presented in Figure 3.12 to indicate the nature of soil behaviour under such irrigation events in terms of suction pressure, but the values cannot be used in the interpretation of the soil moisture characteristic curve due to the unreliable values of soil moisture over the same period.

It can be seen from Figure 3.11 that for the drying limb of 1999 suction is first recorded at 43% and that at -30 kPa, the constant of field capacity, the soil moisture is recorded at 41% over the drying curve. Similar values are recorded for -30 kPa on the wetting curve also. These values are higher than the value of 32% recorded at 40 kPa using the tensiometer (moisture average of the upper 0.8 m). This is to be expected for the surface layer due to its peaty characteristics enabling an enhanced water holding capacity.

The soil continues to dry to a value of 15% at pressure -700 kPa. Much data output of the Equitensiometer had to be rejected as the values were outside the upper calibration limit i.e. exceeded –1000 kPa; this is the reason for data range of 0 to –1000 kPa rather than to the wilting point 1500 kPa in Figure 3.11. The minimum value of soil moisture recorded over the summer period from the electrical resistance blocks was in the order of 7-8 % and it is believed that the soil moisture over the range –1000 to -1500 kPa would not fall further than these very low moisture contents. Thus it is estimated that the soil moisture would decline further from 10 to 7% to -1500 kPa, the wilting point constant.

The rewetting of soil over winter 1999 exhibits hysteresis i.e. the moisture characteristic curve differs from the drying limb, with a suppressed magnitude of potential relative to the drying curve over a soil moisture range of 12-50%.

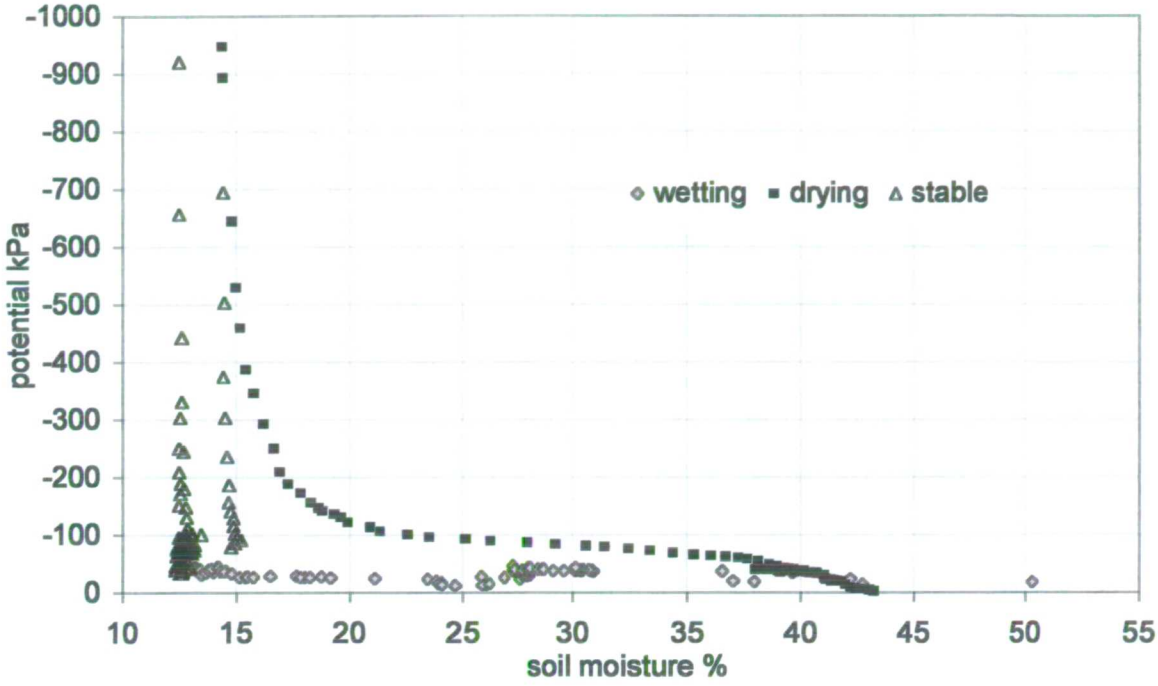


Figure 3.11. The θψ relationship of the surface soil observed with the ThetaProbe and Equitensiometer. The graph is displayed to highlight hysteresis of the drying and wetting limb and period of stable soil moisture.

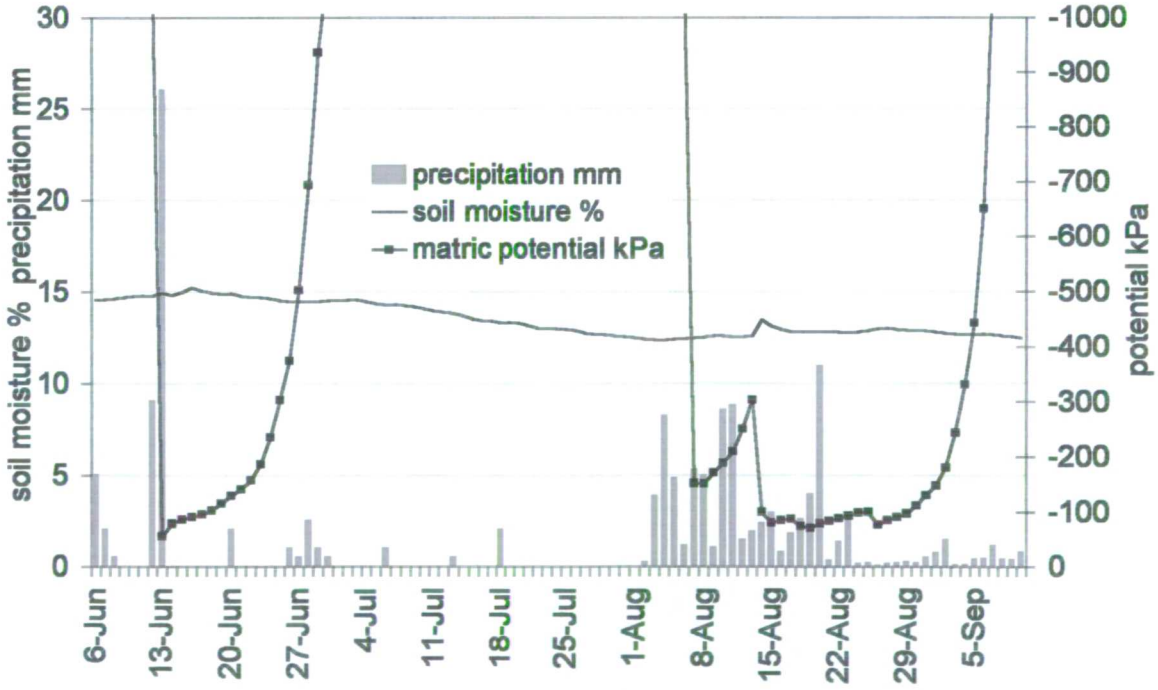


Figure 3.12. Fluctuation of matric potential (measured by an Equitensiometer) and steady response of soil moisture (measured by a ThetaProbe) caused by precipitation events over summer 1999. The upper range of the Equitensiometer calibration is –1000 kPa.

3.3.3.4.1 Relationship

The soil moisture characteristic curve of the surface soil was measured *in situ* using 185 data pairs (excluding the period of fluctuating potential but steady moisture) derived from computing daily averages of matric potential and soil moisture datapairs from the instruments (logged hourly) and clearly illustrates the change in soil moisture with pressure and the degree of hysteresis. The soil moisture characteristic curve should be monitored in this way over a number of wetting and drying cycles to establish the natural variability of the relationship.

Attempts were made to fit a function to the drying limb data so that soil potential may be predicted from moisture values. Following the approach of Hutson and Cass (1987), it was found that a two part function best described the data. The fitted curve employs a third degree polynomial (Equation 3.15) and a rational function (Equation 3.16) with the point of inflection between the two curves at 25%. Thus the former is employed to predict potential at moistures between 43% to 25%, and the latter below this threshold to a minimum moisture volume of 14.5% after which the curve diverges. Correlation coefficients are high within the specified soil moisture ranges with $r^2$ above 0.99 for both functions. The function is displayed against observed data in Figure 3.13. Details of the measurement error for the fitted function are displayed in Table A.11 in Appendix A.

When $25 > \theta < 43$:

The third degree polynomial:

$$\psi = a + b\theta + c\theta^2 + \theta x^3 \qquad \text{Equation 3.15}$$

Where:
$\psi$ is potential in kPa
$\theta$ is volumetric moisture content %
and the constants a, b, c, d have the value -565.51, 45.18, -1.48, and 0.02 respectively.

When $14.5 > \theta < 25$:

The rational function:

$$\psi = \frac{a + b\theta}{1 + c\theta + d\theta^2} \qquad \text{Equation 3.16}$$

Where:
the constants a, b, c, d have the value $3.03x10^9$, $-2.75x10^8$, -2214048.8, and 156833.3 respectively.

### 3.3.3.5 The derived relationship for the soil moisture characteristic curve

Figure 3.14 displays the fitted soil moisture characteristics curve for the surface soil and layer 0-0.8 m deep from saturation to a maximum of –1000 kPa. Note that while a good relationship has been derived from the tensiometer results to determine the matric potential at a given moisture content of the profile, it must be stated that this provides a reference only due to the few data pairs available, especially at low soil moistures.

The surface layers are saturated at 42% and experience a gradual decrease in matric potential to 100 kPa at 22%. After this point potentials increase rapidly with further moisture loss to –1000 kPa at 14%. The deeper layers fall below saturation at 34% and attain a potential of –100 kPa at 29%, much faster than the surface layers. The curve becomes more steep reaching a value of –700 kPa reached by 25%, after which the slope become less steep attaining a value of –1000 kPa to 17%. It can be seen that shape of the two curves exhibits a marked difference and serve to highlight the distinct difference in texture structural and other soil characteristics between the surface and rest of the soil profile.

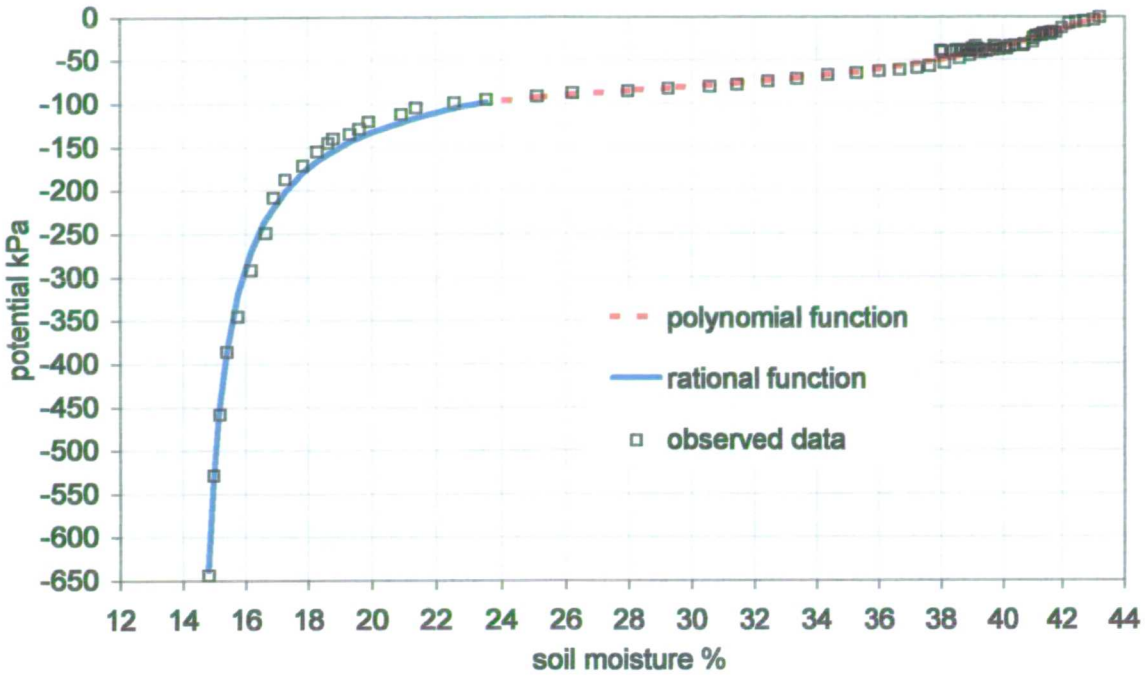


Figure 3.13. The two-part soil moisture characteristic curve fitted to the $\theta\psi$ observations of the surface soil. The change from the polynomial to rational function occurs at the intercept at 24% moisture content. Confidence intervals are not shown for clarity as they are very close to the values of fitted function (7 kPa and 26 kPa for the polynomial and rational function at the 95% confidence interval).

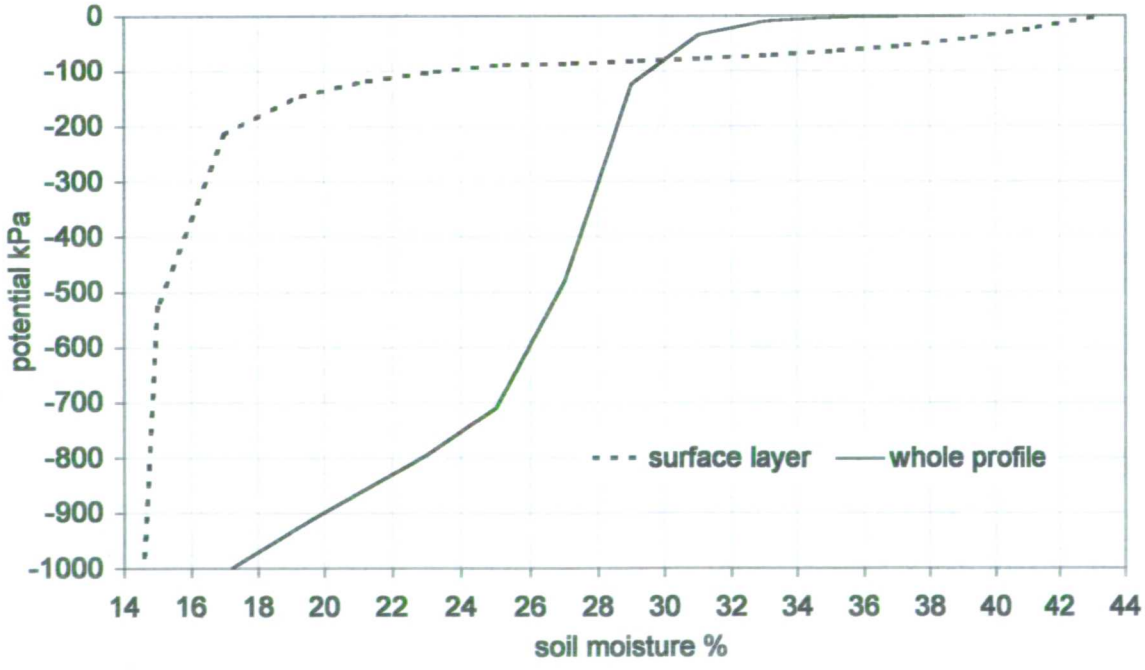


Figure 3.14. The two derived functions of the soil moisture characteristic curve for the surface soil and the whole profile from 0-0.8 m depth.

# Chapter 4 Ditch water: soil water relationships. Part 2: Soil Hydraulics

This chapter continues from Chapter 3 to present research results and analysis for Research Question 1: *What is the relationship between ditch water levels and the water table and soil moisture in the adjacent field?* In this chapter can be found the results of monitoring the water table and ditch stage, and modelling performed to quantify and predict the relationship between ditch water levels and the position of the water table, and recharge fluxes. The water table is modelled using the Dupuit-Forchheimer approach and also using the DITCH model, Drain Interaction with Channel Hydrology. Appendix A contains details pertinent to this chapter relating to the design and layout of the piezometers and stageboards (section A.3) and precipitation from the Automatic Weather Station (section A.1.5).

This chapter is organised into the following subsections:

- Relationship between the water table and potentiometric head (section 4.1) and the relationship between ditch levels and saturation in the soil, over piezometer transects west to east and north to south.
- Dupuit-Forchheimer analysis (section 4.2).
- Discussion of the DITCH model, simulation of the water table of the study area, and computation of the ditch recharge and discharge functions (section 4.3).

Chapter 5 details moisture monitoring of the soil profile and the results of modelling together with an investigation into the spatial and temporal change in surface soil moisture.

## 4.1 Results of monitoring water table and ditch water levels

### 4.1.1 Relationship between the water table and potentiometric head

The piezometer layout (Figure 1.3) and construction is detailed in section A.3.2; in brief each piezometer site possesses a nest of three piezometers (Figure A.7) at depths 1 m, 1.5 m, and 2m. The water level in piezometers represents the potentiometric level created by the hydraulic head or hydrostatic pressure at the screen of the pipe. In unconfined aquifers with homogenous properties this should equal the phreatic

surface or water table. There were initial concerns over whether the water levels in the piezometers at the study site represented the water table due to two factors. Firstly, the actual water level and response differed between the different depths of piezometers, leading to uncertainty over which piezometer best represented the water table (Figure 4.1). Secondly, the results of soil sampling and pump tests revealed an inhomogeneous soil system with depth and that the screen of the piezometers is sunk into the blue/grey unripened clay suggesting locally confined conditions.

The difference in water level between piezometers of different depths indicates heterogeneity with depth of the saturated zone. The water levels in the 2 m piezometers (Figure 4.1c) exhibit no seasonal change but steadily rise over the monitoring period. This trend is unrepresentative of the seasonal change in water level as shown by the 1 m and 1.5 m piezometers (Figure 4.1a and b). These piezometers exhibit similar values but consistent differences of up to 0.2-0.3 m are apparent, with a lower water level always recorded in the 1.5 m piezometers representing the dominance of downward gradients. It was decided to employ the data from the 1 m depth piezometers to indicate the position of the water table of the study field.

The relationship between the piezometer water levels and the water table needs to be clarified so that it can be stated that the potentiometric level of the piezometer equates the phreatic level. The relationship is ascertained by linking the position of the potentiometric head with the point at which soil saturation occurs. Figure 5.1 shows that there is no change in soil moisture measured by neutron scattering at depths greater than 0.7 m (1.36 m O.D.). The soil moistures at this point are within the range of 40-50%, which accords to saturation (Figure 3.3). Figure 4.2 shows the potentiometric level measured from the piezometer site B at a distance of only 20 m from the main enclosure. A decrease is seen over the monitoring period of April to October 1998 (the monitoring period of the neutron probe) to a minimum value of 0.74 m below the surface (1.12 m O.D.). This depth tallies with the measurement of saturated soil from neutron scattering in the main enclosure. Further, the soil moisture measurements start to show a gradual decline from May until September when the moisture levels then recover. This trend is mirrored by the potentiometric level that fell from the surface to 0.34 m below the surface (1.52 m O.D.) from late April to early May and continued to decline to 0.74 m before recovering.

a:

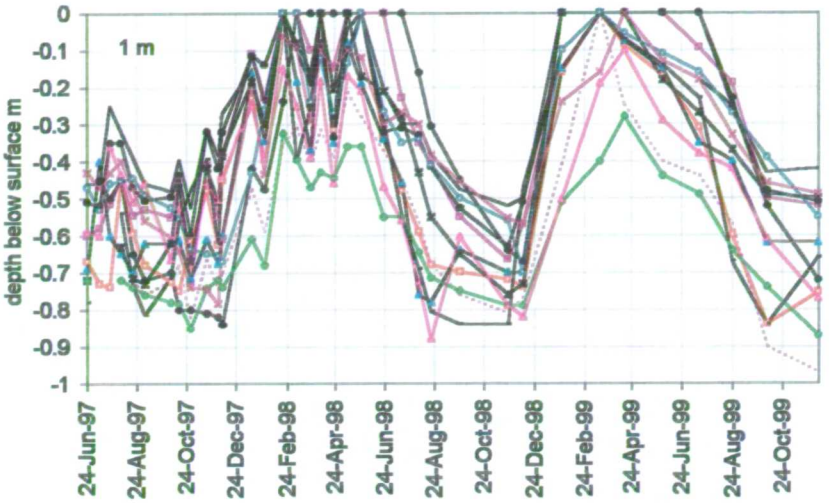


b:

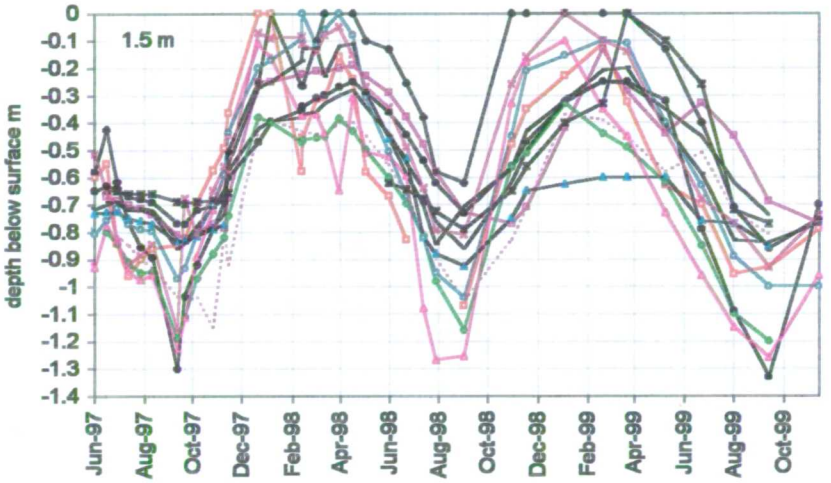


c:

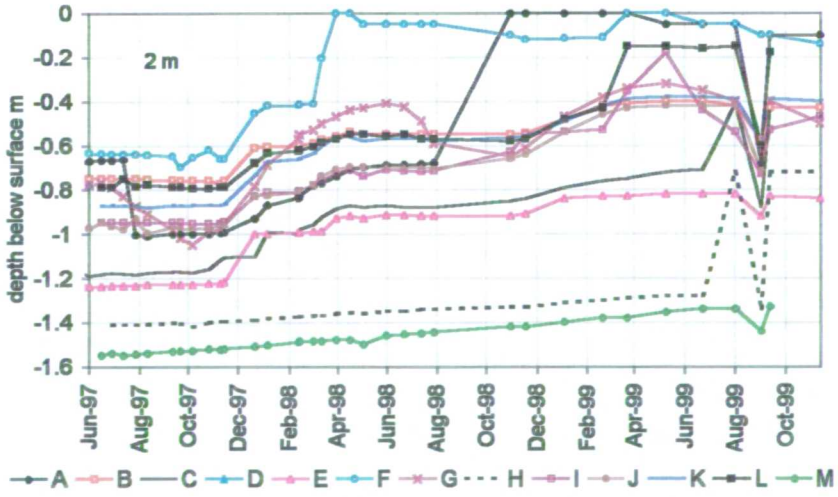


Figure 4.1. Water level change in the transect piezometers A-M over the study period at a: 1 m, b: 1.5 m and c: 2 m depth. See Figure 1.3 for their location within the study field. Water levels are relative to the surface.

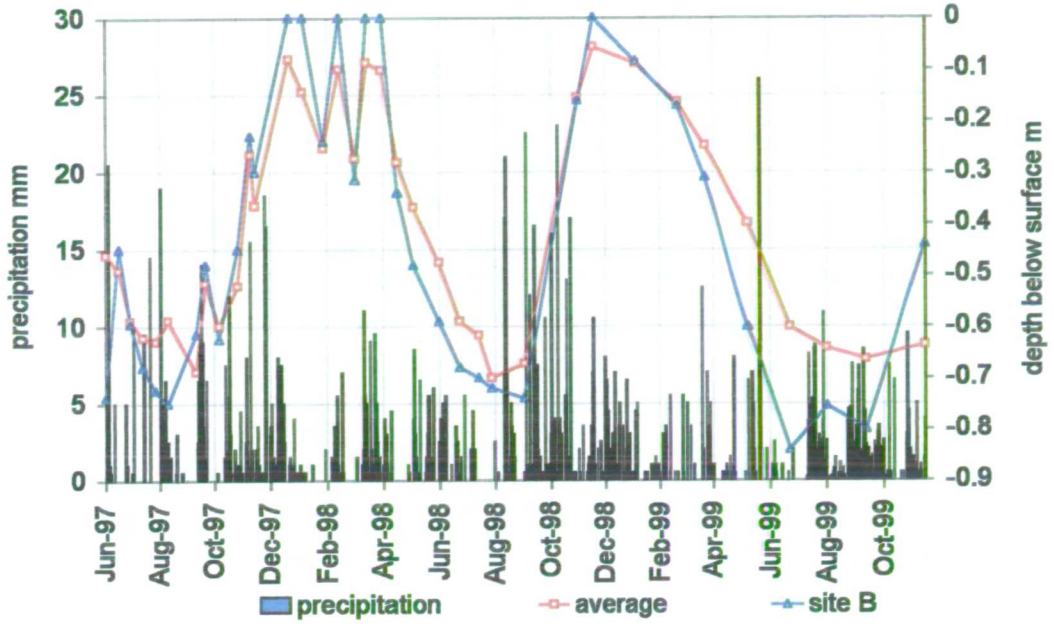


Figure 4.2. Water level change in the transect piezometer B at 1 m and the average change at 1 m depth over the study period expressed as depth below the surface. The daily precipitation totals are expressed to illustrate the effects upon the groundwater level.

These results illustrate the potentiometric level measured in the 1 m wells does equate with the phreatic surface and so the water levels in these piezometers can be used to point to the position of the water table over the marsh. The term water table will be subsequently used in the text when referring to the water level in the 1 m piezometers.

### 4.1.2 Overall trend of the water table

Figure 4.1a illustrates the change of the water table as measured in all 1 m transect piezometers in the study field. The rise and decline of the water table closely follows the pattern of precipitation. The water table is positioned at 0.5-0.8 m below the surface, 1.4-0.8 m O.D., declining to 0.6 to 0.9 m depth by October 1997. The water table then rises to the surface by January 1998 and fluctuates within 0.2 m of the surface until mid April when a steady decline is observed to the summer low of 0.6 to 0.9 m depth from August to September 1998. The water table then rises rapidly to the surface throughout December 1998 to January 1999, before falling to 0.5 to 0.9 m depth the surface by late July 1999. After this point most sites exhibit further decline until September and show recovery to the end of monitoring in December 1999. It

can be seen that in additional to a marked seasonal flux there is also a spatial difference between the piezometer sites up to approximately 0.4-0.5 m.

Figures 4.1a and 4.2 show that the decline of the water table over the time period studied is a gradual process. For example the decline of the water table measured in piezometer B from 0.34 to 0.74 m below the surface took place over 138 days over May to September 1998. These results confirm the calculation of slow hydraulic conductivities for the Elmley Marshes controlling the loss of water (section 3.3.2) although soil cracking would enable water to be lost at rates faster than the hydraulic conductivity. Rapid change following heavy precipitation (Figure 4.2) however characterises the recovery of the water table when water levels in the 1 m piezometers rise from 0.4 m depth to the surface. Again using the data from piezometer B, only just over half the time, 77 days, is required to replenish the water table from the low of 0.74 m depth to the surface over September to December 1998. As this rate of recharge is faster than the rate of the hydraulic conductivity, it points to the presence and importance of macropores in water movement. Such pronounced temporal changes due to macropores are indicative of bypass flow (Baird 1995), and suggest that traditional Darcy flow based models of water movement would be subject to errors in this environment, especially after dry spells when macropores flow predominate.

Further, it can be seen that the average water level of all 1 m depth piezometers, Figure 4.2, reaches the surface for example by January 1998, drops by February before coming back to the surface by early March. The water table again falls by late March before coming to the surface in April 1998. This pattern directly matches that of precipitation. Baird (1995, p123) also noted this phenomenon in a clay alluvial groundwater gley under permanent pasture, similar to the Wallasea soils series of the Elmley Marshes, and suggested possible reasons for the temporal change in response rate and fluctuation of the water table at the surface:

> 'First the autumn response could be more rapid because of crack flow which is [then] reduced by swelling of the soil and partial closure of the larger voids and cracks as the soil wets up fully. Secondly if the clay had not re-wetted fully in the autumn then it is possible that the fall of the water table was due to absorption of water into the soil peds as well as drainage to the ditch'.

The formation of large cracks in the soil through shrinking due to soil moisture loss, together with bioturbidation by ants and burrowing animals for example creates

macropores and cracks which can transport water to depths at faster rates than water moving through the soil matrix. Such cracks are a common observation at the study site (Figure 3.5). Soil swelling (section 3.3.1.10) due to soil moisture gain in winter is slow allowing the transportation of water through the macropores for a considerable period of time. Water is redistributed through the soil profile both from infiltration from the surface layers and also through the walls and bottom of macropores. Reid and Parkinson (1984a, 1984b) confirm this explanation for clay soils noting that the difference in drainage responses is explained by the fact that complete re-wetting and therefore swelling of the soil peds does not occur until late winter.

### 4.1.3 Relationship between ditch levels and saturation in the soil

The changes in water level of the four ditches bordering the field of the study site have been monitored by stageboards. The stageboards have been installed in the ditches that border the study field and act as boundaries at the ends of the piezometer transects (Figure 1.3, Appendix A.3.1). Data exists for the period December 1997 to December 1999. The change in water level of the four ditches that borders the study field relative to Ordnance Datum (O.D.) can be seen in Figure 4.3.
The ditches display a marked seasonal flux in response to precipitation and evaporation. The north ditch is a major ditch of the marshes, (Figure 2.4) with a larger cross section (Figure 4.4) compared to the other three ditches, but all exhibit water levels at similar elevations. The ditches are interconnected by control structures which are managed to ensure water levels are maintained at mean field height by distributing water around the ditch network (Figures 2.2-2.4). There is also a pronounced microtopography of former salt marsh rills. When the ditch levels exceed a certain elevation, water can flow into the rill features creating surface flooding; Figure 4.3 shows that if the rill features were not present cutting through the raised banks, the period of flooding from overtopping would be considerably reduced for the north and south ditches, and would not occur from the east and wet ditches.

In order to examine the relationship between the ditch water levels and water table in the field, it is necessary to plot the water table from each transect of piezometers together with the water level of the boundary ditches relative to ordnance datum. The piezometers and stageboards were surveyed to a triangulation pillar close to the study

field (section A.3.3). In order to test whether the water table is influenced by the relative position of the ditch water level, only a selection of monitoring dates is graphed for clarity for each transect over 1998 and 1999.

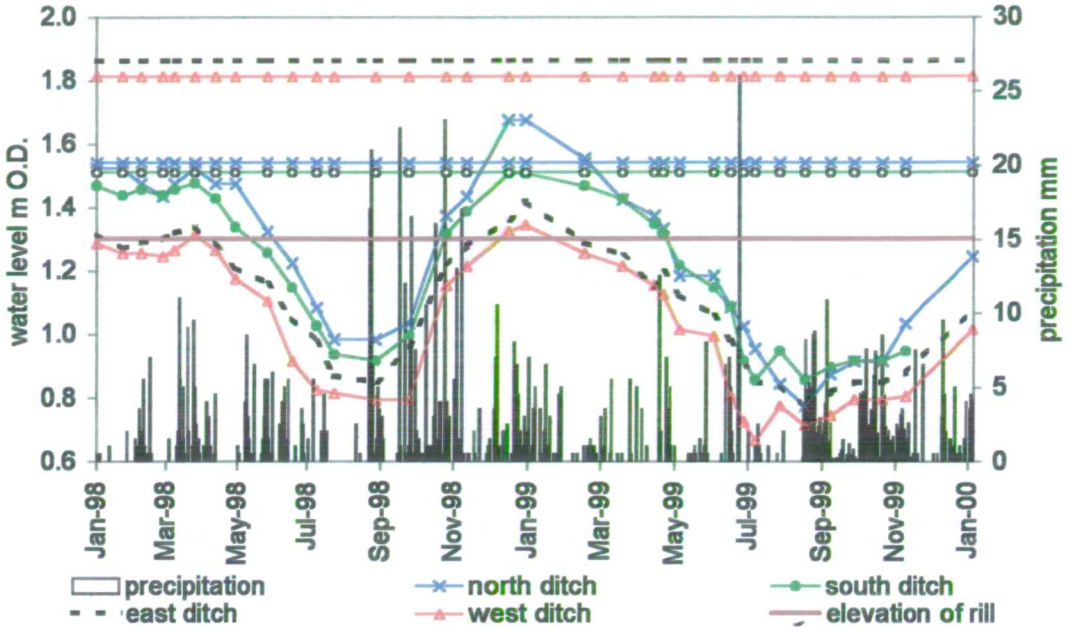


Figure 4.3. Change in water level of the four ditches surrounding the study field with precipitation (mm). The chart also displays the elevation of each ditch bank (patterned straight line) and rill elevation. The rill elevation is true for the north, south and west ditches; the east ditch has a rill at 1.4 m O.D. All the ditches fulfil the requirements of the ESA Tier 1a and 1b of at least 0.3 m water depth over summer.

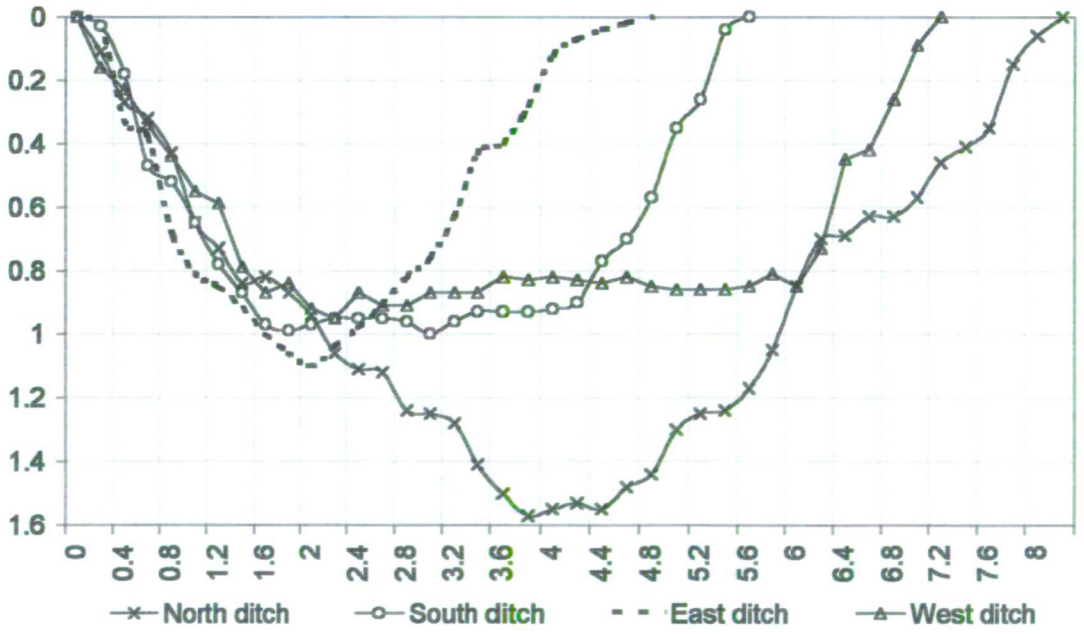


Figure 4.4. The cross section of the four ditches surrounding the study field, with width and depth (m) on the x and y axes respectively. The north ditch is the deepest and widest, with the other three having similar depth but differing widths.

### 4.1.4 Transect west to east

Figure 4.5 shows the trend of the water table and ditch water levels for the west to east transect, piezometers H to M, in 1998 and 1999. The saucer shaped topography of the field is visible, created by silt dredgings being deposited on the bankside.
Figure 4.5a displays the data for 1998. The water table is at the surface in January, apart from at the east ditch where it is 0.4 m below the surface. The water table remains at this position or falls slightly (the west edge particularly) by April. The water table then falls over the marsh by approximately 0.5 m by July, falling lower by September at the edges of the fields, and rising slightly in the middle. By November the water table has recovered to near April values and has reached the surface by December. The ditch levels are at maximum in January, falling progressively until minimum ditch levels are reached by September. The stage then recovers back up to near maximum levels by December.

Figure 4.5b displays the data for 1999. It can be seen that continuing from December 1998, the water table is at the surface except again adjacent to the east ditch, which is 0.5 m below the surface. By April 1999 the position of the water table has fallen, especially at the west edge, and it falls further by July to summer minimum levels of approximately 0.7 m below the surface. The water table remains fairly static at this level until December 1999, apart from a slight rise at site L, 370 m along the x axis, which exhibits a small rise. A very similar pattern is displayed by the ditch stage that remains at the same level over December 1998 to April 1999, falls to the summer low in July staying at this level, or in the case of the east ditch falling further by the end of monitoring. As in 1998, the ditch water levels are constantly lower than the position of the water table in the field creating a hydraulic gradient of water movement towards the ditch. The water table at the edges of the east ditch and up to 160 m inland of the west ditch slope towards the ditches, except for December 1998 by the west ditch. Again the water table fluctuates in mid field between 160 and 370 m from the west ditch which does not follow the hydraulic gradient imposed by the position of the ditch water levels.

a:

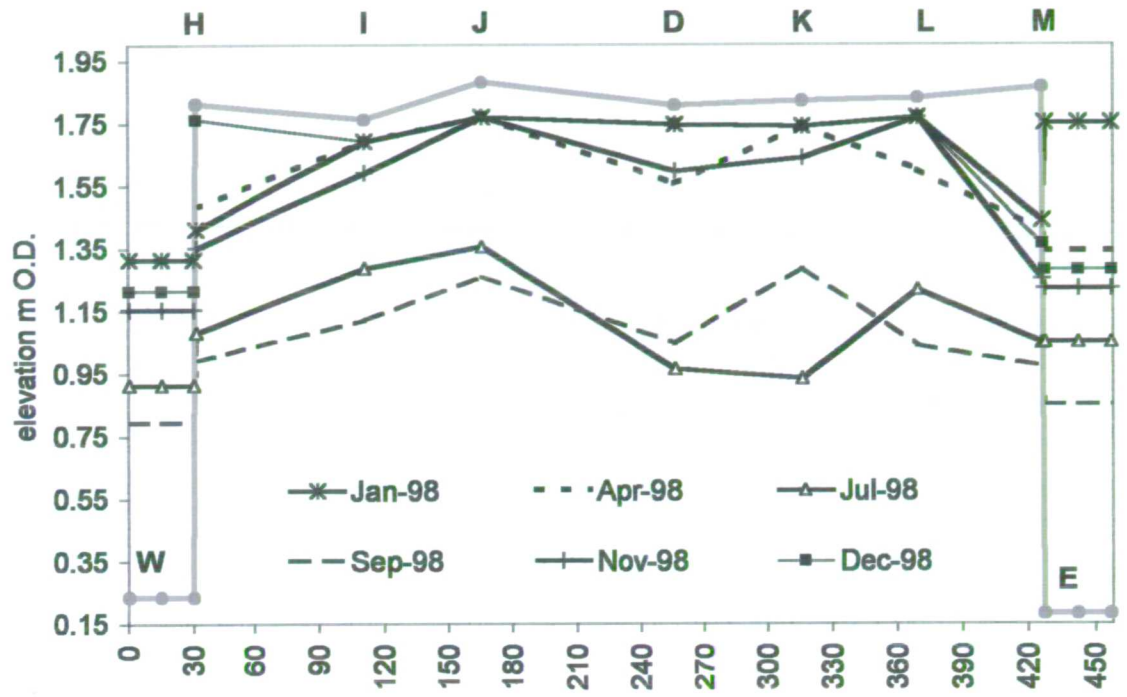


b:

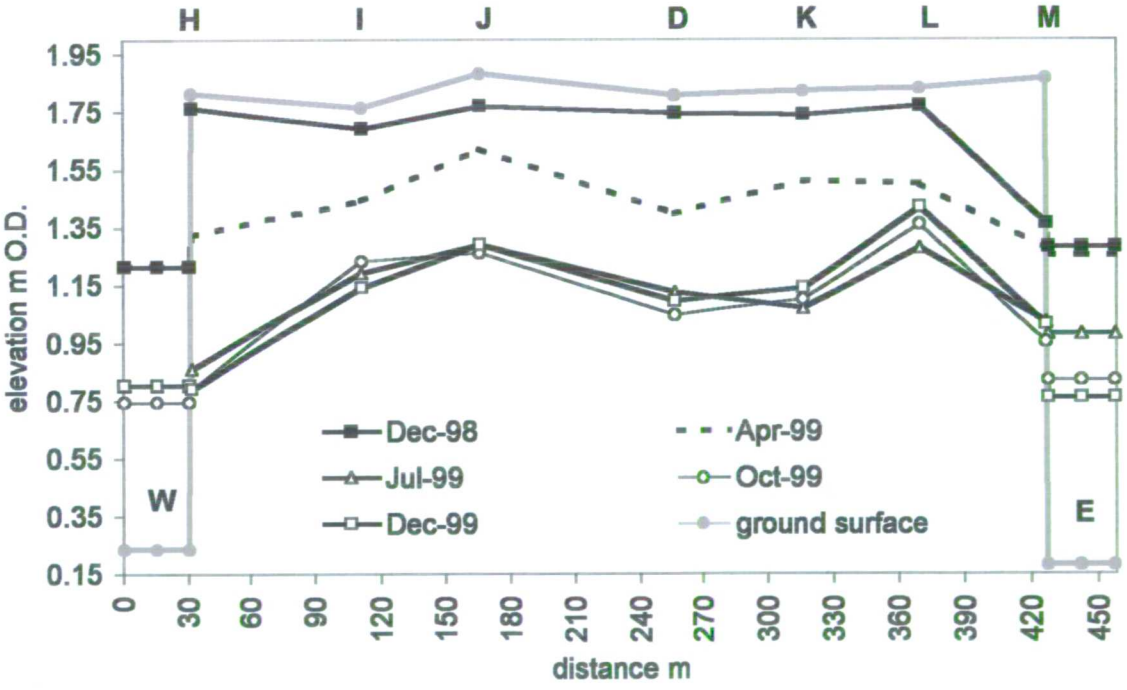


Figure 4.5. The change in water table and ditch stage over the study field in the west-east direction; a: 1998; b: 1999. Note that the x axis illustrates the distance (m) from the west and should be used as a reference starting from the edge of the marsh, 30 m along the axis; the ditches are not 30 m wide (Figure 4.4) but it was necessary to assign this width for graphical reasons so that the ditch stage could be illustrated. Water table data have been obtained from the west-east transect piezometers at 1 m depth and the stageboards at the transect end. Letters refer to the piezometer sites; see Figure 1.3 for location.

The water levels of both the west and east ditches are always lower than the groundwater during the same time period. Thus theoretically the ditches function as a drain as the relative position of the ditch water level and the water table creates a hydraulic gradient towards the ditch. The influence of this drain function can be seen at the piezometers adjacent to the ditches at the edge of the field, and up to site J, 160 m along the x axis, in that the position of the water table slopes toward the ditches. Alternatively this sloping could be influenced by the surface topography alone.

Nevertheless the pattern of the water table being lower at the ditch edge than the field interior points to the existence of a hydraulic gradient (due to the high banks relative to the ditch water surface) for the marsh edges at least. Within the field the water table change cannot be associated with any influence of the ditch, as the water table between sites J to L fall and recover independently of the movement at the edges.

In addition, the level of water in the west and east ditch in relation their banks shows that there is an insufficient volume of water to obtain a ditch level 'not less than mean field height' as specified in the ESA prescription for Tier 1a. The period of time at which the ditch stage is sufficiently high to flow into the rills (Figure 4.3) is also very short. Thus the function of the east and west ditches, at least at the field margins, is to act as a drain, the opposite of the desired ESA management effect.

### 4.1.5 Transect north to south

The ditches to the north and south of the field are observed in winter to achieve bank full capacity and thus fulfil the ESA requirement of being 'not less than mean field height', flooding the marsh interior. The surface topography of this north to south transect differs from that above with low levels at the north ditch edge rising to site B thereafter sloping towards the south ditch. There is no appreciable saucer effect of high banks with lower field interiors for this transect. The lower elevation of the banks allows flooding of the marsh through overtopping (north ditch) and via the rill channels (south ditch).

Figure 4.6a displays the trend of the water table in the north to south transect during 1998. The water table is at the surface from the start of monitoring in January except for a slight dip at site E, at 320 m along the x-axis, and either remains at this level by

April or falls in places, for example at the north edge. The water table then lowers substantially by July and further still by September before rising by November. By the end of monitoring in December 1999 the water table has recovered back to the surface. The water level in both ditches is at bankfull capacity from January to April 1998, dropping approximately 0.30 m by July and by 0.6 m by September, the minimum observed stage at 0.92 – 0.98 m O.D. The water levels then recover by November and are near the marsh surface by December 1998.

In contrast to the west – east transect, the ditch water levels in this transect are mostly higher than the position of the water table; note from Figure 4.3 that the stage levels rise higher than the marsh surface between the dates displayed in Figure 4.6 allowing water to flood over the marsh edge inland. Thus the ditches theoretically function as a source of water and act to irrigate the marsh through the hydraulic gradient created by the difference in head between the ditch water level and the water table. However the influence of this irrigation function cannot be seen from Figure 4.6 which actually displays the downward sloping of the water table to the ditches and the position of the water table at greater depth than the ditch levels at the edge of the marsh. This is an indication of the lack of lateral water movement, as otherwise the maximum depth of the water table should equate to that of the ditches. There is a consistent dip of the water table at site E, 320 m along the x-axis that cannot be explained by ditch influence or surface elevation.

Figure 4.6b displays the water table and ditch levels monitored over 1999. Continuing from December 1998 the water table is at the surface, bar a dip at site E, and falls to an even level between 1.35-1.55 m O.D. by April 1999. By July the water table falls lower, with low levels of 0.95 m O.D. at the ditch edges, peaking at 1.35 m O.D. at site C. This shape is retained through to October with further lowering at the ditch edges, and some recovery is evident by the end of monitoring in December.
The water levels in both ditches remain at bankfull capacity from December 1998 to April 1999, before falling progressively to 1.1 m O.D. by July. Stage levels fall to minimum observed levels by October of 0.87 - 9 m O.D. and recovering slightly by December.

a:

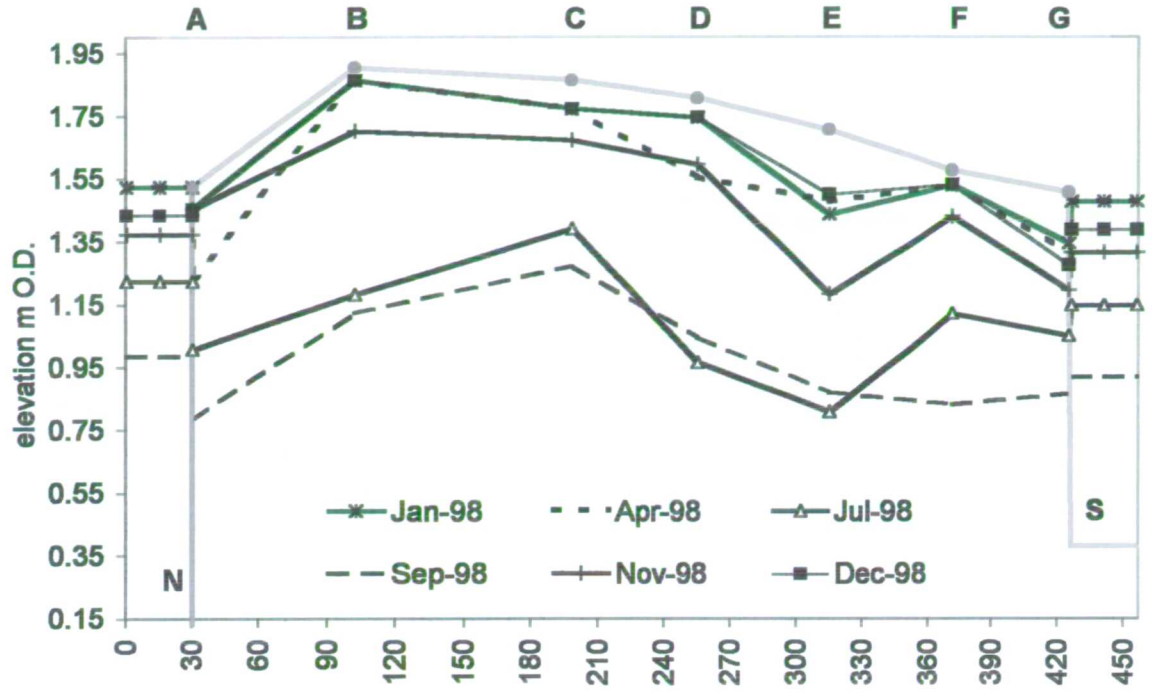


b:

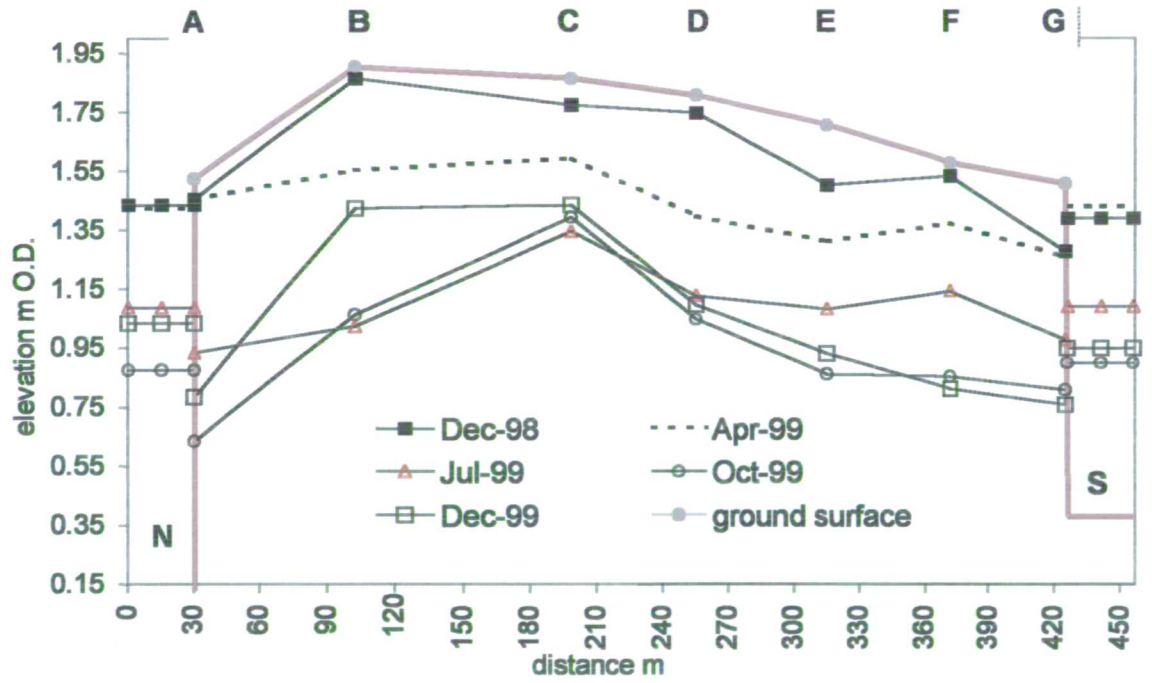


Figure 4.6. The change in water table and ditch stage over the study field in the north-south direction; a: 1998, b: 1999. Note that the x axis illustrates the distance (m) from the west and should be used as a reference starting from the edge of the marsh, 30 m along the axis; the ditches are not 30 m wide (Figure 4.4) but it was necessary to assign this width so that the ditch stage could be illustrated. Water table data have been obtained from the north-south transect piezometers at 1 m depth and the stageboards at the transect end. Letters refer to piezometer sites; see Figure 1.3 for location.

The data shows that as in 1998, the water levels in the ditches are higher than the position of the water table except for December 1998, and again act as an irrigation source during 1999. However the position of the water table does not seem to be influenced by the ditches. While there seems to be a levelling of the water table over the marsh inline with the water level of the north ditch in April 1999, the water table is lower than the level of the south ditch. In fact the water level of the south ditch actually increased slightly from December to April yet the water table adjacent to the ditch was lowered over the same period. After April the water table at the edge of the marsh slopes down towards the ditches indicating discharge even thought the levels in the ditches are higher. There is also non-uniform movement of the water table over the season in particularly between sites D and F.

### 4.1.6 Conclusion

Overall it can be seen from these results that the mechanism of obtaining high water tables in the marsh through high ditch water levels does not seem to be effective. In cases where the ditches have insufficient water volume for levels to rise to mean field level, for example in the west and east ditches, the ditches function as drains and this function can be seen especially at the edges of the marsh but only to a certain distance within. However the drain function is also seen in the north south transect where the ditches have sufficient water to overtop the banks and are always higher than the water table. These ditches should perform an irrigation function, but this is not illustrated by the incline of the water table sloping towards rather than away from the ditch edge.

Observations of the relative change of water table and ditch stage indicate that there is no relationship between them, except perhaps at the field edges of the west-east transect i.e. where there is a considerable hydraulic head promoting drainage. The position of the water table generally mirrors the surface elevation indicating that the mechanics of change operate on a localised fashion; i.e. lateral movement of water is slight.

Further analysis of these data has been achieved through Dupuit-Forchheimer analysis and applying the DITCH model. The results of these analyses are presented below in sections 4.2 and 4.3.

The objective of the ditch water level manipulation, advocated in the ESA prescriptions, is to achieve high water table to create 'soft moist ground conditions'. To assess the nature and change of ground conditions the soil moisture content of the surface soil and depth were monitored. These results are presented in Chapter 5 together with further analysis through modelling the soil profile, and an investigation into the spatial and temporal change in surface soil moisture.

## 4.2 Dupuit-Forchheimer analysis

### 4.2.1 Introduction

Following the conclusion of little relationship between the water table and ditch water levels from data observations, attempts were made to verify this by calculating the water table height using the principles of groundwater flow theory. Detailed accounts and derivation of equations relating to the principles of groundwater flow can be found in the accounts of Fetter (1994), Hillel (1971, 1998), Freeze and Cherry (1979) and other texts. In confined aquifers, steady state flow can be modelled using Darcy's law. However flow calculations are complicated under conditions of an unconfined aquifer where the position of the water table acts as the upper boundary of flow. Non steady state conditions exist due to the changes in hydraulic head and slope of the hydraulic head in space and time. Under such circumstances, for example, when the groundwater slopes towards a shallow sink such as ditches or drainage tubes, resting on an impermeable bed (Figure 4.7), such as the Elmley Marshes, groundwater flow can be determined using the Dupuit-Forchheimer seepage theory (Dupuit 1863, Forchheimer 1886) (section 3.2.1). Although care has to be used in the application of the Dupuit-Forchheimer theory it does allow for an approximation of the height of the water table and has been widely used. Youngs (1991) successfully employed Dupuit-Forchheimer theory to model the water table of fields intersected by ditches in the Somerset Levels and Moors. The relevance of this investigation proved that not only could the Dupuit-Forchheimer approach could be used in a flat low-lying lands intersected by ditches, but also that the theory could be used to assess different management strategies for the control of soil moisture conditions through the control of the water table throughout the ditch water level.

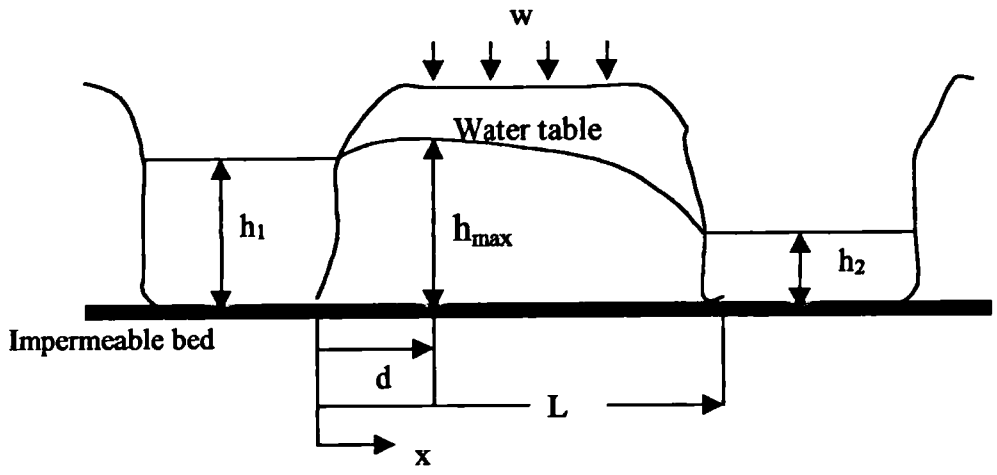


Figure 4.7. Example of an unconfined aquifer resting on an impermeable base where the position of the water table acts as the upper boundary of flow and the slope of the groundwater is in the direction of a shallow sink such as ditches. Nomenclature is discussed in the text (Figure 4.1).

### 4.2.2 Theory

The Dupuit-Forchheimer equation is derived from the integration of Darcy's law with boundary conditions of L and h (Figure 4.7) (Fetter 1994):

$$q = \frac{1}{2}K\left(\frac{h_1^2 - h_2^2}{L}\right) \qquad \text{Equation 4.1}$$

Where:

$q$ is the flow per unit width $m^3\ day^{-1}$
$K$ is the hydraulic conductivity $m\ day^{-1}$
$h_1$ is the head at the origin m
$h_2$ is the head at L m
$L$ is the flow length distance from the origin where $h_2$ is measured (m)

Under steady flow conditions, flow through the groundwater system must be equal to a gain or loss across the water table in the form of precipitation or evaporation. The net addition or accretion is at the rate of $w$. It has to be assumed that the addition of water in this way travels vertically from the surface to the water table with little delay. Under conditions of unidirectional flow the elevation of the water table at distance x from the origin can be found:

$$h = \sqrt{h_1^2 - \frac{(h_1^2 - h_2^2)x}{L} + \frac{w}{K}(L-x)x} \qquad \text{Equation 4.2}$$

Under conditions of no recharge i.e. no infiltration or evaporation, $w = 0$, Equation 4.2 reduces to:

$$h = \sqrt{h_1^2 - \frac{(h_1^2 - h_2^2)x}{L}} \qquad \text{Equation 4.3}$$

The position of the watershed can be determined using Equation 4.3. The substitution of d for x in Equation 4.2 will enable the calculation of the water table at the watershed i.e. the maximum level of the water table:

$$d = \frac{L}{2} - \frac{K}{w}\frac{(h_1^2 - h_2^2)}{L} \qquad \text{Equation 4.4}$$

Where:
$d$ is the distance from the origin to the watershed m
$L$ is the distance from the origin where $h_2$ is measured m
$K$ is the hydraulic conductivity m day$^{-1}$
$w$ is the recharge rate m day$^{-1}$
$h_1$ is the head at the origin m
$h_2$ is the head at L m

4.2.3 Application to the study area

Dupuit-Forchheimer theory was applied in an attempt to determine the flow rate (Equation 4.1), watershed of the study field (Equation 4.4) and the elevation of the water table under conditions of no recharge (Equation 4.3), accounting for recharge (Equation 4.2). A simplified two-dimensional drainage case was taken by employing the north - south piezometer transect data (ditch stage and water table elevations) as input values.

An average value of the hydraulic conductivity of the subsurface soil was used (section 3.3.2) and precipitation and potential evaporation values were totalled for 1998 and 1999 to obtain recharge values for each year. Evaporation was computed using the Penman Monteith formula using reference resistance values for a grass surface (section 7.2.2). Table 4.1 lists the values of the parameters employed in the analysis.

Table 4.1. The parameters employed in the Dupuit-Forchheimer simulations for 1998 and 1999.

| Parameter | Value | Comments |
|---|---|---|
| $L$ | 426 m | Distance in m between the north and south ditch |
| $K$ | $6.316 \times 10^{-4}$ m day$^{-1}$ | The average hydraulic conductivity of the clay soil m day$^{-1}$ |
| $w$ | $7.507 \times 10^{-4}$ m day$^{-1}$ | Value for recharge rate in 1998.<br>$w$ = (rainfall (m) –evaporation (m))/365<br>$w$ = (0.576 – 0.302)/365 |
| $w$ | $5.055 \times 10^{-4}$ m day$^{-1}$ | Value for recharge rate in 1999<br>$w$ = (0.512-0.3275)/365 |
| $h_1$ | 0.98 m | Lowest water depth of north ditch in 1998 |
| $h_1$ | 0.77 m | Lowest water depth of north ditch in 1999 |
| $h_1$ | 1.52 m | Highest water depth of north ditch in 1998 |
| $h_1$ | 1.67 m | Highest water depth of north ditch in 1999 |
| $h_2$ | 0.92 m | Lowest water depth of south ditch in 1998 |
| $h_2$ | 0.86 m | Lowest water depth of south ditch in 1999 |
| $h_2$ | 1.48 m | Highest water depth of south ditch in 1998 |
| $h_2$ | 1.51 m | Highest water depth of south ditch in 1999 |

Table 4.2. Result of calculating the flow rates for the water heights listed in Table 4.1.

| Flow rate m day$^{-1}$ | Conditions |
|---|---|
| $1.44 \times 10^{-8}$ | Low water depth in 1998 |
| $1.85 \times 10^{-8}$ | Low water depth in 1999 |
| $1.14 \times 10^{-8}$ | High water depth in 1998 |
| $6.42 \times 10^{-8}$ | High water depth in 1999 |

For the simulation of the water table accounting for recharge, the lowest and highest recorded stage data for 1998 and 1999 were used so that change in position of the water table at the watershed could be assessed. For the simulation of no recharge, the position of the water table was calculated at each location at a transect piezometer monitoring point. Table 4.3 and 4.4 lists the results of the simulations of no recharge and recharge respectively.

The water table elevations for the locations of the piezometers in the north-south transect were calculated firstly assuming no recharge. When recharge is not assumed to occur the elevation of the water table is determined based on the difference in the water level of the two sinks.

Comparison with the observed water table data from the piezometers in the north-south transect, Table 4.3 and Figure 4.8, show that the water table can be calculated within the range 0.02-0.56 m; an average difference of 0.15 m. It can be seen that the

Dupuit-Forchheimer approach can be used to approximate the position of the watershed assuming no recharge. However to asses if these results are accurate, Figure 4.8 illustrates that the predicted water table takes a linear form which matches that observed at the ditch edges (piezometer sites A and G) but not inland. The deviation of observed data from the predicted water table shows the influence of recharge and discharge fluxes upon the position of the water table and so Equation 4.2 needs to be used to calculate the water table.

Table 4.4 lists the results of the simulation accounting for recharge. The watershed is exactly half the distance between ditches in this simplified one-dimensional approach. The calculated values of the water table at the watershed in 1998 and 1999 are extremely high compared to the actual elevation of the marsh surface at approximately 2 m O.D. For both high and low ditch water levels there is no difference in the elevation of the water table within each year. There is however a difference between years with the water table at a lower position in 1999 due to the smaller input of precipitation and greater evaporative demand of that year compared to 1998 resulting in a smaller value of recharge in 1999.

The calculated water table can be interpreted to indicate major flooding of the marsh surface, but to a much deeper extent than what naturally occurs. Due to the positive recharge (i.e. net precipitation) and very low hydraulic conductivity, the flow is so slow that the water table becomes extremely high, greater than 250 m O.D. Interrogation of the calculation indicates that, under the assumption of no vertical water movement, the system would need a hydraulic conductivity of 30 m $day^{-1}$, or the ditches would have to be spaced at intervals less than 4 m for the calculated water table to mirror the observed water table.

With the knowledge that the marsh surface does not exceed 2 m O.D., and that the hydraulic conductivity of the soil matrix is very low, it has to be concluded from these results that the predominate water movement over the marsh must be in the vertical direction composed of precipitation and evaporation fluxes. In addition the rate of water movement must be faster than the hydraulic conductivity of the soil matrix i.e. water transport through macropores must be a dominant process.

Table 4.3. Results from the Dupuit-Forchheimer analysis under conditions of no recharge. The position of the watershed is at 196 m from the north ditch. The piezometer site is in brackets in the second column.

| Condition of calculation | Distance from the north ditch m (piezometer site in brackets) | Elevation of the water table m O.D. | | |
|---|---|---|---|---|
| | | Observed | Predicted | Difference |
| 1998 low water levels | 1 (A) | 0.78 | 0.98 | -0.20 |
| | 72 (B) | 1.12 | 0.97 | 0.15 |
| | 168 (C) | 1.27 | 0.96 | 0.32 |
| | 255 (D) | 1.05 | 0.94 | 0.10 |
| | 285 (E) | 0.60 | 0.94 | -0.34 |
| | 342 (F) | 0.83 | 0.93 | -0.10 |
| | 395 (G) | 0.87 | 0.92 | -0.06 |
| 1999 low water levels | 1 (A) | 0.68 | 0.77 | -0.09 |
| | 72 (B) | 1.09 | 0.79 | 0.30 |
| | 168 (C) | 1.37 | 0.81 | 0.56 |
| | 255 (D) | 1.09 | 0.83 | 0.26 |
| | 285 (E) | 0.86 | 0.84 | 0.02 |
| | 342 (F) | 0.92 | 0.85 | 0.07 |
| | 395 (G) | 0.88 | 0.86 | 0.02 |
| 1998 high water levels | 1 (A) | 1.45 | 1.52 | -0.07 |
| | 72 (B) | 1.86 | 1.51 | 0.35 |
| | 168 (C) | 1.77 | 1.51 | 0.26 |
| | 255 (D) | 1.56 | 1.50 | 0.06 |
| | 285 (E) | 1.44 | 1.50 | -0.06 |
| | 342 (F) | 1.53 | 1.49 | 0.04 |
| | 395 (G) | 1.35 | 1.49 | -0.15 |
| 1999 high water levels | 1 (A) | 1.45 | 1.67 | -0.22 |
| | 72 (B) | 1.78 | 1.64 | 0.13 |
| | 168 (C) | 1.77 | 1.60 | 0.17 |
| | 255 (D) | 1.67 | 1.57 | 0.10 |
| | 285 (E) | 1.59 | 1.56 | 0.03 |
| | 342 (F) | 1.48 | 1.53 | -0.06 |
| | 395 (G) | 1.44 | 1.51 | -0.08 |
| Maximum and minimum difference between observed and predicted | | | | 0.56 – 0.02 |
| Average difference | | | | 0.15 |
| Standard deviation | | | | 0.13 |

Table 4.4. Results from the Dupuit-Forchheimer analysis under conditions of recharge.

| Parameter | Calculated Value | Comments |
|---|---|---|
| *d* position of the watershed | 198 m from north ditch | 1998 |
| *d* position of the watershed | 198 m from north ditch | 1999 |
| *h* water table at the watershed 1998 | 542 m O.D. | Same result for both high and low values of the stage |
| *h* water table at the watershed 1999 | 445 m O.D. | Same result for both high and low water depths |

### 4.2.4 Conclusion

The overall conclusion from these results is that under the assumption of no vertical water movement there would need to be a very large hydraulic head to ensure

groundwater flow from the watershed towards the ditches. The reality of flat hydraulic gradients with low hydraulic conductivity, together with the calculation of extremely low flow rates, and predominant vertical water movement testify to the disconnected nature of the water table to the ditch water levels.

From this it can be argued that the fluctuation in the water table and ditch water level over the year is a function of recharge and discharge through the *vertical water movement of precipitation and evaporation only.* Ergo under conditions of a reversed hydraulic head with recharge from the ditch into the soil (the objective of water level management for conservation purposes) the fluctuation of the groundwater over the interior of the marsh is again a function of precipitation and evaporation due to negligible recharge from the ditch. The ESA prescription of raised ditch water levels to promote a high water table can clearly be seen to be ineffective and does not reach its objectives.

The conclusion is reached that the Dupuit-Forchheimer assumption cannot be applied for Elmley. This due to the following points:

- Soil cracking and shrinkage allows vertical water movement at rates faster than the hydraulic conductivity of the marsh soil matrix
- Direct recharge/discharge of the groundwater occurs through these cracks and macropores

These factors cause the application of the Dupuit-Forchheimer theory to Elmley to fail. Due to these findings, the DITCH model, Drain Interaction with Channel Hydrology, devised to predict the movement of water between ditches and surrounding fields was applied to Elmley to simulate the change in the water table. This enables an examination of the change in the water table over time in response to precipitation and evaporation that could not be simulated using the Dupuit-Forchheimer analysis when accounting for recharge. This analysis is presented in section 4.3.

a:

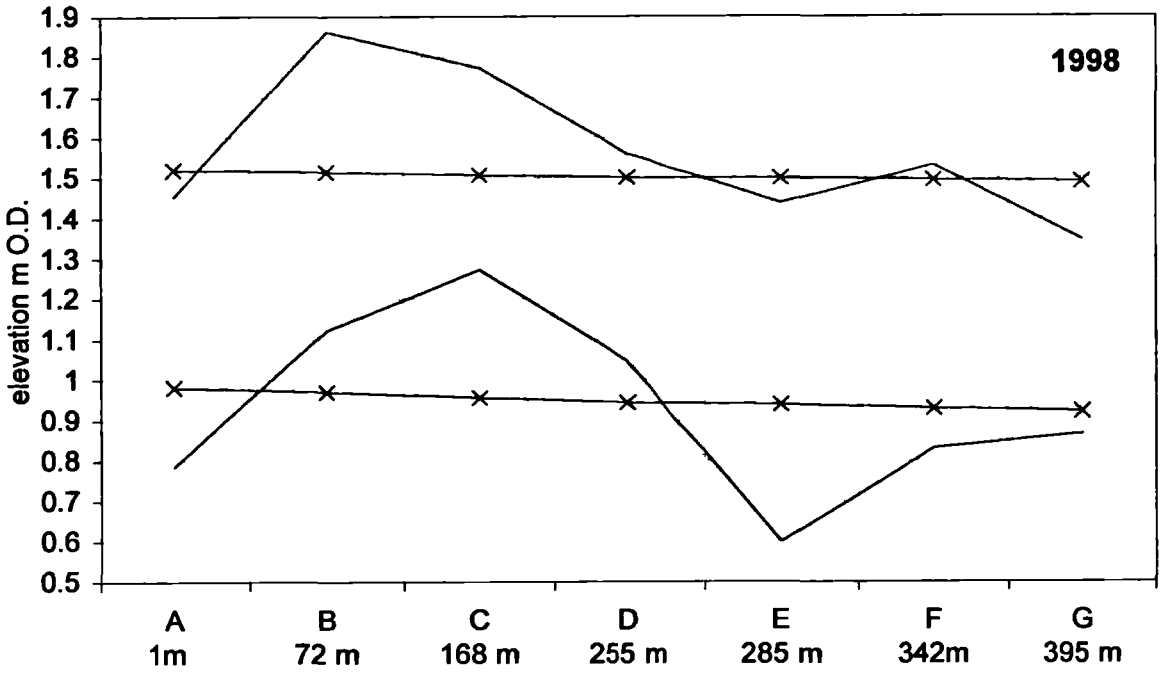


b:

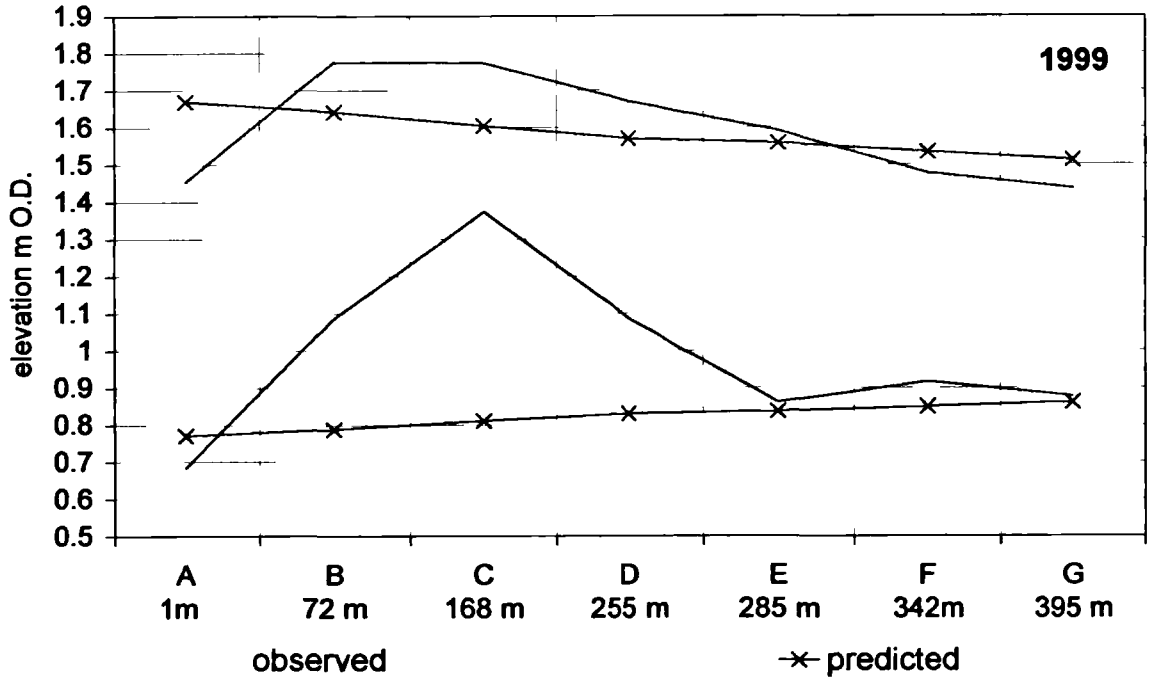


Figure 4.8. The observed and predicted water table from the Dupuit-Forchheimer approach assuming no recharge (Equation 4.3) for the north-south piezometer transect for 1998 and 1999. Each graph shows a pairing of observed and predicted data for maximum (green) and minimum (blue) ditch water levels. The distance of each piezometer site from the north ditch is shown.

## 4.3 DITCH model

### 4.3.1 Introduction

Armstrong (1993), Armstrong and Rose (1998), and Swetnam *et al.* (1998) detail the model Drain Interaction with Channel Hydrology, DITCH, which was devised to predict the movement of water between ditches and surrounding fields and to examine the consequence of various ditch management regimes. The authors present the results of the model when applied to the Somerset Levels and Moors, and Halvergate Marshes. The model successfully simulates the water table in the study area when compared to observed data and was used to simulate the ability of the ditch management schemes in these areas to generate desired field conditions. The analysis showed that soils with high hydraulic conductivity such as the peat soils employed, the model proved it was possible to manipulate in-field water tables through ditch water levels. However soil of low hydraulic conductivity, the recharge flux through the ditch systems is such that it is difficult to control the in-field water table and that the water regime is dominated by the summer evaporative demand.

The Somerset levels and Moors, and the Halvergate marshes, are both covered by an ESA with the similar objectives as the North Kent Marshes ESA, and are therefore subject to the same ditch management regime and objectives as Elmley. In addition the soil type of Halvergate marshes, Newchurch (Armstrong and Rose 1998), is very similar to the Wallasea soil type of Elmley except the former possesses calcareous subsoil above 0.4 m depth. The success of the DITCH model to simulate the water table regime at the Halvergate Marshes indicates its suitability to simulate the conditions of the Elmley Marshes. The water table regime of the study field at Elmley in relation to the ditch stage has been described in section 4.14 and 4.15. By applying DITCH to Elmley, the ability of the model to simulate the effects of ditch stage manipulation upon the in-field water table, in a field with ditch spacing greater than the Halvergate marshes, can be assessed. The magnitude of the recharge and discharge fluxes from the ditch system can also be quantified.

### 4.3.2 Theory

The following account of the ditch model is taken from the account of Armstrong and Rose (1998) and Armstrong (1993, 2000). The water table of the field can be determined through a calculation of the input through the water balance and flux from the ditch system. It assumes that the loss and gain of water through evaporation and precipitation from the soil profile causes the water table to fall and rise respectively. This is a simplification as water is lost and gained over the whole profile, but it allows for the avoidance of using the Richards equation of unsaturated flow (Richards 1931), which is 'notoriously difficult [to solve]...and imposes excessive demands upon computing resources" (Armstrong and Rose 1998 p209).

The water table is thus modelled under the assumption that the soil moisture can be directly related to the depth of the water table. This was investigated in section 4.1.1 which details the coupling of measurements made in piezometers at 1m depth to moisture levels recorded by neutron scattering, with the result that the position of the water level in the piezometers represents the water table and therefore saturated conditions.

The simplification that the loss and gain of water from the soil profile causes a direct change in the water table is achieved through the use of the specific yield. The specific yield, $f$, is generally defined as the ratio of the volume of soil to the volume of water extracted when the water table is lowered a unit distance. The value is raised to unity when the water table exceeds the surface i.e. under flooded conditions. The concept of a drainable porosity, from which water will withdraw instantaneously, causing the water table to fall, is an approximation (Hillel 1998). Assuming a constant value of specific yield ignores the forces of suction that accompany moisture loss that induces a gradual increase water extraction and lowering of the water table. However the alternative standard method to model unsaturated flow, Richards equation, also has many assumptions of which one is that the soil is isotropic, homogenous and non-swelling (Youngs 1988, Feddes *et al.* 1988, Narasimhan 1989). The clay fraction of the Wallasea soil series at Elmley is composed of 60% smectite (Hazelden *et al.* 1986). Such significant fractions of smectite have extensive volume change properties (Rowell 1994) which is seen at Elmley Marshes (section 3.3.1.10, Figure 3.5). Under such circumstances, it can be argued that the application of the Richards equation is invalid and the simplified approach of specific yield can be applied as a surrogate to

modelling macropore flow. Such flow situations are difficult to obtain which necessitate the use of a simplified approach such as the DITCH model, and so make it ideal for application to Elmley Marshes.

Further to the conjecture that the soil moisture can be directly related to the position of the water table, the constraint upon evaporation through the deficit of soil moisture is also modelled using the position of the water table. In the DITCH model, wilting point is defined as a factor of the water table; wilting point is at 1 m below surface; permanent wilting point at 3 m below the surface (Armstrong and Rose 1993). Should this approach be valid however, the position of the water table at wilting point and permanent wilting point must be linked to the particular soil under investigation to account for the influence of its textural properties.

The DITCH model:

$$M_t = M_{t-1} + \frac{(R - ET - Q_d)}{f} \qquad \text{Equation 4.5}$$

$$Q_d = 4K\frac{\left(M_{t-1}^2 - D_t^2\right)}{L^2} \qquad \text{Equation 4.6}$$

Where:
$M_t$ is water elevation in the field on day $t$ m
$R$ is rainfall m
$ET$ is evapotranspiration m
$Q_d$ is discharge though the drainage systems
$f$ is specific yield, approximated by the drainable porosity of the soil, becoming unity when water level is above the soil surface.
$D_t$ is the level of the ditches on day t m
$K$ is hydraulic conductivity m day$^{-1}$
$L$ is the ditch spacing m

In order to initiate the model, the observed value of the water table at the start of the data record is input as $M_{t-1}$ in order to find $M_t$ and $Q_d$. Thereafter the predicted value of the water table from the model is input as $M_{t-1}$. In this way the model computes the water table independently from the observed data. Equation 4.6 to find $Q_d$ is the Donnan Drainage Equation (International Institute for Land Reclamation and Improvement 1973) and refers to steady state conditions. Armstrong (1993) suggests that a timestep of one hour is sufficiently small to allow the change of water table to be modelled as a series of steady states with numerically stable results. The value of

$Q_d$ depends upon the difference in the position of the ditch water levels and the groundwater and its sign refers to the flux of water from the ditch (negative sign) or from the soil into the ditch (positive sign).

### 4.3.3 Application to the study area

The application of DITCH was made using two sets of data. The first set comprises the hourly data from pressure transducers located in the north ditch and three piezometers adjacent to this ditch. The piezometers were used for hydraulic conductivity tests (section 3.3.2.1) which necessitated the removal of water by pumping. It was necessary therefore to select periods of time over the data record that represented the actual water table. This was undertaken by comparing the record for the piezometers measured by the pressure transducers, with the nearest transect piezometer that was measured during field visits. From this analysis the following time periods were selected: 14 October to 18 November 1997, 22 April to 23 June 1998, and 26 January to 15 July 1999. Preliminary modelling attempts demonstrate that the model was successful in simulating the water table when compared to observed data from the pressure transducer record. However due to the short time periods of the selected data and the limited distance of the furthest piezometer from the ditch, it was decided to focus attention on the second set of data.

The second set of data comprises the water table measured over the marsh from the two transects of piezometers together with the stage levels of the four ditches which border the study field. A much longer time period is available from 13 January 1998 to 7 December 1999, but the time step is much greater than with the pressure transducers with an average of 21 days between observation dates in 1998 and 45 days in 1999. This has implications as to whether the change in water table heights can still be considered as succession of steady states but as the change in the observed water table is slow it is thought that steady state conditions can be applied.
The data from the north-south transect of piezometers was employed as the observations of the water regime of this transect revealed that there is sufficient water in the ditches to maintain the stage to mean field height to comply with the ESA prescriptions (section 4.1.5). DITCH was used to simulate the water table regime and calculate the drainage and recharge fluxes at each of the piezometer sites in this

transect and thereby assess the influence of the ditches across the whole field. As the whole field was simulated, the average water level was taken of the north and south ditches bordering the piezometer transect.
Values of precipitation were totalled for each timestep as were values of evaporation calculated from the Penman Monteith formula (using grass reference resistances, section 7.2.2).

Sensitivity analyses of the model were undertaken to find the optimum value of the specific yield. Armstrong (1993) employs a value of 0.05 for clay soil, which accords to literature values (Fetter 1994, Brassington 1988, taken from Johnson 1967). However a value of 0.1 or 0.15 (Table 4.6) was found to be optimum, depending on each transect piezometer, which is indicative of a silt/fine sand soil. It is postulated that while a value of 0.05 may be characteristic of many clay soils, the shrinkage of the Wallasea series creates fissures and macropores which act to increase the specific yield. The model calculations were written to change the value of the specific yield to unity when the modelled water table exceeds the surface elevation. An average value of hydraulic conductivity was used in DITCH, as employed in the Dupuit-Forchheimer analysis. Values for the parameters in the DITCH model are presented in Table 4.5.

Statistical analysis of the model output follows the six-step goodness of fit criteria of Zepp and Belz (1992). The rationale of using six measures is that a more reasoned assessment of model reliability is achieved, rather than simple visual fitting between measured and calculated data, or the sole use of commonly employed lumped criteria such as the correlation coefficient, r, between the observed and simulated data. This is affirmed by Gupta 1998, Gupta *et al.* 1998, Yapo *et al.* 1998, and Bastidas *et al.* 1999.
The following symbols are employed in the formulae below: $i$ is the time index with $i = 1,...n$, $x_{im}$ is the measured variable, $x_{is}$ is the simulated variable, $\bar{x}_m$ is the arithmetic mean of the measured variable, $\bar{x}_s$ is the arithmetic mean of the simulated variable.

1. Correlation coefficient, r, between measured and simulated data; the standard statistical procedure to asses the functional relationship between variables.

2. Mean Percental Error (MPE):

$$MPE = \frac{1}{n}\sum_{i=1}^{n}\left(\frac{|x_{im} - x_{is}|}{x_{im}}100\right)$$

This is the mean of percental deviations between measured and simulated values. The mean of the positive and of the negative deviations is calculated separately to prevent mutual elimination. The advantage of the mean error is that is not as sensitive to outliers as the coefficient of correlation.

3. Standard Percental Error (SPE):

$$SPE = \sqrt{\frac{1}{n-1}\sum_{i=1}^{n}\left[\left(\frac{|x_{im} - x_{is}|}{x_{im}}100\right) - MPE\right]^2}$$

The standard deviation of the percentage deviations between measured and simulated variables is an Index expressing the variability of the mean percental deviations. It is computed separately for the positive and negative mean percental deviations.

4. Range Index:

$$RI = \frac{\sqrt{\frac{1}{n-1}\sum_{i=1}^{n}(\bar{x}_s - x_{is})^2}}{\sqrt{\frac{1}{n-1}\sum_{i=1}^{n}(\bar{x}_m - x_{im})^2}}$$

The Range Index is the ratio of the standard deviation of both measured and simulated water contents. An optimal Index of 1 indicates that the variability or range of the simulated variable matches perfectly that of the measured variable. Dissimilarity between the range causes the Index to fall above or below unity depending upon the magnitude of the simulated range to the observed data range.

5. Level Index:

$$LI = \bar{x}_s - \bar{x}_m$$

This is a much simpler criterion and expresses the difference between the means of the simulated and measured water contents. As with the Range Index, a Level Index of 1 indicates a perfect match between the two means, while differences between the means causes the Index to fall above or below unity depending upon the magnitude of the simulated range to the observed data range.

6. Storage Index:

$$SI = \frac{(x_{im} - x_{nm})}{(x_{is} - x_{ns})}$$

This indicates the difference between the first and last value of the dataset for both measured and simulated values. The Index can be used to assess the model performance over different time periods to ascertain any lag between simulated and observed data. As with the above Indexes, a Storage Index of 1 indicates a perfect relationship with differences causing the Index to fall above or below unity depending upon the magnitude of the simulated range to the observed data range. A negative Index is created when the observed last datapoint is greater than the initial measurement, while this situation is not matched by the simulated data.

The results of statistical analysis are presented in Table 4.6.

Table 4.5. Parameters used in the DITCH model

| Parameter | Value |
|---|---|
| $M_t$ | First data value of the observed record is input as $M_{t-1}$ in order to find $M_t$. Thereafter the predicted value of the water table from the model is input as $M_{t-1}$. Data unit: m O.D. |
| $R$ | Data taken from the tipping bucket rain gauge attached to the automatic weather station and summed per time step. Data unit: m. |
| $ET$ | Data computed from the Penman formula and summed per time step. A comparison of simulated water table using input evaporation values computed from Penman and Penman Monteith (using conditions for Elmley) demonstrated the closer agreement to the observed water tables when using the Penman values. Data unit: m. |
| $Q_d$ | First data value of the observed record is input as $M_{t-1}$ in order to find $Q_d$. Thereafter the predicted value of the water table from the model is input as $M_{t-1}$. Data unit: m. |
| $f$ | Value of 0.1 or 0.15 raised to unity when the predicted water table exceeds the ground surface elevation. |
| $D_t$ | An average value of the stage level measured in the north and south ditch was taken. Average values was used rather than employing the data for one ditch so that the spatial influence upon the water table could be assessed over the entire field. The water levels of the two ditches were very similar in magnitude and change with only an average of 0.15 m difference in stage. Data unit m. |
| $K$ | Value of $1.0 \times 10^{-4}$ m $day^{-1}$; a weighted average value from the results of the pump tests and Guelph permeameter. |
| $L$ | Value of 396 m; the length of the study field in the north-south direction (compared to 70 m in the Halvergate marshes). |

### 4.3.4 Results of modelling

DITCH was used to simulate the water table at the seven locations over the north – south transect where the water table is monitored using piezometers, and the results of modelling are overall very good.

At the start of monitoring the observed water table at each of the seven piezometer sites was given as input data. Thereafter the model computed the water table independently using the values specified in Table 4.5. The success of the model in predicting the elevation of the water table compared to observed data over the modelling period February 1998 to December 1999 can be seen in Figure 4.9. Figure 4.9 shows that the model closely predicts the observed water table fluctuations in 1998, but the closeness of fit was not as good in 1999 when the modelled water table is considerably higher than observed values. The two years of modelling are discussed separately below. Manipulation of the specific yield per site was undertaken to improve the fit of the simulated water table. A value of 0.1 or 0.15 was found to be optimal with higher values allowing too little water loss and thus an overestimation of the water table i.e. simulated water table was higher than observed. Lower values have the opposite effect with considerable water loss and an underestimation of the water table.

Table 4.6 lists the results of the statistical analysis of the model data for the six goodness of fit criteria for the whole dataset; 1998-1999 and 1998 alone. These results quantify the differences in the model's ability to predict the water table per piezometer site and between different years. Site C displays the best overall goodness of fit criteria followed by sites A and B for both 1998 and 1998-1999. The goodness of fit criteria also quantify that the results of modelling are better overall for 1998 compared to the whole dataset over 1998-1999 which is due to the underestimation in 1999.

The correlation coefficient for all piezometer sites is equal to 0.75 and 0.79 for 1998 alone, which indicate a good fit between the observed and simulated data, which generates confidence in the modelled output. Sites D and E have the lowest correlation coefficients; Figure 4.9 shows that the underestimation of the water table at these sites over summer periods is quite considerable and there is a long lag over

winter for the simulated water tables to recover to observed values. At these sites the modelling results suggest that using a simple model with specific yield as a substitute for the spatial and temporal variability introduced by macropore flow can predict only an approximation of the observed water table, and that a more sophisticated model is required for greater accuracy.

For all sites there exist positive and negative Mean and Standard Percental Errors (MPE and SPE) hence the simulated water table fluctuates both above and below the true elevation. Overall the positive deviations are associated with higher errors than the negative deviations, which mean that the amount of underestimation (i.e. modelled water table is higher than observed) is more significant and the model results are less accurate in this direction. The 1998 positive and negative MPE have equal magnitudes compared to the 1998-1999 period indicating that the unequal distribution of negative deviations in the latter are caused by the underestimation of the model in 1999. To give an indication of the accuracy of the DITCH model, the values of the positive and negative MPE over 1998-1999 are 7.24% and –17.07%. For a simulated water table of 1.5 m O.D. this corresponds to a range of only 0.11 m O.D. and 0.26 m O.D. about the true value of the water table according to whether the simulated water table is lower or higher than observed.

The Range Index assesses the variability of the modelling output (i.e. rise and fall of the water table) to the observed data. The optimal value is 1; Indexes less than 1 indicate greater variability (greater range of the water table) in the simulated data set; Indexes greater than 1 indicate greater variability in the observed dataset. All sites exhibit a similar degree of variability resulting in Index values around the optimum, with average values of 0.87 and 0.99 for 1998-1999 and 1998 respectively. Low values are computed for site A however indicating lower variability of the simulated dataset. In 1998 this is due to lag as the simulated water table has not recovered to the surface like the observed water table. While other sites also exhibit this lag, they also show a trough in the water table in August 1998. This trough increases the simulated range of the water table resulting in a higher variability of water table elevations that act to compensate for the lag factor when computing the Range Index. Over 1998-1999, Figure 4.9, the observed water table at site A greatly exceeds that simulated water table thus again resulting in a low Range Index.

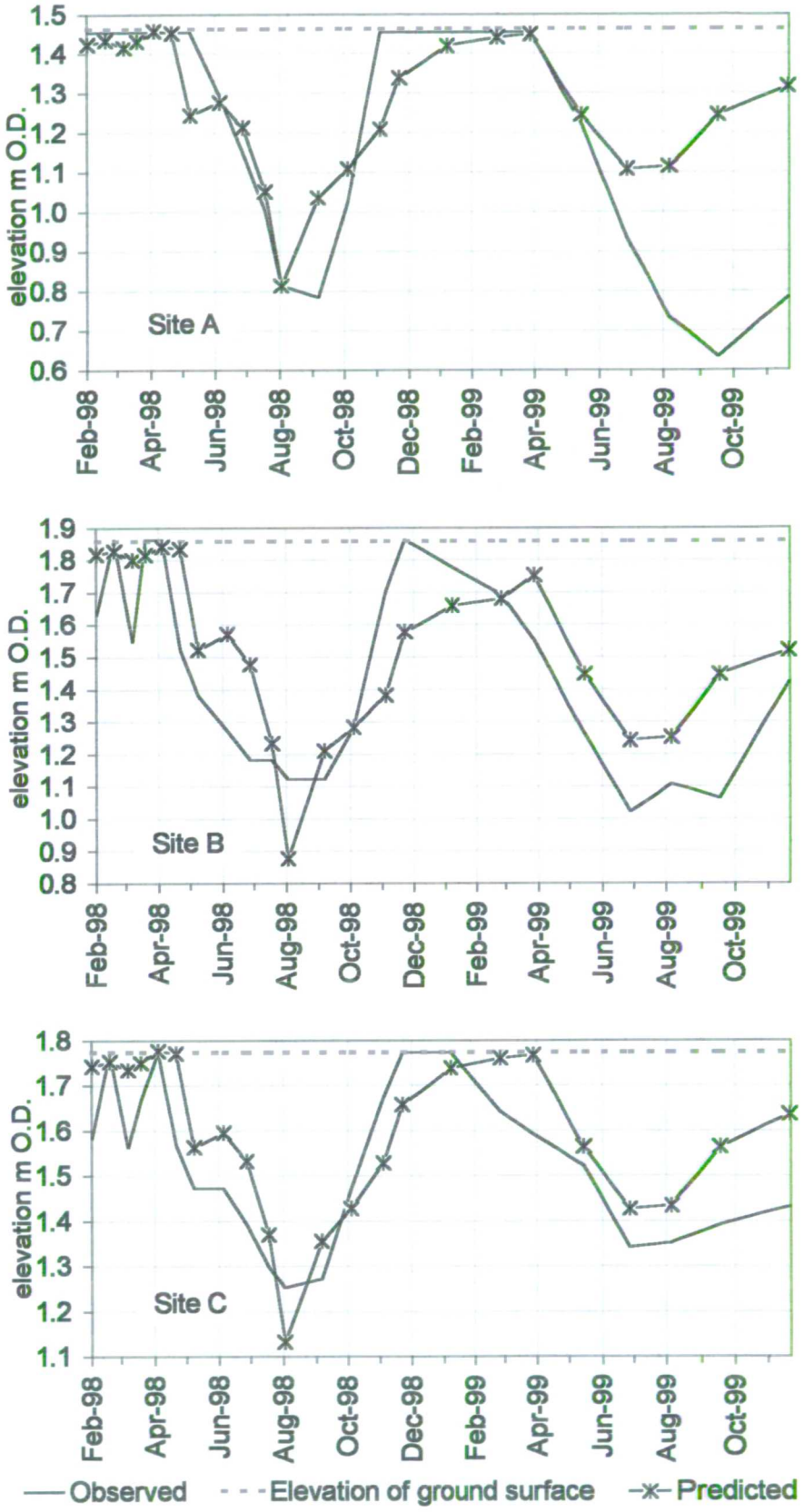


Figure 4.9. The results of modelling water table elevations with the DITCH model for the north-south transect. Piezometer sites A-C are shown above and sites D-G are overleaf. The period of modelling extends over February 1998-December 1999.

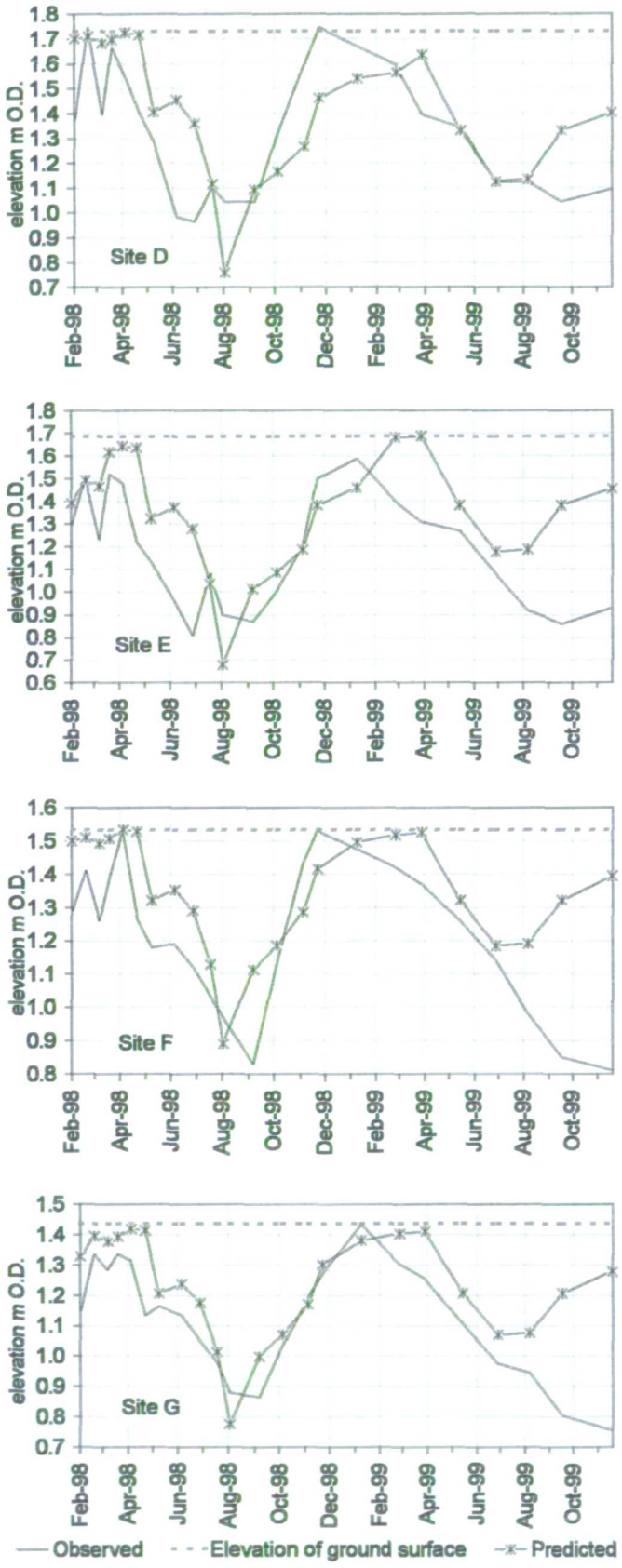


Figure 4.9. continued. Results of simulating the water table elevation for piezometer sites D-G.

Table 4.6. Results of the statistical tests of the model fit to observed data. The value of specific yield employed per site is in brackets in the first column, and optimal values for each criterion are in brackets in the relevant columns. The definition of each criterion is discussed in the text.

| 1998-1999 | | | | | | | | |
|---|---|---|---|---|---|---|---|---|
| Site | Correlation coefficient (1) | Mean Percental Deviation (0) | | Standard Percental Deviation (0) | | Range Index (1) | Level Index (1) | Storage Index (1) |
| | | +ve | -ve | +ve | -ve | | | |
| A (0.15) | 0.74 | 4.77 | -30.34 | 6.00 | 35.99 | 0.58 | 1.04 | 6.33 |
| B (0.1) | 0.76 | 8.60 | -14.96 | 8.81 | 9.49 | 0.89 | 1.05 | 0.70 |
| C (0.15) | 0.81 | 5.12 | -7.99 | 4.28 | 10.09 | 1.03 | 1.04 | 1.42 |
| D (0.1) | 0.62 | 11.07 | -17.11 | 10.54 | 15.04 | 1.01 | 1.06 | 0.94 |
| E (0.1) | 0.63 | 8.46 | -23.94 | 9.71 | 20.77 | 1.12 | 1.15 | -5.86 |
| F (0.15) | 0.66 | 8.60 | -16.89 | 2.15 | 18.12 | 0.78 | 1.11 | 4.53 |
| G (0.15) | 0.71 | 5.82 | -14.37 | 5.53 | 17.00 | 0.90 | 1.10 | 8.10 |
| All | 0.75 | 7.24 | -17.07 | 7.11 | 17.70 | 0.87 | 1.08 | 3.65 |
| 1998 only | | | | | | | | |
| A | 0.90 | 4.40 | -11.22 | 6.69 | 14.50 | 0.26 | 0.98 | 0 |
| B | 0.74 | 9.50 | -10.13 | 9.67 | 9.56 | 1.01 | 1.03 | -0.97 |
| C | 0.82 | 5.54 | -4.98 | 17.40 | 10.65 | 1.07 | 1.03 | -2.24 |
| D | 0.59 | 15.17 | -13.66 | 12.40 | 16.06 | 1.08 | 1.06 | -1.55 |
| E | 0.70 | 8.39 | -16.72 | 9.240 | 18.46 | 1.10 | 1.15 | -17.20 |
| F | 0.77 | 8.60 | -9.19 | 1.26 | 18.47 | 0.94 | 1.11 | -2.84 |
| G | 0.88 | 6.88 | -6.33 | 26.41 | 9.60 | 1.21 | 1.10 | -4.83 |
| All | 0.79 | 8.36 | -13.25 | 7.65 | 10.84 | 0.99 | 1.05 | 5.08 |

The Level Index is the ratio of the simulated and observed mean water table elevations. This Index therefore complements the Range Index by accounting for the range of the water table in absolute values. Overall the results of the Level Index are very good with values close to the optimum of 1, average values are 1.08 and 1.05 over 1998-1999 and 1998. This indicates that the mean of the simulated water tables is close to observed data; with 1998 performing slightly better. To give an indication of the magnitude of the Index, an Index of 1.08 represents simulated water table of 1.39 m O.D. compared to an observed level of 1.29 m O.D., while an Index of 1.05 represents a simulated water table of 1.39 m O.D. compared to the observed level of 1.32 m O.D.

A Storage Index of 1 indicates that the overall change in storage is the same for both observed and simulated water table i.e. that the both the observed and simulated water table at the last timestep have changed by the same magnitude compared to the initial timestep. The actual position is not accounted for, so if the simulated water table were consistently overestimated by a constant amount, provided the overall change in

storage is the same, the Storage Index will be 1. Storage Indexes of less than 1 indicate that the simulated storage change is greater than observed, while an Index greater than 1 indicates the reverse situation. A negative Index indicates that the water tables are moving in opposite directions. The results of the Index overall per piezometer site are good with average values of 3.65 and 5.08 for 1998-1999 and 1998. There is an element of lag for some piezometer sites over winter periods whereby the simulated water table reaches observed levels over a longer time period, which increases the value of the Index. Particularly high values are computed for sites A and E in 1998, and A and G over 1998-1999, and site E in 1998. Sites A and G have high values for 1998-1999 analysis due to the large difference between water tables at the end of monitoring period in December when the modelling water table has begun to recover to 0.2 m below the surface while the observed water table remains at 0.6 – 0.7 m below the surface. This large storage change is represented by high Storage Indexes. The high value in 1998 of site E is due to a small simulated storage change with a water table of 1.39 and 1.38 m O.D. at the initial and last timesteps of 1998 respectively. This contrasts with the large storage change in observed data from 1.3 to 1.5 m O.D. The Index is negative while the observed data has a positive change i.e. the end water table has surpassed the simulated water tables is just below its initial position. An Index of zero for site A results from the identical position of the observed water table at the beginning and end of the simulation in 1998.

Overall the statistical analysis illustrate the good performance of the DITCH model despite spatial differences between piezometer sites. The results of modelling are more accurate over 1998 than 1999 highlighting the discrepancy between the simulated and observed water table for all sites over 1999. This is discussed further below in section 4.3.6.

### 4.3.5 Recharge and discharge fluxes over 1998

The success of the model in modelling the water table in 1998 allows the quantification of the recharge and discharge fluxes from the ditches for this year i.e. the irrigation and drainage function of the ditches respectively. A negative value of $Q_d$ (Equation 4.6) indicates recharge from the ditch due to higher ditch level than the

water table creating a hydraulic gradient to irrigate the marsh. A positive $Q_d$ indicates the reversal of this, i.e. discharge from the marsh. The fluxes were calculated by totalling the contribution of positive and negative $Q_d$ calculated at the piezometers closest to the ditches, site A and G, over the respective time periods. Table 4.7 lists the contributions and it can be seen that they are so small as to be considered insignificant. Substituting a value of zero for $Q_d$ in the DITCH calculations result in such trivial changes to the position of the water table that it can be concluded for Elmley Marshes, any irrigation from the ditches is irrelevant and could be excluded from the calculations.

Table 4.7. Recharge and discharge fluxes from the north and south ditch over the time period measured in 1998.

| Sum of recharge/irrigation from the ditches Negative Qd mm | Sum of discharge/drainage by the ditches Positive Qd mm | Net recharge from the ditches mm |
|---|---|---|
| $4.004 \times 10^{-3}$ | $8.26 \times 10^{-5}$ | $3.29 \times 10^{-3}$ |

### 4.3.6 Model performance over 1999

The reason for the poor performance of the model in 1999 is linked to the accuracy of the input potential evaporation data. The precipitation data can be considered reliable as it is measured directly by the AWS tipping bucket gauge logging hourly and totals are checked by comparison to a standard Met Office gauge within the main enclosure (Appendix A.1.5). However potential evaporation is not measured directly but computed using the Penman Monteith formula (section 7.2.2).

The predicted water table does not fall as low, and is also seen to recover earlier than the observed water table. Manipulation of the specific yield can force the predicted water table closer to actual data. This suggests that the degree of soil cracking is greater in 1999 than 1998 creating larger pores through enhanced macropores and fissures.

Figure 5.5a indicates that the moisture to 0.8 m depth monitored through soil sampling in 1999 can be seen to be somewhat drier compared to the results of neutron

scattering in the enclosure, Figure 5.4a. However, as ditch recharge has been shown to be negligible away from the ditch edge, soil desiccation is a function of the potential evaporative demand of the atmosphere. Even with changes to the specific yield the predicted water table is still higher than observed, so that the computed values of potential evaporation need to be assessed.

Potential evaporation values were computed from the Penman Monteith approach using standard grass references (section 7.2.2) rather than the open water rate. This was due to a consideration of resistance factors involved in the release of water from the marsh. Open water surfaces can evaporate freely in contrast to water in soil that must overcome plant-induced resistances or the retention properties of the soil. This is expressed in the fact that the potential rate of a grass surface is lower than that of open water due to a consideration of such resistances.

It was expected that as the water table declined, analogous to an increase in the soil moisture deficit, the evaporation of water from the marsh would decrease to rates below that of potential (the premise of the second research investigation, Chapter 7). This would result in the observed water table being exceeded by that of the model, as the model continues to predict using potential values of evaporation. This is exhibited by most piezometer sites over summer of 1998. The one exception is site A at only 1m distance from the north ditch edge. At this site, the proximity of the ditch would maintain moisture levels as exhibited by the results of neutron scattering in the small enclosure (section 5.1, Figure 5.1) allowing the water table to fall governed by the potential evaporative rate of water loss.

It is understood that, as the modelled water table is higher than observed data in 1999, the values of evaporation employed were not sufficiently high enough despite the use potential rates. A possible explanation for the rate of water loss being higher than grass reference potential rates in 1999 could be due to more energy being available in the system than expected. This is discussed further in the results of investigations for the second and third Research Questions, Chapters 7 and 8.

### 4.3.7 Conclusion

In conclusion, provided that there is confidence that the input values of evaporation accurately represent the actual losses from the system, it has been demonstrated that DITCH can be used successfully to generate values of the water table at different locations across the marsh. The recharge and discharge fluxes of the north and south ditch are so small as to be ignored and it can be concluded from this result that there is no existence of lateral water movement from the ditches into the marsh soil matrix.
It is difficult to model hydrological processes in dynamic soils which crack and swell and which have pronounced macropore flow. A widely accepted method is to employ a two domain approach to simulate water flow in clay soils with macropores under the assumption that the matrix and macropore are separate domains with vertical flow and horizontal exchange from macropore walls into the matrix (Hoogmoed and Bouma 1980, Beven and Germann 1982). This approach is used successfully by Chen and Wagenet (1992) for example. By using the specific yield in the simple model DITCH as a surrogate for macropore flow, together with low saturated hydraulic conductivity of the soil matrix, it has been possible to successfully simulate the rise and fall of the water table of the study site. Leeds-Harrison *et al.* (1986) have also used value of specific yield as a measure of the macroporosity of a swelling clay soil. A value of specific yield characteristic of silt/fine sandy soils to represent macropore flow optimises the goodness of fit between the predicted and observed water table. If a longer dataset were available it may be possible to determine a seasonal change in the specific yield value to represent the soil shrink and swell cycles.

The results of modelling prove that vertical water movement is dominant and that horizontal movement is negligible. The position of the water table is little influenced by the ditch water level due to the extremely limited recharge capability. From this it can be stated that the ESA Tier 1a prescription of maintaining high water tables to promote high water tables over the marsh is ineffective. The position of the water table has been shown to be in response to precipitation and evaporation fluxes; thus the only method to raise water levels is to increase vertical water flow through enabling flooding of the marsh from ditches or pumping water onto the surface.

# Chapter 5 Ditch water: soil water relationships. Part 3: Soil moisture

This chapter continues from Chapter 4 to present final research results and analysis for the Research Question 1: *What is the relationship between ditch water levels and the water table and soil moisture in the adjacent field?* In this chapter can be found the results of monitoring the soil profile with the neutron probe, electrical resistance blocks and soil sampling over 1998 and 1999. The soil profile was modelled with BUDGET to ascertain the dominant water fluxes. Results are presented of the investigation into the spatial and temporal change in moisture content of the surface soil and inundation. Appendix A contains details pertinent to this chapter relating to the principles of operation and calibration of the neutron probe, electrical resistance blocks and Surface Capacitance Insertion Probe.

This chapter is organised into the following subsections:

- Results of monitoring the soil moisture over time and space identifying the trend of soil moisture (section 5.1).
- Modelling the soil profile with the BUDGET model and an assessment of its performance to simulate observed soil moisture change for moisture contents at the ditch edge and at distance (section 5.2).
- Inundation mapping of the study area and the change in extent of the surface 'types' i.e. land cover of the marsh. The monitoring strategy undertaken to identify spatial surface soil moisture change is discussed. Results are presented of regular measurements of a grid adjacent to the north ditch of the study area (section 5.3).

## 5.1 Results of monitoring the soil moisture over time and space

The objective of the ESA prescription is to create soft moist penetrable ground conditions through the manipulation of ditch water levels. Although the water table and ditch stage have shown little relationship with the water table receding up to 1 m below the surface of the marsh (Figure 4.1 and 4.2), the soil in the unsaturated zone may remain soft and moist from winter inundation (precipitation and ditch overflow, Figure 4.4) as implied in the Tier 1b prescriptions (section 3.1). Information is

therefore needed of flood extent and the change in soil moisture with depth and space over time. The flood extent of the study site was mapped and soil moisture levels were monitored on field visits using a variety of methods. The surface soil (0-0.2 m depth) was monitored using a Surface Insertion Capacitance Probe, SCIP, electrical resistance blocks, ERB, and soil sampling. The deeper layers (0.2-1.7 m depth) were monitored using neutron scattering and soil sampling. Details of the instruments including their calibration are found in Appendix A sections A.5 (neutron scattering), A.6 (SCIP) and A.8 (ERB).

Data was collected for two purposes:

- To understand the variability of soil moisture with depth and space. Neutron scattering was used at two locations: one site at 2 m from the north ditch in the small enclosure and two sites within the main enclosure at 35 m distance from the north ditch (Figure 1.3). The former is considered to be representative of the marsh edge, and the latter representative of the marsh interior. ERB and soil sampling were used to obtain moisture values in the surface 0.2 m adjacent to the neutron probe access tubes in the enclosure and next to the north ditch respectively.
- To assess the change in flooding extent and surface soil moisture. The area of the study field covered by open water was mapped over time and the SCIP was employed to generate moisture values in a grid 90 x 90 m stretching away from the north ditch. The monitoring strategy was determined through a geostatistical investigation.

The following section considers these two elements in turn. First, data generated from neutron scattering coupled to observations from the electrical resistance blocks is discussed. The data is examined to determine the overall trend for the two locations; the influence of the ditch; and, for the enclosure, the large range of moisture content in the surface soil. Second, the results of mapping inundation extent and change in land cover over the inundation cycle are presented. This is followed by results of surface soil moisture monitoring with the SCIP, after an explanation of the sampling strategy employed. Finally the effectiveness of flooding to obtain moist conditions are discussed.

### 5.1.1 Response of neutron scattering and resistance blocks

Figures 5.1 and 5.2 shows the results of soil moisture monitoring with the neutron probe combined with surface soil measurements taken with the ERBs or soil sampling. The data has been used to ascertain the relationship between the potentiometric water level and the water table (section 4.1.1). The figures reveal that changes in moisture trend occur with depth, distance from the north ditch and with time.

It can be seen from the figures, that the trend of the water content curve changes with depth. There is a contrast between the magnitude and pattern of moisture measurements taken in the surface 0.2 m to the deeper measurements taken with neutron scattering. While this behaviour could be due to the use of data derived from different methods (even though all instruments were calibrated to the soil, see Appendix A), it is thought that it is more a function of the textural and structural difference between the surface soil layer and the soil at greater depths. The physical differences between the soil layers are described in section 3.3.1, and are most marked between the upper 0.2 m and that below. The surface organic layer exhibits a very large moisture range (8-70%), and it is believed that it acts as a protective mulch or buffer restricting the loss of water from the clay soil below. The difference in structure and greater porosity of the upper layer would inhibit the movement of capillary water at depth from the clay soil into the organic layer causing the surface to dry out but allow the soil beneath to remain relatively moist. The reverse situation also occurs with higher moistures recorded by the ERBs at 0.2 m depth relative to lower values below this depth, for example 3 April 1998, can be explained by structural differences, as water infiltrating the soil flows through the porous organic layer but ponds at the interface with the clay soil due to its slower transmission capabilities. The difference is also visible in the data from the site by the ditch where the surface layers exhibit much higher moisture contents than the soil below.

Further to this there is a depth below which moisture change is insignificant. For the main enclosure, this depth is at 0.65 m compared to 0.5 m for the tube near the ditch. These depths mark the boundary of saturated soil and have been linked to the position of the water table (section 4.1.1).

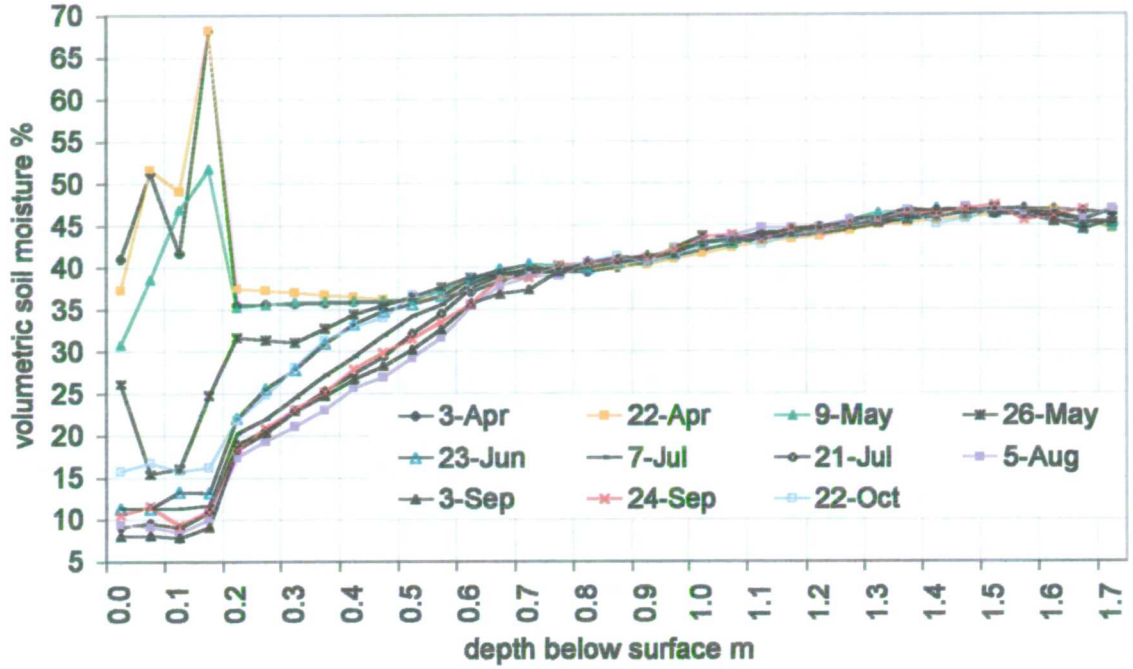


Figure 5.1. Change in volumetric soil moisture measured in the access tubes in the main enclosure. The two tubes are 0.8 and 1.7 m in length; data is averaged to 0.8 m depth after which data for the long tube alone is used. The difference in response between the surface organic layer and clay soil below can be seen clearly with saturated conditions below 0.6 m depth.

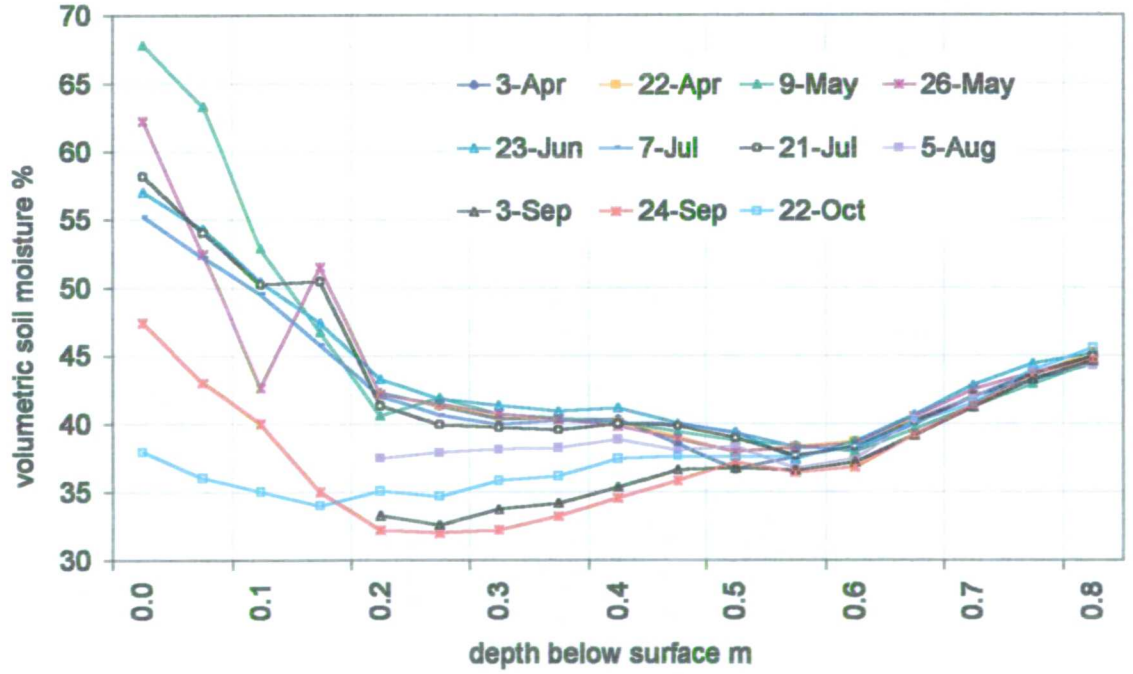


Figure 5.2. Change in volumetric soil moisture measured in the access tube adjacent to the north ditch. Moisture values are higher than those exhibited by the soil in the enclosure. Note that surface measurements are not available for some dates.

5.1.2 Trend of soil moisture with depth and location over time

The soil moisture in the enclosure shows a trend of increase with depth (Figure 5.1). At the start of monitoring in early April 1998, the moisture level in the surface increased from 40% to 68 % at 0.2 m depth, dropped and remained at 36% over 0.2 – 0.5 m depth thereafter increased to 47% at 1.55 m depth. After an increase in moisture by the end of April from 0.1 m depth, the soil moisture profile showed a steady progressive decrease until minimum values were reached by early August. Minimum values of 8-10% were recorded at the surface which, after a jump to 16% at 0.2 m, steadily increased with depth. The soil moisture then increased throughout September and by late October had recovered to June levels.

The soil moisture measured adjacent to the north ditch (Figure 5.2) shows a trend of high levels at the surface, which fall smoothly to approximately 0.25 m depth. The moisture levels then remain steady until 0.45 m depth when the moisture level dips before increasing at 0.5 – 0.6 m depth to the maximum measured depth of 0.8 m. At the start of monitoring in early April, the moisture level at 0.2 m was 42%; it decreased to 38% at 0.55 m, then increased to 45% at 0.8 m depth. Very high moisture levels at the surface were recorded; in early May the soil moisture at the surface was 68% decreasing to 41% at 0.25 – 0.55 m depth after which it increased to 46% at 0.8 m depth. By early July the soil moisture at the surface had dropped to 55% declining to 41% at 0.2 m depth. Over April to July the moisture values from 0.2 m depth were stable exhibiting only small changes and the change in moisture at the surface is also small.

These observations contrast with the data from the main enclosure where drying of the soil with depth was exhibited from May onwards; only from August did soil moistures adjacent to the ditch start to decline to minimum levels in September. The data for the ditch margin in September show moisture levels reduced to 48% at the surface lowering to 38% at 0.2 m depth, increasing up to 37% at 0.55 m after which depth change is insignificant. By the end of monitoring in October, the soil moisture at the surface dropped further to 38%, but below 0.15 m, the moisture levels recovered to above September's values. So while a decrease in moisture is observed, moisture content of the riparian stretch is very high relative to soil inland as measured in the enclosure.

In contrast to the soil moisture recorded in the enclosure, the soil bordering the ditch experienced near saturated conditions at all depths at the start of monitoring. Moisture depletion from 0.2 m depth is only initiated by August, a lag of three months after the enclosure soil. At all depths the soil by the ditch does not experience desiccation to the same degree as the enclosure and the moisture values are substantially greater than in the enclosure for all depths. This difference in the magnitude and rate of soil water loss between the two measurement sites points to the influence of the ditch in maintaining higher moisture contents along its border.

A comparison can be made between the change in ditch water level of the north ditch and the depth at which soil moisture is depleted adjacent to the ditch to further determine the influence of the ditch. From Figures 4.3 and 4.6a it can be seen that in April 1998 the north ditch was at bankfull capacity. At this time, field observations were made of the ditch flooding its banks and surface rills, which would have raised the soil moisture content to saturation levels. The ditch water levels fell by 15 July to 0.3 m below the field surface. This is concomitant with the decrease in surface soil moisture from April and the decline in water level of the north ditch after July. The water level of the north ditch fell further to 0.55 m below the field surface in September, which also tallies with the observation that the soil profile continues to dry above this depth over this period. By October the ditch water level has started to increase slightly as has the soil moisture content.

### 5.1.3 Conclusion

From these results it seems that the north ditch does influence the moisture content of soil adjacent to its edge but at a distance of 35 m in the enclosure, the influence is negligible. Soil analyses of structure, porosity, organic matter and hydraulic conductivity (sections 3.3.1 - 3.3.2) reveal heterogeneity with depth, with the result that water movement is extremely slow at depth but that the infiltration at the surface is substantially faster. Thus the movement of water from the ditch through the subsoil is extremely limited but should the ditch water interact with the organic surface layer of the field, water could move horizontally through the latter. This would promote high moisture creating soft moist ground conditions as desired by the ESA scheme.

In order to examine further the soil moisture flux of the marsh and ditch recharge along its riparian border the BUDGET model was employed (section 5.2). In addition, to assess the spatial influence of the ditch in the surface layer, the focus of soil moisture monitoring changed to examine the moisture content of the surface with increasing distance from the north ditch. This was undertaken using the Surface Capacitance Insertion Probe, SCIP, and is discussed in section 5.3.2. The malfunction of the neutron probe in October 1998 curtailed its further use.

## 5.2 Modelling the soil moisture profile using BUDGET

The observations of the interactions between the ditches, water table, and soil moisture, together with soil structure and hydraulic conductivity data enables an assessment of the ESA management prescriptions. As a further exercise in data analysis the results of the investigations have been modelled using BUDGET. This model can simulate the change in soil moisture through the input and output of precipitation and potential evaporation respectively. If the model can simulate the conditions at Elmley Marshes then it can be assumed that only these data are important in soil moisture change i.e. there is no influence of the ditch water level upon soil moisture. The effects of flooding with brackish ditch water upon soil salinity can also be addressed.

### 5.2.1 Theory

The following description of the model is taken from its manual (Raes 1996); few investigations have been undertaken using the model and it is believed that this is the first time it has been employed for a wetland environment. BUDGET calculates the water storage in a soil profile, composed of a series of soil layers each with specific characteristics, as affected by input (precipitation and/or irrigation) and withdrawal (evaporation) of water for a given period. The soil profile is simulated as a two-dimensional grid of soil depth and time, with grid node increments of space and time, $\Delta z$ and $\Delta t$ (Figure 5.3).

The value of $\Delta t$ is fixed at one day but $\Delta z$ can be varied; the soil profile in the BUDGET model is composed of a number of homogenous soil layers with thickness $\Delta z$. The flow equation is solved for each node at different depth $z_i$ and time intervals $t_j$ so that the soil moisture content is determined for each grid node for every time step. In BUDGET Richards's differential flow equation is replaced by a set of finite difference equations or submodels written in terms of the dependant variable, soil moisture $\theta$, Equation 5.1. Each submodel concerns a different process of infiltration, surface runoff, internal drainage, and deep percolation losses, and evaporation. Soil water flow is calculated only in the vertical direction. At the beginning of each timestep the drainage submodel is executed and the soil moisture content is updated per grid node according to the computed soil moisture variation $\Delta\theta$, per submodel (Equation 5.2. Next the rainfall and or irrigation inputs are stored in the soil profile after the subtraction of water lost by surface runoff. After the soil moisture is again updated, the evaporation and transpiration losses are removed.

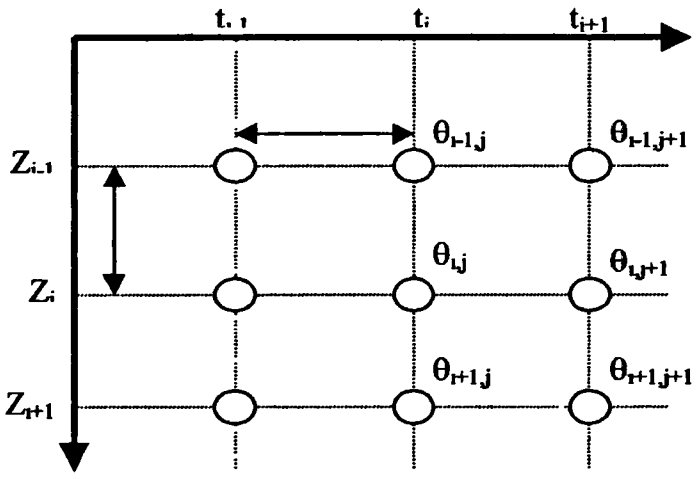


Figure 5.3. The time depth grid of BUDGET for the numerical solution of the one-dimensional flow equation.

$$\theta_{i,j+1} = \{[(\theta_{i,j} + \Delta\theta_{i,drain}) + \Delta\theta_{i,inf}] + \Delta\theta_{i,evap}\} + \Delta\theta_{i,transp} \qquad \text{Equation 5.1}$$

Where:
$\theta_{i,j}$ is the soil moisture at the node i at time j
$\theta_{i,j+1}$ is the soil moisture at the node i at time j+1
$\Delta\theta_{i,drain}$ is the drainage submodel
$\Delta\theta_{i,inf}$ is the precipitation and infiltration submodel
$\Delta\theta_{i,evap}$ is the soil evaporation submodel
$\Delta\theta_{i,transp}$ is the transpiration submodel

Raes (1996) acknowledges that as the calculated value of $\Delta\theta$ in each of the submodels depends upon the actual soil moisture content, the sequence or order of the calculations will influence the results of each submodel and subsequently the final total soil moisture variation. However this influence is considered to be negligible as the timestep is small leading to small changes after each day. In addition the dependency of each submodel upon the actual soil moisture content differs. For example, the drainage submodel depends upon the wetness of the soil and is at its maximum when the soil is saturated at which point the evaporation and transpiration submodels are independent of the soil moisture content.

An account is given below of the drainage, infiltration, transpiration submodels and salt transport subroutine as these have been employed when applying the model to the study site.

5.2.1.1 Drainage submodel

In a uniform soil of equal wetness the change in soil moisture per day, $\Delta\theta/\Delta t$, is assumed to be constant over the profile. The drainage ability of the soil is given by the exponential equation and is related to the soil moisture content of each soil compartment:

$$\frac{\Delta\theta_i}{\Delta t} = \tau(\theta_{SAT} - \theta_{FC}) - \frac{e^{(\theta - \theta_{FC})} - 1}{e^{(\theta_{SAT} - \theta_{FC})} - 1} \qquad \text{Equation 5.2}$$

$$IF \quad \theta_i = \theta_{FC} \quad THEN \quad \frac{\Delta\theta_i}{\Delta t} = 0$$

$$IF \quad \theta_i = \theta_{SAT} \quad THEN \quad \frac{\Delta\theta_i}{\Delta t} = \tau(\theta_{SAT} - \theta_{FC})$$

Where:

$\theta_i$ is moisture content $m^3\ m^{-3}$

$\tau$ is a drainage function representing the percolation of water by free drainage as a function of time for any moisture content between saturation and field capacity. The value of the function (dimensionless) depends upon the textural properties of the soil with a high value of 1 for coarse sands and low value of 0.1 for basin clay.

$\theta_{SAT}$ is the soil moisture at saturation $m^3\ m^{-3}$

$\theta_{FC}$ is the soil moisture at field capacity $m^3\ m^{-3}$

The amount of water draining out of the profile at the end of one day is given by Equation 5.3:

$$D = 1000 \frac{\Delta\theta}{\Delta t} \Delta z \quad \Delta t \qquad \text{Equation 5.3}$$

To simulate the flow process in the soil profile composed of non-uniformly wetted and heterogeneous soil compartments, the procedure of BUDGET is to compare the different drainage ability of the soil compartments. The amount of water that drains out of the top soil compartment at the end of the time step is given by Equation 5.4:

$$D_1 = 1000 \frac{\Delta\theta_1}{\Delta t} \Delta z_1 \quad \Delta t \qquad \text{Equation 5.4}$$

Where:
$D_1$ is the flux of water between soil compartments 1 and 2, mm
$\Delta\theta_1$ is the change in moisture content of the top compartment
$\Delta z_1$ is the thickness of the top compartment, m
$\Delta t_1$ is the timestep day

The soil moisture of the top compartment is updated and the calculations repeated for the successive compartments to the end of the soil profile. The drainage ability, (Equation 5.2) is dependant upon the soil moisture content of the compartment; water will only flow if the soil moisture of the compartment is greater than the value set as field capacity. The cumulative drainage amount will pass through each compartment provided the drainage ability of that compartment is equal to or greater than overlying compartment. Should the drainage ability of the compartment be smaller, the cumulative drainage amount is stored within the compartment thus raising its soil moisture and consequently its drainage ability. Should the soil moisture of the compartment be raised so that values greater than field capacity are reached, BUDGET allows drainage to the next, underlying compartment; if field capacity is not exceeded no water will drain to the underlying compartment.

5.2.1.2 Infiltration submodel

Water infiltrating the soil is modelled as being stored in the top compartment until the soil moisture of the compartment exceeds the threshold moisture content of field capacity. After which point the infiltration drains from the top compartment into the

one beneath and so on. The infiltration capacity of each compartment can be set within BUDGET.

5.2.1.3 Transpiration submodel

Water extracted by transpiration is taken out of the root zone; the depth of which can be set within the model. The root extraction or sink term, S, expresses the water uptaken by the roots per unit volume of soil per day ($m^3\ m^{-3}\ day^{-1}$) (Equation 5.5). S depends upon a maximum sink term, Smax, and a dimensional variable, $\alpha$, whose values depends upon the soil moisture content:

$$S_i = \alpha\, S\max \qquad \text{Equation 5.5}$$

Where:
$S_i$ is the sink term of compartment $i$ $m^3\ m^{-3}\ day^{-1}$
$\alpha$ is the dimensionless sink term variable
*Smax* is the maximum sink term $m^3\ m^{-3}\ day^{-1}$

BUDGET allows the maximum sink term to be defined in either of two ways by employing the solution methods by Feddes *et al.* (1978) or Hoogland *et al.* (1981).
Smax can be defined as a function of the root depth and independently of the potential transpiration rate using a linear decrease from the highest set value of Smax at the top of the soil profile to a minimum value at the bottom of the rooting depth.
Alternatively Smax can also be defined as the ratio of the potential transpiration rate $T_{pot}$ (mm $day^{-1}$) to the rooting depth $Z_{rootzone}$ (m), Equation 5.6:

$$S\max = \frac{T_{pot}}{Z_{rootzone}} \qquad \text{Equation 5.6}$$

This simulates the extraction of water by transpiration as equally distributed over the entire root zone.

The sink term $\alpha$ is a function of the soil moisture content of the compartment under consideration. When the compartment exceeds a critical moisture content $\alpha = 1$; $\alpha$ decreases with continued soil moisture decline becoming zero at the wilting point. The critical moisture content is determined by the *p* value, which is the proportion of the Total Available Water, TAW, which is Readily Available for water uptake and

crop transpiration, RAW. TAW is the water content between field capacity and wilting point. When the readily available fraction of soil water has been depleted, RAW–0, the critical soil moisture content is reached. The value of $p$ is influenced by the potential transpiration rate, *Tpot*, dictated by the climate; $p$ is larger (i.e. the RAW fraction is greater) when *Tpot* is small at less than 3 mm $day^{-1}$, compared to high values of greater than 8 mm $day^{-1}$ for example. The value of $p$ can be set within the model but the default value is equal to 0.6 when *Tpot* is low and this value has been used in the simulations. The transpiration submodel is also influenced by the salt transport subroutine discussed below.

5.2.1.4 Salt transport subroutine

BUDGET simulates flow movement in the vertical direction through pores only; solutes contained in the draining water consequently bypass the soil water in the matrix. In order to account for the horizontal transfer of solutes, a diffusion process is included within BUDGET to describe the redistribution of solutes from pores into the soil matrix under a salt concentration gradient.

To simulate the diffusion of salts from the macropores into the soil matrix, the soil compartment is vertically divided into a number of cells in which salts can be stored. Salts can be transported between cells if the cell contains water and a concentration gradient exists. Each cell within the soil compartment is representative of a certain pore diameter and the number of cells containing water, and therefore active in the salt diffusion process, depends upon the wetness of the soil. Under dry conditions, i.e. less than field capacity, only the cells representing small pore diameter are active in diffusion and the salt is redistributed in a horizontal plane. At soil moistures above field capacity the macropores become active and salt is also transported vertically down the profile.

The rate of horizontal diffusion of the salt depends not only on the salt concentration gradient but also the pore size diameter. Equilibrium is reached quickly between cells of large pore diameter compared to pores with smaller pores and therefore lower values of hydraulic conductivity and higher adsorption forces such as clay soils. In such soils equilibrium is reached much more slowly. BUDGET simulates this process with a 'global diffusion factor' that varies between 100% for macropores (no

limitation upon on salt diffusion; response is based solely upon the concentration gradient) and 0% for the smallest pores (salts cannot diffuse between cells). The value of the diffusion factor can be specified within the model; the default value is 20%, which has been employed in the simulations.

The effect of salt within the soil in increasing the osmotic pressure and thereby reducing the water available for transpiration is simulated within BUDGET by adjusting the maximum sink term, Smax with a relative soil salinity factor, Equation 5.7:

$$S\max_{adjusted} = S\max\left(1 - \frac{EC_{sw}}{EC_{e\max}}\right) \qquad \text{Equation 5.7}$$

Where:
$Smax_{adjusted}$ is the value of Smax adjusted to the salinity of the root zone $m^3\ m^{-3}\ day^{-1}$
$EC_{sw}$ the electrical conductivity of the soil water solution dS $m^{-1}$
$EC_{emax}$ the electrical conductivity of the soil saturation extract at which level crop yield is presumed to become zero dS $m^{-1}$

An increase in salt accumulation in the root zone and/or a reduction in soil water content increases the electrical conductivity of the soil water solution $EC_{sw}$. An increase in $EC_{sw}$ causes a corresponding increase in the relative soil salinity and therefore reduces $Smax_{adjusted}$, the amount of water that can be extracted by the roots. $EC_{emax}$ is used to describe the reduction in crop transpiration due to salinity due to the linear relation between crop yield and water stress.

### 5.2.2 Application of BUDGET to the study site

The modelling procedure involves setting the initial conditions of soil moisture and soil electrical conductivity for the first day of the simulation from observed data. A climate file is needed comprising daily values of precipitation and evaporation for the simulation period. The model determines the change in soil moisture in the designated soil compartments (i.e. depth layers) based on the flux of water expressed in the input file and the values set for the soil parameters.

The model was calibrated using soil moisture data collected in 1998 in the enclosure from the electrical resistance blocks at the surface and neutron scattering from 0.2 –

1.0 m depth. Validation was performed using the moisture data obtained in 1999 from electrical resistance blocks at the surface and soil sampling from 0.2 – 0.8 m depth in the main enclosure. Values of soil conductivity determined in section 3.3.1.7 were also used in the model. Table 5.1 shows the parameters modified during model calibration and validation and the final optimal values of these parameters. A simulation was also performed to assess the change in the soil moisture at the ditch edge.

The calibration, validation and ditch edge simulations are discussed below together with statistical analyses of the model output for each simulation. The statistical analysis followed the six-step goodness of fit criteria of Zepp and Belz (1992) as applied for the DITCH model (section 4.3). The goodness of fit criteria are detailed in section 4.3.3 and are applied to the simulated soil moisture datasets of 1998 and 1999. A closer examination of the model results over April to August 1998 was also performed to assess the accuracy over the drying phase of that year for both the simulations of the enclosure and ditch riparian area.

5.2.2.1 Sensitivity analysis

A sensitivity analysis has been performed of the model (Table 5.1), using soil characteristics determined for the Elmley Marshes, and reveals that there is an insignificant effect on the simulation accuracy in changing the value of the RAW: TAW ratio in the transpiration model, and the global diffusion factor of the salinity submodel.

The most sensitive parameter is the root water uptake, Smax, with optimal maximum values of 0.015 $m^3 m^{-3} day^{-1}$ at the top and 0.001 $m^3 m^{-3} day^{-1}$ at the bottom of the rooting depth. The highest permitted setting of 0.05 $m^3 m^{-3} day^{-1}$ at the top evaporates too much water with up to 10% difference in moisture values when using 0.015 $m^3 m^{-3} day^{-1}$. The lowest allowed setting of 0.01 $m^3 m^{-3} day^{-1}$ suppresses soil drying through evaporation with up to 40% difference in soil moisture values when using the optimal value.

The first compartment of the soil layers is set at 0.2 m depth compared to the remainder, which are set at 0.1 m. It was necessary to deepen the surface layer to avoid the tendency of the model to simulate very high moistures in the 0-0.1 m layer and then lower values in the 0.1-0.2 m layer. Optimal values of $\tau$ were found to be 0.5

for the surface layer and 0.1 thereafter. These are reference values for a fine sandy loam and basin clay respectively highlighting the difference in the soil with depth.

The infiltration rate/hydraulic conductivity is the next most sensitive parameter. The values derived from field experiments (section 3.3.2) were input into the model but the simulated moisture levels were too wet when compared to observed moisture data. Through repeated simulations, optimal values were found to be 1 mm from the surface to 0.4 m depth, and 0.1 mm in all subsequent layers. These values are lower than measured infiltration rates (section 3.3.2.2.2).

Similarly, it was found that employing values of field capacity, taken from the soil moisture characteristic derived for the study site (section 3.3.3), resulted in too much water draining out of the profile (i.e. the simulated soil moisture was lower than observed). It was necessary to set the value of field capacity artificially high to counter this effect. These two effects result in the model being able to simulate the drying process well but not the wetting of the profile. This is discussed further in subsequent sections. Values for the wilting point were based on the minimum moisture values observed for each soil moisture layer over 1998-1999.

Table 5.1. Parameter settings of the BUDGET model found optimal to simulate Elmley Marshes.

| Crop description | | | | | |
|---|---|---|---|---|---|
| Rooting depth | Constant value of 0.62 m | | | | |
| $\tau$ | 0.5 in surface layer, 0.1 thereafter | | | | |
| RAW: TAW | 0.6 (default value) | | | | |
| Global diffusion factor | 20% (default value) | | | | |
| Root water uptake | 0.015 $m^3 m^{-3} day^{-1}$ at the top, 0.001 $m^3 m^{-3} day^{-1}$ at the bottom | | | | |
| Soil description | | | | | |
| Soil profile split into layers of 0.2 m depth (each comprising two compartments of 0.1 m depth except for the surface layer with one compartment of 0.2 m depth) | | | | | |
| | Saturation % | Field Capacity % | Wilting Point % | $\tau$ | Infiltration mm $day^{-1}$ |
| Layer 0.0-0.2 m | 51 | 40 | 7 | 0.52 | 1 |
| Layer 0.2–0.4 m | 44 | 40 | 12 | 0.5 | 1 |
| Layer 0.4-0.6 m | 47 | 44 | 18 | 0.1 | 0.1 |
| Layer 0.6-0.8 m | 47 | 44 | 18 | 0.1 | 0.1 |
| Layer 0.8-1.0 m | 47 | 44 | 18 | 0.1 | 0.1 |

5.2.2.2 Calibration

In order to calibrate the model, surface soil moisture from the electrical resistance blocks and neutron scattering in the enclosure in 1998 were employed. Soil conductivity values per soil layer in the main enclosure were taken from Table 3.10. These data are listed in Table 5.2.

Table 5.2. Input soil moisture and soil conductivity data to initiate the calibration simulation of the marsh field interior. Data are for 3 April 1998.

| Soil Layer | 0-0.2 | 0.2-0.3 | 0.3-0.4 | 0.4-0.5 | 0.5-0.6 | 0.6-0.7 | 0.7-0.8 | 0.8-0.9 | 0.9-1.0 |
|---|---|---|---|---|---|---|---|---|---|
| Soil moisture % | 45 | 37 | 36 | 36 | 36 | 37 | 39 | 40 | 40 |
| Soil conductivity dS $m^{-1}$ | 2.61 | 2.83 | 2.83 | 3.91 | 3.91 | 3.74 | 3.74 | 7.86 | 7.86 |

The simulation output, soil moisture content per soil compartment, are then extracted for the dates for which soil moisture is available from the monitoring equipment. The success of the model is determined by its success to independently replicate observed soil moisture content. Tables 5.3 and 5.4, and Figure 5.4 show the observed and modelled soil moisture values over time and the difference between them.

Over the time period modelled, the model output is extremely accurate up to 3 September 1998. After this date observed data shows the soil moisture increasing which is not shown by the BUDGET model except in the top layer 0-0.2 m. After the 3 September there is a large input of water through precipitation which initiates the wetting of the soil profile at depth. At the study site, precipitation falls both onto the soil matrix and also cracks in the soil, created by soil shrinkage and macropores which allow the penetration of the rainwater to depths of 0.6 m which is shown in the observed rapid change in the position of the water table (section 4.1.2). BUDGET does not compute partitioning of precipitation into fractions that fall onto the soil matrix and into macropores, like other models such as SWATRE (Belmans *et al.* 1984). Rather, the model assumes that the soil profile is wetted through infiltration at the surface permeating the soil matrix to depth. Thus BUDGET simulates an increase in moisture only at surface which makes the difference between simulated and observed moisture contents very large after the 3 September particularly at 0.3-0.6 m depth.

a:

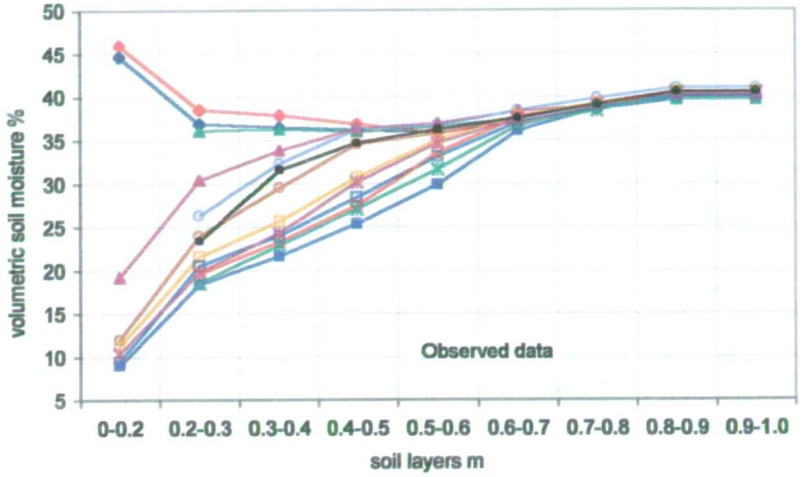


b:

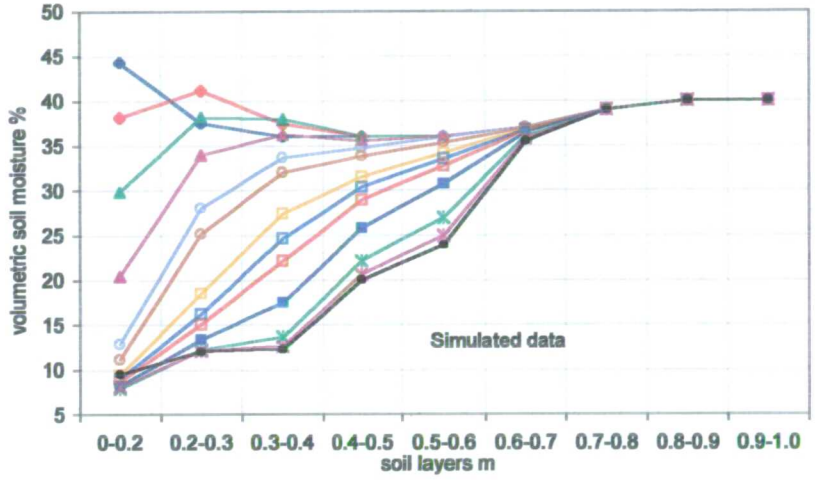


c:

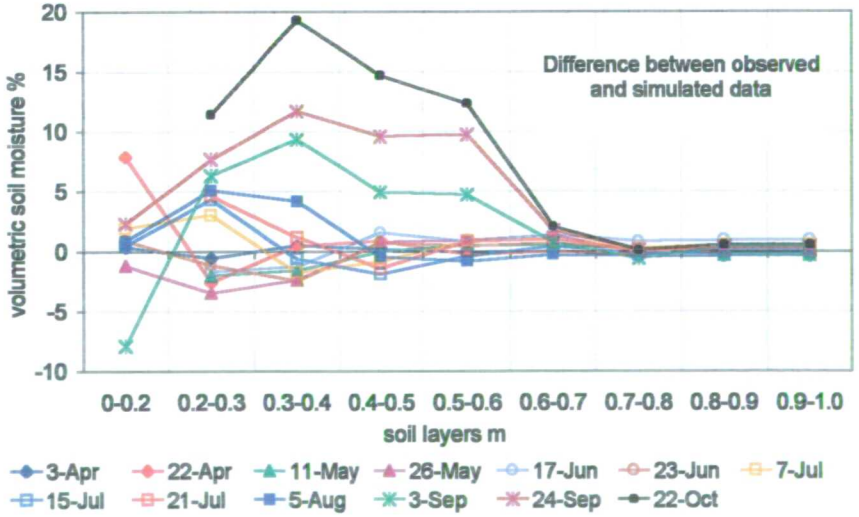


Figure 5.4. Soil moisture change in the main enclosure in the study field in 1998, with a: observed data, b: the BUDGET simulation and c: difference. The legend shown is common to all charts. Figure c has been obtained by subtracting simulated moisture content from observed data so that a positive difference indicted that the marsh is wetter than simulated, negative values indicate the reverse situation.

The statistical analysis of the 1998 simulation is presented in Table 5.5. The simulation performs extremely well with a correlation coefficient of 0.91. Positive Mean and Standard Percental Errors (MPEs and SPEs) are greater than negatives, which indicate that simulated moistures are lower than observed data. The positive Errors are reduced considerably when only the period April to August 1998 is analysed indicating the model is successful in simulating the drying phase; only when the soil wets again are significant errors produced.

The MPE is interpreted in the following manner. For a moisture content of 30% for example, a negative MPE of -3.23% and positive MPE of 5.83% (results of the simulation of April to August 1998 in the main enclosure), results in a simulated moisture content in the range 29-32% respectively. This contrasts with the MPE for the whole 1998 dataset in the main enclosure of –3.19 and 12.02 resulting in a simulation moisture range of 29-34%. This is still an accurate range as the loss of accuracy once the soil begins to wet is masked by the overall average.

Table 5.3. Temporal change in observed soil moisture % per depth increment at the main enclosure over 1998 used to calibrate the BUDGET model. Soil moisture values, %, are expressed per depth layer, m, and date of monitoring. The surface 0.2 m layer data was monitored with electrical resistance blocks with neutron scattering below this depth; note there are some dates with no surface measurement.

| | Soil compartments m | | | | | | | | |
|---|---|---|---|---|---|---|---|---|---|
| 1998 | 0-0.2 | 0.2-0.3 | 0.3-0.4 | 0.4-0.5 | 0.5-0.6 | 0.6-0.7 | 0.7-0.8 | 0.8-0.9 | 0.9-1.0 |
| 3 April | 45 | 37 | 36 | 36 | 36 | 37 | 39 | 40 | 40 |
| 22 April | 46 | 39 | 38 | 37 | 36 | 37 | 39 | 40 | 40 |
| 9 May | 39 | 37 | 36 | 37 | 36 | 38 | 39 | 40 | 40 |
| 11 May | | 36 | 36 | 36 | 37 | 37 | 39 | 40 | 40 |
| 26 May | 19 | 30 | 34 | 36 | 37 | 38 | 39 | 40 | 40 |
| 17 June | | 26 | 32 | 36 | 37 | 38 | 40 | 41 | 41 |
| 23 June | 12 | 24 | 30 | 35 | 36 | 38 | 39 | 40 | 40 |
| 7 July | 11 | 22 | 26 | 31 | 35 | 38 | 39 | 41 | 41 |
| 15 July | 9 | 21 | 24 | 28 | 33 | 37 | 39 | 40 | 40 |
| 21 July | | 20 | 23 | 27 | 33 | 38 | 39 | 40 | 40 |
| 5 August | 9 | 18 | 22 | 25 | 30 | 36 | 39 | 40 | 40 |
| 3 September | | 18 | 23 | 27 | 32 | 37 | 38 | 40 | 40 |
| 24 September | 10 | 20 | 24 | 30 | 35 | 37 | 39 | 40 | 40 |
| 22 October | | 23 | 32 | 35 | 36 | 38 | 39 | 41 | 41 |

Table 5.4. Simulated soil moisture % per depth increment at the main enclosure over 1998 from the BUDGET model for comparison against Table 5.3. Soil moisture values are listed for the dates for which observed soil moistures are available.

| | Soil compartments m | | | | | | | | |
|---|---|---|---|---|---|---|---|---|---|
| 1998 | 0-0.2 | 0.2-0.3 | 0.3-0.4 | 0.4-0.5 | 0.5-0.6 | 0.6-0.7 | 0.7-0.8 | 0.8-0.9 | 0.9-1.0 |
| 3 April | 44 | 38 | 36 | 36 | 36 | 37 | 39 | 40 | 40 |
| 22 April | 38 | 41 | 37 | 36 | 36 | 37 | 39 | 40 | 40 |
| 9 May | 31 | 39 | 38 | 36 | 36 | 37 | 39 | 40 | 40 |
| 11 May | 30 | 38 | 38 | 36 | 36 | 37 | 39 | 40 | 40 |
| 26 May | 20 | 34 | 36 | 36 | 36 | 37 | 39 | 40 | 40 |
| 17 June | 13 | 28 | 34 | 35 | 36 | 37 | 39 | 40 | 40 |
| 23 June | 11 | 25 | 32 | 34 | 35 | 37 | 39 | 40 | 40 |
| 7 July | 9 | 19 | 27 | 32 | 34 | 37 | 39 | 40 | 40 |
| 15 July | 9 | 16 | 25 | 30 | 34 | 37 | 39 | 40 | 40 |
| 21 July | 9 | 15 | 22 | 29 | 33 | 37 | 39 | 40 | 40 |
| 5 August | 8 | 13 | 18 | 26 | 31 | 36 | 39 | 40 | 40 |
| 3 September | 8 | 12 | 14 | 22 | 27 | 36 | 39 | 40 | 40 |
| 24 September | 8 | 12 | 13 | 21 | 25 | 36 | 39 | 40 | 40 |
| 22 October | 10 | 12 | 12 | 20 | 24 | 36 | 39 | 40 | 40 |

Table 5.5. Six-step goodness of fit between measured and simulation soil moisture for the calibration of the BUDGET model. Optimal values for each criterion are in brackets in the relevant columns. The definition of each criterion is discussed in section 4.3.3.

| | Correlation coefficient (1) | Mean Percental Error (0) | | Standard Percental Error (0) | | Range Index (1) | Level Index (1) | Storage Index (1) |
|---|---|---|---|---|---|---|---|---|
| | | +ve | -ve | +ve | -ve | | | |
| 1998 | 0.91 | 12.02 | -3.19 | 15.37 | 3.12 | 1.27 | 0.92 | 0.26 |
| 1998 until August | 0.97 | 5.83 | -3.23 | 7.68 | 3.14 | 1.12 | 0.97 | 0.91 |

As the 1998 simulation is successful in recreating the low summer moisture content, the Range and Level Indexes are close to optimal as expected. This is also true for the Storage Index of the truncated 1998 dataset (April to August). A much lower value of 0.26 for the Storage Index is calculated when considering the whole 1998 dataset due to the inability of BUDGET to successfully simulate the re-wetting of the soil. This results in final simulated moisture contents much lower than observed creating a low Storage Index.

5.2.2.3 Validation

The calibrated model was subsequently validated using input data from 1999 to ascertain if the success of BUDGET to simulate the soil moisture in 1998 could be repeated. Unfortunately soil moisture data from neutron scattering was not available

in 1999 and soil samples were taken using augers instead. This introduces greater variability in the soil moisture data for 1999 due to two reasons. Firstly, the soil moisture at the exact location cannot be monitored over time. In addition, as the soil dries out and becomes hard and brittle, it is very difficult to extract a soil sample using augers, and the depth to which a sample is taken cannot be precisely determined.

This leads to moisture values for irregular depth increments that cannot be precisely compared against each other. However it was possible to average values to describe the same soil layers as the calibration data set. Soil samples were taken over July to November 1999 resulting in a shorter database and modelling period compared to 1998. As with model calibration, soil conductivity measurements with depth for soil in the enclosure were taken from Table 3.10. These data are listed in Table 5.6.

Table 5.6. Input soil moisture and soil conductivity data to initiate the validation simulation of the marsh field interior. Data are for 8 July 1999.

| Soil Layer | 0-0.2 | 0.2-0.3 | 0.3-0.4 | 0.4-0.5 | 0.5-0.6 | 0.6-0.7 | 0.7-0.8 |
|---|---|---|---|---|---|---|---|
| Soil moisture % | 14 | 18 | 23 | 26 | 25 | 32 | 39 |
| Soil conductivity dS $m^{-1}$ | 2.61 | 2.83 | 2.83 | 3.91 | 3.91 | 3.74 | 3.74 |

Tables 5.7 and 5.8, and Figure 5.5 show the observed and modelled soil moisture content for the validation simulation over time and the difference between them. It was found that the parameter settings as employed in the 1998 simulation run also provided the best fit between simulated and observed soil moistures for 1999. The statistical analysis of the 1999 simulation is presented in Table 5.9. The correlation coefficient for the simulation is good but lower than 1998 which is expected from the model results presented in Figure 5.5. The error values are much higher than for 1998 due to the under-prediction of moisture loss at depth. In addition the moisture dataset in 1999 has a shorter period of drying, which is the period over which the model performs best, and so MPE and SPE are high. Again positive Errors are greater than negatives, indicating that the simulated moistures which are lower than the observed data are of greater significance. Negative Errors are comparable to the 1998 dataset. This indicates that for all simulations performed, the consistent problem of the model is overestimation of the evaporative loss which results in low soil moistures.

a:

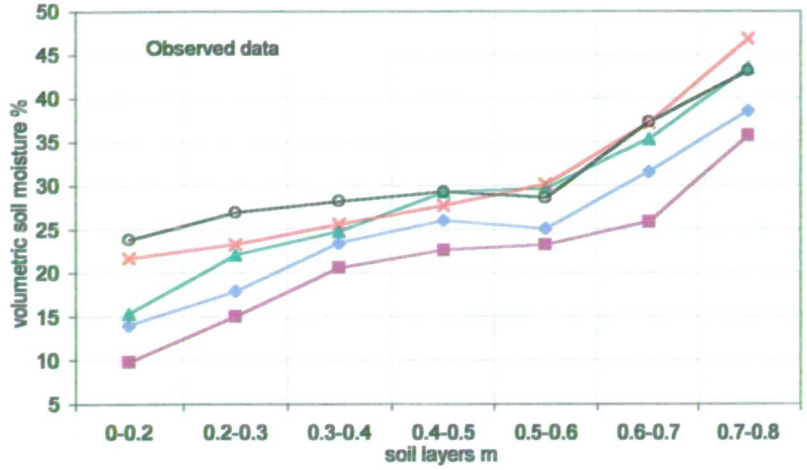


b:

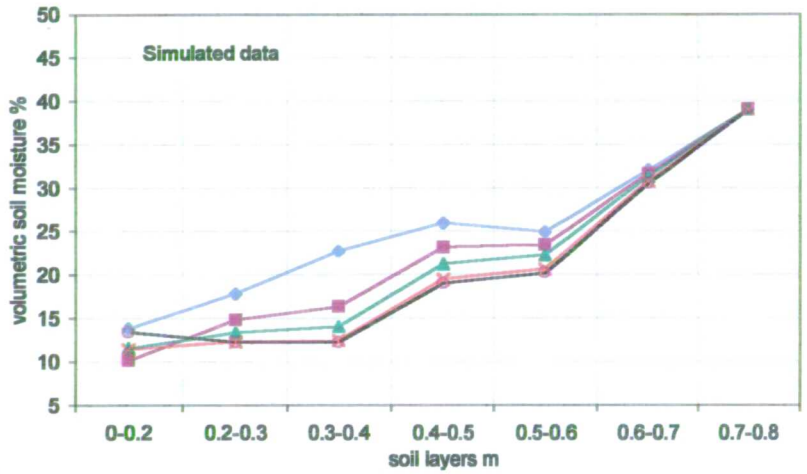


c:

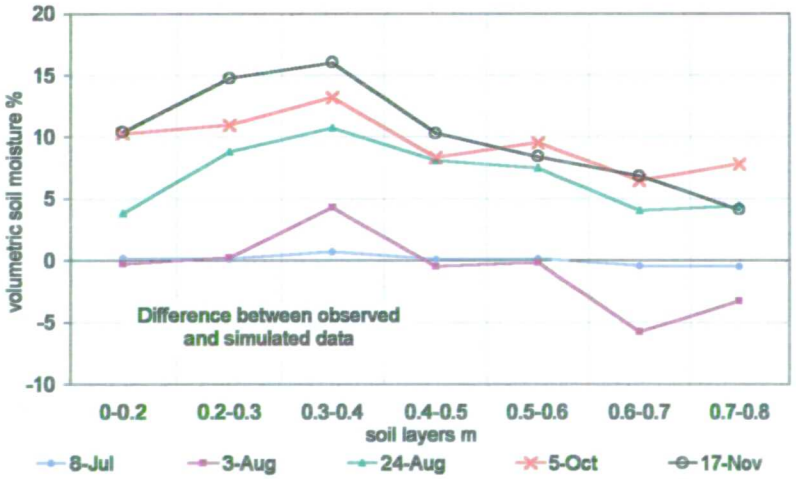


Figure 5.5. Soil moisture change in the main enclosure in the study field in 1999 with a: observed data, b: the BUDGET simulation and c: difference. The legend shown is common to all charts. Figure c has been obtained by subtracting simulated moisture content from observed data so that a positive difference indicted that the marsh is wetter than simulated, negative values indicate the reverse situation.

Table 5.7. Observed soil moisture at the main enclosure over 1999 used to validate the BUDGET model. Soil moisture values, %, are expressed per depth layer, m, and date of monitoring. The surface 0.2 m layer data was monitored with electrical resistance blocks with neutron scattering below this depth.

| Soil compartments m | | | | | | | |
|---|---|---|---|---|---|---|---|
| 1999 | 0-0.2 | 0.2-0.3 | 0.3-0.4 | 0.4-0.5 | 0.5-0.6 | 0.6-0.7 | 0.7-0.8 |
| 8 July | 14 | 18 | 23 | 26 | 25 | 32 | 39 |
| 3 August | 10 | 15 | 21 | 23 | 23 | 26 | 36 |
| 24 August | 15 | 22 | 25 | 29 | 30 | 35 | 43 |
| 5 October | 22 | 23 | 26 | 28 | 30 | 37 | 47 |
| 17 November | 24 | 27 | 28 | 29 | 29 | 37 | 43 |

Table 5.8. Simulated soil moisture at the main enclosure over 1999 from the BUDGET model. Simulated soil moisture output of the BUDGET model in 1999. Soil moisture values are listed for the dates for which observed soil moistures are available.

| Simulated soil moisture % from electrical resistance soil sampling | | | | | | | |
|---|---|---|---|---|---|---|---|
| Soil compartments m | | | | | | | |
| 1999 | 0-0.2 | 0.2-0.3 | 0.3-0.4 | 0.4-0.5 | 0.5-0.6 | 0.6-0.7 | 0.7-0.8 |
| 8 July | 14 | 18 | 23 | 26 | 25 | 32 | 39 |
| 3 August | 10 | 15 | 16 | 23 | 23 | 32 | 39 |
| 24 August | 12 | 13 | 14 | 21 | 22 | 31 | 39 |
| 5 October | 11 | 12 | 12 | 19 | 21 | 31 | 39 |
| 17 November | 13 | 12 | 12 | 19 | 20 | 31 | 39 |

Table 5.9. Six-step goodness of fit between measured and simulation soil moisture for the validation of the BUDGET model. Optimal values for each criterion are in brackets in the relevant columns. The definition of each criterion is discussed in section 4.3.3.

| | Correlation coefficient | Mean Percental Error (0) | | Standard Percental Error (0) | | Range Index | Level Index | Storage Index |
|---|---|---|---|---|---|---|---|---|
| | (1) | +ve | -ve | +ve | -ve | (1) | (1) | (1) |
| 1999 | 0.82 | 24.92 | -5.84 | 32.33 | 4.56 | 1.11 | 0.81 | -1.38 |

The Range and Level Indexes perform well. The Storage Index has a negative value as the final moisture values are in different directions than the initial moisture levels. This means that while observed moisture recovered to 31% by end of the simulation, wetter than the initial moisture level of 25%, the simulated dataset remains at a low of 21% by the end of modelling from the same initial moisture content.

It can be stated that the model has not been sufficiently validated and that it needs to be compared against data over a number of years. However, it has been shown that the model successful replicates the change in soil moisture observed in 1998 based on the input data of precipitation and evaporation.

5.2.2.4 Ditch recharge

In order to examine the recharge of soil moisture along the ditch edge, a simulation was performed with BUDGET using soil moisture data from neutron scattering adjacent to the north ditch of the study field in 1998. Surface soil moistures next to the neutron access tube were determined by either taking samples or using the SCIP. Under conditions of no recharge from the ditch, the model should be able to simulate the change in soil moisture as accurately as the calibration simulation over the same time period. The ditch edge simulation spans the period May to October 1998, over which period there are certain dates for which surface soil moisture was not available. Values for the soil conductivity of the ditch edge with depth were taken from Table 3.10. These data are listed in Table 5.10. The simulation parameters determined as optimal during model calibration and validation simulation were employed. The results of modelling are presented in Figure 5.6 and Tables 5.11 and 5.12.

The results of the simulation exhibit a major overestimation of the moisture decline i.e. BUDGET simulates a decline in soil moisture, based on the fluxes of precipitation and evaporation, that is not observed by regular monitoring. Differences between simulated and observed moisture contents of up to 42% are observed at the surface. Over May to July the difference below 0.2 m depth is considerably lower in the range 0-6%. After July however, the model simulates a decrease in soil moisture, due to the lack of rain for three weeks during August, but a decrease in soil moisture to the same extent is not observed by neutron scattering. These results indicate recharge from the ditch is maintaining higher moisture levels. After the three-week period of no rain, precipitation received over the marsh is intense with 158 mm recorded over 23 August to 22 October. The model however continues to simulate a fall in soil moisture albeit at a reduced rate with an increase only in the surface layers. This is in contrast with observed data that exhibits a slight increase in moisture values through recharge via macropores.

Table 5.10. Input soil moisture and soil conductivity data to initiate the ditch recharge simulation adjacent to the north ditch. Data are for 9 May 1998.

| Soil Layer | 0-0.2 | 0.2-0.3 | 0.3-0.4 | 0.4-0.5 | 0.5-0.6 | 0.6-0.7 | 0.7-0.8 |
|---|---|---|---|---|---|---|---|
| Soil moisture % | 65 | 41 | 41 | 39 | 38 | 43 | 46 |
| Soil conductivity dS $m^{-1}$ | 6.19 | 5.16 | 5.16 | 4.69 | 4.69 | 4.75 | 4.75 |

a:

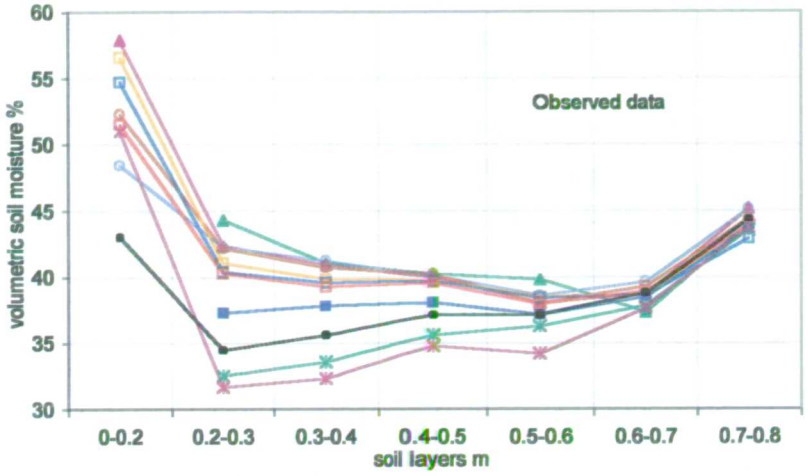


b:

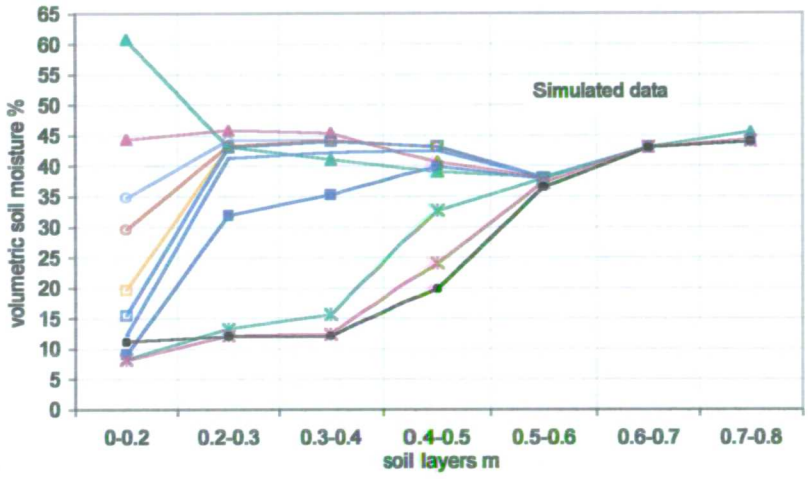


c:

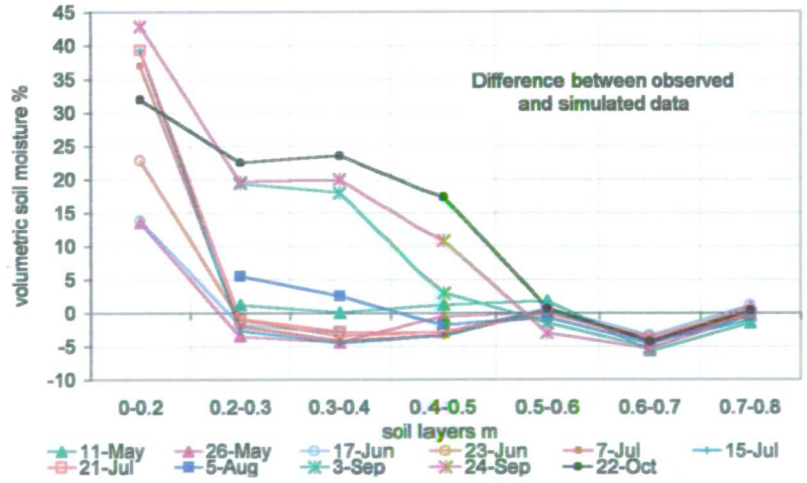


Figure 5.6. Soil moisture change adjacent to the north ditch of the study field in 1998 with a: observed data, b: BUDGET simulation and c: difference. The legend shown is common to all charts. Figure c has been obtained by subtracting simulated moisture content from observed data so that a positive difference indicted that the marsh is wetter than simulated, negative values indicate the reverse situation.

That BUDGET does not simulate the observed values of soil moisture indicates that there is some lateral movement of water taking place from the ditch maintaining the high soil moistures along its border. The large differences between the simulated and observed moisture data of the surface soil highlights the influence of the ditch in maintaining high moisture values in this layer.

The statistical analysis of this simulation is presented in Table 5.13. The correlation coefficient of the ditch riparian area simulation is extremely low, which is to be expected due to the poor performance of the model in this simulation. The simulation of the soil moisture adjacent to the north ditch of the study field gives poor performances on all criteria in Table 5.13 though most results are improved if only the period April to August is analysed. In particular the MPE is reduced, and the Range, Level and Storage Indexes are closer to unity. The high positive Mean Percental Errors of 29.2 and 17.6, for the dataset entire and truncated (April to August), indicate the underestimation of the moisture content (i.e. simulated soil moisture is lower than observed) as seen in Figure 5.4. With an MPE 29.27 and –5.99% the simulated soil moisture is in the range of 28-39% from an observed value of 30%. The percental nature of this index means that the higher the moisture content the greater the error.

Table 5.11. Change in observed soil moisture % per depth increment at the north ditch over 1998. Soil moisture at the surface was determined by soil sampling or using the SCIP and values of moisture below this layer measured by neutron scattering.

| | Soil compartments m | | | | | | |
|---|---|---|---|---|---|---|---|
| 1998 | 0-0.2 | 0.2-0.3 | 0.3-0.4 | 0.4-0.5 | 0.5-0.6 | 0.6-0.7 | 0.7-0.8 |
| 9 May | 65 | 41 | 41 | 39 | 38 | 43 | 46 |
| 11 May | | 44 | 41 | 40 | 40 | 37 | 44 |
| 26 May | 58 | 42 | 41 | 40 | 38 | 39 | 45 |
| 17 June | 48 | 42 | 41 | 40 | 39 | 40 | 45 |
| 23 June | 52 | 42 | 41 | 40 | 38 | 39 | 44 |
| 7 July | 57 | 41 | 40 | 40 | 38 | 39 | 44 |
| 15 July | 55 | 40 | 40 | 40 | 38 | 39 | 43 |
| 21 July | 51 | 40 | 39 | 40 | 38 | 39 | 44 |
| 5 August | | 37 | 38 | 38 | 37 | 38 | 44 |
| 3 September | | 33 | 34 | 36 | 36 | 38 | 44 |
| 24 September | 51 | 32 | 32 | 35 | 34 | 38 | 44 |
| 22 October | 43 | 34 | 36 | 37 | 37 | 39 | 44 |

Table 5.12. Simulated soil moisture at the north ditch over 1998. Soil moisture values are listed for the dates for which observed soil moistures area available.

| | Soil compartments m | | | | | | |
|---|---|---|---|---|---|---|---|
| 1998 | 0-0.2 | 0.2-0.3 | 0.3-0.4 | 0.4-0.5 | 0.5-0.6 | 0.6-0.7 | 0.7-0.8 |
| 9 May | 64 | 42 | 41 | 39 | 38 | 43 | 46 |
| 11 May | 61 | 43 | 41 | 39 | 38 | 43 | 46 |
| 26 May | 44 | 46 | 45 | 41 | 38 | 43 | 44 |
| 17 June | 35 | 44 | 44 | 43 | 38 | 43 | 44 |
| 23 June | 30 | 43 | 44 | 43 | 38 | 43 | 44 |
| 7 July | 20 | 43 | 44 | 43 | 38 | 43 | 44 |
| 15 July | 15 | 43 | 44 | 43 | 38 | 43 | 44 |
| 21 July | 12 | 41 | 42 | 43 | 38 | 43 | 44 |
| 5 August | 9 | 32 | 35 | 40 | 38 | 43 | 44 |
| 3 September | 8 | 13 | 16 | 33 | 38 | 43 | 44 |
| 24 September | 8 | 12 | 12 | 24 | 37 | 43 | 44 |
| 22 October | 11 | 12 | 12 | 20 | 37 | 43 | 44 |

Table 5.13. Six-step goodness of fit between measured and simulation soil moisture for the assessment of ditch recharge. Optimal values for each criterion are in brackets in the relevant columns. The definition of each criterion is discussed in section 4.3.3.

| | Correlation coefficient (1) | Mean Percental Error (0) | | Standard Percental Error (0) | | Range Index (1) | Level Index (1) | Storage Index (1) |
|---|---|---|---|---|---|---|---|---|
| | | +ve | -ve | +ve | -ve | | | |
| 1998 ditch | 0.17 | 29.27 | -5.99 | 29.62 | 4.91 | 2.11 | 0.90 | 0.31 |
| 1998 ditch until August | -0.14 | 17.58 | -5.70 | 32.00 | 4.94 | 1.55 | 0.96 | 0.57 |

To conclude it can be seen that maintenance of high levels of soil moisture from recharge from the ditch does occur but that it is extremely limited in spatial extent to only a few metres. Away from this zone of influence along the edges of ditches that overtop their banks, the change in soil moisture of the marsh is characterised by the fluxes of precipitation and evaporation only.

5.2.2.5 Soil electrical conductivity

Finally a brief examination of the change in salt electrical conductivity can be examined using BUDGET. The accuracy of the model to simulate change in soil electrical conductivity cannot be established, unlike the soil moisture simulations, as only average data per soil layer are available rather than the required relationship with soil moisture content (Table 3.10). However the model provides an opportunity to

ascertain the effect on soil conductivity from flooding with brackish ditch water which is stipulated in the ESA management prescription Tier 1b.

The procedure employed was to examine the change in soil conductivity of soil that is not normally susceptible to brackish floodwaters. To this end a model simulation was performed using 1998 soil moisture and electrical conductivity data for the enclosure as has been used for the calibration of the model. Precipitation was assigned an electrical conductivity of 0.1 dS $m^{-1}$, as measured in the Met. Office gauge (Table 3.10). A second simulation was also performed with the same input data but assigning a value of 3.6 dS $m^{-1}$ to precipitation. This value of electrical conductivity is that measured in the north ditch of the study field. It must be stated that these simulations do not represent the field conditions totally by treating the inundation of ditch water as precipitation rather than ponded water, however this was the most suitable method to employ the model to this end. Figure 5.7 shows the result of the two simulations. Results are expressed per soil layer to a depth of 0.4 m (for subsequent soil layers, no change was observed in electrical conductivity and so these data have been excluded from Figure 5.7 for clarity).

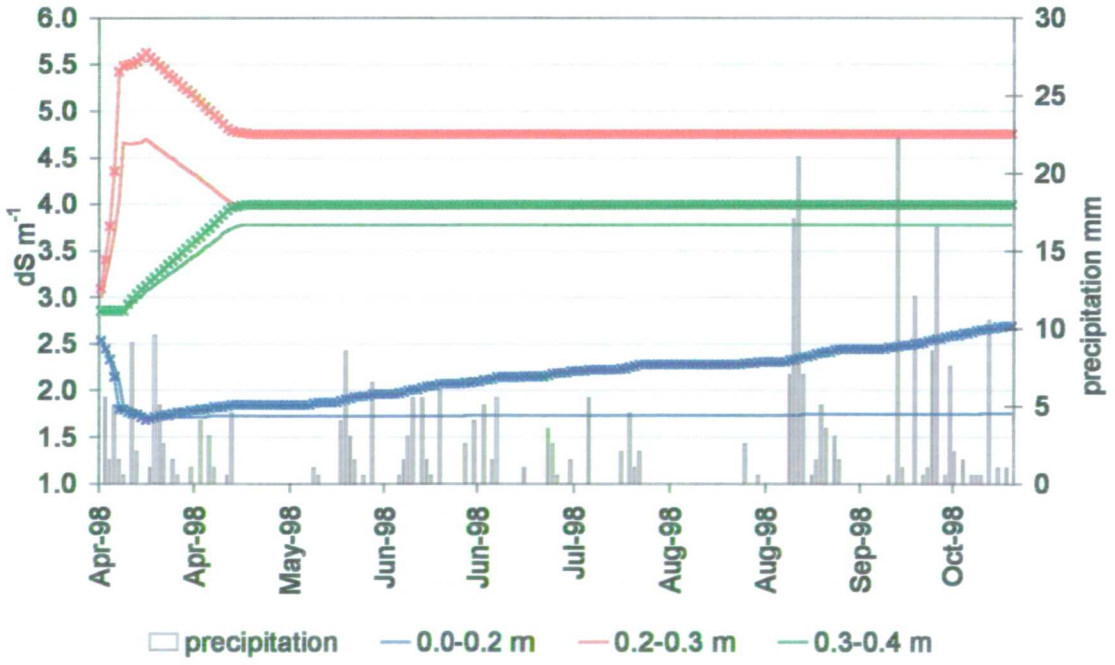


Figure 5.7. Results of BUDGET simulation to examine change in soil electrical conductivity with precipitation used to represent flooding from the north ditch. Results are shown over time per soil layer. The simulation with precipitation of measured conductivity, 0.1 dS $m^{-1}$ shows soil layers with smooth lines. The simulation with precipitation of higher conductivity, 3.6 dS $m^{-1}$ shows soil layers with crossed lines.

Figure 5.7 shows with precipitation of 0.1 dS $m^{-1}$, the action of the incoming water is to leach salt from the surface layer deeper into the profile. This causes the salt content in the deeper layers, 0.2-0.3 m and 0.3-0.4 m to increase accordingly. The salt of the top layer, 0-0.2 m deep is flushed quickly due to the rain at the beginning of the simulation and thereafter remains constant. The salt content rises in the 0.2-0.3 m layer concomitant to the decrease of the upper layer. The salt is leached further as the 0.2-0.3 m soil layer reaches saturation and drains to the 0.3-0.4 layer. This pattern of salt transport is linked to the soil moisture of the soil layer as described in section 5.2.1.4.

With precipitation of 3.6 dS $m^{-1}$, a similar pattern is observed but the change in magnitude of electrical conductivity is greater. The greater influx of salt causes higher soil conductivity in all soil layers particularly the layer 0.2-0.3 m deep. The most marked deviation from the first simulation is the steady increase in conductivity of the surface soil with continued precipitation over the time period illustrated.

It can be inferred from these results that with repeated flooding of the marsh with water of higher electrical conductivity (and sodicity), the electrical conductivity of the soil will increase. The elevated soil electrical conductivity of the 0.2-0.3 m soil layer in Figure 5.7 reach levels that have been observed alongside ditch margins and areas of the study field that experience regular inundation (Figure 3.4, Table 3.10). Widespread flooding causing an increase in soil conductivity over large areas could prove to have deleterious feedbacks with a change in flora and soil structural properties. This is discussed further in section 6.4.

### 5.2.3 Conclusions

The BUDGET model accurately simulates the moisture content of the field interior when the soil is drying out, using only rainfall and evaporation as input data. However it cannot account for the rapid re-wetting of the marsh which occurs by preferential flow along cracks and macropores. The model needs to be validated using a longer time period, which is outside the scope of this project. However the successful simulation results from 1998 highlight the fact that the change in soil

moisture over the marsh can be simulated using only precipitation and evaporation over the drying phase.

Maintenance of high soil moisture from ditch recharge does occur, as illustrated by the simulation of soil adjacent to the north ditch of the study field, but it is extremely limited in spatial extent of only a few metres. Away from this zone of influence, the change in soil moisture of the marsh is characterised by the fluxes of precipitation and evaporation only which can be simulated by BUDGET.

The statistical analyses in Tables 5.5 and 5.9 show that the number of positive Mean Percental Errors (simulated soil moisture is lower than observed), outnumber negative differences and are of much larger magnitude. This means that the marsh is actually wetter than simulated indicating that too much water is being evaporated in the model.

The evaporation data used in the BUDGET simulations is computed from Penman Monteith using reference conditions of grass height and surface resistance. The transpiration submodel within BUDGET is discussed above, and the default setting of $p$ has been employed i.e. 60% of the TAW fraction is readily available. In brief, transpiration will occur at the potential rate until the readily available fraction has been depleted. After this critical point, actual transpiration loss will be less than potential at a rate dependant upon the moisture content of the soil, becoming zero at the wilting point.

In order to reduce the predicted evaporative loss from the marsh, the value of $p$ could be set higher so that the RAW fraction is depleted more quickly so that the actual transpiration become less than potential rates. However, sensitivity analysis of this parameter revealed little improvement in the fit of simulated to observed data. Alternatively, the value of field capacity could be reduced for each soil layer to a value more akin to field observations, which will reduce the TAW fraction. However, changing the value of this parameter from the values used in the calibration and validation simulations have a negative feedback in the drainage submodel resulting in less accurate simulations overall.

Evaporation loss from the marsh is explored in more detail in Chapters 7 and 8 as the results of the research detailed so far confirm that the dominant fluxes over the marsh

are vertical. The evaporative flux is the dominant loss of water from the system and needs to be investigated in more detail, particularly the adaptation of the Penman Monteith model to the wet grassland conditions. In addition, as the results of the BUDGET simulations have indicated, the relationship between potential evaporation computed by Penman Monteith and decreasing soil moisture needs to be examined. The second and third research investigations focus upon this important dominant process.

## 5.3 Inundation of the marsh and surface soil moisture

As discussed in section 3.1, the ESA review introduced an evolution of Tier 1a in Tier 1b which stipulates that a proportion of the land surface be inundated either through pumping or flooding of ditch water into surface rills. The objective is to create soft ground conditions together with areas of open water for feeding and breeding waterfowl. The FRCA (1997, p15) state that land entered into Tier 1b must follow the guidelines of:

- shallow (up to 0.2 m) surface water over at least 20% of the area from 1 December to 31 March
- shallow surface water over at least 15% of the site during April
- shallow surface water over 10% of the site to the end of May
- at least 300 mm depth of water in ditches during the summer and autumn months

### 5.3.1 Inundation of the marsh

As discussed in section 4.1 the study field (and the Elmley Marshes overall) experiences inundation over the winter months and subsequently dries out over the summer. The spatial extent of flooding of the study field was monitored over the winter of 1998 throughout 1999, and can be seen in Figure 5.10. The figure shows flood extent for four occasions over November 1998 to June 1999; start of inundation (November); maximum period of inundation (January); drying off (March) and the effective end of water on the marsh (June). Inundation occurs chiefly through the flooding of surface depressions and rills, creating a patchwork effect of open water

and grass areas. Figure 5.11 presents a selection of 'typical' flood scenes. The study field has a natural relict system of saltmarsh channels into which water can flow from the ditches. The most controlled method to achieve surface flooding is to enhance this natural microtopography by creating channels to transport water from ditches to spill into surface rills and depressions, rather than rely upon flooding through heavy winter precipitation. Figure 4.3 shows the elevation of these natural rills, and the level in each ditch to which water levels must rise to enter the channels. The proportion of time that the east and west ditches exceed the rill elevation is less than the other ditches in most part due to the high banks caused by silt deposition and lower water levels.

Figure 5.8 demonstrates the change in the extent of land cover of the study field over the inundation cycle. Using detailed maps of the study area, the extent of open water and bare soil on the land surface of the field was sketched on field visits over the period November 1998 to October 1999. The areas of these surface types were computed using the counting square method. The extent of grass covered marsh was determined as a residual of the remaining area of the land surface. The areal extent of open water in the ditch channels was determined using wet width: stage relationships formulated for each of the four ditches that border the study field. The cross section of each ditch was measured at bankfull capacity (Figure 4.4), allowing the derivation of third order polynomial relationships relating the wet width of the water surface to water level (Figure 5.9). This enabled the area of the water surfaces of each ditch to be computed from its water level and length, which was added to the area of open water from the land surface. A fall in ditch water level causes a reduction in the area of open water, due to the sloping sides of the ditch banks, exposing bare soil. The area of bare soil, determined as the difference between the maximum ditch water area and its current area, is added to the area of bare soil on the land surface.

Prior to inundation, the marsh is nearly completely covered by grass with a small area of bare soil located at gates or alongside ditch margins where the cattle trample the soil. With increased flooding, the area of open water increases to 50% of the field in January. As the flood waters recede or dry off, the area of ground previously under water become patches of bare soil as the vegetation has died. As open water areas dry

off so the proportion of bare soil increases in tandem. This process continues until a point is reached in late April when the area of bare soil decreases in extent as it is starts to be re-colonised by vegetation. The change in extent of the surface flooding of the study area exceeds the prescription of Tier 1 b.

The effect of the changing proportion of different land cover also has an effect upon the processes operating to evaporate water from the marsh. This is investigated further as the third research investigation, Chapter 8.

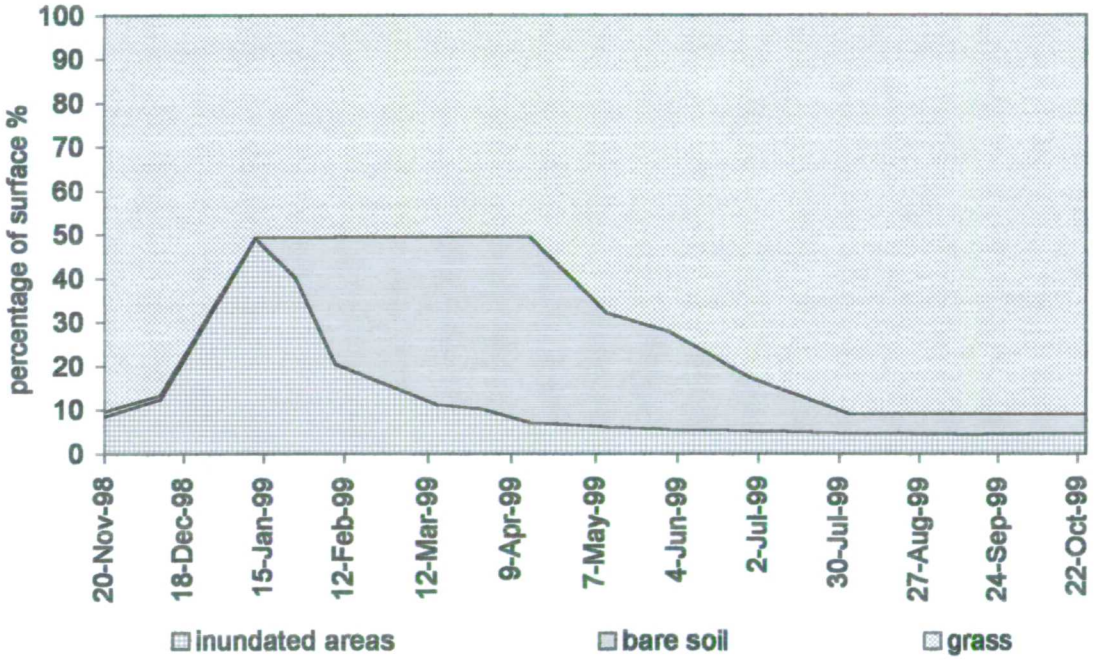


Figure 5.8. The change in extent of the land cover of the study field over the cycle of inundation (see Figures 5.10 and 5.11). The extent of flooding and bare soil was mapped on field visits and the area computed by the counting square method. Open water areas include the surface area of the water in the four ditches surrounding the study field. The proportion of grass was computed as the remainder from the total area of the field.

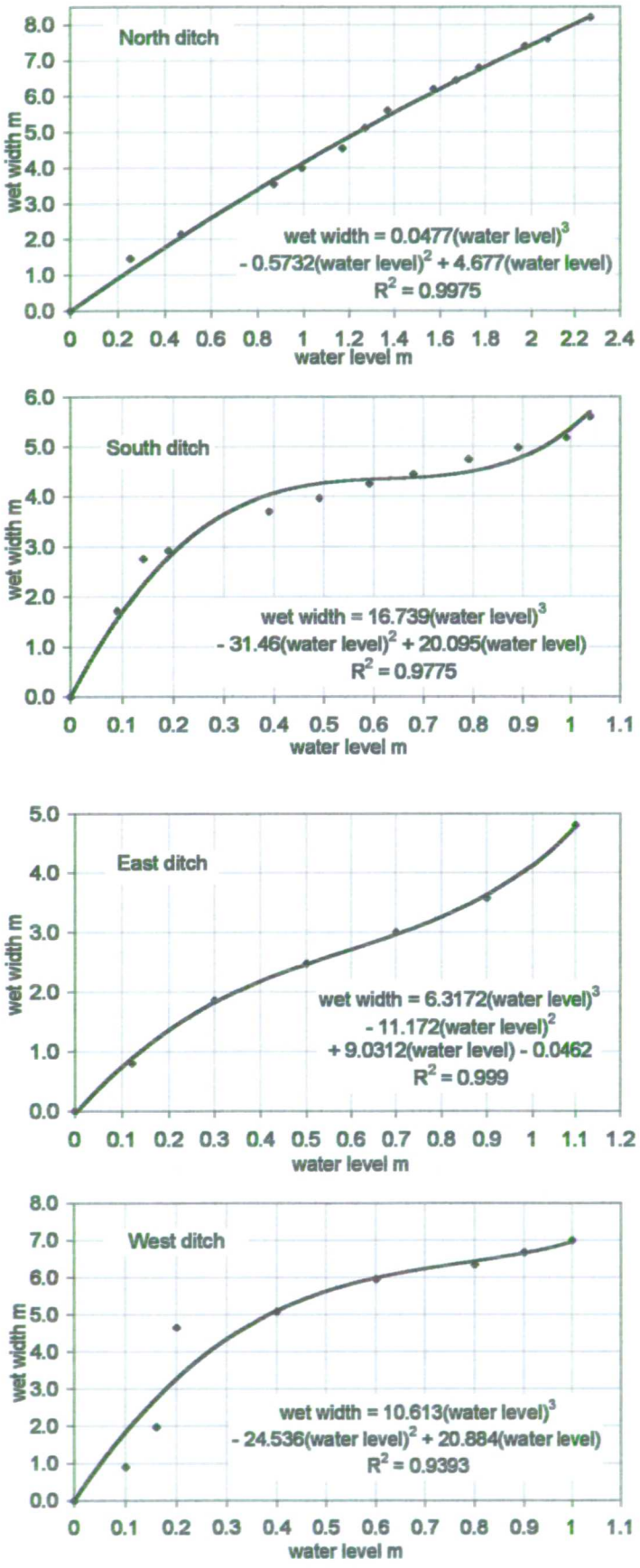


Figure 5.9. The third order polynomial relationship between the wet width of the water surface and water level of the four ditches bordering the study field.

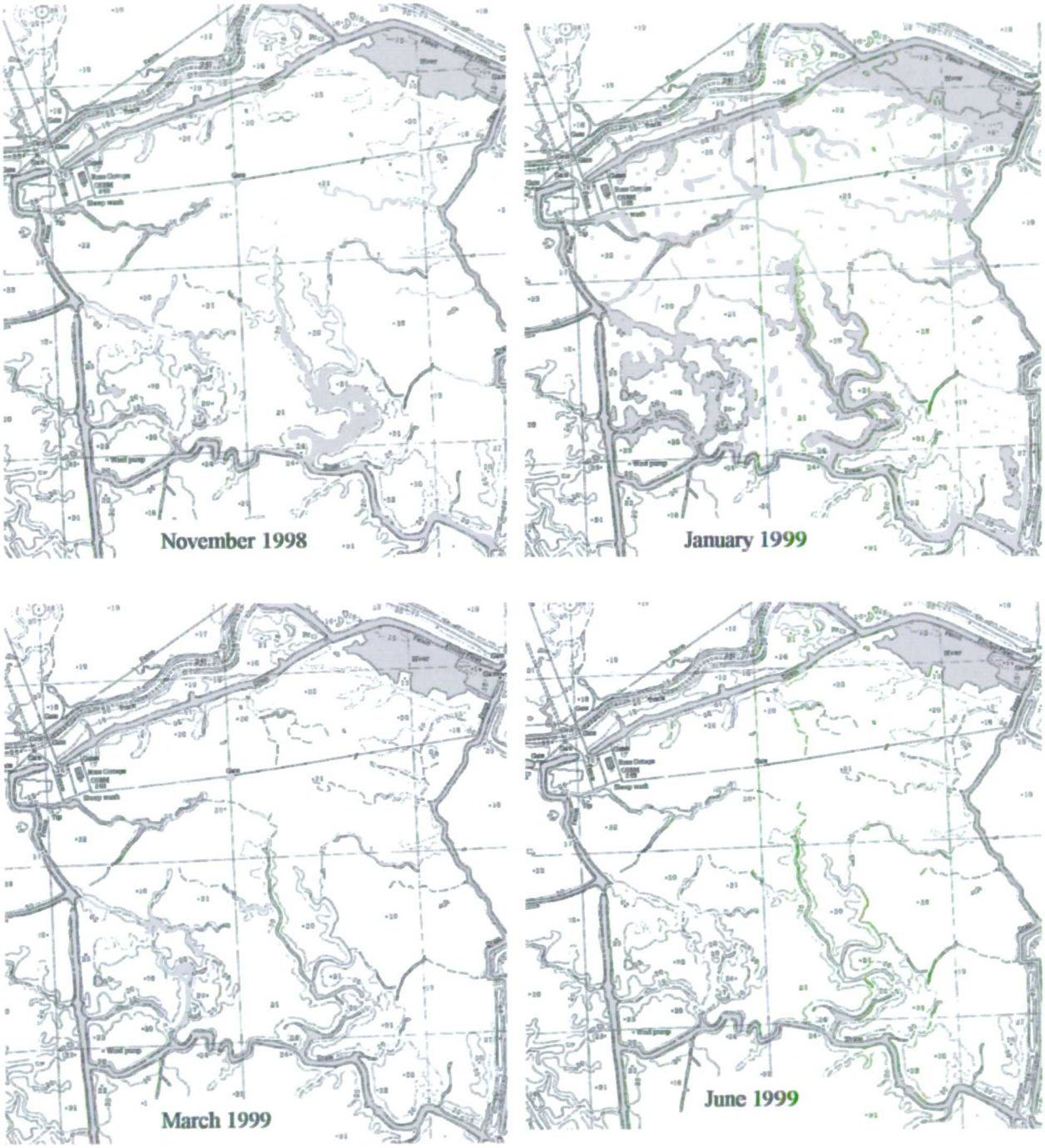


Figure 5.10. The inundation extent of the study field over winter 1998/1999. Shaded areas indicate flooding. The first instance of flooding was recorded in November 1998 with the maximum cover of floodwater in January 1999. Water patches started to dry up after January until only a small extent remained in June 1999. Inundation is a combination of flooding from the ditches through surface rills (south and north ditches respectively) and standing water from precipitation. Figure 5.11 also illustrates flooding of the study field, and Figure 5.8 shows the change in extent of land cover (grass, open water, bare soil) over the same period. As an idea of scale, each square on the map represents 200 m x 200 m.

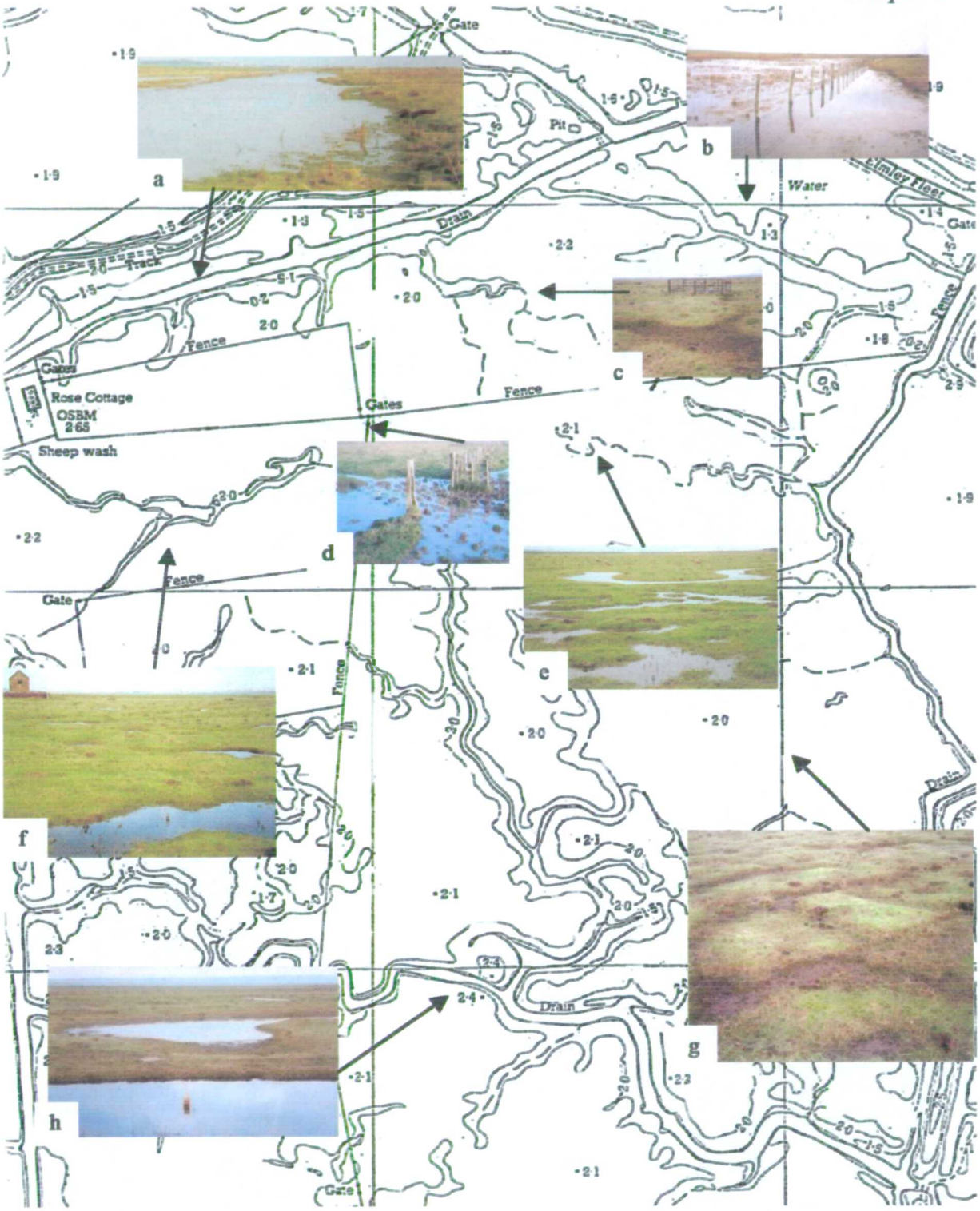


Figure 5.11. Visual display of the inundation of the study field showing areas under flood and drying out. Images a and b show the north ditch flooding over the bank edge and into the top right corner of the field; d shows flooding over bare soil through access points such as gates. Images e, f and h are examples of flooded rill features of the field which serve as natural conduits to collect both precipitation and ditch water. Images c and g show previously inundated area drying out; the grass has died so that patches of bare soil are produced. Images e and g indicate the 'chessboard' variability of the surface when under water with the juxtaposition of patches of grass and open water, replaced by grass and bare soil when the floodwater subside. The bare soil is quickly colonised reducing the extent of cover of bare soil (Figure 5.8).

### 5.3.2 Surface soil moisture monitoring

To examine the moisture content of the surface with increasing distance from the north ditch, a monitoring program was established using the Surface Insertion Capacitance Probe, SCIP, within a regular grid to obtain repeated measurements of moisture of the upper 0.1 m at the same locations over time. Appendix A.6 details the instrument design, functioning and calibration to the Wallasea soil series.

#### 5.3.2.1 Determination of sampling strategy

Due to the constraints upon time and effort, the whole of the study field could not be monitored with the SCIP to determine the spatial change of surface soil moisture coupled with observation of inundation. A sampling strategy had to be determined to ensure soil moisture was being sampled in a way that could identify spatial change, and the tool of geostatistical sampling was employed. See Appendix B for a wider discussion on the theory of geostatistical sampling.

As little was known about the variability of the soil moisture of the surface, a balanced nested sampling scheme was adopted in order to encompass larger lag distances than would have possible using transects or grids. This approach is widely used and 'most published accounts of reconnaissance spatial surveys involve nested designs' (Pettitt and McBratney 1993 p191). Oliver *et al.* (1989b p 277) succinctly summarise the problem:

> 'It often happens that local estimates and quantitative maps are required for little known regions. How should such a region be sampled? If a given sampling interval is sparse relative to the intensity of the variation there might be no dependence in the data: neighbouring sites might be beyond the range of the semivariogram. On the other hand if the semivariogram has a long range then a similar sampling intensity may be unnecessary dense and so waste resources. Thus in many instances uniform sampling over the whole region must be a hit or miss affair. Some means is needed of identifying the spatial scale of variation economically and surely, albeit only roughly, before sampling uniformly to map. This can be achieved using a nested sampling and hierarchical analysis of variance as part of a two-stage survey.'

The principle of the nested approach is that an individual observation embodies variation from each stage in a hierarchy, including unresolved variance from the lowest stage and the contributions from each stage is estimated by the analysis. These contributions are the components of variance. While only a few lags (distances) can be sampled, the great advantage of the technique is that the variation over orders of magnitude can be covered in a single sampling attempt. The nested design employed in the study field is illustrated in Figure 5.12. It comprised six stations each with five nested stages. Each station was located in different areas of the study field in the same surface type (grass) in order to encompass as much of the field as possible to integrate the maximum variance. At each sampling node within the nested design the soil moisture level was measured with the SCIP. The components of variance were then computed (Table 5.14).

It can be seen from Table 5.14 that the components of variance per stage increases from 0.5 m lag to 10 m. Between 10 m – 30 m the variance stays stable, but increases between 30 m and 60 m lag. These results indicate spatial independence at short and long lags and to confirm these findings a 90 x 90 m grid was sampled at a lag of 5 m to determine the semivariance more precisely. The experimental semivariogram (Figure 5.13) was calculated using the shareware geostatistical modelling software gstat (Pebesma 1997). Figure 5.13 illustrates a spatial dependence at small sampling distances (less than 20 m), followed by spatial independence between 20 m – 80 m, and increasing variability from 80 m. Thus sampling with a small grid (less than 20 m) will give most information however this would involve considerable time and effort to cover the entire field. A more economical sampling scheme would be a wide grid width with nodes every 80 m however this would not allow an appraisal of small-scale changes. In view of these results, in order that the soil moisture of the marsh around flooded areas from ditch overtopping and surface could be examined, it was decided to sample only a portion of the field keeping the 90 x 90 m grid with measurements at 10 m nodes.

The grid was positioned with the north ditch at the grid's north edge (Figure 1.3). The north ditch was chosen as it floods along its edge, and the results of neutron scattering (section 5.1.2) have illustrated an influence of the ditch in maintaining high moistures alongside its riparian border. In addition the grid would encompass the two enclosures, so the moisture value generated by the SCIP could be cross-referenced with the other soil moisture instruments. The size of the grid was set at 90 x 90 m due

to a barbed wire fence running adjacent to the ditch at this distance that made further measurements more difficult.

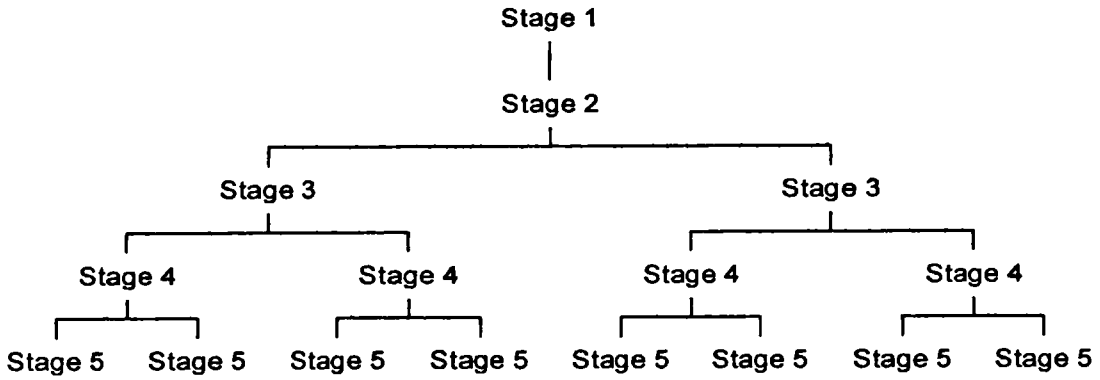


Figure 5.12. The balanced design of the geostatistical nested sampling; only one half of one station is shown due to lack of space. The design comprises six stations, each with 5 stages. Each stage represents a different lag, in total rendering a total of 186 sampling points: stage 1 = 60 m lag, 6 measurements; stage 2 = 30 m, lag 12 measurements; stage 3 = 10 m lag, 24 measurements; stage 4 = 2m lag, 48 measurements; stage 5 = 0.5 m lag, 96 measurements.

Table 5.14. The components of variance CV, expressed as a percentage.

| Lag m | Stage | CV as % contribution per stage |
|---|---|---|
| 0.5 | 5 | 3.5 |
| 2 | 4 | 6.6 |
| 10 | 3 | 17.5 |
| 30 | 2 | 19.2 |
| 60 | 1 | 53.2 |

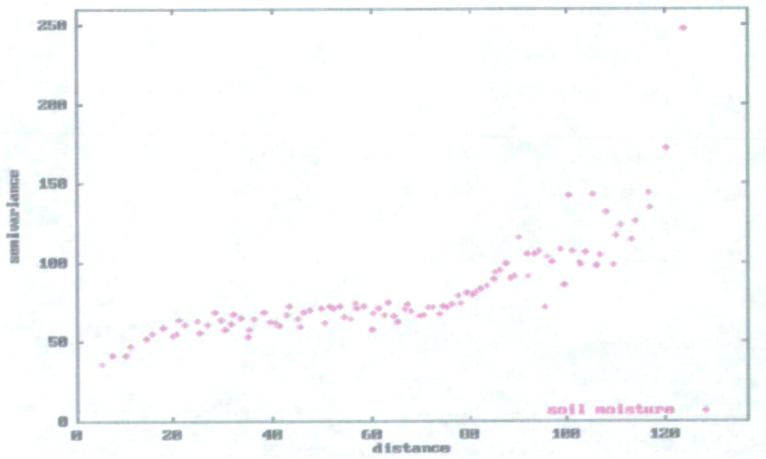


Figure 5.13. The experimental semivariogram of the grid sampled soil moisture data (image imported from the software gstat). Distance is in units of m. Measurements of soil moisture were taken at 5 m interval over a 90 x 90 m grid and the semi variance calculated for different lag i.e. distance).

5.3.2.2 Soil moisture grid mapping

Figure 1.3 displays the location of the regular sampling grid as a red square, bordered to the north by the ditch and the fence to the south and encompassing the two enclosures. Figure 5.14 is a plot of the surface elevation of the grid. The ground level slopes from approximately 1.6 m O.D. to 2.1 m O.D. by 10 m away from the ditch edge thereafter remaining relatively constant. While the change is topography is slight, micro relief can be seen, the rills present on Figures 5.10 and 5.11 (image c) can be distinguished within Figure 5.14 skirting upper right corner of the grid. As seen in Figure 5.10 (January) this rill connects with the rill from the north ditch adjacent to the enclosure when the ditch water level is high enough to flow into it. There is another rill that floods which stretches in a fairly straight line from the ditch inland.

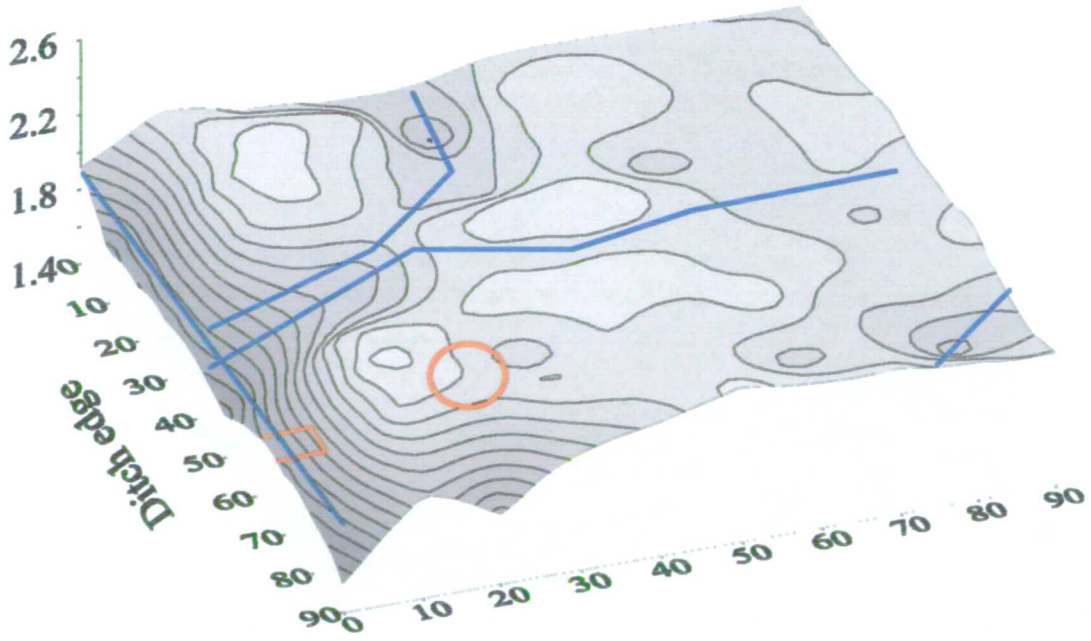


Figure 5.14. The elevation of the SCIP monitoring grid produced from surveying each node. Distance unit is m; elevation unit is m O.D. with grid contours every 0.05 m. The red square and circle represent the relative position of the small and main enclosure. The blue lines indicate areas of the grid that become inundated.

5.3.2.2.1 Method

Soil moisture plots (Figure 5.15) were produced by using the SCIP over the grid at nodes every 10 m. At the start of monitoring the grid, tapes were laid over the marsh to determine the points at which measurements should be taken, and confidence was soon gained so that distances were paced between each grid node using a compass. This was necessary to reduce the time taken and impracticality of using a number of short tapes especially in windy conditions. This means that the actual position of measurement at each node varies between grids but is within one metre or so. The grid was measured starting at the most western point at the edge of the north ditch. Measurements were taken along this line away from the ditch until the end node at 90 m, before returning to the ditch edge and continuing down the next line, 10 m along. If a regular monitoring node of the grid was covered by water, a measurement was taken as near as possible at a location that was not inundated. These measurement points are seen in Figure 5.15 as high peaks. Four fibreglass poles were inserted alongside the ditch edge to mark the start and end of the grid and two places in between. These poles were inserted into the ground, so that a permanent marker of the start of the grid was available.

The values of soil moisture at nodes 10 m apart were interpolated in the Surfer surface mapping software to produce smoothed soil moisture relief plots. Seven grids are displayed in Figure 5.15. The grids illustrate the change in soil moisture of the surface soil layer from the start of winter inundation in October 1998 through to the end of monitoring in December 1999.

5.3.2.2.2 Results

A comparison of the moisture values generated by the capacitance probe from a measurement point next to the position of the electrical resistance blocks in the enclosure is presented in Appendix A.9. While the SCIP records slightly lower moistures over the winter of 1998/1999 overall the close agreement between the two methods gives confidence in the values of moisture generated.

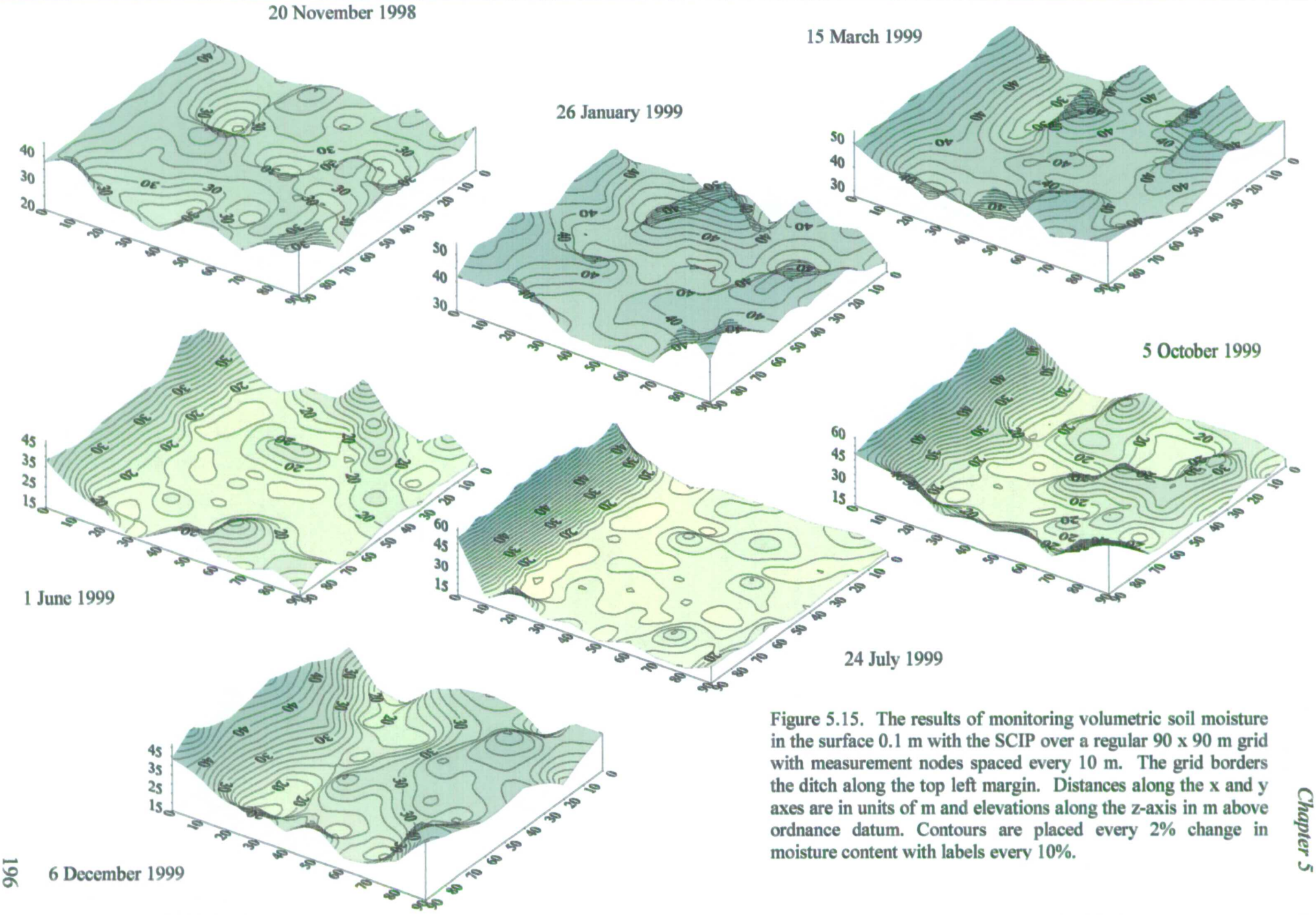


Figure 5.15. The results of monitoring volumetric soil moisture in the surface 0.1 m with the SCIP over a regular 90 x 90 m grid with measurement nodes spaced every 10 m. The grid borders the ditch along the top left margin. Distances along the x and y axes are in units of m and elevations along the z-axis in m above ordnance datum. Contours are placed every 2% change in moisture content with labels every 10%.

The grids are useful to show the variability of soil moisture over a regular area of ground and the impact of the ditch and flooded rills upon the moisture content. The seven grids in Figure 5.15 illustrate the change in soil moisture from November 1998 to December 1999 and it can be seen that there is a marked change with space and time, with high variable moisture levels in winter becoming low and uniform over summer. Over the duration of monitoring with the SCIP, the inundation of the study field changed in extent (section 5.3.1 and Figure 5.10) from small patches of inundation in November 1998 increasing to maximum flood levels in January 1999. The flood patches then started to diminish and was largely absent from the grid by March and from the study field by June 1999. The position of the water table measured at piezometer site B (which is within the SCIP grid) is at the surface or within 0.2m below the surface over November to March, falling below 0.8 m depth over summer before rising from October 1999 to 0.5 m depth at the end of monitoring in December 1999.

Particular features to note from Figure 5.15 are threefold. Firstly, the grid node 90,90 is located in a patch of bare soil (Figure 5.11d). Figure 5.10 shows that this area remains under ponded water for longest, and after flooding the soil starts to dry out and crack. However as shown in Figure 3.5 the soil dries to a depth of 2 cm below which moistures remain high. The SCIP pins penetrate the wetter soil, being 10 cm in length and the grid node of this point exhibits a higher moisture content relative to the remainder of the grass covered grid.

The next two features are linked and are related to the influence of surface topography. The rill skirting the top left corner of the grid (Figure 5.14), is inundated by January 1999 and the area around the rill displays an elevated moisture pattern. Over time, with the reduction in flood extent and soil drying through evaporation, higher moistures are maintained around the rill at all times except July 1999 where the soil moisture level is uniformly low inland. The other inundated channel stretching inland from the ditch (Figure 5.14) can also be identified in the January grid.

The last feature of the grids is the trend of higher moisture along the ditch edge. Over winter, elevated moisture extend inland from the ditch edge due to the overflow of ditch water into the rills. In summer however higher moistures are restricted to the ditch edge; the first monitoring nodes. There is therefore an influence of the ditch at its edge maintaining high moistures of the surface soil.

5.3.2.2.3 Conclusion

To conclude, the grids illustrate that the soil moisture of the sampled area changes in space and time and is quite variable in winter becoming more uniform over summer away from the ditch edge. Moisture values range from over 60% to 14% over the monitoring period, with higher moistures along the ditch edge and rills. These higher moisture levels were created by the water level of the north ditch being at field surface level maintaining saturation of the soil and overflowing into the rills to extend inland. The remainder of the grid experiences an uneven pattern of high moisture contents. With water loss through evaporation, moisture levels decline substantially, not uniformly but in a pattern that is influenced by the small scale changes in topography. Eventually the soil moisture relief becomes uniformly flattened from 10 m distance from the north ditch bordering the grids.

A definite tend of elevated moistures can be seen therefore extending from the ditch inland through lateral seepage, to a spatial extent determined by the presence of rills in winter reduced to the ditch edge in summer.

# Chapter 6 Discussion of Research Question 1

This chapter synthesises the results of the investigation of Research Question 1: *What is the relationship between ditch water levels and the water table and soil moisture in the adjacent field?* and discusses the effectiveness of the ESA management prescriptions.

## 6.1 Introduction

To recapitulate, the environment objective of the North Kent ESA of particular interest to this investigation is Objective 2: 'To maintain and enhance the wildlife conservation value of grazing marsh without detriment to the landscape by maintaining high water levels in ditches and dykes' MAFF (1994). The management prescription to obtain this objective at the start of the ESA project was outlined as Tier 1a:

> 'During the period 1 December to 30 April maintain water levels in ditches and dykes at not less than mean field level so as to create shallow pools and do not let water out of the ditches and dykes until this has been achieved except under flood warning conditions. Provide at least 30 cm of water in the bottoms of ditches and dykes from 1 May until 30 November.'

A mid-term review of the scheme highlighted that "a better understanding of water relationships on the marshes is needed and the continuing drought has highlighted the need to re-appraise Tier 1a. There is a consensus that objectives must be re-set in the light of the existing and growing constraints in terms of water resources' ADAS (1997, p. 6).

The prescription Tier 1a was modified into Tier 1b (FRCA 1997) which has the specific aim of encouraging breeding waders through promoting high soil moisture through surface flooding. Land entered into Tier 1b must follow the management prescriptions:

> 'There must be shallow (up to 0.2 m) surface water over at least 20% of the area from 1 December to 31 March. Shallow surface water must cover at least 15% of the site during April and over 10% of the site to the end of May. There must be at least 300 mm depth of water in ditches during the summer and autumn months.'

The following discussion synthesises research results presented in Chapters 3-5 in order to answer Research Question 1 and the effectiveness of the ESA in meeting its environmental objective by considering the Tier 1a and Tier 1b prescriptions in turn.

## 6.2 Synthesis of results relating to Tier 1a

- Soil analyses indicate that with depth the soil exhibits a change in texture, increasing electrical conductivity and decreasing organic content and hydraulic conductivity.
- The soil is dynamic, shrinking in summer and swelling in winter. Water movement occurs faster than the computed matric hydraulic conductivity through macropores and soil cracks in summer, allowing rapid recharge of the water table.
- Observations of the water table and the results of modelling with Dupuit-Forchheimer analysis and DITCH confirm the dominant fluxes are in the vertical direction i.e. precipitation and evaporation. The water table fluctuation is in response to these fluxes with negligible recharge from the ditches.
- The importance of macropores in transporting water mean that when modelling the position of the water table with DITCH, the specific yield parameter needs to be employed as a surrogate for macroporosity.
- Attempts to model soil moisture with BUDGET is hampered by the dynamic nature of the soil i.e. shrinking and swelling. Good results are obtained when the soil is drying and poor results are obtained when wetting.

To answer to Research Question 1: *What is the relationship between ditch water levels and the water table and soil moisture in the adjacent field?*, it has to be stated, from the results presented above, that there is no relationship between the change in water table to the ditch water levels. The position of the water table moves in response to the vertical fluxes of precipitation and evaporation. The dynamic shrink-swell nature of the soil allows the position of the water table to change at rates faster than the matrix soil hydraulic conductivity due to the creation of soil cracks and macropores.

The implications for Tier 1A is that high ditch water levels are maintained for no effective purpose as the objectives are not met.

## 6.3 Synthesis of results relating to Tier 1b

- Soil moisture of the upper surface organic layer has a greater seasonal and spatial range than the deeper soil layer as seen by the ERB and neutron scattering results. A different SMC curve characterises the surface soil from deeper layers due to the differences in texture and organic matter. The surface layer may act as mulch to prevent moisture loss from the deeper soil.
- Overtopping of ditch water and flooding the marsh surface lengthens the period of open water on the marsh and elevated soil moistures.
- The SCIP soil moisture grids illustrate heterogeneity caused by microtopography and rainfall. Soil moisture is uniformly low over summer due to evaporative loss, however higher soil moistures are recorded along the ditch edge.
- Inundation of the marsh through ditches can create controlled soil moisture conditions (i.e. through the creation of splashback areas and surface rills).
- Bank overtopping by brackish ditch water increases the soil salinity and sodicity. This causes a deterioration of the soil structure through defloculation. Through enhanced soil salinity a different flora is established which may not be of sufficient quality for grazing.

To answer to Research Question 1: *What is the relationship between ditch water levels and the water table and soil moisture in the adjacent field?*, it has to be stated, from the results presented above, that there is an influence of the ditch in maintaining high soil moisture levels along its edge when bankfull. This influence is restricted to a very narrow riparian border of only a few metres in extent. When the ditch overtops its banks and floods the surface, this ditch water is highly influential in maintaining surface moisture contents, as the ditch water moves into the middle of the field via the surface rills.

The implications for Tier 1b is that high ditch water levels do promote high surface soil moisture particularly through overtopping of the ditch channel to flooding of the marsh surface. In this way the ESA prescription is successful.

## 6.4 Discussion of Tier 1b

The success of the Tier 1b management prescription needs to be examined in further detail. The study site at Elmley Marshes has an environment as particularly favourable for breeding and nesting waders, and is home for large numbers of snipe, lapwing and redshank and others that feed by probing the surface soil for invertebrates. The results of monitoring the surface moisture in a regular grid show that the level of moisture, and therefore the penetrability of the soil and potential habitat, changes in space and time and is quite variable in winter becoming more uniform over summer. Soil moisture values range from over 60% to 14% over the monitoring period, with higher moistures along the ditch edge and rills. These enhanced moisture levels were created by the ditch water at field surface level maintaining saturation of the surface along its edge and overflowing into the rills to extend inland. A definite tend of elevated moistures can be seen extending from the ditch inland through lateral seepage, to a spatial extent determined by the presence of rills in winter reduced to the ditch edge in summer.

These conditions meet the hydrological requirements specified of the ESA Tier 1b; and it needs to be determined whether or not this management regime is effective in achieving its objectives of attracting waders. Research by T. Milsom (personal communication) at Elmley Marshes between 1995 – 1997 investigated the link between management of the grazing marsh habitat and ground nesting birds. Results indicated that functional relationships between the distribution of the key species, lapwing and redshank, were related to surface topography, especially the presence of rill features, their wetness in spring and, for redshank, the rate at which rills dried out during the breeding season. Thus the approach of Tier 1b is successful in achieving its objectives.

However, while flooding from the ditch into the rill network is shown to promote desired higher moistures levels of longer duration, there are deleterious impacts upon

the soil and vegetation characteristics of the marsh that need to be examined. A distinctly different flora, of reduced quality for grazing, occupies the area of marsh next to the north ditch edge and other areas that are regularly inundated by ditch water such as the relict saltmarsh channels and rill features. This can be seen clearly in Figure 1.3 as a darker colour for the rill stretching from the south ditch but is not as clear on the image for the north ditch on its southern bank. (The rill at the middle right of the SCIP grids (Figure 5.15) is only slightly distinguishable being a very faint brown strip.)

Harpley (1999) identifies the typical species of these regularly inundated areas as being the more salt tolerant marsh foxtail *Alopecurus geniculatus*, salt marsh grasses *Puccinellia spp.* saltmarsh rush *Juncus gerardi* and lesser sea spurrey *Spergularia marina.* These plants contrast with the predominant vegetation community of the less salt tolerant *Lolium perenne-Cynosurus cristatus* grassland, *Lolium perenne* leys and *Festuca rubra-Agrostis stoloifera/Potentilla anserina* grassland (ADAS 1997).

This change in vegetation is dependant upon the duration of flooding with ditch water and the soil electrical conductivity. The presence of salt tolerant flora in the areas inundated by ditch water contrasts with other areas inundated by rain water reflecting the higher conductivity of the water from the ditches compared to the incoming precipitation (Table 3.10). The four study ditches exhibit a conductivity in the range 3.4 – 6.0 dS $m^{-1}$, classified as very slightly saline to slightly saline, compared to the value of the precipitation of the marsh at 0.09-0.11 dS $m^{-1}$, classified as non saline.

Further to this floral change due to enhanced salinity, prolonged extensive saturation of the soil causes implications for grazing of the land. There are health implications for grazing animals, and low stocking densities are required to prevent soil compaction. Creation of an optimal habitat is dependant upon the grazing regime; ungrazed land can become dominated with woody flora ceasing to be unattractive to the desired species (Armstrong *et al.* 1995, P. Merricks, pers. comm.).

A similar change in plant communities in flood affected areas of the Somerset Levels and Moors ESA to tussock forming grasses, sedges and rushes has been noted by Glaves (1998). Glaves notes that while the change in plant community was potentially beneficial in providing a diversity of structure and cover for nesting birds, they may pose a threat to floristically rich wet grasslands.

Research upon the influence of hydrological regime upon plant communities has identified that the key factor is the ability of species to tolerate a range of drought and aeration stresses (Silvertown *et al.* 1999, Gowing *et al.* 1998, Gowing and Youngs 1997). Drought and aeration stresses refer respectively to periods of soil moisture deficit when plant communities cannot access sufficient moisture and so close stomata and become less competitive, and waterlogging conditions with insufficient levels of oxygen to supply the respiratory demands of the roots.

Research by Swetnam *et al.* 1998 was undertaken at Southlake Moor within the Somerset Levels and Moors, an area subject to a raised water level regime through ESA prescription, and identified as being of botanical interest under threat. The site comprises up to 7% of the national resource of *C. cristatus-C. palustris* grassland NVC vegetation community MG8 (Rodwell 1992). The response of the plant community to drought and aeration stress was determined, and the tolerance to aeration stress was found to be exceeded due to the imposed flooding regime. The authors point to the national implications of potential damage to this botanical resource as over 70% of the MG8 community are situated within the area liable to spring floods under raised water level management. They state that 'landowners may be receiving subsidies which ultimately lead to a decline in species diversity... and recovery or re-instatement is difficult and expensive'.

A case study by Gowing and Youngs (1997) found similar findings at Cricklade meadow, a National Nature Reserve on the Thames floodplain. The flood meadow is a classic example of *Alopecurus pratensis-Sanguisorba officinalis* grassland, vegetation type MG4; some 80% of the British population of Snakeshead Fritillary are found at the site. Two other communities are present, MG13 *Agrostis stolonifera-Alopecurus geniculatus* grassland and MG 5 *Cynosurus cristatus-Centaurea nigra* grassland. A spatial investigation was undertaken across the meadow linking the water table to the drought and aeration stress tolerances of the plant community. The conclusions drawn from the analysis in terms of hydrological management was that the greatest threat to the MG4 community stems from an increase in spring floods, which will favour the competitiveness of the MG13 community. At the same time however results indicate that MG4 requires a high water table in spring if the community is to be sustained and not tend into an MG5 community.

A change in the hydrological regime at Elmley Marshes through the creation of splashback areas and pumping water onto the marsh surface, will induce vegetation

change. The mechanism of change found in other wet grasslands by Swetnam *et al.* (1998), and Gowing and Youngs (1997), is the intolerance of the current plant communities to the changed drought and aeration stresses. In addition at Elmley Marshes there is the important factor of soil salinity with brackish ditch water being used to flood the marsh. Differences exist of elevated soil electrical conductivity and sodicity adjacent to ditches where flooding occurs regularly. Using ditch water to flood the marsh will cause an increase in electrical conductivity and sodicity over larger areas of the marsh causing defloculation and soil structural degradation

To conclude, it can be seen that while the ESA Tier 1b attains its objectives to promote habitat availability for target bird species, there are unappreciated negative feedbacks that impinge upon other ecological aspects. As such management guidelines for the conservation of valuable habitats as a whole need to become more sophisticated to ensure that problems such as soil and botanical degradation are avoided while targeting ornithological objectives. Armstrong *et al.* (1995) stress the importance of conservation measures to preserve whole ecosystems including the food chains and habitats for all life stages rather than focus on single faunal (mainly ornithological) components. Management of land is the key to success and it is necessary to abandon extensive, uniform, single target schemes in favour of more complex, mixed management regimes within a wetland area to maintain ecosystem.

# Chapter 7 Wetland evaporation. Part 1 Soil moisture: surface resistance relationship

The investigation for the first research question, presented in Chapters 3-5 prove that the dominant water movement of the wet grassland is vertical and that evaporation is the dominant water loss from the system. The evaporative loss therefore needs to be quantified and this comprises the second and third research investigation.

## 7.1 Introduction

The evaporation from a vegetated surface can be determined by use of the Penman Monteith model (Monteith 1965, 1981) which has been widely reviewed and employed. It is now the definitive model of calculating evaporation and has been recommended by the FAO and adopted by the UK Met Office through its use in MORECS (Met Office Rainfall and Evaporation Calculation System). The Penman Monteith combination equation 'includes all parameters which govern, in a major way, energy exchange and corresponding latent heat flux (evapotranspiration) from uniform expanses of vegetation' (Allen *et al.* 1994 p5). The Penman Monteith method was proven best, in terms of mean accuracy and standard error of estimate, in a comparison of 20 methods of determining evaporation with actual evaporation values from lysimeters (Jensen *et al.* 1990). Allen *et al.* (1994) report another study comparing nine evaporation calculation methods performed by Choisnel *et al.* (1992) which also favours Penman Monteith as the definitive evaporation equation. In view of these results and the wealth of research supporting the use of the Penman Monteith method, Allen *et al.* (1994, p18) state:

> 'The FAO Expert Consultation on Revision of FAO Methodologies for Crop Water Requirements (Pereira and Smith 1989; Smith *et al.* 1992) recommend the Penman Monteith method as the primary ET [reference evaporation] method for determining grass ET and for determining crop coefficients. The Penman Monteith method was selected because it closely approximates grass ET, is physically based, and explicitly incorporates both physiological and aerodynamic parameters.'

Calculations of evaporation for water balance and irrigation studies have largely been concerned with agricultural crops and commercial tree plantations due to economic

considerations (Kelliher *et al.* 1993 p154). While it is true to say that the evaporation of grass has been investigated, it is mostly under 'reference conditions'. Grass reference evaporation has been defined as 'the rate of evapotranspiration from an extensive surface of 8-15 cm tall, green grass cover of uniform height, actively growing, completely shading the ground and not short of water' (Doorenbos and Pruitt 1977; Jensen *et al.* 1990). Few studies have examined the spatial variability of the grass cover, including areas of that do not meet the reference condition, and in this respect it can be stated that 'there is little or no testing of the model in naturally vegetated areas' (Wessel and Rouse 1994, p111) for example Elmley Marshes.

### 7.1.1 Application of the Penman Monteith model to the Elmley Marshes

Research undertaken for Research Question 1, presented in Chapters 3-5, shows that the hydrological cycle of the grazed wet grassland study site is characterised by a strong seasonal trend of water levels and soil moisture from inundation during the winter months to ditch water depletion and soil desiccation during summer. Spatial heterogeneity is evident with ditches and former saltmarsh channels on the marsh resulting in a mosaic of different vegetation communities that reflect the underlying differences in moisture level of the soil, together with patches of bare soil and temporary areas of standing water. The close assemblages of such different microhabitats, or surface types, result in an inhomogeneous surface, and the use of the marsh for grazing produces temporal changes in sward height unrelated to the normal growth pattern.

As the area is spatially diverse in terms of soil moisture and grass height, it does not meet the reference conditions above in terms of grass height and unlimited soil moisture. There are thus two obstacles in the application of the Penman Monteith method to the study site, which need consideration:

1. The conditions of reference grass evaporation assume constant supply of water to the evaporating vegetation.
2. Penman Monteith simulates the evaporating surface in the form of a 'big leaf' and is applicable to homogenous stands of vegetation whose physiological properties can be represented by this approach.

### 7.1.2 Availability of water to the evaporating surface

The seasonal depletion and replenishment of soil moisture is considered to have an impact upon the rate of evaporation from the marsh. The effect of change in soil moisture upon evaporation can be ascertained through the surface resistance term of the Penman Monteith model. Surface resistance can be defined as the amalgamation of leaf stomata resistance, which represent the resistance to vapour transfer from the leaf stoma of the plant to the atmospheric sink. This produces a value of bulk resistance for the whole canopy.

A decrease in soil moisture causes the leaf stomata to close (Turner 1991) and thus invokes an increased resistance to water vapour movement. The influence of the soil moisture status is felt in two possible pathways. Firstly soil dehydration induces a 'drought stress' reducing the ability of the plant to maintain maximum turgor pressure and leaf water potential and so the stoma close to regulate the amount of water lost. Secondly, the balance of phytohormones produced by the roots and transported to the leaf, such as abscisic acid (Zhang *et al.* 1987), is affected by soil moisture status, but actual response to soil water deficits will vary between plants (Jones 1992).

The sensitivity of the Penman Monteith model to the surface resistance factor employed to represent the surface has been well noted in the literature (Shuttleworth 1975, Beven 1979, Kelliher *et al.* 1993). Figure 7.1 displays the sensitivity of the model to changes in surface resistance with other meteorological conditions held constant. This has been compiled after the method of Raupach and Finnigan (1988) by computing evaporation with the Penman Monteith formula, changing the value of the surface resistance and keeping other all variables constant. Graphing the ratio AE: PE against surface resistance illustrates the change in evaporation computed with different resistance values. The fractional change in the evaporation rate that occurs with a step resistance increase or decrease can be computed. A fairly linear relationship is evident between surface resistance and change in evaporation except during the range 0-30 $sm^{-1}$ where an increased sensitivity is apparent. Thus, while it is important to have accurate surface resistance values over the whole range of values experienced, it is especially necessary to characterise the resistance over the initial drying phase from inundation.

Relating to this research, there is a need to derive a relationship between surface

resistance and soil moisture so that the water loss from actual evaporation of the study site can be computed over the range of soil moistures experienced by the marsh.

This research forms the second research investigation to answer Research Question 2: *What is the effect of decreasing soil moisture upon the evaporation rate?* (Table 7.1). Results are presented in this chapter.

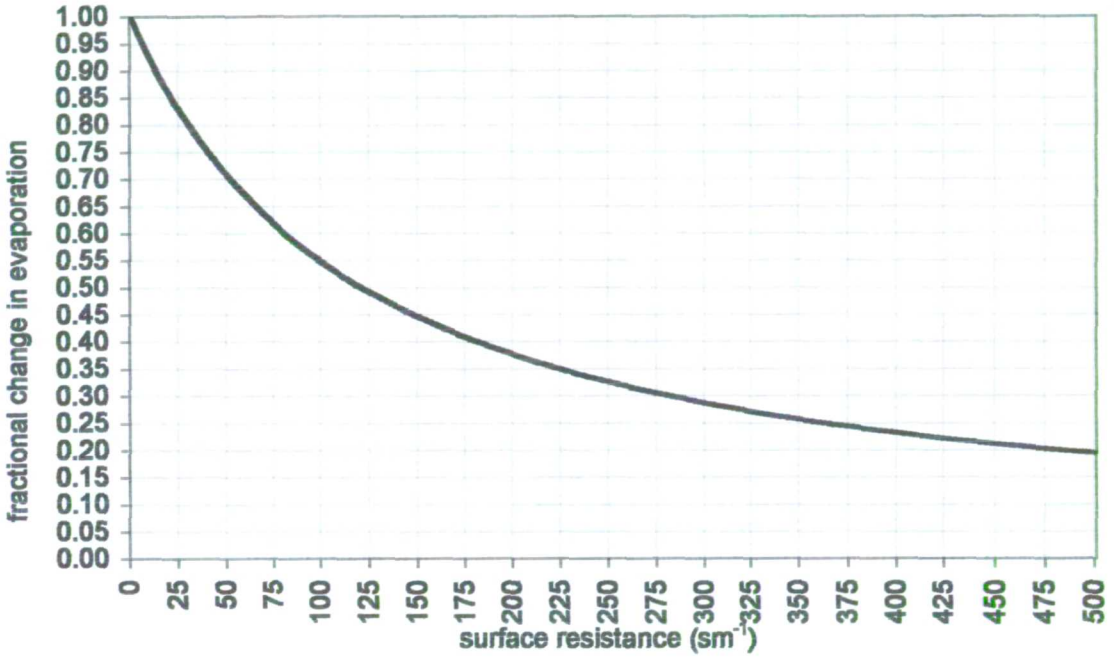


Figure 7.1. The sensitivity of the Penman Monteith model to changes in surface resistance. The chart illustrates that the fractional reduction of evaporation with increased resistance is non-linear, being greatest at low values of resistance.

### 7.1.3 Application of the Penman Monteith model to a heterogeneous surface

Once a relationship between soil moisture and surface resistance has been established, the calculation of the evaporative loss from the marsh accounting for the heterogeneity of the surface forms the third research investigation, expressed as Research Question 3: *What is the actual evaporation loss from the heterogeneous wetland surface?* (Table 7.1).

Either a value for surface resistance can be attributed for the entire marsh surface, or more accurately for each 'surface type'. Wetland environments are usually comprised of a variety of 'surface types', for example open water, wet inundated grass, bare soil

and the Elmley Marshes are no exception. A study to investigate the evaporation of different surface areas of a tundra wetland was undertaken by Wessel and Rouse (1994) who calculated the evaporation from each surface 'type'. The values of evaporation are then weighted according to the proportion of land occupied by each surface type and summed to generate an amalgamated value of evaporation for the total surface. As evaporation is the major driving force of water loss from Elmley Marshes, this method is applied in order to obtain accurate representative evaporative fluxes from the total surface. The surface types of Elmley Marshes can be classified as bare soil, grass, and open water, and the extent of each varies in space and time.

Thus in order to characterise the evaporative loss using the Penman Monteith model, the Weighted Penman Monteith, WPM, (Wessel and Rouse 1994) is employed to asses whether the method can compute an accurate representative value of evaporation for the marsh surface. The WPM method relies upon accurate surface resistance values for each surface type. The difference in resistance values from each grass surface type (i.e. wet/inundated and dry) is considered, for simplification, to be a function of soil moisture alone allowing the designation of resistance values depending upon the moisture content. This is a simplification as the value of surface resistance could also depend upon the different grass species present in different areas. The results of modelling with the WPM approach are referenced against actual evaporation data from the Bowen Ratio Energy Balance approach, which are available from March to November 1999 for the study site. The results for this investigation are presented in Chapter 8.

## 7.2 Evaporation formulae

A common definition of the term evaporation is the process by which liquid, in this case water, is changed into a gas. Transpiration is the process whereby water in plants is transferred as water vapour to the atmosphere. Total evaporation or evapotranspiration is the term given to represent both evaporation and transpiration but in this thesis, the term evaporation is used to describe the two forms of water loss for simplification, after Monteith (1981).

'The process can only occur naturally if there is an input of energy either from the sun or from the atmosphere itself, and is controlled by the rate as which the energy, in the form of water vapour, can diffuse away from the earth's surface' (Shuttleworth 1979). Thus 'evaporation in the natural environment can be considered to be a result of a balance between...atmospheric demand and the availability of water at the evaporating surface' (Calder 1990).

Table 7.1. The Logical Framework Diagram of the research investigation. The Research Question is stated and the investigation detailed in terms of approach, data collected and equipment used and data analysis. The three investigations link together as shown in Figure 1.2.

| Research Question 2:<br>*What is the effect of soil moisture upon the evaporation rate?* | |
|---|---|
| Justification | Research of this type for grass surfaces in the UK is limited. Original research. Research findings will promote a better understanding of the hydrological processes aiding more effective management. |
| Approach | Derive the parameters of the Penman Monteith formula to best simulate the Elmley Marshes environment in terms of wetness levels. Determine the effect of soil moisture levels by computing values of actual evaporation by the water balance referencing against potential evaporation. Establish whether a relationship can be made between soil moisture and surface resistance so that actual evaporation can be computed using the Penman Monteith formula. |
| Data | A Soil moisture data in with depth in space and time.<br>B Actual and potential evaporation |
| Equipment | A Electrical resistance blocks, neutron probe soil sampling equipment<br>B Automatic Weather Station |
| Analysis | Quantification of a relationship will enable computation of actual evaporation from the Penman Monteith model over a range of soil moisture levels. |

| Research Question 3<br>*What is the actual evaporation loss from the heterogeneous wetland surface?* | |
|---|---|
| Justification | Research of this type for wetland environments is limited. Original research |
| Approach | Establish whether the Weighted Penman Monteith approach can be used obtain a spatially distributed value of evaporation over the marsh. . Determine the change in surface types of the wetland over the time period and assign surface resistance values depending upon moisture levels. Reference against AET from the BREB method. Assess the relationship to the equilibrium evaporation and effects of local heat advection |
| Data | A Actual and potential evaporation<br>B Spatial and temporal change in extent of the surface areas of grass, open water and bare soil. |
| Equipment | A Bowen Ratio Energy Balance station and Automatic Weather Station |
| Analysis | The results link together the relationship between actual and potential evaporation and the inundation of the marsh. Employs the results of the second investigation to assign surface resistance values to the grass areas. The results indicate if the Weighted Penman Monteith approach can be used to simulate the actual evaporation from the wetland taking account of its spatial heterogeneity. |

The management of wetland systems focuses on the conservation of the ecological variables or attributes, and most do not have any formal hydrological monitoring programmes established. However, especially in rain-fed wetlands such as Elmley Marshes, an understanding of the hydrological regime and in particular the evaporative flux of the wetland is required to achieve the best use of the water resource for ecological purposes.

Many physically based models to calculate evaporation have been developed due to its importance in water balance calculations (Wessel and Rouse 1994). However most 'evaporation models have been developed for agriculture and forestry purposes and there has been relatively little testing in naturally vegetated areas' (Wessel and Rouse 1994 p111). Many formulae have been devised to calculate potential evaporation from a range of standard meteorological variables such as air temperature, humidity and wind speed for example.
The first successful formula that combined both aerodynamic (turbulent) and energy balance approaches was initially proposed by Penman (1948).

### 7.2.1 Penman

Penman's model (1948) combines the aerodynamic and energy budget methods for calculating evaporation. A constant supply of water is assumed and thus, is representative of the potential rate of evaporation from open water.
Penman's equation for natural evaporation from an open water surface:

$$E = \frac{\frac{\Delta}{\gamma} H + Ea}{\frac{\Delta}{\gamma} + 1} \qquad \text{Equation 7.1}$$

Where:
$E$ = evaporation from an open water surface mm $day^{-1}$
$\Delta$ = the slope of the vapour pressure curve kPa $°C^{-1}$
$\gamma$ = psychometric constant kPa $°C^{-1}$
$Ea$ = f(u) (ea-ed)

### 7.2.2 Penman Monteith

Penman's formula uses commonly measured meteorological variables and as such has been used extensively. However, no account of the influence of vegetation is taken and the original Penman equation has been modified extensively to represent water loss via transpiration. The most widely used model that incorporates an evaluation of the loss of water via transpiration is the Penman-Monteith model, Equation 7.2, which is a development of the original Penman model by Monteith (1965). This model assumes a homogenous closed canopy of vegetation and negligible contributions from the substrate and simulates evaporation by treating the canopy as a single leaf (Allen *et al.* 1989):

$$\lambda ET = \frac{\Delta(Rn-G)+\frac{\rho cp(ea-ed)}{ra}}{\Delta+\gamma(1+\frac{rs}{ra})} \qquad \text{Equation 7.2}$$

$$\Delta = \frac{4098 e_a}{(T+237.3)^2} \qquad \text{Equation 7.2a}$$

$$e_a = 0.611 \exp\left(\frac{17.27T}{T+237.3}\right) \qquad \text{Equation 7.2b}$$

$$e_d = e_{a(Twet)} - \gamma_{asp}(T-T_{wet})P \qquad \text{Equation 7.2c}$$

$$\gamma = \frac{c_p P}{\varepsilon\lambda} \times 10^{-3} \qquad \text{Equation 7.2d}$$

$$ra = \frac{\ln\left(\frac{Z_m-d}{Z_{om}}\right)\ln\left(\frac{Z_h-d}{Z_{oh}}\right)}{k^2 U_z} \qquad \text{Equation 7.2e}$$

$$d = \frac{2}{3}h_c \qquad \text{Equation 7.2f}$$

$$Z_{om} = 0.123 h_c \qquad \text{Equation 7.2g}$$

$$Z_{oh} = 0.1 Z_{om} \qquad \text{Equation 7.2h}$$

Where:
$\lambda ET$ is the latent heat flux of evaporation kJ $m^{-2}$ $s^{-1}$
$Rn$ is the net radiation kJ $m^{-2}$ $s^{-1}$
$G$ is the soil heat flux kJ $m^{-2}$ $s^{-1}$
$\Delta$ is the slope of the vapour pressure curve (kPa°$C^{-1}$
$T$ is the air temperature °C
$T_{wet}$ is the wet bulb temperature °C
$e_a$ is the saturation vapour pressure at temperature T kPa
$e_d$ is the actual vapour pressure at temperature $T_{wet}$ kPa
$e_a$-$e_d$ is the vapour pressure deficit kPa

$\gamma$ is the psychrometric constant kPa°C$^{-1}$
$\gamma_{asp}$ is the aspirated psychrometric constant, 0.0008 for natural ventilation kPa°C$^{-1}$
$c_p$ is the specific heat of moist air = 1.013 kJ kg$^{-1}$°C$^{-1}$
$P$ is the atmospheric pressure kPa
$\varepsilon$ is the ratio of molecular weight of water vapour to dry air = 0.622
$\lambda$ is the latent heat of vaporisation MJ kg$^{-1}$
*ra* is the aerodynamic resistance sm$^{-1}$
*rs* is canopy resistance s m$^{-1}$
$Z_m$ is the height of windspeed measurement m
$Z_h$ is the height of temperature and humidity measurements m
$k$ is the von Karman constant = 0.41 m
$U_z$ is the windspeed measurement at height Zm ms$^{-1}$
$d$ is the zero plane displacement of wind profile m
$h_c$ is the crop height m

The effect of the physical roughness of the vegetation affecting the upward transfer of energy and water vapour away from the evaporating surface, and the plant control of transpiration via stomata control, are represented by the aerodynamic resistance factor, ra and the canopy or surface resistance, rs, respectively. Resistance exerted by soil in non-vegetated surfaces can also be represented using the rs resistance term. Values for the resistance terms can be taken as standard values derived for reference conditions or can be calculated empirically. Under reference conditions and correct resistance values, the Penman Monteith equation generates values of actual evaporation loss. Reference conditions can be described as the rate of evapotranspiration from an extensive surface of 8-15 cm tall, green grass cover of uniform height, actively growing, completely shading the ground and not short of water (Doorenbos and Pruitt 1977; Jensen *et al.* 1990).

### 7.2.3 Weighted Penman Monteith

Wessel and Rouse (1994) have developed the Penman-Monteith model by introducing the concept of heterogeneity of surface cover types. The 'Weighted Penman-Monteith' or 'WPM' model estimates total evaporation by the calculation of each surface type within the study area, which are weighted according to their proportional land cover. The model was used to simulate seasonal evaporation change for a tundra sedge wetland. "Theoretically this is the best approach for representing evaporation from areas which have a variety of surfaces" Wessel and Rouse 1994 p111).

In an analysis of WPM and Penman-Monteith, Wessel and Rouse (1994) concluded that the former provided the best overall simulation when compared to calculations of actual evaporation from the Bowen Ratio Energy Balance BREB measurements.
The proportions of the surface types (hummock, hollow and open water) were determined by a series of surveys throughout the study period with interpolation of the rate of change in-between surveys. The model is defined as:

$$AE = G \times AEc + S \times AEs + W \times AEw \qquad \text{Equation 7.3}$$

Where:
G, S and W are the proportion of grass, soil and open water respectively
AE is total actual evaporation loss
Ec is actual evaporation from the canopy using Penman Monteith
AEs is actual evaporation from the soil using Penman Monteith
AEw is actual evaporation from the water using Penman-Monteith

### 7.2.4 Energy balance method

The energy balance method apportions the total incoming energy into sensible and latent heat fluxes in order to determine the amount used in evaporation. The Bowen Ratio Energy Balance (BREB) (Bowen 1926) is commonly used to determine the components of the energy balance. The BREB method is a combination of transport and energy balance equations and is considered to be superior to the direct use of turbulent transfer equations for estimating transfers of water vapour above a surface (ASCE 1996). The principles of the BREB approach are described in section 8.3.

## 7.3 Typical meteorological data from Elmley Marshes

It is useful to illustrate the basic meteorological fluxes of the study site before an examination of the effects of soil moisture is examined in detail. The following discussion covers briefly the radiation, temperature and vapour pressure deficit and precipitation experienced at the study site. Reference levels of evaporation are computed for open water (rs = zero) and reference grass (rs = 70).

### 7.3.1 Solar and net radiation

Figure 7.2 shows the mean daily solar and net radiation from sensors of the AWS. Appendix A.1.4 demonstrates the seasonal cyclic pattern with solar radiation received

by the marsh increasing from minimum values of 2 MJ $m^2$ in winter to 26 MJ $m^2$ in summer. Basic statistics are outlined in Table 7.2 and show that the receipt of energy is very similar over the two years. The radiative efficiency (net radiation/incoming solar radiation) was in the order of 60% which accords with values found over similar surfaces (Den Hartog *et al.* 1994, Lafleur *et al.* 1987).

### 7.3.2 Air temperatures

The mean daily wet and dry bulk thermometer measurements of the AWS are presented in Figure 7.3, and Table 7.3 describes the average minimum and maximum temperatures over 1998-1999. Air temperatures range from below 0°C in winter periods to above 21°C in summer. The temperature pattern is similar between the two years. The vapour pressure deficit follows a similar pattern over 1998-1999 (Figure 7.4) rising from 0.1-0.2 kPa approaching to 1 kPa in summer periods.

Table 7.2. Basic statistics of the net radiation (Net) and solar radiation (Solar) received by the study site over 1998 and 1999. Units of MJ $m^2$.

| | Mean daily totals | | Minimum daily values | | Maximum daily values | |
|---|---|---|---|---|---|---|
| | Net | Solar | Net | Solar | Net | Solar |
| 1998 | 4.83 | 9.79 | -2.41 | 0.42 | 15.64 | 28.00 |
| 1999 | 4.57 | 8.86 | -3.84 | 0.38 | 16.60 | 27.69 |

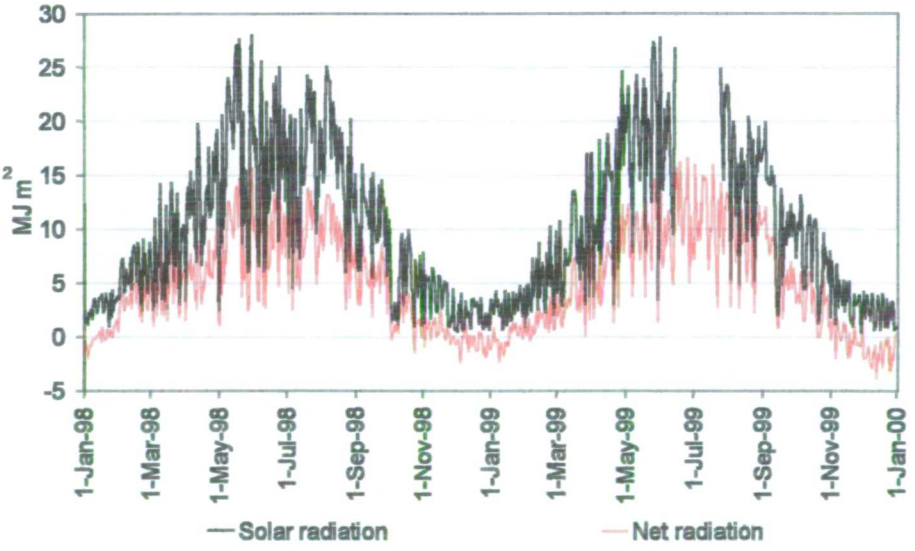


Figure 7.2. Mean daily solar and net radiation from the AWS. The period of 15 June and 24 July 1999 was characterised by malfunction of the solarimeter and net radiometer of the AWS. This is represented as a gap in the solar radiation trend while substitute values of net radiation have been used from the Bowen Ratio station net radiometer. See also Figure A.3 in Appendix A.

### 7.3.3 Precipitation

Precipitation data have been obtained from the gauge of the Automatic Weather Station, and for comparison, three additional gauges on the Isle of Sheppey. Figure 7.5 illustrates the location of the gauges and the data is displayed in Figures 7.6 and 7.7. Figure 7.6 displays the daily precipitation totals recorded by the tipping bucket rain gauge within the main enclosure of the study site. The elevation of this gauge is 2 m O.D. Figure 7.7 shows the spatial and temporal record of an additional three Met Office gauges near the study site on the Isle of Sheppey in addition to the AWS gauge. The Kingshill gauge is located on higher ground of the Elmley Marshes at 11 m O.D. Wallend is at 5 m O.D. with available data covering the period 1969 to 1977. Barnland station is on the northern edge of the Isle of Sheppey at 49 m O.D. with available data covering 1961 to 1999. These data have been obtained from the British Atmospheric Data Centre (BADC). In Figure 7.7 gaps in the record for each gauge indicate periods when data was unavailable and so annual totals could not be computed.

Figure 7.7 shows that the three gauges, despite difference in location and elevation, record similar annual precipitation totals. The average annual total over the period 1961 to 1998 from these three gauges equals 525 mm. The record of the AWS gauge is too short to allow any interpretation as to the similarity to the other gauges in rain totals. There are also gaps in the available data for the other gauges, which mean there is only a total for 1998 from the Barnlands gauge and no value for 1999. However it can be seen that the total for 1998, 576 mm, is above the mean of 525 mm and that for 1999, 438 mm, is substantially below the average. These values are within the natural fluctuation of annual rain totals displayed by Figure 7.7 in the range 343 mm to 719 mm. These values of precipitation are very low relative to the whole of the British Isles (Figure 7.8) due to the position of the marshes in the south east; in the rain shadow of Atlantic frontal depressions and orographic uplift (Goudie and Brunsden 1994).

Table 7.3. Basic statistics of the wet and dry bulb temperatures at the study site over 1998 and 1999. Units of °C.

| | Mean daily values | | Minimum daily values | | Maximum daily values | |
|---|---|---|---|---|---|---|
| | Wet | Dry | Wet | Dry | Wet | Dry |
| 1998 | 9.18 | 10.75 | -1.63 | -1.29 | 18.25 | 22.53 |
| 1999 | 9.29 | 11.05 | -2.87 | -2.25 | 18.99 | 21.62 |

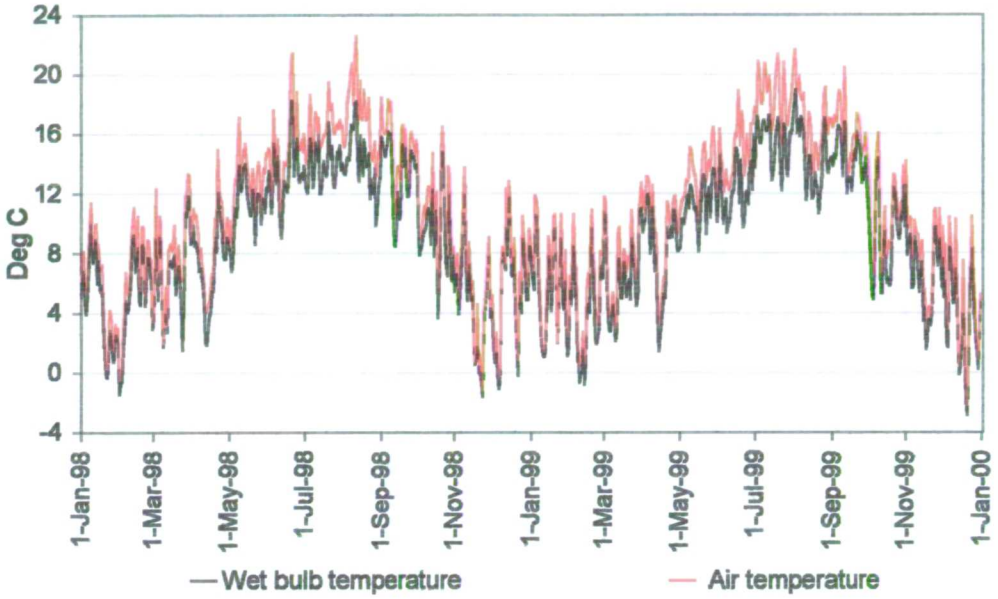


Figure 7.3. Range of temperatures at the study site over 1998 and 1999 with data derived from the wet and dry thermometers of the AWS.

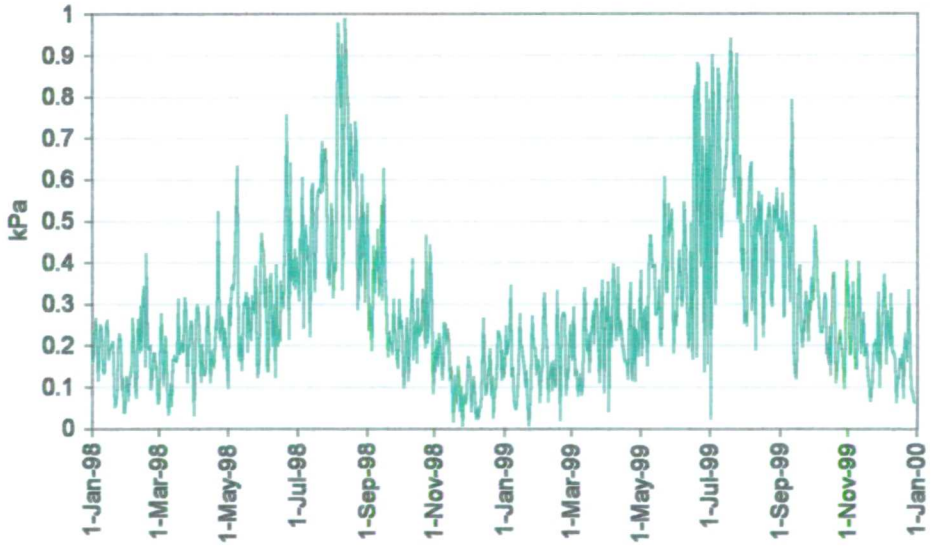


Figure 7.4. Vapour pressure deficit, kPa, computed for the wet and dry bulb thermometers of the AWS.

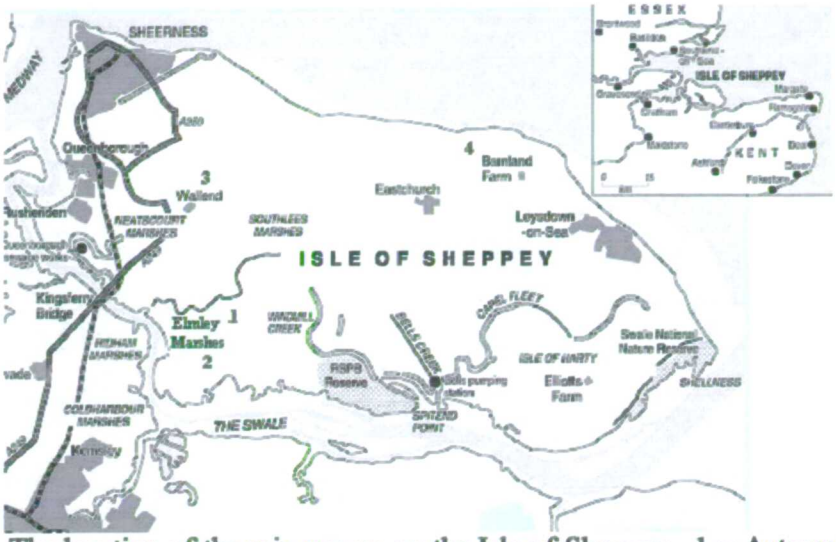


Figure 7.5. The location of the rain gauges on the Isle of Sheppey. 1 = Automatic Weather Station (2 m O.D.), 2 = Kingshill (11 m O.D.), 3 = Wallend (5m O.D.), 4 = Barnland (49 m O.D.).

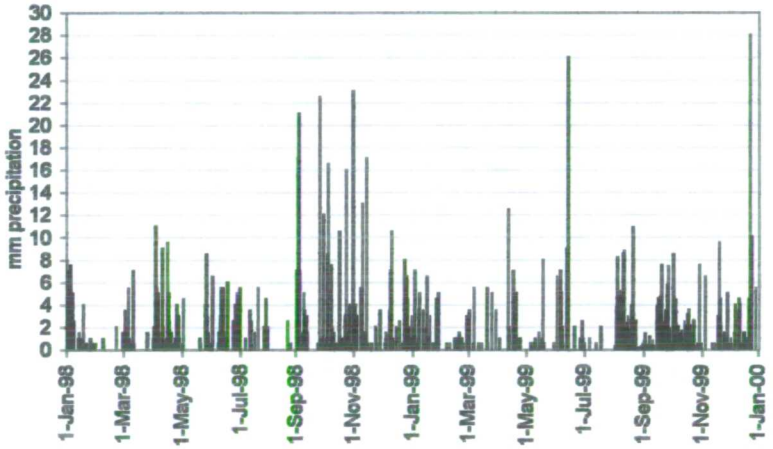


Figure 7.6. The daily totals of precipitation (mm) recorded by the AWS at the study site over 1998-1999.

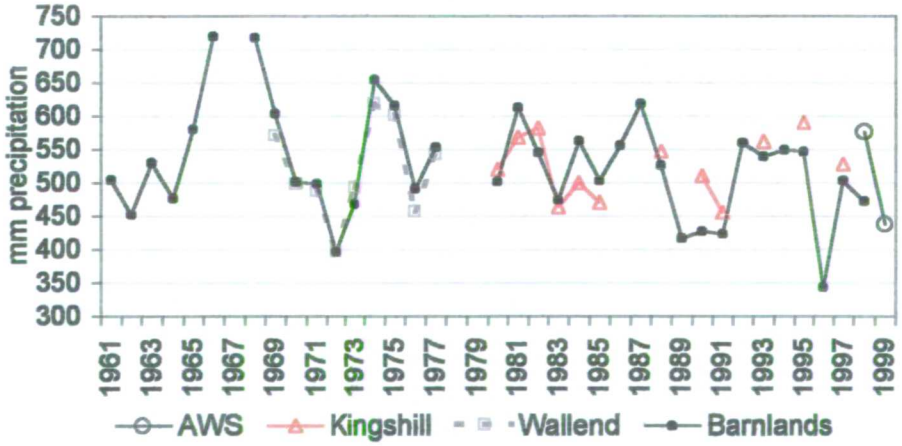


Figure 7.7. The annual precipitation total (mm) recorded by the AWS and three other gauges located near the study site on the Isle of Sheppey over 1961-1999.


**Figure 7.8. Mean annual rainfall (mm) of the UK and Ireland for the period 1931-1960. Source: Goudie and Brunsden (1994) (based on data provided by the UK Meteorological Office and the Eire Meteorological Service).**

## 7.3.4 Evaporation

Figures 7.9 and 7.10 show reference potential evaporation from grass and open water surface displayed daily and cumulatively over 1998-1999. Reference grass evaporation rate is lower than the open water due to the higher surface resistance (rs = zero for water, rs = 70 for reference grass). The difference between the two evaporation rates is seen more clearly in Figure 7.10 and indicates the annual cycle of water depletion and replenishment. Evaporation from the reference open water surface is in the order of 429 mm and 450 mm for 1998 and 1999, and loss from the grass reference surface is 302 mm and 327 mm for the two years respectively.

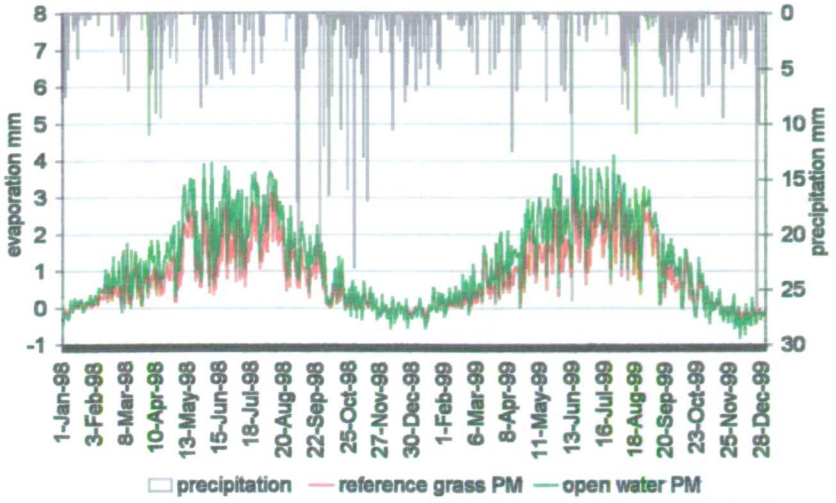


Figure 7.9. Precipitation and evaporation over 1998 and 1999 at the study site.

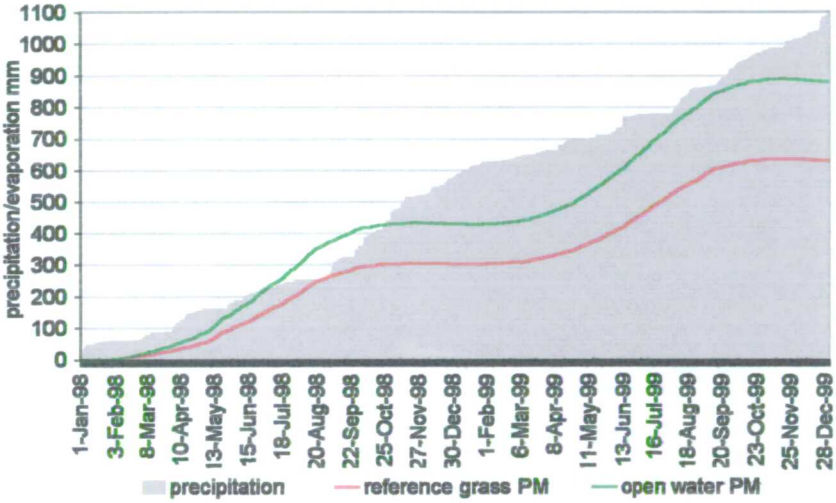


Figure 7.10. Cumulative precipitation and evaporation totals over 1998 and 1999.

## 7.4 Investigation of the influence of soil moisture upon surface resistance

### 7.4.1 Introduction

Cain (1998) reviews research undertaken to assess the effect of soil moisture deficit on the surface resistance term of the Penman Monteith formula, both overall and specifically for grass surfaces. Published research exhibit 'considerable variation' and Cain (1998 p20) declares that 'given the importance of grass cover in the UK it seems surprising that there has been no definitive study of the surface conductance [inverse of resistance] of UK grassland and its dependence on soil moisture'. While

the research presented here does not constitute a definitive study, Cain's view highlights the need for continued research in this area, which this investigation addresses.

### 7.4.2 Published relationships between evaporation, soil moisture and surface resistance

A number of experimental relationships have been published in the literature to obtain surface resistance, and from these data, actual evaporation linked to a consideration of the soil moisture deficit. Data from the research at Elmley Marshes of a link between surface resistance and soil moisture will be compared to these published relationships.

The discussion below focuses upon the research findings of Szeicz and Long (1969), Russell (1980), Saugier and Katerji (1991), Eagleman (1971), Linacre (1973, 1993) and the MORECS approach (Hough *et al.* 1997). Each piece of research is discussed in detail below, summarised in Table 7.4, and is followed by the results of the original research performed at Elmley Marshes. A functional relationship is derived and compared to the discussed published models.

#### 7.4.2.1 Szeicz and Long (1969)

An early key paper by Szeicz and Long (1969) used a number of methods to calculate the surface resistance, rs, with the conclusion that the heat or energy balance method offers the most convenient solution. To employ this method the aerodynamic resistance, ra, and the energy balance of the vegetation must be known, with rs calculated for the ratio of potential to actual evaporation:

$$rs = ra\left[1+\left(\frac{\Delta}{\gamma}\right)\left[\left(\frac{PE}{AE}\right)-1\right]\right] \qquad \text{Equation 7.4}$$

Where:
*rs* is surface resistance $sm^{-1}$
*ra* is aerodynamic resistance $sm^{-1}$
$\Delta$ is the slope of the vapour pressure curve kPa $°C^{-1}$
$\gamma$ is the psychrometric constant kPa $°C^{-1}$
*AE* is actual evaporation computed from the water balance method mm
*PE* is potential evaporation calculated using the Penman Monteith formula mm

Potential evaporation is determined from the Penman Monteith formula using setting surface resistance to zero. Theoretically surface evaporation proceeds at the potential rate when saturated when surface resistance is minimal. The choice of zero surface resistance, the resistance for open water rather than rs = 70 which is the FAO recommended resistance for reference grass surface (Doorenbos and Pruitt 1977; Jensen *et al.* 1990) is due to the fact that the calculation of potential evaporation also includes the evaporation of intercepted water when the canopy is wet; rs is reduced to zero in these situations. Values of actual evaporation can be calculated from three sources: lysimeters, the water balance and the energy balance approach.

An analysis was undertaken by Szeicz and Long (1969) of the value of mean monthly surface resistance from the ten years of data published by Aslyng (1965) for a grass clover crop with increasing soil moisture deficit. The soil type is not identified. The analysis was examined using a soil moisture characteristic derived in the laboratory between the soil matric potential, $\psi$, of the surface 0.25 m layer and the soil moisture deficit of the soil profile to 1.25 m depth. This was done under the assumption that stomata behaviour, and therefore the value of surface resistance, is mainly affected by leaf potential which is governed in turn by the soil water potential in the top layer (Rawlins *et al.* 1968), as water extracted by plant roots tends to begin at the surface progressing downwards as the soil dries (Gardner 1983). Szeicz and Long report that the mean value of surface resistance for the clover grass crop stays constant at 26 $sm^{-1}$ as the soil water potential in the top layer reduces from 0 to –350 kPa, thereafter decreasing almost linearly. The authors compare these results to those of van Bavel (1967) who also found no significant change with resistance for an alfalfa crop until a potential of –400 kPa was reached. When plotted against $\psi$ the relative evaporation ratio AE: PE is at unity i.e. actual evaporation is equal to potential evaporation until -350 kPa is reached. After this critical threshold the ratio falls below unity, initially quite steeply to a value of 0.6 at –600 kPa, then more gradually with decreasing $\psi$ to a value of 0.38 at –1200 kPa. The authors claim that although not strictly comparable the ratio curve is in agreement with those by Gardner and Ehlig (1963), Denmead and Shaw (1962) and van Bavel (1967). Based on this, Szeicz and Long offer a 'universal relation' that for a temperate climate with moderate rates of evaporation (2-3 mm $day^{-1}$), the surface resistance of a grass clover crop is maintained at a minimum until the $\psi$

in the top 0.25 m layer falls to between –300 and –400 kPa. After this threshold rs increases almost linearly to a value of 350 $sm^{-1}$ at a matric potential of –1200 kPa.
The production of such relationships allows the easy computation of actual evaporation through the use of correct resistance values in the Penman Monteith equation, or the multiplication of potential evaporation by the correct ratio of relative evaporation at the given soil water potential. The observation of a critical moisture level after which resistances increase is common with examples provided later of other researchers who have observed this phenomenon. It can be related to the available water capacity which is often conceptually partitioned into an 'easily or readily available' fraction that is used initially by the plant roots, and the remainder that is used only after the former has been depleted. This is the premise of the MORECS approach discussed below.

7.4.2.2 Russell (1980)

Russell (1980) followed the same approach as Szeicz and Long (1969) to investigate the evaporation of grass pasture and soil water status of a sandy loam and a clay soil over four years. Neutron scattering was used to monitor soil moisture, with matric potential was determined in the laboratory. Russell also obtained a soil moisture characteristic curve by linking the potential measured in the upper 0.3 m layer of soil with soil moisture measured deeper than this. Russell claims that although $\psi$ varies down the profile most of the roots are located in the surface and using the potential at 0.3 m depth therefore constitutes a 'good index'. The same approach was taken in thesis to determine the soil moisture characteristic of the study site, section 3.3.3.
Russell's results for pasture indicate that mean rs = 40 $sm^{-1}$ until a soil moisture deficit, SMD, of 40 mm is reached. Thereafter resistance increases linearly to 180 $sm^{-1}$ at 100 mm SMD. The results from the clay and sandy loam soil follow the same trend, although the SMD for the sandy loam is deeper than the clay above. The ratio AE: PE for pasture declined gradually from 0.77 at zero SMD to 0.74 at 50 mm and then more sharply to 0.45 at 100 mm, although with considerable variation. The value of the ratio of 0.77 at zero SMD is confirmed by Monteith (1965) who reports a range of 0.62 to 0.76 for crops adequately supplied with water.

While Russell's results are comparable to Szeicz and Long's analysis of Aslyng's (1965) data, they cannot be directly linked without reference to the soil moisture characteristic curve, SMC. The SMC is influenced by the soil physical and textural properties with the result that a deficit of, for example, 40 mm in sandy loam does not equal the same deficit in a clay soil in terms of water availability. By relating surface resistance to matric potential, the results can be transferred and compared to other studies. Russell (1980) report values of resistance for the sandy loam remaining at 40 $sm^{-1}$ until –150 kPa is reached; thereafter increasing linearly to a mean value of 160 $sm^{-1}$ at -1500 kPa. The critical point after which resistance starts to increase was found to occur at much earlier than the data presented by Szeicz and Long (1969). Unfortunately potentials for the clay soil, which would have been comparable to the research undertaken at Elmley Marshes, were not measured.

Russell's results differ from the proposed 'universal relation' of Szeicz and Long (1969). Russell issues a caveat that although the SMD and matric potential can be used to predict rs, both can give misleading results under certain circumstances. The SMD is distorted when rain falls onto dry soil especially near the end of the timestep; if an input of water occurs just before the end of the time step and the time delay in change in soil moisture is greater than the computation period due to slow infiltration for example, the water will be computed as having evaporated. In reality only a portion of this water may evaporate, the remainder acting to change the moisture level of the soil. Further, the use of matric potential derived for the surface soil layer may be inappropriate if a significant proportion of water loss originated from the subsoil.

The same methodological approach taken by Russell and Szeicz and Long is followed in the research at Elmley Marshes so that a relationship between surface resistance and matric potential for the clay soil can be established. From this, a method for obtaining AE can be determined either through the input of correct surface resistance values in Penman Monteith formula, or the application of a coefficient from the ratio AE: PE.

### 7.4.2.3 Saugier and Katerji (1991)

Saugier and Katerji (1991) present a model to account for the effect of water shortage upon evaporation, which is also the approach employed in the BUDGET model (Raes

1996) used to simulate soil moisture change of Elmley Marshes (section 5.2). The ratio AE: PE is linked to the ratio of readily available water to total available water in the soil RAW:TAW, where AE: PE has the value of 1 until the readily available fraction has become depleted. Subsequently AE: PE falls below unity with continued soil moisture decline as outlined in Figure 7.11.

Saugier and Katerji (1991) state that the value for the threshold or critical soil moisture value, i.e. the ratio RAW:TAW, is often taken to be between 0.5 and 0.7. A default value of 0.6 is employed in the BUDGET model employed to simulate soil moisture change at the study site, (section 5.2). The threshold of 0.5 is employed in the CROPWAT model of the FAO (Smith 1992). Slabbers (1980) presents a method to derive the ratio from leaf water potential. Alternatively the value of the RAW:TAW ratio can be undertaken from the approach of Russell (1980) and Szeicz and Long (1969).

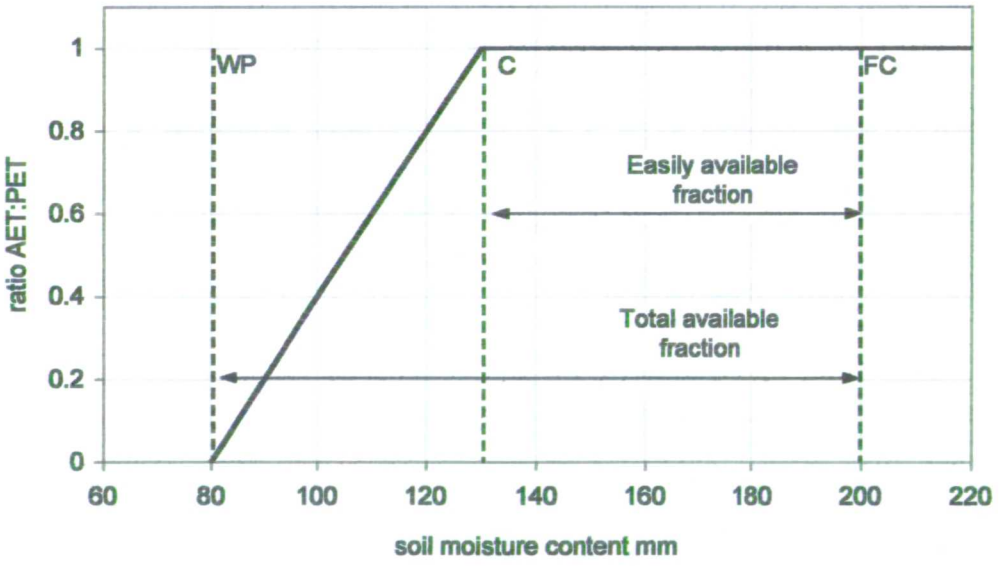


Figure 7.11. The relationship between the ratio AE: PE to soil moisture availability. The total amount of water available is that between field capacity (FC) and the wilting point (WP). Of this quota, that deemed easily available is found between FC and the critical threshold (C). In the figure, C = 130 mm which is 60% of the total available between FC and WP. The ratio of AE: PE is at unity until the critical moisture level has been reached after which point the ratio decreases.

7.4.2.4 Eagleman (1971)

Eagleman (1971) developed a relationship from regression analysis using published experimental data from several different climatic regions and vegetation covers (Denmead and Shaw 1962, Pierce 1958, Eagleman 1963, Van Bavel 1967), to determine actual evaporation from the variables of soil moisture and potential evaporation. His model takes the form of a cubic relationship, following the results of researchers such as Denmead and Shaw (1962) which indicate that the ratio AE: PE as a function of soil moisture exhibits this type of behaviour. The ratio remains high over an initial period of soil moisture decline, decreasing more sharply with increased decline. Eagleman's model takes the form:

$$\frac{AET}{PET} = A + B(MR) + C(MR)^2 + D(MR)^3 \qquad \text{Equation 7.5}$$

$$MR = \left( \frac{\theta - \theta_{wp}}{\theta_{fc} - \theta_{wp}} \right) \qquad \text{Equation 7.5a}$$

Where:
MR is the moisture ratio or fraction of the available water content
$\theta$ is soil moisture with subscripts WP, FC pertaining to soil moisture content at wilting point and field capacity respectively.
A to D are regression coefficients. Eagleman derived each of the coefficients as a function of potential evaporation (PE) so:

A = 0.732-0.05(PE) Equation 7.5b
B = 4.97-0.661(PE) Equation 7.5c
C = -8.57+1.561(PE) Equation 7.5d
D = 4.35-0.880(PE) Equation 7.5e

Eagleman (1971) tested the model by comparing computed AE to measured water loss in a soybean field. While the model overestimated the soil moisture content of two occasions by 5% and 6%, the model output was very accurate on other occasions, but the period of comparison was short. Eagleman concludes that a good relationship derived for the regression coefficients despite the difference in climatic conditions within the data implying a similar overall response is observed by the different vegetation types to soil moisture stress.

In a response to Eagleman's model, Linacre (1973, 1993) published a simplified model supported by Johns and Smith (1975) based on the same dataset. Linacre's

approach states that AE equals PE until the moisture level had fallen below a critical threshold. Linacre's MR is defined as:

$$MR = 0.25\left(\sqrt{PE}\right) \qquad \text{Equation 7.6}$$

Thereafter :

$$AE = 16(MR)^2 \qquad \text{Equation 7.6a}$$

Where:
*AE* and *PE* are in mm

7.4.2.5 MORECS Hough *et al.* (1997)

Hough *et al.* (1997) present the Meteorological Office Rainfall and Evaporation Calculation System, MORECS, a method for determining actual evaporation from a consideration of the surface resistance and soil moisture stress:

$$rs = rs(x)\left(\frac{2.5}{1-\left(\frac{(y\max - y)}{y\max}\right)} - 1.5\right) \qquad \text{Equation 7.7}$$

Where:
rs is the surface resistance ($sm^{-1}$)
x is the value for surface resistance when moisture is not limiting, changing monthly: January and February =89, March =69, April =57, May =40, June and July =64, August =74, September =75, October =78, November =87, December =89.
y is the soil moisture expressed as the available water mm
ymax is the critical threshold of the available water capacity when soil moisture becomes limiting mm

The monthly rs values linked to Equation 7.7 constitute the recommended values of surface resistance for a reference crop when soil moisture is not limiting. The values change monthly, accounting for the influence of leaf senescence upon resistance, with higher values in winter and spring due to young and old leaves having less conductance to vapour flow. Under limiting availability of soil moisture MORECS calculates rs following Equation 7.7. The available water content (AWC) of the soil is conceptually segregated into two reservoirs, x and y, characterised by the ease of the plant roots to extract water.

All water in reservoir x is termed easily available to the plant due to the greater density of plant roots in x compared to reservoir y which holds water that is

correspondingly less accessible to the plant. Surface resistance values are minimal, i.e. follow the monthly figures given above, until the amount of water in reservoir x is depleted. After reservoir x is depleted, water in reservoir y is used. The extent of the depletion of the moisture in reservoir y influences the increase in resistance values according to the formula given in Equation 7.7. The method of soil water extraction used in MORECS is that described by Thomasson (1995). A number of crops can be delineated by a characteristic rooting depth and associated proportion of soil water that is freely available. Reservoir x holds water from –5 to -200 kPa whereas water held at –200 to -1500 kPa contained within reservoir y.

A critical factor in the comparison of MORECS to other relationships between soil moisture availability and surface resistance is the definition of the available water content, AWC, and the allied soil moisture deficit, SMD. The traditional definition of the AWC is the difference between field capacity and wilting point; the amount of water held in the soil at -30 kPa and -1500 kPa respectively (Birkeland 1984). MORECS calculates the AWC as the water held in the soil from just below saturation to the wilting point through the use of -5 kPa as the point of field capacity (Hough *et al.* 1997, p19). This is confirmed by research by Gowing (pers. comm.) that has indicated that plants can detect even small decreases in soil moisture levels from saturation inducing stress and shape change of the stomata.

#### 7.4.2.6. Summary of published models

The above discussion of the published models can be summarised for reference in Table 7.4, which shows the complexity of the studies discussed above with researchers expressing the relationship between soil moisture and evaporation in different forms.

### 7.4.3 Research at Elmley Marshes

The results of the investigation at the study site to derive a relationship between soil moisture and the surface resistance term of the Penman Monteith formula are presented below. The derivation of surface resistance that account for soil moisture stress upon the grass vegetation can, when input into the Penman Monteith model, enable the calculation of actual evaporation.

Table 7.4. Summary of published models relating soil moisture and evaporation rate.

| Authors | Conditions |
|---|---|
| Szeicz and Long (1969) | Surface resistance of 26 $sm^{-1}$ over matric potentials of 0 to –350 kPa. Surface resistance increase linearly thereafter to 350 $sm^{-1}$ at a matric potential of -1200 kPa. |
| Russell (1980) | Surface resistance of 40 $sm^{-1}$ over a soil moisture deficit of 0-40 mm. Surface resistance increase linearly thereafter to 180 $sm^{-1}$ at an SMD of 100 mm. |
| Saugier and Katerji (1991) | Ratio AE: PE = 1 until 60% of the available water content has been depleted. Thereafter the ratio AE: PE declines to zero at the wilting point. |
| Eagleman (1971) | Ratio AE: PE follows a cubic relationship based on the available water content and rate of potential evaporation. |
| Linacre (1973, 1993) | Ratio AE: PE = 1 until available water falls below a function of potential evaporation. Thereafter AE is a function of the available water content. |
| MORECS Hough *et al.* (1997) | Surface resistance based on monthly crop growth stages until available moisture falls below a matric potential of –200 kPa. Surface resistance is then defined as a function of available water. |

### 7.4.3.1 Methods

In order to calculate surface resistance, the Penman Monteith formula was rearranged to find rs (Russell, 1980; Szeicz and Long, 1969):

$$rs = ra\left[1+\left(\frac{\Delta}{\gamma}\right)\right]\left[\left(\frac{PE}{AE}\right)-1\right] \qquad \text{Equation 7.4}$$

Where:
*rs* is surface resistance ($sm^{-1}$)
*ra* is aerodynamic resistance ($sm^{-1}$)
$\Delta$ is slope of the vapour pressure curve (kPa $°C^{-1}$)
$\gamma$ is psychrometric constant (kPa $°C^{-1}$)
*AE* is actual evaporation computed from the water balance method (mm)
*PE* is potential evaporation calculated using the Penman Monteith formula with surface resistance set to zero (mm).

This approach requires *a priori* values of actual evaporation together with potential evaporation, aerodynamic resistance, vapour pressures and values of the psychometric constant, summed per timestep. A database was constructed for each timestep to solve Equation 7.4, see Table 7.5.

7.4.3.1.1 AE and soil moisture

With the assumption that runoff is negligible due to the flat terrain, values of actual evaporation loss, AE, have been obtained by employing a simple soil moisture balance approach:

$E = P + \Delta S$ Equation 7.8

Where:
E is actual evaporation (mm) per time step
P is the input of water through precipitation (mm)
$\Delta S$ is the change in soil moisture (mm)

The soil moisture was measured on twelve occasions during the period April to October 1998, and on eight occasions between March and October 1999 allowing the calculation of actual evaporation for eleven and seven timesteps for 1998 and 1999 respectively. The time steps range in duration from 7 to 50 days.

For 1998, soil moisture data was obtained from electrical resistance blocks embedded in the upper 0.2 m layer and by neutron scattering for the remainder of the soil to 0.80 m depth. While other studies have averaged neutron probe data to depths of 1 m and more to obtain a representative moisture value for the whole soil profile (Dolman *et al.* 1988, Kim and Verma 1991) it was decided to compute the water balance only to the depth of 0.80 m. While neutron scattering data suggest that soil moisture change is insignificant beyond 0.65 m (section 5.1.2), soil moisture loss extended to a depth of 0.8 m in 1999. This depth is therefore used as a standard for both years.
Malfunction of the neutron probe resulted in the use of the soil sampling method to determine the moisture of the marsh in 1999. Data from the electrical resistance blocks were taken for the surface, as it was difficult to take moisture samples at regular depths in the surface layer when the soil became dry and hard.

7.4.3.1.2 PE and other variables

Daily values of potential evaporation, PE, were computed using the Penman Monteith formula (Equation 7.2) setting surface resistance to zero. These values were then summed to give total values per time step. The choice of zero resistance, effectively the open water evaporation rate, is due to the fact that the calculation of potential

evaporation also includes the evaporation of intercepted water when the canopy is wet; rs is reduced to zero at these points. All subsequent references to the potential evaporation rate relate therefore the open water rate unless otherwise stated.
Precipitation was measured daily by the tipping bucket gauge connected to the automatic weather station and summed to generate a total per time step.
Values of the aerodynamic resistance, slope of the vapour pressure curve and the psychometric constant (Equations 7.2a and b) were computed using daily averages of temperature and wind speed from the automatic weather station at the study field. Aerodynamic resistance (Equation 7.2c - f) were computed using the actual grass height over the study area. Values were then summed per timestep.

#### 7.4.3.2 Results

The input parameters of Equation 7.4 and the surface resistance obtained are presented in Table 7.5. The first observation to make from Table 7.5 is that there are nine time steps when a negative surface resistance is computed. This is due to values of actual evaporation from the water balance being higher than potential values. These data points are discussed in further detail in section 8.4.2.2, and is the focus of the third research investigation into the effects of small scale wetness heterogeneity on the evaporation of the wetland. The following sections discuss the positive resistance values obtained where actual evaporation is lower than potential values.

##### 7.4.3.2.1 Effect of decreasing soil moisture on surface resistance.

Figures 7.12 to 7.17 displays the relationship between surface resistance and the relative evaporative rate against various forms of expressing the soil moisture content in order that the relationship of decreasing soil moisture upon evaporation loss can be assessed. For all these Figures, each data point is expressed as a range according to the parameter of the x axis to indicate the magnitude of change of that parameter over the timestep. The measurement at the end of the timestep is indicated as an open square. In this way the length of the timestep can be easily identified in addition to whether the soil is drying or wetting. Data points from timesteps with a large input precipitation are marked with filled squares. Matric potential was computed using a

relationship derived for the soil characteristic of the upper 0.8 m of soil, see section 3.3.3.5.

Table 7.5. The variables (summed over the timestep except soil moisture and matric potential that are averaged over the timestep) required to determine surface resistance (Equation 7.4).

| Date (no of days per timestep in brackets) | Mean θ over timestep | ψ | Precipitation | AE | PE | ra | Δ | γ | rs |
|---|---|---|---|---|---|---|---|---|---|
| 1998 | % | kPa | mm | mm | mm | $sm^{-1}$ | $kPa°C^{-1}$ | $kPa°C^{-1}$ | $sm^{-1}$ |
| 3 - 21 April (19) | 40.7 | 0 | 56 | 49.9 | 21.6 | 1028.4 | 1.2 | 1.3 | -60.7 |
| 22 April - 8 May (17) | 39.7 | 0 | 14 | 35.4 | 25.1 | 837.5 | 1.3 | 1.1 | -31.2 |
| 9 – 25 May (17) | 35.1 | -3 | 1.5 | 53.4 | 41.9 | 1181.6 | 1.6 | 1.1 | -35.7 |
| 26 May - 16 June (22) | 30.2 | -51 | 42 | 68.4 | 42.5 | 1169.9 | 2.0 | 1.5 | -48.0 |
| 17 – 22 June (6) | 28.0 | -222 | 6 | 15.4 | 16.3 | 369.2 | 0.7 | 0.4 | 9.2 |
| 23-June - 6 July (14) | 26.7 | -583 | 19.5 | 31.5 | 32.2 | 784.0 | 1.4 | 0.9 | 3.3 |
| 7 – 14 July (8) | 25.5 | -682 | 6.5 | 13.1 | 15.4 | 467.6 | 0.8 | 0.5 | 25.8 |
| 15 – 20 July (6) | 25.1 | -706 | 7 | 7.1 | 14.9 | 466.6 | 0.6 | 0.4 | 213.3 |
| 21 July - 4 August (15) | 24.1 | -751 | 9.5 | 24.6 | 37.1 | 1056.5 | 1.5 | 1.0 | 90.1 |
| 5 August - 23 September (50) | 23.9 | -762 | 70 | 57.7 | 92.3 | 3516.7 | 5.1 | 3.4 | 98.6 |
| 24 September - 22 October (28) | 26.9 | -465 | 88 | 25.8 | 19.5 | 2201.9 | 2.4 | 1.9 | -109.5 |
| 1999 | | | | | | | | | |
| 15 March – 14 April (31) | 38.9 | 0 | 30 | 47.6 | 31.2 | 3668.6 | 2.2 | 2.0 | -85.0 |
| 15 April – 31 May (47) | 33.5 | -8 | 34 | 103.6 | 92.3 | 4094 | 3.8 | 3.1 | -21.2 |
| 1 June – 6 July (36) | 27.8 | -294 | 64.5 | 88.7 | 83.7 | 3754.1 | 3.5 | 2.4 | -14.3 |
| 7 July - 2 August (27) | 24.8 | -732 | 6.5 | 30.9 | 72.3 | 2760.4 | 3.1 | 1.8 | 369.9 |
| 3 - 23 August (21) | 25.5 | -667 | 70 | 29.8 | 46.0 | 2145.5 | 2.1 | 1.4 | 140.0 |
| 24 August – 4 October (42) | 29.0 | -97 | 78 | 62.1 | 69.7 | 4634.6 | 4.3 | 2.8 | 34.3 |
| 5 - 24 October (20) | 29.0 | -116 | 35 | 52.0 | 12.7 | 2119.6 | 1.5 | 1.3 | -171.6 |

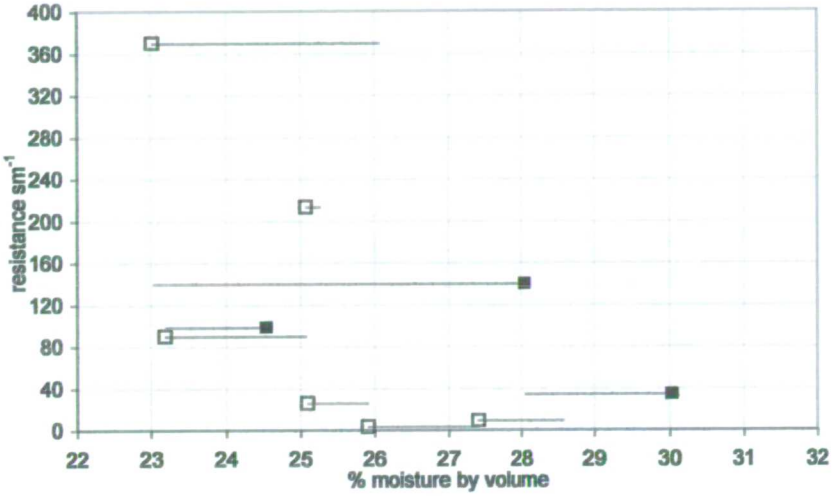


Figure 7.12. Surface resistance against soil moisture decline over the study period.

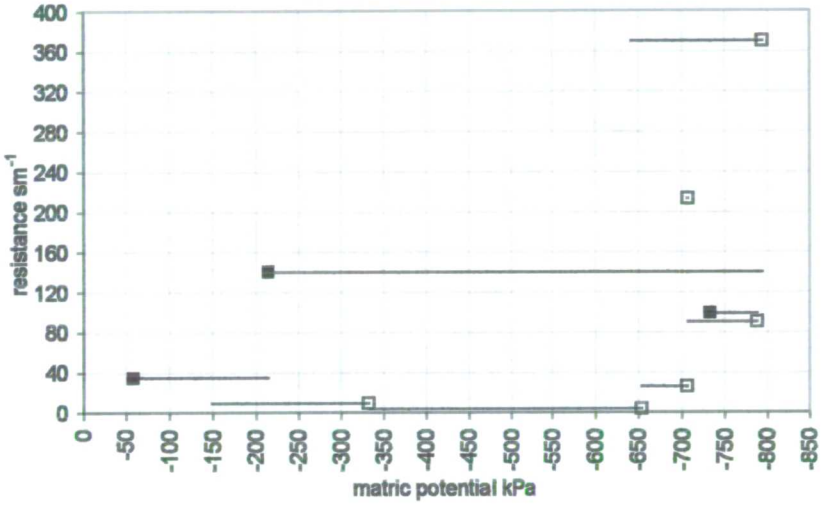


Figure 7.13. Surface resistance against matric potential.

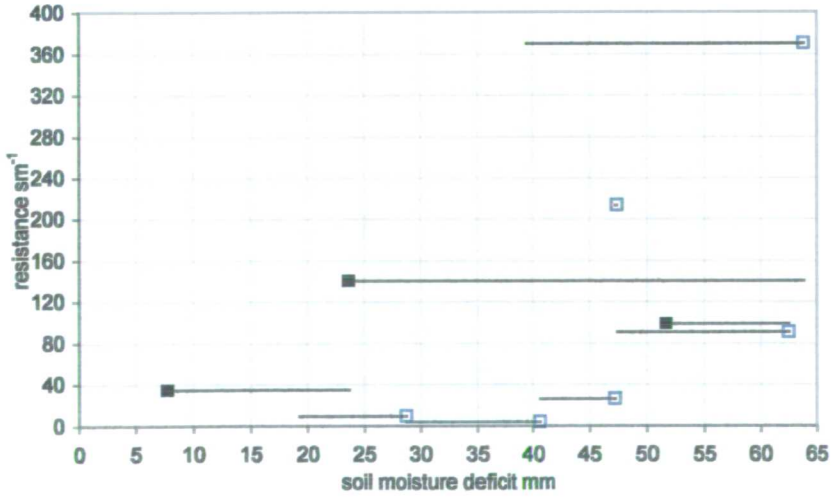


Figure 7.14. Surface resistance as a function of the soil moisture deficit (using values of the field capacity and wilting point as 31% and 10% volumetric soil moisture).

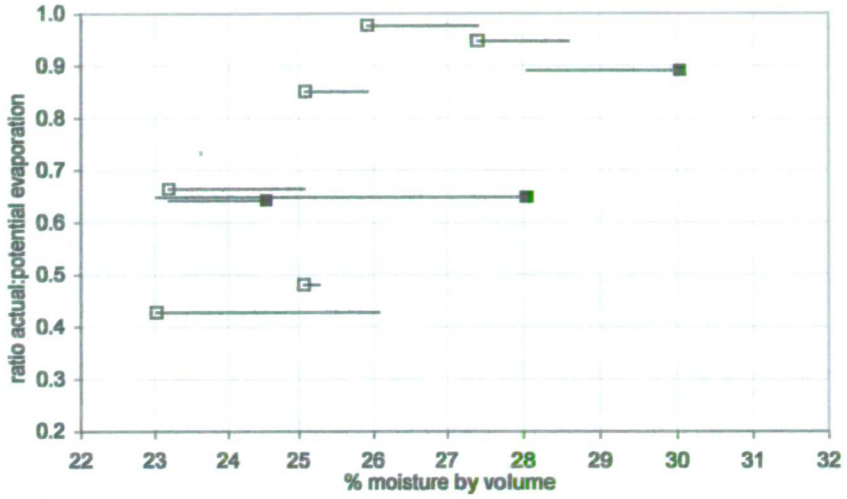


Figure 7.15. Ratio of AE: PE as a function of matric potential.

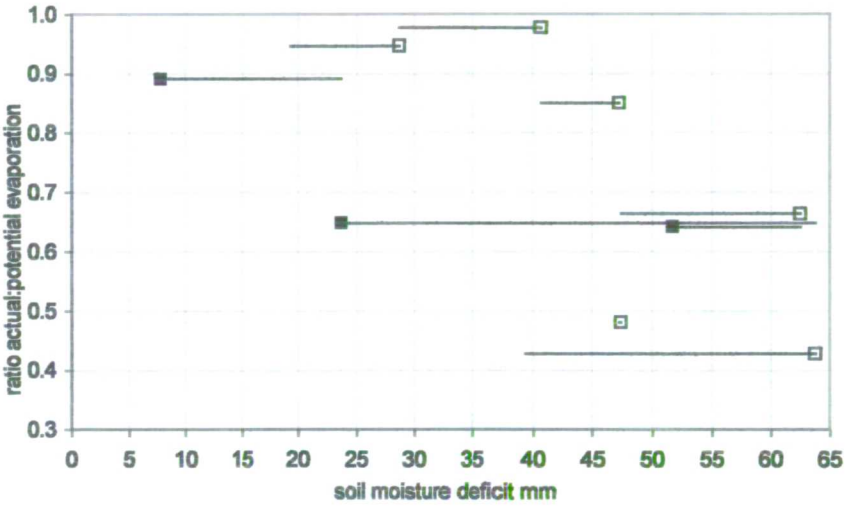


Figure 7.16. Ratio of AE: PE as a function of the soil moisture deficit.

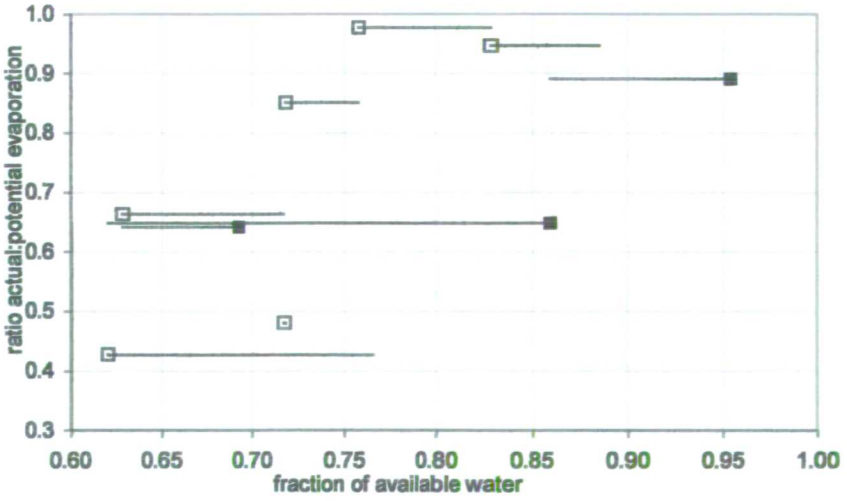


Figure 7.17. Ratio of AE: PE as a fraction of the available water or Linacre's Moisture Ratio.

7.4.3.2.2 General trend

The data points presented in Figures 7.12 to 7.17 are each expressed as a range according to the parameter of the x axis to indicate the change of that parameter over the time step. The measurement at the end of the time step is indicated as an open square. Data points from time steps with a large input precipitation are marked with filled squares. In this way the span of the time step can be easily identified in addition to whether the soil is drying or wetting. There is one time step (3-24 August 1999) which received a large precipitation input and exhibits a large range (5% moisture increase) as the soil wetted. This data point seems out of step compared to the others, which show more restricted changes.

The results indicate that there is a relationship, albeit complex, between surface resistance and soil moisture. The results in Figures 7.12 and 7.13 can be summarised as follows. Minimum resistance values (range 3-34 $sm^{-1}$) are maintained until a soil moisture of 26%, corresponding to a matric potential of –650 kPa or soil moisture deficit of 40 mm. Resistance increases with moisture contents below this threshold but the lack of data points prevent identification of a definite trend. However it is postulated that the data follow a linear form reaching a high value of 370 $sm^{-1}$ at 23% moisture content equivalent to –800 kPa and 64 mm deficit.

7.4.3.2.3 Ratio of actual to potential evaporation

The data in Figures 7.14 to 7.17 show the change in the ratio AE: PE for various forms of expressing the moisture content. The data demonstrate that the ratio is within the range 0.89-0.98 until a soil moisture of 26% is reached which is equal to a deficit of 40 mm or when the fraction of available water (FC-WP) has fallen to 0.75. After this critical threshold the data suggest that the ratio falls lower with greater moisture deficit in a fairly linear trend. A ratio of 0.43 is reached at 23% volumetric moisture equal to 64 mm deficit or 0.62 faction of available water.
As discussed in section 7.4.2.3 Saugier and Katerji (1991) state that the threshold or critical soil moisture value is often taken to be between 0.5 and 0.7 fraction of available moisture. The results in Figure 7.17 suggest a slightly higher value of 0.75.

This threshold marks the point at which the easily accessible portion of the total available water has been depleted.

The MORECS soil moisture extraction model (Hough *et al.* 1997) for a grass crop on clay soil is based on the easily available fraction constituting 62% of the total available water i.e. the ratio of actual potential evaporation remains at unity until only 0.38 fraction of available moisture remains. This is considerably lower than the values above, partially explained by the difference in calculation of the available water content. MORECS computes the available water as between matric potential of –0.05 to –1500 kPa; the traditional definition used above is the water available between –30 to –1500 kPa. The MORECS approach is applied to the data collected at the Elmley Marshes in section 7.6.3.

7.4.3.2.4 Effect of evaporative demand

Many authors have noted the different rates of water loss under different potential evaporation conditions (Denmead and Shaw 1962, Kristensen and Jensen 1975, Eagleman 1971, Linacre 1993, Raes 1996). At given moisture levels, an area with a high atmospheric evaporative demand will lose moisture faster than a low evaporative demand, and thus the critical moisture threshold is reached at a higher moisture level. For example the classic results of Denmead and Shaw (1962) demonstrated that at low atmospheric demand of 1.4 mm $day^{-1}$, the potential evaporation rate was maintained up to -500 kPa, while at a high rate of 7.4 mm $day^{-1}$ potential rate was maintained only up to -30 kPa. A moderate demand of 3-4 mm $day^{-1}$ could be maintained until approximately -200 kPa. These results were obtained with daily measurements from corn crops in controlled experiments employing lysimeters in order to ensure uniformity of soil moisture within the lysimeter and to restrict the root zone.

It not feasible to employ lysimeters at Elmley Marshes and so the results presented for this study are based on measurements taken at intervals of several days from undisturbed marsh soil. As such, it is not possible to distinctly classify the results into group according to the atmospheric demand as meteorological conditions would be variable over each timestep, especially for long periods. However, as the link between surface resistance and soil moisture content is indirect, with leaf water status identified as the controlling factor, it is necessary to assess the relative importance of

the evaporative demand of the atmosphere. Table 7.6 contains the range of potential demand for the periods that yield positive values of surface resistance. The range of potential evaporation over the entire period studied is in the order of 0.1 to 4.1 mm $day^{-1}$, which could be classified as low to moderate demand. Such a large range is expected not only from the natural variability of meteorological conditions but also the duration of the study period extending from May to October. The average rate is presented to allow comparisons between timesteps and it can be seen that there is an overall range of 1.7 to 3.1 mm $day^{-1}$; values much lower than those reported by Denmead and Shaw (1962). There seems to be a weak positive relationship of surface resistance with increasing potential evaporation; however there is considerable scatter with high potential rates, 2.9 mm, being coupled to both high and low resistances 370 and 9 $sm^{-1}$ respectively.

The lack of a strong relationship between surface resistance and potential evaporation in Figure 7.18 indicates that the former was affected by soil moisture availability independently of evaporative demand; a trend also found by Russell (1980). As the range of potential evaporation over the time period studied is quite restricted (between 0.1-4.1 mm) compared to other studies, the uptake of water by roots at the marsh is more limited by soil factors such as the low hydraulic conductivity, soil structure and salt content and osmotic potential.

Table 7.6. The daily average and range of potential evaporation per timestep.

| Date (no of days per timestep in brackets) | Average | Range Max-Min |
|---|---|---|
| 1998 | mm $day^{-1}$ | mm $day^{-1}$ |
| 17 – 22 June (6) | 2 9 | 3.8-1.9 |
| 23-June - 6 July (14) | 2.4 | 3.7-0.9 |
| 7 – 14 July (8) | 2.1 | 3.2-1.1 |
| 15 – 20 July (6) | 2.7 | 3.6-2.0 |
| 21 July - 4 August (15) | 2.7 | 3.7-1.3 |
| 5 August - 23 September (50) | 2.0 | 3.7-0.4 |
| 1999 | | |
| 7 July - 2 August (27) | 2.9 | 4.1-0.8 |
| 3 - 23 August (21) | 2.3 | 3.4-1.0 |
| 24 August – 4 October (42) | 1.8 | 3.3-0.1 |

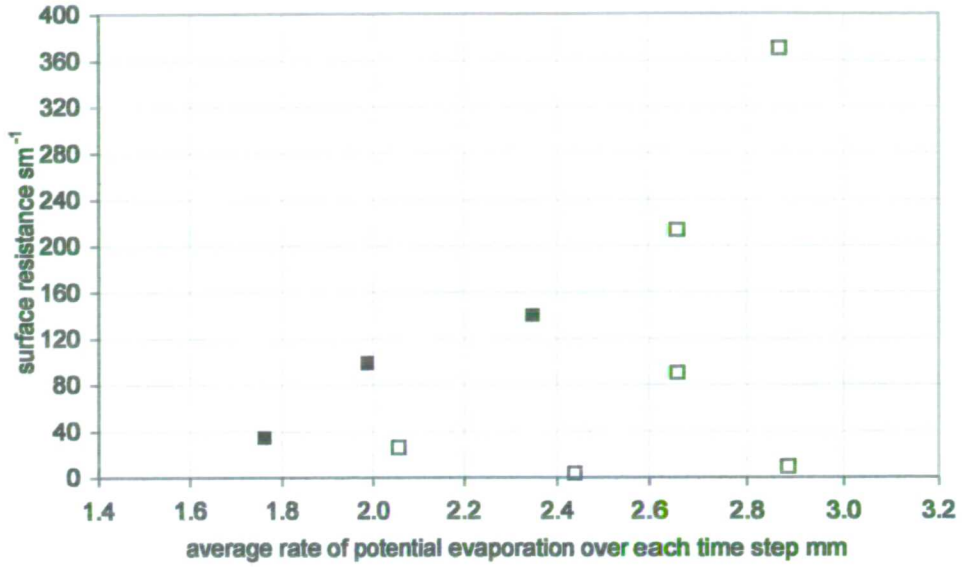


Figure 7.18. Surface resistance plotted as a function of the average rate of potential evaporation per timestep.

## 7.5 Derivation of a functional relationship

The general trend observed in Figures 7.12 to 7.14 follows the same pattern as the observations reported in Szeicz and Long (1969), and Russell (1980), with computed values of resistance of the same magnitude, Figure 7.19. The threshold moisture content of 26% is similar to that reported by Kelliher *et al.* (1993) for pasture.

The research presented by Russell (1980) and Szeicz and Long (1969) to determine the relationship between resistance and soil moisture deficit, was undertaken over a period of 4 and 9 years respectively generating considerably larger datasets (49 and 56 data pairs respectively) than that from the investigation at Elmley Marshes (9). Both authors found a minimum resistance was maintained (26 – 40 $sm^{-1}$) until a threshold moisture content was reached after which the resistance increased linearly. Szeicz and Long (1969) expressed the critical threshold as being between –300 to –400 kPa or 30 mm SMD, with surface resistance increasing thereafter to –1200 kPa or 85 mm.

As the results of this study span two summers resulting in only nine data pairs, there are insufficient data points to establish conclusive trends, however a general trend can be observed which is similar to the results of the authors above. To clarify this similarity, the data of Szeicz and Long (1969) and Russell (1980) are reproduced in

Figure 7.19 illustrating change in surface resistance with moisture deficit. It can be seen that despite is considerable scatter, the two datasets are comparable until a deficit of 40 mm is reached. Thereafter the relationship follows a similar curve form but the gradient differs, with higher resistances exhibited by the Szeicz and Long dataset. The results from the investigation at Elmley Marshes are also presented in Figure 7.19c and it can be seen that although the dataset is small, the scatter of datapoints falls within those about the Szeicz and Long dataset, and it can be said to follow their 'universal relationship'.

As the data from the Elmley Marshes fits the universal relationship proffered by Szeicz and Long (1969) rather than try to derive a formula from the small Elmley dataset alone, it is valid to quantify the relationship between resistance and soil moisture deficit using all observations presented in Figure 7.19c. Such a formula would allow the determination of correct resistances for a given soil moisture content, which would enable the computation of actual evaporation for the grass surface when employed in the Penman Monteith equation. Figure 7.19b shows trend lines fitted to the mean of moisture deficit classes at 15 mm intervals. This trend line has been recalculated to all the data shown in 7.19c to account for the additional data from the investigation at Elmley Marshes. This adjusted trendline is shown as a dashed line in Figure 7.19c. The trend line follows an exponential form:

$$rs = ae^{b(x)} \qquad \text{Equation 7.9}$$

Where:
$rs$ is surface resistance $sm^{-1}$
$x$ is the soil moisture deficit mm
$a$ and $b$ are constants of value 21.31 and 0.031 respectively.
The correlation coefficient is high with $r^2 = 0.79$ and due to the scatter of the data, the standard error has a value of 66.46.

The data obtained from the investigation at Elmley Marshes and the 'updated universal relationship' is also compared below to the models of Eagleman (1971) Linacre (1973, 1993) and MORECS (Hough *et al.* 1997).

The 'updated universal relationship' is used in the third research investigation to determine actual evaporation from the marsh surface according to the moisture status of the marsh over 1999, Chapter 8.

a:

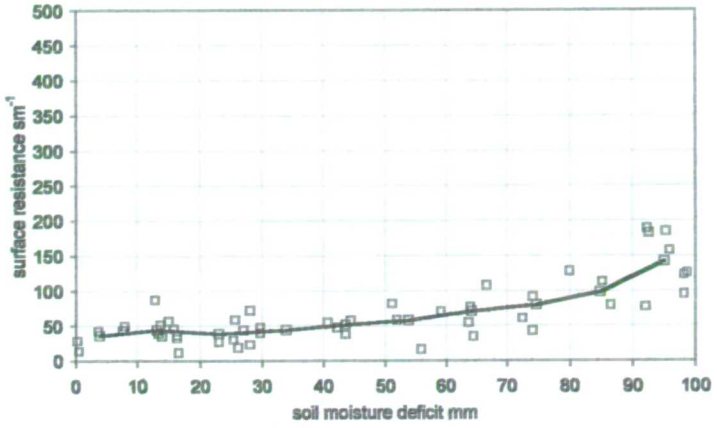


b:

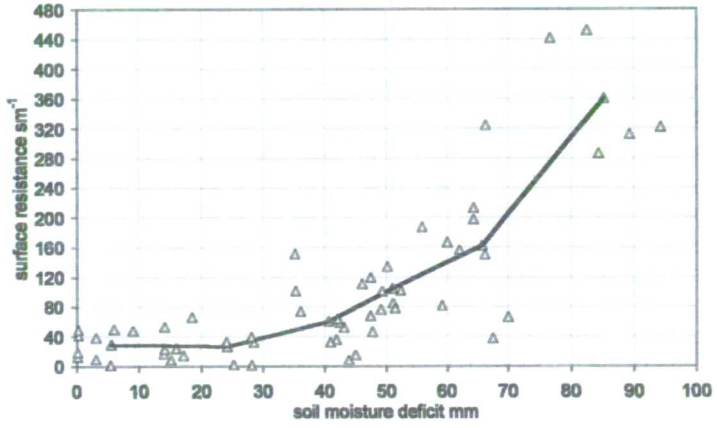


c:

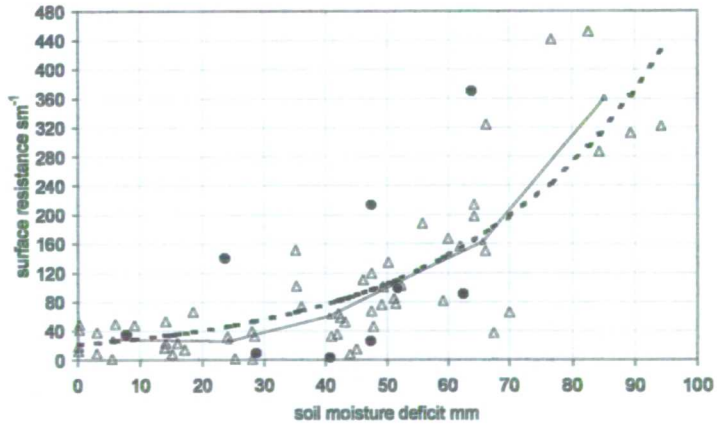


Figure 7.19. Derivation of a functional relationship; the 'updated universal relationship'. Observations of surface resistance ($sm^{-1}$ y axis) and soil moisture deficit (mm x-axis) by a: Russell (1980), and b: reproduction in Szeicz and Long (1969) of data by Aslyng (1965). The lines are fitted to SMD class on of intervals 10 mm and 15 mm respectively. Chart c illustrates Aslyng's data together with the results of this study. The dashed line is fitted to all the data points in chart c and takes an exponential form: surface resistance ($sm^{-1}$) $=ae^{b(x)}$ where the constant a = 21.31 and b = 0.032. The correlation coefficient is high with $r^2 = 0.79$ and the standard error is 66.46.

## 7.6 Comparison of the derived relationship with published models

### 7.6.1 Eagleman (1971)

Eagleman's relationship to determine actual evaporation from the variables of soil moisture and potential evaporation is a regression analysis taking the form of a cubic relationship. Eagleman's model (Equation 7.5 section 7.4.2.4), was applied to the soil moisture and potential evaporation data of the nine time steps where the ratio of potential to actual evaporation did not exceed unity. Values of field capacity and wilting point were taken as 31% and 10% volumetric moisture content, taken from the derived soil moisture characteristic curve for the Wallasea soil series of the study site, section 3.3.3.3.5.

Figure 7.20 reveals an overestimation of the actual evaporation loss computed from Eagleman's model compared to the water balance. The overestimation is pronounced at periods of low evaporative loss 1-2 mm $day^{-1}$, becoming less at higher evaporative loss. The range of overestimation is on the order of 0.1 to 1.5 mm $day^{-1}$.

The overestimation by the model is due the fact that the potential rates experienced in the Elmley Marshes dataset are lower than those employed by Eagleman in deriving the relationship: Eagleman states that the experimental data used to derive the relationship was in the range 2.0 to 9.0 mm of PE (1971, p390) and that generated curves were extrapolated outside this range. As a result, "at the low end of the scale at a PE of 2.0 mm the calculated rate is 2.20 mm. This difference is not very significant in terms of amount but is greater in terms of percent error". Over long time periods however overestimation as much as 1.5 mm $day^{-1}$ can be substantial. It can be concluded that for areas with comparatively low potential evaporative rates, the model by Eagleman will overestimate AE and the model is not recommended.

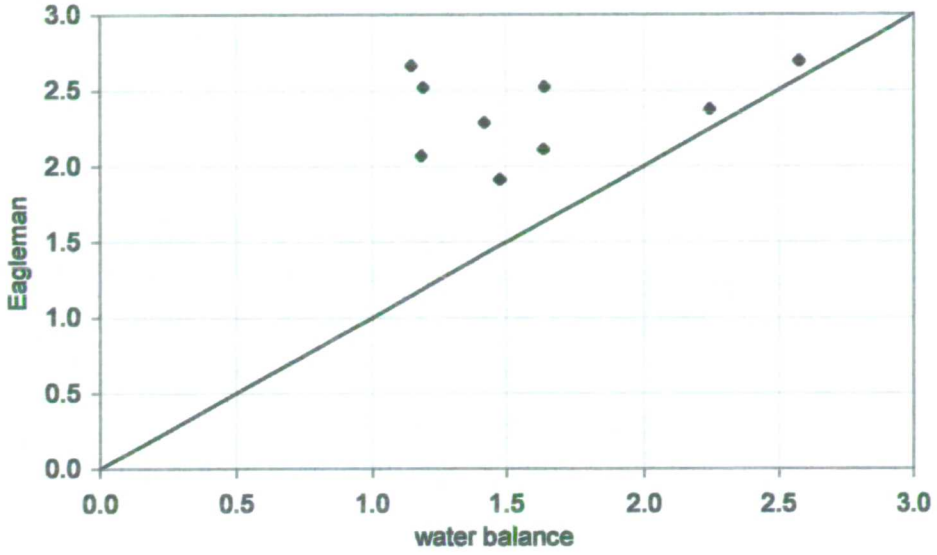


**Figure 7.20. Values of actual evaporative loss (mm day$^{-1}$) computed by the water balance at Elmley Marshes and the model of Eagleman. A 1:1 line is shown for guidance.**

## 7.6.2 Linacre (1973, 1993)

Linacre's model, Equation 7.6, section 7.4.2.4, is an adaptation of the data used by Eagleman (1971) using the same input variables of soil moisture and potential evaporation. Linacre's adaptation states that the ratio AE: PE is equal to 1 until the critical threshold is reached defined as the fraction of the AWC that equals $0.25\left(\sqrt{PE}\right)$. Then AE = 16(MR$^2$) where MR is the fraction of the AWC when it has become limiting.

Linacre's model was applied to the soil moisture and potential evaporation data of the nine time steps where the ratio of potential to actual evaporation did not exceed unity. Values of field capacity and wilting point were taken as 31% and 10% volumetric moisture content for a soil profile to 0.8 m depth, as for Eagleman's model application.

The value of the critical threshold was determined both per timestep and as an average. For the former the threshold varied from 0.21 to 0.41 depending upon the evaporative power of the atmosphere. For the latter the overall critical point was computed to be 0.36 i.e. the AWC would be reduced to 36%, which is very low

equating to a moisture content of 18% or a moisture deficit of 108 mm before AE became less than PE.

In both approaches, the critical threshold was never exceeded and for all timesteps, the actual evaporative loss would have equalled the potential loss according to Linacre's model. As the model was based on the dataset of Eagleman (1971), it can be stated again that that the potential rates experienced in the Elmley Marshes dataset are lower than those employed by Eagleman and so outside the range for which Linacre's model should be applied.
Linacre's empirical model thus generates a critical threshold that is low compared to the water balance, and overestimates the loss when this is exceeded. In conclusion it cannot be seen to work well for the conditions at Elmley Marshes.

### 7.6.3 MORECS

The MORECS method (Hough *et al.* 1997), Equation 7.8, section 7.4.2.5 was first applied using the information given for Square 163, which covers the Elmley Marshes, using the median AWC (i.e. clay soil) for a grass crop. The AWC equalled 114 mm for a profile of 0.8 m depth and the value of ymax, the critical moisture threshold perceived to be at a matric potential of –200 kPa, calculated to be 43 mm, i.e. 38% of the AWC. This value of reservoir y is low due to the perceived high rooting density of the theoretical grass crop ensuring that the majority of the soil water is readily available i.e. reservoir x is large. Should the AWC fall below this threshold, surface resistance will increase from given monthly values.
Equation 7.8 was applied to the moisture deficit data of Elmley Marshes for the nine time steps that generated positive surface resistance values (Table 7.5), employing the theoretical value of the critical threshold. It was found that the actual deficit did not fall below this threshold and consequently resistance followed monthly values. This does not accord with the updated universal relationship derived above that shows resistances exceeding the MORECS monthly values for the same Elmley Marshes moisture deficit dataset.

The next application of the MORECS approach used the actual value of ymax for Elmley Marshes, rather than derive it from the information from MORECS Square

163. A value of ymax was computed according to the observed point at which resistances are seen to increase in the updated universal relationship. Figure 7.21 illustrates that resistances start to increase substantially after a deficit of approximately 40 mm has been exceeded. This equates to 26% volumetric moisture content or a matric potential of –650 kPa. The soil moisture deficit in Figure 7.21 has been computed as the water held between matric potentials of -30 to –1500 kPa, 31% to 10% soil moisture, and thus the threshold of 40 mm deficit renders only 24% of the total available water (168 mm) to be readily accessible.

The MORECS approach however expresses the available water content as between the range –5 to –1500 kPa. This covers the soil moisture range of 34 - 10%, an available water content of 192 mm. Taking the threshold moisture content of 26%, 64 mm are now readily available, the x reservoir; 33% of the total amount available, leaving 128 mm in the y reservoir. Computing the available water content for actual conditions at Elmley Marshes results in a much lower readily available fraction at a lower matrix potential than that proposed for the theoretical Square 163.
Using ymax = 128 mm in Equation 7.8 with moisture deficit data from the nine timesteps as above causes the x reservoir to become depleted and surface resistances increase with increasing moisture deficit. Figure 7.19 shows the result together with resistances computed from the updated universal relationship. Also shown for comparison are the MORECS resistances when the available water is not limiting where change is influenced by leaf senescence on a monthly time-scale.

Figure 7.21 shows that, when compared to the updated universal relationship, MORECS overestimates surface resistance at moistures higher than the threshold ymax by mirroring given monthly values. There is also an underestimation when ymax is exceeded. The given monthly values approximate to the value of 70 $sm^{-1}$ given by Smith *et al.* (1992) for the 'reference grass crop not short of water'. The question to be answered from this result is whether or not the amount of deviation from the universal relationship by the MORECS results is significant? The objective of deriving surface resistance values from soil moisture data is to derive input values for the Penman Monteith formula to determine actual evaporation. The Penman Monteith model has greatest sensitivity to surface resistance over initial increases of the latter from zero (Figure 7.1). The result is that change in resistance over the initial

drying phase from soil inundation corresponds to a greater magnitude of change in the value of evaporation computed than if the same change was made when the soil is drier. For the overestimation by MORECS at the wetter moisture contents, Figures 7.1 and 7.21 shows that an increase in resistance from 30 to 78 $sm^{-1}$ invokes a fractional decrease in evaporation, computed by Penman Monteith, of 0.2. For the underestimation by MORECS at the drier end, an increase in resistance from 120 to 155 $sm^{-1}$ invokes a much lower fractional decrease in evaporation of 0.07. Thus the difference in resistance values is more significant over the drying phase from soil inundation.

In conclusion applying the theoretical values of the available water and critical threshold for the MORECS Square covering the Elmley Marshes results in a poor prediction of the resistance values compared to the updated universal relationship due to the large readily available water fraction. Determining the water availability and critical threshold from site-specific observations produces resistance values of the same trend as the universal relationship with some degree of over and underestimation. The sensitivity of the Penman Monteith formula indicates that the difference at drier moisture content is of less significance than at the wetter moisture contents.

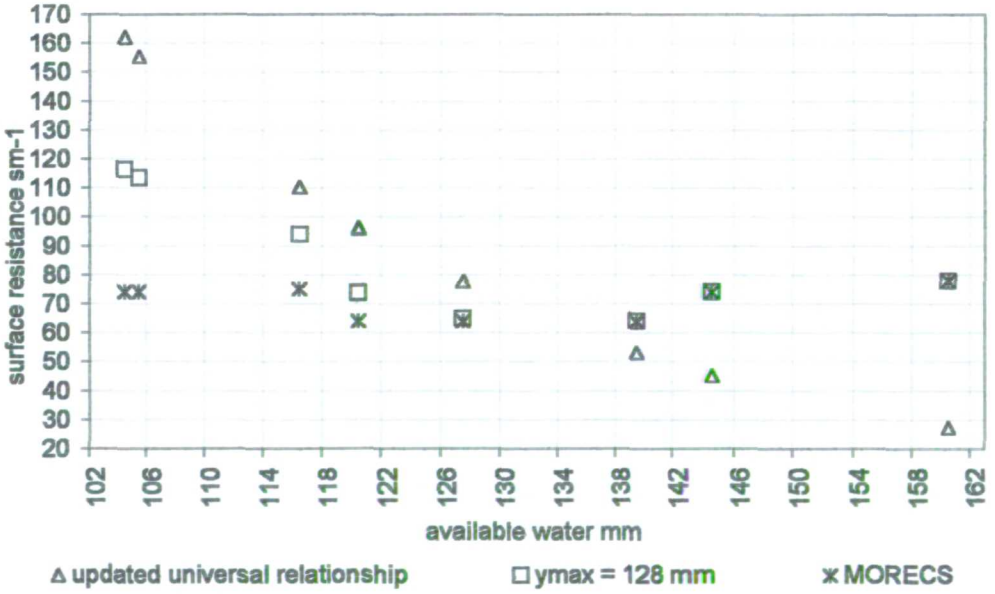


Figure 7.21. Results of the MORECS approach to compute surface resistance ($sm^{-1}$) from the available water content of Elmley Marshes (mm) using derived values of the threshold ymax =128 mm together with resistances computed from the updated universal relationship. Also shown are the MORECS resistances when the available water is not limiting where change is influenced by leaf senescence on a monthly time-scale.

## 7.7 Conclusions

The original research undertaken at Elmley Marshes have proven that there is an influence of decreasing soil moisture upon the surface resistance. As the number of data pairs from the study site were few, observations from Elmley Marshes were combined with the data by presented by Szeicz and Long (1969) described as the 'universal relationship'. With the additional data from this investigation, this relationship was re-quantified as the 'updated universal relationship'. When compared against this relationship, published models, particularly the MORECS approach, are observed to over and underestimate values of surface resistance using the same soil moisture database.

Consequently the 'updated universal relationship' is recommended as a method to designate 'appropriate' values of surface resistance based on soil moisture content. Through inclusion in the Penman Monteith model, an estimate of actual evaporation can be made.

This approach is undertaken as part of the third research investigation, Chapter 8, to compute a value of actual evaporation that is representative for the heterogeneous wetland.

# Chapter 8 Wetland evaporation. Part 2 Actual evaporation loss

Building upon the results from second research question presented in Chapter 7, this Chapter presents the investigation to determine actual evaporation loss from the marshland to answer Research Question 3 *'What is the actual evaporation loss from the heterogeneous wetland surface?* (Table 7.1).

## 8.1 Introduction

Quantification of the relationship between soil moisture and surface resistance in Chapter 6 allows the computation of actual evaporation from the grassed marsh accounting for moisture availability. The wetland surface is characterised by small scale patches of open water and bare soil in addition to the grassed marsh and evaporation from these surface types need to be considered when attempting to compute a representative evaporative flux.

The approach taken in this investigation follows that of Wessel and Rouse (1994) who computed the evaporation of a Canadian high subarctic tundra wetland characterised by patches of vegetated hummocks of sedges and grasses, bare soil hollows and ponds of standing water that change in extent over time. Their method, the Weighted Penman Monteith approach (WPM) applies the Penman Monteith formula to each surface type, weighting each component calculation for the surface area of each surface type, and summing the components to give the total evaporation from the site. Wessel and Rouse (1994, p111) claim that 'theoretically this is the best approach for representing evaporation for areas which have a variety of surface types'.
The WPM is presented here for a new environment; a temperate wet grassland in an area of water shortage. The surface types of Elmley Marshes can be classified as bare soil, grass, and open water.

As discussed in section 7.1.3, the WPM method relies upon accurate surface resistance values for each surface type. The resistance from the grass surface type is considered to be a function of soil moisture alone, allowing the designation of

resistance values depending upon the moisture content determined using the 'updated universal relationship' (section 7.5).

The results of computing the evaporative flux with the WPM approach are referenced against actual evaporation data from a Bowen Ratio Energy Balance station on the study site. The equipment was installed on site at the beginning of 1999 and data to determine actual evaporative loss by the Bowen Ratio Energy Balance, BREB, was available for the period 24 March to 30 September 1999. This is the period of the investigation presented here. The investigation was confined to this period so that the accuracy of the WPM model could be assessed by comparison to the BREB data.

## 8.2 Method

In order to perform the Weighted Penman Monteith model a number of steps need to be followed. To ascertain the changing areas of the surface types in time and space it is first necessary to examine the fetch requirements for the micrometeorological equipment in the main enclosure of the study field, the AWS and BREB station, and to ascertain the predominant wind direction over the marsh. The proportion of areas in the dominant wind direction are then mapped and quantified. Surface resistance values are designated to each surface type. The data from the BREB station needs to be examined and screened. These steps are discussed below.

### 8.2.1 Fetch

A commonly suggested ratio for the necessary upwind fetch for boundary layer instrumentation, is in the order of 100 m for each m depth of the turbulent boundary layer that is in equilibrium and therefore representative of the surface energy exchange being measured (Oke 1987). For measurements made at a maximum height of 2 m in the main enclosure from this simple ratio it can be seen that there is sufficient fetch over the marsh except due west, 250-260°, where at the edge of the field 180 m away is a brick building and small concrete paved area.

Brutsaert (1982) developed a method for determining the fetch requirements based on a consideration of surface roughness. With the common assumption that the lower 10% of an internal boundary layer downwind of a surface discontinuity has reached a new equilibrium the minimum fetch can be determined as:

$$x_f = \left( \frac{30(z-d)}{(z_{om})^{0.125}} \right)^{1.14} \qquad \text{Equation 8.1}$$

Where:

$x_f$ is the minimum fetch required for complete boundary layer development m

$z$ is the maximum sensor height above the ground m

$d$ is the zero plane displacement of wind profile (m) estimated as $d = \frac{2}{3}h$ where h is the canopy height (m)

$z_{om}$ is momentum roughness height of the surface (m) estimated as $z_{om} = 0.123h$

Equation 8.1 is formulated for near-neutral conditions; for situations of increasing or decreasing stability the exponent (1.14) should be increased or decreased respectively. Equation 8.1 was employed to compute the minimum fetch requirements for the study field. The height of the grass sward of the study field was monitored on field visits, kept short by animal grazing ranging between 0.02 and 0.09 m with an average value of 0.04 m over the period. The fetch was determined for all heights and a value for water was also computed with a value of $z_{om}$=0.0001 after ASCE (1996). Results are presented in Table 8.1 and show that as surface roughness increases, i.e. with an increase in canopy height, the fetch requirement decreases due to the greater turbulence and associated convective mixing.

The minimum fetch requirements under stable conditions for the grass surface is in the range 249 to 195 m depending upon sward height. For the average sward height of 0.04 m the required upwind fetch length is 224 m which is fulfilled in all directions from the location of the meteorological instrumentation except for 250-260°, as mentioned above.

Data when the wind direction is 250-260° have been rejected due to insufficient fetch for the period 24 March to 30 September 1999. This is the period of comparison between the results of computing actual evaporation using the WPM approach against the BREB method. A total of 5 data days were rejected see Table 8.4 (section 8.3.2).

Table 8.1. Minimum upwind fetch distances for the range of canopy heights experienced over the study field 1999 (Equation 8.1). Results using the average grass height (0.04 m) over the period are in bold. All parameters have units in m.

| Canopy height | $z$ | $d$ | $z_{om}$ | $x_f$ |
|---|---|---|---|---|
| 0 (water) | 2 | 0 | 0.0001 | 396 |
| 0.02 | 2 | 0.0133 | 0.0025 | 249 |
| 0.03 | 2 | 0.0200 | 0.0037 | 234 |
| **0.04** | **2** | **0.0267** | **0.0050** | **224** |
| 0.05 | 2 | 0.0333 | 0.0062 | 216 |
| 0.06 | 2 | 0.0400 | 0.0074 | 209 |
| 0.07 | 2 | 0.0467 | 0.0086 | 204 |
| 0.08 | 2 | 0.0533 | 0.0098 | 199 |
| 0.09 | 2 | 0.0600 | 0.0111 | 195 |

An estimate of the fraction of λE sensed from a specific distance of upwind fetch as 'seen' at a specific instrument height can be calculated after Gash (1986), Schuepp *et al.* (1990) and Shuttleworth (1992):

$$F = \exp\left[\frac{(z-d)\left(1-\ln\left(\frac{(z-d)}{z_{om}}\right)\right)-z_{om}}{k^2 x_f\left(1-\frac{z_{om}}{(z-d)}\right)}\right] \qquad \text{Equation 8.2}$$

Where:
$F$ is the fraction of vapour and sensible heat flux densities at height z contributed by a fetch of upwind length $x_f$ m
$k$ is von Karman constant (0.41)
Other terms as above

The equation represents F for conditions with neutral stability with a tendency to over-predict F for stable conditions and under-predict for unstable conditions.
It is a useful simple method to generate an estimation of the quality of measurements by the BREB method where F represents the fraction of λE or H generated by the fetch of surface cover over which the sensors were located. F should be close to 1 in order for measurements to be completely representative of the measurement surface.

Equation 8.2 was applied to determine F for the study field using the range of values of $x_f$ generated by the differences in sward height. Results are presented in Table 8.2 and indictae that there is little sensitivity over this narrow range of height with 0.76-0.77 of λE generated from the computed fetch using Equation 8.1. From this result it can be seen that Equation 8.2 is more conservative than Brutsaert's Equation 8.1 i.e. a

longer fetch is required to ensure measurements are representative of the surface. The effect of increasing the fetch upon F was examined by increasing the $x_f$ term in Equation 8.2 and keeping other factors constant as for a sward height of 0.04 m. Figure 8.1 shows that the relationship between $x_f$ and F follows an 'inverse exponential' curve with a fetch far greater than 224 m to attain F=1 ($x_f$ would need to be in excess of 5 km in stable conditions).

Table 8.2. Estimation of the fraction F of λE (Equation 8.2) sensed at certain upwind fetch distances (m). Fetch is expressed over the range of grass sward height (m)(Table 8.1). Results using the average grass height (0.04 m over the period studied) are in bold.

| Canopy height m | $z$ | $x_f$ | $F$ |
|---|---|---|---|
| 0.02 | 2 | 249 | 0.763 |
| 0.03 | 2 | 234 | 0.766 |
| **0.04** | **2** | **224** | **0.769** |
| 0.05 | 2 | 216 | 0.771 |
| 0.06 | 2 | 209 | 0.774 |
| 0.07 | 2 | 204 | 0.776 |
| 0.08 | 2 | 199 | 0.778 |
| 0.09 | 2 | 195 | 0.780 |

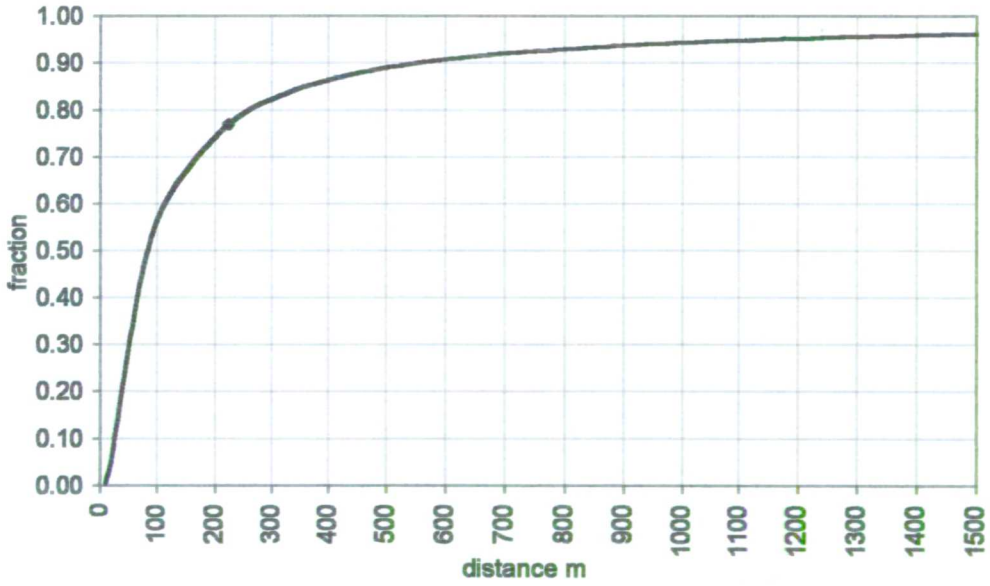


Figure 8.1. The change in the fraction of λE with increasing fetch distance for the conditions at the study site (z=2 m, mean grass height = 0.04 m). The data point represents the fetch distance for the mean grass height = 0.04 m.

### 8.2.2 Wind direction and speed

The daily average wind direction and speed, recorded by the AWS anemometer at 2 m height within the main enclosure, over the same period as field mapping are plotted as wind roses, Figure 8.2. The predominant wind direction is south to south-west-west, with 44% of the total wind direction between 180 to 240°.

Figure 8.3 shows the wind rose diagrams (Figure 8.2a) superimposed upon a map of the study field to illustrate the predominant contributing area upwind of the main enclosure. This area is enclosed between the extended lines on the figure, and the change in extent of the surface types in this zone has been determined, see Figure 8.4. As the predominant wind direction is from the south to south-west-west, the extent of each surface type in the 180 - 240 ° segment stretching over the field from the main enclosure was determined.

Figure 8.2c shows the percentage distribution of wind speeds over the period of field mapping. The range of wind speed experienced over the marsh is in region 0-10.8 $ms^{-1}$. The average wind speed is 3.9 $ms^{-1}$ and it can be seen from Figure 8.2c that there is fairly equal distribution of wind speeds between 2-6 $ms^{-1}$ which accounts for 67% of the time represented. Wind speeds below 3 $ms^{-1}$ are uncommon accounting for only 2%, with the remaining 15% of the period representing winds higher than 6 $ms^{-1}$. Average wind speed is fairly equally distributed (3 to 5 $ms^{-1}$) from all directions, except for lower values from the direction 60-100°.

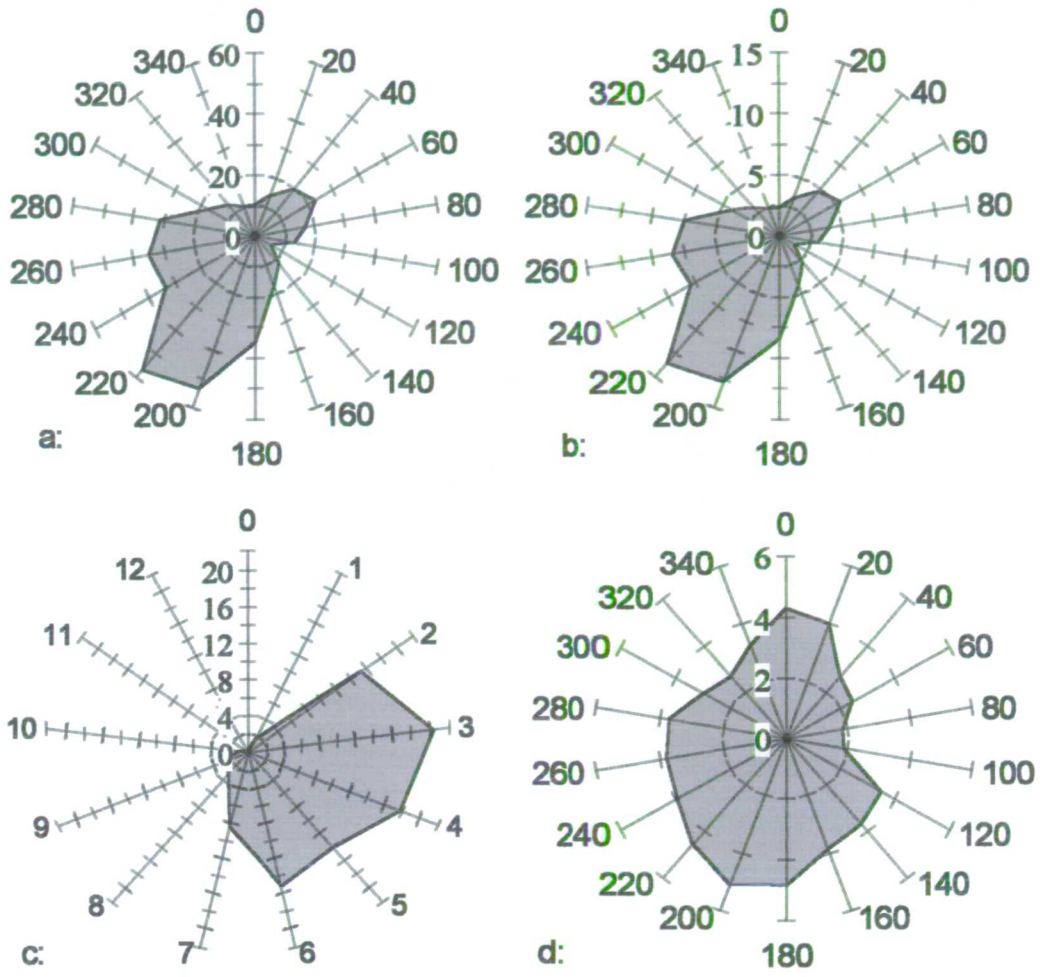


**Figure 8.2. The daily average wind direction and speed recorded by the AWS in the main enclosure of the study field. The figures are constructed using data covering the period November 1998 to October 1999 with a: the frequency (number of days) and b: the percentage (% of total number of days) distribution of wind direction. Figure c: shows the percentage distribution of wind speed ($ms^{-1}$) and d: displays the average wind speed recorded according to wind direction. The frequency and percentage is marked along the vertical scale.**

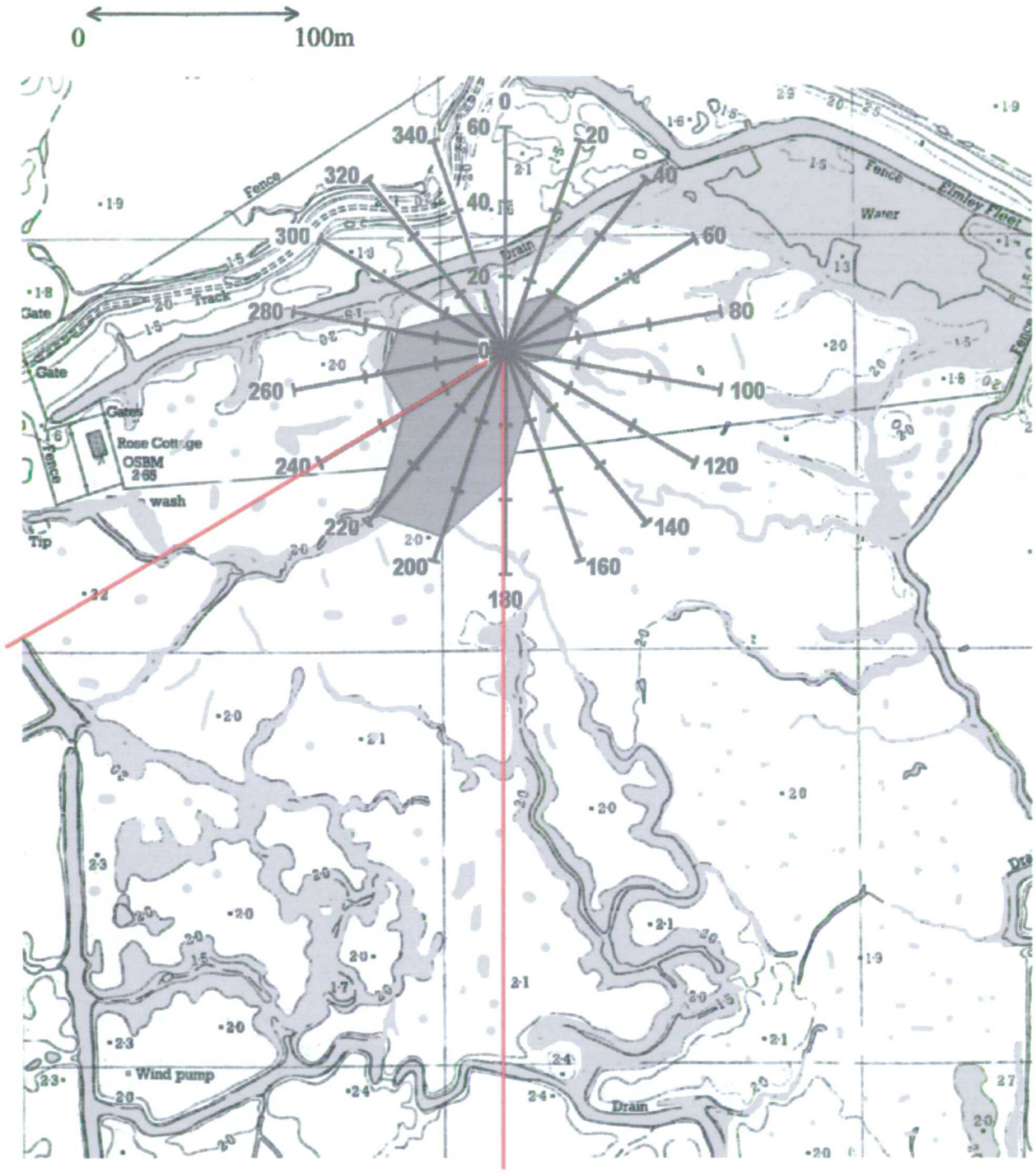


Figure 8.3. The wind rose frequency diagram (Figure 8.2 a) showing the predominant daily average wind direction for the same period as field mapping superimposed on the map of the study field. The extent of the surface types of open water (shaded above), grass (white space above), and bare soil areas (not shown above) between the extended red lines of 180 and 240° within the study field has been computed for the WPM approach. The map shows the scene of 12 January 1999; time of maximum flooding with shaded areas representing open water with the white space as grassed marsh. Numbers on the map refer to elevation (m O.D.).

### 8.2.3 Mapping of inundated areas

Central to the WPM approach is the quantification of the areal extent and change over time of each surface type of the wetland. Figure 8.3 shows the wind rose diagram (Figure 8.2a) superimposed upon a map of the study field to illustrate the predominant contributing area upwind of the main enclosure between 180 and 240°. This area is enclosed between the extended lines on the figure to the ditches bordering the corner of the field, and the change in extent of the surface types in this zone has been determined, see Figure 8.4. The required fetch, calculated from Equation 8.1 under near neutral conditions, of 224 m indicates that it would be sufficient to confine attention to within 224 m from the enclosure. However as Figure 8.1 illustrates that an increased fetch results in a greater proportion of the vapour and sensible fluxes controlled by the measurement surface under inspection, it was decided to extend the zone of monitoring to the opposite banks of the ditches bordering the field. At the maximum distance of 360 m in the direction 210° from the main enclosure to the outer bank of the junction of the south and west ditches, this increases the fraction of fluxes generated by the surface to 0.85 with the average grass sward of 0.04 m. It was not considered practical to extend the zone further due to the lack of surface cover measurements mapped outside the study field, and as Figure 8.1 highlights, increasing fetch beyond this distance result in very little increase in the fraction of $\lambda E$.

To simplify the application of WPM, the area of surface types computed in the zone 180-260° will be employed in the model despite daily variation in the wind direction. Wessel and Rouse (1994) also used this simplification using a representation of the general tundra area from transects undertaken south of the instrument set-up regardless of wind direction. The transects extended along the eight cardinal directions from a central point located 50 m south from the instrument site.

In this investigation a different approach was taken that did not involve the use of transects. On field visits the extent of flooding and bare soil patches on the whole study field was recorded from November 1998 to December 1999 onto detailed maps of the study area (Figure 5.10 illustrates four inundation maps). For logistical reasons only the inundation of the study field was mapped. The study field is taken here to be the parcel of land containing the main enclosure to the far side of the bank of the

ditches that border the edges. The method and results of mapping the extent and change of surface type over the study field has been discussed in section 5.3.1, and the main points are repeated below. The area of each surface type was computed for the entire field (Figure 5.8) and for the 180 - 240° zone (Figure 8.4). This method of mapping is suitable for the small area involved in this investigation however would be not practical for larger areas. For extensive sites, mapping could be undertaken using remotely sensed imagery as discussed by Gilvear and Watson (1995).

The area of inundation and bare soil on the marsh was computed from the maps using the counting square method. The extent of grass covered marsh was determined as a residual of the remaining area of the field. As the floodwaters recede or dry off, patches of bare soil are exposed as the vegetation has withered and decomposed from being inundated. As open water areas dry off so the proportion of bare soil increases in tandem until a point is reached in late April when the area of bare soil decreases in extent as it is starts to be re-colonised by vegetation. The areal extent of open water in the ditch channels bordering the study field was determined using wet width stage relationships formulated for each of the four ditches that border the study field. The cross section of each ditch was measured at bankfull capacity, allowing the derivation of a polynomial relationship relating the wet width of the water surface to water level (Figure 5.9). Thus the area of the ditch water surfaces could be computed from consideration of the water level and ditch length. The area of ditch open water is then added to the area of inundation of the field. A fall in ditch water level causes a reduction in the area of open water, due to the sloping sides of the ditch banks, exposing bare soil. The area of bare soil, determined as the difference between the maximum ditch water area and its current area, is added to the area of bare soil on the marsh surface.

### 8.2.4 Surface resistance measurements

The WPM method depends upon the use of accurate surface resistance value for each surface type in Penmen Monteith so that the actual evaporative loss can be determined for the entire surface. The resistance values given to each surface type are outlined below.

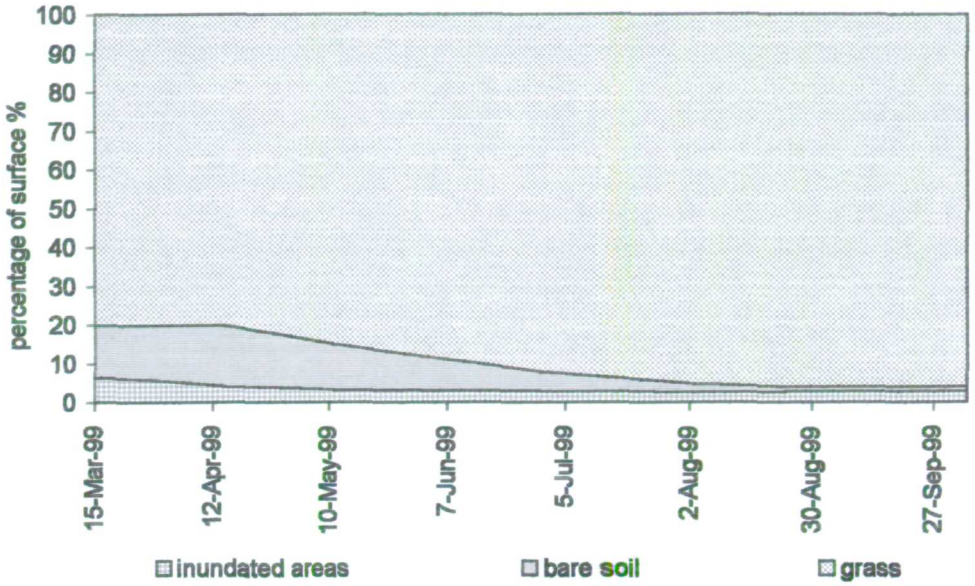


**Figure 8.4. The change in percentage extent of surface types over March to September 1999 in the 180-260° zone of the study field identified on Figure 8.3.**

### 8.2.4.1 Open water

A surface resistance of zero is given to the open water surface type according to common practice.

### 8.2.4.2 Grass surface

Surface resistance values for the grass surface will be generated from the soil moisture of the marsh by the 'updated universal relationship' formulated in section 7.5.

Over 1999 the soil moisture of the marsh was measured by soil sampling to 0.8 m depth on field visits over March to September. The soil moisture and computed surface resistance values are presented in Table 8.3. The change in allocated surface resistance for the grass surface can be seen in Figure 8.5. The poor results of the BUDGET model to simulate daily soil moistures over 1999 (section 5.2.2.3) has meant that only soil moisture data recorded on field visits has been used, so that resistances can be seen to change in a stepped manner over time. While the designation of resistance values could have been applied in a more smooth way, the 'step' approach was used as it is operationally simpler.

Table 8.3. The soil moisture of the marsh over the 1999 study period. Moisture was determined from soil sampling adjacent to the main enclosure. The value of surface resistance is computed from the 'updated universal relationship' (Equation 7.5, section 7.5).

| Date of measurement 1999 | Soil moisture of profile 0 – 0.8 m depth % | Surface resistance $sm^{-1}$ |
|---|---|---|
| 15 March | 40.0 | 21.3 |
| 15 April | 37.8 | 21.3 |
| 1 June | 29.1 | 34.1 |
| 7 July | 26.5 | 65.1 |
| 3 August | 23.0 | 155.0 |
| 24 August | 24.8 | 98.8 |
| 5 October | 30.0 | 27.3 |

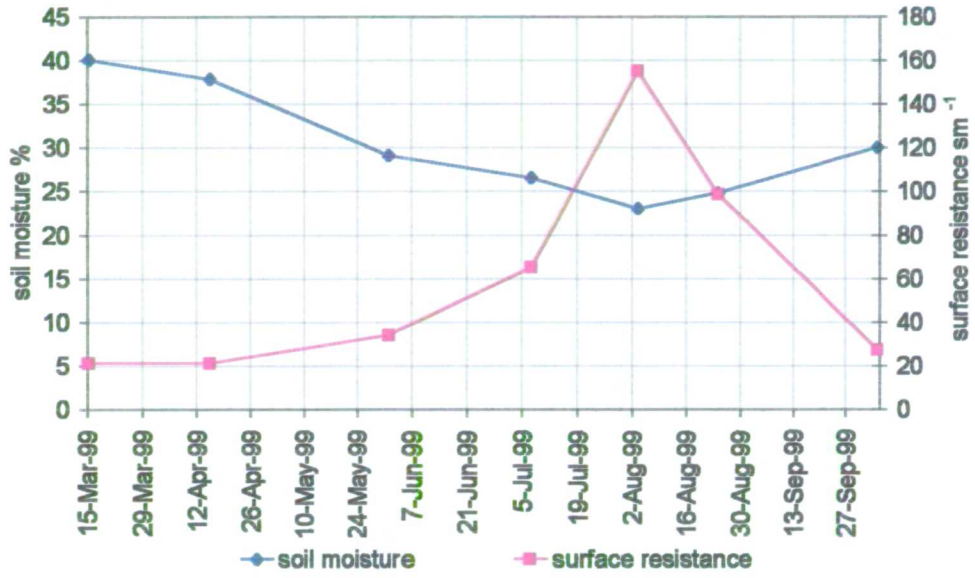


Figure 8.5. Change in soil moisture and corresponding value of surface resistance for the grass surface type of the marsh (see Table 8.3).

### 8.2.4.3 Bare soil

The resistance to evaporation of bare soil varies significantly with its moisture content. When the soil surface is moist, water is transported to the surface by capillary action in response to the atmospheric demand and resistances are minimal. Once the surface starts to dry as hydraulic transport to the surface lags the evaporative demand and becomes constricted due to the decreasing moisture content, so evaporation becomes constricted and the resistance of the soil increases. The soil moisture, if not replenished by precipitation, will eventually desiccate to below the wilting point and the resistance will be such that evaporation effectively ceases.

The approach of MORECS (Hough *et al.* 1997) to generate a surface resistance for bare soil conditions of limiting soil moisture is to apply the same method as

vegetation as detailed in section 7.4.2.5 (Chapter 7). This method applies minimum resistance values (in this case 100 $sm^{-1}$) until the easily available soil moisture fraction of the profile is depleted after which resistance increase following Equation 7.8.

This approach depends upon effective moisture redistribution of the profile in response to the evaporative drying at the surface so that consideration can be given to the moisture status of the entire profile. However it is the moisture content of the surface soil layer that is deemed to have the greatest influence upon resistance. Camillo and Gurney (1986) have noted the importance of the soil moisture content of the uppermost layer, with values of resistance ranging from zero and 600 $sm^{-1}$ for a wet and dry top layer respectively. Mahfouf and Noihan (1991) report that surface resistance could range between zero and several thousands per $sm^{-1}$ depending upon soil texture and moisture content. Van de Griend and Owe (1994) present an exponential relationship between resistance and soil moisture of the upper 1 cm of fine sandy loam. Minimum resistances are maintained at approximately 10 $sm^{-1}$, until the soil moisture of the 1 cm top layer falls below half the value at field capacity (15%). Thereafter resistance increases to 1500 $sm^{-1}$ at 1% moisture content up to 4000 $sm^{-1}$ when dry.

The thickness of the desiccated top layer is a function of soil hydraulic and thermal properties; the propensity of the Wallasea soil series of Elmley Marshes is to produce soil polygons through horizontal cracking, which, with continued water loss cracks in the vertical direction, form discrete dry soil discs of approximately 20 mm depth (Figure 3.5). After the discs have formed some further drying is observed beneath the discs of centimetre depth, but generally the dry upper layer prevents moisture loss from beneath. Regular moisture measurements of a permanent bare soil patch near the main enclosure (Figure 5.11d) have been taken with the SCIP. The pins of the SCIP incorporate the moisture of the upper dry skin and the moist soil below within the upper 10 cm soil layer. The results of monitoring are presented in Figure 8.7 and show the maintenance of high soil moisture contents over September 1998 to December 1999. Over this time period the upper 2 cm of soil had experienced desiccation and cracking of the upper 2 cm in September 1998, saturation and swelling over winter 1998/1999, beginning to dry out in March 1999 and crack widely by April 1999 and thereafter. The data clearly show that the desiccation of the bare soil surface acts as a preventative barrier to the loss of moisture from deeper in the

profile. The higher moisture content beneath the bare soil patch can also be seen in the SCIP monitoring grids presented in Figure 5.15. The bare soil patch is at grid node 90,90 and the elevated moisture content relative to the remainder of the grid covered by grass is clearly seen.

As such the application of the MORECS approach to derive soil moisture resistance values would not be representative, as it is the moisture content of the uppermost 2 cm soil layer which controls evaporative loss rather than the moisture content of the profile as a whole.

In order to include the bare soil patches into the WPM approach a method is required to designate surface resistance values for this surface type in the Penman Monteith model. The relationship of Van de Griend and Owe (1994) cannot be used, as moisture measurements were not made in the top 1 cm of bare soil patches. A simplified approach is used by Raes (1996) in the BUDGET model in which actual evaporation from top layer of bare soil proceeds at potential rates provided the soil moisture is equal to or above the threshold value of half the value of the wilting point. Below this threshold water can no longer be extracted by evaporation. This seems to tally with Figure 8.7 in that moisture in the uppermost layer remain high beneath the dry surface crust.

In terms of resistance, this means that minimal resistances are applied to bare soil surfaces until the threshold is surpassed after which resistances are infinite.

It was decided to take this approach, with a modification for precipitation to designate daily values of surface resistance for the bare soil surface type. As soil moisture information of the top layer was not available an assessment of the moisture content was taken from the degree of desiccation and cracking observed on field visits. As mentioned above the patches of bare soil started to desiccate in March and were fully cracked and dry by April and this governed the magnitude of the surface resistance. It was decided, after the results of van de Griend and Owe (1994), to give a minimal value of 10 $sm^{-1}$ when the soil was observed to be wet over the period January to April 1999; a value of 500 $sm^{-1}$ from April thereafter. Referring to Figure 7.1, which illustrates the sensitivity of the Penman Monteith algorithm to changes in surface resistance, it can be seen that the fractional reduction in evaporation from change in surface resistance from 10 to 500 $sm^{-1}$ is considerable at 0.73.

It was observed that after precipitation events, the surface soil wets up due to the absorption of water and dries off quickly. To account for this evaporation of absorbed water a minimal resistance of 10 $sm^{-1}$ was allocated for two days after a precipitation event regardless of the precipitation total. The allocation of surface resistance to the soil surface can be seen in Figure 8.6.

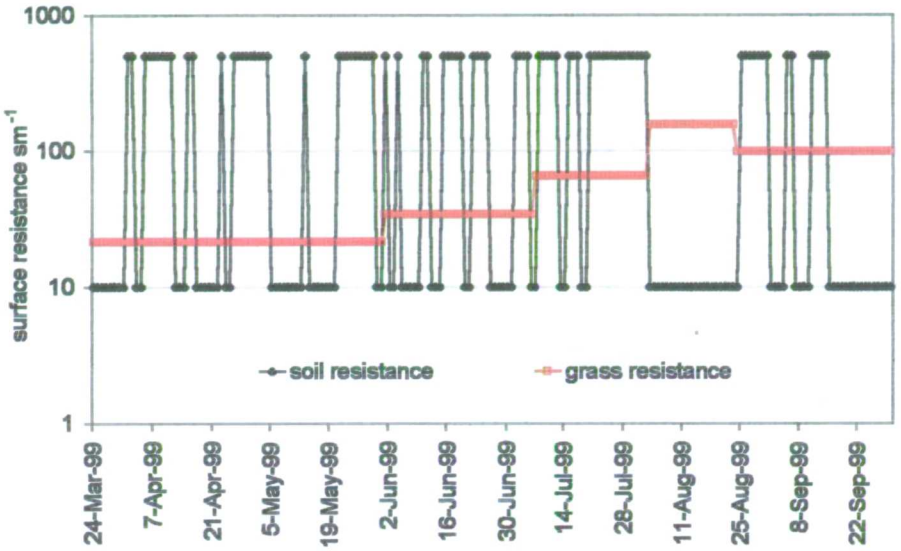


Figure 8.6. The designation of surface resistance value for the soil and grass surface types of the study field. The water surface has an allocation of 0 $sm^{-1}$ at all times. The soil resistance fluctuates between 10 and 500 $sm^{-1}$ based on precipitation input. The grass resistance follows a more step change based on the measurement of soil moisture on field visits.

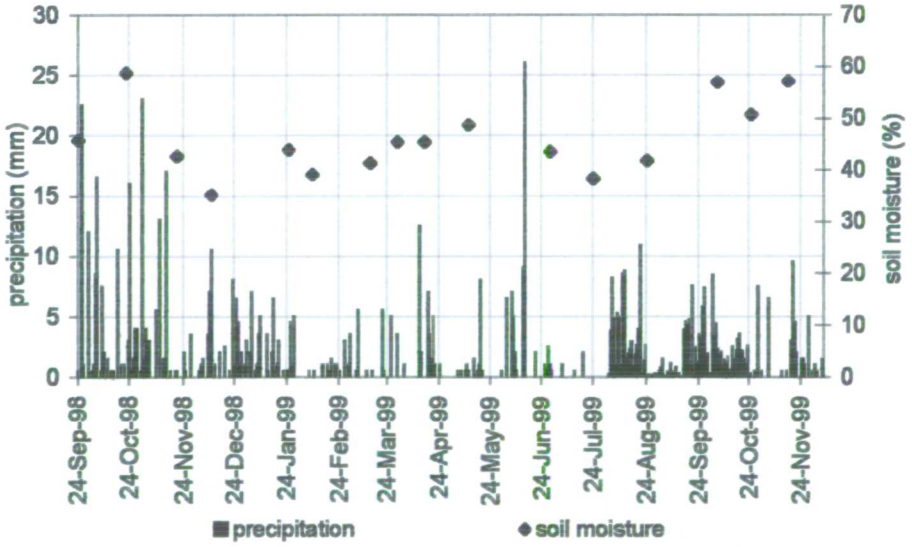


Figure 8.7. Average moisture content of the upper 10 cm of a permanent patch of bare soil on the study field. Daily precipitation totals are also illustrated. Soil moisture data were obtained with the SCIP on each field visit. The soil was observed to become desiccated and crack from mid March 1999 onwards.

## 8.3 Principles of the Bowen Ratio Energy Balance approach

The results of modelling the evaporation over the marsh will be compared to actual evaporation from the Bowen Ratio Energy Balance method, BREB (Campbell Scientific 1995). A station was located within the main enclosure alongside the AWS during 1999. The data available allows an assessment of the accuracy of the WPM approach over the period 24 March to 30 September.

ASCE (1996) state that the BREB method is a combination of transport and energy balance equations and is considered to be superior to the direct use of turbulent transfer equations for estimating transfers of water vapour above a surface. Its superiority is due to constraints provided in the BREB approach by inclusion of the net radiation balance in the method. Errors in estimating gradients of temperature and humidity are not directly related to the estimates of λE or H, as is the case in strictly aerodynamic models.

The assumptions of the BREB are that transport of λE or H is one dimensional (vertical), the surface is homogenous dense and shallow (i.e. heat and water momentum sources and sinks are indistinguishable and steady state conditions exist. The disadvantages of the method are the fragility of sensors, particularly fine wire thermocouples, requirement of necessary upwind fetch, and the numerical instability of Equations 8.6 and 8.7 during periods of $\beta$ near –1. The latter point is discussed in section 8.3.2.

Advantages of the BREB method are the ability to measure λE from non reference surfaces and the elimination of wind and turbulent transfer coefficients. The BREB is therefore considered as one of the most accurate ET equations if $R_n$, G, and the temperature and humidity profiles can be accurately measured with accuracies for well operated BREB systems estimated to be approximately 10% (Sinclair *et al.* 1975).

The theoretical considerations of the BREB approach is covered by many authors including Gay and Stewart 1974, Brutsaert 1982, Den Hartog *et al.* 1994, ASCE 1996, Thompson *et al.* 1999. The BREB method for flux determination is derived from the energy balance of the underlying surface:

$$R_n - G = H + \lambda E \qquad \text{Equation 8.4}$$

Where
$R_n$ is the net radiation W $m^{-2}$
$G$ is the ground heat flux W $m^{-2}$
$H$ is the sensible heat flux W $m^{-2}$
$\lambda E$ is the latent heat flux W $m^{-2}$

The Bowen ratio $\beta$ (Bowen 1926) (dimensionless) is the ratio of sensible to latent heat flux. If $\beta < 1$ latent energy exceeds sensible heat while $\beta > 1$ indicates that sensible heat dominates the energy balance. The former case is characteristic of sites where water is not limiting, the latter when moisture supply is restricted.

$$\beta = \frac{H}{\lambda E} \qquad \text{Equation 8.5}$$

By combining Equations 8.4 and 8.5 the latent and sensible heat fluxes are calculated:

$$\lambda E = \frac{(R_n - G)}{1 + \beta} \qquad \text{Equation 8.6}$$

$$H = \beta \lambda E \qquad \text{Equation 8.7}$$

The sensible and latent heat fluxes can also be expressed as:

$$H = -pC_p K_h \left(\frac{\Delta T}{\Delta z}\right) \qquad \text{Equation 8.8}$$

$$\lambda E = -\left(\frac{p\lambda\varepsilon}{P}\right) K_v \left(\frac{\Delta e}{\Delta z}\right) \qquad \text{Equation 8.9}$$

Where:
$p$ is air density kg $m^{-3}$
$C_p$ the specific heat capacity of the air 1.013 kJ $kg^{-1}$ °$C^{-1}$
$K_h$ and $K_v$ eddy diffusivity for heat and water vapour respectively $m^2$ $s^{-1}$
$\frac{\Delta T}{\Delta z}$ and $\frac{\Delta e}{\Delta z}$ is the temperature, °C, and vapour pressure gradient, kPa, respectively
$P$ is air pressure kPa
$\varepsilon$ is the ratio of the molecular weight of water to that of air (0.622).

Substituting 8.6 and 8.7 into 8.5, with the assumptions that the eddy diffusivities of heat and vapour are equal, the similarity principle, (Ibanez *et al.* 1999) $\beta$ becomes:

$$\beta = \gamma \frac{\Delta T}{\Delta e} = \gamma \frac{T_2 - T_1}{e_2 - e_1} \qquad \text{Equation 8.10}$$

Where:

$T_1$ and $e_1$ are air temperature and vapour pressure at height $z_1$ (°C and kPa respectively)
$T_2$ and $e_2$ are air temperature and vapour pressures at height $z_2$
$\gamma$ is the psychrometric constant (Equation 7.2b) kPa °C$^{-1}$

The energy budget measurements of the latent and sensible heat fluxes can therefore be computed from the measurement of net radiation, ground heat flux, and the air temperature and moisture at a minimum of two heights.

So that measurements are taken within the equilibrium layer the $z_1$ height should be at least 0.3m above a canopy for a smooth dense canopy and raised higher for tall spare crops; the $z_2$ height is 1 to 2 m above (ASCE 1996). Gay (1974) uses the rule of thumb of Lettau (1959) that for low smooth crops the lower sensor level should not be lower than five times the average momentum roughness height $z_{om}$ above the surface (estimated as $z_{om} = 0.123h$). Practical concerns relating to sensor damage may mean that it is not possible to place the sensor at low heights however.

### 8.3.1 BREB station

The BREB station (Campbell Scientific) used at the study site to compute evaporation every 20 minutes, monitors vapour pressure at each height by routing air samples drawn through filters of 1 μm pore size to a chilled mirror hygrometer. Air drawn through the mirror is switched between heights every two minutes and after an allowance of 40 seconds for stabilisation, the dew point temperature is measured every second. Air temperature $T_2 - T_1$ is measured using naturally aspirated differentially wired fine wire thermocouples at heights of 0.4 m and 1.6 m above the ground for the lower and upper height respectively. These heights fulfil the requirements described above to ensure measurements are taken in the equilibrium layer.
Net radiation is monitored with a NR-Lite Teflon covered sensor, however data has been taken from the AWS bubble domed sensor, see Appendix A.2.1. Ground heat flux is monitored with heat flux plates buried at 8 cm depth and thermocouples in the soil layer above. The ground heat flux G (W m$^{-2}$) is computed as:

$$G = G_p + \Delta S \qquad \text{Equation 8.11}$$

$$\Delta S = d\frac{\Delta T_s}{t}\rho_b(c_s + wc_w) \qquad \text{Equation 8.12}$$

Where:

$G_p$ is the average measurement from the ground heat plates (W $m^{-2}$)

$\Delta S$ is the rate of heat storage in the soil layer between the heat plates and the surface (W $m^{-2}$)

$d$ is the thickness of the soil layer (m)

$\Delta T_s$ temperature change in the soil layer (°C)

$t$ is the time between consecutive measurement of the soil temperature (seconds)

$\rho_b$ is bulk density (kg $m^{-3}$)

$c_s$ and $c_w$ is dry soil specific heat and specific heat of water respectively (J $kg^{-1}$ $°C^{-1}$)

$w$ is gravimetric soil moisture content (fraction)

### 8.3.2 Data Inspection

The numerical instability as $\beta$ approaches –1 (indicating sensible heat transport toward the surface is in near equilibrium with latent transport away from the surface) when calculation of λE and H becomes impossible, is a major limitation of the technique. Such situations arise when H is small for example at night and when there is little energy available i.e. $R_n - G$ is small. If data is not rejected over these periods errors can result; when $\beta$ approaches zero the computed $\lambda E$ approaches infinity unless $R_n - G$ is zero. In a comprehensive error analysis Angus and Watts (1984) showed the potential for error in calculation of $\lambda E$ increases rapidly as $\beta$ drops below –0.2. In this study it was found that $\beta$ approaches –1 during the conditions mentioned above and also during periods of rainfall and mists.

In addition to $\beta$ approaches –1, data screening is required to detect periods of very slight, zero and negative vapour gradients. Overall data were excluded (also performed by Campbell and Williamson 1997, Burba *et al.* 1999. and Dugas and Hicks 1998) according to the following criteria:

- When $-0.7 < \beta > 10$, $\beta$ was set to zero
- When the vapour pressure gradient was zero, evaporation was set to zero
- When evaporation was negative, evaporation was set to zero

- When the vapour pressure gradient were negative values were set to zero

Normally these criteria exclude short periods (timesteps of 20 minutes) but a certain number of daily values were rejected. These days are given in Table 8.4 together with those days rejected due to limited fetch. The days listed in Table 8.4 have been completely excluded from the database and further analyses, and are the reason for gaps in the Figures.

Table 8.4. The total number of days rejected from the database due to periods of limited fetch and 4 step data correction criteria of the BREB approach.

| Rejected days (1999) | |
|---|---|
| 25 March | BREB criteria |
| 26 March | Limited fetch |
| 29 March | BREB criteria |
| 2 April | BREB criteria |
| 19 April | BREB criteria |
| 17 May | BREB criteria |
| 29 May | BREB criteria |
| 9 June | Limited fetch |
| 13 July | Limited fetch |
| 9 August | BREB criteria |
| 19 August | Limited fetch |
| 31 August | Limited fetch |

## 8.4 Results and Discussion

The results of modelling the evaporative water loss from the wetland study site over the time period 24 March 30 September 1999 are displayed in the following figures. To give a consideration of the range of evaporation, Figure 8.8 shows the values of actual evaporation computed for each surface type applying relevant surface resistance values as discussed in section 8.2.4. Initially all surface types exhibit the same evaporative rate, i.e. close to the open water rate. The actual evaporative loss of the bare soil area becomes restricted early on from April, with the evaporative trend fluctuating according to the designated surface resistance (Figure 8.6). Evaporation from the grass area becomes restricted after June 1999 when soil moisture falls below the threshold level of 31% (168 mm SMD).

A value for the actual evaporative loss from the wetland was then taken by weighting these values according to surface extent (Figure 8.4). The wetland actual evaporative loss computed from the WPM method is displayed in Figure 8.9 with actual

evaporation computed from the BREB method for reference. The difference between the rates is displayed in Figure 8.10. The value of actual evaporation by BREB is considered to be the reference value against which the success of the WPM approach can be based.

Table 8.5 details the actual evaporation computed for each surface type and for the WPM and BREB methods (the computation of equilibrium evaporation is discussed below in section 8.4.2.2). It can be seen that the dominant contributor to the WPM method of the grass surface due to its extensive spatial extent, and that the soil and water surface areas have fairly equal contributions.

Table 8.5. Evaporation computations over the period 24 March to 30 September 1999 for each method and surface type. Derivation of equilibrium evaporation is discussed in section 8.4.2.2.

| Total actual evaporation per surface type mm | | Contribution to WPM mm | WPM mm | BREB mm | Equilibrium evaporation mm $\alpha = 1$ | Equilibrium evaporation mm $\alpha = 1.25, 0.8$ |
|---|---|---|---|---|---|---|
| Soil | 278.1 | 11.2 | 326.9 | 387.1 | 404.0 | 391.2 |
| Water | 404.8 | 13.5 | | | | |
| Grass | 332.8 | 302.2 | | | | |

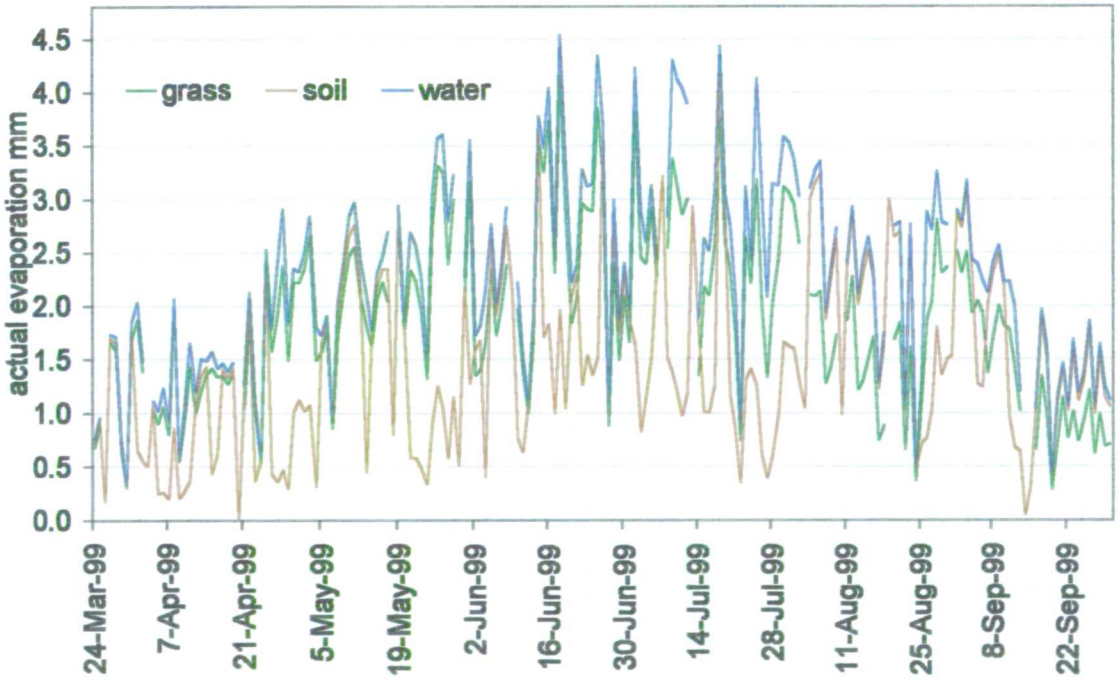


Figure 8.8. Daily actual evaporation (mm) computed for each surface type of the study area using the appropriate resistance values.

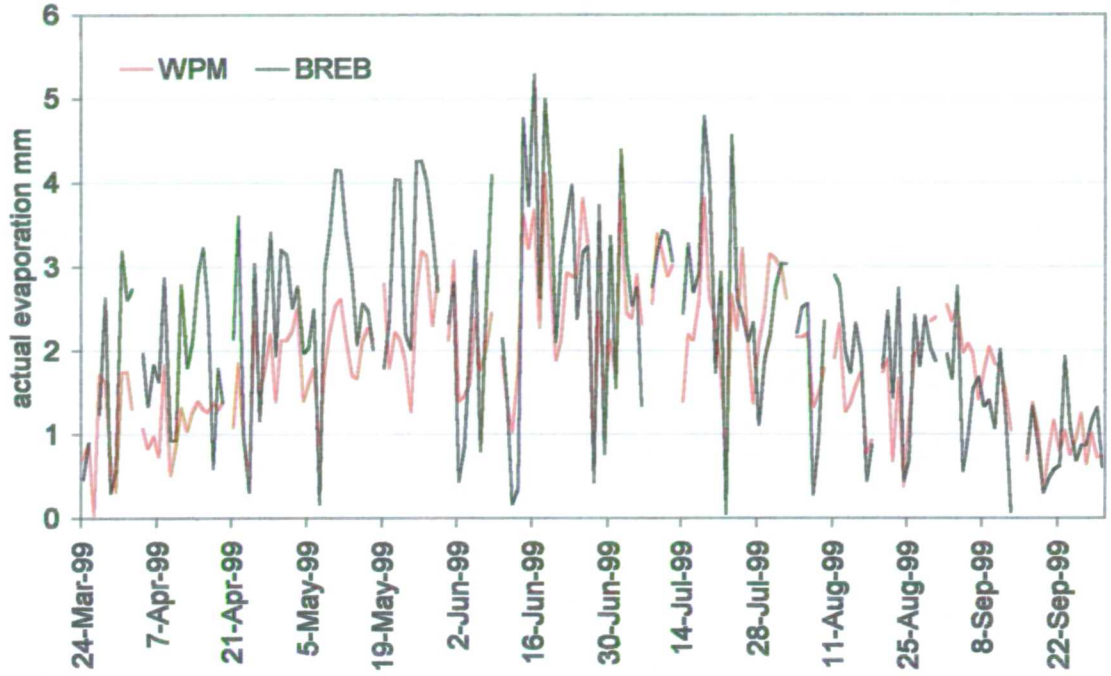


Figure 8.9. The actual evaporative loss for the study area computed by the Weighted Penman Monteith approach (WPM) and the Bowen Ratio Energy Balance method (BREB).

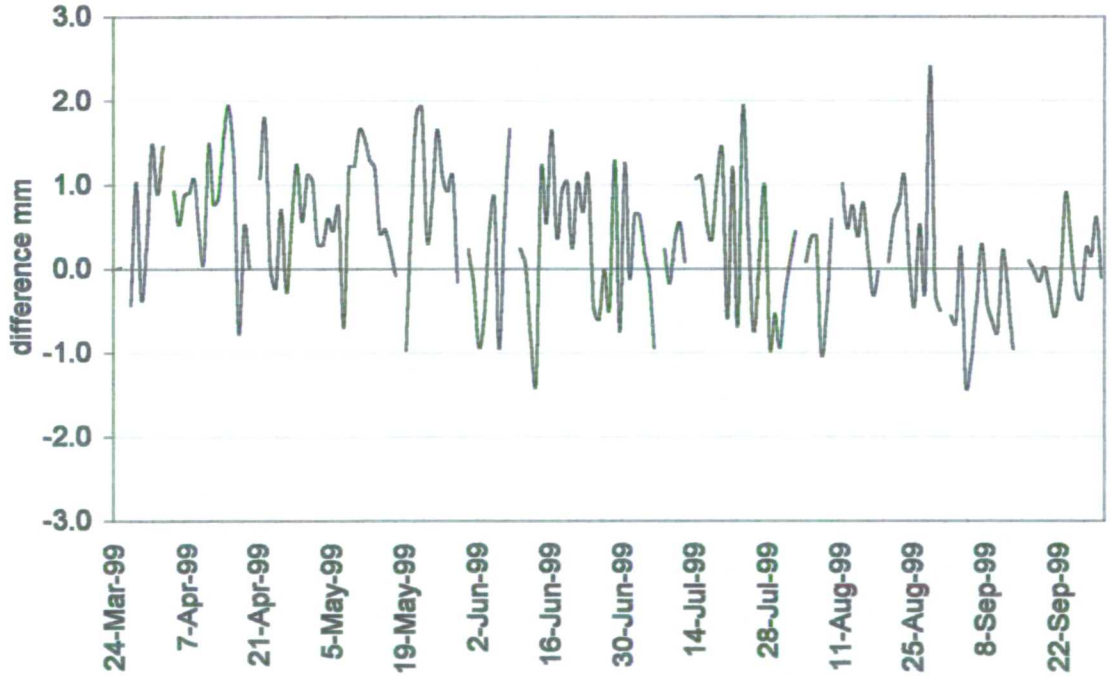


Figure 8.10. The difference (mm) in actual evaporation computed by the WPM and BREB method. Positive values indicate higher values of evaporation from the BREB and negative values the reverse situation.

Figures 8.9 and 8.10 show that there is a discrepancy between the WPM and BREB methods for the first half of the study period (March to June) with the BREB recording higher values of evaporation than the WPM. From June onwards however

the trend of AE by the WPM and BREB methods are very similar. The discussion of the results below firstly focuses on the overall results and the good fit between WPM and BREB after June, and then the discrepancy prior to this date is examined. June is the time by which all patches of open water and inundation had disappeared from the marsh surface.

### 8.4.1. Overall similarity of WPM and BREB

There is great similarity between the BREB and WPM post June, which validates the use of the WPM to compute actual evaporative flux over a wetland surface. The closeness of fit is evidence of the accuracy of the surface resistance values particularly for the grass surface, which is the dominant type after June. The relationship between soil moisture and surface resistance developed using the water balance method in this investigation is corroborated by its goodness of fit against AE by the BREB.

While a five step method of evaluation (Zepp and Belz 1992) has been used to assess the DITCH and BUDGET models (sections 4.3 and 5.2 respectively), it is appropriate to use only two indicators to asses the performance of the evaporation models over the time period studied due to the difference in nature of the data. The performance of the evaporation models was evaluated against the BREB by the Root Mean Square Error, RMSE, and 'index of agreement' $d_i$, (Willmott and Wicks 1980) (as used by Wessel and Rouse (1994):

$$RMSE = \sqrt{\frac{1}{n}\sum_{i=1}^{n}(P_i - O_i)^2} \qquad \text{Equation 8.13}$$

$$d_i = 1 - \left[\frac{\sum_{i=1}^{n}(P_i - O_i)^2}{\sum_{i=1}^{n}\left(|P_i'| + |O_i'|\right)^2}\right] \qquad \text{Equation 8.14}$$

Where:
$n$ is the number of time steps (days)
$P_i$ is the predicted evaporation (mm)
$O_i$ is the observed evaporation by the BREB (mm)
$P_i' = P_i - O_m$ and $O_i' = O_i - O_m$ where $O_m$ is the mean of the observed evaporation
$d_i$ varies between 0 and 1 such that the model with the highest value of $d_i$ is considered to have the best simulation.

The results of the evaluation are presented in Table 8.6. It can be seen that the WPM provided the best overall simulation of actual evaporation relative to BREB with the highest $d_i$=0.88. Using Penman Monteith for the grass and open water surfaces separately have equal values of $d_i$=0.82. Values of RMSE are fairly equal for these three methods. Using Penman Monteith for the soil surface alone results in poor fit to the BREB.

These results indicate that WPM is marginally the best method to determine the actual evaporation from an area with a heterogeneous surface rather than compute Penman Monteith, if the areas of surface types are known. Given the underestimation of evaporation at times of inundation of the marsh (discussed below) the optimal performance of the WPM model highlights the very good fit to the BREB data once water is no longer on the surface.

At the study site over the period March to September, the grass surface type dominates the WPM with only between 16% to 3% of the area occupied by soil and open water. Table 8.6 indicates that the higher overall total produced by the WPM through inclusion of freely evaporating water surfaces renders the final evaporation total closer to that of the BREB. This result show that the WPM approach does produce a slightly closer fit to the BREB but that the actual evaporation loss from the grass surface alone also produces similar results due to its dominance of spatial extent.

Figure 6.12 shows that the rate of AE from the grass surface closely matches the BREB data, Figure 8.12, show that the surface resistance values applied according to the soil moisture status are accurate. The relationship between soil moisture and surface resistance was determined using the water balance approach (section 7.4.3.1), and the good daily comparison against the BREB displayed in Figure 8.9 after June show the validity of the 'updated universal relationship'. June marks the point at which the soil moisture of the marsh falls below the threshold level and consequently resistances for the grass surface start to increase (Figure 8.6).

Table 8.6 shows similar index of agreement and RMSE for the open water surface relative to grass, and the predicted total is the closest to the BREB total. These results would suggest that the open water rate could also be used to predict the actual

evaporative loss from the marsh. However inspection of Figure 8.11, which illustrates the trend of BREB and open water evaporation, reveals considerable over- and under- estimation with the conclusion that proximity to the BREB total evaporation is, in effect, a product of cancellation of these extremes, and that as a method to predict the actual evaporative loss it is only suitable for long time steps.

Table 8.6. Evaluation of the WPM model performance for the study period (excluding rejected days (Table 8.4). $n$ is the number of timesteps (days) and RMSE is the root mean square error. PRED is the predicted actual evaporation (mm) and $d_i$ is the index of agreement to actual evaporation (BREB) (mm).

| Parameter | Soil | Open Water | Grass | WPM |
|---|---|---|---|---|
| $n$ | 179 | 179 | 179 | 179 |
| PRED | 278.1 | 404.8 | 332.8 | 326.9 |
| BREB | 387.1 | 387.1 | 387.1 | 387.1 |
| RMSE | 1.40 | 0.80 | 0.80 | 0.82 |
| $d_i$ | 0.36 | 0.82 | 0.82 | 0.81 |

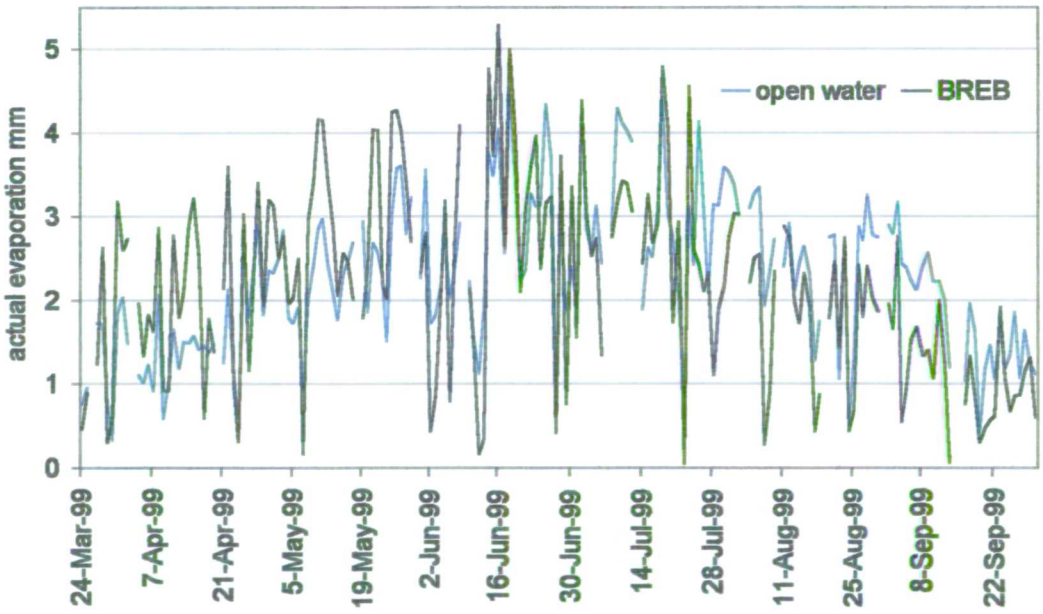


Figure 8.11. Actual evaporative loss computed from the BREB approach and Penman Monteith for open water using 'correct' surface resistances.

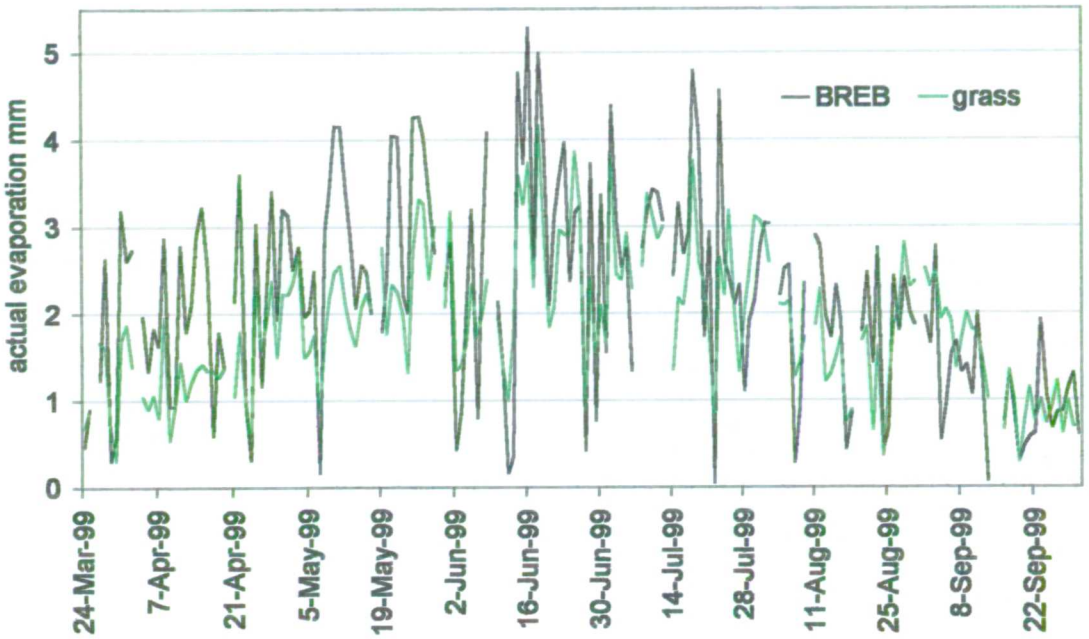


**Figure 8.12. Actual evaporative loss computed from the BREB approach and Penman Monteith for grass using 'correct' surface resistances**

### 8.4.2 Dissimilarity of BREB and WPM prior to June

The observation of higher BREB values over March until June are interesting as June marks the time at which there is no longer any surface inundation of the marsh with water confined to ditch channels.

Possible reasons for WPM<BREB could include inaccurate surface mapping and unrepresentative surface resistances, and the effects of heat advection. These are discussed below.

#### 8.4.2.1 Inaccurate surface mapping and incorrect resistances

From the period March to June 1999 the BREB records higher evaporative loss than the WPM. If the mapping of surface areas were adjusted so that there was a greater proportion of open water, this would increase the evaporative loss due to the lower resistances of this surface type.

However comparison of AE from BREB and evaporation from open water computed using Penman Monteith (with rs = zero), Figure 8.11, show that the latter still exhibits higher evaporation values prior to June. This means that even if the percentage of

open water was increased to 100%, the value of evaporation computed from the WPM approach would still be lower than the BREB values. After June the open water evaporation becomes higher than the BREB indicating that restriction of the evaporation rate is required through increased surface resistance in the WPM approach.

8.4.2.2 Equilibrium evaporation

Considering the AE from the BREB exceeds the potential evaporation rate of open water prior to June (Figure 8.11), it is useful to examine the relationship to the equilibrium evaporation rate. The Penman Monteith model (Equation 7.2) can be simplified for cases where air in the lower meter or so is saturated or nearly saturated (Slatyer and McIlroy 1961) i.e. under conditions of zero vapour pressure deficit and surface resistance as the aerodynamic term drops out to (Price 1991):

$$\lambda E_{eq} = \left(\frac{\Delta}{\Delta+\gamma}\right)(R_n - G) \qquad \text{Equation 8.15}$$

This is termed the equilibrium evaporation, and $\lambda E_{eq}$ approximates $\lambda E$ when 'conditions are not too dry or too wet' (Wilson and Rouse 1972). The equilibrium evaporation is advantageous over the use of Penman or Penman Monteith to derive potential evaporation as it is less dependant on local energy partitioning and has been used in a number of studies to demonstrate the level of dependence of evaporation on the net radiation (Thompson *et al.* 1999).

Actual evaporation is related to equilibrium evaporation by a coefficient of evaporability $\alpha$ (Priestly and Taylor 1972):

$$\lambda E = \alpha\left(\frac{\Delta}{\Delta+\gamma}\right)(R_n - G) \qquad \text{Equation 8.16}$$

By the inclusion of $\alpha$ the Priestly-Taylor (1972) model provides a compromise between the equilibrium evaporation and the requirement of including an aerodynamic term typical of combination aerodynamic – energy balance equation. The parameter $\alpha$ can be determined:

$$\alpha = \frac{\lambda E_{eq}}{\lambda E} \qquad \text{Equation 8.17}$$

When $\alpha \approx 1$ Equation 8.16 represents the equilibrium evaporation (Equation 8.15) i.e. conditions where the surface which is neither excessively wet nor dry, under conditions of zero advection; the equilibrium evaporation is equivalent to the open water rate computed with Penman or Penman Monteith with rs = zero (Crago and Brutsaert 1992).

Saturated surfaces, not necessarily just open water areas (Monteith and Unsworth 1990) that evaporate at the potential rate under conditions of minimal advection have been found to have $\alpha = 1.26$ (Priestly-Taylor 1972, Brutsaert 1982). Researchers in wetland systems have found a variety of values for $\alpha$; Stewart and Rouse (1976) found a value of 1.26 for wet sedge, Price *et al.* (1991) discovered $\alpha = 1.1$ characterised peat ridges in a Labrador bog. A Florida cattail marsh had a value of 1.18 (Abtew and Obeysekera 1995), a Kansas prairie expressed $\alpha = 1.16$ (Crago and Brutsaert 1992). Other researchers found lower values of $\alpha$; Souch *et al.* 1996) computed a value of 1.03 for the Lake Michigan lacustrine environment, $\alpha = 0.63$ represented lakeside peatlands adjacent at the Hudson Bay lowlands (den Hartog *et al.* 1994) and values ranging from 0.34 to 0.58 were calculated from two peat bogs in New Zealand (Thompson *et al.* 1999).

To display the results from this study, actual evaporation computed by WPM and BREB is plotted against the equilibrium evaporation as a time series and also as a scatter graph to determine the value of $\alpha$. The change in value of $\alpha$ and soil moisture over the study period is also presented.

Figures 8.13 and 8.14 show that the actual evaporation computed by the WPM method is a very close fit to the equilibrium evaporation if slightly lower until June; after this point the WPM falls below the equilibrium evaporation as moisture availability becomes restricted. The relationship between the two is very strong with $r^2$=0.91 yielding $\alpha = 0.81$. The increasing restriction of moisture is reflected in a decline in $\alpha$ over the study period from 0.93 to 0.7 (Figure 8.15).

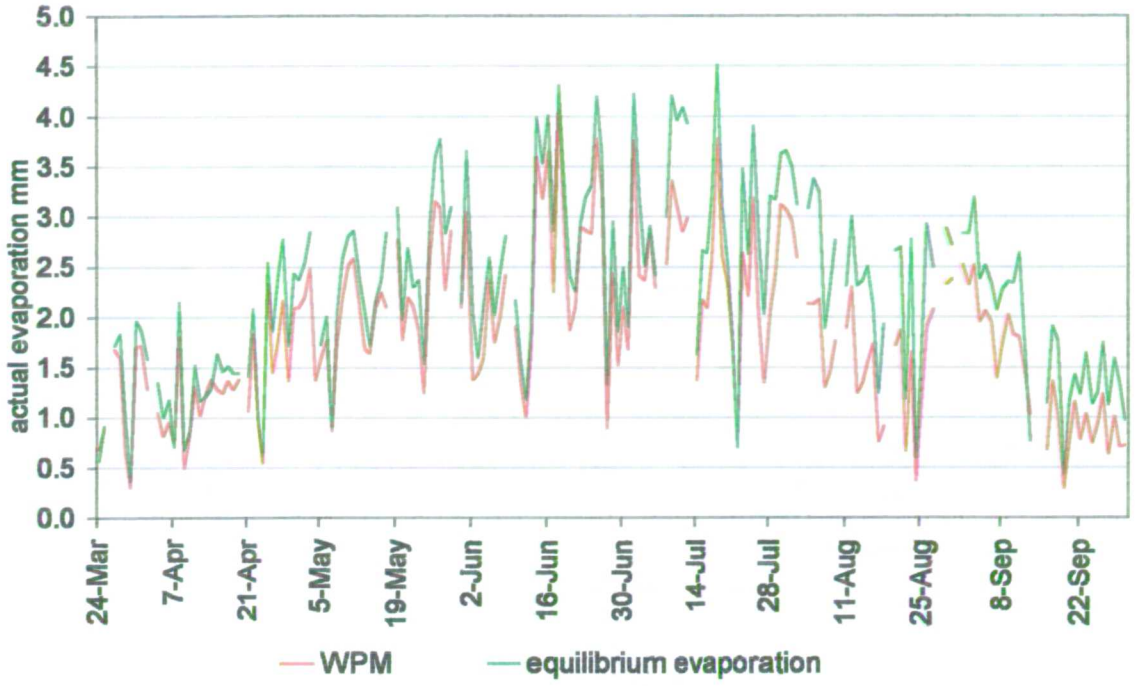


Figure 8.13. Trend of actual evaporation computed by the WPM approach and equilibrium evaporation.

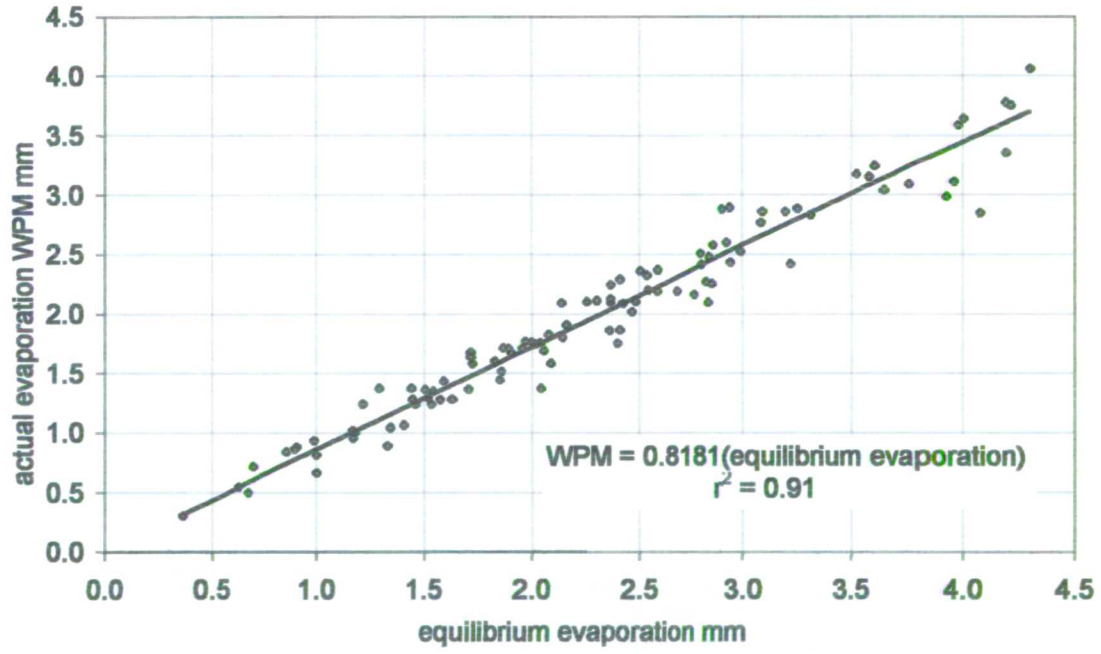


Figure 8.14. Actual evaporation (WPM) against equilibrium evaporation over March to September 1999. The relationship is very strong with $\alpha = 0.81$.

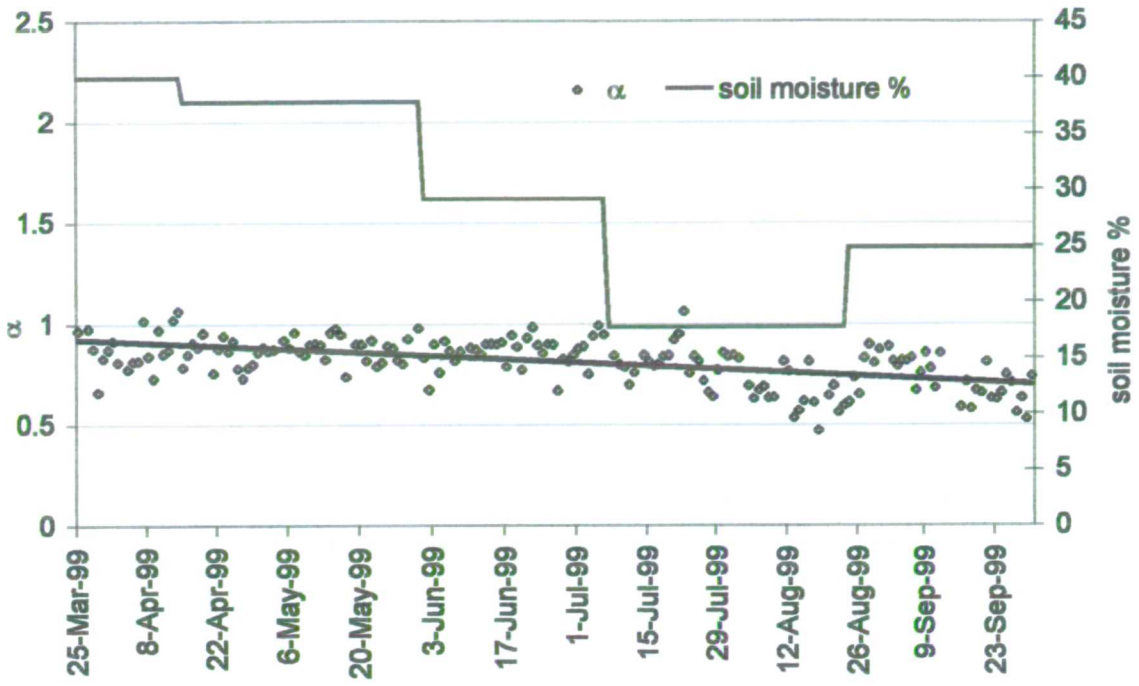


Figure 8.15. Change in α (WPM) and soil moisture over the study period. The trend line shows a decrease in α from 0.93 to 0.7.

Figures 8.16 and 8.17 display BREB against equilibrium evaporation and show a pattern of higher AE until June and lower thereafter. The relationship is not as strong as for WPM with $r^2$=0.53 and $\alpha = 1.01$. The value of $\alpha$ declines markedly over the study period from 1.37 to 0.55 concomitant to the change in soil moisture. The average value of $\alpha$ over the period of inundation of the marsh (March to June) is 1.25, which accords closely with Priestly and Taylor (1972), but there is great variability. The average drops to 0.80 when the wetland starts to dry (June to September). The values clearly show the influence of inundation and open water patches on the equilibrium evaporation rate in this wetland environment.

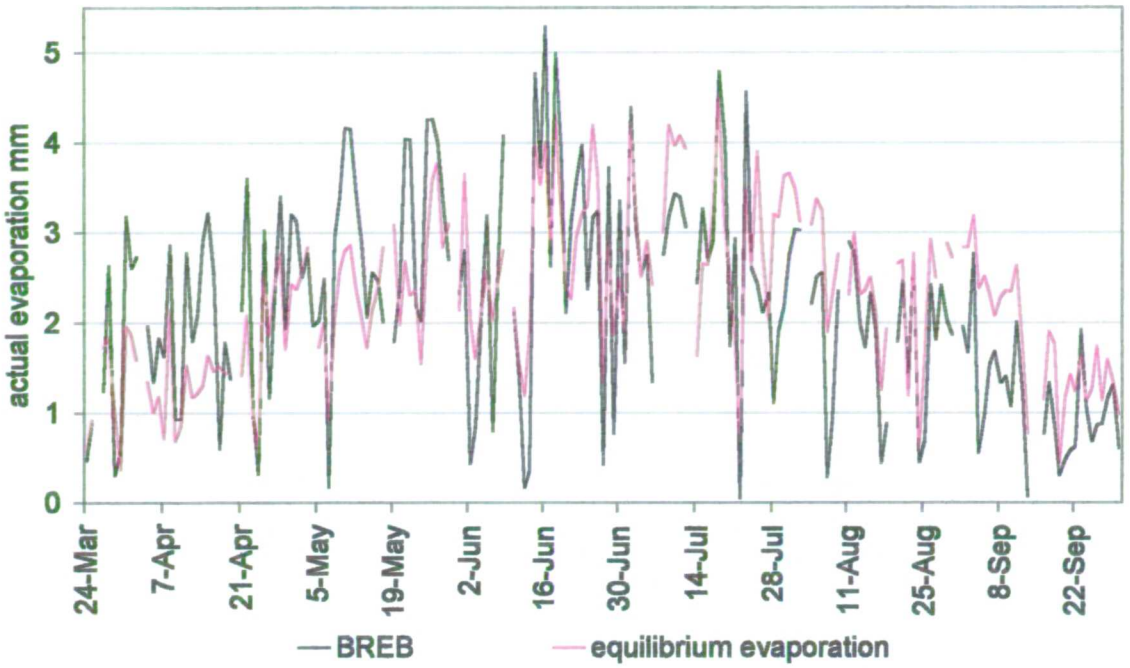


Figure 8.16. Trend of actual evaporation computed by the BREB approach and equilibrium evaporation.

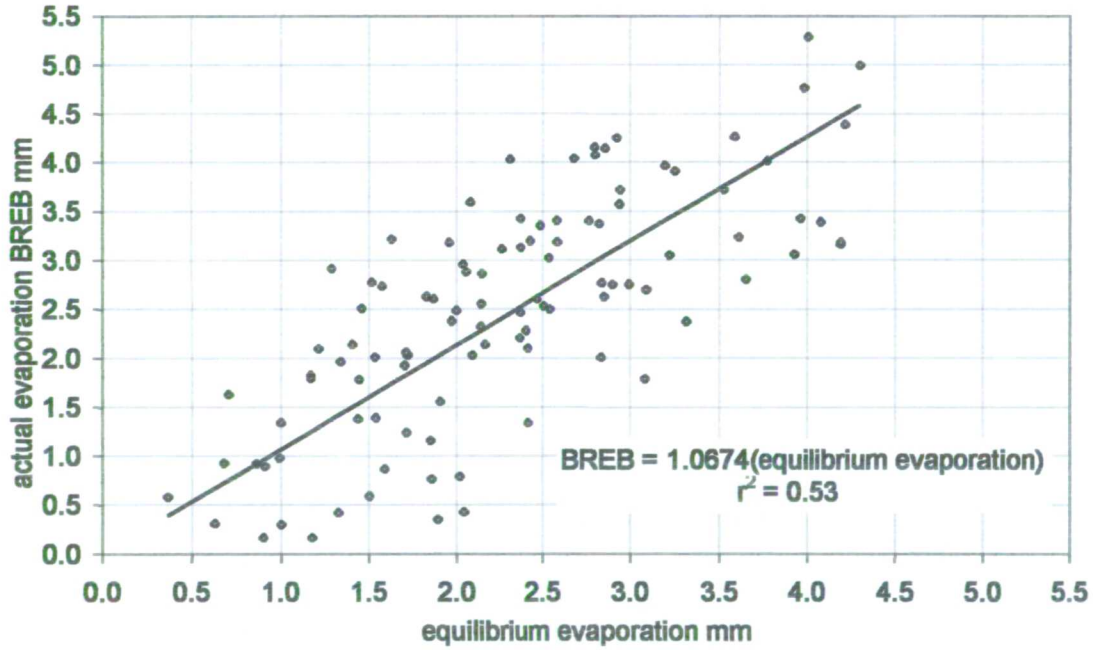


Figure 8.17. Actual evaporation (BREB) against equilibrium evaporation over March to September 1999. The relationship is moderate with $r^2 = 0.53$ and $\alpha = 0.96$ overall. Application of an F test to test the variance between the samples indicates the results were highly significant however with an F ratio of 191.17 against a critical value of $1.02 \times 10^{-29}$.

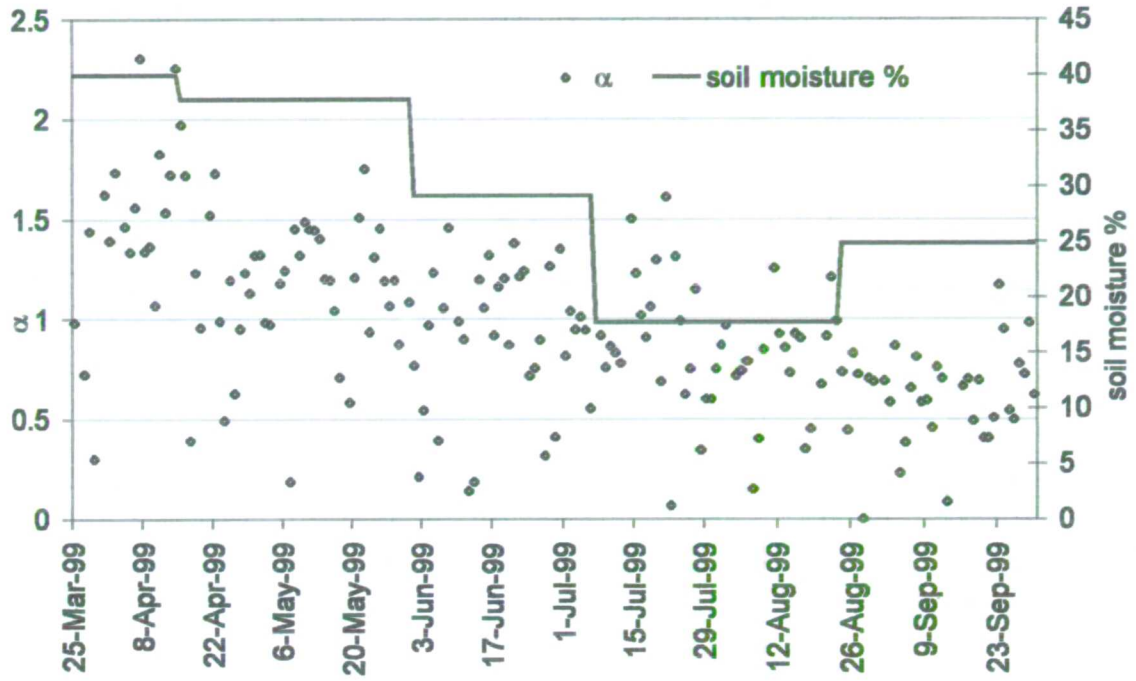


**Figure 8.18. Change in $\alpha$ (BREB) and soil moisture over the study period.**

The principle observations from Figures 8.13 to 8.18 can be summarised:

- AE (BREB) from the marsh occurs above the equilibrium evaporation rate with $\alpha$=1.25 under conditions of freely available moisture and surface inundation
- As patches of open water are lost from the marsh surface and soil moisture becomes limiting, the AE (BREB) falls below the equilibrium rate with $\alpha$=0.80

Three conclusions can be made from the results above.

Firstly it can be inferred that an estimation of the actual evaporation from the wetland can be made using the equilibrium evaporation approach, using appropriate values of $\alpha$ according to the level of inundation and available water of the marsh. In order to assess if this approach could be followed, the equilibrium evaporation, or strictly, the Priestly Taylor model was employed with $\alpha$=1.25 at periods of inundation (24 March to 17 June) and $\alpha$=0.80 (18 June to 30 September) when there are no patches of water present on the marsh surface. Results are presented against the BREB in Figure 8.19 and show that relative to Figure 8.16, BREB and equilibrium evaporation with $\alpha$=1, the goodness of fit is greatly approved with the equilibrium rate closely following the trend of the BREB.

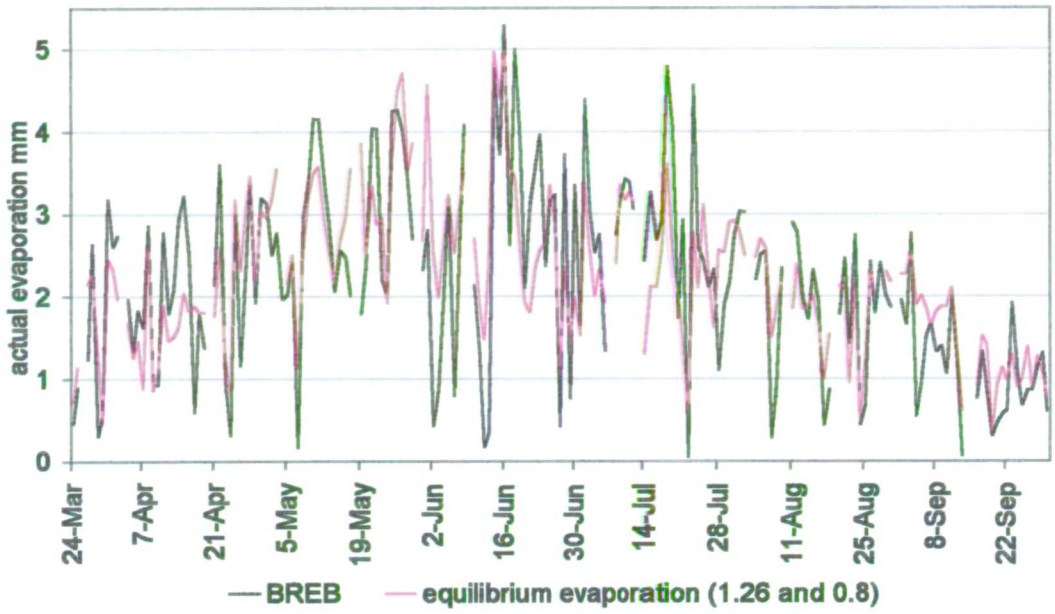


**Figure 8.19. The relationship between BREB and equilibrium evaporation with $\alpha$=1.25 at periods of inundation and $\alpha$=0.80 when there are no patches of water present on the marsh surface.**

Secondly, areas of open water should be computed using the Priestly Taylor approach (Equation 8.16) with $\alpha$=1.25. When incorporating this into the calculations of the WPM approach this should have the effect of increasing the actual evaporation loss. However as the proportion of open water areas is very low, there is no discernible difference/better fit of the trend of WPM to BREB and no change in the value of $d_i$; the use of $\alpha$=1.25 results in an increased contribution of only 3.4 mm. This confirms that 'saturated surfaces' refer not only to open water areas but also to soil.

This leads onto the third conclusion which is that there are implications for the values of potential evaporation used in the investigation to establish the relationship between surface resistance and soil moisture, $\theta$ *rs*, at the study site (Chapter 7). Use of potential evaporation computed by Penman Monteith with rs = zero is shown in Figure 8.11 to be lower than the BREB. For some timesteps of the investigation, it was found that actual evaporation computed from the water balance approach was in excess of the potential evaporation (Table 7.5). Should the 'true' potential evaporation have been computed using $\alpha$=1.25 over the duration of saturated conditions and $\alpha$=1 at other times, theoretically this would have the effect of

matching or exceeding the AE by the water balance. This adjustment may have an impact upon the values of surface resistance obtained.

The adjustment was made to the calculations of potential evaporation of the $\theta rs$ database (Table 7.5) by multiplying by 1.25. This resulted in a change in only one timestep, 9 to 25 May 1998 that was previously lower than the AE computed by the water balance. With the adjustment, the value of potential evaporation increased from 43.4 mm to 54.3 mm over the timestep, slightly exceeding the AE of 53.4 mm. This resulted in an increase in the value of surface resistance for the timestep from -31 $sm^{-1}$ to 2.5 $sm^{-1}$. This new resistance value with a soil moisture deficit of 0 mm (average moisture = 30%) fits within the scatter of points of the 'updated universal relationship' (Figure 7.19). The $\theta rs$ relationship does not therefore need to be recomputed.

8.4.2.3 Dependence of evaporation upon net radiation

A possible reason for the change to only one data point in the $\theta rs$ relationship when using adjusted values of potential evaporation could be due to the variability of $\alpha$ as illustrated in Figure 8.18 (BREB and $\alpha$) as $\alpha$=1.25 is the average value computed over saturated surfaces (March to June 1999), and variability is high.

Values of $\alpha$>1 are indicative of conditions of minimal advection and the value of the parameter can be used to demonstrate the level of dependence of evaporation on the net radiation (Thompson *et al.* 1999, Campbell 1989). The change in $\alpha$ over March to September (Figure 8.18) illustrates the change in dependence of evaporation upon net radiation. Primarily evaporation proceeds at the level of net radiation falling when the soil moisture becomes limiting and the wetland cannot evaporate at the equilibrium rate.

The energy closure and evaporation efficiency can be computed to further assess the dependence of evaporation upon the net radiation. For both closure and efficiency rates, values vary between 0 and 1 with the latter implying a perfect relationship.

After Lafleur *et al.* (1997) (units in W $m^{-2}$):

$$Energy\ balance\ closure = \frac{(H + LE)}{(Rn - G)} \qquad \text{Equation 8.18}$$

$$Energy\ efficiency = \frac{(LE)}{(H + LE)}$$ Equation 8.19

High evaporation efficiency signifies that energy is being expended upon latent energy to evaporate water. The evaporative efficiency can fall below 1 if available water is limiting and transpiration is reduced so sensible heat become more significant (Lafleur *et al.* 1997).

The data used to compute the energy closure and evaporation efficiency for the study site comprises only the daylight periods of each day over March to September 1999. It was not possible to use set periods of the day for example 06:00 to 20:00 hours as the start and length of daylight hours changed over the long time period. In order to account for this change, the data were automatically filtered so that only periods of Rn>0 were employed. The components of the energy balance, Rn, G, H and LE were then summed over these periods to generate daily totals.

Figure 8.20 and 8.21 shows the daily energy closure and evaporation efficiency at the study site. The energy closure is very high; a near perfect balance. The evaporation efficiency is also high at 0.9 i.e. 90% of the available energy is used for the latent heat flux. The evaporation efficiency does fluctuate daily however between 0.5 and 1.5. The dominance of the latent heat flux is to be expected as the study site is a wetland environment.

Kelliher *et al.* (1993) report the evaporative efficiency of two New Zealand grassland sites from studies by Ripley and Saugier (1978) and McAeney and Judd (1983). Both sites observed an evaporation efficiency of 0.78 until a critical soil moisture content is reached thereafter the efficiency declines to 0.2 indicating a change in dominant energy flux from latent to sensible heat.
It was thought perhaps that the loss of water and desiccation of the marsh experienced at the study site would impinge upon the efficiency rate to have a similar effect as reported by Kelliher *et al.* (1993) but no discernible influence can be detected. This is also confirmed in Figure 8.22, which presents the daily average value of the Bowen ratio β (Equation 8.5).

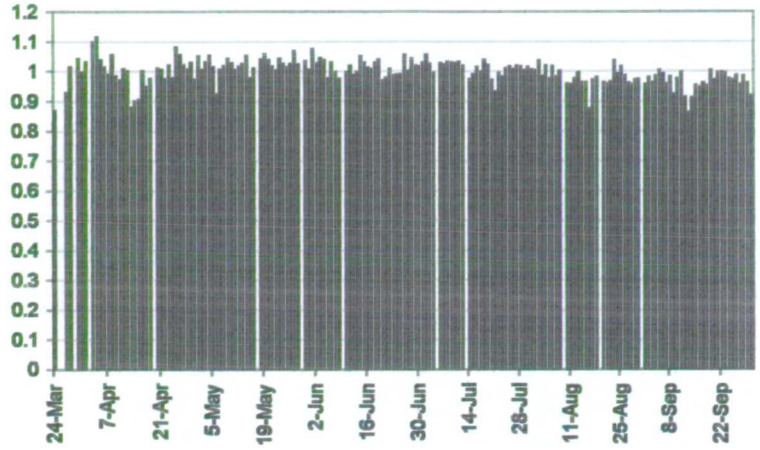


**Figure 8.20. Daily energy closure (Equation 8.18). The average closure rate over the study period is very high at 0.997.**

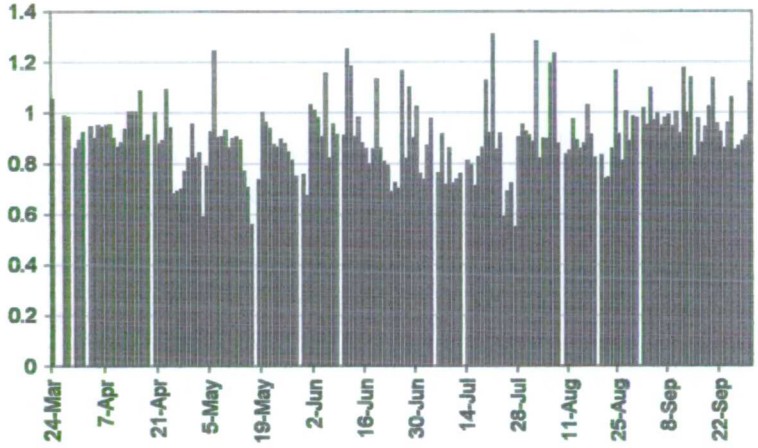


**Figure 8.21. The daily evaporation efficiency (Equation 8.19) at the study site. The overall average efficiency rate is high at 0.90.**

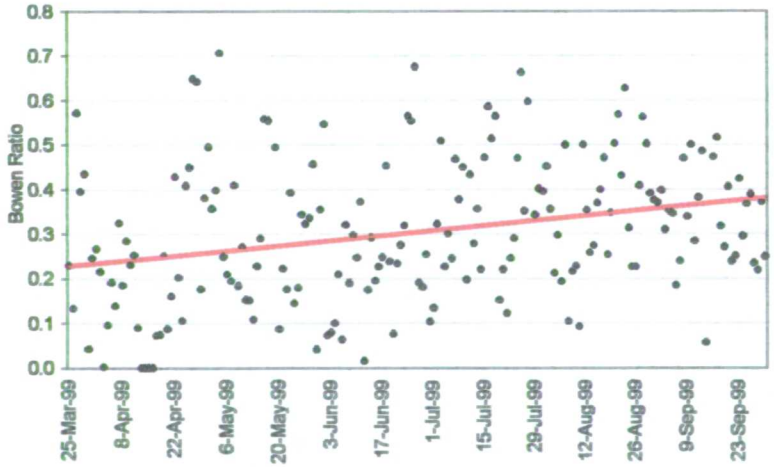


**Figure 8.22. Daily average values of the Bowen ratio, β, over the period March to September 1999. The overall average value is 0.30 with the trend line showing an increase from 0.23 and 0.38 over the period shown.**

Values of β reported for wetland environments are variable between studies and also within studies depending upon the change in wetness levels. For example Lafleur *et al.* (1997) report β for a northern tundra wetland changing from 0.7 during spring thaw, to 0.1-0.2 during early vegetation development increasing to 1 during senescence. Price (1991) report average β of 0.8 for a coastal blanket bog wetted by fog drip rising to 1 when dry. Large values of 2 were common for peat bogs studied by Thompson *et al.* (1999) explained by the inability of capillary rise to replenish the upper surface moisture content, as the ratio fell to below 1 when the bog was wetted. Campbell and Williamson (1997) found similar results at the same site with β in the range 3-5. Souch *et al.* (1996) recorded mean values of 0.35 for an Indiana lakeshore wetland which contrasts against the mean value of 1.11 of a Hudson Bay lakeshore wetland measured by den Hartog *et al.* (1994). Moore *et al.* (1994) found a diurnal trend with values varying between 0.2 to 0.8 for a subarctic fen, and Lafleur and Rouse (1988) found $\beta<1$ but varied over three adjacent wetland systems according to the vegetation growth stage and wind direction

For the Elmley Marshes the value of β over the time period is scattered but always less than 0.7; the overall average over March to September is 0.3. There is a slight trend over the time period with the average value of β increasing from 0.23 to 0.38. Such low β relative to the published values above confirm the dominance of latent heat flux over March to September 1999 despite the difference in saturation level of the grassed marsh; the dominant surface type of the study site.

8.4.2.3.1 Advection

Conditions of $\alpha>1$ are indicative of minimal advection (Priestly and Taylor 1972). It is common to assume an absence of advected energy when calculating evaporation loss but this is rare in the natural environment. Given the values of $\alpha>1$ computed in this study it is instructive to examine the energy advection over the period March to September 1999 at the study site.

A common procedure to identify periods of advection is to use the criteria of LE>Rn-G (Dunin 1991). Figure 8.23 and Table 8.7 shows that LE is very close to Rn-G over

March and April and August to September. LE exceeds Rn-G on 33 days, which comprises 18% of the data period. On those days LE Rn-G exceeded Rn-G by an average of 606 W $m^{-2}$ (high standard deviation at 496 W $m^{-2}$). These days are scattered through the study period.

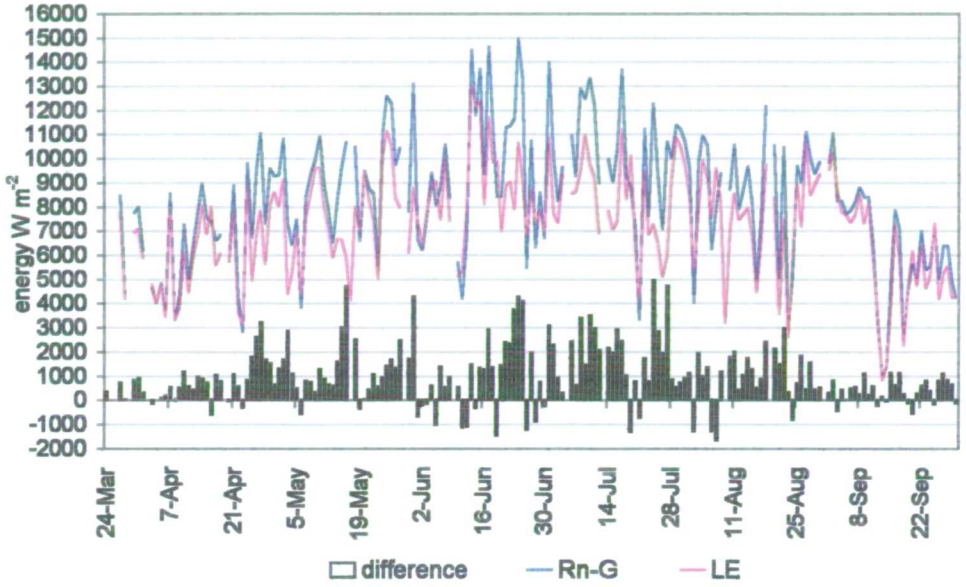


Figure 8.23. The trend of Rn-G and LE as a measure to identify periods of advection.

Table 8.7. The distribution of the 33 days when LE exceeded Rn-G.

| | |
|---|---|
| April | 3, 4, 8, 16, 20, 23 |
| May | 6, 19 |
| June | 1, 2, 3, 5, 11, 12, 14, 19, 26, 28, 30 |
| July | 19, 21 |
| August | 2, 6, 7, 23, 24 |
| September | 3, 12, 14, 19, 20, 25, 30 |

Local heat advection accompanies spatial variability or surface discontinuities over the landscape (Dunin 1991) and enhances the capacity for evaporation (Lafleur and Rouse 1988). The Elmley Marshes landscape can be conceptualised as changing from one with 'merged' margins between open water in ditches, saturated ground and inundated patches, to progressively dry ground areas with sharp boundaries to the water in ditch channels from June onwards.

The latter situation of dry-warm (ground) and wet-cool (ditch water) patches or strips can generate local heat advection (Guo and Schuepp 1994a and b). Inspection of Table 8.7 and Figure 8.23 show that advection days are greater in number and of increased magnitude from June onwards when there are no inundated areas over the

marsh (except for water in ditches). The juxtaposition of patches with differing wetness and therefore heat capacity levels may cause the reallocation of a portion of sensible heat from the dry to the wet patch, enhancing the evaporation from the latter. Guo and Schuepp (1994a) examine this effect in detail investigating the magnitude of enhanced evaporation at various dry and wet patch sizes. Taking their results and applying factors to characterise the Elmley Marshes, based on dry and wet patches or strips of 400 m and 5 m respectively and a temperature difference of 20°C between the patches (dry = 40°C and water = 20°C), the effect of local heat advection is to promote a relative increase in the evaporation rate by >50% and lower $\beta$ by 55% which is considerable.

Enhanced evaporation by local heat advection between the dry marsh and wet ditches in this way could be a major reason for the high values of $\alpha$ and low $\beta$ recorded for this investigation at Elmley Marshes, relative to the values discussed above from other wetland systems.

## 8.5 Conclusions

The aim of this investigation has been to investigate the actual evaporative loss from the wetland surface and invoke fresh insights from original empirical data. The ability of the WPM approach to compute AE using BREB data as the reference AE has been evaluated. Results show that over the entire time period the WPM has the marginally strongest performance to the BREB, with the daily trend becoming close after inundated patches on the marsh surface has disappeared.

The BREB expressed against the Priestly-Taylor approach (1972) is in excess of equilibrium evaporation with $\alpha$=1.25 falling to $\alpha$=0.80 after the end of surface inundation. Computation of Priestly Taylor with these values of according to the level of saturation reveal a very close fit to the BREB indicating that this simple method can be used method to estimate the actual evaporation from the wetland.

To conclude, while it has to be stated that the analysis covered in the investigation covers only a period of seven months and is therefore a short dataset, there is

nevertheless an opportunity to discuss operational methods of determining actual evaporation from wetland surfaces based on the research results of this investigation. This is discussed below and illustrated in Figure 8.24.

A common approach to determine evaporation is to employ the Penman Monteith approach using reference resistances (Allen *et al.* 1989, 1994). Evaporation can be computed in this way for a variety of crops and vegetation communities with standard meteorological data. For wetlands with heterogeneous wetness levels in time and place, such as wet grassland environments the results of this investigation highlight problems with the standard application of Penman Monteith. It can be stated that the application of Penman Monteith with grass reference resistances can lead to an underestimation of the actual evaporation loss when the wetland is saturated, and an over estimation over periods of non-saturation. The heterogeneity of wetland surfaces is also disregarded when employing this approach.

Consideration can be made of the spatial heterogeneity of the wetland on two levels. Firstly the temporal change in spatial extent of representative surface types can be accounted for by employing the Weighted Penman Monteith approach. Secondly, for wetlands that experience substantial annual variation in wetness, the application of WPM is much improved if the relationship between actual evaporation loss and moisture status for each surface type is considered. This enables the designation of surface resistances appropriate to the moisture level to better estimate actual evaporation. The relationship taken for this investigation employed the 'updated universal relationship' (section 7.5).

To follow the Weighted Penman Monteith method however is extremely data intensive, requiring information on the change in extent of surface types over time and space which is not routinely collected in wetland environments. This is an acute problem for large wetland sites where it is unfeasible to estimate surface types by hand mapping. In such cases remote sensing techniques are useful (Al-Khudhairy *et al.* 1999, in review, Gilvear and Watson 1995), but are expensive which may prohibit their use.

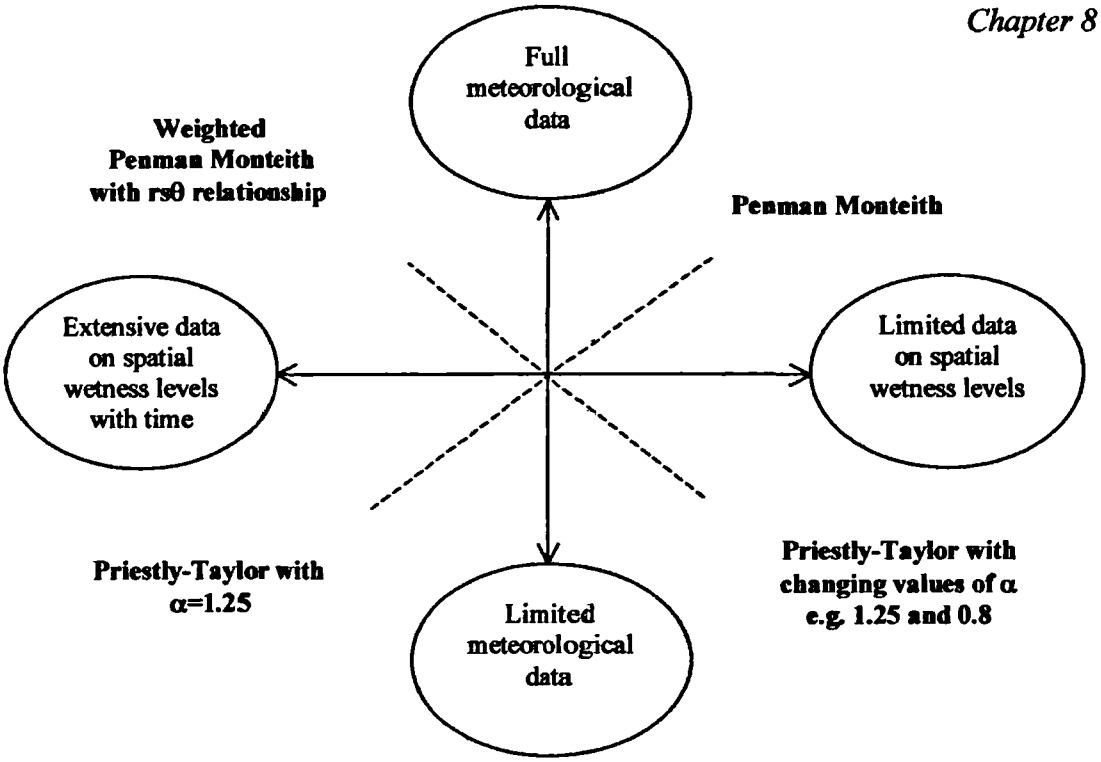


Figure 8.24. Diagram to illustrate the operational methods (bold) to compute evaporation based on data availability (ovals).

For wetlands where data is scarce a simpler approach is required. It has been shown by this research that the Priestly-Taylor method, with 'appropriate' values of $\alpha$ to represent the levels of surface wetness, provides accurate estimates of actual evaporation when compared to BREB data. The Priestly-Taylor approach can also be used if only temperature and net or solar radiation data are available, which would be insufficient to compute Penman Monteith (Equation 7.2).

In this study, the average value of $\alpha$ was found to be 1.25 when the wetland experienced surface wetness or inundation, a value near identical to that found by Priestly and Taylor (1972) and many researchers (section 8.4.2.2). These results verify the 'appropriate' value of $\alpha$=1.25 to represent wetlands with a degree of surface flooding and may be used with some confidence.

An average value of $\alpha$= 0.80 was calculated for the wetland when free from surface inundation. Published values indicate a range of $\alpha$ for different wetland systems under conditions of no surface flood indicating the importance of wetland type and local conditions. As such care must be take when applying a single value of $\alpha$ to represent a wetland in a non-saturated state, but the original empirical results of this investigation provide a standard or guide for wet grassland environments.

# Chapter 9 Summary and conclusions

This thesis has presented the results of a comprehensive hydrological study of an ecologically important wet grassland site, Elmley Marshes located within the North Kent Marshes, UK. The North Kent Marshes are covered by an Environmentally Sensitive Areas scheme that specifies hydrological manipulation for ecological conservation aims. The rationale of the research was to investigate the hydrological implications of the management of the wetland.

## 9.1 Summary of research

Research was initiated to establish the effectiveness of the management prescriptions of the ESA, Tier 1a and 1b, the 'Wet Grassland' tiers that stipulated management of ditch water levels. Attention has started to focus upon the success of agri-environment schemes. Morris and Potter (1995, p52) remark that 'questions are rightly being asked about the extent and quality of the environmental protection and improvement that "conservation by contract" is able to bring about'. Further to this, Wilson (1997, p304) notes that while the socio-economic implications of the ESA scheme have been intensively researched, 'studies on the ecological and environmental conservation impacts of ESA schemes have been scarce'.

Research into wetland hydrology remains a priority area (Clymo *et al.* 1995, Armstrong *et al.* 1995), and Gilman (1994, p91) argues that 'without a clear understanding of the hydrology of the site it is impossible to predict the effects of changes in adjoining land to confirm the long-term variability of existing or created wetlands, or to improve on the management of the land to increase its habitat value'.

The approach undertaken at the Elmley Marshes to assess the ESA management prescription was to commence a monitoring programme of ditch water level, groundwater level, soil moisture, precipitation and evaporation, to examine change in time and space. The research was split into three separate but interlinked investigations:

- Research Question 1: *What is the relationship between ditch water level and the water table and soil moisture in the adjacent field?*
- Research Question 2: *What is the effect of soil moisture upon the evaporation rate?*
- Research Question 3: *What is the actual evaporation loss from the heterogeneous wetland surface?*

The research findings have been discussed after each investigation and a summary is presented below.

Work undertaken for Research Question 1 is presented in Chapters 3-5 and discussed in Chapter 6. Results prove that due to the clay soil texture and low hydraulic conductivity of the marsh substrate, little relationship exists between the position of ditch water levels and groundwater. Thus the manipulation of ditch water levels to promote high water table as proposed by the ESA Tier 1a is ineffective.

The effect of flooding the marsh surface with ditch water as proposed by ESA Tier 1b does promote high surface soil moisture content and optimal habitat for waterfowl. However the deleterious effects upon soil structure and floristic diversity of regularly flooding large areas have been noted. These effects are enhanced due to the brackish water quality of the ditch water, and need to be taken in consideration for the sustainable management of the wetland.

The research above demonstrated that the dominant water fluxes over the Marshes are in the vertical direction; precipitation and evaporation. The rise and fall of the ground water is seen to be in direct response to these variables, with rates of response faster than measured rates of hydraulic conductivity would suggest. This is due to the dynamic soil properties of the clay soil by shrinking when drying, allowing the creation of large macropores that act as bypass channel for incoming rainwater.

These observations lead to the examination of the evaporative loss of the water from the marshes, Research Questions 2 and 3.

Research Question 2, presented in Chapter 7, examined the relationship between evaporation and soil moisture of the wet grassland, and was initiated due to the large moisture range of the marshland over the seasons. Research focused on the relationship between surface resistance and soil moisture content, so that 'correct' surface resistance values could be input to the Penman Monteith method to compute actual evaporation according to the wetness of the marsh. Research results showed a complex relationship between soil moisture loss and rates of actual evaporation decreasing below potential rates. Data compiled at the Elmley Marshes fitted the relationship of Szeicz and Long (1969), and so the datasets were combined. In this way a functional relationship was quantified, termed the 'updated universal relationship'.

Research Question 3, presented in Chapter 8, comprised an investigation to compute the actual evaporation of the wetland taking into account the small-scale heterogeneity of surface wetness conditions. The Weighted Penman Monteith approach was followed referencing results against data by the Bowen Ratio Energy Balance method. Research results show that the WPM method could be used to compute the actual evaporation loss, however the adoption of the Priestly-Taylor approach with suitable values of $\alpha$ is a simpler method, computationally much less demanding and of equal if not greater accuracy. Using the latter method, research results showed that actual evaporation follows a rate equivalent to that of equilibrium evaporation with $\alpha$=1.25 (compared to 1.26 of Priestly and Taylor (1972)) over periods when surface water was present on the marsh. Actual evaporation was observed to decline below the equilibrium rate once surface water was no longer present on the marsh. For other wet grasslands and similar wetlands where meteorological and surface wetness data are scarce, the computation of $\alpha$ in this investigation provides a reference for the application of this technique to compute actual evaporation.

It is believed that the research undertaken and presented in this thesis has fulfilled its objective of increasing the scientific understanding of wetland hydrology not only for the study site but also for wet grassland environments generally.

## 9.2 Conclusion

Gilvear *et al.* (1993, p311) express that 'a knowledge of wetland hydrology and quantification of water inputs and outputs are a necessary prerequisite to (a) understanding wetland environments and (b) developing wetland hydrological models for vulnerability assessment'. Research to further the scientific understanding of wetland environments should be essential for areas prior to being covered by agri-environment schemes, and would enhance the understanding of the system to determine the best mechanisms for meeting desired objectives through hydrological ends. Research presented in this thesis has shown that the hydrological management of the North Kent Marshes has not yielded success in a sustainable manner. The implications of the management on *all* aspects of the site, for example amelioration of habitats for waterfowl, aquatic invertebrates, and floristic diversity should be assessed, rather than the present focus upon ornithological preferences.

This would ensure compensatory payments are not misspent and instead put to optimal use. The existing situation of standard hydrological prescriptions imposed to achieve ecological aims without prior research or scientific understanding of the site has been shown to be ineffective. As such the need for hydrological research in wetland environments remains a priority to ensure their conservation and protection for the future.

# Appendix A Data acquisition and quality

This appendix contains details relating to instruments used in the research presented in this thesis. Many of the instruments required a soil specific calibration and the results are presented in this chapter. Steps taken to deal with periods of data loss are also detailed. Most datasets do not cover the entire study period due to unavailability or malfunction for example (Table A.1). The hydrological investigation presented here focuses upon one representative field within the Elmley Marshes (Figure A.1). Instrumentation was shielded from grazing animals within two enclosures, donated by the Elmley Conservation Trust. The layout of the main enclosure can be seen in Figure A.1 (a reproduction of Figure 1.3) and Figure A.2. All references to the 'enclosure' in the text refer to the main one 35 m from the north ditch of the study field.

This chapter is organised into the following subsections:

- Automatic weather station – data availability and quality of the AWS sensors and tipping bucket rain gauge.
- Bowen Ratio Energy Balance – adjustments made to the net radiometer
- Ditch and ground water levels – details of the stage board set-up, piezometers and pressure transducers.
- Soil moisture monitoring equipment and calibration – details of the calibrations of the neutron probe, SCIP, ThetaProbe and Equitensiometer, and electrical resistance blocks.

## A.1 Automatic weather station

### A 1.1 Data availability

The Institute of Hydrology loaned for the duration of the project, a Didcot Automatic Weather Station (AWS) with Campbell CR10X data logger and Solarex solar panel. This has been installed within the enclosure in the field site (Figure A.1 and A.2). The AWS records the meteorological variables required for calculating evaporation on an hourly and daily basis The station comprises a solarimeter, net radiometer, wind run sensor and direction vane,

temperature screen housing wet bulb and dry bulb sensors and a tipping bucket rain gauge. The logger is programmed to average data at hourly and daily intervals.

Table A.1. The period of data collection.

| Dataset | 1997 | | | | 1998 | | | | | | 1999 | | | | | |
|---|---|---|---|---|---|---|---|---|---|---|---|---|---|---|---|---|
| | M J | J A | S O | N D | J F | M A | M J | J A | S O | N D | J F | M A | M J | J A | S O | N D |
| Water table | | | | | | | | | | | | | | | | |
| AWS | | | | | | | | | | | | | | | | |
| Ditch water level | | | | | | | | | | | | | | | | |
| Neutron scattering | | | | | | | | | | | | | | | | |
| Electrical resistance blocks | | | | | | | | | | | | | | | | |
| Tensiometer | | | | | | | | | | | | | | | | |
| ThetaProbe and Equitensiometer | | | | | | | | | | | | | | | | |
| Vegetation monitoring | | | | | | | | | | | | | | | | |
| SCIP | | | | | | | | | | | | | | | | |
| Inundation mapping | | | | | | | | | | | | | | | | |
| Bowen Ratio Energy Balance | | | | | | | | | | | | | | | | |
| Soil moisture samples | | | | | | | | | | | | | | | | |

## A.1.2 Data quality

There have been periods when the AWS has generated erroneous data due to malfunctions caused by water entering the connections of the cables. Data has been lost chiefly from the dry bulb, solarimeter, net radiation and precipitation sensors. The proportion of error values with the AWS account for 4.5% of the time over 1997-1999 (5886 data hours from a total of 140448) which can be considered a good data capture rate. These values include the period when the logger malfunctioned over a period of 9 days, from 14 to 22 July 1999 when the data from all sensors was lost. Table A.2 details the loss of data per sensor. The procedures employed to generate data for periods when the sensors were malfunctioning are outlined below.


Figure A.1. The study area in detail.
An aerial view (above: overlay of two photographs) and diagram (right) of the layout of the main enclosure (blue shield shape above) and smaller enclosure (blue open-ended square above) adjacent to the north ditch of the study field (also known as Elmley Fleet).
Marked upon the aerial photograph are the transect piezometers (small white squares) aligned north-south (A-G) and west-east (H-M). Also marked are the location of the stageboards (marked with S), positioned at the end of the piezometer transects and are referred to in the text as the east, south and west ditches.
The red square outlines the grid in which the surface soil moisture was monitored with the SCIP.
On the diagram the shaded squares are the piezometers 1, 2, 3 in which a pressure transducer is located. These piezometers were subject to pump tests performed to determine the saturated hydraulic conductivity.
The main enclosure houses most of the instruments used in this research. The ThetaProbe, Equitensiometer and pressure transducers are wired into the logger in the main enclosure. In the small enclosure the position of the stageboard (S), pressure transducer (P) in the north ditch, and the neutron access tube are labelled.

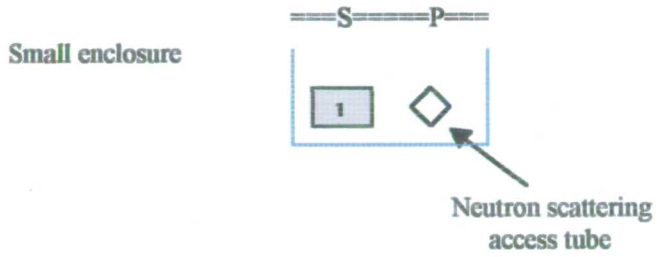


**Main enclosure**

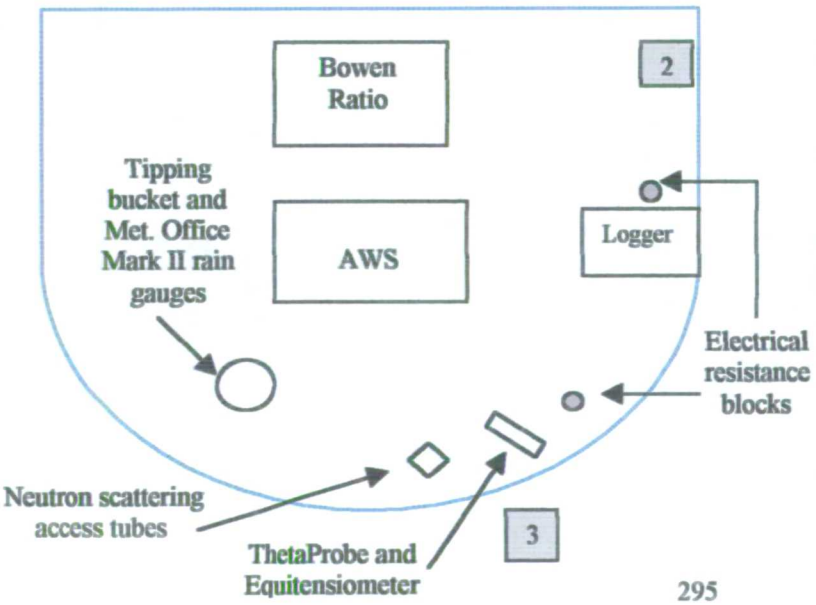

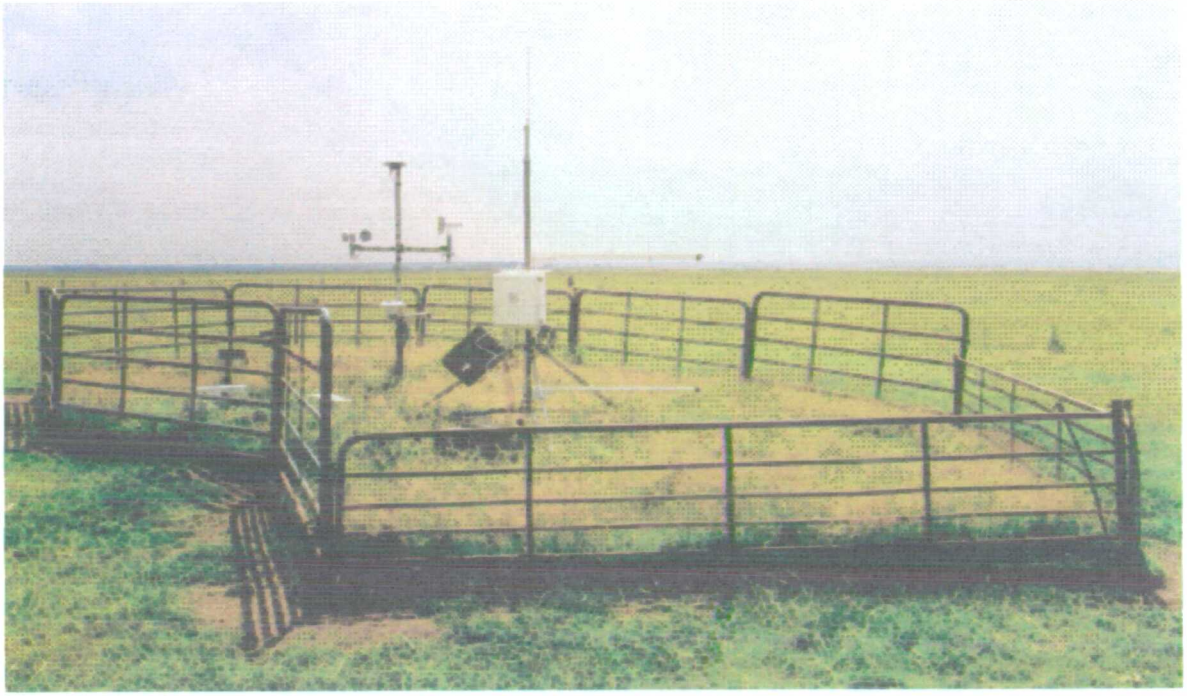

Figure A.2. A view of the main enclosure taken facing towards the south. The AWS (left) and Bowen Ratio Energy station (right) are visible, with the former in the background; other instruments are at ground level and cannot be seen. The difference in sward height inside the ungrazed enclosure and the grazed field can be substantial and the grass around the instruments was cut inside the enclosure on field visits to mean field height.

Table A.2. The number of data hours for each sensor, which have yielded erroneous data over the monitoring period 24th June 1997 to 6 December 2000.

| Sensor | Number of erroneous data hours | Plus the number of hours the logger was removed (14 to 22 July 1999) | Percentage of time that erroneous data has been recorded |
|---|---|---|---|
| Solarimeter | 868 | 1088 | 5.4 |
| Net radiometer | 946 | 1166 | 5.8 |
| Wet bulb | 2 | 222 | 1.1 |
| Dry bulb | 907 | 1127 | 5.6 |
| Rain | 2063 | 2283 | 11.4 |
| Wind speed | 0 | 220 | 1.1 |
| Wind direction | 0 | 220 | 1.1 |
| 5886 | Total number of erroneous data hours | | |
| 20064 | Total number of hours over the period of data collection | | |
| 140448 | Total number of data hours collected by the sensors | | |
| 4.5% | Overall percentage of time an error was observed from the sensors | | |

### A.1.3 Wet and dry bulb temperature

The procedure to derive data for the dry bulb temperature sensor for periods of malfunction involved interpolating a value based on previous and subsequent entries. For some error days, the data loss concerns only a few hours and so interpolation can be inferred from hourly temperature data recorded on the same day. On other occasions, larger time periods of data loss are involved lasting from one to several days. On these occasions, only the dry bulb sensor had failed and so values can be derived from the wet bulb by interpolating the general relationship between the two sensors measured over the preceding days. When the logger malfunctioned for nine days in July 1999, both air temperature and wet bulb temperature were taken from the nearest station recording these variables, which was at Sheerness, on the Isle of Sheppey. Relative humidity was assumed to remain the same between the two stations. Comparisons between the temperature data at Sheerness and from the automatic weather station show good agreement and so the temperature data is used in confidence.

### A.1.4 Net Radiation

In order to derive values for a period when the net radiometer sensor was malfunctioning, the relationship between the solarimeter and the net radiometer sensor was established (Figure A.3) so that substitute values can be generated from the solarimeter for short periods. The relationship between the two variables is strong, as expected with the radiative efficiency of 62% which accords with values found over similar surfaces (Den Hartog *et al.* 1994, Lafleur *et al.* 1987).

Over the period 27 February to 17 March 1998 however both the solarimeter and the net radiometer sensors failed. As with the temperature data, it is only possible to derive values for these parameters using values from another weather station recording this variable. Substitute values were taken from the East Malling weather station near Maidstone, Kent. For the logger failure in July 1999 net radiation values were available from the Bowen Ratio Energy Balance station within the enclosure.

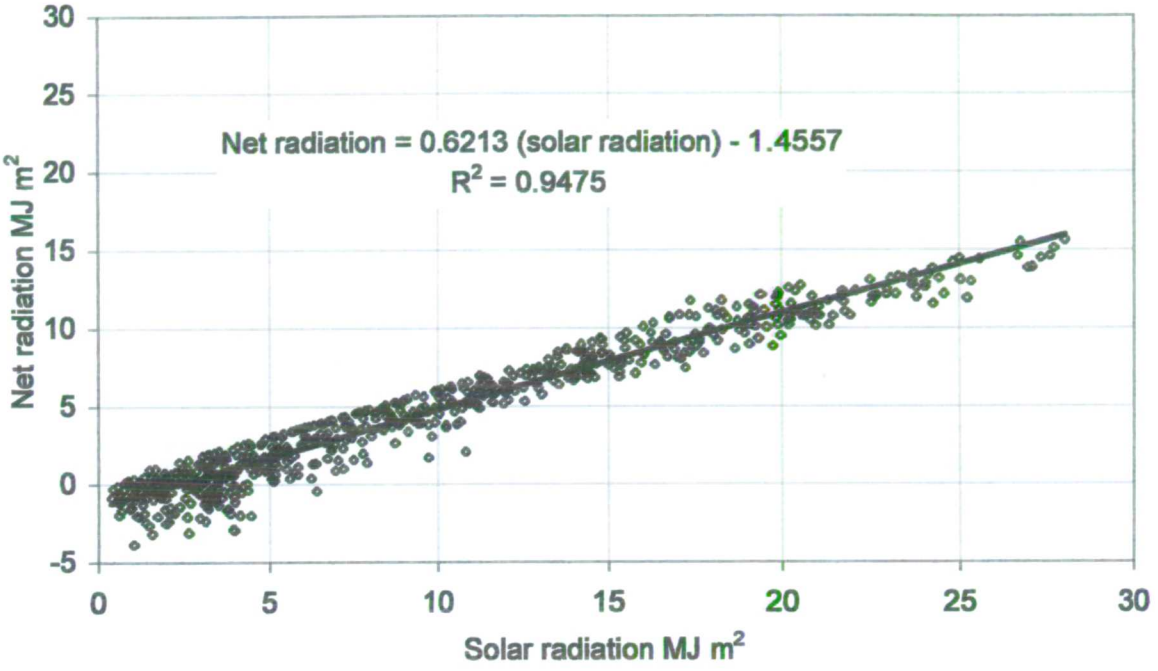


**Figure A.3. The relationship between solar radiation and net radiation of the AWS. At times of malfunction of the net radiometer, substitute values were taken from the solarimeter using the relationship above.**

## A.1.5 Rainfall

The rain gauge of the AWS is a tipping bucket design with a minimum recording volume of 0.5 mm and is logged every hour. In order to provide a check on the accuracy of the tipping bucket a standard Met Office Mark II rain gauge was installed next to the tipping bucket. This rain gauge was measured manually on field visits and Figure A.4 displays precipitation totals measured by the two gauges over the study period. For most periods the difference in precipitation totals is negligible and the Met Office gauge and tipping bucket can be considered to record similar values. This has meant that over periods when the AWS logger and tipping bucket itself malfunctioned (16 to 24 July 1999 and 4 August to 26 October 1999 respectively), values of precipitation could still be measured during this period from the Met Office gauge. The tipping bucket malfunctioned after moisture entered the cable but functioned normally after treatment.

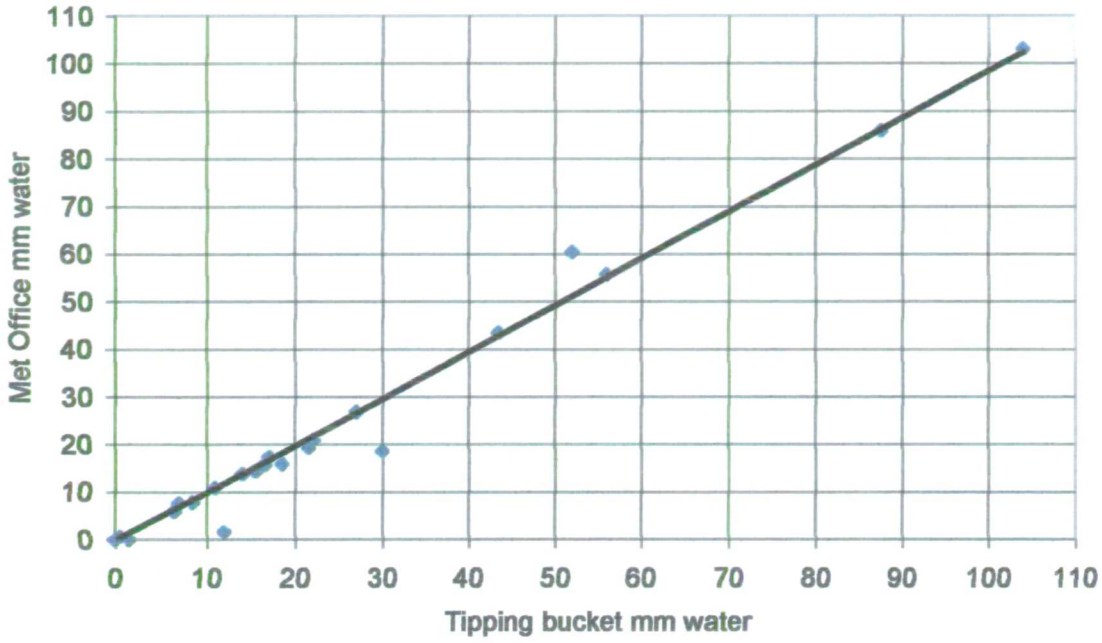


Figure A.4. Measurements of precipitation by the AWS tipping bucket gauge and the standard Met Office Mark 11 gauge. Correlation is strong with $r^2 = 0.98$.

## A.2 Bowen Ratio Energy Balance

A Bowen Ratio Energy Balance station has been installed on Elmley marsh within the enclosure next to the AWS (Figures A.1 and A.2). Data employed in this research covers the period 25 March to 15 October 1999. The BREB data are employed in the investigation into small-scale wetness heterogeneity of the surface and to validate the values of the Weighted Penman Monteith approach (Chapter 8).

### A.2.1 Net radiation

The net radiometer (NR-Lite) of the BREB station gave initial concern when compared to the output of the sensor of the AWS, a Didcot Instruments bubble dome. Initial comparisons showed that the NR-Lite recorded substantially lower values than the AWS. This was checked however by the manufacturers who issued an adaptation of the calibration factor by 10%. While the NR-Lite manual (Campbell Scientific 1998) stated that the Teflon coated

surfaces results in a robust design giving good sensor stability, it noted that 'this design is slightly less accurate than the more traditional radiometers which use plastic domes...[and has a] particularly a higher sensitivity to windspeed with a subsequent lessening of accuracy'. This is due to the calibration of the sensor being performed at zero windspeed levels. The decrease in sensitivity is effectively independent of the radiation level and less than 1% of the reading per $ms^{-1}$ wind speed.

A windspeed adjustment was also performed on the net radiometer data in accordance to the instrument manual. Hourly windspeed data were available from the AWS, however as the BREB station was programmed to output data at 20 minute intervals it was necessary to use the same hourly data value for the extra timesteps within the hour. The assumption of constant windspeed was made to simplify the procedure. The windspeed adjustment to the net radiation data was made following the correction in the manual:

$$correction\ multiplier = 1 + 0.0082u \qquad \text{Equation A.1}$$

Where:
$u$ is the windspeed $ms^{-1}$ at the sensor level.

Figure A.5 displays the values of net radiation from the Didcot Instruments sensor, the NR-Lite, and the results of the adjustments applied to the latter sensor. It can be seen that the effect of the correction applied to the NR-Lite is to increase the value of net radiation more closely to that of the Didcot Instruments sensor, especially in higher windspeeds. At low windspeed the NR-Lite slightly underestimates the net radiation compared to the Didcot sensor. Figure A.6 shows the value of daily net radiation recorded by the adjusted NR-Lite and Didcot sensor over a longer time period together with the difference in net radiation recorded by the two sensors. The magnitude of the difference in energy recorded is up to 2 $MJ\ m^{-2}\ day^{-1}$.

Net radiation is an important parameter in evaporation calculations. The presence of an anomaly in recorded values by two different sensors in very close proximity presents problems when comparing values of evaporation computed by the Bowen Ratio Energy Balance and Weighted Penman Monteith approach (Chapters 7 and 8). Comparisons

between evaporation totals can not be made with confidence due to the variability of the net radiation measurements. Therefore it was decided to reject values of net radiation recorded by the NR-Lite sensor and use those from the AWS Didcot sensor in the BREB calculations. This would ensure that the values of evaporation computed from different methods had the same common reference of net radiation data. Similarly to the situation with windspeed above, hourly measurements of net radiation are available from the AWS while data at 20 minute intervals are required for the BREB computations so the same approach was followed as for the windspeed data. For the periods of malfunction of the Didcot Instrument sensor, and the AWS logger was removed (14- 22 July 1999) data from the NR-Lite was used to ensure a continuos data record, as it was considered that the potential for error as discussed above was small over this short time period, and that an alternative data source was unavailable.

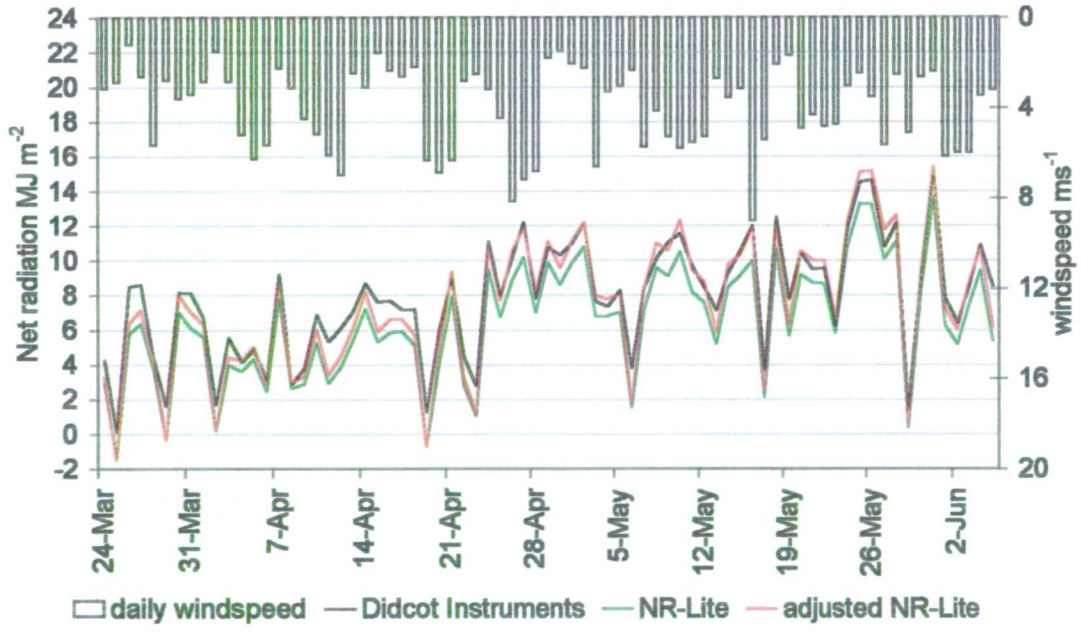


Figure A.5. The values of net radiation from the AWS sensor, the NR-Lite, and the NR-Lite adjusted with the manufacturer correction and the windspeed multiplier (Equation A.1).

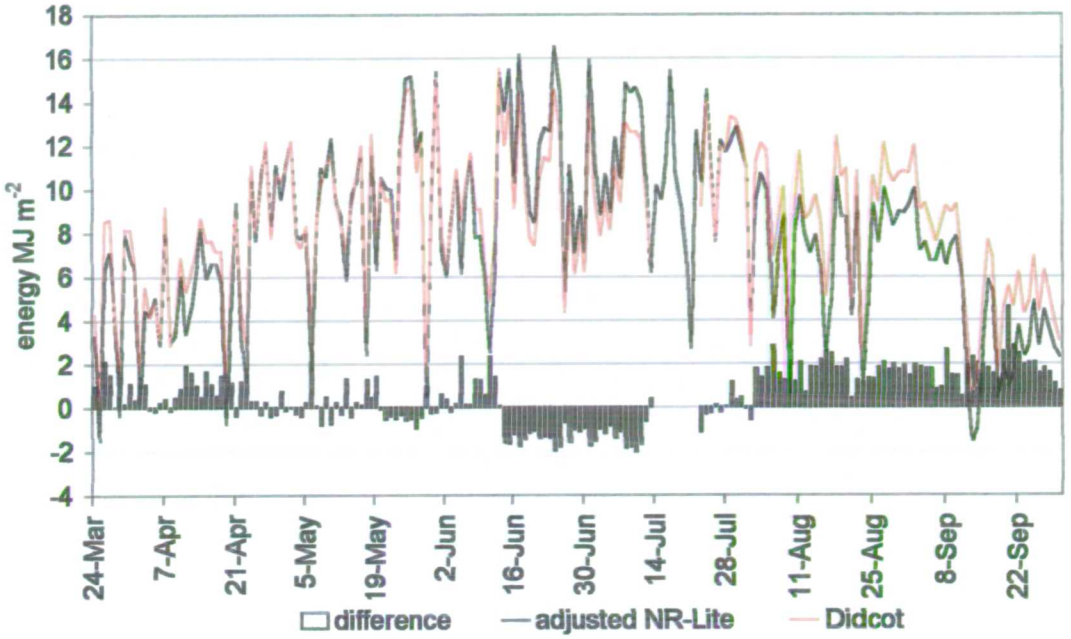


Figure A.6. The trend of daily net radiation recorded by the two sensors over the period March to September 1999 and the magnitude of difference displayed as a histogram. The gap in the record of the Didcot Instruments sensor is due to the removal of the AWS logger over this period.

## A.3 Ditch and ground water levels

### A.3.1 Stage boards

In order to obtain accurate measurements of water levels within the ditches of the Elmley Marshes, stage boards have been constructed and installed at the end of the north-south and west-east piezometer transects, see Figure A.1 and Table A.3 for their location. Readings were made to an accuracy of within ± 0.01 m.

The stage boards have been constructed from 2.5 mm thick PVC sheets cut into 1.0 m by 0.1 m sections. These sections have been painted to provide centimetre graduations using the design provided by Shaw (1987). The installation of the stageboards at Elmley Marshes was undertaken in December 1997 at which time, ditches were at bankfull capacity making conditions difficult. The stageboards were fixed onto wooden stakes, which were then knocked into the ditch. The depth of burial of the bottom of the stageboard into the silt was determined to account for this error when taking a stage reading. As the stage boards were installed relatively near to the bank edges due to logistic reasons, the cross section of the

ditches were measured to relate the stage reading to the maximum water depth. Water depths reported are therefore the maximum water levels of the ditch.

A 3 2 Piezometers

There exists two series of piezometer nests in Elmley Marshes, the 'transect' series installed in 1995, and the 'pumped' series installed during May 1997 (Figure A.1 and Table A 3). The pumped series were installed so that pump test could be performed to determine saturated hydraulic conductivity rates. Both series share the following characteristics. Each piezometer site possesses a nest of three piezometers The first has its base at approximately 1 m below the soil surface, the second at 1.5 m and the third at 2 m. Data used in this thesis has been taken from the 1 m piezometers Each piezometer consists of a length of plastic pipe sealed at one end with a rubber bung. Above the bung the pipe is perforated for a length of approximately 0.1 m. Screw augers were used to create an access hole in the soil into which the piezometer was inserted. The use of this auger resulted in a close fit between the hole and piezometer tube. Once installed the open ends of the piezometers were sealed with a removable rubber bung to prevent the entry of surface water, and a layer of bentonite put down over the surface of the access hole to prevent soil cracking and ingress of water down the side of the piezometers. The immediate area around the top of each nest of three piezometers was excavated to a depth of around 0.05 m. A stone paving slab was placed in this access hole to prevent damage to the piezometers from trampling by the animals that graze the area. Figure A.7 shows a typical piezometer nest

Of the pumped series, three piezometers were used in this investigation. The piezometers are located along a transect running approximately north-south along a line normal to the north ditch of the study field (Figure A.1). The spacing of these piezometer nests is shown below in Table A 4

Figure A.7. The piezometer nest design of an access hole covered by a paving stone to fit flush with the ground to protect the piezometers from grazing animals. However, as shown, the access hole design is susceptible to inundation at times of surface flooding which necessitates pumping before a measurement can be taken. The piezometers are bunged to prevent water and soil entering the tube.

### A.3.3 Surface elevation

The elevation of the stage boards, piezometers, and neutron access tubes have been determined relative to Ordnance Datum using a level from a triangulation point close to the study field (seen in Figure 3.5 b and d). Table A.3 lists the elevation of the upper surface of the covering stone of each piezometer nest and the ditch bed where the stage board is inserted. The surveying accuracy was checked by standard procedure of computing the sum of all the foresight measurements and subtracting the sum of the backsights. When subtracted from the starting elevation the result should equal the elevation of the last point. When checked the surveying results were accurate to millimetre precision.

## A.4 Pressure Transducers

Druck PDCR830 pressure transducers were placed in the 1.5 m depth piezometers no. 1, 2 and 3. An additional transducer was also placed in the north ditch adjacent to the stageboard. The pressure transducers were installed to obtain continuous measurements of the change in groundwater levels, so that pump tests to establish the hydraulic conductivity of the soil at depth could be undertaken. The ditch water level data recorded by the transducer in the north ditch was used in the DITCH model (section 4.3.3).

Table A.3. Elevation at the base of the stageboards (ditch bed at point of stage board insertion) and upper surface of the slabs covering the piezometer nests (ground surface)

| Feature | Elevation m O D. | Grid reference |
|---|---|---|
| Triangulation Pillar | 1.5 | 594400 168400 |
| Upper surface of the stone covering each piezometer nest | | |
| 1 | 0 74 | 594701 168885 |
| 2 | 1 05 | 594701 168860 |
| 3 | 1 05 | 594701 168851 |
| A | 1.52 | 594796 168887 |
| B | 1.90 | 594754 168821 |
| C | 1 86 | 594755 168692 |
| D | 1 80 | 594793 168654 |
| E | 1 70 | 594769 168604 |
| F | 1.58 | 594749 168549 |
| G | 1.50 | 594731 168485 |
| H | 1 81 | 594485 168585 |
| I | 1.76 | 594585 168639 |
| J | 1.88 | 594667 168638 |
| K | 1 82 | 594836 168635 |
| L | 1.83 | 594891 168672 |
| M | 0.90 | 594934 168663 |
| Maximum depth of the ditches where the stage boards are inserted | | |
| North ditch | -0.77 | Adjacent to piezometer 1 |
| South ditch | 0.18 | Adjacent to piezometer G |
| East ditch | 0.23 | Adjacent to piezometer M |
| West ditch | 0.38 | Adjacent to piezometer H |

Table A.4. The spacing of the piezometers used for pump tests.

| Piezometer Nest | 1 | 2 | 3 |
|---|---|---|---|
| Distance from the north ditch (m) | 1 | 25 | 35 |

The transducers were connected to a Campbell CR10X logger recharged by a Solarex solar panel. A shallow trench was dug from the logger to the piezometer nests in order to bury the cables for protection. The pressure transducers operate by converting the pressure head of water above the sensor to a water depth Using this equipment hourly readings of water level in the ditch and piezometers has been recorded since October 1997. Some interruptions to the data set have occurred when reprogramming the logger for other uses and when two pressure transducers were removed to allow other instruments access to the logger. To ensure the pressure transducers were functioning normally, water levels were checked periodically by comparing logger output to measured water depths using a welldipper.

## A.5 Neutron probe

The use of the neutron probe, or neutron scattering meter, has become widely used in hydrology for non-destructive, repetitive measurements of soil moisture in the field to a high level of precision (Evett and Steiner 1995). In order to obtain direct measurements of soil moisture by the use of the neutron probe, three aluminium neutron probe access tubes have been installed at Elmley Marshes. Two tubes of depth 0 7 m were installed in December 1997, one in the main enclosure and the other alongside the north ditch, (Figure A.1). A tube of depth 1.7 m was installed in the main enclosure alongside the 0.7 m tube, in early April 1998. All neutron access tubes were installed in close fitting holes created with screw augers to ensure a close fit The neutron probe allows measurements of volumetric soil moisture of the soil from 0.2 m below the surface to the depth of the access tube. A dataset has been collected on field visits from 23 June 22 October 1998 before the probe malfunctioned due to a breakage in the $BF_3$ tube. The time taken to repair the neutron probe has been considerable, extending outside the monitoring programme, resulting in no further data collection with this instrument.

### A.5.1 The operation of the neutron probe

The principles and theory of neutron probe operation are discussed more fully by Bell (1981). Briefly the probe emits fast/high energy neutrons from an Americium-Beryllium radioactive source, which are slowed upon collision of the nuclei of (predominantly) atoms within the soil (thermalisation) (Chanasyk and Naeth 1996). The energy loss is greater upon collision with atoms low atomic weight than heavier atoms. In soils, the former is predominantly hydrogen with the result that the subsequent cloud of slow neutrons is a function of water content. A slow neutron detector within the probe counts the density of slow neutrons around the source, and thus the water content of the soil can be determined from the ratio of count rate at a given depth to a water standard.

A 5 2 Calibration

As calibration curves provided by probe manufacturers are frequently cited in the literature as incorrect (Carneiro and De Jong 1985), calibration of the instrument to the study soil is necessary. This can either be done in the laboratory using drums filled with soil and taking measurements under different water contents or preferably in the field, by taking samples upon installation of a neutron access tube, or from the near vicinity of the tube. The calibration is performed between volumetric soil moisture and the ratio of count rate at a given depth to a water standard rate takes the form of a linear regression.

$$\theta = m\frac{R}{RW} + c \qquad \text{Equation A.2}$$

Where:
$\theta$ is volumetric soil moisture $m^3\ m^{3\text{-}1}$
$m$ is the gradient of the regression line
$R$ is the count rate in the soil per depth increment counts per second
RW is the count rate in the water standard counts per second
c is the intercept on the moisture axis y-axis

Problems associated with gaining adequate calibrations for neutron probes in clay soils are reviewed by Grismer *et al.* (1995) who report results of a wide investigation into the calibration of the neutron probe and error analysis in soils with over 40% clay fraction. The investigation focused upon a number of issues including (of relevance to this study), whether calibrations based on soil samples taken from inside the access hole are better than those taken outside, the effect of swelling soils, and possible impact of chloride interference. The authors found that calibration using samples from the access hole during installation and those taken outside on later dates, had similar regression coefficient and estimation errors, but the number of samples required to characterise the soil moisture content increased with the latter. Provided soil was not compacted during tube installation, it was found that measurement errors were reduced when taking samples from the access hole. This approach has the advantages of being the simplest providing a more consistent calibration compared to other methods. The authors also found that regression improved when the neutron count was measured when the upper soil layers had begun to dry out, due to the calibration being based upon wider range of moistures and count ratios. Moreover the authors found that for field

calibrations, corrections for the volume changes due to swelling and shrinkage may not be necessary and correction did not always result in greater errors in water counts estimated from neutron count data. The reasons being that the entire profile shrinks and swells more or less consistently as the soil dries and is rewetted; that is, the field calibration reflects the combined effects of moisture content and volume change. Mitchell and van Genuchten (1993) also found that linear regression is suitable for moderately swelling clay soils with 30-40% clay fractions, but soil cracking adjacent to the access tube may be a significant factor adversely affecting the linear calibrations when developing a field calibration for a particular access tube. In addition Grismer *et al.* (1995) found that while salinity levels of their soil samples substantially increased with depth, a regression between count rate and chloride concentration was poor, with the chloride having little or no effect so that no adjustment is needed to reflect chloride adsorption.

### A 5 3 Sphere of influence

The volume of soil, 'sphere of influence', sensed during measurement is an important factor to be considered and is influenced by the soil water content. The concept of the sphere of influence was first proposed by van Bavel (1956), and developed by Mortier *et al.* 1960 and Olgaard (1965) cited in Visvalingham and Tandy (1972). It can be defined as the sphere which, if all the soil and water outside the sphere be removed, would yield 95% of the flux obtained in an infinite medium.

The sphere of influence is important as it affects accurate measurement of soil moisture at or near the soil surface, where the radius of the sphere extends above the dry-wet interface of the soil surface and atmosphere. Chanasyk and Naeth (1996) state that under such conditions, neutrons that pass out of the soil are not deflected back by the air in significant amounts leading to a lower count than is characteristic for the particular moisture content. This necessitates additional measurements of soil moisture to be made for the surface layer. Chanasyk and Naeth (1988) determined the sphere of influence to be approximately 0.2 m by comparing near-surface neutron probe readings with and without bags of water placed around the access tube. They found that the sphere radius remained unchanged for soil moistures in the range 16% to 32% by volume. Other attempts to measure the near surface

soil moisture content have been made Grant (1975) proposed taking neutron counts before and after a 0.1 m depth layer of soil about the access tube has been removed. After a comparison of the neutron readings, a correction for depth can be made. Other methods involve the use of aluminium or fibreglass trays (low neutron thermalisers) stored on site and filled with soil (Parkes and Siam 1979, Hanna and Siam 1980) They are placed over the access tube, flush with the soil surface, thus ensuring the sphere of influence does not extend into the air. Grismer *et al.* 1995 however report that for fine textured heavy clay soils measurements at depths between 0.15-0.30 m deep can be taken with confidence despite theoretical neutron losses at the surface.

A.5 4 Sources of measurement error

Haverkamp *et al.* (1984) stated that the estimation variance of determining a value of soil moisture using neutron scattering is composed of two terms: instrument and calibration components, with the former contributing the least source of error. Instrument error variance, the random counting error, can be minimised by increasing the counting time.
The random counting error, i.e. the distribution of individual estimates of mean count rate about the true mean count rate, is determined according to the formula (after Bell and Eeles 1967):

$$\sigma\theta = m\frac{R}{RW}\left(\frac{1}{Rt}+\frac{1}{RW\,tW}\right)^{0.5} \qquad \text{Equation A.3}$$

Where:
$\sigma\theta$ is the standard deviation of the soil moisture estimate
$t$ is the counting time seconds

The error variance about the soil moisture prediction of the regression calibration can be determined by an appreciation of the standard error of the estimate of soil moisture with the required confidence limits (Shaw and Wheeler 1998, Spiegel 1980):

$$\hat{Y} \pm SE_{\hat{Y}} \times t \qquad \text{Equation A.4a}$$

$$SE_{\hat{Y}} = \sqrt{\frac{\sum\left(Y-\hat{Y}\right)^2}{n}} * \sqrt{\frac{n}{n-2}} \qquad \text{Equation A.4b}$$

Where.
$\hat{Y}$ is the prediction of Y (volumetric soil moisture)
$SE_f$ is the standard error of the prediction of Y
$t$ is the critical statistic of the t-distribution for the given degrees of freedom and required confidence level.
$n$ is the number of observations

A.5.5 Calibration to the Wallasea soil series of the study site.

To calibrate the relationship between neutron scattering and soil moisture, soil samples were taken to a depth of 1.8m when installing the access tubes with a screw auger. Volumetric water content determined by oven drying, using bulk density values obtained from previous soil analysis, section 3.3.1.5. Soil samples were taken every 0.05 m from the surface to 0.7 m depth, thereafter every 0.1 m down to 1.8 m depth. A count, R, was performed immediately after the tube was installed. Counts were taken with a length of 64 seconds from 0.2 m depth, to account for the sphere of influence, at intervals in accordance with the soil samples taken. A standard water count, RW (value = 872.9), was taken in the adjacent ditch (north ditch), using a 16 minute count time. These count times were used when taking all measurements and chosen to maximise the precision of the count after Haverkamp *et al.* (1984).

Figure A.8 shows the linear regression applied to the calibration dataset. The correlation co-efficient is very strong at $r^2$=0.95. Also presented on Figure A.8 is the supplied manufacturer's calibration for clay soils. While it has been recognised that the use of the supplied calibration can yield incorrect values of soil moisture, it has been suggested that it can be used to determine the relative change in soil moisture over time rather than absolute. Chanasyk and McKenzie (1986) found that this to be incorrect however as the slope of the calibration derived by the authors differed from the manufacturers. The shift in slope indicates a difference in the count rate response to soil moisture, meaning that when using the manufacturer's curve, neither absolute values of soil moisture, nor soil moisture change over time can be determined accurately resulting in calibrations that are not directly comparable. The same situation is also found in this study where the supplied calibration not only overestimates, but also becomes steeper with increasing soil moisture relative to the derived calibration.

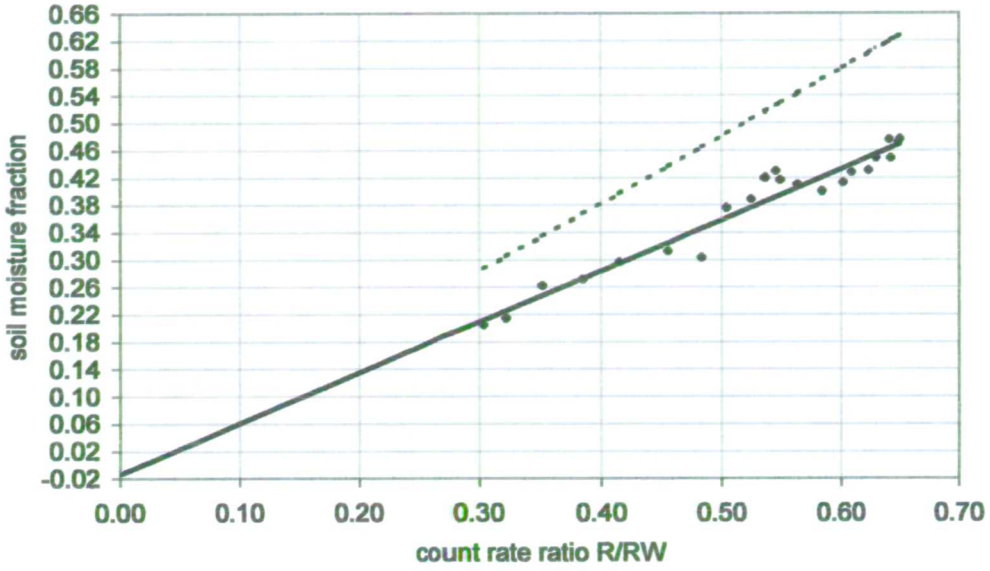


Figure A.8. The solid line represents the linear regression applied to the calibration dataset extended to intercept the y axis, with the observed soil moisture data. The correlation co-efficient is very strong at $r^2$=0.95. The dashed line represents the manufacturer's calibration for the same dataset.

The random counting error of the neutron probe was also determined after Equation A.2:

$$\sigma\theta = m\frac{R}{872.9}\left(\frac{1}{R\ (16)} + \frac{1}{872.9\ (16*60)}\right)^{0.5}$$

The regression between R/RW and volumetric soil moisture, and the random counting error can be seen in Figure A.9. As an example, using the average count rate over the soil profile, the random counting error for the 95% confidence interval is equal to 0.46% volumetric soil moisture. That is, there is a 95% probability that the soil moisture determination is within 0.46% either side of the mean. This is extremely precise due to the choice of long count rates. It can be seen from Figure A.9 that the random counting error of the neutron probe falls well within the 95% confidence levels of the regression line fitted to the R/RW and volumetric soil moisture data. The 95% confidence levels of the regression line indicate estimated moisture contents calculated from the regression equation are within ±4.2% at the

95% level. Details of the measurement error for the regression calibration and random counting error of the neutron probe are displayed in Table A.5.

## A.6 Capacitance Technique

The theory of the capacitance method, of such instruments as the Surface Capacitance Insertion Probe (SCIP) and ThetaProbe, is based on the differences between the dielectric constants of water (80), soil solids (2-4) and air (1) (Robinson and Dean 1993). Soil is composed of varying proportions of air, soil solids and water and thus the dielectric content of soil is sensitive to the amount of water due to the high value of its dielectric constant compared to other components. The sensitivity of soil dielectric constant to water is well known; Dean *et al.* (1987) cite a volume of literature that covers the dielectric constant of soil and instruments designed to measure soil moisture using this approach. The term 'dielectric' refers to the free electrical charges contained by a substance and thus the dielectric constant is positively related to the conductivity of the substance. A poor conductor has few free electrons and thus has a low value for its dielectric constant (Curran 1985).

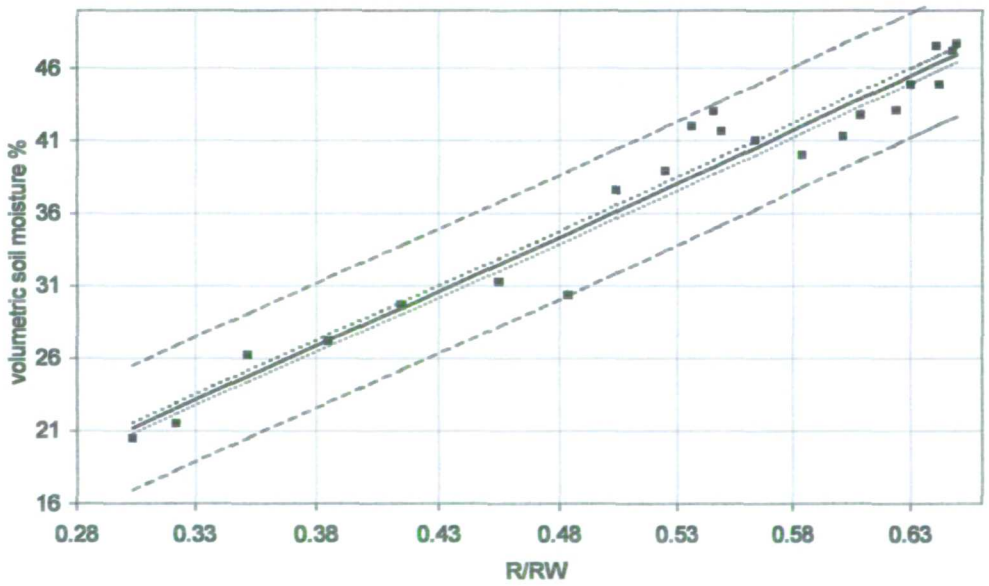


Figure A.9. The regression between R/RW and volumetric soil moisture, and the random counting error of the neutron probe. The solid line represents the regression line applied to the calibration dataset with the observed soil moisture data represented as dots. The correlation co-efficient is very strong at $r^2$=0.95. The outer and inner dashed lines represent the 95% confidence interval of the regression line and the standard counting error respectively.

Table A.5. Details of the regression error (Equation A 4) and the random counting error (Equation A.3) for the neutron probe per depth increment. Both errors are expressed at the confidence level 95%

| Depth below surface m | R/RW (RW 872.9) | Observed Vol. Soil Moisture % | Predicted Vol. Soil Moisture % | Regression error ± Vol. Soil Moisture % | Random counting error ± Vol. Soil Moisture % |
|---|---|---|---|---|---|
| 0.2 | 0.30 | 20.47 | 21 19 | 4.29 | 0.35 |
| 0.25 | 0.32 | 21.50 | 22 55 | 4 29 | 0.36 |
| 0.3 | 0 35 | 26 21 | 24 77 | 4 29 | 0.38 |
| 0.35 | 0.38 | 27.15 | 27.24 | 4.29 | 0.40 |
| 0 4 | 0.41 | 29 64 | 29 46 | 4 29 | 0.41 |
| 0 45 | 0.45 | 31.24 | 32.44 | 4.29 | 0.43 |
| 0.5 | 0.48 | 30.32 | 34 57 | 4.29 | 0.45 |
| 0.55 | 0.50 | 37.57 | 36 11 | 4.29 | 0.46 |
| 0.6 | 0.52 | 38.88 | 37 64 | 4.29 | 0.47 |
| 0.65 | 0.54 | 42.00 | 38 5 | 4.29 | 0.47 |
| 0.7 | 0.55 | 43.00 | 39.18 | 4.29 | 0.48 |
| 0.8 | 0.55 | 41.63 | 39.44 | 4.29 | 0.48 |
| 0.9 | 0.56 | 41.00 | 40 5 | 4.29 | 0.48 |
| 1 | 0 58 | 40.00 | 42 04 | 4.29 | 0.49 |
| 1.1 | 0.60 | 41.29 | 43 36 | 4 29 | 0.51 |
| 1.2 | 0.61 | 42.76 | 43.91 | 4.29 | 0.50 |
| 1.3 | 0.62 | 43.09 | 45 02 | 4.29 | 0.51 |
| 1.4 | 0.64 | 44 86 | 46 39 | 4.29 | 0.52 |
| 1.5 | 0.65 | 47.68 | 46.94 | 4.29 | 0.52 |
| 1.6 | 0.65 | 47.15 | 46 81 | 4.29 | 0.52 |
| 1 7 | 0 64 | 47 52 | 46 3 | 4 29 | 0.52 |
| 1.8 | 0 63 | 44.87 | 45 48 | 4.29 | 0.51 |
| Details of the regression calibration | | | | | |
| Gradient m | 74 44 | | | | |
| Intercept c | -1.4139 | | | | |
| Analysis of variance | Sum of squares | Degrees of freedom | Variance | F-ratio. Critical (95%) = 4 35 | |
| Regression | 1421.92 | 1 | 1421.922 | 368 3 | |
| Residual | 77 21 | 22-1-1 | 3 86 | | |
| Total | 1499.14 | 22-1 | | | |
| $r^2$ | 0 95 | | | | |

## A 6 1 Surface Capacitance Insertion Probe

As the neutron probe does not accurately quantify the soil water in the top 0 2 m soil layer, a Surface Capacitance Insertion Probe, Figure A.10, was employed to monitor this important surface organic soil layer. The development of the capacitance probe by the Institute of

Hydrology in the early 1980s was initiated by this inability of the neutron probe to accurately measure the surface moisture content (Dean 1994). Two probe designs were produced, an access tube probe and a surface probe (SCIP). The access tube probe is designed to be used in pipes inserted into the soil, similar to the neutron probe set-up. It is the SCIP that is used in this project and all subsequent referrals to the 'capacitance probe' refer to this design. The probe allows the measurement of the surface 0.05 m and 0.1 m soil water content based on a calibration relating the dielectric constant of soil and water. The traditional method of obtaining soil moisture data is from oven drying samples is destructive to the site, and time and resource intensive. In view of these drawbacks, the method is unsuitable for regular sampling over large areas. The SCIP technique allows a non radioactive and non-destructive method of obtaining soil moisture measurements quickly and easily in space and time
Dean (1994) contains a full description of the physics of the measurement of dielectric constant by the capacitance probe; only a short summary is presented here. In order to obtain a value of the dielectric constant of a material, it is introduced into the electrical field of a capacitor, and the change in capacitance from air to that of the material recorded The rods of the SCIP act as the capacitor through which an alternating current of frequency 100 MHz is applied. As the capacitor is part of an oscillator circuit, the change in oscillator frequency results from the dielectric constant of the soil. Thus in order to take a measurement in soil, the rods are pushed into the ground ensuring full contact of the rods with the soil, and a reading taken immediately. Readings may range from 90-150 MHz for wet and dry soil respectively (Robinson and Dean 1993).

The range of sensitivity of the probe is approximately 0 04 m diameter around the rods; this is compared to 0.15 - 0.50 m of the neutron probe (depending upon soil type) but does not vary with soil moisture content unlike the neutron probe (Robinson and Dean 1993). The length of the rods is 0.1 m but the use of the polyacetate spacer will reduce this length to 0.05 m if required. The probe measures the arithmetic average of soil moisture along the length of the rods (Dean 1994). In this study only measurements using the full rod length of 0.1 m were of interest and so only a calibration for this depth has been undertaken.

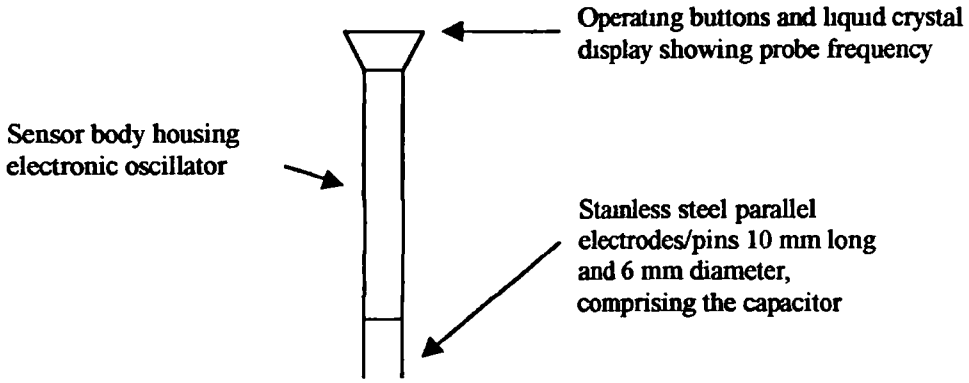


Figure A.10. The design of the Surface Capacitance Insertion Probe.

## A.6.2 Calibration procedure

Dean (1994) separated the response of the capacitance probe to oscillation frequency into two parts:

Function 1 Oscillation frequency = $f$ Er

Function 2 $\theta = f$ Er

Where:
*Er* is the dielectric constant
$\theta$ is volumetric soil moisture

The first function relates to the laboratory calibration of the probe oscillation frequency to dielectric constant. This function has been theoretically and empirically tested and is determined in the laboratory using four liquids of known dielectric constant: chloroform, acetone, ethanediol and water. As the liquids used can be treated as standards, the probe stability and the precision of the calibration can be determined This calibration, specific to each individual probe and for both 0.05 and 0.1 m depth, then allows the derivation of constants a, b and c for the conversion of the displayed reading of oscillator frequency to dielectric constant. This calibration is done by the manufacturer for each probe.

The second function involves the calibration of the dielectric constant to soil moisture content. Calibration is achieved using soil samples covering a range of soil moisture contents. Field calibration was undertaken by taking a reading and collecting a soil core sample immediately afterwards from the exact area covered by the rods to ensure the water content of the same area of soil obtained.

This exact match is favoured over taking several measurements close together and using an average as it avoids the introduction of spatial variability (Dean 1994). The core obtained is of the same length of the rods of the probe. The volumetric soil moisture of the core was determined by gravimetric drying and employing bulk density values, Er. The probe reading, R, is input into Equation A.5 to determine the dielectric constant, $Er$. The calibration is then found using a non-linear equation plotting $\sqrt{Er}$ as a function of volumetric water content θ and dry bulk density $\rho d$ (Equation A.6).

$$Er = \frac{a}{(R^2 - b) - c} \qquad \text{Equation A.5}$$

$$\theta = \frac{\left(\sqrt{Er} + d - f.\rho d\right)}{e} \qquad \text{Equation A.6}$$

Where:
$Er$ is dielectric constant
$R$ is oscillator frequency (probe output/10000)
$a$, $b$, $c$ are coefficients specific to each probe and depth (i.e. 0.05 m or 0.1 m)
$d$, $e$, $f$ are regression parameters
$\theta$ is volumetric soil moisture $m^3\ m3^{-1}$
$\rho d$ is dry bulk density of the soil layer $g\ cm^{-3}$

A.6 3 Problems of calibration

Bell *et al.* (1987) issued a caveat that the traditional definition of soil water, and the water in the soil that is measured by the capacitance probe may not be the same. The traditional method for gravimetric soil moisture defines water content as the amount of water expelled by oven drying at 105 °C for 24 hours This method succeeds in evaporating most water held by surface tension forces in varying pore sizes and shapes, water films on particle surfaces in addition to water from the hydration of certain minerals. Soil type is important through its

influence of particle size and moisture retention characteristics. The frequency response of the capacitance probe depends upon the water molecules that are least strongly held by surface absorption forces, as these molecules are the ones that have a degree of relaxation to allow dipole response to the electrical field of the capacitor. Thus only part of the total water content as determined by gravimetric sampling is responsible for the probe response. The neutron probe is also identified by Bell *et al.* 1987) as not sharing the same definition as gravimetric soil moisture. In this case, the neutron probe responds to all forms of hydrogen in the soil, a significant proportion of which may not be expelled by standard gravimetric drying procedures. Bell *et al.* (1987) state however that until the development of calibration procedures that are independent of soil type, calibration against gravimetric methods is satisfactory for operational use if the user is prepared to accept the need for calibrating each soil.

A.6 4 Calibration to the Wallasea Series

The calibration procedure as described above was undertaken. Soil samples were taken from the study field covering a range of moisture contents. The samples were taken using a core tube to ensure that the exact length of sample could be obtained. Calibration was only undertaken for the 0.1 m rod length.

As discussed in section 3.3.1.5, the dry bulk density of Elmley soils is a variable that has proven difficult to measure. The holes in the soil produced by the action of pushing the rods of the probe into the soil were retained when the probe is withdrawn. The volume of the holes may have resulted in soil compression which, although its effect may be slight, may be significant due to the narrow core taken (taken due to the narrow sphere of influence of the probe) and the sensitivity of the bulk density of the clay soil. Also the creation of voids in the sample would have produced unreliable bulk density values.
In view of this, it was decided to use an average value of dry bulk density calculated from sampling efforts prior to capacitance sampling, as these samples were handled with the utmost care.

In order to calibrate dielectric constant to θ, the calibration of the frequency oscillation was firstly undertaken using the calibration specific to the instrument. Then Er was related to θ, using Function 2

As there is some debate over the comparative soil water contents of standard gravimetric techniques and the capacitance method and that the calibration for Elmley concerns a clay soil that has strong moisture retention characteristics, it was decided to conduct an experiment into the length of drying time required for Elmley soils. This was undertaken to ascertain whether or not 24 hours was a suitable time period for drying the samples.
The 15 calibration samples were oven dried at 105 °C as standard but weighed after drying periods of 5, 24, 26, 27, and 46 hours had been completed. There was negligible change in weight, i.e. increased water loss, after 24 hours, which meant this was a suitable time period for drying soil samples.

Use of Equation A.6 and a value of bulk density of 0.7 g $cm^{-3}$ to derive a relation between $\sqrt{Er}$ and volumetric soil moisture produces the formula:

$$\theta = \frac{\left(\sqrt{Er} + 0.92 - 1.11.\rho d\right)}{0.23}$$

Figure A.11 shows the linear regression applied to the calibration dataset. The co-efficient of determination is very strong at $r^2$=0.98. The 95% confidence intervals of the regression line are also presented and it can be seen that the variance is relatively high compared to the neutron probe calibration, due to the smaller sample size. Details of the measurement error for the regression calibration are displayed in Table A.6.

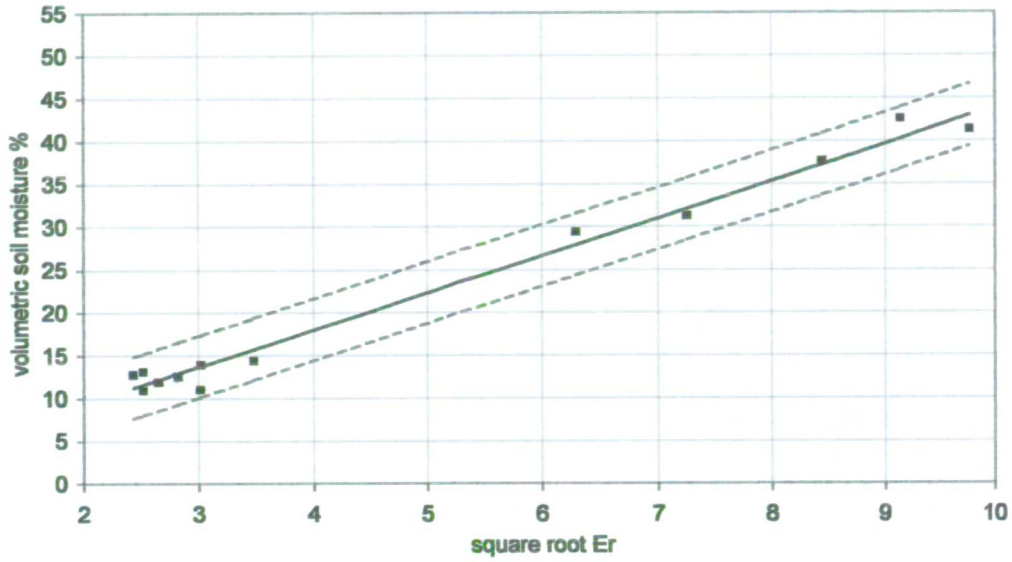


Figure A.11. The regression between √Er and volumetric soil moisture for the SCIP. The solid line represents the regression line applied to the calibration dataset with the observed soil moisture data represented as dots. The co-efficient of determination is very strong at $r^2$=0.98. The dashed lines represent the 95% confidence interval of the regression line.

Table A.6. Details of the regression error (Equation A.4) for the SCIP. Regression errors are expressed at the confidence level 95%.

| Sample | $\sqrt{Er}$ | Observed vol. soil moisture % | Predicted vol. soil moisture % | Regression error ± vol. soil moisture % |
|---|---|---|---|---|
| 1 | 3.02 | 13.88 | 13.72 | 3.6 |
| 2 | 3.47 | 14.30 | 15.68 | 3.6 |
| 3 | 3.02 | 10.95 | 13.70 | 3.6 |
| 4 | 2.65 | 11.89 | 12.12 | 3.6 |
| 5 | 2.52 | 13.06 | 11.56 | 3.6 |
| 6 | 2.43 | 12.70 | 11.17 | 3.6 |
| 7 | 2.52 | 10.89 | 11.56 | 3.6 |
| 8 | 2.82 | 12.50 | 12.87 | 3.6 |
| 9 | 6.29 | 29.32 | 27.91 | 3.6 |
| 10 | 7.25 | 31.26 | 32.06 | 3.6 |
| 11 | 8.44 | 37.62 | 37.24 | 3.6 |
| 12 | 9.77 | 41.28 | 43.00 | 3.6 |
| 13 | 9.14 | 42.51 | 40.25 | 3.6 |
| Details of the regression calibration | | | | |
| Analysis of variance | Sum of squares | Degrees of freedom | Variance | F-ratio. Critical (95%) = 4.84 |
| Regression | 1835.38 | 1 | 1835.38 | 788.28 |
| Residual | 25.61 | 13-1-1 | 2.33 | |
| Total | 1860.99 | 13-1 | | |
| $r^2$ | 0.98 | | | |

## A.7 ThetaProbe and Equitensiometer

The ThetaProbe design (Delta-T Devices 1998a) resembles a smaller version of the SCIP with four steel pins, of length 0.06 m, which is inserted in the soil and left *in situ* to determine the volumetric water content at the same point over time. Like the SCIP, the device works on the principle of the difference in dielectric constant between soil and water with the steel pins acting as a capacitor.

The Equitensiometer (Delta-T Devices 1998b) comprises a ThetaProbe whose pins are embedded in a porous media, and which, like the ThetaProbe, is inserted into the soil and left *in situ*. The porous media has a known stable relationship between water content and matric potential. When inserted in the soil, the matric potential within the equilibrium body equilibrates to the surrounding soils. The water content of the porous material is measured by the ThetaProbe and output as a voltage which can be converted to matric potential using the calibrate curve specific to each instrument. It is not necessary to undertake any further calibration.

These instruments became available for use in this project from May 1998 and were monitored during field visits until connected to a datalogger from January 1999 to output continuos measurements. They are buried in the soil so that the pins cover a soil depth of 0.1 – 0.16 m.

### A.7.1 Calibration of the ThetaProbe to Wallasea soil series

The calibration of the ThetaProbe follows the same approach as the SCIP in that the relationship between probe output and the square root of dielectric constant, $\sqrt{Er}$, follows the manufacturer's relationship (Equation A.7), and soil specific calibration relates $\sqrt{Er}$ to volumetric soil moisture (Equation A.8). The calibration procedure outlined in the instrument manual (Delta-T Devices 1998a) involves taking a voltage reading of the wet soil sample and again when dried. The $\sqrt{Er}$ is determined for the wet and dry sample readings, $a_1$ and $a$ respectively.

$$\sqrt{Er} = 1.07 + 6.4V - 6.4V^2 + 4.7V^3 \qquad \text{Equation A.7}$$

Where:

$\sqrt{Er}$ is the square root of dielectric constant
V is the voltage output of the ThetaProbe

The relationship between volumetric water content and the square root of dielectric constant:

$$\theta = \frac{\sqrt{Er} - a}{a_1}$$ Equation A.8

Where:
$\theta$ is the volumetric water content
$a_0$ is the dielectric constant of the soil sample when dried
$a_1$ is the dielectric constant of the soil sample when wet

When following the above approach, the predicted soil moisture values generated by Equation A.8 as both high soil moistures were underestimated and low soil moistures overestimated when compared to observed soil moisture of the samples. It was found that the following linear approach instead provided a closer fit to observed data:

$$\theta = b + a_1\left(\sqrt{Er} - a_0\right)$$ Equation A.9

Where:
b is a constant of value –9.3056
$a_1$ and $a_0$ have a value of 14.02 and 1.48 respectively.

The regression between √Er and volumetric soil moisture using Equation A.9 can be seen in Figure A.12, which also displays the 95% confidence levels of the regression line. The confidence levels of the regression coefficient indicate predicted soil moisture calculated from the regression equation is within ±5.9% at the 95% level. This is high due to the small number of samples. Details of the measurement error for the regression calibration of the ThetaProbe are displayed in Table A.7.

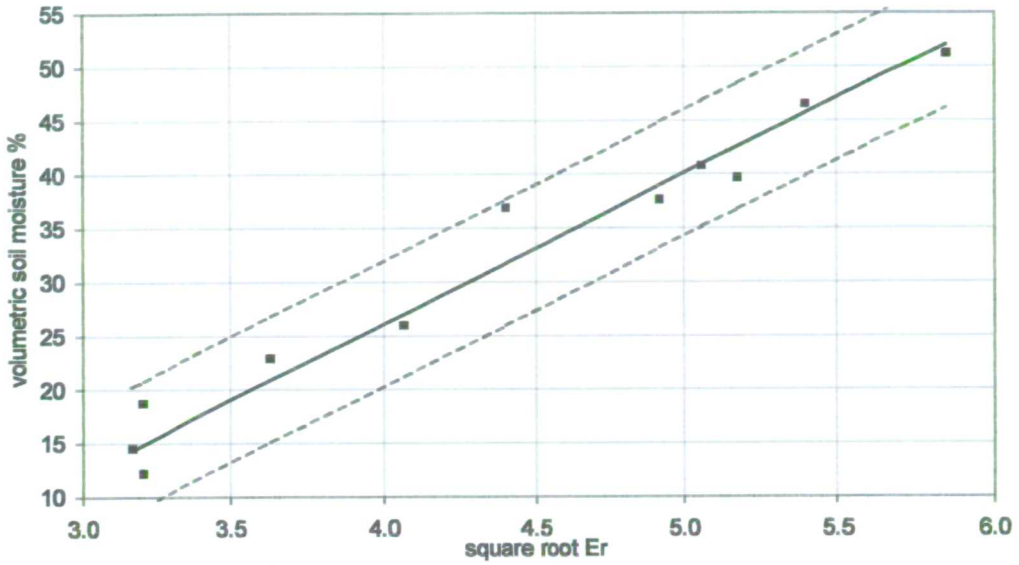


Figure A.12. The regression between √Er and volumetric soil moisture for the ThetaProbe. The solid line represents the regression line applied to the calibration dataset with the observed soil moisture data represented as dots. The co-efficient of determination is very strong at $r^2$=0.97. The dashed lines represent the 95% confidence interval of the regression line.

Table A.7. Details of the regression error (Equation A.3) for the ThetaProbe. Regression errors are expressed at the confidence level 95%.

| Sample | $\sqrt{Er}$ | Observed vol. soil moisture % | Predicted vol. soil moisture % | Regression error Volumetric soil moisture % |
|---|---|---|---|---|
| 1 | 4.40 | 36.87 | 31.75 | 5.92 |
| 2 | 5.40 | 46.47 | 45.68 | 5.92 |
| 3 | 5.85 | 51.14 | 52.01 | 5.92 |
| 4 | 5.17 | 39.64 | 42.57 | 5.92 |
| 5 | 5.06 | 40.76 | 40.95 | 5.92 |
| 6 | 4.92 | 37.61 | 38.98 | 5.92 |
| 7 | 4.07 | 25.93 | 27.01 | 5.92 |
| 8 | 3.63 | 22.87 | 20.91 | 5.92 |
| 9 | 3.20 | 12.18 | 14.90 | 5.92 |
| 10 | 3.20 | 18.68 | 14.88 | 5.92 |
| 11 | 3.17 | 14.49 | 14.42 | 5.92 |
| 12 | 3.16 | 13.16 | 14.34 | 5.92 |
| Details of the regression calibration | | | | |
| Analysis of variance | Sum of squares | Degrees of freedom | Variance | F-ratio. Critical (95%) = 4.96 |
| Regression | 2127.56 | 1 | 21.27.56 | 352.92 |
| Residual | 66.31 | 12-1-1 | 6.0284 | |
| Total | 2193.87 | 12-1 | | |
| $r^2$ | 0.97 | | | |

## A.8 Electrical resistance blocks

Bouyoucous and Mick (1940) were the first to embed electrodes onto a porous medium block which when buried in soil provided a method of monitoring soil moisture indirectly through the measurement of soil electrical resistance. Reynolds *et al.* (1987 p237) describes the operation of the blocks or cells as operating 'on the principle that water content within a cell responds to the suction from the water content of the surrounding soil, which results in a change in the electrical resistance between the electrodes embedded in the porous medium'. King (1967) state that the 'resistance between the electrodes depends on the amount of water in the surrounding porous material, which in turn depends upon the relative affinity of the soil and porous material for moisture, the amount of moisture present, the rate that water transfer can be made from one material to the other, and the electrical conductivity of the moisture or solution that is within the electrical influence of the electrodes'.

The most important of these factors, for the employment of the units in the Wallasea soil series, is the effect of the electrical solution i.e. the soil solution salinity. Originally composed of gypsum, blocks composed of alternative porous materials exist such as, for example, nylon, fibreglass and plaster of Paris, each of which have d'fferent advantages (Kings 1967). For example, gypsum blocks create an electrolyte by self-dissolution and so erode over time, but are insensitive to changes in soil salinity. Plaster of Paris blocks maintain a saturated solution in the bock and so are likewise affected less by changes in the salt content of the soil solution compared to fibreglass units, but the latter are often selected for long term burial due to their relative stability. Fibreglass cells have been used at the study site.

The susceptibility of the electrical resistance blocks (ERB) to salinity is one of the great disadvantages of using this technique Other disadvantages include the variability that can exist between cells, degradation of certain blocks and loss of contact with the block and soil, slow reaction to soil water change which can give rise to hysteresis effects during wetting and drying cycles, and the difficulties of establishing suction equilibrium with the soil for highly porous blocks (Livingston 1993).

However the advantages of the blocks include the facts they are inexpensive and easy to install and use, and can provide regular soil moisture data in the surface soil layers not monitored by the neutron probe. This has lead to the installation of two sets of four fibreglass cells in the AWS enclosure on the Elmley Marshes. The cells were inserted into the soil at parallel depths of 0-0.05 m, 0.05 - 0.1 m, 0.1 – 0 15 m and 0.15 – 0.2 m, with one set buried close to the neutron probe tubes in the enclosure and the other set buried few metres away.

In order to assess the effect of soil salinity of the Wallasea Series at Elmley Marshes upon the resistance blocks, soil samples have been taken to determine the electrical conductivity (section 3.3.1.7). The method outlined by Rowell (1997) and Hazelden *et al.* (1986) of a 1.5 soil: water extract of the soil was followed. The results of the experiments are presented in Table 3.10 and show that the surface soil electrical conductivity can be classified as non-saline to very slightly saline. This is the soil layer in which the ERBs are buried, and so it is assumed that at this depth the level of salinity is low enough to enable the blocks to function as normally as in a soil classified as non-saline.

### A.8.1 Calibration to the Wallasea series

The relationship between resistance and volumetric soil moisture follows a linear form after both variables have been transformed through a natural log:

$$\ln(\theta) = a \ln(\Omega) + b \qquad \text{Equation A.10}$$

Where:
$\ln(\theta)$ is the natural log of predicted volumetric soil moisture %
$\ln(\Omega)$ is the natural log of resistance ohms
$a$ and $b$ are constants

The resistance blocks were installed within the main enclosure of the study field (Figure A.1) before a calibration was performed. While the standard procedure is to calibrate the individual cells to be employed prior to burial, in this case calibration after a period of use allowed the examination of whether the cells could withstand the soil conditions However this also meant that as the cells performed well, it was decided to keep them embedded in the soil and use spare cells to generate a calibration equation. Reynolds *et al.* (1987) issues the

caveat that although cell manufacture is standardised, each individual cell may contain differences in response, which could warrant generating a calibration equation for each individual cell, employed However 'theoretically, if differences among cells are random and minimal, a random sample of cells can be used to generate a calibration curve for a population of cells in a particular soil type' (Reynolds *et al.* 1987 p237) It is assumed that the differences in response between the cells used to produce a calibration with an undisturbed soil block in the laboratory can be used to indicate the variability of the cells *in situ*. This would allow data to be collected from the cells buried *in situ*, while the calibration procedure is being undertaken, allowing a longer period of monitoring

In addition, while the conductivity of the upper soil layers in the main enclosure can be classified as only very slightly saline, section 3.3.1.7, the influence upon the resistance cells of any physical change of the soil within the top 0.2 m of soil needs to be examined. The upper 0.2 m of the soil profile can be divided into two horizons, 0-0 1 m and 0.1–0.2 m based on the greater intensity of roots and organic matter in the upper layer, section 3.3.1.4.

It was the aim of the calibration exercise therefore to ascertain whether or not one regression equation could be employed to predict soil moisture regardless of depth and individual cell. This would allow a simplified approach to predict soil moisture from the eight cells at the study field. Thus the null hypothesis was stated that there is neither a significant variability in response between individual cells nor a significant difference in the calibration between the two soil horizons.

A.8 2 Procedure

Two large blocks of soil of 0.3 m depth dug from within the main enclosure were subsampled in the laboratory to provide four undisturbed soil blocks for calibration. Two electrical resistance cells were inserted into the soil block cut from the 0-0.1 m depth soil layer and similarly for the block cut from the 0.1-0.2 m layer. The blocks were soaked in distilled water to achieve maximum saturation. Measurements were taken only as the soil blocks dried out i.e. the drying limb of the soil moisture curve, due to the problem of ensuring the soil block is uniformly wetted when taking measurements on the wetting limb.

This procedure was undertaken twice i.e. the blocks were soaked and dried twice to generate data point for calibration, before the samples were oven dried to obtain volumetric water contents. Of 80 data points generated by the calibration procedure 31 (39%) had to be rejected due to resistance reading of infinity. As stated by Reynolds *et al.* (1987) the values of infinity represent values of soil moisture for which no calibration is required as they are very low (for example approximately 3%) and so below the wilting point. Due to the non-linear response of resistance and soil moisture, the moisture and resistance data were log normally transformed before the start of data analysis.

Regression equations for each cell employed in the analysis were derived, and all resistance: soil moisture observations were bulked to derive a relationship regardless of depth or cell. For all cases the correlation was strong with $r^2$ above 0.9; the small unexplained variability between the resistance and soil moisture generated by chemical and structural heterogeneity in the soil and also the existence of cell to cell variability together with random sampling errors.

Next the regressions were applied to generate predictions of volumetric soil moisture, from the entire dataset of resistance readings, upon which analysis of variance was performed to test the significance of the difference in response. The results indicate with F below the critical level the null hypothesis can be accepted i.e., variability between cells and with depth is insignificant, and that a sole regression can be employed for the cells *in situ* (Figure A.13). Table A.8 displays the ANOVA results and Table A.9 has the regression details of the final calibration.

Table A.8. The results of ANOVA. The critical values of F and P value are expressed to the 95% confidence level.

| Groups | No. of observations | Sum | Mean | Variance | |
|---|---|---|---|---|---|
| Cell 1 0-1 m | 47 | 147.81 | 3.14 | 0 33 | |
| Cell 2 0-1 m | 47 | 161.04 | 3.43 | 0.31 | |
| Cell 3 0 1-0.2 m | 47 | 163.58 | 3.48 | 0.65 | |
| Cell 4 0 1-0 2 m | 47 | 163 84 | 3.49 | 0 47 | |
| All | 47 | 160 14 | 3 41 | 0 40 | |
| Source of Variation | Sum of squares | Degrees of freedom | Variance | F-ratio | F critical value |
| Between Groups | 3 72 | 4 | 0 93 | 2.15 | 2.41 |
| Within Groups | 99 62 | 230 | 0.43 | | |
| Total | 103 33 | 234 | | | |

Table A.9. Details of the regression error (Equation A.3) for the electrical resistance blocks. Regression errors are expressed at the confidence level 95%

| Sample | ln(resistance ohms | Observed ln(vol soil moisture % | Predicted ln(vol. soil moisture % | Regression error ln(soil moisture) Volumetric soil moisture % given in square brackets |
|---|---|---|---|---|
| 1 | -2 30 | 4 36 | 4 22 | 0 23 [1.25] |
| 2 | -2 30 | 4 19 | 4 22 | 0 23 [1 25] |
| 3 | -2 30 | 3 98 | 4 22 | 0.23 [ .25] |
| 4 | -1 74 | 4 41 | 4 09 | 0 23 [ 25] |
| 5 | -1 74 | 4 38 | 4 09 | 0 23 [1 25] |
| 6 | -1 74 | 3.99 | 4 09 | 0 23 [1.25] |
| 7 | -1 74 | 3 86 | 4 09 | 0 23 [1 25] |
| 8 | -1 66 | 4.23 | 4 07 | 0.23 [1 25] |
| 9 | -1.66 | 3 87 | 4 07 | 0 23 [1 25] |
| 10 | -1 66 | 3 80 | 4 07 | 0.23 [1 25] |
| 11 | -1 61 | 4 19 | 4 06 | 0 23 [1 25] |
| 12 | -1 61 | 4 13 | 4 06 | 0 23 [1.25] |
| 13 | -1.61 | 4 13 | 4 06 | 0 23 [1.25] |
| 14 | -0 92 | 3.62 | 3 89 | 0 23 [1.25] |
| 15 | -0.69 | 3.88 | 3 84 | 0 23 [1.25] |
| 16 | -0 51 | 3 78 | 3 80 | 0 23 [1.25] |
| 17 | -0.11 | 3 99 | 3.70 | 0 23 [1 25] |
| 18 | 0 00 | 3 99 | 3.68 | 0.23 [1.25] |
| 19 | 0 33 | 3 10 | 3 60 | 0 23 [1.25] |
| 20 | 0.34 | 3 31 | 3.60 | 0.23 [1.25] |
| 21 | 0.47 | 3 81 | 3.57 | 0.23 [1.25] |
| 22 | 0.59 | 3.75 | 3.54 | 0 23 [1 25] |
| 23 | 0 59 | 3.27 | 3.54 | 0.23 [1.25] |
| 24 | 0 69 | 3.74 | 3.51 | 0.23 [1.25] |
| 25 | 0.92 | 2 93 | 3 46 | 0.23 [1.25] |
| 26 | 0 99 | 3.08 | 3.44 | 0.23 [1.25] |
| 27 | 1 01 | 3 42 | 3 44 | 0 23 [1.25] |
| 28 | 1.25 | 3 64 | 3.38 | 0.23 [1.25] |
| 29 | 1.32 | 3 48 | 3.36 | 0.23 [1.25] |
| 30 | 1.50 | 3.39 | 3.32 | 0.23 [1.25] |
| 31 | 1.50 | 3.14 | 3.32 | 0.23 [1.25] |
| 32 | 1 61 | 3 46 | 3 30 | 0 23 [1.25] |
| 33 | 2 44 | 3 30 | 3.10 | 0 23 [1.25] |
| 34 | 2.48 | 3 35 | 3.09 | 0 23 [1.25] |
| 35 | 2 48 | 3 07 | 3 09 | 0 23 [1.25] |
| 36 | 2.77 | 2 80 | 3.02 | 0.23 [1.25] |
| 37 | 3 00 | 3 05 | 2.97 | 0.23 [1 25] |
| 38 | 3 40 | 2 97 | 2 87 | 0 23 [1 25] |
| 39 | 3 69 | 3.06 | 2 80 | 0 23 [1.25] |
| 40 | 4 79 | 2 49 | 2 54 | 0 23 [1.25] |
| 41 | 5 19 | 2 66 | 2 45 | 0 23 [1.25] |
| 42 | 5 19 | 2 61 | 2 45 | 0 23 [1 25] |
| 43 | 5 70 | 2 01 | 2 33 | 0.23 [1.25] |
| 44 | 5 86 | 2 20 | 2 29 | 0 23 [1.25] |
| 45 | 6 21 | 2 27 | 2 21 | 0 23 [1.25] |
| 46 | 6 21 | 2 02 | 2 21 | 0.23 [1.25] |
| 47 | 7 31 | 1 91 | 1 95 | 0 23 [1.25] |

| Details of the regression calibration | | | | |
|---|---|---|---|---|
| Analysis of variance | Sum of squares | Degrees of freedom | Variance | F-ratio Critical (95%) = 4 052 |
| Regression | 121 5205 | 1 | 121 5205 | 9538 00 |
| Residual | 0 5733 | 47-1-1 | 0 0127 | |
| Total | 122 0939 | 47-1 | | |
| $r^2$ | 0 99 | | | |

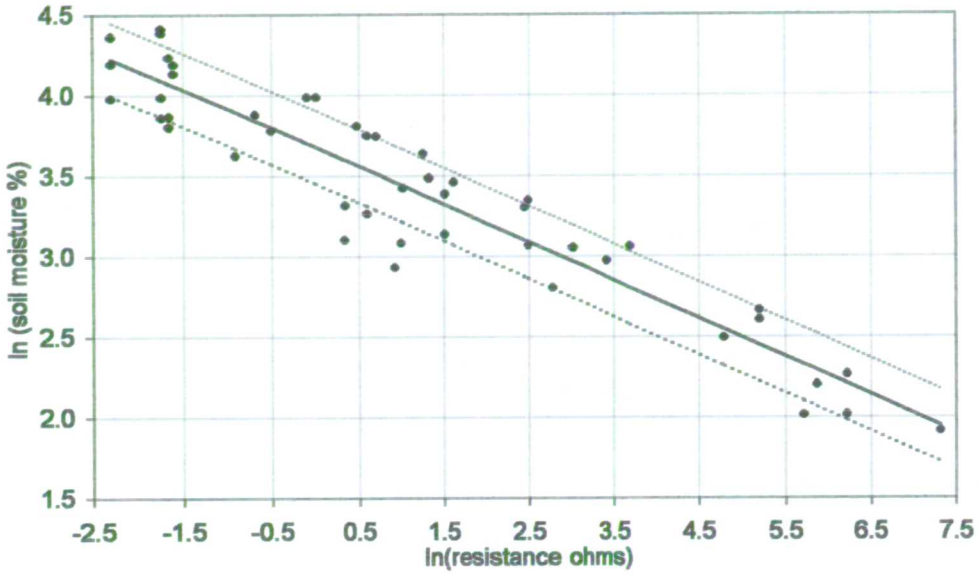


Figure A.13. The regression between ln(soil moisture) and ln(resistance) moisture for all cells regardless of depth for the ERBs. The solid line represents the regression line applied to the calibration dataset with the observed soil moisture data represented as dots. The co-efficient of determination is very strong at $r^2$=0.99 The dashed lines represent the 95% confidence interval of the regression line and has the equivalent value of 1.24% volumetric soil moisture; precision is high due to the large number of samples.

## A.9 Review of soil moisture monitoring in the surface layer of soil

Four methods have been employed to monitor the soil moisture in the surface layer (top 0.2 m) of soil and all are located in the space of a few metres in the enclosure:

1. Neutron scattering. The data of the two tubes (0.8 m and 1.8 m depth) for the 0.2 m layer have been averaged to represent the moisture content of the surface layer.
2. SCIP. Used to investigate the spatial variation of soil moisture of the surface 0.1 m on a 90$m^2$ grid since October 1998. The grid is located normal to the north ditch and includes the enclosure within its extent (Figure A.1).
3. ThetaProbe. Installed at 0.1 – 0.15 m depth and used since July 1998. Until January 1999 measurements were taken from the ThetaProbe during field visits; thereafter the probe was connected to the datalogger.
4. Electrical resistance blocks. Two sets of four cells are installed at 0.05 m depth intervals from the surface. Measurements have been taken on field visits since April 1998.

It is instructive to compare the sets of measurements to see if there are any discrepancies in the soil moisture values being monitored. Figure A.14 displays the results of each method of soil moisture monitoring together with some soil sampling results. The monitoring period shown starts in early April 1998 with electrical resistance blocks (averaged to produce a value for the upper 0.1 and 0.2 m) and neutron scattering results, until July 1998 when the ThetaProbe was installed. Neutron scattering data is available until October 1998. SCIP data is included from the start of data collection in late November 1998. The hiatus in measurements for the ThetaProbe between November 1998 to January 1999 was caused by problems connecting the instrument to the datalogger. Gravimetric samples were taken during July to December 1999. Gaps in the other datasets are due to logistical problems of taking the measurements on particular field visits due to for example severe weather or insufficient time especially in winter.

It can be seen from Figure A.14 that the ThetaProbe, SCIP and resistance blocks give comparable results. These values are similar to those obtained by gravimetric sampling in 1999. Over the winter period, the moisture values from the SCIP from the monitoring node within the enclosure are up to 10% lower than those derived from the 0-0.1 m average of the resistance blocks, but exhibit comparable values after April 1999. Both instruments have strong calibrations to the soil and are located close together; the difference can only be explained by small scale variability of surface moisture. This can be seen on a larger scale by the soil moisture grids produced by the SCIP, section 5.3.2.2.

The maximum discrepancy between the moisture measurements taken in 1999 is between the ThetaProbe and other methods from September to the end of sampling in December 1999 when the ThetaProbe remained at a low value of 12% moisture content compared to the other methods which recorded an increase up to 20-25%. It can be seen that the ThetaProbe exhibits a steady unchanging nature from June onwards. Monitoring after the end of the time period presented in this thesis have revealed recorded an increase in moisture levels recorded by the ThetaProbe to comparable levels to the electrical resistance blocks. It is possible that the time delay in response of the ThetaProbe could be due to dry conditions in 1999 leading to soil cracking around the pins of the ThetaProbe. This could have resulted in only partial

connection with the soil until swelling established full contact and a response in the ThetaProbe. Air pockets around the pins of the ThetaProbe can lead to values of soil moisture that are lower than reality (Delta-T Devices 1988a) However the good agreement of the ThetaProbe until September 1999 to soil moisture values generated by other methods show that this has not happened before, and that the ThetaProbe can be used with confidence before this date.

The quite large difference between the average moisture in the surface layer measured by the ERBs and the moisture content at 0.2 m by the neutron probe in 1998 can be explained by consideration of the actual soil depth and method of measurement by the two instruments. The ERB measurement is an average of eight resistance cells buried in the surface 0.2 m and therefore incorporates the lower surface measurements and slightly higher moisture contents deeper in the profile. Neutron scattering was performed from 0.2 m depth, but the 'sphere of influence' of the probe about this depth could incorporate higher moisture levels at depth into this measurement. In addition the surface organic layer could act as a mulch or protecting layer to the clay soil below preventing moisture being lost, which would result in the slightly deeper measurement of the neutron probe generating higher moistures. This seems to be illustrated by the observation that at the start of monitoring, the resistance cells record much higher moisture contents indicating the ability of the surface organic layer to retain water, and the subsequent rate of loss much more rapid compared to the neutron probe.

Overall it can be seen from Figure A.14 that the different techniques used to monitor soil moisture give comparable results. These values are also similar to those obtained by soil sampling in 1999. Thus it can be stated that the data is reliable and can be used in confidence in further analysis.

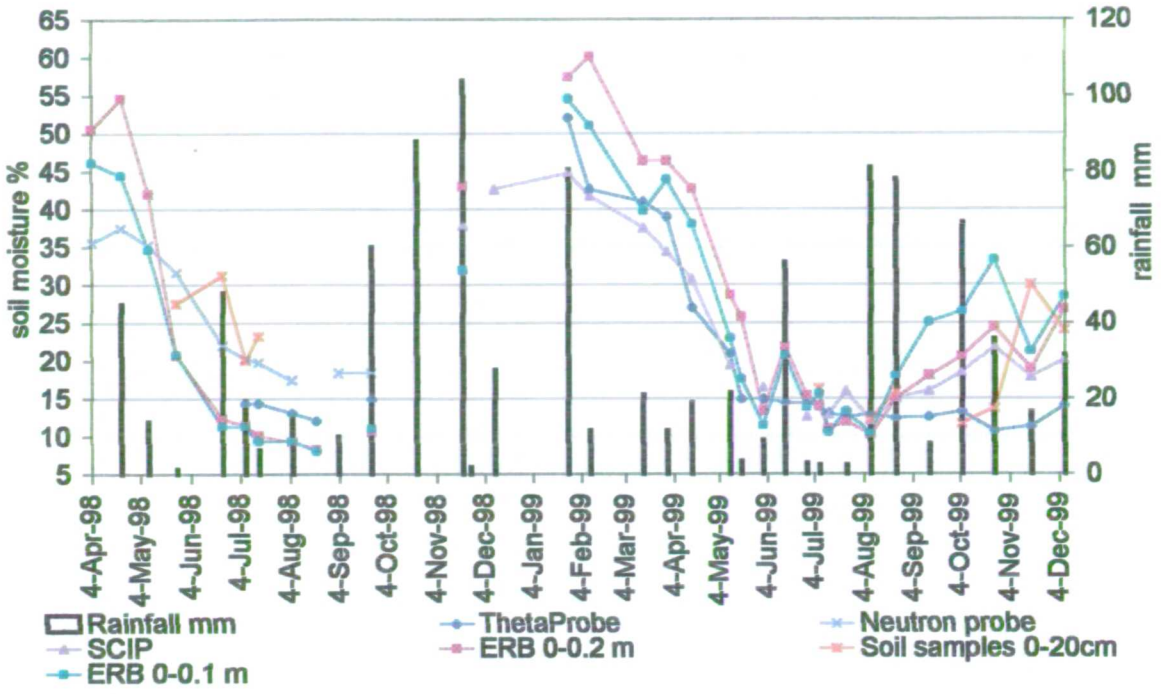


Figure A.14. Results of soil moisture monitoring in the surface soil layer together with precipitation totalled per field visit. See text for discussion.

## A.10 Soil moisture characteristic curve.

Soil moisture and matric potential data were coupled from neutron scattering and tensiometer (section 3.3.3.3.1), and the Theta probe and Equitensiometer (section 3.3.3.4.1) in order to derive the soil moisture characteristic curve. The procedure and results are outlined in the respective sections. Table A.10 details the measurement error for the fitted function using the neutron probe and tensiometer for the soil profile of 0-0.8 m depth. Table A.11 details the measurement error for the fitted function using the ThetaProbe and Equitensiometer for the surface soil layer, 0-0.2 m.

Table A.10. Details of the regression error (Equation A.3) for the fitted function to the soil moisture characteristic observations for the soil averaged over 0 – 0.8 m depth Matric potential was recorded using a tensiometer, and soil moisture content by neutron scattering and electrical resistance blocks.

| Data pair | Observed vol. soil moisture % | Observed matric potential kPa | Predicted matric potential kPa | Regression error ± Vol. matric potential kPa |
|---|---|---|---|---|
| 1 | 37 4 | 0 | -1.0 | 72.1 |
| 2 | 34.0 | 0 | -6 0 | 72 1 |
| 3 | 31.9 | -40 | -20 9 | 72.1 |
| 4 | 28.8 | -130 | -140 6 | 72.1 |
| 5 | 27.3 | -450 | -464 0 | 207 3 |
| 6 | 26.5 | -670 | -607.1 | 207.3 |
| 7 | 26 0 | -630 | -647 2 | 207.3 |
| 8 | 24.7 | -680 | -724 0 | 207.3 |
| Details of the regression calibration for the parabolic curve (data pairs 1-4) | | | | |
| Analysis of variance | Sum of squares | Degrees of freedom | Variance | F-ratio. Critical (95%) = 18 51 |
| Regression | 35741.3 | 1 | 35741.3 | 139.0 |
| Residual | 514.4 | 4-1-1 | 257.2 | |
| Total | 36255.7 | 4-1 | | |
| $r^2$ | 0.99 | | | |
| Details of the regression calibration for the rational function (data pairs 5-8) | | | | |
| Analysis of variance | Sum of squares | Degrees of freedom | Variance | F-ratio. Critical (95%) = 18 51 |
| Regression | 1657215.5 | 1 | 1657215.5 | 520.0 |
| Residual | 6375 5 | 4-1-1 | 3187.8 | |
| Total | 1663590.9 | 4-1 | | |
| $r^2$ | 0 99 | | | |

Table A 11. Details of the regression error (Equation A.3) for the fitted function to the soil moisture characteristic observations for the surface soil layer. Matric potential was recorded using an Equitensiometer, and soil moisture content by a ThetaProbe.

| Data pair | Observed vol. soil moisture % | Observed matric potential kPa | Predicted matric potential kPa | Regression error ± Vol. matrix potential kPa |
|---|---|---|---|---|
| 1 | 43.2 | 43.2 | -0 4 | 7 2 |
| 2 | 43 0 | 43 0 | -2 9 | 7 2 |
| 3 | 42.7 | 42.7 | -6 6 | 7 2 |
| 4 | 42.4 | 42.4 | -9 8 | 7.2 |
| 5 | 42.2 | 42.2 | -12 3 | 7.2 |
| 6 | 42.0 | 42 0 | -15 0 | 7.2 |
| 7 | 41.8 | 41 8 | -17 1 | 7 2 |
| 8 | 41.7 | 41.7 | -18 2 | 7.2 |
| 9 | 41.6 | 41 6 | -18 9 | 7.2 |
| 10 | 41.6 | 41.6 | -19 4 | 7.2 |
| 11 | 41.5 | 41 5 | -20 4 | 7.2 |
| 12 | 41.4 | 41.4 | -21 3 | 7.2 |
| 13 | 41 4 | 41 4 | -21.5 | 7.2 |
| 14 | 41.3 | 41.3 | -21.9 | 7.2 |
| 15 | 41.3 | 41.3 | -21.9 | 7.2 |
| 16 | 41.3 | 41 3 | -22.7 | 7.2 |
| 17 | 41.1 | 41.1 | -24.1 | 7 2 |
| 18 | 41.1 | 41.1 | -24.7 | 7.2 |
| 19 | 41.0 | 41.0 | -24.8 | 7.2 |
| 20 | 41.0 | 41.0 | -25.0 | 7.2 |
| 21 | 40.7 | 40.7 | -27.8 | 7.2 |
| 22 | 40.7 | 40.7 | -28.2 | 7.2 |
| 23 | 40.4 | 40.4 | -30.6 | 7.2 |
| 24 | 40.2 | 40.2 | -32.3 | 7.2 |
| 25 | 40.1 | 40.1 | -33.1 | 7.2 |
| 26 | 40.1 | 40.1 | -33.5 | 7.2 |
| 27 | 39.9 | 39.9 | -35.3 | 7.2 |
| 28 | 39.8 | 39.8 | -36.1 | 7.2 |
| 29 | 39.7 | 39.7 | -36.7 | 7.2 |
| 30 | 39.7 | 39.7 | -37.0 | 7.2 |
| 31 | 39.6 | 39.6 | -37.9 | 7.2 |
| 32 | 39.5 | 39.5 | -38 6 | 7.2 |
| 33 | 39 3 | 39.3 | -40 2 | 7.2 |
| 34 | 39.2 | 39.2 | -40.5 | 7.2 |
| 35 | 39.2 | 39 2 | -40.9 | 7.2 |
| 36 | 39.1 | 39.1 | -41.4 | 7.2 |
| 37 | 39.1 | 39.1 | -41 8 | 7.2 |
| 38 | 39.0 | 39 0 | -42.3 | 7 2 |
| 39 | 39 0 | 39 0 | -42.7 | 7 2 |
| 40 | 38.9 | 38.9 | -42.8 | 7.2 |
| 41 | 38.9 | 38 9 | -43.4 | 7 2 |
| 42 | 38.6 | 38 6 | -45.0 | 7.2 |
| 43 | 38.6 | 38 6 | -45.2 | 7 2 |
| 44 | 38 6 | 38 6 | -45 2 | 7 2 |
| 45 | 38 5 | 38 5 | -46.0 | 7 2 |
| 46 | 38 4 | 38 4 | -46.9 | 7.2 |

| Table A 11. Continued | | | | |
|---|---|---|---|---|
| 47 | 38 1 | 38 1 | -48 5 | 7 2 |
| 48 | 38 1 | 38 1 | -48 9 | 7 2 |
| 49 | 38 0 | 38 0 | -49 4 | 7 2 |
| 50 | 37.6 | 37 6 | -51 6 | 7 2 |
| 51 | 37.2 | 37 2 | -54 0 | 7.2 |
| 52 | 36.7 | 36.7 | -57.1 | 7 2 |
| 53 | 36.0 | 36 0 | -60 5 | 7 2 |
| 54 | 35 3 | 35.3 | -63.9 | 7.2 |
| 55 | 34.4 | 34.4 | -67 6 | 7.2 |
| 56 | 33.4 | 33 4 | -71 3 | 7 2 |
| 57 | 32.5 | 32 5 | -74 1 | 7.2 |
| 58 | 31.4 | 31.4 | -77 0 | 7.2 |
| 59 | 30.6 | 30.6 | -79.2 | 7.2 |
| 60 | 29.3 | 29 3 | -82 4 | 7 2 |
| 61 | 28.0 | 28.0 | -85 5 | 7.2 |
| 62 | 26 2 | 26.2 | -90.0 | 7 2 |
| 63 | 25 1 | 25.1 | -93 3 | 7.2 |
| 64 | 23.5 | -96.1 | -99.0 | 26.0 |
| 65 | 22.6 | -99.8 | -106.2 | 26 0 |
| 66 | 21.4 | -105.4 | -117 0 | 26 0 |
| 67 | 20.9 | -113.1 | -122 0 | 26.0 |
| 68 | 19.9 | -121.6 | -135 1 | 26.0 |
| 69 | 19.6 | -130.3 | -139.7 | 26.0 |
| 70 | 19 3 | -135.9 | -144.7 | 26.0 |
| 71 | 18.8 | -141.2 | -154 6 | 26.0 |
| 72 | 18.7 | -146 4 | -158 2 | 26.0 |
| 73 | 18.3 | -155.9 | -166 6 | 26.0 |
| 74 | 17.8 | -172.0 | -179 9 | 26.0 |
| 75 | 17.3 | -188 1 | -201 0 | 26.0 |
| 76 | 16.9 | -209.3 | -219.7 | 26.0 |
| 77 | 16.6 | -249 7 | -234.7 | 26.0 |
| 78 | 16.2 | -292.2 | -270 6 | 26.0 |
| 79 | 15.8 | -345.7 | -319 8 | 26.0 |
| 80 | 15.4 | -386.7 | -385 4 | 26.0 |
| 81 | 15.2 | -459 3 | -454 5 | 26.0 |
| 82 | 15 0 | -529 0 | -536 4 | 26.0 |
| 83 | 14.8 | -644.1 | -639.3 | 26 0 |
| Details of the regression calibration for the polynomial curve (data pairs 1-63) | | | | |
| Analysis of | Sum of squares | Degrees of freedom | Variance | F-ratio Critical (95%) |
| Regression | 416563 0 | 1 | 416563 0 | 32092.3 |
| Residual | 791 8 | 63-1-1 | 13 0 | |
| Total | 417354 8 | 63-1 | | |
| $r^2$ | 0 99 | | | |
| Details of the regression calibration for the rational function (data pairs 64-83) | | | | |
| Analysis of | Sum of squares | Degrees of freedom | Variance | F-ratio. Critical (95%) |
| Regression | 1768974 7 | 1 | 1768974.7 | 11184.4 |
| Residual | 2847.0 | 20-1-1 | 158 16 | |
| Total | 177182 6 | 20-1 | | |
| $r^2$ | 0.99 | | | |

# Appendix B Geostatistics

## B.1 Introduction

The Theory of Regionalised Variables, also known as geostatistics, was first developed in 1960 by Georges Matheron and was created from demand by the mining industry. The estimation techniques of geostatistics, which aim to produce a 'best' estimation of the unknown value at some location, are collectively known as kriging (Clark 1979). The aim of geostatistics is to study any phenomenon which can be quantified and which develops in a structured way in space and/or time. Despite the foundations of geostatistical theory in the mining industry, the estimation techniques can be used whenever a measure is made of 'properties distributed over the earth's surface to assess their spatial variation' (Oliver *et al.* 1989b). Thus the use of geostatistics has been established in physical geography, which include the fields of soil science (Webster 1977, Webster and Burgess 1984, Oliver and Webster 1986), hydrogeology (Kitandis 1997) and earth sciences (Isaaks and Srvastaven 1989).
The steps in a geostatistical study include exploratory data analysis, structural analysis (calculation and modelling of semivariograms), and making predictions (kriging or simulations).

## B.2 Use of geostatistics in soil science

The application of geostatistics for soil analysis has been demonstrated by the research into the following areas: thickness of loam cover, stone content of topsoil (Oliver *et al.* 1989b), soil characteristics and texture (Oliver *et al.* 1987a; Oliver *et al.* 1989a), soil chemistry (Weitz *et al.* 1993), soil pH (Corsten *et al.* 1994), and infiltration rates (Jetten *et al.* 1993) The spatial and temporal variability of water content in the surface layers of soil can also be examined using geostatistics. Soil moisture can be considered a 'property that is distributed over the earth's surface' due to its influence from factors of precipitation and evaporation, vegetation uptake, soil structure, texture and drainage for example.

In this study, geostatistical theory is applied to the problem of determining the spatial variability of surface soil water content within the study field at Elmley Marshes, measured using a Surface Insertion Capacitance Probe, SCIP, (section 5 3.2)

## B.3 Theory

The basic assumptions of the theory of geostatistics has been listed by Clark (1979 p10) and Oliver *et al.* (1989a):

- The difference between the values of pairs of samples is determined by the relative spatial lag, h, of the samples, where h is a vector that separates the samples in distance and / or direction
- There is no trend of the variable within the scale of the sample i e. the mean of any spatially dependant random component is zero at lag h=0.
- As the mean and variance are derived from the same probability distribution, the difference between pairs of samples depends only on the lag. This is the concept of stationarity.

From these assumptions Matheron formulated his 'intrinsic hypothesis' which defines the variance between the sample pair as:

$$\gamma^*(\mathrm{h}) = \frac{1}{2n(h)} \sum_{i\ 1}^{n(h)} [z(xi) - z(xi+h)]2$$

Equation B.1

Where:
n(h) = number of samples at lag (h)
z(xi) and z(xi+h) = measured values of z, the variable at xi and xi+h respectively

$\gamma^*(h)$ is the observed semivariance of the samples at lag (h) (half the expected squared difference between the samples). A distinction is made between the experimental and theoretical semivariogram by the inclusion of an asterisk in the former The former is computed from observations the latter is the fitted function derived from the experimental semivariance that relates $\gamma$ to h. By varying h, a set of semivariances for discrete distances can be obtained.

## B.4 Kriging

The use of geostatistical techniques allows the prediction of a spatially distributed variable from adjacent values while considering the interdependence expressed in the semivariogram (Henley 1981) Such kriging techniques, named after D G Krige who developed the technique are at their simplest, linear, unbiased, weighted moving average techniques. Other linear unbiased estimators exist but kriging has the advantage of being a minimum variance estimator, i e it minimises the variance of the estimation errors and takes into account the spatial process. Furthermore, kriging allows the quantification of the precision of the predictions via the kriging variance. Kriging can be termed an exact interpolator i.e. the value of a sampled point corresponds exactly with the measured value As there are many ways in which the weighting can be attributed, kriging is a method of determining the combination of weights that will produce the minimum estimation variance. The process involves solving a series of simultaneous equations with the inclusion of a Lagrangian multiplier.

Kriging therefore has advantages over other methods of estimation, of being unbiased, producing the lowest estimation variance and, from the knowledge of the estimation variances, can be used with known confidence. The comparison of techniques of interpolation by Laslett (1987) showed kriging to be the most reliable.

## B.5 Problems

Henley (1981) identifies certain problems with the assumptions required by geostatistical theory. The concept of stationary, Matheron's 'Intrinsic Hypothesis' is the major problem as it is rarely found in the real world. It can be argued that as local stationarity can be assumed, deviations of stationarity are of no practical concern. However there is no test to produce proof to ascertain this Another flaw is that the fitting of an experimental semivariogram to a theoretical model is not straightforward and a degree of skill is required, especially when datasets do not resemble any of the accepted models.

In view of these criticisms however, the advantages of geostatistics remain over other

spatial analysis techniques: of no bias, minimum variances, linearity and of allowing an estimation of the quality of estimates produced by kriging

## B.6 The semivariogram

The semivariogram is the central tool of geostatistics and used to model the way two values in space or time are correlated. It is intuitive that two values in space that are close together tend to be more similar than two values farther apart. Two distributions might have the same mean and variance, but differ in the way they are correlated with each other. Thus geostatistics allows the quantification of the correlation between any two values separated by a lag distance h and uses this information for kriging i.e. to make predictions at unsampled locations. Semivariogram modelling is a prerequisite for kriging.

Semivariograms are usually described using two parameters. For example, the spherical model, Figure B.1, is considered the equivalent in geostatistics to the normal distribution. The model is bounded (attains a peak value), and consists of two separate functions; the range and the sill. The range is the extent of influence of a semivariogram; beyond this distance the mean square deviation between z(xi) and z(xi+h) no longer correlated upon the lag h and thus the quantities are independent of each other. The sill of the semivariogram is the point at which the value of $\gamma$ at the semivariance becomes stable. The sill value is numerically equal to the sum of the ordinary sample variance.

The calculation of the semivariogram from equation 1 is fully described in Clark (1979) and Henley (1981). If a grid of observations is used with a regular lag h between observations, the semivariance for the lag h0 is calculated. Semivariances for other lag spacing are also calculated from Equation B.1 using the samples that are separated by the distance of 2h 3h etc. In addition, provided that there is a sufficient number of samples (Webster and Oliver 1992, McBratney and Webster 1983) anisotropy can be detected by computing $\gamma$ in different directions.

Lag, h, always starts at zero and cuts the $\gamma$ ordinate at zero in accordance with the basic assumptions of geostatistics; 2 samples taken at exactly the same place must

have the same value ergo γ and γ * equal zero. With increasing h, γ will increase until the sample values become independent of each other.

The semivariogram computed from observations is termed an experimental semivariogram, and depending upon the noise of the data, may appear irregular in form. The experimental semivariogram is then compared against a number of established curves, theoretical semivariograms. It is usually the theoretical semivariogram that is then used in further geostatistical estimation techniques.

Figure B.1. The ideal shape for the semivariogram; the spherical model where c = sill, a = range. Source: Clark 1979 p7.

### B.6.1 Nugget variance

A line drawn through the first two point of the semivariogram to intercept the γ axis can give an indication of any random components of the variable under study. If the line intersects the γ axis at values greater than zero (even though the line of the semivariogram must theoretically pass through the origin) a proportion of the variation of the variable under investigation is due to random factors. This is termed nugget effect and is due both measurement errors and spatially dependant variation on scales smaller than the smallest lag (Oliver *et al.* 1989a). As the sill is equal to the sample variance then:

Percentage variation = Intersection of γ axis / value of sill Equation B.2

The mathematical form of the semivariogram treats the nugget variance as a constant:

$\gamma(0) = 0$

$\gamma(h) - C_o + \gamma(h)$ Equation B 2

Where:
$C_o$ = value of nugget variance
$\gamma(h)$ = normal model function

In this way a new sill is calculated by subtracting the value of the nugget effect

B 6.2 Number of samples required

A large number of samples are required to compute the semivariogram reliably. Webster and Oliver (1992) determined approximate confidence intervals for the semivariogram. The authors created a dense field of values representing a soil variable using a plausible exponential and spherical model the field was sampled using sample sizes of 25, 49, 100, 144, 225, and 400. Using this approach the semivariograms of the sampling efforts could be computed against the original model to assess their accuracy. Two scenarios were explored; firstly the range of the semivariogram was a large proportion of the distance across the simulated field employed a grid-sampling scheme The second scenario involved sampling a small range of the semivariogram using transects. Results show a clear trend of decreased standard error with increased sample size for both models and sampling strategies. The authors ascertain that in order to obtain a reasonably precise estimate at least 144 measurements were needed while a sample of 400 would give a very precise estimate for the semivariogram. While also showing an increase in precision with sample size, sampling with transects produced more fluctuations resulting in larger confidence intervals than the grid method. However this can be explained by the greater area of the field being sampled compared to shorter range of the semivariogram thus more variance in the region was experienced. Overall the conclusion from both scenarios is that a sampling range of 150-200 points is required to reliably estimate the semivariogram in isotropic conditions; anistrophic conditions require larger sampling sizes The authors also observe that the shorter the lag distances the narrower the confidence interval therefore a more precise semivariogram is created which is

optimal for kriging Thus attempts to obtain the same number of samples for longer lags as for smaller lags is unnecessary.

## B.7 Nested sampling

> 'It often happens that local estimates and quantitative maps are required for little known regions How should such a region be sampled? If a given sampling interval is sparse relative to the intensity of the variation there might be no dependence in the data: neighbouring sites might be beyond the range of the semivariogram. On the other hand if the semivariogram has a long range then a similar sampling intensity may be unnecessary dense and so waste resources. Thus in many instances uniform sampling over the whole region must be a hot or miss affair. Some means is needed of identifying the spatial scale of variation economically and surely, albeit only roughly, before sampling uniformly to map. This can be achieved using a nested sampling and hierarchical analysis of variance as part of a two-stage survey ' (Oliver *et al.* 1989b p277 )

> 'Most published accounts of reconnaissance spatial surveys involve nested designs' (Pettitt *et al.* 1993 p191).

Nested sampling designs offer a way of obtaining information about the scale of variation of the variable under investigation in an area in which variability is unknown. These designs are based on hierarchical systems of comprising stages of differing spatial / lag intervals (Weitz *et al.* 1993, Jetten *et al.* 1993). In this way an economic initial approximate estimation of the spatial dependence is obtained is obtained in terms of time, effort and resources (Oliver *et al* 1989a, Oliver *et al* 1987b)

There are two variations of nested designs, balanced and unbalanced. A balanced design involves a doubling density at subsequent stages in the hierarchy after the first (Oliver *et al.* 1987b) and is symmetrical in form which results in a large number of samples at the lower stages. An unbalanced design is unsymmetrical in form with some stages of the hierarchy containing the same number of replications as the preceding stage. Such designs can reduce the sampling effort required; the unbalanced design using by Oliver *et al* (1989b) to examine the spatial distribution of soil

properties in the Wyre Forest achieved a reduction of 25% of sampling effort when compared to a fully balanced design.

Nested designs can be either grid based (Jetten *et al* 1992) or transect based (Pettitt *et al.* 1993, Weitz *et al.* 1993). Nested analysis can also be used to identify the range or lag over which most of the spatial variation of the variable occurs The components of variance for differing spatial scale at each stage in the hierarchy can be computed, see Table B.1

Table B.1. Calculation of the components of variation for a four-stage design. Source Weitz *et al.* 1993, after Webster 1977.

| Source | Degrees of freedom | Component of variation estimated by mean square |
|---|---|---|
| Stage 1 | n1 | $\sigma_4^2 + n_4\sigma_3^2 + n_3 n^4 \sigma_2^2 + n_2 n_3 n_4 \sigma^2$ |
| Stage 2 | n1(n2-1) | $\sigma_4^2 + n_4\sigma_3^2 + n\, n^4 \sigma_2^2$ |
| Stage 3 | n1n2(n3-1) | $\sigma_4^2 + n_4\sigma_3^2$ |
| Stage 4 | n1n2n3(n4-1) | $\sigma_4^2$ |
| Total | n1n2n3n4 | |

# References


Abtew, W., and Obeysekera, J 1995 Lysimeter study of evapotranspiration of cattails and comparison of three estimation methods. Transactions of the ASAE 38 (1): 121-129

Adams W A. 1973 The effect of organic matter on the bulk and true densities of some uncultivated podzolic soils Journal of Soil Science 24(1) 10-17.

Adamus, P.R. Stockwell, L.T. 1983 A method for wetland functional assessment: Volume 1 Critical review and evaluation of concepts. Federal Highway Administration, Washington DC

ADAS (Agricultural Development Advisory Service) (1998) Environmental Monitoring in The Essex Coast ESA 1994-1997. ADAS report to MAFF.

ADAS (Agricultural Development Advisory Service) 1997 Environmental monitoring in the North Kent Marshes ESA 1993 - 1996 ADAS report to the Ministry of Agriculture Fisheries and Food. MAFF.

Al-Khudhairy, D.H.A., Shepherd, I.M., Langhoff, A., Calaon, R., Hoffmann, V., Thompson, J.R., Agnew, C.T, Gavin, H., Gasca-Tucker D., Zalidis, G., Bilas, G., Hadjikiannis, S., Refsgaard A., and Refstrup Sørensen, H. (1999) 'New Integrated Technologies for Wetland Management and Protection', Paper presented at the 3rd DHI Software Conference, Helsingør, Denmark, 7th- 11th June 1999.

Al-Khudhairy, D.H A., Leemhuis, C., Hoffmann, V, Calaon, R., Shepherd, I M., Thompson, J.R., Gavin, H. and Gasca-Tucker, D.L. (in review) 'Monitoring wetland ditch water levels in the North Kent Marshes, UK, using Landsat TM imagery and ground-based measurements', Hydrological Sciences Journal.

Allen, R G., Jensen, M.E., Wright, J L. and Burman, R.D. 1989 Operational estimates of reference evapotranspiration. Agronomy Journal 81 650-662.

Allen, R.G , Smith, M., Perrier, A and Pereira, L.S. 994 An update for the definition of reference evapotranspiration. ICID Bulletin 43 (2), 1-32.

Allerup, S. 1960 Transpiration changes and stomatal movements in young barley plants. Physiol Plantarum 13. 112.

American Society of Civil Engineers ASCE 1996 Hydrology Handbook. ASCE Manuals and Reports in Engineering Practice No. 28 ASCE New York.

Amoozegar, A. 1989 Comparison of the Glover solution with the simultaneous equations approach for measuring hydraulic conductivity. Soil Sci Soc. Am. J. 58 1362-1387.

Andreas, E L. and Cash, B A. 1996 A new formulation for the Bowen ratio over saturated surfaces Journal of Applied Meteorology 35 1279-1289

Angus, D.E. and Watts, P.J. 1984 Evapotranspiration – How good is the Bowen ratio method? Agric Water Mgmt 8· 133-150.

Armstrong, A C. 1986 Drainage Benefits to Land Workability. In Smith, K.V.H. and Rycroft, D W (ed ) Hydraulic Des'gn in Water Resources Engineering Land Drainage Proceedings of the 2nd International Conference Southampton University UK.

Armstrong, A C. 1993 Modelling the response of in-field water tables to ditch levels imposed for ecological aims a theoretical analysis. Agriculture, Ecosystems and Environment 43: 345-351.

Armstrong, A.C. 2000 DITCH: a model to simulate field conditions in response to ditch levels managed for environmental aims. Agriculture, Ecosystems and Environment 77: 179-192.

Armstrong A C., Caldow, R., Hodge, I D, and Treweek, J 1995 'Re-creating wetlands in Britain. the hydrological, ecological and socio-economic dimensions'. In Hughes, J.M R. and Heathwaite, A.L. Hydrology and hydrochemistry of British Wetlands. John Wiley and Sons Ltd

Armstrong A.C., and Rose S. 1998 Managing Water for Wetland Ecosystems· A Case Study in Joyce, C.B, and Wade, P M, (eds) European Wet Grasslands: Biodiversity, Management and Restoration. John Wiley and Sons Ltd.

Armstrong, A.C. and Tring, I. 1980 The estimation of sub-soil hydraulic conductivity. Field Drainage Experimental Unit, Report no 4. MAFF

Arya, L.M. and Paris, J.F. 1981 A physico-empirical model to predict the soil moisture characteristic from particle size distribution and bulk density data. Soil Sci. Soc. Am. J. 45.1023-1030.

Asare, S N., Rudra, R.P, Dickinson, W.T and Wall, G J 1993 Seasonal variability of hydraulic conductivity. Transactions of the ASAE 36 (2)·451-457.

Aslyng, H.C. 1965 Evaporation, evapotranspiration and water balance investigations at Copenhagen 1955-1964. Acta Agr Scand. 15: 284-300.

Assoglou, N, Kosmos, C.S, Moustakas, N., Tzianis, E and Danalatos, N G., 1994 Cracking in recent alluvial soils as related to easily determined soil properties. Geoderma 63: 289-298.

Avery, B.W. and Bascombe C.L. (eds.) 1974 Soil Survey Laboratory Methods Technical monograph No. 6 Soil Survey Harpenden.

Bailey, V. 1980 'Climate'. In Fordham, S.J. and Green, R.D. 1980 Soils of Kent. Harpenden.

Baird, A.J. 1995 'Hydrological investigations of soil water and groundwater processes in wetlands'. In Hughes, J M R and Heathwaite, A L. Hydrology and hydrochemistry of British Wetlands. John Wiley and Sons Ltd

Baird, A.J. 1997 Field estimation of macropore functioning and surface hydraulic conductivity in a fen peat. Hydrological Processes 11. 287-295.

Barham, A J., Bates, M R. and Whittaker, K. 1991 North Kent Marshes, historic and cultural resources: The archaeological and historical significance of the North Kent Marshes. Unpublished report by the Geoarcheology Service Facility, Institute of Archaeology, University College London.

Barrs, H D 1968 Determination of water deficits in plant tissues In Kazlowski, T.T., Water deficits and Plant growth. Vol. 1· Development, contr l and measurement. Academic Press.

Bascombe, A.D., Crawley, C.J.A., Fitzpatrick, A.P., and Seager-Smith, R.H 1995 Birds and Salterns. The A249 Iwade bypass to Queenborough Kent UK. In Cox, Straker, and Taylor (eds ) Wetland archaeology and nature conservation HMSO

Bastidas, L.A., Gupta, H.V, Sorooshian, S., Shuttleworth, W J., and Yang Z L 1999 Sensitivity analysis of a land surface scheme using multicriteria methods. Journal of Geophysical Research – Atmospheres 104. (D16) 19481- 9490

Bell, J P 1981 Neutron Probe Practice Institute of Hydrology Report no 19. Institute of Hydrology.

Bell, J P. and Eeles, C.W.O. 1967 Neutron random counting error in terms of soil moisture for non-linear calibration curves Soil Science 103 (1) 1-3

Bell, J P., Dean T J, Hodnett M G., 1987 Soil moisture by an improved capacitance technique, Part 2 field techniques, evaluation and calibration. Journal of Hydrology 93· 67-78.

Belmans, C , Wesseling, J G. and Feddes, R.A., 1984 SWATRE Simulation model of the water balance of a cropped soil providing different types of boundary conditions Institute for Land and Water Management Research Wageningen, Netherlands, ICW Nota 1257.

Beven, K. 1979 A sensitivity analysis of the Penman-Monteith actual evaporation estimates Journal of Hydrology 44 (3) 169-190

Beven, K. and Germann, P. 1982 Macropores and water flow in soils Water Resources Research 18 (5)· 1311-1325.

Birkeland, P W. 1984 Soils and Geomorphology OUP

Black, T.A., Gardner, W.R. and Thurtell, G W. 1969 The prediction of evaporation, drainage and soil water storage for a bare soil. Soil Sci. Amer. Proc. 33. 655-660.

Black, T.A., Spittlehouse, D L., Novak, M.D. and Price, D.T. (eds ) 1987 Estimation of areal evaporation. Proceedings of an international workshop held during the XIXth General Assembly of the International Union of Geodesy and Geophysics at Vancouver, British Colombia, Canada, 9-22 August 1987. IAHS Publication No. 177.

Boelter, D H. 1972 Water table drawdown around an open ditch in organic soils. Journal of Hydrology 15:329-340.

Boonyatharokul, W and Walker, W.R. 1979 Evaporation under depleting soil moisture. Proc. ASCE Irrigation and Drainage Division 105. 391-402.

Boorman, L.A. 1992 The environmental consequences of climatic change on British salt marsh vegetation' Wetlands Ecology and Management 2 (1-2). 11-21

Bouma, J. 1980 Field measurement of soil hydraulic properties characterising water movement through swelling clay soils. Journal of Hydrology 45.149-158.

Bouma, J and Dekker L.W. 1981 A method for measuring the vertical and horizontal $K_{sat}$ of clay soils with macropores. Soil. Sci. Am. J. 45 662-663.

Bouma, J. and Dekker, L.W. 1978 A case study on infiltration into dry clay soil. 1 Morphological observations. Geoderma 20.27-40.

Boussinesq, J. 1904 Recherches théorétiques sur l'écoulement des nappes d'eau infiltrées dans le sol et sur débit de sources. J. Math. Pure et Appl 10 363-394.

Bouwer, H and Rice, R.C. 1976 A slug test for determining hydraulic conductivity of unconfined aquifers with completely or partially penetrating wells. Water Resources Research 12 (3). 423-428.

Bouwer, H and Rice, R.C. 1989 The Bouwer and Rice slug test- an update. Groundwater 27: 304-309.

Bouwer, H. 1996 Discussion of the Bouwer and Rice slug test review articles Groundwater 34· 171.

Bouwer, H., and Jackson R.D. 1974 Determining soil properties In Drainage for Agriculture. ASA Monograph 17, Chapter 23, Section 10, Van Schilfgaarde, J. (ed ) p611-672, American Society of Agronomy Madison Wisconsin

Bouyoucous, G J. and Mick, A.H 1940 An electrical resistance method for the continuos measurement of soil moisture under field conditions. Michigan Exp Stn. Tech. Bull 172.

Bowen, I S. 1926 The ratio of heat losses by conduction and evaporation from any water surface. Phys Rev. 27: 779-787.

Bradford, R.J., Hsiao, T.C. 1982 Stomatal behaviour and water relations of water logged of tomato plants. Plant Physiology 70, 1508-1513.

Brady, N C. 1990 The nature and propertie of s ls. Macmillan.
Brassington, R 1988 Field Hydrogeology John Wiley and Sons
Brereton, A.J., Danielov, S.A., Scott, D. 1996 Agronomy of grass and grasslands for middle latitudes Tech. Note No. 197 World Meteorological Organisation.
Briscoe, B., 1998 Nature conservation sites in Kent. Kent County Council Planning Department.
Bronswijk, J J B 1988 Modelling of water balance, cracking and subsidence of clay soils Journal of Hydrology 97 (5) 199-212
Brooks, R.H., and Corey, A.T. 1966 Properties of porous media affecting fluid flow. Journal of Irrigation and Drainage Division American Society of Civil Engineers 92, 61-88.
Brown, A F., and Grice, P.V. 1993 Birds in England: Context and Priorities English Nature Research Report No. 67, Peterborough, UK.
Brown, D L., Narasimhan, T.N , and Demir, Z. 1995 An evaluation of the Bouwer and Rice method of slug test analys s Water Resources Research 31 (5). 1239-1246.
Bruggeman, G.A. 1987 Chapter 5. Methods of calculation. In Custodio, E. and Bruggeman, G A (Eds ) Groundwater problems in coastal areas Studies and reports in hydrology no. 45. UNESCO.
Brunt, D. 1952 Physical and dynamical Meteorology, 2nd ed. University Press, Cambridge 428pp.
Brutsaert W. 1975 The roughness length for water vapour, sensible heat and other scalars. J Atm. Sci. 32.2028-2031
Brutsaert, W. 1982 Evaporation into the atmosphere. Theory, History and Applications. D. Reidel Publishing Co. Dordrecht, Holland 299 p
Buckingham, E. 1907 Studies on the movement of soil moisture USDA Bru Soils Bull 38.
Buitendijk, J. 1984 FLOWEX A numerical model for simulation of vertical flow of water through unsaturated layered so l. Note 1494. ICW Wageninnen.
Bultot, F., Duprez, G.L. and Gellens, D 1990 Simulation of land use changes and impacts upon water balance a case study for Belgium. Journal of Hydrology 114 (1-4) 327-348
Burba, G.G , Verma, S B , and Kim, J. 1998 Energy fluxes in a mid-latitude prairie wetland Boundary Layer Meteorology 91 495-504
Burba, G.G., Verma, S.B., and Kim, J 1999 A comparative study of the surface energy fluxes of three communities *Phragmites australis, Scirpus acutis* and open water in a prairie wetland ecosystem. Wetlands 19 (2). 451-457.
Burgess T.M. Webster R. McBratney A.B 1981 Optimal Interpolation and Isarithmic Mapping of soil properties. IV Sampling Strategy Journal of Soil Science 32 643-659
Burnham, C P 1973 'Climate'. In McRae S G and Burnham C P (eds ) The rural landscape of Kent Wye College
Burke, W 1961 Drainage investigations on bogland. Irish Journal of Agricultural Research 1: 31-34
Ca n, J D. 1998 Modelling evaporat n from plant canopies Inst tute of Hydrology Report no. 132 Institute of Hydrol gy
Calder, I R. 1990 Evaporation in the up ands John Wiley and Sons
Camillo, P J and Gurney, R.J, 1986 A resistance parameter for bare soil evaporation models. Soil Science 141 95-105.

Campbell Scientific 1995 Bowen Ratio System (Standard Version) User Guide. Campbell Scientific Ltd.

Campbell Scientific 1998 NR-Lite Net Radiometer User Guide. Campbell Scientific Ltd

Campbell, C.M. and Fritton, D.D. 1994 Factors affecting field-saturated hydraulic conductivity measured by the borehole permeameter technique. Soil Science Society of America Journal 58. 1354-1357.

Campbell, D.I. 1989 Energy balance and evapotranspiration from tussock grassland in New Zealand Boundary Layer Meteorology 46: 133-152

Campbell, D.I., and Williamson, J.L. 1997 Evaporation from a raised peat bog Journal of Hydrology 193: 142-160.

Campbell, G S 1974 A simple method for determining unsaturated conductivity from moisture retention data. Soil Science 117 (6): 311-314.

Campbell, G S and Norman, J.N. 1998 An introduction to Environmental Biophysics Second Edition. Springer-Verlag. New York.

Campbell, G.S, 1985 Soil physics with BASIC Transport models for soil – plant systems Elsevier.

Carlson, T.N. 1991 Modelling stomatal resistance: an overview of he 1989 workshop at the Pennsylvania State University. Agricultural and Forest Meteorology 54, 103-106.

Carneiro, C., and De Jong, E. 1985 *In situ* determination of the slope of the calibration curve of a neutron probe using a volumetric technique. Soil Sci. 139 (3): 250-254.

Carter E. 1982 'Land drainage' Farming and wildlife Advisory Group Newsletter Spring/Summer 1982.

Chanasyk, D.S. and McKenzie, R.H. 1986 Field calibration of a neutron probe. Can. J Soil. Sci. 66: 173-176.

Chanasyk, D.S. and Naeth, M.A. 1988 Measurement of near surface soil moisture with a hydrogenously shielded neutron probe. Can. J. Soil Sci. 68: 171-176.

Chanasyk, D.S. and Naeth, M A. 1996 Field measurement of soil moisture using neutron probes. Canadian Journal Of Soil Science 76. 317-323.

Chen, C. and Wagenet, R.J. 1992 Simulation of water and chemicals in macropore soils. Part 1 Representation of the equivalent macropore influence and its effect on soil water flow. Journal of Hydrology 130: 105-126.

Choisnel, E., de Villele, O. and Lacroze, F. 1992 Une approache uniformise'e du calcul de l'évapotranspriation potentielle pour l'ensemble des pays de la Communauté Europeene Com Commum, Européenne, EUR 14223 FR, Luxembourg.

Clark I. 1979 Practical Geostatistics Applied Science Publishers Ltd.

Clifford Evans G, 1972 The quantitative analysis of plant growth Blackwell Scientific Publications.

Clymo, R.S D., F.H., Bertram, B C.R., Burt, T.P., Gilman, K., Ingram, H A.P., James, R., Kirkby, M J, Lee, J.A., Maltby, E, Wheeler, B.D, and Wilcock, D. 1995 Conclusion: direction for research on wetlands in Britain IN Hughes, J M R, and Heathwaite, A.L, (Eds) Hydrology and hydrochemistry of British Wetlands Wiley Chichester

Collin, P. 1991 'Elmley Reserve'. In Oliver, P. Bird watching on the North Kent Marshes Cinque Port Press

Corsten L.C.A. Stein A, 1994 Nested Sampling for estimating Spatial semivariograms compared to other designs. Applied Stochastic Models and Data Analysis 10.103-122.

Crago, R D. and Brutseart, W 1992 A comparison of several evaporation equations. Water Resource Research 28 (3): 951-954.

Crescimanno, G., Iovino, M., and Provenzano, G. 1995 Influence of salinity and sodicity on soil structural and hydraulic characteristics. Soil Sci Soc Am. J 59: 1701-1708.

Curran P.J. 1985 Principles of remote sensing Longman

Curtis, L.F., Trudgill, S. 1975 The measurement of soil moisture British Geomorphological Research Group Technical Bulletin No. 13.

Custodio, E. 1987 Chapter 2: Coastal aquifers In Custodio, E. and Bruggeman, G.A. (Eds.) Groundwater problems in coastal areas. Studies and reports in hydrology no. 45. UNESCO

Department of the Environment (D.o.E.) 1992 Policy Planning Guidance. Coastal Planning.

Darcy, H 1856 Les Fontaines Publiques de la ville de Dijon. Dalmont Paris.

De Jong, R. and Loebel, K. 1982 Empirical relationship between soil components and water retention at 1/3 and 15 atmospheres. Can J. Soil Sci. 62: 343-350.

Dean and Robinson 1993 Measurement of near-surface soil-water content using a capacitance probe. Hydrological Processes 7:1, 77-86

Dean, T.J. 1994 The IH capacitance probe for measurement of soil water content. IH Report no. 125 Institute of Hydrology.

Dean, T.J., Bell, J.P., Baty A.J B. 1987 Soil moisture measurement by an improved capacitance technique 1: Sensor design and performance. Journal of Hydrology, 93.67-78

Deardrorff, J.W. 1978 Efficient prediction of ground surface temperature and moisture within inclusion of a layer of vegetation. Journal of Geophysical Research 83 (C4): 1889-1903.

Dekka, L.W. and Ritsema, C.J 1996 Uneven moisture patterns in water repellent soil. Geoderma 70. 87-99.

Delta-T Devices 1988a ThetaProbe, Soil Moisture Sensor, Type ML2 User Manual. Delta-T Devices Cambridge

Delta-T Devices 1988b Equitensiometer, Soil Matrix Potential Sensor, Type EQ1 User Manual. Delta-T Devices Cambridge.

Den Hartog, G, Neumann, H H., King, K.M, and Chipanshi, A C 1994 Energy budget measurements using eddy correlation and Bowen ratio techniques at the Kinosheo Lake tower site during the Northern Wetands Study. Journal of Geophysical Research 99 (D1). 1539-1549.

Denmead, O.T. and Shaw, R.H. 1962 Availability of soil water to plants as affected by soil moisture content and meteorological conditions. Agronomy Journal 54: 385-390.

Devitt, D A., Sala, A., Smith, S D , Cleverly, J., Shaulis, L.K , and Hammett, R. 1998 Bowen ratio estimates of evapotranspiration for *Tamarix ramosissima* stands on the Virgin River in southern Nevada. Water Resources Research 34 (9) 2047-2414.

Dolman, A.J., Stewart, J B., Cooper, JD. 1988 Predicting forest transpiration from climatological data. Agricultural and Forest Meteorology 42, 399-353.

Doorenbos, J. and Pruitt, W O. 1977 Guidelines for predicting crop water requirements. Irrigation and Drainage Paper 24, 2nd edition. UN-FAO, Rome.

Dorsey, J.D., Ward, A.D., Faussey, N.K., Bair, E.S. 1990 A comparison of four field methods for measuring the saturated hydraulic conductivity. Transaction of the ASAE 33 (6): 1925-1931

Dugas, A and Hicks, R.A. 1998 Effect of removal of *Juniperus ashei* on evapotranspiration and runoff in the Seco Creek watershed. Water Resources Research 34 (6): 1499-1506

Dunin, F.X. 1991 Extrapolation of 'point' measurements of evaporation. some issues of scale. Vegetatio 91: 39-47.

Dunn, S.M and Mackay, R. 1995 Spatial variation in evapotranspiration and the influence of land use on catchment hydrology. Journal of Hydrology 171 (1-4): 49-73.

Dupuit, J. 1863 Études théoriques and practiques sur le mouvement des eaux dans le canaux découverts et à travers les terrains permeables, 2nd ed Paris: Dunod.

Eagleman J.R. 1971 An experimentally derived model for actual evapotranspiration rates. Agric. Meteorol. 8. 385-394.

Eagleman J.R. 1973 A simpler expression for actual evapotranspiration rates - a reply. Agric. Meteorol. 11: 453.

Eagleman, J.R. 1963 The influence of the soil moisture potential and unsaturated conductivity upon evapotranspiration. Thesis 64-4800 University Microfilms, Ann Arber, Michigan 111pp.

Elrick, D.E., Reynolds, W.D., Tan, A.K., 1989 Hydraulic conductivity measurements in the unsaturated zone using improved well analysis. Groundwater Monitoring Review 9.184-193.

English Nature 1991 The Swale National Nature Reserve: Wetland Project English Nature Ashford 1pp.

English Nature 1995 A survey of ditch flora in the North Kent Marshes SSSIs. English Nature Research Report No. 167.

English Nature 1997 Wildlife and fresh water An agenda for sustainable management. English Nature.

Environmental Resources Limited ERL 1990 Technical Annex A: Water quality and hydrology - Final Report Lionhope Planning Inquiry.

Eschenbach, C., Kappen, L. 1996 Leaf Area Index determination in an alder forest: A comparison of three methods. Journal of Experimental Botany 47: 1457-1462.

Evans J.H. 1953 Archaeological horizons on the North Kent Marshes' Archaeologia Cantiana 66, 103-46.

Evett, S R. and Steiner, J L 1995 Precision of neutron scattering and capacitance type soil water content gauges from field calibration. Soil Sci. Soc. Am J. 59 (4):, 961-968.

Feddes, R.A., Kabat, P., van Bakal, P.J.T., Bronswijk, J.J.B. and Habertsma, J. 1988 Modelling soil water dynamics in the unsaturated zone – state of the art. Journal of Hydrology 100 (5): 69-111.

Feddes, R.A., Kowalik, P.J , and Zaradny, H. 1978 Simulation of field water use and crop yield Pudoc, Simulation Monographs, Wageningen, the Netherlands.

Fetter, C.W. 1985 Final Hydrogeological report, Seymour Recycling Corp. Hazardous Wastes Site, Seymour, Indiana. Report to United States Environmental Protection Agency.

Fetter, C W. 1994 Applied Hydrogeology Third Edition. Prentice Hall.

Field, R.T., Fritschen, L J , Kanemasu, E T., Smith, E A., Stewart, J B., Verma, S B and Kustas, W.P. 1992 Calibration, comparison and correction of net radiation

instruments using during FIFE. Journal of Geophys'cal Research, 97 (D17): 18681-18695.

Finke, P.A., Bouma, J. and Stein, A. 1992 Measuring field variability of disturbed soils for simulation purposes Soil Sci Soc. Am J 56: 187-192.

Finlayson, M., Moser, M (eds ) 1991 Wetlands. IWRB.

Fitter, A.H and Hay, R K M 1987 Environmental Physiology of Plants Academic Press, London

Fladung, M. and Ritter, E. 1991 Plant leaf-Area measurements by personal computers. Journal of Agronomy and Crop Science 166 69-70.

Forchheimer, P. 1886 Ueber die Ergiebigkeit von Brunnan-Anlagen und Sickerschlitzen. Z. Archit Ing -Verein Konigreivh Hannover, 32.529 – 563.

Fordham, S.J. and Green, R.D. 1980 Soils of Kent Harpenden.

Frazier, S., 1996 An Overview of the World's Ramsar Sites Wetlands International.

FRCA 1997 Proposals for the future of the North Kent Marshes Environmentally Sensitive Area 1998-2003 A Consultative Document. HMSO.

Freeze, R.A., Cherry, J.A. 1979 Groundwater Prentice Hall Inc.

Fuller R.M. 1987 'The changing extent and conservation interest of lowland grasslands in England and Wales: A review of grassland surveys 1930-1984' Biological conservation 39: 243-253.

Fuller, R.J. 1982 Bird habitats in Britain. Carlton Poyser London.

Gallichand, J., Madramootoo, C.A., Enright, P. and Barrington, S.F. 1990 An evaluation of the Guelph permeameter for measuring saturated hydraulic conductivity. ASAE 33 (4). 1179-1184.

Gardner, E.H. 1983 Soil properties and efficient water use: an overview. In Taylor, H.M., Jordan, W.R., Sinclair, T.R. (eds ) Limitations to efficient water use in crop production. American Society of Agronomy. Madison Wisconsin USA.

Gardner, E.R., Ehlig, C.P. 1963 The influence of soil water and transpiration by plants J. Geophys. Res 68. 5719-5724.

Gardner, W.R. 1958 Some steady state solutions of the unsaturated moisture flow equation with application to evaporation from a water table. Soil Science 85: 228-232.

Gardner, W.R., Hillel, D , and Benyamini, Y. 1970a Post irrigation movement of soil water: l. Redistribution. Water Resources Research 6 851-861.

Gardner, W.R., Hillel, D , and Benyamini, Y. 1970b Post irrigation movement of soil water: ll. simultaneous redistribution and evaporation Water Resources Research 6· 1148-1153.

Gash, J.H.C. 1986 A note on estimating the effect of limited fetch on micrometeorological evaporation measurements Boundary Layer Meteorology 35. 409-413.

Gaskin., G.J. Miller, J D. 1996 Measurement of the soil water content using a simplified impedance measuring technique Journal of Agricultural Engineering Research 63. 153-160.

Gavin H , Agnew C.T. 2000 Estimating evaporation and surface resistance from a wet grassland Phys Chem Earth PT B 25. (7-8) 599-603.

Gay, L.W. Stewart, J B. 1974 Energy balance studies in coniferous forests. Institute of Hydrology Report No 23.

Gee, G W. and Bauder, J W 1986 Particle size analysis In Klute (ed.) Methods of soil analysis No 9 Agronomy. American Society of Agronomy. Madison Wisconsin.

Geyger, E. 1977 Leaf Area and productivity in grasslands In Krause, W. (ed) Handbook of vegetation science Part iii Application of vegetation science to grassland husbandry. Dr W Junk The Hague

Gilham E H , Homes R C. 1950 Birds of the North Kent Marshes London: Collins.

Gilman, K, 1994 Hydrology and Wetland conservation. Wiley, Chichester.

Gilvear, D J, Andrews, R., Tellam, J.H., Lloyd, J.W. and Lerner, D.N 1993 Quantification of the water balance ad hydrogeological processes in the vicinity of a small groundwater-fed wetland, East Anglia, UK. Journal of Hydrology 144(3): 311-334.

Gilvear, D J. and Watson, A 1995 The use of remotely sensed imagery for mapping wetland water table depths· Insh Marshes, Scotland. In Hughes, J M R. and Heathwaite, A.L. Hydrology and hydrochemistry of British Wetlands John Wiley and Sons.

Glaves, D.J., 1998 Environmental Monitoring of Grassland Management in the Somerset Levels and Moors Environmentally Sensitive Rae. England. In Joyce, C.B. and Wade, P.M. (Eds.) European wet grasslands· Biodiversity, Management and Restoration. John Wiley and Sons

Gollan, T., Passioura, J.B., Munns, R 1986 Soil water status affects the stomatal conductance of fully turgid wheat and sunflower leaves. Aust. J. Plant Physiol. 13: 459-464.

Goudie, A.S., and Brunsden, D. 1994 The environment of the British Isles – An Atlas. Clarenden Press.

Gower, S.T., Kucharik, C.J., Norman, J.M. 1999 Direct and indirect estimation of leaf area index, f(APAR), and net primary productivity of terrestrial ecosystems. Remote Sensing of Environment 70: 29-51.

Gowing, D.J.G and Youngs, E.G. 1997 The effect of the hydrology of a Thames flood meadow on its vegetation pattern. BHS Occasional paper No.8 British Hydrological Society.

Gowing, D.J.G, Spoor, G., and Mountford O.J. 1998 The Influence of Minor Variations in Hydrological Regime on Grassland Plant Communities: Implications for water management. In Joyce, C.B and Max Wade, P.(ed.) European wet grasslands: Biodiversity and Restoration. John Wiley and Sons

Grant, D.R. 1975 Measurement of soil moisture near the surface using a neutron moisture meter. J. Soil Sci. 26: 124-129.

Green B H. 1971 Report of a Working Party on Wildlife conservation on the North Kent Marshes Nature Conservancy Council.

Green R.D. 1968 'Soils of Romney Marsh' Bull. Soil Survey Gt. Br.

Green R.D. and Burnham C.P. 1973 'Soils'. In McRae S.G. and Burnham C P (eds.) The rural landscape of Kent. Wye College.

Green, R E. 1988 Effects of environmental factors on the timing and success of breeding of common snipe *Gallinago gallinago* (Aves Scolopacidae) Journal of Applied Ecology 25:79-93.

Green, R.E., Hirons, G J.M., and Cresswell, B H. 1990 Foraging habits of female common snipe *Gallinago* during the incubation period Journal of Applied Ecology 27.325-335.

Gregson, K., Hector, D J , and McGowan, M. 1987 A one parameter model for the soil water characteristic. Journal of Soil Science 38. 483-486.

Grismer, M E., Bali, K M. and Robinson F.E 1995 Field scale neutron probe calibration and variance analysis of clay soil. Journal of Irrigation and Drainage Engineering 121 (5): 354-362.

Guo, Y. Schuepp, P H. 1994a On surface energy balance over the northern wetlands 1. The effects of small-scale temperature and wetness heterogeneity. Journal of Geophysical Research 99 (D1) 1601-1612

Guo, Y. Schuepp, P H 1994b On surface energy balance over the northern wetlands 2. The variability of the Bowen ratio Journal of Geophysical Research 99 (D1): 1613-1621.

Gupta, H V. 1998 Multi-criteria methods for improved calibration of hydrological models. Presentation to the American Geophysical Union Fall meeting

Gupta, H V., Sorooshian, S , and Yapo, P.O 1998 Towards improved calibration of hydrological models: Multiple and noncommensurable measures of information. Water Resources Research 34 (4) 751-763.

Gupta, S C. and Larson, W E 1979 Estimating soil water retention characteristics from particle size distribution, organic matter percent and bulk density. Water Resources Research 5 (6): 1633-1635.

Hamm, N.A S. 1998 An investigation into the unsaturated zone in the hydrology of the Elmley Marshes. MRes Thesis UCL.

Hanna, L W., and Siam, N. 1980 The estimation of moisture content in the top 10 cm of soil using a neutron probe. J. Agric. Sci. 94: 215-253.

Harpley, J. 1999 Water Level Management Plan for the Elmley and Spitend Marshes Lower Medway Internal Drainage Board.

Haverkamp, R., Vauclin, M., and Vachuad, G. 1984 Error analysis in estimating soil water content from neutron probe measurements. 1. Local standpoint. Soil Sci. 137. 78-90.

Hazelden J., Loveland P.J. and Sturdy R.G 1986 Saline soils in North Kent. Soil Survey Special Survey No. 14.

Henley, S. 1981 Non parametric Geostatistics. Applied Science: London.

Hillel, D , 1971 Soil and water: physical principles and processes Academic Press.

Hillel, D., 1998 Environmental Soil Physics. Academic Press.

Hills, R.C. 1970 The determination of the infiltration capacity of field soils using the cylinder infiltrometer. British Geomorphological Research Group. Technical Bulleting No.3.

Hollis. G.E , Fennessey, S. and Thompson, J.R. 1993 A249 Iwade to Queenborough Final Report UCL Wetland Research Unit Internal Report.

Hoogland, G.H. and Samani, Z A. 1982 Estimating potential evapotranspiration. Journal of the Irrigation and Drainage Division, ASCE 108 (IR3): 225-230.

Hoogland, J.C., Belmans, C., and Feddes, R.A. 1981 Root water uptake model depending on soil water pressure head and maximum water extraction rate. Acta Hort 119 123-135

Hoogmoed, W.D. and Bouma, J. 1980 A simulation model for predicting infiltration into cracked clay soils Soil Sci. Soc. Am. J. 44. 458-461.

Hough , M., Palmer, S , Weir, A., Lee, M., Barrie, I 1997 The Meteorological Office Rainfall and Evaporation Calculation System: MORECS Version 2.0 (1995). The Met Office

Hudson, J A., and Gilman, K. 1993 Long-term variability in the water balances in the Plynlimon catchments Journal of Hydrology 143 355-180.

Hulme, M and Barrow, E 1997 Climatology of the British Isles Routledge.

Huntingford, C. 1995 Non-dimensialisation of the Penman-Monteith model. Journal of Hydrology 170 (3): 215-232.

Hutson, J L., and Cass, A. 1987 A retentivity function for use in soil-water simulation models Journal of Soil Science 38: 105-113.

Hvorslev, M J. 1951 Time lag and soil permeability in groundwater observations Bulletin no. 56 Waterways Experiment Station US Army Corps of Engineers

Hyder, Z. and Butler, J J , 1995 Slug tests in unconfined formations: An assessment of the Bouwer and Rice technique Groundwater 33.16-22.

Ibanez, M., Perez, P.J., Caselles, V., and Castellvi, F. 1999 Estimation of the latent heat flux over full canopy covers from the radiative temperature. Journal of Applied Meteorology 38 423-431.

Idso, S B., Allen, S G., Kimball, B A. 1987 The peril of porometry. Pages 133-138 in Proc. Ntl. Cnf. On Measurement of soil and plant water stress Vol2 Logan UT 6-10 July 1987 Utah State, Univ. Logan UT.

Ingram, H.A P. 1983 Hydrology In A.J P Gore (ed.) Mires: swamp bog fen and moor. Ecosystems of the World 4a. Elsevier Amsterdam.

Institute of Geological Sciences IGS 1970 Hydrogeological Map of the Chalk and Lower Greensand of Kent: Sheet 1. Chalk, Regional Characteristics and Explanatory Notes Institute of Geological Sciences, London.

Intergovernmental Panel on Climate Change IPCC 1990 The Policy Makers' Summary of the Report of Working Group 2 to the IPCC, UNEP and World Meteorological Organisation IPCC.

Intergovernmental Panel on Climate Change IPCC 1995 Second Assessment Report: Climate Change A Report of the Intergovernmental Panel on Climate Change. IPCC, Geneva, Switzerland. pp 64.

International Institute for Land Reclamation and Improvement 1973 Drainage principles and Applications 4 Vols. ILRI Publication no 16 Wageningen, Netherlands.

Isaaks E.H Srivastava R.M. 1989 An introduction to Applied Geostatistics. Oxford University Press

IUCN 1987 Directory of wetlands of international importance: sites designated under the Convention on Wetlands of International Importance especially as Waterfowl Habitat. International Union for Conservation of Nature and Natural Resources Gland, Switzerland.

Jacobsen, O.H. and Schjønning, P. 1993 Field evaluation of time domain reflectrometry for soil water measurements. Journal of Hydrology 151: 159-172.

Jarvis, P.G. 1976 The interpretation of the variations in leaf water potential and stomatal conductance found in canopies in the field. Phil Trans. R. Soc Lond. B. 273: 593-610.

Jarvis, P.G. 1993 Water losses of crowns canopies and communities. In J A.C Smith and H. Griffiths (ed.) Water Deficits - Plant responses from cell to community. Bios Scientific Publishers pp285-315.

Jassim H.F. 1976 Soils and land use of the North Kent Marshes M Phil. Thesis University of London.

Jaworski, J. 1981 The influence of soil moisture and soil water deficit on the evapotranspiration process. Journal of Hydrological Sciences 8 (1-4): 35-47.

Jaworski, J 1991 Assessment of diffusive crop cover resistance in evapotranspiration simulations by means of mathematical models Hydrological Interactions between Atmosphere Soil and Vegetation (Proceedings of the Vienna Symposium) IAHS Publication no 204.

Jensen, M.E., Burman, R.D., and Allen, R.G. 1990 Evaporation and irrigation water requirements. ASCE Manual No 70

Jetten V.G., Riezebos T.H., Hoefsloot F., Rossum J.V. 1993 Spatial Variability of infiltration and related properties of tropical soils. Earth Surface Process and Landforms 18 177-488

Johns, G G and Smith, R.C G 1975 Accuracy of soil water budget based on a range of relationships for the influence of soil water availability on actual water use. Aust J Agric Res. 26: 871-883

Johnson A.I. 1967 Specific yield – compilation of specific yields for various materials. U S. Geological Survey Water-Supply Paper 1662-D.

Jones, H.G. 1992 Plants and Microclimate: a quantitative approach to environmental plant physiology. Second ed CUP.

Journel A.G. Huijbregts C.J 1979 Mining Geostatistics. Academic Press.

Kelliher, F M., Leuning, R., Schulze, E D 1993 Evaporation and canopy characteristics of coniferous forests and grasslands Oecologia 95 (2)· 153-163.

Kim, J. and Verma, S 1991 Modelling canopy stomatal conductance in a temperate grassland ecosystem. Agricultural and Forest Meteorology 55 (1-2). 149-166.

King C. 1981 The stratigraphy of the London Clay and associated deposits Tertiary Research Special Paper No. 6 Rotterdam: Dr. W. Backhuys.

Kings K.M. 1967 Soil moisture – instrumentation, measurement and general principles of network design. In Proceedings of Hydrology Symposium no. 6 Soil Moisture. Published by Inland waters Branch Department of energy Mines and Resources Canada.

Kirkham 1967 Explanation of paradoxes in Dupuit-Forchheimer seepage theory. Water Resources Research 3, 609-622.

Kitandis P.K. 1997 Introduction to Geostatistics· Applications to Hydrogeology Cambridge Academic Press.

Kovacs, G. 1987 Estimation of average areal evapotranspiration. Journal of Hydrology 95 (3-4): 227-40.

Kristensen K.J., and Jensen, S E., 1975 A model for estimating actual evapotranspiration from potential evapotranspiration. Nordic Hydrology 6: 170-188.

Kristensen, K.J. 1973 Depth intervals and topsoil measurements with the neutron depth probe. Nordic Hydrology 4:77-85.

Kussner, R., Mosandl, R. 2000 Comparison of direct and indirect estimation of leaf area index in mature Norway spruce stands of eastern Germany. Canadian Journal of Forest Research 30 (3). 440-447.

Lafleur, P., and Rouse, W R., 1988 The influence of surface cover and climate on energy partitioning and evaporation in a subarctic wetland. Boundary Layer Meteorology 44 (4) 327-347

Lafleur, P., Rouse, W.R., Hardill, S.G. 1987 Components of the surface energy balance of subarctic wetland terrain units duing the snow free period. Arct. Alp Res 19 (1): 53-63.

Lafleur, P.M, McCaughey, J H., Joiner, D.W., Bartlett, P.A., and Jelinski, D.E. 1997 Seasonal trends in energy, water and carbon dioxide fluxes at a northern boreal wetland Journal of Geophysical Research Atmos 102 (D24). 290009-29020.

Langlands, J.P. and Bennett, I L. 1973 Stocking intensity and pasture production, changes in the soil and vegetation of grown pasture grazed by sheep at different stocking rates. J. Agr Sci. 81.193-204.

Larcher W. 1980 Second ed. Physiological Plant Eology Springer-Verlag.

Laslett, G.M., McBratney, A B., Pahl P J. and Hutchinson, M.F. 1987 Comparison of several spatial prediction methods for soil pH. Journal of Soil Science 38 (2): 325-341

Lee, D.M., Reynolds, W.D , Elrick, D E , and Clothier, B E 1985 A comparison of three field methods to determine saturated hydraulic conductivity Can J Soil Sci. 65 563-573.

Leeds-Harrison, P.B., Shipway, C.J.P , Jarvis, N.J., and Youngs, E.G. 1986 The influence of soil macroporosity on water retention, transmission and drainage in a clay soil. Soil Use and Management 2.47-50

Lemon, E.R., Wright, J.L. 1969 Photosynthesis under field conditions XA Assessing sources and sinks of carbon dioxide in a corn (Zea mays L ) crop using a momentum balance approach Agronomy Journal 61 405-410

Lettau, H. 1959 A review of research problems in micrometeorology. Dept. Meteorology, Univ. Wis. Final report, Contract DA-36-039-SC-80063

Lewis, J.M. 1995 The story behind the Bowen ratio. Bull Amer. Meteor. Soc. 76 (12): 2433-2443.

Lhomme, J. 1991 The concept of canopy resistance· historical survey and comparison of different approaches. Agricultural and Forest Meteorology 54 (2-4): 227-240.

Lilly, A. 1994 The determination of field-saturated hydraulic conductivity in some Scottish soils using the Guelph permeameter. Soil Use and Management 10 (2): 72-78.

Linacre, E.T. 1973 A simpler step empirical expression for actual evapotranspiration rates – A discussion. Agricultural Meteorology 11 (1): 451-452.

Linacre, E.T. 1993 A three resistance model of crop and forest evaporation. Theor. Appl. Clim 48: 41-48

Livingston, N.J. 1993 Soil Water Potential. In Carter, M.R. (ed.) Soil Sampling and Methods of Analysis Canadian society of Soil Science. Lewis Publishers.

Loomis, R.S., Williams, W N. 1969 Productivity and the morphology of crop stands: patterns with leaves. In Eastin, J.D. (ed ) Physiological aspects of crop yields. ASA CSSA and SSA Madison WI.

Loveland, P J., Hazelden, J., Sturdy, R.G., and Hodgson, J.M. 1986 Salt affected soils in England and Wales Soil Use and Management 2 (4): 150-156.

MAFF 1962 The East Coast Floods 1953. HMSO

MAFF 1967 Potential Transpiration Tech. Bull. no. 16 London: HMSO

MAFF 1994 The North Kent Marshes Environmental Sensitive Areas Gu'delines for Farmers, Reading. MAFF. HMSO.

Mahfouf, J.F. and Noilhan, J. 1991 Comparative formulations of evaporation from bare soil using in situ data. J Clim. Appl Meteorol 30 (9):1354-1365

Malek, E and Bingham, G.E. 1993 Comparison of the Bowen ratio-energy balance and the water balance methods for the measurement of evaporation Journal of Hydrology 146 (1-4)· 209-220.

Malek, E. 1992 Night-time evaporation vs. daytime and 24h evaporation Journal of Hydrology, 138 (1-2) : 119-129

Malek, E. 1993 Rap'd changes of the surface soil heat flux and its effects on the estimation of evaporation. Journal of Hydrology, 142: 89-97

Marks M J. and Robins D J. 1986 Field drainage and soil management. In Hazelden J., Loveland P.J. and Sturdy R.G Saline soils in North Kent Soil Survey. Special Survey No. 14.

Marshall, D C.W. 1989 The Instrumentation of Flat, Low-Lying Catchments for Hydrological Research Institute of Hydrology Report No 105, Wallingford.

Martinez-Cobb, A. and Cuenca, R H 1992 Influence of elevation on regional evapotranspiration using multivariate geostatistics of various climatic regimes in Oregon Journal of Hydrology 13(1-4): 353-380.

Mas-Pla, J , JimYeh, TEC , Williams, T.M , McCartney, J F 1997 Analyses of slug tests and hydraulic conductivity variations in the near field of a two well tracer experimental site Groundwater 35 (3) :492-501.

McAneney, K J., K.J. Judd, M.J. 1983 Pasture production and water use measurement in the central Waikato, New Zealand. J. Agric Res. 26 (1): 7-143.

McBratney A.B. Webster R. 1983 How many observations are needed for regional estimation of soil properties? Soil Science 135 (3): 177-183.

McBratney A.B. Webster R. 1986 Choosing functions for semi-variograms of soil properties and fitting them to sampling estimates Journal of Soil Science 37 (4): 617-639.

McRae S G 1973a 'Geology'. In McRae S.G. and Burnham C.P. (eds.) The rural landscape of Kent. Wye College.

McRae S.G. 1973b 'Agriculture and horticulture'. In McRae S.G. and Burnham C.P. (eds.) The rural landscape of Kent. Wye College.

Mendez, J., Hinzman, L.D. and Kane, D L. 1998 Evapotranspiration form a wetland complex on the Arctic coastal plain of Alaska. Nordic Hydrology 29 (4-5): 303-330.

Merricks, P. (Elmley Conservation Trust). Personal communication regarding grazing regime and saturated fields at Elmley Marshes

Messing, I., Jarvis, N.J. 1990 Seasonal variation in field saturated hydraulic conductivity in two swelling clay soils in Sweden. Journal of Soil Science 41 (2): 229-237.

Miller, R.W. and Gardiner, D.T. 1997 Soils in our environment Eight edition. Prentice Hall.

Milsom, T. (Central Services Laboratory, York ) Personal communication regarding research undertaken by Milsom at Elmley Marshes over 1995-1997. (Research to be published in the Journal of Applied Ecology, and Biological Conservation)

Mitchell, A R. and van Genuchten, M.T. 1993 Flood irrigation of a cracked soil. Soil Sci. Soc. Am. J. 57 (2): 490-497.

Mitsch, W J., Gosselink, J G. 2000 Wetlands Third Edition Wiley

Monteith, J.L. 1965 Evaporation and environment, Symp. Soc. Exp. Biol. XIX Cambridge University Press

Monteith, J.L. 1981 Evaporation and surface temperature Quarterly Journal of the Royal Meteorological Society 107 (451): 1-27.

Monteith, J L., and Unsworth, M 1990 Principles of Environmental Physics Second Edition. Arnold

Moore, K.E., Fitzjarrald, D R., Wofsy, S C., Daube, B C., Munger, J W., Bakwin, P.S. and Crill, P. 1994 A season of heat, water vapour, total hydrocarbon and ozone fluxes at a subarctic fen. Journal of Geophysical Research 99 (D1): 1937-1952.

Morris, C., and Potter, C. 1995 Recruiting the new conservationists. Farmers' adoption of agri-environment schemes in the UK. J. of Rural Studies 11 (1): 51-63.

Mortier, P., DeBoodt, M., Donsercoer, W. and DeLeenheer, L. 1960 The resolution of the neutron scattering method for soil moisture determination. Trans 7th Intern. Congr Soil Sci. 1.321-329.

Moss B. 1992 'Potential effects of greenhouse warming on freshwater systems in the UK with special references to coastal lowlands' Wetlands Ecology and Management 1 (1-2): 51-53.

Murray, F.W. 1967 On the computation of saturation vapour pressure. J Appl. Meteor 6: 203-204.

Narasimhan, T N. 1989 Numerical simulation of Richards' equation· current approaches as an alternative perspective. In Morel-Seytoux, H.J. (ed.) Unsaturated Flow in Hydrological Modelling· Theory and Practise Kluwer Academic Publishers London

Nash, J.E. 1989 Potential evaporation and the complementary relationship. Journal of Hydrology 111. 1-7.

National Rivers Authority (NRA) 1991 NRA Policy Implementation Guidance Note No. TE/ED001: Climate Change - Sea Level Rise and Isostatic Variations NRA Bristol.

Nature Conservancy Council (NCC) 1984 Nature Conservation in Great Britain Shrewsbury; Nature Conservancy Council.

Nature Conservancy Council (NCC) 1990 The Swale: Site of Special Scientific Interest Citation File reference TQ-96-2. 2pp and map.

Nicholson, I.A., Robertson, R.A. and Robinson, M. 1989 The effects of drainage on the hydrology of a peat bog. International Peat Journal 3: 59-83.

Oke, T.R. 1987 Boundary Layer Climates Second Edition Routledge.

Olgaard, P.L. 1965 On the theory of the neutronic method for measuring the water content of soils. Danish Atomic Energy Comm. Res. Est. Riso. Rept. 97.

Olier, B. d' 1972 'Subsidence and sea level rise on the Thames estuary' Phil. Trans. Roy. Soc. (A) 272: 121-30

Oliver M, Webster R, Gerrard J. 1989b Geostatistics in physical geography Part II: application. Trans Inst. Br Geogr N S 14: 270-286.

Oliver M., Webster R., Gerrard J. 1989a Geostatistics in physical geography Part I: theory. Trans. Inst. Br. Geogr. N S. 14. 259-269.

Oliver M.A., Webster R. 1986 Combining Nested and Linear Sampling for determining the scale and form of Spatial Variation. Geographical Analysis 18 (3)· 227-242.

Oliver M.A., Webster R. 1986 Semi-variograms for modelling the spatial pattern of landform and soil properties Earth Surface Process and Landforms 11 (5): 491-504.

Oliver M.A , Webster R. 1987 The elucidation of soil pattern in the Wyre Forest of the West Midlands, England. I Multivariate Distribution. Journal of Soil Science 38 (2): 279-291.

Oliver M.A., Webster R. 1987 The elucidation of soil pattern in the Wyre Forest of the West Midlands, England. II Spatial Distribution. Journal of Soil Science 38 (2) 293-307.

Oliver P. 1991 Bird watching on the North Kent Marshes St. Leonards-on-sea: Cinque Port Press

Oppenheimer, H R. 1951 Physiological behaviour of maize under irrigation Palestine J. Botany Rehovot Ser 8: 32

Ortega-Farias, S O , Cuenca, R.H. and English, M. 1995 Hourly grass evapotranspiration in modified maritime environment. Journal of Irrigation and Drainage Engineering 121· 6, 369-373

Ould Mohammed S., Bertuzzi P., Bruand A., Raison, L., and Bruckler, L., 1998 Field evaluation and error analysis of soil water content measurement using the capacitance probe method. Soil Sci. Soc. Am. J. 61 (2): 399-408.

Parker, J. 1968 Drought resistance mechanisms. In Kazlowski, T.T., Water deficits and Plant growth. Vol. 1: Development, control and measurement. Academic Press.

Parkes, M E, and Siam N. 1979 Error associated with measurement of soil moisture change by neutron probe J Agric Eng. Res 24. 87-93

Pebesma, E.J. 1997 gstat user's manual. Downloaded from the World Wide Web· http://www.frw uva.nl/~pebsema/gstat/

Pegg, R.K. and Ward, R.C. 1972 Evapotranspiration from a small clay catchment. Journal of Hydrology 15: 149-165.

Penman, H.L. 1948 Natural evaporation from open water, bare soil and grass. Proc. Roy Soc Lon. A 193: 120-145.

Pereira, L.S. and Smith, M. 1989 Proposed procedures for revision of guidelines for predicting crop water requirements Land and Water Use Div. FAO Rome.

Persson, G. and Lindroth, A. 1994 Simulating evaporation from short rotation forest: variations within and between seasons. Journal of Hydrology 156 (1-4): 21-45.

Pettersen, O.W., Cunningham, R L., and Matelski, R.P. 1968 Moisture characteristics of Pennsylvanian soils: 1 Moisture retention as related to texture. Soil. Sci. Soc. Am J. 32:271-275.

Pettitt A.N., McBratney A.B. 1993 Sampling Designs for Estimating Spatial Variance Components. Appl. Stat. J. Roy. St. C42 (1). 185-209.

Phersson, M. and Pettersson, O. 1997 Energy and water balance of a bog in central Sweden. Nordic Hydrology 28 (4-5) 163-272.

Philip, J.R 1985 Approximate analysis of the borehole permeameter in unsaturated soil. Water Resources Research 21 (7): 1025-1033.

Pierce, L.T., 1958 Estimating seasonal and short term fluctuations in evapotranspiration from meadow crops. Bull. Am. Meteorol. Soc. 39: 73-78.

Pitcher W.S. 1958 'The geological setting of the lower Tertiary deposits of the London region'. In Wells A.K. (ed ) Geologists Association Guides No. 30: The London Region Colchester: Benham and Company Limited.

Price, J.S. 1991 Evaporation from a blanket bog in a foggy coastal environment. Boundary Layer Meteorology 57 (4): 391-406.

Price, J.S., Maloney, D.A., and Downey, F G. 1991 Peatlands of the Lake Mellville Coastal Plain, Labrador. Proc. Northern Hydrol. Symp , Saskatoon, July 2000.

Priestly, C.H B., and Taylor, R.J., 1972 On the assessment of surface heat flux and evaporation using large scale parameters. Monthly Weather Rev. 100 81-92.

Puckett, W.E., Dane, J H, and Hajek, B.F. 1985 Physical and mineralogical data to determine soil hydraulic propert es Soil. Sci. Soc. Am J. 49 (4): 831-836.

Raes D., 1996 BUDGET A field water balance model Reference manual K U. Leuven University, Belgium.

Ragab, R. and Cooper, J D 1993a Variability of unsaturated zone water transport parameter: implications for hydrological modelling 1. In situ measurements Journal of Hydrology 148 (1-4) 109-131.

Ragab, R. and Cooper, J D. 1993b Variability of unsaturated zone water transport parameter: implications for hydrological modelling. 1 Predicted vs. in situ measurements and evaluation of methods. Journal of Hydrology 148 (1-4): 133-147.

Ragab, R. Finch, J. and Harding, R. 1997 Estimation of groundwater recharge to chalk and sandstone aquifers using simple soil models. Journal of Hydrology 190 (1-2): 19-41

Raupach, M R., Finnigan, J.J. 1998 Single-layer models of evaporation from plant canopies are incorrect but useful, whereas multi-layer models are correct but useless - Discuss Aust J. Plant Physiol. 15 (6): 705-716

Rawlins, S.L. Gardner, W R., Dalton, F.N. 1968 In situ measurements of soil and leaf water potential Proc. Soil Sci Soc Amer. 32. 468-300.

Rawls, W.J., Brakensiek, D.L. 1982 Estimating soil water retention from soil properties. Transactions of the ASAE 108 (2) 166-171.

Rawls, W.J, Brakensiek, D.L. and Saxton K E. 1982 Estimation of soil water properties. Transactions of the ASAE 25 (5): 1316-1320 &1328.

Reeve, R.C. 1982 Soil Permeability – Auger Hole Method. Technical Note no 2-118 Advanced Drainage Systems Columbus OH.

Reid, I, and Parkinson, R.J. 1984a The nature of the tile drain outfall hydrograph in heavy clay soils Journal of Hydrology 72 (3-4): 289-305.

Reid, I, and Parkinson, R.J. 1984b The wetting and drying of a grazed and ungrazed clay soil. Journal of Hydrology 35 (4): 607-614.

Reynolds, T.D., Shepard, R B., Laundré, L.W. and Larrabee Winter, C. 1987 Calibrating resistance-type soil moisture units in a high clay-content soil. Soil Science 144 (4): 237-241.

Reynolds, W.D., 1994 Comments on 'Comparison of three methods for assessing soil hydraulic properties' by G G Paige and D. Hillel. Soil Science 157: 116-119.

Reynolds, W.D., and Elrick, D.E. 1986 A method for simultaneous in situ measurement in the vadose zone of field-saturated hydraulic conductivity, sorptivity and the conductivity-pressure head relationship. Ground Water Monitoring Review 6 (1): 84-95 WIN.

Reynolds, W.D., and Elrick, D.E. 1987 A laboratory and numerical assessment of the Guelph permeameter method. Soil Sci 144 (4): 282-292.

Reynolds, W.D., and Elrick, D.E. 1990 Ponded infiltration from a single ring 1: Analysis of steady flow. Soil Sci Soc. Am J. 54 (5):1233-1241.

Reynolds, W.D., Elrick, D.E. and Clothier, B.E. 1985 The constant head well permeameter; effects of unsaturated flow. Soil Science 139:172-180.

Reynolds, W.D., Elrick, D E. and Topp, G C. 1983 A re-examination of the constant head well permeameter method for measuring saturated hydraulic conductivity above the water table Soil Sci. 136 (4). 250-268.

Richards, L.A. 1931 Capillary conduction of liquids through porous medium Physics 1:318-333

Riezebos H.Th. 1989 Application of nested analysis of variation in mapping procedures for land evaluation. Soil Use and Management 5 (1): 25-30.

Ripley E.A., and Redmann, R.E. 1976 Grassland. In Monteith, J L. (ed ) Vegetation and the Atmosphere. Volume 2 Case Studies. Academic Press

Ripley, E A., Saugier, B 1978 Biophysics of a natural grassland: evaporation. J Appl. Ecol 15: 459-479.

Ritchie, J.T. and Adams, J E 1974 Field measurement of soil evaporation from soil shrinkage cracks Soil Sci Soc Am Proc. 38:131-134.

Roberts, A.M. 1989 The Catchment Research Data Base at the Institute of Hydrology. Institute of Hydrology Report no 106 Institute of Hydrology.

Robinson D.A., Bell J.P., and Batchelor C.H 1994 Influence of iron minerals on the determination of soil water content using dielectric techniques Journal of Hydrology 161 (1-4)· 169-180.

Robinson, M. and Beven, K.J. 1983 The effect of mole drainage on the hydrological response of a swelling clay soil. Journal of Hydrology 64(4):205-223.

Robinson, M and Dean T.J. 1993 Measurement of near surface soil water content using a capacitance probe. Hydrological processes 7 (1): 77-86.

Rodwell, J S. 1992 British plant communities. Volume 3 Grassland and montane communities pp550. Cambridge Cambridge University Press.

Roth, C.H., Malicki, M.A., and Plagge R. 1993 Empirical evaluation of the relationship between soil dielectric constant and volumetric water content as the basis for calibrating soil moisture measurements by TDR. Journal of Soil Science 43 (1): 1-13.

Roulet NT., Munro, S. and Mortsch, L 1997 In Bailey, W., Rouse, W R., and Oke, T.R (eds) Surface climates of Canada. McGill-Queen Prees Montreal Canada.

Rowell, D.L. 1997 Soil Science: Methods and Applications. Longman.

Royal Society for the Protection of Birds (RSPB) 1992 'Time for a Greater Thames' RSPB.

RSPB, EN and ITE 1997 The Wet Grassland Guide RSPB.

Russell, G. 1980 Crop evaporation, surface resistance and soil water status. Agricultural Meteorology 21, 213-226.

Salverda, A.P. and Dane, J.H. 1993 An examination of the Guelph permeameter for measuring the soil's hydraulic properties. Geoderma 5 (4). 405-421.

Saugier, B. and Katerji, N. 1991 Some plant factors controlling evapotranspiration. Agricultural and Forest Meteorology 54 (2-4), 263-277.

Schincariol, R.A. and Schwartz, F.W. 1990 An experimental investigation of variable density flow and mixing in homogenous and heterogeneous media. Water Resources Research 26 (10): 2317-2329.

Schmid H.P., Oke, T.R., 1990 A model to estimate the source area contribution to turbulent exchange in the surface layer over patchy terrain. Quarterly Journal of Research of the Meteorological Society 116 (494): 965-988.

Schuepp, P H. Leclerc, M Y., Macpherson, J I., and Desjardins, R.L. 1990 Footprint prediction of scalar fluxes from analytical solutions of the diffusion equation. Boundary Layer Meteorology 50 (1-4): 355-373.

Sene, K.J., Gash, J.H.C. and McNeil, D.D. 1991 Evaporation from a tropical lake: comparison of theory with direct measurement. Journal of Hydrology 127 (1-4)· 193-217.

SERPLAN 1988 Development potential in the Eastern Thames Corridor The London and Southeast Regional Planning Conference, London.

Shaw, E.M. 1994 Hydrology in practise. Third Edition. Chapman and Hall.

Shaw, G. and Wheeler, D. 1994 Statistical Techniques in Geographical Analysis Second edition. David Fulton Publishers Ltd London.

Shennan, I. (ed ) 1989 'Late Quaternary sea level changes and coastal movements in the British Isles' Journal of Quaternary Science 4. 1 94

Shuttleworth, W.J. 1975 Experimental evidence for the failure of the Penman Monteith equation in partially wet conditions Boundary-Layer Meteorology 10: 91-94.

Shuttleworth, W.J. 1979 Evaporation Institute of Hydrology Report no. 56 Institute of Hydrology.

Shuttleworth, W.J. 1992 Evaporation Chapter 4 in Maidment (ed ) Handbook of Hydrology. McGraw-Hill Inc New York NY.

Silvertown, J., Dodd, M E., Gowing, D.J.G, and Mountford O J. 1999 Hydrologically defined niches reveal a basis for species richness in plant communities. Nature 400 (6739): 61-63.

Sinclair, T.R., Allen, L.H , and Lemon, E R. 1975 An analysis of errors in the calculation of energy flux densities above vegetation by a Bowen ratio profile method. Boundary-Layer Meteorology 8.129-139.

Slabbers, P J 1980 Practical prediction of actual evapotranspiration. Irrigation Science 1, 185-196.

Slatyer, R O, and McIlroy, I C. 1961 Practical Microclimatology C S.I R.O , Melbourne, UNESCO, Paris. 340 p.

Smith K.W. 1983 The status and distribution of waders breeding on wet lowland grassland in England and Wales. Bird Study 30 (NOV). 177-192.

Smith, M., Allen, R.G., Monteith, J L., Perrier, A., Pereira, L. and Segeren, A. 1992 Report of the expert consultation on procedures for revision of FAO guidelines for prediction of crop water requirements UN-FAO, Rome, Italy.

Smith, M. CROPWAT A computer program for irrigation planning and management. FAO Irrigation and Drainage Paper no. 46.

Soil Moisture Equipment Corp. 1987 Guelph permeameter, Model2800K1 operating and instruction manual. Santa Barbara, CA Soil Moisture Equipment Corp.

Souch, C., Wolfe, C.P. and Grimmon, S B., 1996 Wetland evaporation and energy partitioning. Indian Dunes National Lakeshore. Journal of Hydrology 184 (3-4): 189-208.

Spiegel, R.G. 1980 Schuam's Outline of Theory and Problems of Probability and Statistics SI (Metric) Edition. McGraw-Hill.

Stalfelt, M.G. 1961 The effect of the water deficit on the stomatal movements in a carbon dioxide free atmosphere. Physiol. Plantarum. 14: 826

Stamp D. 1943 Report of the Land Utilisation Survey of Britain Part 85: Kent. Geographical Publications London.

Stephens, D.B., Unruh, M., Havlena, Knowlton, R.G, Mattson, E., and Cox, W. 1988 Vadose zone characterisation of low-permeability sediments using permeameters. Ground Water Monitoring Review 8 (2). 59-65 Spring

Stewart, J.B 1988 Modelling stomatal conductance of pine forest. Agricultural and Forest Meteorology 43, 19-35

Stewart, R.B , and Rouse, W.R. 1976 Simple models for calculating evaporation from dry and wet surfaces. Arctic and Alpine Res. 8: 263-274.

Swartz, C.H. and Schwartz, F.W. 1998 An experimental study of mixing and instability development in variable density systems. Journal of Contaminant Hydrology 34 (3): 169-189

Swetnam, R.D., Mountford, J O., Armstrong, A.C , Gowing, D J G, Brown, N J., Manchester, S J. and Treweek, J R. 1998 Spatial relationships between site hydrology and the occurrence of grassland of conservation importance: a risk assessment with GIS. Journal of Environmental Management 54 (3): 189-203.

Szeicz, G. and Long, I F. 1969 Surface resistance of crop canopies. Water Resources Research 5 (3): 622-633.

Szeicz, G., Endrodi, G., Tajchman, S., 1969 Aerodynamic and surface factors in evaporation. Water Resources Research 5: 380-394.

Tanner, C.B., Fuchs, M. 1968 Evaporation from unsaturated surfaces: A generalised combination method. Journal of Geophysical Research 73 1299-1304.

Tetens, O. 1930 Uber einige meteorologische Begriffe. Z Geophys 6. 297-309.

Thames Estuary Project (TEP) 1996 Thames Estuary man gement Plan Draft for Consultation

Thompson, J R. and Hollis, G E. 1996 Hydrological Functioning of the North Kent Marshes Report for the Joint Research Centre Ispra.

Thompson, M A , Campbell, D I , Sproken-Smith, R.A 1999 Evaporation from natural and mod fied raised peat bogs in New Zealand Agricultural Forest Meteorology 95 (2) 85-98

Thornley, J H.M 1996 Modelling water in plants and ecosystems Annals of Botany 77 (3) 261-265

Thornton D. and Kite D J 1990 Changes in the extent of the Thames estuary grazing marshes Nature Conservancy Council.

Tomer, M.D. and Anderson J.L. 1995 Field evaluati n of a soil water-capacitance probe in a fine sand Soil Science 159 (2) 90-98

Topp, G C., Davis, J L , Annan, A.P. 1980 Electromagnetic determination of the soil water content. Water Resources Research 16 574-582

Towner, G.D , Youngs, E G., 1986 Application of drainage theory in the field. Soil Use and Management 2 (2) 44-47

Treweek, J.R., Mountford, J.O., Brown, N.J., Manchester, S.J., Sparks, T.H., Stamp, T R , Swetnam, R.D , Caldow, R.W G , Gowing, D J G, Lambourne, R. 1996 Effects of Managing Water Levels to Maintain or Enhance Ecological Diversity within Discrete Catchments. Institute of Terrestrial Ecology Final Report to the Ministry of Agriculture, Monks Wood, Abbots Ripton, Huntington, Cambridgeshire, UK.

Tsuda, M. 1999 Errors in leaf Area Measurement with an automatic Area Meter due to Leaf Chlorophyll in crop plants Annals of Botany 84 (6) 799-801

Turner, N.C. 1991 Measurement and influence of environmental and plant factor on stomatal conductance in the field. Agricultural and Forest Meteorology 54 (2-4): 137-154.

Van Bavel, C.H M 1956 Neutron and gamma radiation applied to measuring physical properties of soil in its natural state. Trans 6th Intern Congr Soil Sci. B pp355-360

Van Bavel, C H.M 1967 Changes in canopy resistance to water loss from alfalfa induced by soil water depletion Agr Meterorol 4 165-176

Van de Griend, A.A. and Owe, M. 1994 Bare soil surface resistance to evaporation by vapour diffusi n under semiarid conditions. Water Resources Research 30(2): 181 188)

Van Genuchten, M. Th 1980 A closed form equation for predicting the hydraulic conductivity of unsaturated soi s Soil Sci Am J 44 8 2-899

Vereecken, H , Maes, J , Feyen, J and Darius, P 1 89 Estimating the soil moisture retention characteri tic from texture, bulk dens ty, and carbon content. Soil Science 1 8 (6) 389-403

Visvalingham, M. and Tandy, J D 1972 The neutron method for measuring soil moisture content A review J Soil Sci 23 499-511

Waggoner, P E , and Zel tch, I Transpiration and the stomata of leaves Sc ence 150 1413

Ward, R C and Rob nson, M 1990 Principles of Hydrology Third Edition McGraw-Hill

Warrick A.W , Myers D E. 1987 Optimization of Sampling Location for variogram calculations Water Resources Research 23 (3) 496-500

Watson, D J , 1947 Annals of Botany 11, 41-76

Webster R., Burgess T.M 1984 Sampling and bulking strategies for estimating soil properties in small regions. Journal of Soil Science 35 (1)· 127-140.

Webster R., Oliver M.A. 1992 Sample adequately to estimate variograms of soil properties. Journal of Soil Science 43 (1): 177-192.

Webster, R. 1977 Quantitative and numerical methods in soil classification and survey. Monograph of Soil Survey Clarenden Press, Oxford.

Weitz A., Bunte D , Herseman H., 1993 Application of Nested Sampling Technique to Determine the Scale of Variation in Soil Variation and Chemical Properties. Catena 20 (1-2): 207-214.

Wessel, D A. and Rouse, W R. 1994 Modelling evaporation from wetland tundra. Boundary Layer Meteorology 68 (1-2). 109-130.

Williams G, Henderson A., Goldsmith L. and Spreadborough A. 1983 'The effects on birds of land drainage improvements in the North Kent Marshes' Wildfowl 34: 33-47.

Williams, G. and Hall, M. 1987 The loss to arable agriculture of coastal grazing marshes in south and east England with special reference to east Essex. Biological Conservation 39: 243-253.

Williams, J., Prebble, R.E., Williams, W.T. and Hignett, C.T. 1983 The influence of texture, structure and clay mineralogy on the soil moisture characteristic. Australian Journal of Soil Research 21 15-32.

Willmott, C.J., and Wicks, D.E. 1980 An empirical method for the spatial interpolation of monthly precipitation within California. Phys Geogr. 1.59-73.

Willock C. 1993 'Farming wildfowl on Elmley Island' The Field pp82-83.

Wilson, G.A, 1997 Assessing the Environmental Impact of the Environmentally Sensitive Area Scheme: a case for using farmer's knowledge? Landscape Research 22: No3. 303-326.

Wilson, R.G., and Rouse, W.R. 1972 Moisture and temperature limits of the equilibrium evapotranspiration model. J. Appl. Meterol. 11, 436-442.

Wind, G P., and Van Doorne, W. 1975 A numerical model for the simulation of unsaturated vertical flow of moisture in soil. Journal of Hydrology 24:1-20.

Woo, M , and Rowsell, D. 1993 Hydrology of a prairie slough. Journal of Hydrology 146 (1-4). 175-207

Wosten, J.H.M. and van Genuchten, M.TH. 1988 Using texture and other properties to predict the unsaturated soil hydraulic functions. Soil Sci. Soc Am J. 52 (6): 1762-1770.

Wright, I.R and Harding, R.J. 1993 Evaporation from natural mountain grassland. Journal of Hydrology 145 (3-4): 267-263.

Wright, J L., Lemon, E.R. 1966 Photosynthesis under field conditions IX vertical distribution of photosynthesis with a corn crop. Agronomy Journal 58: 265-268.

Wu, K. 1998 Measurement of soil moisture change in spatially heterogeneous weathered soils using a capacitance probe. Hydrological Processes 12. 135-146.

Yapo, P O., Gupta, H.V and Sorooshian, S. 1998 Multi-objective global optimisation for hydrologic models. Journal of Hydrology 204: (1-4) 83-97

Yassoglou, N., Kosmas, C.S , Moustakas, N , Tzianis, E. and Danalatos, N G. 1994 Cracking in recent alluvial soils as related to easily determined soil properties. Geoderma 63 (3-4). 289-298.

Youngs E.G. 1990 An examination of computed steady-state water table heights in unconfined aquifers. Dupuit-Forchheimer estimates and exact analytical results. Journal of Hydrology 119 (1-4): 210-214

Youngs, E.G. 1965 Horizontal seepage through unconfined aquifers with hydraulic conductivity varying with depth. Journal of Hydrology 3.283-296

Youngs, E G. 1998 Soil physics and hydrology Journal of Hydrology 100 (1-3): 411-431.

Youngs, E.G., Leeds-Harrison, P.B., and Chapman, J M. 1989 Modelling water table movement in flat low lying lands. Hydrological Processes 3 (4): 301-315.

Youngs, S.E.G., Chapman, J M, Leeds-Harrison, P.B. and Spoor, G. 1991 The application of a soil physics model to the management of soil water conditions in wetland environments in wildlife conditions Hydrological basis of ecologically sound management of soil and groundwater IAHS Publ No. 202

Zepp, H. and Belz, A. 1992 Sensitivity and problems in modelling soil moisture conditions. Journal of Hydrology 131 (1-4)· 227-238.

Zhang, J., Schurr, U., Davies, W.J. 1987 Control of stomatal behaviour by abscisic acid which apparently originates in the roots Journal of Experimental Botany 38 (192): 1174-1187.

Ziemer, R.R. 1979 Evaporation and Transpiration. Reviews of Geophysics and Space Physics 17 (6): 1175-1186.

Zlotnik, V. 1994 Interpretation of slug and packer tests in anisotropic aquifers. Ground Water 32 (5): 761-766.